Creation and improvement of solid fuel piston internal combustion engines.

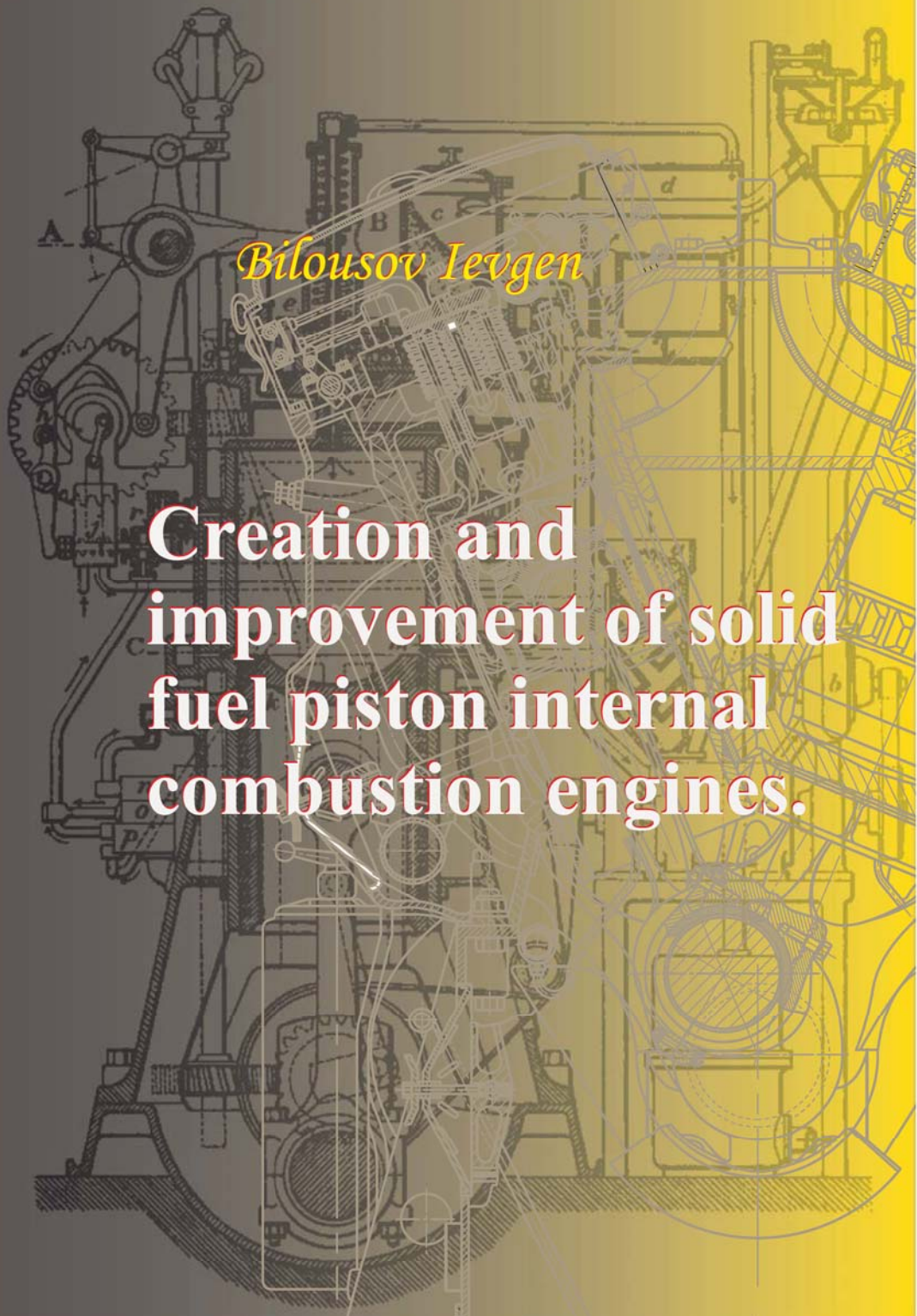

Bilousov Ievgen

Creation and improvement of solid fuel piston internal combustion engines.

I. Bilousov

CREATION AND IMPROVEMENT OF SOLID-FUEL PISTON INTERNAL COMBUSTION ENGINES

Odesa
"Astroprint"
2026

UDK 621.435
B 43

Bilousov I. V.

B 43 Creation and improvement of solid-fuel piston internal combustion engines : [monograph] / I. Bilousov. — Odesa : Astroprint, 2026. — 400 p.

ISBN 978–617–8569–78–5

This monograph outlines the historical background and the evolution of direct solid-fuel combustion techniques within reciprocating internal combustion engines. It offers an in-depth review of the current technological state and proposes solutions for the primary issues regarding the practical application of such engines. The work explores the theoretical aspects of solid-fuel burnout within the engine's combustion chamber, examining both volumetric and layered combustion methods.

The book is intended for specialists focused on the research and advancement of internal combustion engines, as well as a broad audience interested in this field of engineering.

UDK 621.435

У монографії висвітлено історичні передумови та еволюцію методів прямого спалювання твердого палива в поршневих двигунах внутрішнього згоряння. Наведено поглиблений огляд сучасного стану технологій та запропоновано рішення основних проблем практичного застосування таких двигунів. Досліджено теоретичні аспекти вигорання твердого палива в камері згоряння двигуна, розглянуто методи як об'ємного, так і шарового спалювання.

Книга розрахована на фахівців, які займаються дослідженням і вдосконаленням двигунів внутрішнього згоряння, а також на широке коло читачів, які цікавляться цією галуззю техніки.

ISBN 978–617–8569–78–5

© Bilousov I. V., 2026

CONTENTS

INTRODUCTION to the 2026 edition 7
INTRODUCTION to the 2006 edition 8
Chapter 1 Direct combustion of solid fuel in internal combustion engines 10
1.1. History of the issue 10
1.1.1. Period from 1893 to 1939 12
1.1.2. Period from 1945 to 1970 23
1.1.3. The period from 1970 to the present 27
1.2. Analytical research 65
Chapter 2 Economic aspects of the problem of direct combustion of solid fuels in piston internal combustion engines 70
2.1. World fuel resources and the problem of searching for alternative fuels for internal combustion engines 70
2.2. Selection of the method and efficiency of using solid fuels in piston internal combustion engines 74
2.3. Areas of application of engines using direct combustion methods of solid fuel 77
2.4. Economic prerequisites for the conversion of piston engines to coal fuel 77
2.5. Prospects for the use of solid-fuel piston engines in railway transport. 79
2.6. Prospects for the use of solid-fuel piston engines in stationary power generation 81
2.6.1. Increased engine cost and operating costs when using WCS 82
2.6.2. WCS production costs 83
2.6.3. Costs of combating harmful emissions 84
Chapter 3 Solid fuels and fuel suspensions based on them used in internal combustion engines 86
3.1. Raw materials for the production of pulverized coal fuel 86
3.2. Purification of raw materials from mineral impurities 88
3.3. Use of purified pulverized coal fuel 88
3.4. Use of coal suspensions 89
3.4.1. Selecting a liquid carrier 90
3.4.2. Rheological characteristics of the CS 91
3.5. Use of fuel-coal suspensions 102
3.6. Use of coal-water suspensions 106
3.6.1. Influence of source fuel characteristics on WCS propertie 110
3.6.2. Effect of particle size on the combustion behavior of WCS 113
3.6.3. Influence of source fuel parameters on WCS flammability 117
3.6.4. Use of additives to improve WCS performance 117
3.6.5. Storage and transportation of fuel 119
3.6.6. Engine characteristics when running on WCS 120
3.7. Water-methanol-coal suspensions (WMCS) 121
Chapter 4 Injection of suspensions into the engine combustion chamber 125
4.1. Schematic and design solutions for fuel injection system 125
4.1.1. Fuel injection system with pulse feed (plunger pumps) 126
4.1.2. Using pump-nozzles for injection of coal suspension 136

4.1.3. Accumulator fuel injection system ... 138
4.2. Pilot diesel fuel injection system ... 145
4.3. Research of the injection process of suspension ... 149
4.4. Coal suspension injection proces ... 153
4.4.1. Formation and development of the spraying plume and stages of the injection process ... 153
4.4.2. Spray characteristics and aerosol droplet structure ... 159
4.4.3. Change in average particle size along the spraying plume lengt ... 161
4.4.4. Changing the spray cone angl ... 163
4.5. Factors affecting CS spraying quality ... 167
4.5.1. The influence of injection pressure on the spraying quality of WCS ... 169
4.5.2. The influence of air charge density on spray quality ... 171
4.5.3. The influence of the geometric parameters of the sprayer hole on the quality of CS spraying and the characteristics of their combustion ... 172
Chapter 5 Features of the operating process of a piston engine with self-ignition of coal-based fuels under compression ... 182
5.1. Spontaneous self-ignition and combustion of FCS ... 182
5.2. Spontaneous self-ignition and combustion of WCS ... 182
5.2.1. Determination of the WCS self-ignition delay period ... 182
5.2.2. Factors influencing the WCS self-ignition delay valu ... 184
5.3. Study of self-ignition processes of FCS and WCS ... 188
5.4. Ways to improve the self-ignition and combustion of coal fuel ... 191
5.4.1. The influence of injection advance angle on the self-ignition and combustion characteristics of WCS ... 192
5.4.2. The influence of the air charge state at the end of the compression process on the self-ignition and combustion efficiency of coal fuel ... 193
5.4.3. The influence of particle size and polydispersity of coal fuel on its self-ignition and completeness of combustion ... 202
5.4.4. The influence of coal fuel properties on their self-ignition and combustion efficienc ... 204
5.4.5. Increasing the self-ignition of WCS by adding additive ... 204
Chapter 6 Operating process of a coal-based forced ignition piston engine ... 206
6.1. Forced combustion activation. Ignition coefficient ... 206
6.2. Methods of forced ignition of coal fuel in the combustion chamber of a piston engine and their influence on the working process ... 206
6.2.1. Thermal ignition method ... 207
6.2.2. Pilot ignition method ... 208
6.2.3. Stratified ignition method ... 211
6.2.4. Plasma ignition method ... 215
6.3. The influence of air charge parameters at the engine inlet on the efficiency of the working process ... 217
6.3.1. The influence of excess air coefficient on the efficiency of the engine working process ... 218
6.3.2. Effect of engine inlet air temperature on WCS combustion efficiency. 218
6.3.3. The influence of engine inlet air pressure on the WCS ignition process ... 224

6.4. The influence of the injection angle of the pilot DF and WCS on the efficiency of the working process of the engine with pilot ignition ... 227
6.4.1. The influence of the pilot fuel IAA on the efficiency of the working process ... 233
6.4.2. The influence of IAA WCS on the efficiency of the engine working process ... 246
6.5. The influence of spark angle on the efficiency of the working process of an engine with plasma ignition ... 250
6.6. The influence of pilot fuel quantity on the efficiency of the pilotignition engine ... 252
6.7. Regulation of engines operating on WCS ... 256
6.8. Fuel consumption in engines working on WCS ... 261
Chapter 7 Theoretical foundations of burning coal fuel in the working space of a piston engine ... 264
7.1. The process of combustion of solid fuel in the working space of the engine ... 264
7.2. Model of the state of the working body in the engine cylinder ... 265
7.3. Stages of the combustion process of coal suspensions in the working space of a piston engine ... 267
7.4. Formation of active zones ... 270
7.5. Evaporation of the liquid carrier ... 272
7.5.1. Evaporation of DF when using FCS ... 272
7.5.2. Evaporation of water when using WCS ... 273
7.6. Removal of volatile substances ... 274
7.7. Burnout of coke-coal residue ... 281
7.7.1. Burnout of a single coke-coal massif in the working space of a piston engine ... 283
7.8. The combined effect of various factors on the combustion process of coal-water fuel in the engine working space ... 287
7.9. The influence of rotational speed on the efficiency of the engine working process ... 289
Chapter 8 Wear and mitigation methods for solid fuel-based piston engines ... 291
8.1. Wear mechanisms operating in solid fuel-based ICEs ... 291
8.2. Wear of injection system elements ... 294
8.3. Wear of engine components ... 302
8.3.1. The influence of particle size and ash content on the wear rate of cylinder-piston group parts ... 307
8.3.2. Composition of mineral residues and their influence on the rate of engine wear ... 308
8.3.3. The mechanism of wear of engine elements in direct contact with abrasive materials ... 311
8.4. Ways to reduce wear in engines running on solid fuels ... 311
8.4.1. Selection of materials for elements of the engine cylinder-piston group ... 311
8.4.2. Protection of valve timing components, turbocharger blades and pressure-lubricated parts ... 318

Chapter 9 **Environmental aspects of direct combustion of solid fuels in piston internal combustion engines. Methods for reducing harmful emissions** ... 321
9.1. Content of harmful substances in the exhaust gases of piston engines using coal fuel ... 321
9.1.1. Nitrogen oxide content in exhaust gases ... 325
9.1.2. Content of carbon monoxide and hydrocarbons in combustion products ... 328
9.1.3. Sulfur oxide content in exhaust gases ... 331
9.1.4. Content of solid particles in exhaust gases ... 335
Chapter 10 **Layered combustion of solid fuels in reciprocating internal combustion engines** ... 344
10.1. The method of cyclic gasification of solid fuel in the working space of a piston engine ... 344
10.2. The process of layer burning of solid fuel in an internal combustion engine by means of forced purging of the layer ... 346
10.3. Flow of the working process in SFPE with forced controlled blowing of the layer ... 352
10.3.1. Compression process ... 353
10.3.2. The process of heat supply ... 356
10.3.3. The influence of the layer blowing mode on the nature of heat supply in the thermodynamic cycle ... 358
10.4. The process of feeding fuel into the SFPE combustion device ... 359
10.5. Fuels for layer combustion in SFPE ... 360
10.6. The burnout process of solid fuel in a SFPE reactor ... 361
10.6.1. General characteristics of the solid fuel combustion process. Layer structure ... 361
10.6.2. Methods of organizing layered combustion of fuel in a SFPE reactor and their influence on the rate of formation, composition and properties of combustion products ... 363
10.6.3. The process of combustion of solid fuel within the oxygen zone ... 364
10.6.4. The rate of reactions in the layer ... 366
10.6.5. Activation of the fuel layer ... 372
10.6.6. The influence of pressure at the end of the compression process and charge density on the fuel burnout process in the SFPE reactor ... 373
10.6.7. Fuel layer aerodynamics in the SFPE reactor and its influence on the process of working fluid production ... 374
10.7. Ways to improve SFPE with layered combustion of fuel ... 374
10.8. Advantages of layer combustion of solid fuels in internal combustion engines over other methods ... 376
List of references ... 378
Appendix A List of references containing information regarding the direct combustion of solid fuels in piston internal combustion engines ... 384

INTRODUCTION to the 2026 edition

This book authored over twenty years ago. Since then, much has changed, and the primary issues raised herein have largely lost their immediate relevance. However, for this English translation, we deliberately chose not to adapt the text to modern realities. This decision preserves the spirit of an era when scientists were striving to realize a concept that had persisted for over a century: the use of solid fuels in reciprocating heat engines. Although these efforts did not result in the commercial adoption of solid-fuel piston engines, specific solutions developed during these projects paved the way for advancements in other engine types. Notable among these is pilot ignition for fuels with high activation energy or low cetane numbers – a method now widely utilized in dual-fuel gas engines, as well as those running on methanol or ammonia. Furthermore, research into mitigating wear in solid-fuel engines led to the development of specialized coatings that significantly extend the service life of engines operating under standard conditions. The use of coal-water suspensions demonstrated that the presence of water in the combustion chamber substantially reduces nitrogen oxide emissions, forming the basis for modern emission control strategies. It is also worth noting that while Common Rail electronic injection not invented for this specific engine class, it underwent substantial refinement within these projects. Thus, the efforts of scientists and engineers have transformed into modern engine manufacturing, which continues to offer humanity the cheapest mobile energy sources. They have evolved to meet contemporary challenges, remaining the most efficient prime movers available to humanity. The author hopes this book allows readers to appreciate how even an «unsuccessful» attempt at solving an extreme problem can fundamentally reshape a field of science.

INTRODUCTION to the 2006 edition

Piston internal combustion engines (ICEs) are today the most economical primary heat engines, which has contributed to their widespread use in all spheres of human economic activity. A significant disadvantage of piston engines is that the vast majority of them operate on oil and gas fuels, due to which the prospects for their further development and use directly related to the changes taking place in the global oil and gas complex. The practice of recent decades shows that with an increase in the need for oil and gas fuels, their cost, although it fluctuates within significant limits, is, on average, steadily increasing. It is easy to foresee that this trend will continue in the future. This is due to a number of objective reasons related to the limited reserves of these energy resources, as well as the result of various political combinations, and sometimes-outright speculation. All the energy crises that have occurred over the past decades have primarily concerned crude oil and liquid hydrocarbon fuels derived from it.

An objective reason that should take into account when determining priorities for the development and improvement of internal combustion engines is the fact that crude oil and natural gas are non-renewable energy sources. Their reserves may exhausted already in this century, but even now, many countries feel a lack of oil and gas to ensure the functioning of their energy and transport systems. At this stage, the problem is local in nature and explained by the uneven distribution of oil across regions. There are very few countries in the world that cover their oil needs through their own production, and even fewer countries that are able to export oil to foreign markets. This once again shows how vulnerable the world economy as a whole and the transport system in particular are, how dependent it is on the conditions of the global oil market and how important and difficult it is to solve the problem of finding alternative fuels for internal combustion engines.

An analysis of the world's resources of non-renewable fuels allows us to conclude that coal is the most promising for use in the energy sector. The amount of proven coal reserves, converted to equivalent fuel, is more than ten times greater than proven oil reserves. For this reason, many experts see the transfer of some part of internal combustion engines to the use of various types of solid fuels as one of the alternative ways of their development. The most effective method of using solid fuels in internal combustion engines is their direct combustion in the working cylinder of the engine. This method allows you to most fully realize the advantages that distinguish piston engines from other types of heat engines. However, it is this method that is also the most difficult to implement, as it is associated with the need to solve

a number of serious problems: the difficulty of implementing an effective thermodynamic cycle using solid fuel; high abrasive wear of working cylinders, pistons, fuel supply equipment and other engine parts; the need to comply with environmental requirements, etc.

The purpose of this book is to show the current state of the issue, systematize the available information on research devoted to the problem of direct combustion of solid fuels in piston internal combustion engines, analyze the results obtained, and identify ways for further development and improvement of solid fuel piston engines. The book intended for a wide range of readers familiar with the structure and operation of piston internal combustion engines; it may be useful to specialists in the field of engine design, as well as students and graduate students studying in the specialty «Internal Combustion Engines» and «Marine Power Plants».

Chapter 1

Direct combustion of solid fuel in internal combustion engines

1.1. History of the issue.

The history of the development of internal combustion engines (ICE) inextricably linked with attempts to create engines capable of operating on various types of solid fuel. Suffice it to remember that the first piston engine was proposed in 1678 the outstanding Dutch mathematician, mechanical engineer and physicist Christiaan Huygens (1629-1695). It assumed that black powder would use as fuel for such an engine. This engine did not reciprocate, but rather operated with a single downward stroke of the piston, driven by the vacuum created in the cylinder after the propellant gases released. A propellant charge used to raise the piston to its upper position. This meant that the engine's power stroke achieved not by the expansion of the propellant gases, which pushed the piston upward, but by the subsequent drop in pressure in the working cylinder. In 1682, a prototype engine capable of lifting several people created [12].

Christiaan Huygens
1629-1695

Demonstration of Huygens' prototype gunpowder engine in 1682

Proposed in 1860 by the Belgian engineer Etienne Lenoir (1822-1900), the engine ran on so-called city gas, which in those days produced at special gas stations by gasifying coal [18].

The idea of using generator gas later borrowed by Eugen Langen (1833-1895) and Nikolaus Otto (1832-1891) for their four-stroke engine, which used precompression of an air charge. This engine consumed four times less generator gas than the Lenoir engine and was the first efficient piston internal combustion engine [18].

The use of generator gases had a great inconvenience – gas generator engines could only installed in the immediate vicinity of gas generator stations. The use of gas engines in transport was associated with a number of both design and operational inconveniences. Because of numerous searches for universal fuels for internal combustion engines, the choice fell on

petroleum products. This type of fuel was subsequently associated with significant improvements in Otto engines and their widespread use in transport.

Despite the fact that by the end of the 19th century, Otto engines had already become widespread in industrial enterprises and in some vehicles, the idea of creating an engine capable of running on solid fuel remained relevant and continued to interest specialists as one of the alternative ways for the further development of internal combustion engines. In addition, this idea had very definite economic prerequisites.

At that time, the coal industry of many economically developed countries, such as the United States of America, Britain, Germany, Russia, was in a booming stage, and the oil industry was just emerging. In addition, large oil fields by this time either had not yet been discovered (as, for example, in the USA), or were located outside those countries in which the pace of industrial development was the greatest (for example, Britain, Germany and France). Therefore, along with the use of generator gas and petroleum products, some specialists of that time attempted to directly fine coal dust to power internal combustion engines operating on the Otto cycle.

The idea of using coal dust as fuel, in general, lay on the surface, since by that time it well known about the ability of coal dust to form a rather explosive mixture with air. This was the repeated cause of accidents in coalmines, and it this property of the coal-air mixture that suggested the possibility of using it as fuel for internal combustion engines. However, the designers had to face serious technical difficulties, which included poor carburation of coal dust, as result of which it was not possible to achieve a stable dosage of the composition of the coal-air mixture. In addition, external mixture formation led to the fact that coal dust entered the cylinder at the beginning of the compression process, and its particles exposed to almost the entire internal surface of the working cylinder. As a result, some of the coal dust abundantly deposited on the oil-coated walls, forming a coating that did not take part in combustion and, accumulating, quickly disables the engine [16].

These circumstances turned out to be practically insurmountable and forced the abandonment of the use of coal dust in engines with external mixture formation, so almost all-further research carried out on engines with internal mixture formation.

In total, the problem of using solid fuels for internal combustion engines remains relevant and has attracted the interest of specialists for more than a hundred years. The bulk of the research conducted during this time was experimental in nature, and only in recent decades attempts been made to

provide a theoretical basis for these studies. Throughout the entire designated period, views on the problem have repeatedly changed, and therefore, approaches to solving it have changed accordingly. Apart from scattered attempts to use coal dust in engines operating on the Otto cycle, all research carried out during this time can be divided into three main stages.

The first stage began with the work of R. Diesel to create a rational heat engine. This period characterized by the fact that most of the work on creating a piston internal combustion engine capable of running on solid fuel carried out in Germany. At the same time, the main efforts of researchers aimed at studying the possibility of burning coal fuels in the form of fine dust. This period lasted until the outbreak of the Second World War.

The second period, which began after the Second World War, lasted until the energy crisis of 1972-73.

The third period continues to the present day and characterized by the fact that the main attention in the ongoing research is on the use of coal fuels in the composition of fine solutions with water, diesel fuel, various alcohols, vegetable oils, and synthetic liquid fuels.

1.1.1. Period from 1893 to 1939. The first attempt to create a piston internal combustion engine capable of running on solid fuel made in 1892 by the German engineer Rudolph Diesel (1858-1913). On February 28, 1892, he received patent No. 67207 for «Working process and method for making a single-cylinder and multi-cylinder engine» [11, 12, 16]. About a year after receiving the patent, the publishing house of technical literature Julius Springer in Berlin published a brochure by Diesel entitled «Theory and design of a rational heat engine designed to replace the steam engine and other engines currently existing» (*Theorie und Konstruktion eines rationellen Wärmemotors zum Ersatz der Dampfmaschine und heute bekannten Wärmemotoren*). In this brochure, Diesel, analyzing the experience of creating piston engines, as well as the basic theoretical principles of thermodynamics, including those developed by Sadi Carnot in his work «On the driving force of fire and on machines capable of converting this force», and proposed the concept of creating a rational heat engine. At the same time, the use of solid fuel in the form of fine coal dust, blown into the cylinder at the end of the compression process using a jet of compressed air, considered as the main design advantage of the new engine. Diesel based on the belief that the energy of the air charge as result of strong compression can exceed the threshold for activating the combustion process of coal particles, and, as consequence of this, self-ignition of the coal-air mixture will occur in the

engine cylinder. To achieve this, it proposed to increase the compression ratio of the air charge several times compared to the Otto engine.

Rudolph Diesel
(1858-1913)

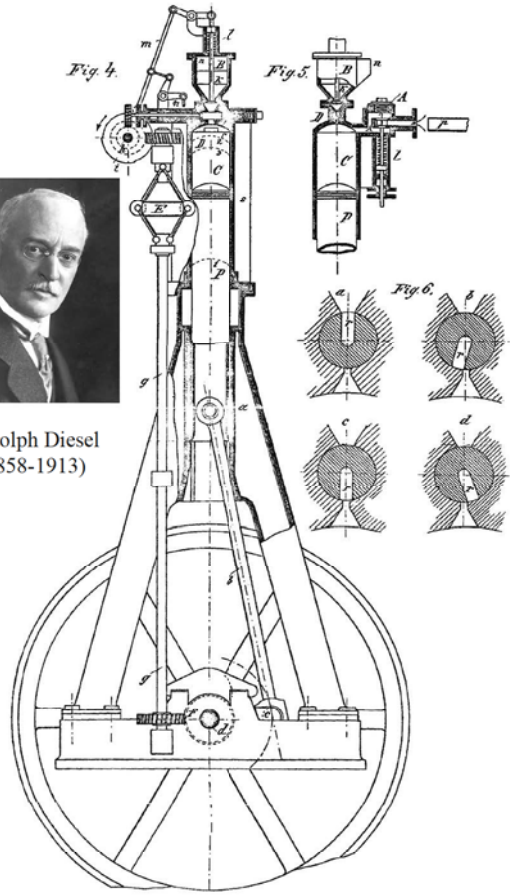

Original design of a diesel engine with a device for feeding coal dust (German Patent No. 67207)

Further, Diesel believed that slowly burning coal dust would enter the cylinder in certain quantities gradually, over a certain period, so that the heat released during the combustion process would compensate for the consumption of internal energy of the working fluid to perform external work as the piston moves.

Such a solution, as the inventor believed, would make it possible to obtain an isothermal supply of heat to the working fluid, as result of which the change in pressure in the engine cylinder would occur smoothly. During the subsequent expansion process, this would allow the temperature of the exhaust gases to reduce as much as possible, thereby reducing the amount of heat removed during the thermodynamic cycle. According to Diesel's calculations, it turned out that the average temperature operating in the engine would be at the level of the average temperature of the operating cycle of steam engines. In this regard, he considered it possible to abandon the cooling system of the working cylinder and engine head in the engine he was designing [12].

In his brochure, Diesel did not limit himself to describing theoretical premises and design solutions. In order to make his project attractive, he examined in detail the economic aspects of the creation and introduction into industry of a solid fuel piston engine. The developing German industry required a new, economical, highly efficient engine mover capable of using cheap solid fuels.

Diesel's work aroused great interest among specialists, finding both supporters and opponents. In fact, a fundamentally new type of engine proposed with the gradual combustion of coal dust sprayed in an air charge. Many assessed the provisions set out in the brochure as extremely interesting in theoretical terms, but hardly feasible in practice. Nevertheless, no one doubted that if the theoretical premises described by Diesel could implemented in practice, then the engine obtained in this way would have undeniable advantages over all heat engines known at that time.

To promote his project, Diesel enlisted the support of the most authoritative scientists of his time, in particular, his former teacher at Westbaden Technical University, Professor Lidne, known as the creator of the method of liquefying air, and the largest authorities in the field of technology, Professors Stehr and Zeiner. Diesel sent copies of the brochure, along with copies of reviews from Lidne, Stehr and Zeiner, to a number of machine-building plants in Germany, Austria and Switzerland. After negotiations in February 1893, the Augsburg Engineering Plant (Maschinenfabrik Augsburg, now part of the MAN concern) agreed to allocate funds for the construction of an experimental engine. Later, in April of the same year, the largest steelmaking company of Friedrich Krupp in Essen joined in financing the project [12, 28]. The most attractive thing about the Diesel project for the two largest companies in Germany was precisely the fact that the designed engine was supposed to run on coal, the reserves of which the latter provided with more than any other energy source. In the context of the looming redivision of the world and the numerous wars that Germany regularly waged with its neighbors, energy independence acquired decisive military and political importance. From the same point of view, this work aroused interest in other countries and, first, in England, which, like Germany, did not have any significant oil reserves. Subsequently, Diesel's brochure translated into English, and the work carried out at the Augsburg plant observed by specialists from England, France, the USA and Russia.

Consistently from 1893 to 1897, R. Diesel produced three prototypes. The first fully complied with the principles set out in his patent, however, faced with difficulties in feeding dust into the combustion chamber, the inventor decided to first test the engine on liquid fuel – lamp kerosene. This measure

considered by Diesel as temporary, necessary to perfect the work process. After the basic principles of operation of the new engine studied, the inventor intended to return to studying the issue regarding the use of solid fuels. The third engine, built by Diesel, running on kerosene, showed an efficiency of about 26.2%, which was two to three times higher than the efficiency of other heat engines known at that time. Therefore, even in this form, the Diesel engine began to be in commercial demand, and the main efforts of the inventor, like most other engineers, aimed at improving the work process based on the use of liquid fuels. R. Diesel returned to the idea of using pulverized coal fuel only once in his practical work. On one of the experimental engines, an attempt made to burn coal dust by feeding it into the working cylinder through the intake manifold. There is no information about what kind of fuel it was. However, knowing the composition of the coals that Germany had and the methods of grinding them characteristic of that time, we can assume that it was coal dust with an ash content of about 10% and a particle size of about 100 μm. The engine ran for approximately 7 minutes before the piston seized in the cylinder. Disassembly of the engine showed that unburned coal dust, mixed with lubricating oil, clogged the entire space between the piston rings. Regarding the tests carried out in this way, Diesel made the following entry in the laboratory journal: «A real pulverized coal engine must be specially studied and constructed from parts specifically designed for this fuel. It is necessary that the piston lubrication allows for the systematic purging of dust particles trapped between the piston rings». R. Diesel did not return to the issue of using solid fuels in his practical work [40].

Technical difficulties associated with the preparation, storage and supply of pulverized fuel, with high wear of cylinders, pistons and piston rings, turned out to be insurmountable at that time. However, the idea of practical implementation of Diesel's theoretical developments to create a rational engine running on pulverized coal fuel has attracted the attention of many specialists throughout the entire time that has passed since the publication of his brochure.

***

The first who managed practically implement the working cycle of a piston engine using solid fuel was the German engineer Rudolf Pawlikowski, formerly one of Diesel's assistants. At the machine-building plant in Görtlitz, starting in 1916, he spent forty years studying issues related to the use of solid fuels. During this time, he built a number of engines that worked quite well on coal dust and were practically not inferior to diesel engines in fuel efficiency.

Rudolf Pawlikowski (1868-1942)

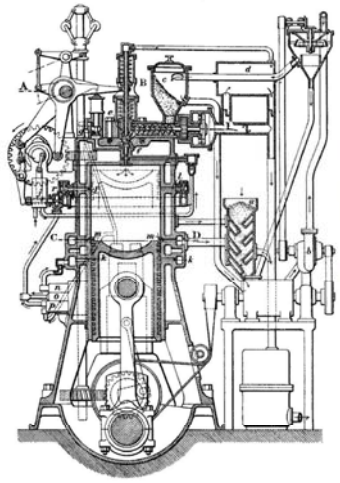

The design of the Rupa engine running on pulverized coal

Following the example of their former mentor, such engines were called «Rupa-motors», that is, Rudolf Pawlikowski's motors [11, 16, 40]. The inventor managed to build the first working engine in 1928. It was a single-cylinder engine with dimen-sions D/S=420/630 mm, which developed a power of 59 kW at a rotation speed of 167min^{-1}. The equivalent fuel consumption was 440 g/(kWh), which corresponded to an engine efficiency of 31%.

Following the first successful model, the inventor created a second engine, which already had three cylinders with dimensions D/S=320/520 mm and a power of 110 kW at a rotation speed of 215 min^{-1}.

In 1936, German technical journals reported that Pawlikowski had succeeded in eliminating the main obstacle to the widespread use of pulverized coal fuel in piston engines – the problem of abrasive wear. An attempt even made to produce a small industrial batch of such engines. The first industrial engine was, as if all previous Pawlikowski engines manufactured at the Kosmos plant, because of which it received the name «Cosmos-Rupamotor». The engine had one cylinder with dimensions D/S = 500/720 mm and developed a power of 103 kW at a rotation speed of 166 min^{-1}. The engine was equipped with an original system for blowing piston rings with compressed air, which, according to the inventor, made it possible to obtain wear comparable to diesel engines running on liquid fuel.

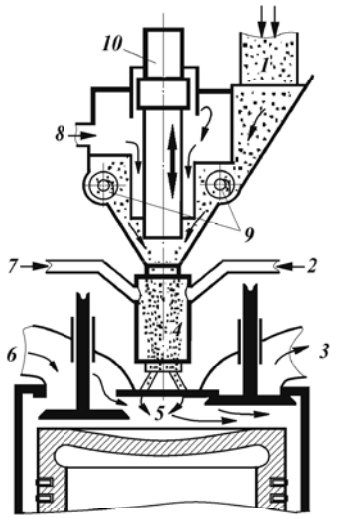

Fig. 1.1. Scheme for feeding coal powder into the combustion chamber of R. Pawlikowski's engine

In addition to increased abrasive wear, when creating his engine, Pawlikowski faced with the problem of supplying fuel to the combustion chamber. Mechanical feed proved unsuitable due to the difficulty of synchronizing the speed of the feeder with the air fluctuations in the intake manifold. Preference given to a scheme with pneumatic fuel supply to the combustion chamber, which, in general, looked like this (Fig. 1.1) [16].

During the period when gas exchange occurs in the working cylinder, coal dust from the fuel supply funnel 1 with intermediate air supplied through the annular space 8 entered the prechamber 4 through the open spool valve 10. At the end of compression, the spool valve went down, isolating the supply system from the working engine space. After this, compressed air and ignition fuel 7 were supplied to the prechamber under a pressure of 5.9 MPa through channel 2, which then, mixed with coal powder, entered the combustion chamber of engine 5 through the channels.

The air required for fuel combustion sucked in through the intake manifold 6, and the exhaust gases removed through the exhaust manifold 3. To prevent the coal dust from being subjected to compression, which could cause briquetting or a decrease in volume, and to avoid caking, two rotating rippers 9 were installed in the supply chamber.

The inventor claimed that he managed to increase the engine life to 11 thousand hours, if the rings were replaced after every thousand hours of operation [11, 16, 40].

The engine featured a number of original design features, both in terms of the choice of materials for the cylinder-piston assembly and fuel supply equipment, and in terms of design solutions aimed at reducing wear. Despite this, there is every reason to believe that the claimed service life of this engine is significantly overstated. Furthermore, all tests not properly recorded.

In addition to R. Pawlikowski, four other large German companies have been conducting their independent research since 1925 in the field of creating an engine running on pulverized coal fuel [38, 40]. Five engines were built and tested by Farben Industrie between 1925-29. The main goal pursued in this case was the creation of a factory power plant capable of generating cheap energy. During testing, the company's specialists, like their predecessors, encountered large abrasive wear. To reduce it, the design of the pistons was changed. The piston rings installed in the cylinder liner so that the ring's protrusion from the groove could adjust as wear occurred. To clean the cylinder walls from coal particles, they blown with compressed air and flushing with water or liquid petroleum products tried. In addition to measures aimed at reducing abrasive wear, a system for supplying pulverized

coal fuel to the engine cylinder tested. Initially, the fuel supply system borrowed from Pawlikowski, but it turned out to be insufficiently reliable and did not provide normal engine regulation, as result of which it subsequently abandoned. Subsequently, compressed air under pressure up to 6.0 MPa, obtained from a three-stage compressor, used to supply fuel to the engine combustion chamber.

Between 1930 and 1932, Schichau Werke tested a version of the engine manufactured by the «Cosmos» plant. The company's engineers faced with the fact that the fuel supply system did not make it possible reliably regulate the engine, and did not provide stable ignition.

Based on the existing design, the company's specialists developed their own, for the manufacture of which special wear-resistant materials used. However, as in previous designs, the fuel supply system remained pre-chamber. According to the company's specialists, they managed to increase the engine life to 6 thousand hours, but there is currently no other information confirming this result.

Subsequently, the company's management curtailed all work on creating an engine using pulverized coal fuel, considering this work to economically unjustified.

***

Bruenner Machinenfabrik manufactured 6 solid fuel engines designed to run on coal dust. At first, the engines had a fuel supply system to the working cylinder the same as in Pawlikowski's engines, however, having encountered the same difficulties as Schichau, this system abandoned, replacing it with a more advanced one, developed at the Dresden Technical University. The new fuel supply system made it possible to significantly turbose the flows of the air-fuel mixture in the engine combustion chamber, which made it possible to increase the burning rate of coal particles to values comparable to the burning rate of liquid fuel. As a result, a rotation speeds of about 1200 min^{-1} obtained on one of the engines. In this case, lignites with an ash content of up to 21% and a particle size of about 60 μm used as fuel. The use of wear-resistant materials made it possible to increase the engine service life to 4000 hours. The Second World War interrupted the company's research

***

HANOMAG (Big German automobile company) has created one engine designed to run on coal dust. No reports regarding the engine test results have been preserved, although the specialized literature reported that the engine operated for 700 hours. It is also known that the company's specialists attempted to improve the method developed by Pawlikowski of feeding coal

dust into the cylinder. At the same time, the possibility of supplying fuel to the working space of the engine without spraying at all, using a special pre-chamber method considered. The essence of the process was that fuel filled a special pre-chamber, usually during the suction process. During the compression stroke, air from the working cylinder, entering the pre-chamber through a special channel, actively mixed with coal dust, resulting in the preparation of a dust-air charge. The prechamber volume was set within 0.4...0.7% of the engine cylinder volume. This solution made it possible to reduce the air pressure required to supply fuel to the prechamber to 2.4...2.9 MPa, which made it possible to reduce energy costs for the compressor drive. When testing on a real engine equipped with such a fuel supply system, the researchers encountered the problem of premature ignition of pulverized coal fuel. In addition, the remnants of unburned coal dust were not completely blown out of the prechamber, so an additional stream of air had to be introduced to remove them. Based on the research carried out, the company's specialists came to the conclusion that this engine power supply circuit most likely cannot be used in further developments, since it is unable to provide effective engine control under changing load-speed conditions. The engine was later upgraded to include a coal dust injection system that used high pressure air. The engine built by HANOMAG was destroyed during the Second World War.

***

It was not possible to find any reliable information regarding the use of solid fuel during the Second World War. At the same time, it known that the German government planned to transfer an order to one of the engineering firms for the construction of a 447 kW diesel engine designed to operate on coal dust. This fact indirectly indicates that by this time German machine technology had reached a level allowing the transition to the commercial use of this type of engine [40].

In addition to Germany, research on the use of pulverized coal fuel for internal combustion engines carried out at the Carnegie Institute (USA). Here, higher fuel efficiency indicators were obtained, the consumption of which, in terms of conventional fuel consumption, amounted to 380 g/(kWh), which corresponded to an effective efficiency of 32.5% [16].

There is also information that before the Second World War, the English Institute of Fuels Research conducted a series of experiments to study the wear of the cylinder-piston group in the presence of abrasive material in the lubrication zone of the rubbing pair. For these experiments, a 6-cylinder gasoline engine with a power of 56 kW and a rotation speed of 2000 min^{-1} used. A mixture of coal dust and gasoline used to power the engine.

Based on the results of the first stage of research, it should note that, thanks to the joint efforts of scientists and engineers, a number of important issues were resolved by the beginning of World War II. Some solutions were notable for their originality, so it makes sense to dwell on some of them in more detail.

Specific problems include the problem of transporting fuel to the feeder.

As studies have shown, mechanical feeding, using screw conveyors and sluice devices, turned out to be unsuitable due to the difficulties of regulating the speed of the feed screw and synchronizing its rotation speed with load changes.

Supplying fuel with compressed air had advantages. However, during testing of engines with this method of transporting dust, several major accidents occurred, as a result of which it was abandoned due to the risk of explosion.

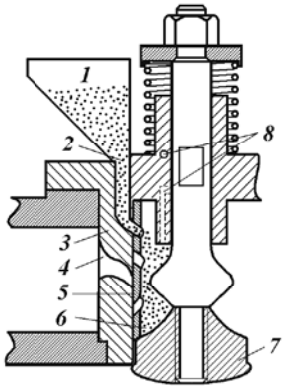

Fig. 1.2. Coal dust dosing device

The simplest and most reliable way to supply coal dust from a tank to the engine feed device is to move it under the force of its own weight with the appropriate arrangement of tanks and fuel supply devices.

The entire process of supplying fuel to the engine consists of two stages that are distinct from each other. The first is the supply of dust, and the second is its blowing into the combustion chamber. In Fig. 1.2 shows one of the design schemes for dust supply [16].

From the funnel 1, the dust, under the influence of gravity, through the supply channel 2 in the body of the supply chamber 3 and the channel in the spool sleeve 5, enters the cavity 6, which serves to accumulate dust prepared for combustion. The second stage begins, associated with the blowing of dust into the combustion chamber at the end of the compression stroke. When valve 7 opens, the spool sleeve moves downward, closing channel 2 and opening channel 4, through which compressed air is supplied to chamber 6. Coal dust is picked up by a stream of compressed air and blown into the

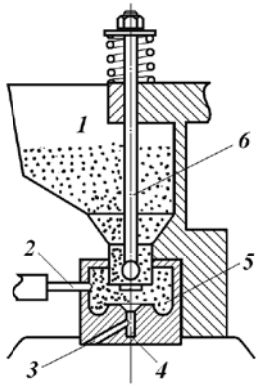

Fig. 1.3. Coal dust feeding device

combustion chamber of the engine, where it ignites upon contact with heated air. Before closing the valve, its rod is blown with compressed air through aeration channels 8 to avoid jamming.

In Fig. 1.3 shows another version of the device for supplying pulverized fuel into the combustion chamber by directly injecting it with compressed air [16]. The device consists of a sealed chamber 1 with a supply of pulverized fuel, a sealed chamber 5 for fuel prepared for combustion, a channel for the intake of compressed air 2 and exhaust channels 3 and 4. The beginning of spraying and the amount of fuel entering the cylinder is determined by the moment and time of valve opening 6. The valve opening period can vary depending on the crankshaft angle, starting 15° before TDC and continuing up to 45° after.

In the field of organizing the working process of a pulverized coal internal combustion engine, it was found that the most favorable conditions for mixture formation are created by pneumatic spraying of coal dust.

As already noted, the most difficult problem in using pulverized coal fuel in internal combustion engines is the increased abrasive wear of parts of the cylinder-piston group. It is enough to note that with an hourly consumption of 50 kg of pulverized coal fuel with an ash content of about 1%, 0.5 kg of abrasive material passes through the working cylinder. At the first stages of the study, with a cylinder diameter of 420 mm, wear reached 0.05 mm/h, while in diesel engines running on heavy oil fuels this figure does not exceed 0.001...0.003 mm/h. During the period under review, encouraging results achieved in addressing issues of extending engine life. The fight against wear carried out in two main directions:

• design changes are aimed at reducing the impact of abrasive materials on engine parts.

Such events include:

– the presence of a special blowing system designed to remove abrasive material;

– the presence of a system for adjusting the extension of the rings sealing the gas joint as they wear out;

– modernization of the lubrication system, aimed at reducing the ingress of pulverized coal particles into the oil and more effectively cleaning it.

• appropriate selection of wear-resistant materials for the manufacture of parts that have direct contact with abrasive particles.

In addition to design changes, it found that chromium-nickel cast iron, as well as cast irons with molybdenum additives, have significantly higher wear resistance. Schichau specialists, according to their information, thanks to the selection of materials, managed to achieve wear on parts of the cylinder-

piston group that is almost comparable to that of liquid-fuel internal combustion engines.

In terms of improving the work process, it was possible to reduce the consumption of equivalent solid fuel from 380...400 g/(kWh) to 280...300 g/(kWh). As a result, the efficiency of pulverized coal engines approached the efficiency of diesel engines, but operating costs associated with the need to grind coal and increased lubricating oil consumption were significantly higher than for diesel engines [16].

Despite some progress in improving designs and working processes, these engines did not become widespread during the period under review. The reasons for this were both purely technical factors and political aspects of the time.

Technical reasons include the fact that neither R. Pawlikowski nor other engineers were able to solve the entire complex of problems formulated by R. Diesel regarding the creation of a rational engine. The heat engines created during this period differed from diesel engines only in the type of fuel used; the thermodynamic cycles underlying their operation remained unchanged. At the time of their creation, their fuel efficiency was practically no different from that of diesel engines. In addition, diesel engines had undergone significant improvements in the period leading up to World War II. In particular, starting in 1907, the cumbersome air fuel injection system, which required significant energy costs to drive the compressor and actually created to use pulverized coal fuel, replaced by a more advanced and less energy-intensive mechanical injection system. This made it possible to increase the engine efficiency by an average of 2...4%. However, the most important factor was that by this time, the infrastructure for the production of both the engines themselves and the fuels for them had created, and a system for maintaining and operating plants equipped with diesel engines had established.

Political factors include the fact that by the time engines powered by coal dust created; Germany had mastered the production of synthetic liquid fuels obtained by processing coal. Since Germany was actively preparing for war at that time, a radical restructuring of the entire fuel and energy complex was practically impossible. An important circumstance that significantly influenced the decline in interest in the problem of direct combustion of solid fuels in piston engines was the fact that the methods for producing synthetic liquid fuels, mastered by German industry on the eve of the Second World War, aimed at producing light motor fuels. As a result, the main bet in the upcoming war placed on Otto engines running on both synthetic fuel and generator gas.

Thus, the period preceding the Second World War was characterized by the development and testing of design solutions related to the organization of the work process in a pulverized-coal piston engine. Experimental studies carried out, during which issues of fuel dosage, its supply to the cylinders, and methods for activating combustion processes studied. The selection of materials for the manufacture of main engine parts has carried out. Some generalizations made; conclusions and recommendations formulated for further improvement of pulverized coal internal combustion engines. The foundations have developed that laid the foundation for theoretical methods for calculating the combustion processes of pulverized coal fuel in the working space of the engine. The most promising fuels have been identified, the processes of preparing them for combustion have been worked out, the basics of operating pulverized coal internal combustion engines have been developed, as well as other aspects of the problem that are important for continuing work to improve the design and operating process of the engine.

1.1.2. Period from 1945 to 1970. The first post-war attempt to use coal fuel in internal combustion engines apparently made Hanse D.J. at North Carolina State University (1949). Experiments were carried out with fuel-coal suspensions (FCS) on a serial four-stroke Hill engine (model R-4) with D/S = 89/133 mm [38, 40]. The suspension consisted of 20% bituminous pulverized coal particles with an average size of 45...75 μm and diesel fuel (DF). To supply the suspension to the engine combustion chamber, a standard Bosch mechanical injection system with an injection pressure of 12.4 MPa used.

During the first tests, frequent jamming of the spray needle observed. The engine speed was unstable when the rack was in a fixed position. Omissions of work processes observed. The average engine speed was 1200 min^{-1}, and power measured during testing. During four consecutive experiments, the power gradually decreased and amounted to 12.4, 10.3, 7.8 and 6.0 kW, respectively. The test time is unknown, and it is unknown how many coal particles burned out as result of the working process. After the tests, the engine disassembled. During inspection, no significant wear of parts found, with the exception of the plunger pair of the fuel pump. According to the researcher, this is what caused the decrease in power.

Based on the test results, a number of recommendations developed aimed at further improving the operating processes of engines operating on fuel-coal suspensions. In particular, it indicated that it was necessary to refine the spray nozzle, adjust the start of injection within a wider range, and optimize the valve timing and the shape of the combustion chamber.

***

Despite the general trend towards the use of solid fuels in internal combustion engines as part of liquid dispersed solutions, during this period some researchers continued to study certain aspects of the problem of using pulverized coal fuel in internal combustion engines. In particular, the work carried out in the USSR in 1952 by V.V. Esin devoted to the issues of supply and spraying of pulverized coal fuel, as well as to the study of factors influencing mixture formation and the nature of development of the pulverized coal torch jet. [16]. The studies were carried out in a special camera made of transparent material and adapted for direct observation and high-speed film photography. The experiment was set up in such a way that the chamber simulated actual conditions characteristic of a motor vehicle diesel engine. At the same time, the influence of individual parameters on the process of development of the jet of the fuel-air torch assessed, keeping other factors constant. During the study, it found that the range of the dust-air torch should be relatively small in the initial stage of the injection process and reach its maximum in the final stage. The torch should direct along the cylinder axis. This creates more favorable conditions combustion of the pulverized fuel. It has also been established that the range and speed of movement of the fuel flame front depends on the pressure of the atomizing air, the back pressure in the cylinder, the lifting speed of the nozzle needle, the fineness of the dust grinding, the type of fuel used, the shape and size of the sprayer nozzles. In this case, the grinding fineness is not the decisive factor determining the size of the particles entering the combustion chamber, since during pneumatic spraying, when the pressure is released, the particles are ruptured by compressed air located in the intrapore space of the particle. In addition, the grinding fineness increases due to friction between the particles as they move in the compressed air stream.

***

In 1957 at the Southwest Research Institute (USA) Tracy E.W. and others conducted experiments aimed at studying the possibility of using FCS for a diesel locomotive engine [38, 40]. The fuel used in the tests contained up to 30% coal dust, various initial solid fuels with particle sizes of the order of 20 μm. It decided to conduct initial research on a small 3.4-liter four-stroke Caterpillar engine using a standard injection system. During the first three and a half hours of testing, the engine power decreased from 17.9 to 8.9 kW at a speed of 1000 min^{-1}. During the experiments, the engine had to stop many times to eliminate sticking of the nozzle needle or fuel pump plunger. It found that the wear rate of piston rings and cylinder liner is 35 times higher than that for an engine running on pure diesel fuel. No influence

of the type of initial solid fuel on engine performance detected. Tests have shown that the plunger pairs of the fuel pump are subject to the greatest wear. It was found that at a sufficiently high rotation frequency, coal particles do not have time to burn out completely, as a result of which large mechanical entrainment is observed. Significant deposits consisting of unburned fuel particles and ash found in the engine exhaust ports.

The main conclusion drawn from the results of the experiments was that rational combustion of carbon fuel is possible only in low-speed engines, in which the time for combustion of coal particles is much longer. For medium- and high-speed engines, efficient combustion of suspensions is a technically difficult task. Even if it is successfully resolved, it is unlikely that this will reduce the costs of operating such engines in railway conditions. Based on these findings and due to the uncertainty of the prospects for commercial use of this type of fuel, further funding for research stopped.

***

In 1959, despite the first unsuccessful results obtained by Tracy E.W., Marshall H.P. and Shelton C., at Virginia tech (USA) carried out a new study aimed at studying the possibility of using FCS in diesel locomotive diesel [38]. The experiments were carried out on a single-cylinder nordberg engine with cylinder dimensions D/S=114/133 mm and a rotation speed of 1700 min^{-1}. During the experiments, a certain part of diesel fuel injected into the combustion chamber using a fuel pump, and coal dust in an amount of 50% of the mass of liquid fuel supplied to the working cylinder through the intake manifold by mechanical spraying in the airflow entering the engine. Initially, it planned to test for 100 hours, but after 6 hours, the exhaust valve jammed in the engine, resulting in a broken pusher rod. In addition, there was serious envelopment of the metal of the aluminum piston onto the cylinder liner. The piston rings extremely worn and the top ring broken. The crankshaft bearings worn as if there was an abrasive material in the oil. After replacing the piston, liner and rings, the test continued. After 7 hours, the engine stopped, and it was impossible to start it later. Compression measurements showed a twofold decrease. After the next repair, the engine worked continuously for 22 hours and failed because the channels supplying oil to the crankshaft bearings clogged with carbon particles. After this, the original goal of conducting research for 100 hours abandoned, and the entire test lasted no more than 45 hours. The main conclusion drawn from the results of the study was that for the successful operation of diesel engines at FCS, it is necessary to modernize the lubrication system in such a way as to prevent the ingress of coal particles into the lubricating oil. Only in this case can continuous engine operation achieved.

In 1959, despite the first unsuccessful results obtained by Tracy E.W., Marshall H.P. and Shelton C., at Virginia Tech (USA) carried out a new study aimed at studying the possibility of using FCS in diesel locomotive diesel [38]. The experiments were carried out on a single-cylinder Nordberg engine with cylinder dimensions D/S = 114/133 mm and a rotation speed of 1700 min^{-1}. During the experiments, a certain part of diesel fuel injected into the combustion chamber using a fuel pump, and coal dust in an amount of 50% of the mass of liquid fuel supplied to the working cylinder through the intake manifold by mechanical spraying in the airflow entering the engine. Initially, it planned to test for 100 hours, but after 6 hours, the exhaust valve jammed in the engine, resulting in a broken pusher rod. In addition, there was serious envelopment of the metal of the aluminum piston onto the cylinder liner. The piston rings extremely worn and the top ring broken. The crankshaft bearings were worn as if there was an abrasive material in the oil. After replacing the piston, liner and rings, the test continued. After 7 hours, the engine stopped, and it was impossible to start it later. Compression measurements showed a twofold decrease. After the next repair, the engine worked continuously for 22 hours and failed because the channels supplying oil to the crankshaft bearings clogged with carbon particles. After this, the original goal of conducting research for 100 hours abandoned, and the entire test lasted no more than 45 hours. The main conclusion drawn from the results of the study was that for the successful operation of diesel engines at FCS, it is necessary to modernize the lubrication system in such a way as to prevent the ingress of coal particles into the lubricating oil. Only in this case can continuous engine operation achieved.

***

Subsequently, the possibility of using coal fuel in diesel locomotive diesel studied Rich L.L., and Walker M.L. [40]. The study carried out at Harvard University in 1969. The main objective was to study the effect of fuel composition on the wear of engine parts. The diesel locomotive SD-45 considered as an object of modernization. It was assumed that when using FCS with a bituminous coal content of about 45% and an average particle size of about 75 μm, its effective performance would deteriorate by no more than 25% compared to the use of liquid fuel. All studies carried out, as in the previous case, on a single-cylinder Nordberg engine with cylinder dimensions D/S = 114/133 mm, but the rotation speed was limited to 1000 min^{-1}. As in the experiments conducted by Marshall and Shelton, coal dust supplied mechanically through the intake manifold. Based on the results of their predecessors, Rich and Walker changed the lubrication system, increasing its performance. For this purpose, an external oil pump installed,

which circulated oil through an additional cleaning and cooling system. Holes made in the connecting rod through which lubricant supplied to the cylinder liner. Oil rings not used on the engine, but instead wider additional piston rings made of wear-resistant material installed. As result of changes made to the design, the researchers were able to complete a full test cycle within 100 hours, but individual time intervals between failures ranged from 25 minutes to 2 hours. The most difficult task was to achieve a uniform mass flow of coal dust in a pulsating flow when feeding it through the engine intake manifold. The dust fed using a screw and during the movement, it was partially compacted and partially slipped between the feed screw and the conveyor body. It found that the initial type of fuel used had a significant effect on engine performance. The thermal efficiency of the cycle dropped from 27% to 11%. Approximately 30% of the coal dust entering the cylinder did not burn and deposited in the exhaust manifold. During the first 33 hours, the exhaust valve jammed several times, and the pressure in the lubrication system dropped significantly. After 33 hours of testing, the engine could no longer operate under load. Disassembly of the engine showed significant wear on the cylinder liner and piston rings, despite the fact that fresh oil constantly added to the engine every hour, and it completely replaced every 10 hours of operation. In addition, a special additive introduced into the oil to reduce friction the mating parts. The amount of wear, according to the results of the study, was 18 μm/h, while for the same engine running on liquid fuel it does not exceed 0.16 μm/h.

Tests have shown that the engine requires routine maintenance (replacement of the piston, liner, piston rings) approximately every 30 hours. However, according to researchers, with further improvement of the design, the task of extending the service life was quite achievable.

1.1.3. The period from 1970 to the present. The renewed interest in the problem of using solid fuels in piston engines is associated with the energy crisis of 1972-73. This time characterized by a fundamental change in the concept of using coal fuel in internal combustion engines. If in the pre-war period the possibility of direct combustion of coal dust in the working space of the engine mainly studied, then subsequently the main emphasis placed on studying the possibility of using coal fuel as part of dispersed solutions with liquid motor fuel or water.

***

At Virginia Tech (USA), Marshall H.P. and Walters D.C. continued earlier research on a single-cylinder Nordberg engine (D/S=114/133) [40]. This time they studied the possibility of using SRC-II liquid synthetic fuel as

a carrier for FCS. A standard injection system used to supply the suspension to the combustion chamber.

It found that a coal dust content of up to 15% had virtually no effect on engine operation, but an increase in concentration led to frequent jamming of the spray needle. Thermally, the engine efficiency when using a suspension at a rotation speed of 1800 min^{-1} dropped from 21 to 17%, and the wear of the spray needle exceeded the permissible value after 2 hours of operation. As result of the tests, it was possible to establish that for complete burnout of coal particles it is necessary to increase the injection advance angle by approximately 20° relative to the injection advance angle for diesel engines. The total test time not recorded. The main conclusions drawn from the study were the following:

– a decrease in the ash content of fuel generally leads to a reduction in abrasive wear, but the coal particles themselves lead to the formation of scuffing on parts of fuel equipment;

– even particles with a size of about 2 μm lead to jamming of precision pairs of fuel equipment;

– the diesel engine power supply system, designed for liquid fuels, is practically unsuitable for the use of coal suspensions and requires significant modernization.

***

In 1979 Tataiah K. and Lestz S.J. published the results of a study carried out at the Lubricants Research Laboratory of the Southwest Research Institute (Texas) [38, 40]. The possibility of replacing light diesel fuel with a fuel-coal suspension in automobile diesel engines studied. In particular, use of FCS in engines with a divided and undivided combustion chamber. The engine with a split combustion chamber was a pre-chamber four-stroke diesel engine Hatz model E-785, in which the FCS supplied to one of the cylinders, and the rest operated on standard diesel fuel. As an engine with an undivided combustion chamber, a four-cylinder Mercedes engine model OM-314 was tested, with a cylinder dimension D/S = 85/110 mm, a displacement of 3.88 liters, a power of 50.7 kW at a rotation speed of 2600 min^{-1}.

The Hatz engine tested at 12 different steady-state conditions, with the amount of coal dust in the suspension ranging from 10 to 20%, and the particle size did not exceed 10 μm. In addition to coal dust, the fuel included water (approximately 2.8%) and several special additives. To prevent jamming, the gap between the needle and the nozzle body has increased. As result of tests, it found that the use of coal particles worsens the combustion of the base diesel fuel, and this, in turn, leads to a decrease in the thermal efficiency of the engine. The cast-iron rings wore out quite quickly during

operation, but no significant increase in crankcase gas breakthrough observed during the 35-hour test.

For the Mercedes engine, a mixture of diesel fuel with 10, 20 and 50% coal dust used as fuel, which had a particle size of 10 μm, ash content of 9.1%, sulfur content of 1.8%. In the beginning, a standard injection system used to supply the suspension to the undivided combustion chamber of the engine. At the same time, the spray needle jammed almost every minute. To eliminate jamming, the fuel equipment parts were ground in such a way as to increase the mating gap. As result of this modification, jamming no longer occurred during the 8-hour test. After disassembling the fuel pump, no noticeable wear of the fuel equipment parts detected.

Tests showed that as the concentration of coal dust increased, the thermal efficiency of the engine decreased. At a 75% load and a rotation speed of 1200 min^{-1}, it was 34.2, 34 and 26.6% with a weight content of coal dust in the FCS of 10, 20 and 40%, respectively. The thermal efficiency of the diesel engine corresponded to 36.43%. With increasing concentration of coal dust, the temperature of the exhaust gases increased. Compared to diesel fuel, the exhaust smoke increased approximately 2 times. The indicator chart taken from the engine showed that there was no noticeable ignition delay when using the FCS. Most of the carbon particles completely burned when the injection advance was approximately 15° before top dead center (TDC). During the testing process, the total time of which was 14 hours, significant wear of the cylinder-piston group observed. No noticeable ash deposits found in the engine exhaust system, and no significant wear of the exhaust valves observed.

***

Ryan T.W., Likos W.E. and Moses C.A. at the Southwestern Research Institute studied the possibility of using various coal suspensions in a diesel engine (1982). Soot, coke and coal tried as solid fuels [40]. The average diameter of soot particles did not exceed 0.02 μm; however, taking into account agglomeration, the actual size of particles entering the engine was at least 10 μm. The tests were carried out on a single-cylinder CLR engine with a dimension D/S=97/95mm, which had direct fuel injection into the combustion chamber. To avoid jamming between the needle and the nozzle body, the mating gap was increased. When using soot, the engine performance was practically no different from the performance obtained with diesel fuel. The use of other solid fuels has also shown good results. However, the tests were short-lived, and the concentration of solid particles in the suspension was insignificant and ranged from 10...20%. Subsequent work examined the effect of fuel composition on suspension injection

characteristics, as well as on fuel ignition and combustion. Based on these studies, significant changes made to the fuel system and engine design to improve fuel efficiency. The engine modernization consisted of additional swirling of the air charge, increasing the compression ratio from ε = 14 to ε = 17, reducing the spray angle and fuel supply intensity. As a result, it was possible to achieve that the engine efficiency when operating on a soot suspension was higher than when operating on diesel fuel. At the same time, the indicator efficiency of the engine was practically independent of the soot content in the suspension, which indirectly indicated the complete combustion of solid particles. The rate of engine wear not recorded, but it noted that the wear rate of individual parts on a soot suspension and diesel fuel exceeded the same parameter for liquid fuel.

***

A study with tasks similar to those set by Ryan carried out in 1983 by Wakenell J.F. [77]. He studied the possibility of using a mixture of diesel fuel and soot in a two-stroke two-cylinder module of a 567B locomotive engine from Electro-motive Division with a cylinder dimension of D/S= 216/254, a rotation speed of 344...835 min^{-1} and a compression ratio of ε=16. Various types of suspensions consisting of diesel fuel, coal, soot and coke, with a mass content of solid fuel of 5...20%, were studied. Subsequently, a mixture of diesel fuel and soot used experiments. The suspension of soot and diesel fuel (Modul L) had agglomerated particle sizes of the order of 10 μm. The study consisted of two stages. At the first stage, the operation of elements of the engine power system was studied on special stands: low-pressure booster pump, filters, pump-injector. During testing, the fuel suspension was stored in a special tank equipped with a constant mixing system. From the reservoir, the suspension pumped through a system of series-connected filters using a low-pressure pump. The filter element of the first filter was made of cotton fabric; the second one was made of cardboard plates. During the experiment, changes in pump performance and filter resistance assessed. During the experiments, both filters clogged during the first hours of operation on the suspension. Soot particles have completely settled on the filter elements. This allowed the researchers to conclude that FCS filtering was not possible. After 50 hours of operation on a suspension with 10 and 20% soot, the booster pump did not change its performance. However, after disassembly it turned out that its elements had significant wear. When testing the pump injector, the performance and resistance of the drive were determined by measuring the force on the drive rocker arm. The injector pump operated on a suspension, the soot content of which gradually increased from 10 to 20%. Each stage of testing lasted 6.5 hours and ended with disassembly. A 10%

addition of soot did not cause noticeable wear in the pump injector parts. After 6.5 hours of testing on a suspension with 20% soot content, the spray needle jammed so that it could only removed by cutting the housing. Glaze deposits found on the surfaces of the needle and the guide hole of the body. A study of the suspension that passed through the pump nozzle showed that the size of the soot particles in it decreased, which led to an increase in its viscosity. To prevent jamming, the gap between the needle and the body increased to 0.025 mm.

At the second stage of the study, the effect of suspension composition on engine performance studied. At the same time, the filters from the fuel supply system removed. Tests have shown that the power and efficiency of the engine on the FCS have remained virtually unchanged compared to the diesel engine. An increase in exhaust gas opacity observed only when the soot content in the suspension was about 20%. There was no jamming of the pump injector needle after increasing the gap. After 40 hours of operation, the engine disassembled for inspection. The top two piston rings had the most wear. There was significant rubbing on the cylinder liner and on all the rubbing parts of the pump injector. Gelatinous deposits found on the piston group parts. Researchers believe that soot particles get into the oil as a possible cause of cylinder and ring wear.

Thus, the study proved that a high-speed engine can, in principle, operate on a diesel fuel suspension with soot. For commercial use of FCS consisting of diesel fuel and soot, it is necessary to solve a number of issues related to filtration, clogging of fuel system channels, sticking of fuel supply equipment elements, and accelerated wear of parts of the cylinder-piston group.

***

The combustion characteristics of various coal suspensions studied at the National Institute for Petroleum and Energy Research [40]. Initially, the research carried out in a special bomb that simulated the combustion process at a constant volume. Subsequently, the combustion of suspensions studied on a single-cylinder engine with a split combustion chamber. Various types of coal used to prepare suspensions. DF, water and methanol, as well as other additives designed to improve the properties of the fuel suspension, tested as a carrier for coal fuel. It noted that during the tests, engine performance progressively deteriorated, and increased wear and plaque formation observed.

***

Robben F. developed a project for modernizing a diesel engine to run on coal fuel and a unique device for studying the ignition and combustion of a water-coal suspension (WCS) [40]. Using this device, the combustion

characteristics of suspensions were determined under conditions as close as possible to a real engine. In his research, Robben used an engine with transparent flat walls, which made it possible to use high-speed filming to study the processes of fuel spraying and combustion. Combustion parameters studied as a function of engine characteristics and fuel properties.

***

Siebers D.L., Dyer T.M. Sandia National Laboratories (Livermore, California) conducted research aimed at studying the combustion of water-coal suspensions (1986). As in the previous case, the studies were carried out in a cylindrical bomb with optical access [38, 40, 71]. As a result, objective data were obtained regarding the ignition delay of coal suspensions under conditions as close as possible to a real engine. It was found that the ignition delay for various types of coal suspensions was approximately 5 times higher than that for diesel fuel.

***

Back in the late 70s. In the 20th century, the Environmental Protection Agency of the US Department of Energy initiated a special program aimed at studying the possibility of using coal fuels in piston internal combustion engines [64]. According to the ministry's specialists, replacing expensive diesel fuel with cheap coal mined domestically, in utility installations, at thermal power plants and in the transport sector will become economically feasible in the first half of the 21st century. At the first stage, the development program was purely research in nature, but the results obtained allowed the Ministry of Energy by the early 80s. Conclude a number of contracts aimed at creating experimental engines intended for industrial and transport needs. Beginning in 1987, all projects were managed by the Office of Mineral Energy, with the US Department of Energy's Morgantown Energy Technology Center (Morgantown, West Virginia) serving as the program's primary coordinator. During this period, several additional research projects launched aimed at creating an internal combustion engine capable of operating on various types of coal fuels, such as FCS and WCS, fine coal dust and coal gasification products. By studying the combustion of these fuels in laboratory bench tests, the researchers established a number of engine design and fuel requirements that must be met to effectively burn these fuels in the working cylinder. The influence of design features of the injection system and fuel characteristics on the wear of engine parts studied. In addition, information obtained on the wear resistance of various structural materials in the presence of ash particles and on the composition of emissions from coal-fired engines.

Based on the assigned tasks, starting from 1988, the program of the Ministry of Energy included two main directions (Table 1.1):

- study of the features of direct combustion of coal fuels in internal combustion engines;
- testing of new principles of operation of coal fuel engines.

In addition to the main projects, a number of auxiliary developments carried out.

The main work on direct combustion research carried out by General Electric, ADL together with Cooper-Bessemer, General Motors (Electro-motive Division), Detroit Diesel and others. A number of research contracts concluded with foreign firms. Thus, the study of issues related to the use of coal suspensions in low-speed internal combustion engines carried out by Sulzer (Switzerland) together with Thermo Electron (USA).

The second direction developed by Caterpillar, Inc., it involved studying a new approach to the use of coal fuels in diesel engines. This refers to the development of a coal gasification plant that produces high-pressure, low-calorie gas in special replaceable cylinders, used as fuel for a diesel locomotive engine. As part of this research, both fundamentally new methods for producing generator gas and the characteristics of a diesel engine running on gasification products tested.

The intended area of application for such engines is stationary power plants, the utilities sector, railway and marine, and in the future, road transport. The second stage of the US Department of Energy program characterized by the fact that research aimed at creating a diesel engine capable of running on coal fuels began to be systematic. The first attempts made to systematize the results of previous research in order to develop a theoretical basis for the processes occurring in engine cylinders.

Table 1.1.

The main directions and main contractors of the research program for the creation of diesel engines using coal fuel

Company	Application area	Fuel
ADL/Cooper-Bessemer	Industrial and autonomous power plants	Water-coal suspension, coal dust
General Electric General Motors	Locomotive engines, stationary installations	Water-coal suspension
Caterpillar	Locomotive engines, stationary installations	Gasified coal

Unlike previous periods, in addition to experimental studies carried out, as a rule, on engines, works began to appear that in the nature of physical and mathematical modeling of both individual processes and the entire thermodynamic cycle of a coal engine. To achieve this, in addition to

engineering companies, a number of US research organizations were involved in the development, carrying out certain types of research or studying individual processes. Total 9 contractors were involved in the program [38, 79]. To coordinate their efforts, the Morgantown Energy Technology Center held regular technical conferences. Research materials constantly published in the «Internal Combustion Engines» section of the journals of the American Society of Mechanical Engineers and in other specialized publications. Dynamics of changes in the number of reports at conferences and publications in American technical literature for the period from 1984 to 1994 (the period of the most intensive research) presented in Fig. 1.4.

The data presented clearly demonstrate that in the United States, interest in the problem of using solid fuels in internal combustion engines constantly increased over the indicated period, there was an intensive exchange of information, which made it possible to achieve significant results in a fairly short time towards creating a commercially suitable engine [38].

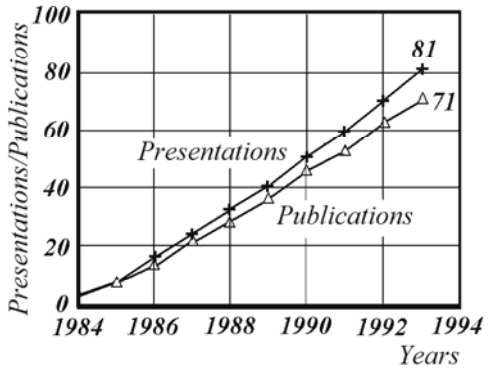

Fig. 1.4. Dynamics of growth of publications and reports on the problem of using solid fuels in piston internal combustion engines

***

Below we will provide brief descriptions of the main areas of research conducted by individual participants in the program, as well as some of the results they obtained during the research.

***

The Sulzer company (Switzerland), which is the largest manufacturer of marine low-speed diesel engines [65, 72], since 1978, together with Thermo Electron (USA), conducted experiments on a single-cylinder installation using a cylinder-piston set of a two-stroke crosshead low-speed diesel engine model 1RSA76 with a loop purge circuit. This choice determined by the desire to avoid increased wear of the gas distribution mechanism parts. The

specialists involved in the project based on the belief that when using coal suspensions, preference should given to engines that do not have timing mechanism.

The tests carried out at the experimental base of the Sulzer Company (Winterthur, Switzerland). The characteristics of the experimental engine presented in Table. 1.2, cross section is shown in Fig. 1.5.

Table 1.2.

Characteristics of the Sulzer 1RSA76 experimental engine

Parameter	Meaning
Cylinder diameter, mm	760
Piston stroke, mm	1550
Power (at 100% load), kW	1471
Rotation speed, min^{-1}	120
Average effective pressure, MPa	1.046
Maximum cycle pressure, MPa	8.43
Compression ratio	10.63
Standard injection advance (before TDC), deg.	6
Standard air inlet temperature, K	350
Boost pressure, kPa	240
Outlet pressure, kPa	200
Number of exhaust ports per cylinder	5
Ports size (height×width), mm×mm	217×110
Opening of exhaust ports (to BDC), deg.	67
Closing of exhaust ports (after BDC), deg.	67
Number of inlet ports per cylinder	8 large /4 small
Ports size (height×width), mm×mm	
Large (height×width), mm×mm	180×55
Small (height×width), mm×mm	103×93
Opening of inlet ports (to BDC), deg.	45
Closing of inlet ports (after BDC), deg.	45

Since 1978, research been focused on studying the possibility of using fuel-coal suspensions in piston low-speed internal combustion engines. Tests have shown that the problem of using these suspensions has much in common with the problem of using heavy oil fuels. At the same time, the composition of the fuel significantly affects its specific consumption and toxicity of exhaust gases. Initially, a mixture of coal dust and diesel fuel in an amount of 30...50% was used as fuel [72]. Subsequently, in addition to liquid fuel, the composition of the fuel suspension included water. It found that the optimal suspension for use in low-speed engines is a suspension consisting of 50% coal dust, 30% water and 20% heavy diesel fuel [65].

Initially, the tests carried out using the standard fuel system of the Bosch engine, which quite often failed when operating on liquid coal suspensions.

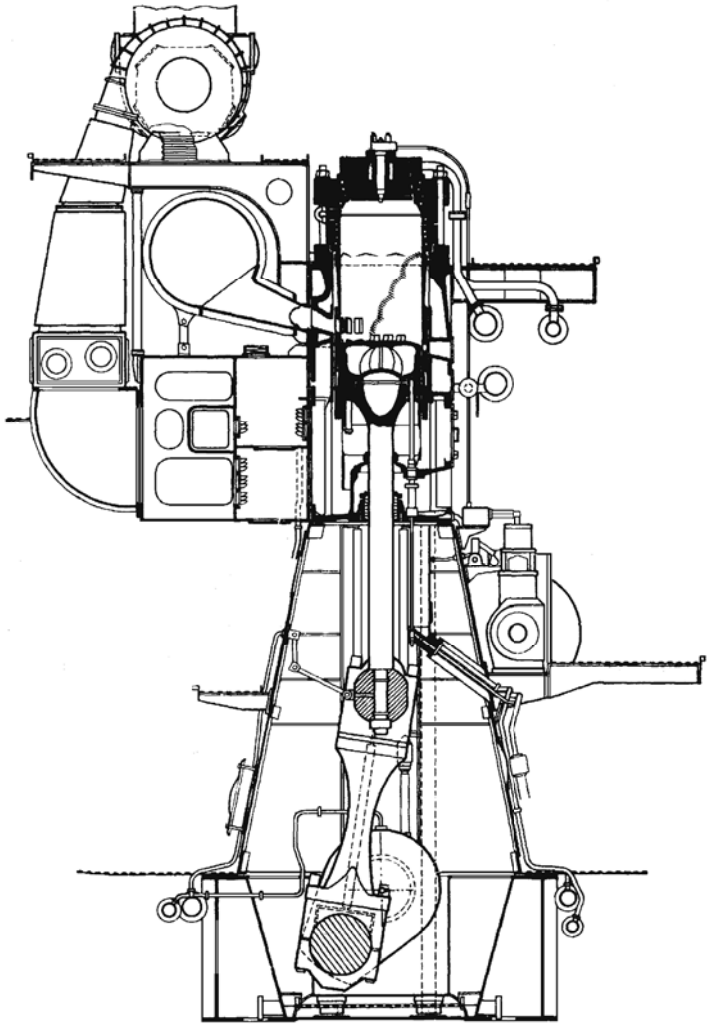

Fig.1.5. Engine 1RSA76 from Sulzer

To increase reliability, design changes made to it in such a way as to prevent the entry of coal particles into the high-pressure fuel pump. For this purpose, the fuel system was equipped with a special accumulator, into which FCS supplied using a low-pressure pump. The accumulator installed directly

in front of the sprayer. The discharge line, which serves to supply the fuel suspension, separated from the accumulator using a special check valve. The accumulator was equipped with a separating diaphragm, which directly acted on the FCS and driven by a special hydraulic system.

The only element of the fuel system that directly exposed to the FCS was the injector nozzle. The system operated reliably during 20 hours of testing. At a rotation speed of 120 min^{-1} and 75% load, the engine efficiency was 41.2% at DF No. 2 and 40.4% at FCS. At maximum load, the engine efficiency decreased to 39% [38]. According to the researchers, the decrease in effective efficiency occurred due to an increase in friction between engine parts, and not due to a deterioration in the parameters of the thermodynamic cycle. Analysis of indicator diagrams did not show any deviations in the flow of the working process on a coal suspension relative to similar parameters when the engine was running on diesel fuel. The sufficiently long time allotted in low-speed engines for the combustion process ensured complete burnout of pulverized coal particles. The observed increase in exhaust smoke, according to researchers, is explained the ash content of coal. The engine freely started from a cold state using the FCS.

The next stage of research, which began in 1982, aimed at studying the possibility of using WCS as a motor fuel for low-speed internal combustion engines. The main goal pursued in this case was to completely abandon the use of petroleum fuels, reduce the combustion temperature and, as a result, reduce the formation of nitrogen oxides.

During the experiments, water-coal suspensions with a mass content of coal particles from 46.5 to 53% and an ash content of 0.5...1.1% tested as fuel. The average particle size ranged from 5 to 16 μm. To activate the WCS combustion process, ignition diesel fuel supplied to the working cylinder.

The total operating time of the single-cylinder test engine on the WCS at loads from 25 to 90% was 50 hours. The previously developed accumulator-based suspension injection system functioned flawlessly. Even with a relatively small amount of ignition fuel (approximately 1% of the total heat of combustion), in experiments with a 90% load, the stability of the engine was quite high. Fluctuations in cylinder pressure from cycle to cycle were no greater than when standard diesel fuel No. 2 burned in the same engine. The correctness of the initial hypotheses confirmed, according to which, firstly, the ignition process depends to greater extent on the parameters of fuel spraying rather than on temperature charge to the end of compression, and secondly, engine parameters optimized for one suspension apply to all others. The engine efficiency when burning water-coal fuels turned out to be approximately the same as when burning diesel fuel No. 2, which confirms

the analytically obtained relationship, according to which when the water content in the suspension is less than 60%, the decrease in engine efficiency becomes negligible.

The maximum value of the derivative of pressure in the cylinder with respect to time when burning WCS was invariably higher than when using diesel fuel. Therefore, the characteristics of the combustion modes of WCS and diesel fuel differ significantly.

As result of the tests, it found that the total time required for complete combustion of WCS is significantly longer than for combustion of diesel fuel. In this regard, it is most rational to use coal fuels in low-speed diesel engines with a rotation speed of about 100...120 min^{-1}, in which the combustion period is on average 60...80 ms. Experiments have shown that in load changing modes in the range of 50...90%, the ignition delay of water-coal fuel is 2.0...4.0 ms versus 0.4...1.0 ms for diesel fuel, and the rate of pressure rise is higher. As for the increased wear of the working surface of the cylinder and piston rings, as result of the study of various design solutions, it was possible significantly slow down the process of their wear by copper plating of the conical working surfaces of the piston rings. The most vulnerable part turned out to be the nozzle nozzles: due to the high content of silicates in the coal fuel (up to 10% by weight of ash), they failed after several hours of operation. As result of the tests, it found that specific fuel consumption over the entire load range increased by no more than 2%. Thus, it proven that Sulzer valveless low-speed engines with central fuel injection, after some modernization, could quite work on coal suspensions.

In addition to diesel fuel and water, liquid synthetic fuels obtained from coal, alcohols, and other liquids can use as carriers for suspensions.

As a result of the research, it was found that low-speed diesel engines have the necessary characteristics to ensure complete and efficient combustion of both fuel-coal and water-coal suspensions. If issues related to fuel spraying and piston ring wear are resolved, such engines can successfully operate on coal suspensions. Based on the research results, it stated that in the future Sulzer plans to produce an experimental low-speed 6-cylinder diesel engine with a power of 16,500 kW, designed to operate on WCS [78]. It assumed that such diesel engines can used as stationary and marine engines, but there is no information on the implementation of these plans.

***

Cooper-Bessemer (Grove City, Pennsylvania) produces a line of medium-speed diesel engines designed for stationary power applications. In 1985, together with the Arthur D. Little company (Cambridge, Massachusetts), it

began a research program codenamed Coal-fueled diesel engine combined-cycle, aimed at studying the possibility of using WCS for a medium-speed diesel engine with a rotation speed of 400 min^{-1} [44, 66]. The studies carried out on a single-cylinder module of a four-stroke diesel engine model JS-1 (Table 1.3).

Table 1.3.

Performance characteristics of the prototype JS-1 engine

Engine's type	Single cylinder, four stroke
Cylinder diameter, mm	330.2
Piston stroke, mm	406.4
Connecting rod length, mm	812.8
Number of valves	4 (2 intake, 2 exhaust)
Valve diameter, mm	104.8
Valve lift, mm	31.8
Inlet valve	Opening 59° before TDC, closing 23° after BDC
Exhaust valve	Opening 50° before BDC, closing 13° after TDC
Shaft rotation speed, min^{-1}	300...450
Compression ratio	10.5
Average effective pressure, MPa	0.686..1.372
Air inlet temperature, °C	27…232
Inlet air pressure, MPa	0…0.17
Power when operating on diesel fuel, kW	180

The experimental engine was equipped with an externally driven air charging system and exhaust throttling, simulating the resistance of a turbocharger turbine. Originally, the top piston ring was made of hard ductile iron; the remaining rings were made of gray cast iron. The cylinder liner coated with porous chromium to increase wear resistance. WCS injection into the undivided combustion chamber carried out by a central closed-type nozzle with 18 spray holes arranged in two rows.

To activate the combustion process, two independent systems installed in the experimental engine. For this, in addition to the main combustion chamber, two side windows made in the cylinder head. In one of the windows, a nozzle for injection of pilot diesel fuel was installed, and in the second, there was an auxiliary chamber into which natural gas supplied, which provided 3...5% of the heat supplied per cycle. The ignition of the gas-air mixture in the auxiliary chamber carried out using a spark plug. For fuel injection, a special system designed with a minimum number of moving parts in direct contact with the WCS. The hydraulic drive of the sprayer carried out through a check valve from a plunger-type fuel pump, developing diesel pressure from 35 to 105 MPa. The WCS supplied to the sprayer using a booster pump. A separating piston made of nitrided steel installed between the nozzle cavities filled with diesel fuel and water-coal suspension. To

prevent the piston from jamming, its surface coated with a layer of titanium nitride. The experiments carried out showed that the most critical element that determines the service life of the engine when operating on WCS is the sprayer. The decisive factor determining the life of the sprayer was the composition of the fuel suspension and the content of mineral impurities in the coal fuel. As an alternative, the use of a poppet valve nozzle considered, which, according to the researchers, could significantly improve engine performance and reduce nozzle wear by reducing injection pressure. When testing the engine, a WCS with a content of coal particles of about 53...55% used, for the preparation of which two types of coal dust with average particle sizes of 11 μm and 8 μm used. Brown coals from several deposits in Kentucky, previously purified to an ash content of 1%, with the same sulfur content, used as the initial solid fuel to obtain suspensions.

As a result of the tests, it was found that, with a coal dust concentration of about 55%, the WCS successfully burns in the engine even in the absence of a combustion activation process. At the same time, the inlet temperature increased to 145...225°C. This, however, according to researchers, did not any way affect the effective efficiency of the engine. An increase in the air temperature at the engine inlet led to an acceleration of self-ignition and improved fuel combustion, which explained by the compensation of heat losses associated with the phase transition of water included in the suspension.

It observed that the use of finer dust in the suspension composition leads to an increase in specific fuel consumption by approximately 4% compared to the use of coarse dust. When operating on WCS, a delay in self-ignition observed, with a constant angle at which the fuel supply began, led to a decrease in engine power. To reduce the auto-ignition delay, an ignition diesel fuel was supplied to the cylinder, providing from 7 to 16% of the heat supplied per cycle. This led to a slight increase in the total specific consumption, but made it possible to obtain stable ignition of the fuel. In Fig. 1.6 shows an indicator diagram of the change in pressure in the working cylinder of the engine when it is running on WCS.

At steady state conditions, the supply of pilot diesel fuel completely stopped, as result of which the total specific consumption decreased. It noted that when the engine was running on WCS, the emission of NO_x with the exhaust gases decreased. In the range of air temperatures at the engine inlet of 38...94°C, the decrease was 68...32% relative to the values obtained when running on diesel fuel. It found that an increase in the temperature at the engine inlet leads to an overall increase in NO_x emissions. A decrease in the NOx content by about 30% was achieved by increasing the diameter of the

nozzle holes from 0.25 to 0.35 mm. A decrease in CO and CH emissions also noted, but the content of sulfur compounds in the exhaust gases was an order of magnitude higher than when using diesel fuel. The total operating time of the experimental engine exceeded 600 hours, but the researchers believe that with further improvements its service life can increased to 6000 hours.

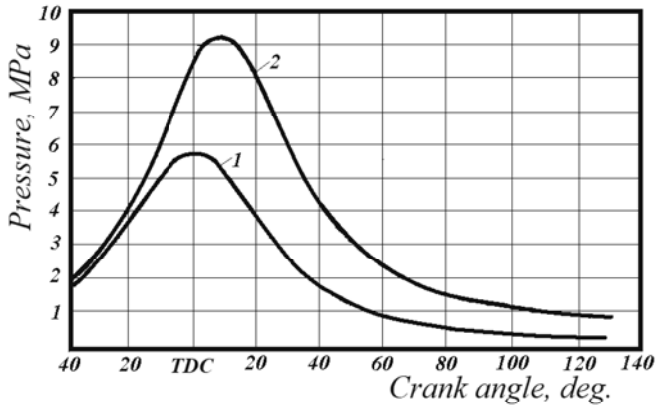

Fig. 1.6. Change in pressure in the working cylinder of the JS-1 engine. 1 – change in pressure in the working cylinder in the absence of fuel supply; 2 – change in pressure in the working cylinder during combustion of the WCS (air temperature at the engine inlet is 224...226.5 °C; the diameter of the nozzle holes is 0.25 mm; pilot fuel is supplied 33° before TDC; maximum heat release rate is 2.64 kJ /deg.)

Based on the results obtained during testing of the single-cylinder JS series engine, in 1992 Cooper-Bessemer began converting a six-cylinder LSB series gas-diesel engine (Fig. 1.7) to run on WCS. The 6- and 8-cylinder LSB series engines are in-line, while the 12, 16, and 20-cylinder engines are V-shaped (LSVB series) [67]. All engines have the same dimensions D/S=393.7/558.8 mm and an operating speed range of 360…400 min^{-1}. Initially, one cylinder subjected to modernization, while the other five ran on diesel fuel. The volumetric supply of WCS by the injection system increased twofold compared to the JS engine. For this purpose, a new cam drive of the fuel pump manufactured, and the diameter of the fuel plunger increased from 26 to 36 mm. The WCS sprayer was located along the cylinder axis and had 37 holes with a diameter of 0.385 mm, arranged in two rows of 18 holes each. One hole was located along the needle valve axis. To activate the combustion process, swirl chambers equipped with pin nozzles for injection of pilot diesel fuel installed in the side windows. The pilot injection system directly into the combustion chamber through a 6-hole sprayer installed in

one of the windows for swirl chambers was also tested. During the tests, the cylinder operating on the WCS developed a full power of 197.6 kW at an average effective pressure of 1.43 MPa. The test result showed high efficiency of coal fuel combustion (Fig. 1.8).

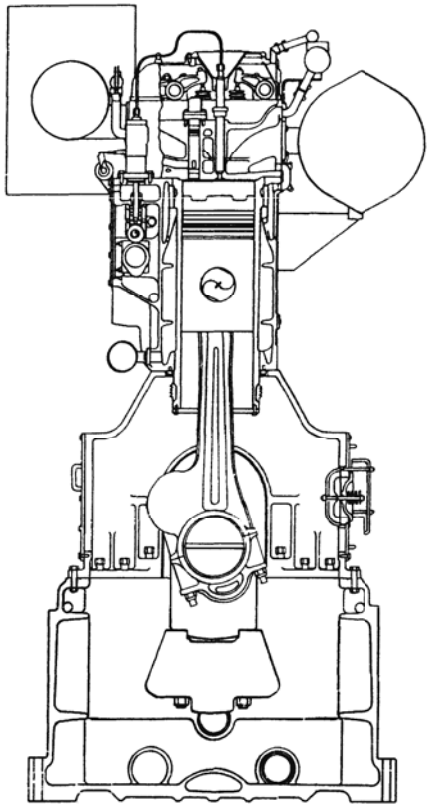

Fig. 1.7. Cross-section of the LSB series engine from Cooper-Bessemer

To extend the service life of the sprayer, its tip made in the form of an insert made of tungsten carbide with the addition of cobalt. Such an sprayer worked on the WCS for more than 100 hours. Sprayers with sapphire and artificial diamond inserts installed in the channels were also tested. Such sprayers also showed good results. Increasing the air temperature at the engine inlet is necessary to compensate for heat loss due to water evaporation. This achieved by eliminating the air cooler from the intake system.

A special system for reducing the toxicity of engine exhaust gases developed. A cyclone installed between the engine and the turbocharger, which protected the turbocharger from relatively large ash particles and unburned fuel. After the turbine, the exhaust gases were passed through a chamber in which ammonia was sprayed in the presence of a ceramic catalyst – zeolite. This made it possible to reduce the NO_x content by 80...90%. Then the gases passed through a heat exchanger simulating a steam generator of the heat recovery system. After the heat exchanger, a sodium-based sorbent was introduced into the gas flow through a Venturi mixer, allowing sulfur to be captured. From the mixer, the gases fed to a special dust collector chamber equipped with porous filters, where the remaining macroparticles filtered along with the sorbent. To compensate for the pressure drop on additional devices of the cleaning system, a centrifugal fan installed directly in front of the exhaust pipe. In addition to the cyclone, in the system for preliminary cleaning of gases from macroparticles, the use of special partition ceramic filters capable of operating at temperatures up to 540 °C also considered.

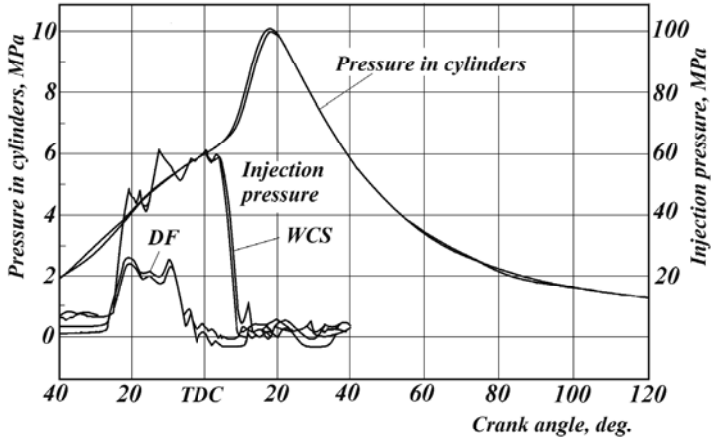

Fig. 1.8. Combined diagram for two working processes in the Cooper-Bessemer LSB series engine when it operates on a WCS

The ultimate goal of the program was to develop a range of medium-speed high-power engines for stationary diesel power plants with a capacity of up to 50 MW, capable of operating on WCS.

***

General Electric-Transportation Systems is one of the largest US manufacturers of diesel engines for diesel locomotives. In the early 80s of the

twentieth century, the company initiated research aimed at creating a piston engine using water-coal fuel. The project financially supported by the Burlington Northern Railroad, along whose highways a large number of coal deposits are concentrated. In the event of a successful implementation of the project, the company's management intended to modernize 67 diesel locomotives for operation on water-coal fuel. The program consisted of four main stages and designed for 7 years, during which it planned to spend 50 million dollars on research. The first stage included the economic development of the project and laboratory research. The second stage was supposed to conduct machine tests on a single-cylinder module. The third stage is the creation of a full-size engine running on water-coal fuel. The fourth stage is the development of the concept of a diesel locomotive equipped with a power plant operating on a WCS [38, 52-55, 72]. In 1985, the Corporate Research Development Center and the Environmental Services Agency joined the research program. General Electric conducted laboratory research and single-cylinder machine tests at the Corporate Research Development Center. This work included the development of equipment for a fuel injection system, and the study of WCS ignition and combustion under real engine conditions. As part of the research program, Leonard G.L. and Fiske G.H. [38] conducted experiments to study the quantitative composition of combustible components in the WCS. First, the possibility of pumping the WCS with high-pressure plunger-type pumps studied. A suspension containing 48% coal by weight, including 2% additives, recognized as optimal. The size of the coal particles was approximately 3 μm. The initial coal purified to an ash content of less than 1%. The ignition and combustion of the WCS also studied, for which the suspension injected into an isolated vessel simulating the combustion chamber of a diesel engine. The temperature in the test chamber maintained at approximately 900 K, and the gas density was 25 kg/m^3. In addition, the gas charge in the chamber was specially turbulized. The studies showed that the fuel mixture self-ignites quite well under conditions simulating engine operation at full load, and does not ignite or ignites very poorly under conditions typical of the partial load mode. First, such deterioration explained by a decrease in injection pressure and, as a consequence, by deterioration in the quality of fuel suspension spraying. In the full load mode, the ignition delay for the WCS was 5 times greater than the same parameter for diesel fuel. In order to reduce the delay period, in partial load modes, the researchers proposed injecting a small amount of pilot diesel fuel into the cylinder.

Based on the results of laboratory studies, a fundamentally new scheme for feeding water-coal solutions into the engine combustion chamber

proposed, which was an accumulator system with electronic control of the injection process [39, 48, 69, 54]. Placing the accumulator in the injector body, in close proximity to the sprayer, made it possible to increase the initial injection pressure to 80 MPa and stabilize its value, regardless of the engine-operating mode. This circumstance favorably distinguished the new system from the initially used volumetric fuel supply system and had a beneficial effect on the ignition process of the WCS in partial load modes. In addition, the electronic control system made it possible to optimally regulate the supply of suspension to the engine combustion chamber in a wide range of changes in its operating modes.

The first stage of the research program completed within two years.

In 1988, the company began machine testing of an engine running on WCS [48]. At this stage, the studies were conducted on a two-cylinder section of a V-shaped four-stroke locomotive diesel engine model 7FDL with D/S = 267/229 mm, n = 1050 min^{-1}, in which one cylinder worked on the WCS, and the other on the diesel fuel (Fig. 1.9).

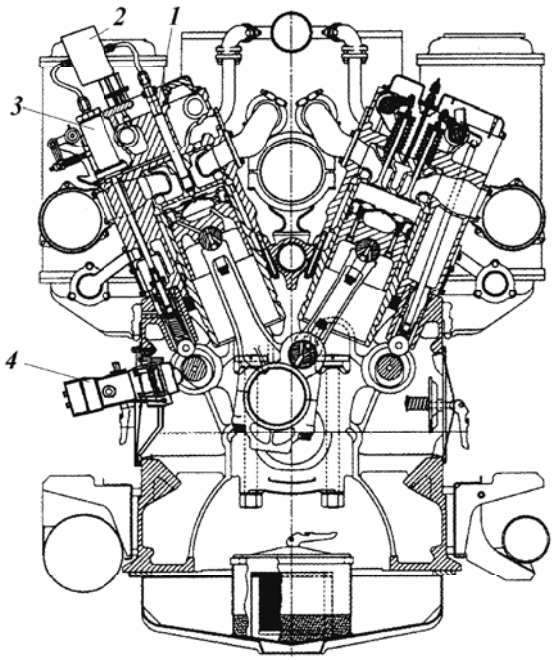

Fig. 1.9. Cross-section of the 7FDL engine, modernized for operation on WCS. 1 – injector for WCS injection; 2 – diaphragm separator; 3 – main fuel pump; 4 – additional fuel pump for pilot diesel fuel injection

In order to obtain the full power of the diesel, the standard fuel equipment of the engine replaced with equipment of greater productivity, providing a higher cyclic supply of the WCS.

In the standard version, the engine is equipped with individual cylinder liners; pistons made of aluminum alloy with steel heads and cast steel cylinder heads. The WCS used contained 47...49% of coal dust, crushed on average to 2.88 μm, with an ash content of no more than 0.36%.

At the first stage of testing the two-cylinder module, three methods of activating the ignition process studied:

- compression ignition (self-ignition);
- ignition with pilot diesel fuel supplied to the combustion chamber by means of a specially installed auxiliary nozzle (pilot ignition);
- sequential supply of pilot diesel fuel first, and then WCS (stratified pilot ignition) through the main fuel injector sprayer.

Ignition achieved by all three methods, but the first case required an increase in the air temperature at the intake. It was found that when the engine is running at full load (186 kW/cyl), stable self-ignition of the suspension occurs with a long delay period (40…45°), due to the time of complete evaporation of water. In addition, it found that self-ignition occurs only if the charge temperature in the cylinder by the end of the delay period is not lower than 890 K.

To ensure effective ignition and combustion, it was sufficient to feed about 3...5% pilot diesel fuel into the engine chamber. Sequential injection of both fuels through a common injector turned out to be especially effective. The intensity of heat release during combustion of the pilot fuel was higher than that of diesel fuel. The amount of NO_x and CO in the exhaust gases was approximately two times less than when operating on diesel fuel. The amount of released heat studied as a function of the temperature and pressure of the air charge, the amount of pilot fuel and the injection pressure.

As result of optimizing the injection process of WCS on the experimental module, a power 186 kW/cyl, at a rotation speed of 1050 min^{-1}, obtained. This practically corresponded to the power of this engine when it was running on liquid fuel. The efficiency of burning out coal particles reached 99.5%.

In parallel with the machine tests on the experimental module, General Electric began developing a full-size multi-cylinder diesel engine running on water-coal fuel. This program included durability testing of an 8-cylinder engine and a 12-cylinder engine as part of a locomotive power plant. The first reports on the results of the tests began to appear around 1990. 8-cylinder V-shaped GE 7FDL engine used for durability testing. It intended to test the

control system and study the operating characteristics. To study the wear dynamics, two cylinders of this engine converted to work on a WCS. The average service life of the engine before repair when running on diesel fuel was 25,000 hours, but when running on a WCS, the standard injection system failed after just 4 hours of operation. This was due to erosion of the injector nozzle channels operating at an injection pressure of up to 140 MPa and a flow rate of 250 m/s. During the tests, the mechanism of wear of the nozzle channels was determined. The information obtained taken into account when creating a 12-cylinder engine [48]. To reduce wear, all spray channels were equipped with diamond inserts with a whole diameter of 0.4 mm, and the needle valve seat was made of tungsten carbide. Laboratory testing of a spray fragment equipped with a diamond insert at the whole outlet, performed on a special stand, showed that for 500 hours under conditions equivalent to the maximum engine load mode, the sprayers can operate without significant wear. It also found that the most optimal droplet sizes of the WCS supplied to the combustion chamber are droplets from 18 to 92 μm. During machine tests after approximately 40 hours of engine operation, no changes in the whole diameter found either.

Initially, the engine was equipped with a plunger-type injection system with separate supply of WCS and pilot fuel (Fig. 1.8), which subsequently replaced with an accumulator with electronic control [39].

The piston rings coated with tungsten carbide. For the upper piston rings and cylinder liners, better wear resistance achieved by applying a tungsten carbide coating with the addition of cobalt. A tungsten carbide layer applied to the surface of the nitrided cast iron cylinder liners by plasma spraying. The second and subsequent piston rings were chrome plated. It found that the use of WCS does not significantly affect the wear resistance of valve stems, bearings and other lubricated parts.

After the described modification, the engine operated for more than 1000 hours at both maximum and partial loads without any serious deviations.

In the first half of 1991, tests of a full-size 12-cylinder engine running on WCS began. As result of laboratory tests, the engine developed a power of 1860 kW at 1050 min^{-1} for more than 10 hours. Subsequently, this engine installed on a diesel locomotive for road tests.

When developing the injection system of the 12-cylinder engine, a mathematical model used to optimize the fuel combustion process. The injection system preliminarily tested on a single-cylinder experimental setup. Eight different injector sprayers tested, including those with diamond inserts at the outlet of the holes. At the first stage of the research, the 12-cylinder engine was equipped with a dual-circuit fuel system. The main system

intended to supply WCS to the cylinders, the auxiliary system – for pilot diesel fuel. A special system for synchronous control of both fuel pumps was also developed. Later, the accumulator injection system developed on the 8-cylinder engine used to supply fuel to the combustion chamber.

After laboratory tests, the 12-cylinder engine installed on a diesel locomotive and the auxiliary equipment placed on a special trailer platform (Fig. 1.10).

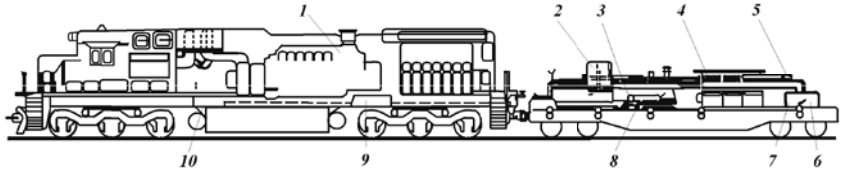

Fig. 1.10. Schematic diagram of an experimental locomotive equipped with a diesel engine running on a WCS. 1 – engine running on a WCS; 2 – electronic control unit; 3 – recirculation pump; 4 – container for the WCS; 5 – cleaning system pump; 6 – tank for purified water; 7 – tank for untreated water; 8 – electric heater and thermostat; 9 – flow-through heat exchanger for heating the WCS; 10 – make-up pump

Initially, the locomotive tested in stationary conditions. At the same time, the whole range of issues related to the introduction of engines running on WCS into practical operation under railway conditions studied. In addition to the tasks directly related to the engine operation, issues of coordinating the characteristics of the power plant with the characteristics of the locomotive also addressed. Methods for controlling the engine and the fuel supply system worked out. As result of the road tests, it found that the emission of NO_x and CO reduced by more than 90%, and a specially designed exhaust gas cleaning system-using sorbents made it possible to reduce the sulfur dioxide content by 85%. Thus, the toxicity of the exhaust gases was significantly lower than the established maximum standards.

In 1993, the main provisions of the program for the development of an engine running on WCS were completed. According to the conclusions of the researchers involved in the implementation of the program, noticeable progress achieved in all areas related to the creation of an engine suitable for commercial use. Despite quite optimistic forecasts, after 1993, due to the decline in oil prices, as well as due to the federal deficit, further work on the creation of a solid-fuel engine by General Electric was suspended.

***

In 1989, General Motors, together with the Southwest Research Institute, studied the possibility of using WCS in a two-stroke diesel locomotive engine [38, 40, 74]. The research program included both the study of WCS

combustion processes in a bomb and machine tests on one cylinder of a two-cylinder engine model EMD 567B (Electro-motive Division, a structural division of General Motors) with a straight-through valve purge system, a cylinder size of D/S= 216/254 mm, ε = 16, N_e = 160 kW/cyl at n = 835 min^{-1}. WCS with a mass content of coal dust of about 50% tested as fuel. The suspension injected by a pump-nozzle located along the cylinder axis. The plunger diameter of the pump-injector was 12.7 mm, and the sprayer had six holes with a diameter of 0.38 mm, located at an angle of 160°. The combustion process activated feeding pilot diesel fuel into the cylinder using a two-jet sprayer located in the head near the cylinder wall. To prevent jamming, the plunger diameter of the pump-injector reduced by 0.013 mm, and the diameter of the sprayer needle reduced by 0.038 mm. The pump-injector body cooled with water.

Table 1.4 shows the results of engine tests when running on diesel fuel No. 2 and WCS. The tests showed that when using the suspension, the engine efficiency, compared to the same parameter for diesel fuel, decreased by an average of 25%. During the experiments, the amount of pilot diesel fuel was 4.5 kg/h, while the amount of WCS fluctuated within the range of 36...42 kg/h. The transition to the use of WCS, the flow rate of which through the main sprayer was 3.5...4 times greater than for diesel fuel (approximately 11.3 kg/hour), led to a change in the volumetric flow rate. As a result, the spray characteristics were far from optimal for this type of fuel. Fig. 1.11, 1.12 show the graphs of the change in pressure and heat release rate in the engine working cylinder when it is running on diesel fuel and WCS. As can be seen from Fig. 1.11, the nature of the pressure change when using WCS is very different from the similar characteristic for diesel fuel.

Table 1.4.

EMD 567B engine test results

Main fuel	**DF №2**	**WCS**
Pilot fuel	DF №2	DF №2
Share of heat supplied by the pilot fuel, %	28	23
Indicator efficiency, %	35	30
Maximum pressure, MPa	7.9	6.2
Start of pilot fuel supply (before TDC), deg.	36	35
Start of main fuel supply (before TDC), deg.	21	26
Duration of pilot fuel supply, deg.	18	16
Duration of main fuel supply, deg.	16	25
Start of pilot fuel combustion (before TDC), deg.	19	18
Start of main fuel combustion (before TDC), deg.	13	9
End of main fuel combustion (before BDC), deg.	23	26
Pilot fuel ignition delay, deg.	17	17
Main fuel ignition delay, deg.	8	17

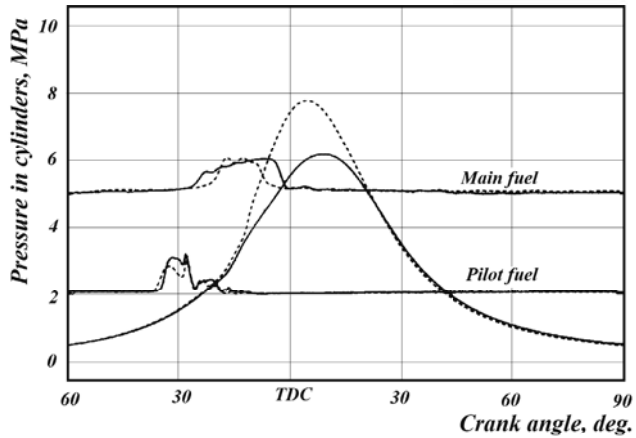

Fig. 1.11. Change in pressure in the engine working-cylinder when using DF and WCS. The feed advance is 25° for WCS, 35° for pilot DF, 20° for main DF. - - - DF; —— WCS

The pressure gradually increases during the entire injection process, but still does not reach the same maximum obtained when using diesel fuel. This indicates that the spray characteristics of WCS were not optimal at the early stages of injection. The nature of the change in the heat release rate (heat stress) for WCS and diesel fuel used as the main fuel shown Fig. 1.12.

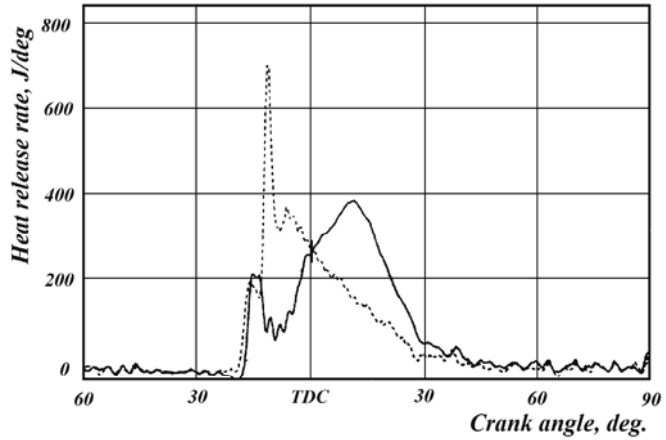

Fig. 1.12. The rate of heat release in the engine working-cylinder when using diesel fuel and WCS. The advance angle of the main fuel supply is 25° for WCS and 20° for diesel fuel. - - - DF; —— WCS

In both cases, the same amount of pilot fuel supplied to the engine combustion chamber, with an injection advance of 35° before TDC. The main difference in the combustion of the WCS is a sharp decrease in the rate of heat release in the initial stage of combustion, which is due to the evaporation of water included in the suspension. The data obtained indicate that the rate of initial combustion of the WCS is very low, most of the carbon particles burn in the diffusion phase. At the same time, a decrease in the temperature in the combustion zone leads to a decrease in the formation of nitrogen oxides and carbon monoxide. Analysis of exhaust gases showed that the emission of NO_x decreased by half, but the content of solid particles increased by an order of magnitude.

After the tests, the engine disassembled for inspection. 600 g of carbon deposits found in the exhaust system, containing approximately 78% carbon and 5% ash. The cylinder head surface was generally clean, without deposits, but the piston and rings showed signs of wear. There were minor carbon deposits on the piston, and traces of abrasion found on the cylinder liner. Based on the results obtained, the researchers came the conclusion that optimization of the engine's operating process can significantly improve its performance. To do this, it is necessary to improve the quality of suspension spraying; clarify the direction of the fuel jets; optimize the start time and duration of suspension and pilot diesel fuel injection; reduce the ignition delay period. The latter can achieved by increasing the charge temperature by the start of fuel injection to 1000 K by heating the air entering the cylinder, increasing the compression ratio, or using combustion chamber thermal insulation. The combustion rate can increase by rational organization of charge movement in the combustion chamber.

The results obtained by General Motors were significantly worse than in other projects, mainly due to the complexity of optimizing the injection process when using pump-injectors. For more or less reliable operation, such a fuel system required a very high degree of purification of the original coal fuel, which contradicted the goals of the program. In connection with this, further research on this type of engine discontinued.

***

Since 1992, ***Detroit Diesel Corporation***, together with the Southwest Research Institute, has been carrying out a research program aimed at creating a model series (model 149) of two-stroke diesel engines with N_e=50 kW/cyl and dimensions D/S= 146/146 mm, intended for operation on WCS [38, 69]. Engines of this series have a valve-slot scavenging scheme with four exhaust valves in the cylinder head. The main goal of the project is to develop a diesel engine with a rotation speed of up to 2000 min^{-1} for trucks

and sea vessels. Economic calculations performed by the company's specialists have shown the commercial attractiveness of the project. Within the framework of the adopted program, a theoretical study was carried out using mathematical modeling methods, as a result of which it was established that in order to achieve a given rotation speed, the average diameter of coal particles entering the engine should not exceed 20 μm. Experimental studies subsequently confirmed the correctness of the theoretical assumptions. To operate on the WCS, the fuel injection system redesigned using a separating piston (similar to the Cooper-Bessemer injection system). Fig. 1.13 shows the dependences of the pressure change and heat release rate in the full load mode in the 8V-149 engine at different angles of the WCS injection start. The pressure and temperature at the engine inlet maintained at 192 kPa and 125°C, respectively.

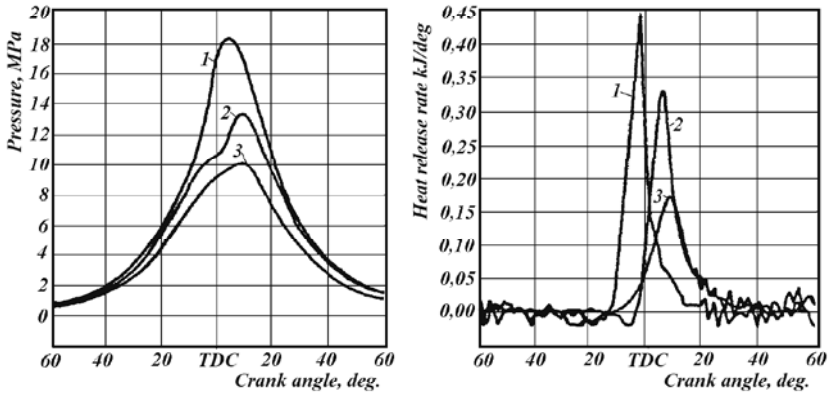

Fig. 1.13. Changes in pressure and heat release rate for different injection angles of the WCS in the 8V-149 engine. 1, 2, 3 – WCS injection 30°, 20°, 40° before TDC, respectively (self-ignition mode)

***

Caterpillar, under contract with the Morgantown Energy Technology Center, spent three years beginning in 1988 studying the injection of WCS into the combustion chamber of a diesel locomotive engine. In addition, work conducted in conjunction with the United Coal Company to prove the practical feasibility of systems for processing coal into low-calorific high-pressure gas intended for direct injection into a diesel locomotive engine. United Coal Company, in collaboration with Caterpillar, developed technology and equipment for producing low-calorific high-pressure producer gas from raw coal. This technology includes coal gasification in a special unit and hot cleaning of the resulting gas. Caterpillar, as part of this

project, conducted research on the combustion of low-calorific gas in a diesel engine with a high compression ratio. Since the use of generator gas does not relate to the processes of direct combustion of solid fuels in internal combustion engines, a detailed consideration of this process is beyond the scope of this work.

***

Individual studies conducted in US research institutions, although not as large-scale as those carried out by engineering companies, nevertheless complemented and refined the work carried out in large projects. The main results of these studies regularly reported at conferences held by the Morgantown Center for Energy Technology.

***

The Morgantown Energy Technology Center, under contract with the U.S. Department of Energy, coordinated all projects carried out within the framework of this program and also studied the production of various types of coal suspensions and the characteristics of their combustion in an isolated bomb. Tests were carried out on a single-cylinder Ricardo Proteous engine with a cylinder diameter of 127 mm [38], the thermal characteristics of which are well known, and from them it is possible to calculate the impact of this or that factor on the working process even before conducting experiments. Based on the obtained data, an attempt made to simulate the working process of the engine on the WCS, and a mathematical model developed at the University of Texas used as the primary modeling tool. Since the range of issues dealt with by the center included the study of all processes associated with the rational use of fuel resources and heat (and diesel engines are only part of the energy system), the work on modeling the diesel engine was combined with modeling of other components (for example, gasification, heat transfer and heat recovery).

***

Southwest Research Institute conducted a number of independent studies and collaborations with major engineering companies between 1983 and 1993. These studies aimed at finding ways to reduce wear in engines running on coal suspensions, as well as studying the characteristics of coal suspension injection, ignition, and combustion [63]. The experiments conducted on a single-cylinder swirl-chamber diesel engine, the characteristics of which given in Table 1.5, and its diagram in Fig. 1.14.

The choice of a swirl chamber engine for this study was due the fact that high airflow rates in the swirl chamber reduce the requirements for spraying quality, which in turn allows the use of lower injection pressures and simpler

sprayer designs. The indirect injection scheme also reduces heat loss, since combustion occurs in the swirl chamber, which can be relatively easily thermally insulated from the rest of the engine.

Table 1.5.

Characteristics of the experimental engine

Engine type	Vortex chamber
Swirl chamber	Cylindrical
Cylinder diameter, mm	96.52
Piston stroke, mm	95.25
Compression ratio	18
Intake valve opening (before TDC), deg.	12
Intake valve closing (before TDC), deg.	136
Exhaust valve opening (after TDC), deg.	136
Exhaust valve closing (after TDC), deg.	12
Swirl chamber volume to combustion chamber volume ratio, %	67.4
Swirl chamber channel area to piston area ratio, %	1.6
Main fuel pump plunger diameter, mm	8
Auxiliary fuel pump plunger diameter, mm	8

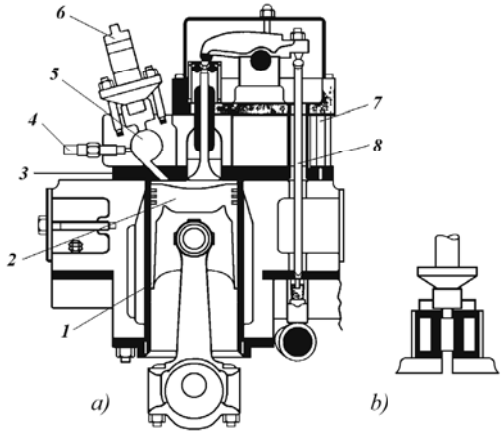

Fig. 1.14. *a* – diagram of the vortex-chamber engine used to conduct the experiments; *b* – diagram of the vortex chamber. 1 – piston; 2 – piston bottom; 3 – heat-insulating gasket; 4 – nozzle for feeding pilot fuel; 5 – vortex chamber; 6 – nozzle for feeding coal suspension; 7 – head mount; 8 – pusher rod

Based on the tasks set, the engine tested in two versions: normal and heat-insulated. For heat insulation of the piston, a special lining installed on its bottom, and the outer surface of the cylinder liner covered with a ceramic layer. The swirl combustion chamber made disassemblable, due to which heat-insulating inserts could installed along its sidewalls. To activate the combustion process in the swirl chamber, two glow plugs with a power of

200 W each installed along the cylinder axis. To ensure stable self-ignition of the suspension, the air supplied to the cylinder heated to 204 °C. The decrease in charge density compensated for by low boost. FCS and WCS with a mass content of coal of about 50%, as well as a water-methanol-coal suspension containing 50% coal, 15% methanol, 35% water were used as fuel. The suspensions injected by a nozzle perpendicular to the axis of the swirl combustion chamber. As one of the options for activating the combustion process, the supply of a pilot portion of diesel fuel to the cylinder studied. For this purpose, an auxiliary nozzle was installed in the head, which injected the pilot diesel fuel perpendicular to the axis of the swirl combustion chamber. Experiments have shown that heating the air at the cylinder inlet or with a glow plug in the combustion chamber ensures the self-ignition of the pilot diesel fuel. FCS for self-ignition requires heating the charge, as result of which combustion worsens. The combustion rate during self-ignition of the pilot diesel fuel and FCS is lower than when activating the combustion process with the help of a pilot diesel fuel. When using a pilot diesel fuel, additional heat supply by heating the air with a glow plug or thermal insulation of the combustion chamber compensates for the latent heat of water evaporation, which allows burning a larger amount of fuel. Excessive heat supply worsens the combustion of the pilot diesel fuel and, accordingly, the ignition and combustion of the suspension. The combustion rate of the suspension was also limited by the cooling of the coal combustion products exiting the swirl chamber into the cylinder. Therefore, to increase the completeness of combustion, most of the fuel should burn a heat-insulated swirl chamber. To do this, the ratio of the swirl chamber volume to the total volume of the combustion chamber should make as large as possible. If the swirl chamber volume for a given engine is 67%, then for effective combustion of coal suspensions it should increased to 90%.

The research showed that the most significant influence engine wear exerted by the particle size of mineral impurities and the thickness of the oil film on the cylinder liner. It also found that with an increase in the injection pressure of the WCS, there were increased torch opening angles, which resulted in a decrease in fuel efficiency.

As part of the cooperation program with General Motors, the Southwest Research Institute conducted a series of tests of a model of a three-cylinder diesel engine made in half the full size. Only one of the three cylinders of the model operated on coal fuel. Water, methanol, diesel fuel, as well as other liquids and their mixtures tested as a carrier for the suspension. The tests provided information on the combustion characteristics of various suspensions and the effect of fuel composition on engine performance.

***

Since 1980, ***Texas A&M University*** has conducted a series of studies aimed at studying the factors affecting the efficiency of combustion of coal suspensions in internal combustion engines. These studies served as the basis for developing a mathematical model of the engine's operating process. Subsequently, based on data obtained by other scientists, the initial models were improved and expanded. As a result, a real opportunity appeared to determine the effective parameters of an engine running on fuel suspensions even during its design process. In addition to theoretical studies, a number of experiments conducted aimed at studying the possibility of organizing the process of feeding suspensions into the combustion chamber of a diesel engine in the form of separate sequential injections. The coefficients of aerosol propagation correlation and the time of break between injections as a function of the distance between the breaks were determined as parameters of intermittent injection. A relationship established between the average size of WCS droplets and the injection pressure, the density of the gas environment and the location of the sprayer relative to the combustion chamber axis.

***

Adiabatics Inc. has carried out a number of studies aimed at improving the fuel supply system, optimizing its combustion and reducing wear. The most interesting in terms of their novelty were the studies aimed at optimizing the combustion of coal fuels in adiabatic (with reduced heat transfer) diesel engines. Higher temperatures of gas and limiting surfaces in engines of this type help to reduce the combustion time of coal particles. This leads to an increase in thermal efficiency and maximum engine speed.

Experimental studies carried out on a single-cylinder engine with a cylinder diameter of 130 mm at speeds of 800...1800 min^{-1}. Bituminous coal used for the experiments, the dry powder of which sprayed in the intake manifold of the engine. Initially, the size of the coal particles did not exceed 10 μm, but subsequently particles up to 21 μm in size used at frequencies up to 1800 min^{-1}. At first, the air heated at the intake to reduce the self-ignition delay time. As a result, the engine efficiency decreased, but it allowed it to operate at higher speeds. In subsequent experiments, an exhaust gas recirculation system was used to regulate the moment of self-ignition, which showed good results. When hot, such an engine easily started on clean coal and continued to operate stably. At the same time, its efficiency was almost the same as that of similar diesel engines.

In addition to the combustion of pulverized coal, some aspects of the engine wear problem studied. In particular, the effect of fuel particle penetration through the gas joint seals into the engine crankcase studied.

***

It is worth noting two more contracts executed within the framework of the research program of the US Department of Energy by the firms Tecogen and Mechanical Technologies, aimed at developing methods of combating wear of piston rings and liners. Tecogen studied ways of improving the system of supplying lubricant to rubbing parts, Mechanical Technologies – investigated the possibility of using dry fine powders as a lubricant.

***

In addition to the United States, studies aimed at studying the problem of using coal fuels in internal combustion engines also conducted in a number of other countries, but there they were of a disparate nature, although individual results of these studies deserve attention.

***

SEMT (France) studied the possibility of using a mixture of coal dust with diesel fuel as a motor fuel, along with various alternative fuels. The studies were conducted on one cylinder of a Pielstick PA6-280 diesel engine with D/S=290/280 mm and N_e = 294 kW/cyl at n = 1000 min^{-1}. FCS and SRC-II (Solvent refined coal) boiler fuel tested as fuel. When using a mixture consisting of 80% SRC-II and diesel fuel in a diesel engine without design changes and additional adjustments, the engine power was practically the same as when running on diesel fuel. However, deterioration of starting properties and delayed ignition of the working mixture in the cylinder were observed. To activate the ignition and combustion process of the FCS, a dual fuel supply system used in the engine, with one injector supplying SRC-II to the cylinder and the other – diesel fuel. In the process of optimizing the timing and fuel injection speed, the amount of SRC-II in the mixture increased to 90%.

***

Murayama T., Miyamoto N. et al. published the results of research conducted at Hokkaido University (Sapporo, Japan) in 1988. They studied the possibility of using soot and dissolved refined coal, produced the USA boiler fuel (SRC-II) as additives to diesel fuels for high-speed internal combustion engines [43, 46]. The soot used to prepare the suspension consisted of particles with an average size of 0.7 μm. The calorific value of a mixture of soot with diesel fuel and SRC-II was equal to 33494 and 39750 kJ/kg, respectively.

Diesel engines with unseparated and separated combustion chambers were used for the study (Table 1.6). During the experiments, the engine operation on fuel mixtures with different component ratios was studied. The diesel engine characteristics, its indicator diagrams, fuel-spraying

characteristics, smoke; operating noise and exhaust toxicity were recorded. All the suspensions and their mixtures studied had a much higher viscosity than diesel fuels. In an engine with an undivided combustion chamber, by increasing the temperature, it was possible to reduce fuel consumption and exhaust smoke to the level of similar parameters for diesel fuel by reducing the viscosity of the suspension. Based on the results obtained, the researchers found that engine performance is determined mainly by the viscosity of the fuel, and not its type. The optimal viscosity value is 0.9...3.0 mm^2/s. When studying the possibility of using soot particles as additives to diesel fuel, their mass content was limited to 20%. This was mainly done for reasons of reducing the abrasive effect on the parts of the fuel system and engine. Since preliminary tests showed that with a soot content of more than 20%, wear of the sprayer and plunger of the fuel pump observed after 50 hours of operation. The study found that, despite the higher viscosity of diesel fuel mixtures with soot, their spraying during injection is better than diesel fuel. Due to this, the mixture burns more intensively, and the combustion duration is reduced (Fig. 1.15). As a result, the specific fuel consumption and smoke decrease, but the noise level and CO emissions with exhaust gases increase (Fig. 1.16). After 50 hours of diesel operation on a mixture of diesel fuel with 5% soot (by weight), no increased wear or carbon deposits noted.

In tests on an engine with a divided combustion chamber, SRC-II fuel and a mixture of diesel fuel with soot showed lower consumption and smoke from exhaust gases, but greater noise and CO and NO_x emissions than on diesel fuel.

Table 1.6.

Characteristics of the engines used in the experiments

Specifications	Engine A	Engine B
Engine brand	KOMATSU ID-105	YANMAR TR-15
Combustion chamber type	Undivided	Antechamber
Cylinder diameter, mm	105	102
Piston stroke, mm	125	106
Cylinder volume, cm^3	1082	866
Compression ratio	17.5	19.5
Power, kW	16	11
Rotation speed, min^{-1}	2500	2600
Fuel pump	Bosch A-type	Bosch A-type
Plunger diameter, mm	9	10
Nozzle brand	ND -DLL A152S32	NP-DN4SD24
Injection start pressure, MPa	24.5	11.8

The increase in the ignition delay period explained by the lower cetane number of SRC-II, as well as the fact that when it is sprayed, smaller aerosol

droplets are formed than when diesel fuel is sprayed. Due to the high combustion rate, the main part of the fuel burns out at a practically constant volume, which leads to a sharp increase in pressure. As a result, the engine experiences large mechanical losses and heat losses to the cooling medium.

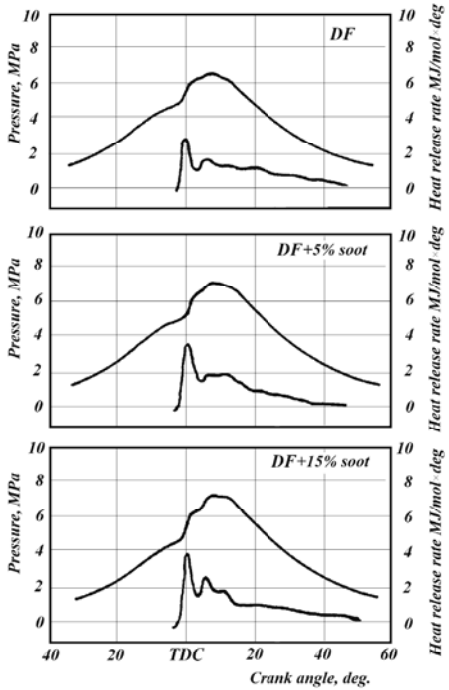

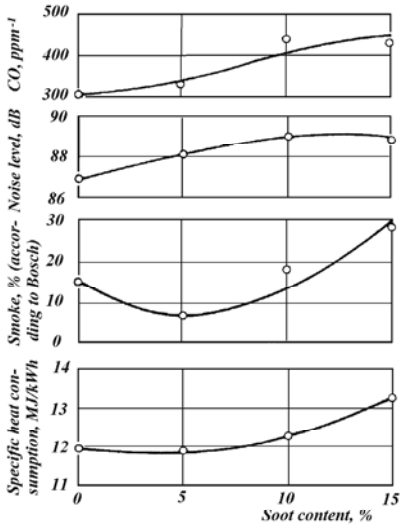

Fig. 1.16. Changing engine parameters depending on the concentration of soot in diesel fuel

Fig. 1.15. Change in pressure (1) and rate of heat release (2) depending on the concentration of soot in diesel fuel

***

In 1998, L.V. Grekhov published the results of a series of studies aimed at studying the patterns of spraying of coal suspensions. The work carried out in the laboratory of the Department of Internal Combustion Engines of the Bauman Moscow State Technical University. Methods for rapid ignition determined selecting the suspension composition and changing the engine design. Based on the experimental data, heat generation characteristics analyzed and methods for accelerating the diffusion combustion of coal particles found [9]. The experimental part of the study was carried out using a single-cylinder vortex-chamber engine with D/S= 85/11 mm as a base. The stand was equipped with a traditional measurement system, as well as an automated measuring complex with high-precision cylinder and fuel supply

equipment indication, with subsequent recording and processing of results on a computer, which made it possible to record and process signals with an accuracy of up to 0.1...0.4% of the amplitude. The design of the fuel supply equipment based on the scheme by N.N. Patrakhaltsev [32]. Fuel suspensions fed into the discharge pipeline through a special feed valve. This made it possible to ensure the operation of the high-pressure fuel pump on pure diesel fuel, assigning it only the role of a control pulse generator and solving the problem of wear of the most expensive unit of the fuel equipment – the plunger pair. The operability of the injector ensured hydraulic locking of the needle, flushing the gap in the sprayer with diesel fuel and using nozzles made of technical diamond, cubic boron nitride, and ruby.

Both FCS and WCS used as fuel for the engine. The maximum particle size was 8...14 μm. Coal dust used to obtain fuel-coal suspensions, and brown coal dust for water-coal suspensions.

During tests on FCS, the diesel engine worked quite stably, although it did not develop rated power. The greatest difficulties at the first stage of the work caused work on WCS. The engine not only did not start, but also did not idle or operate at partial loads. A high instability of the ignition and combustion process observed which led to flashes at the end of compression or at the beginning of exhaust. The latter occurred when the combustible mixture in the exhaust system ignited by the afterburning gases remaining from the previous cycle with misfire. Fig. 1.17 shows a combined diagram including five consecutive cycles, which clearly demonstrates the instability of combustion in the engine cylinder. The operation of the diesel accompanied a sharp knock. All this indicated that the thermal conditions at low loads of a naturally aspirated diesel engine were insufficient for stable ignition of the WCS. After the first series of tests, the engine underwent significant modernization. To heat the air in the intake manifold, an electric heater with a capacity of up to 3.0 kW installed, which made it possible to increase the air temperature to 150 °C. The combustion chamber parts provided with thermal insulation: the bottom of the cylinder head coated with 0.2 mm zirconium dioxide, the piston provided with a heat-resistant EI-283 lining, and a cylinder liner with a heat-insulating insert manufactured. Three high-pressure fuel pumps (HPFP) with plunger pairs of 6.5...12 mm were prepared. Changing the HPFP mount allowed changing the injection advance angle within a wider range. The single-nozzle injector was equipped with replaceable nozzle liners.

When testing a FCS with a coal dust content of approximately 50%, the diesel's effective power (from 4.4 to 2.8 kW) and effective efficiency (from 0.31 to 0.19) dropped sharply. Superimposing the workflow and heat release

diagrams revealed that, despite the earlier fuel injection, a delayed ignition and, most importantly, slower diffusion combustion observed. Even under the highly turbulent working fluid of a swirl-chamber diesel, the combustion rate was unacceptably low.

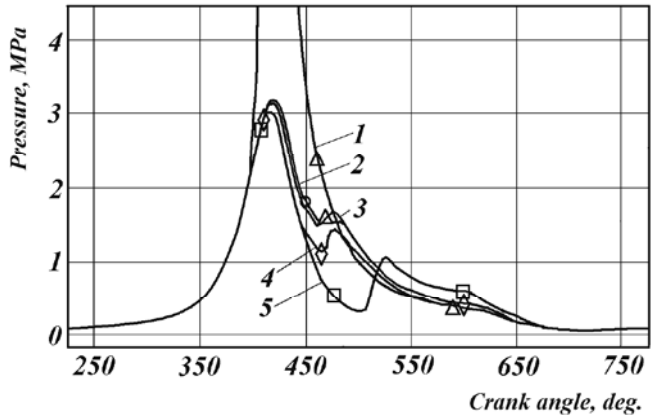

Fig. 1.17. Combined indicator diagram of five consecutive cycles when operating on the WCS (engine load 50%)

According to the author, the relative decrease in effective performance, compared to indicated performance, was due to increased internal losses in the diesel. This also indicated by an increase in indicated pressure at idle.

The increase in internal losses is due to increased friction, which confirmed by microanalysis of the oil, which revealed unburned carbon particles of the same structure as in the original fuel. Experiments demonstrated that increasing the temperature at the end of compression could have a beneficial effect on the ignition and combustion of coal suspension. A minor increase in diesel engine operating characteristics observed when the inlet air temperature raised to 130°C, notwithstanding the concurrent substantial drop in the excess air ratio.

Thus, it confirmed that increasing the intake air temperature accelerates not only self-ignition but also combustion. Therefore, the use of thermally insulated combustion chamber components, particularly for accelerating ignition, is justified. The positive effect of air preheating at idle was significantly greater than at nominal speed due to the high excess air and low thermal state of the working fluid.

When testing the engine with the WCS, an even greater deterioration in operating parameters observed compared to the FCS: a nearly twofold

decrease in power and efficiency. As with the FCS, this explained by increased friction losses and delayed combustion. When operating with the WCS, an even greater ignition delay observed compared to the FCS, along with very slow diffusion combustion. As a result, the engine overheated, and ring seizure occurred in the cylinder liner. After optimizing the suspension composition, power increased from 2.24 to 3.69 kW, and efficiency increased from 0.155 to 0.255. However, this was associated with a significant increase in maximum cycle pressure (6 MPa), resulting in a sharp knocking noise during diesel engine operation. The application of intake air preheating resulted in a simultaneous decrease in ignition delay, maximum pressure, and harshness of combustion. Engine noise significantly reduced. However, due to reduced cylinder filling and excess air ratio, the diesel engine's efficiency and power further reduced.

The WCS composition, optimal for nominal idle operation, made engine operation impossible. Improved idle and low-load performance achieved by heating the air to 130...150°C. In this case, there no excess air or maximum cycle pressure limitations: the diesel engine operated reliably, and the indicator diagram and heat generation approached those typical of a diesel engine.

Based on this, the researcher believes that the heating level should vary according to the diesel engine's operating conditions, even to shutting it down under high loads.

For the normal mixture formation and combustion of coal suspension to occur, the experimental data show that adequate excess air and high injection pressure are critical. To increase the former, it was necessary to reduce the fuel delivery, anticipating a power reduction. The latter overcome by increasing the plunger diameter and decreasing the nozzle orifice diameter. A new high-pressure fuel pump with a 12 mm plunger pair assembled, and the pin injector subsequently replaced with a single-nozzle unit with nozzle inserts of 0.5...0.25 mm diameter, including wear-resistant ones.

Tests of the boosted fuel injection system with various nozzles yielded little variation, despite significant differences in injection pressure and advance angle. This suggests that the selected fuel delivery modes are close to optimal, and an injection pressure of 40 MPa can considered sufficient for a swirl-chamber diesel engine of the speed in question.

To improve ignition stability, the effect of a glow plug studied. Since this required removing the pressure sensor, no indication performed. After installing the glow plug, a significant improvement in diesel engine stability at idle and low loads noted. Stable engine operation at idle even without preheating the intake air was achieved by installing a glow plug and a 12 mm

diameter fuel pump plunger, along with setting the injection advance to 33° BTDC.

Thus, by choosing rational design solutions and operating modes of the engine and, first of all, the fuel supply equipment, it was possible to minimize the impact of the delayed combustion of carbon particles, ensuring heat generation near TDC (Fig. 1.18) [14].

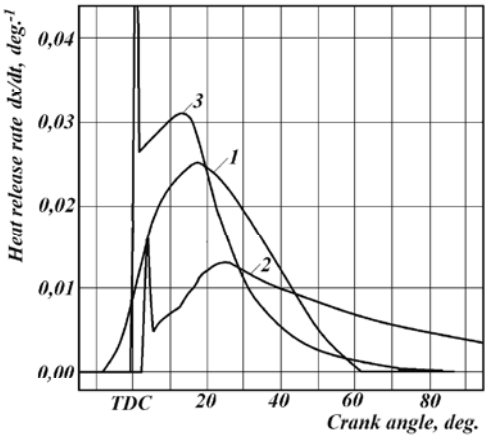

Fig. 1.18. Heat release rate during operation at full load of the original diesel engine on DF (1) and on WCS with standard (2) and forced fuel supply equipment (3)

Because of the modernization, it was possible to achieve a minimal deterioration in the effective indicators compared to the original diesel engine, namely: power decreased by 18%; effective efficiency by 13.5%; indicated efficiency by 3%.

***

The center for research into the use of solid fuels in diesel engines has now moved to the state of Alaska (USA). The main work being conducted at the University of Fairbanks. Like previous projects, this one initiated by the US Department of Energy with the involvement of various investors interested in implementing the program. The total cost of the project estimated at $47.6 million. The involvement of a significant number of investors explained by the fact that Alaska has at least 18 large subbituminous coal deposits, with reserves estimated at between 50 million and 30 billion tons. Stationary diesel power plants are widespread in Alaska, with a combined capacity of 600 MW, generating 22% of the state's electricity. Furthermore, given the low population density, there is a significant need for power plants operating as part of local power grids

covering a relatively small area. The research being conducted using an 18-cylinder, four-stroke Pielstick PC 2.6-400 diesel engines with a cylinder bore and stroke ratio of D/S= 400/460 mm (Fig. 1.19). In its standard configuration, it can run on both light and dark petroleum products. When using diesel fuel, the engine produces 9.6 MW.

The main goal of the project is to prove that this engine can operate on water-coal fuel for 4,000 hours while maintaining efficiency at 41%. The use of water-coal fuel, along with a special catalytic cleaning system, expected to reduce NO_x emissions by 50%, SO_2 by 70%, and CO_2 by 25%.

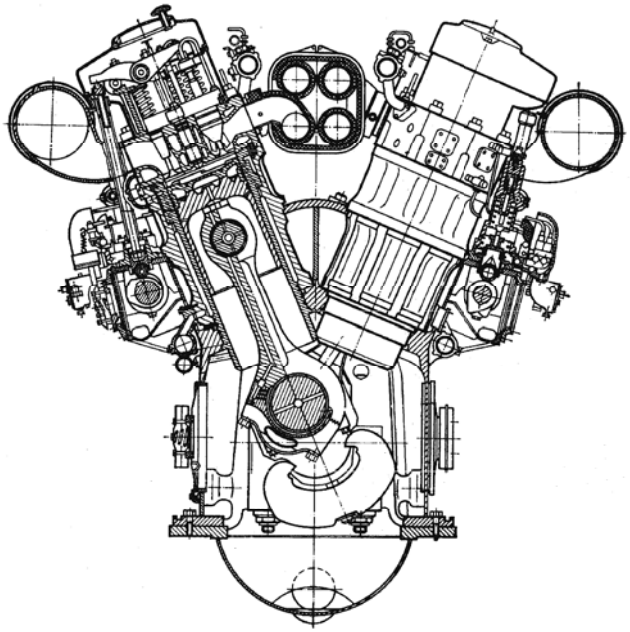

Fig. 1.19. Cross-section of the Pielstick PC2.6-400 engine

The proposed fuel is a water-coal fuel based on low-rank subbituminous coals, which developed by the Mining Research Laboratory and designated LRCWF (low-rank coal water fuel). Engine power expected to drop to 6.4 MW when using this fuel, but the ability to operate on liquid petroleum products also expected to retain. Switching from one fuel to the other will require only minor adjustments to the fuel system. As of the end of 2002, testing of the selective catalytic converter (SCC) exhaust gas purification system for removing NO_x was completed. When running on diesel fuel, NO_x emissions reduced 90%. Three LRCWF mixtures with different compositions

produced. These used to test injectors and other fuel delivery system components. The goal of the testing was to determine the optimal mixture composition to ensure both efficient injection and reliable operation of the fuel delivery system components.

Machine testing initially planned for two cylinders. This would investigate the thermodynamic cycle, the nature and dynamics of wear, and identify optimal coatings and heat treatment methods for critical fuel injection system components, the cylinder-piston assembly, and other engine components.

It anticipated that through further development, the engine's service life could extend to 6,000 hours. The use of a waste-heat recovery system, consisting of a steam boiler producing steam for the turbine, would increase the overall efficiency of the power plant to 48%. This makes the use of water-coal fuel commercially viable and competitive with petroleum-based fuels. The installed capacity of 1.0 kW/h for this type of engine estimated at approximately $1,300. Completion of work this project expected in January 2004.

1.2. Analytical research

The first theoretical studies aimed at studying the combustion of coal fuel in a piston engine performed by Nusselt in 1928. From the heat balance equation, he determined the equilibrium temperature of a particle when exposed to radiative and convective heat flux. Wentzel later continued these studies in 1931 [40]. However, the conclusions reached in these studies based largely on the analysis of experimental data rather than on actual modeling of the ignition and combustion processes. Both studies provided a detailed analysis of the experimental data available at the time on the ignition and combustion of coal dust under real engine conditions, as well as the results of experiments performed by the authors. The experiments conducted using a bomb in which the particles ignited and burned at a constant volume. The main conclusion reached by both researchers was that coal is a fuel with a very low combustion rate, which is due to the heterogeneous nature of the reactions. Based on this, it suggested that the rotation speed of engines using coal fuel could not be more than 400 min^{-1}.

***

Later calculations of the burnout time of a carbon particle in an engine cylinder are largely consistent with each other. At the same time, the high complexity of real processes, as well as their poor study, did not allow for an accurate combustion modeling. According to calculations performed by Rich L.L., Walker M.L. et al. [38, 40], under real engine conditions at a pressure

of 4.5 MPa and an air charge temperature of 2273 K with infinite excess air, a carbon particle of 30...75 μm in size burns out in approximately 10...60 ms. This corresponds to a crank rotation angle of 90...420°. According to the authors, such a combustion time is sufficient to ensure an engine speed of approximately 1000 min^{-1}.

***

Saxton M.J., Creswick F.A., and Kircher J.F. developed a simplified method for analyzing the combustion of carbon particles over a wide range of engine performance. They assessed the effect of carbon particle temperature on its burnout rate [38]. The results of calculations performed using the developed methods are almost completely consistent with the results of calculations obtained by Walker and Rich.

***

Caton J.A., Rosegay K.H. (1983) [37, 68] presented a detailed study of the combustion process of a coal particle in the combustion chamber of a piston engine, carried out using mathematical modeling methods. To study individual phases of the combustion process, they used submodels for the combustion process, the heat exchange process between the particle and the environment, and the mass transfer process. All these submodels combined with a thermodynamic analysis of the engine working cycle. This made it possible to determine the instantaneous value of the state of the parameters of the working fluid in the engine cylinder. The developed model made it possible to determine the optimal parameters of the fuel injection advance and duration, as well as the effect of particle size on the combustion process. Based on the calculations performed, the researchers found that for an engine with a rotation speed of 1500 min^{-1}, the size of coal particles should not exceed 15 μm, only in this case can the optimal combustion characteristics of the fuel suspension ensured. It also found that the combustion rate of coal particles limited, first, by diffusion. As the particle, size decreased, the initial and final reaction rates decreased, but the kinetics of this process remained not entirely clear.

***

In 1986, Kishan S., Bell S.R. and Caton J.A. attempted to model the cycle of a two-stroke piston engine with compression ignition running on water-coal fuel [62]. The study carried out within the framework of the General Motors program for the conversion of the EMD 710 locomotive engine to water-coal fuel. The developed model based on the thermodynamic analysis of the state of the working fluid in the engine cylinder during ignition, combustion, and heat and mass transfer between the working fluid and coal particles. The objective of this study was to develop simple models of the

main processes and integrate them into a complete model of the thermodynamic cycle. The aim of the study is to investigate the combustion process and engine performance when running on WCS. The combustion process of water-coal fuel considered for the conditions of an undivided combustion chamber with direct injection. The entire modeling process structured so that, by modifying the relevant submodels, the model could used to calculate the parameters of the gas exchange process with the environment for both straight-through, valve-slot, and loop scavenging schemes. The submodels for gas exchange, compression, and expansion processes derived from a thermodynamic analysis of the working fluid's state and differed only slightly from similar models used to analyze the operating cycle of a liquid-fuel engine. The combustion submodel underwent the most significant changes.

The thermodynamic analysis yielded a system of nonlinear differential equations, the solution of which allowed us to obtain the instantaneous state of the working fluid, suspension droplets, and carbon particles. To verify the adequacy of the model, the operating cycle of a low-speed Sulzer 1RSA76 engine initially simulated, since at that time, only this engine had objective experimental data reflecting the engine's operating parameters with a WCS. For this reason, an objective evaluation of the modeling results was difficult; however, the experimental data were in good agreement with the calculated results. Having thus confirmed that the model adequately reflects real-world processes, it subsequently used to select optimal operating parameters for the EMD 710 engine during its conversion to water-coal fuel. Testing conducted by General Motors further confirmed the acceptable adequacy of the developed model.

***

To obtain more comprehensive information on the ignition and combustion processes of water-coal fuel, necessary for the development of a piston engine powered a WCS, a group of researchers conducted work between 1986 and 1992 to refine the mathematical model of the cycle. Initially, such models based on the vaporization and combustion of a single suspension droplet in an isolated system with an infinite excess of air. Such models only approximately represented the actual processes occurring in an engine cylinder. Therefore, it became necessary to refine them to account for the effect on ignition and combustion of a large number of suspension droplets, representing a dense cloud of particles burning within a small volume. This approach later became known as group combustion. It allows for the determination of the combustion characteristics of coal particles depending on their location within the cloud, as well as the effect of

vaporization of the liquid carrier contained in the suspension on the ignition and combustion process. This takes into account the effects of decreasing oxygen concentration and increasing the mass fraction of combustion products in the cloud, as well as the influence of the local gas temperature within the cloud on the combustion process. All these factors lead to a decrease in the combustion rate of particles within the aerosol cloud compared to individual particles burning with a significant excess of air.

Annamalai K. and Ramalingam S.C. (1987) [36, 40] were the first to study the influence of the group effect on ignition and combustion processes. They performed a quasi-steady-state analysis of the combustion of a dense cloud of liquid fuel and a WCS. This study based on an analysis of experimental data. As a result, a model developed that allows for acceptable results in assessing the instantaneous state of an aerosol cloud when combustion occurs in the diffusion region.

***

In 1988, T.W. Ryan studied the influence of the group effect on the ignition of water-coal fuel. Pyrolysis of coal particles and the release of volatile substances considered as separate stages preceding the ignition process. The main conclusion reached by the modeling was that the release of volatile substances significantly limits oxygen penetration into the aerosol cloud. The ignition process and the first stage of combustion involving volatile components occur at the cloud boundaries, and only after their burnout does the flame move inward; the second stage the burnout of the coke residue of pulverized coal particles begins.

***

Later, Bell S.R. and Caton J.A. (1986-1992) [33-36] worked on improving the combustion process model taking into account the group influence. All material processes in the engine considered by them as separate submodels. In particular, the formation and propagation of the fuel flame in the air charge environment, heat transfer between the suspension particles and the working fluid, vaporization of the liquid carrier, the release of volatiles from solid particles, the combustion of volatile components and the heterogeneous combustion of solid coal particles were considered as separate submodels. One of the main problems that must solved when modeling the combustion process of the WCS in the cylinder of a piston engine is the zonal distribution of fuel in the air charge environment. Combustion characteristics at different emission levels are different and largely depend on the ratio between the amount of fuel and air inside the local volume, as well as on the effective gas temperature. Thus, the zonal

model makes it possible to take into account various states throughout the cylinder volume with a high degree of accuracy. During fuel injection, a packet is formed droplets of carbon-containing combustible material, entrained air, and combustion products.

The study found that the group effect has a significant impact on the combustion process in the cylinder, but has little effect on the engine's external performance. A reduction in the combustion rate of carbon particles occurs as result of limited air access to the solid fuel surface due to the counter-flow of vapor generated by the evaporation of the liquid carrier, as well as the release of volatile components and CO during combustion. The data also indicate that water evaporation significantly influences the combustion process, the role of which is difficult to assess without considering the group effect.

***

In 1990, the employees of the Ricardo-ITI company Wahiduzzaman S., Blumberg P.N. et al. published the results of a study of the working process in a piston engine running on a coke-coal mixture using mathematical modeling [77]. The working process model developed for a diesel engine with direct injection of a coke-coal mixture and pilot ignition using diesel fuel. The complete combustion model combines the submodels of heat release, mass transfer and chemical kinetics of coke-coal mixture combustion with models of other processes in the cylinder of a diesel engine. It includes a two-stage submodel of vaporization and drying of coke-coal mixture droplets, a global submodel of the kinetics of the release of volatile substances, as well as submodels of coke-coal residue combustion, which contain a description of the surface reactions of coke-coal residue with oxygen, carbon dioxide and water vapor. When considering the combustion process, the volume of the working space divided into many zones, for each of which the thermochemical equilibrium the moment of combustion onset determined by calculations. The model allowed for the precise determination of boundary conditions for the submodels of coal-water droplet combustion and heat release in the gas phase. A submodel of coal-water jet development, entrainment, and mixing used to calculate the mass of unreacted air in each combustion zone. A separate submodel for pilot fuel combustion embedded within the full combustion submodel. The resulting full combustion submodel integrated into the thermodynamic cycle analysis model. The integrated model can use to study the influence of fuel characteristics, fuel injection system parameters, and machine parameters on engine performance, as well as to assess the impact of individual process components on overall engine efficiency and coal fuel burnout.

Chapter 2.

Economic aspects of the problem of direct combustion of solid fuels in piston internal combustion engines.

2.1. World fuel resources and the problem of searching for alternative fuels for internal combustion engines.

Currently, internal combustion engines occupy a leading position in terms of energy production consumed by humanity. This explained by their reliability, comparatively simple operation, and relatively high efficiency. This latter is due to the specifics of the operating process and is achieved largely by supplying heat directly to the working fluid. In terms of efficiency, internal combustion engines surpass all other types of prime movers. A number of objective advantages make these engines a virtually monopolistic source of energy in land and water transport, as well as in small electricity generation markets.

The most significant drawback of piston engines is that the vast majority of them run on oil and gas fuels, which consumed in enormous quantities. Therefore, issues of providing internal combustion engines with fuel and ensuring that reserves of these fuels meet ever-increasing demand have long since gone beyond purely technical or economic concerns. The evolving energy situation requires a change in approaches not only to solving technical issues of providing internal combustion engines with fuel but also to finding fundamentally new ways to utilize it [26].

Problems of rational use of fuel and energy resources have recently had an increasingly noticeable impact on the development of the energy sector and, in particular, on the development and use of piston internal combustion engines. The severity and scale of the problem turned out to be more significant than previously assumed. The growth of energy consumption is increasing disproportionately to their abundance in the earth's crust. Thus, the consumption of oil, the world reserves of which are estimated at 438 billion tons of equivalent fuel [15], has recently increased 5-fold in developed countries, which amounted to about half of all energy consumed [7]. According to various forecasts, the depletion periods of oil and gas reserves vary significantly and fall within the range of 30 to 150 years [7, 15, 19], but even now the problem of a shortage of these energy resources is manifested in their uneven distribution across regions. In the world, just over two dozen countries have the ability to export oil and gas [7], while the rest forced to import part or even all of the hydrocarbon fuel they need. Even an industrialized country like the United States must import up to 50% of its oil

consumption, amounting to approximately 375 million tons per year. 54.5% of this fuel is consumed transportation. By 2000, 97% of global transportation energy consumption met by crude oil.

The uneven distribution of oil and gas across regions demonstrated in Fig. 2.1 [29]. Total production and proven reserves are shown for each region as of 1980. The energy equivalent of estimated potential oil resources is 1.5×10^{22} J, and gas – 1.1×10^{22} J.

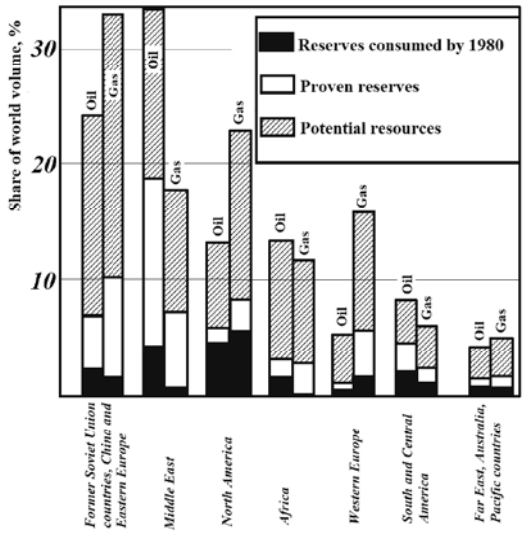

Fig. 2.1. Potential oil and gas resources

Experience over the past decades has shown that as demand for petroleum fuels increases, their cost, although fluctuating significantly, has steadily increased on average. It is easy to predict that this trend will continue. Rising oil prices are already requiring fundamentally new solutions both in terms of finding alternative fuels for internal combustion engines and in terms of their rational use. The lack of any realistic prospects for creating prime movers that are more efficient capable of replacing piston engines, on the one hand, and the potential depletion of oil reserves, on the other, make the search for alternative fuels a global issue [7].

When considering various alternatives to oil and gas, we will dismiss the idea of using renewable energy sources as fuel for internal combustion engines as clearly untenable. Their use for fuel production, while interesting, is quite limited due to the large gap between the production and consumption of these energy resources. For example, if the entire grain harvest in the

United States processed into ethanol, it would only cover 11% of the country's liquid fuel needs [50]. Considering the conversion of potential food products into liquid fuel at a time when more than a billion people on earth are starving is, at the very least, unethical. While such a solution is acceptable for a number of countries with favourable climate conditions, in the foreseeable future of technological development, fuel energy needs will obviously be met by non-renewable fuel resources.

An analysis of global non-renewable fuel resources suggests that coal holds the most promise as an alternative fuel for internal combustion engines. The amount of explored coal reserves, converted to conventional fuel, is 10...15 times greater than the explored oil reserves [7, 15, 19]. The energy equivalent of solid fuels estimated at 21×10^{22} J. The reserves of various fuels (according to MIREK-X data [15]) given in Table 2.1.

Table 2.1.

Characteristics of the world's non-renewable fuel resources

Fuel Type	Non-renewable fuel resources, billion tons of equivalent fuel		
	extracted	forecast	total
Oil	136.5 (12.6)	301.5 (2.6)	438 (3.5)
Natural Gas	108 (10)	222 (1.9)	330 (2.6)
Shale, Heavy Oil, Natural Bitumen	129 (11.9)	553.5 (5.4)	682.5 (5.4)
Solid Fuel	720 (65.5)	10500 (90.1)	11220 (88.2)

The data presented show that coal accounts for 88% of all global non-renewable energy reserves. Geologists believe that the main coal basins already been discovered. Coal reserves in seams thicker than 0.3 m, located at a depth of no more than 2000 m, considered recoverable. Coals that do not meet these requirements classified as potential resources. The geographic distribution of coal reserves on Earth is highly uneven (Fig. 2.2). The majority of recoverable reserves are located in North America, Europe, and Asia. Approximately 43% of the world's coal is located in the countries of the former USSR, 29% in North America, 14.5% in Asian countries, primarily China, and 5.5% in Europe. The rest of the world accounts for only 8% of coal [29].

Based on the above figures, several important conclusions can draw:

- if this pattern of fossil fuel consumption continues, oil reserves will be depleted much earlier than solid fuel reserves. Solid fuels will, however, last for at least several centuries;

- countries located in coal-rich areas should be most interested in exploring the technical feasibility of using solid fuels. As Fig. 2.2 shows, these are primarily economically developed countries capable of undertaking large-scale research programs on this issue;

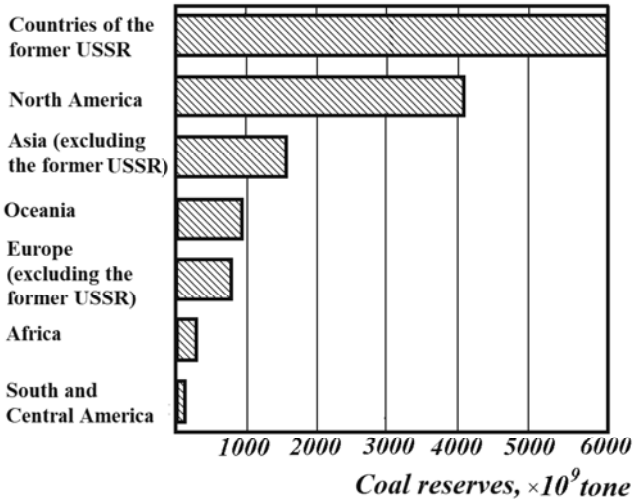

Fig. 2.2. Geographical distribution of coal reserves

- the use of solid fuels for a certain portion of internal combustion engines will, on the one hand, allow for more efficient use of remaining oil, utilizing it only in areas where its replacement is impossible (e.g., the production of fuels for passenger cars and aviation, and in the chemical industry). On the other hand, this will buy time for the development of fundamentally new energy sources unrelated to fossil fuels. Thus, when considering the long-term expansion of the internal combustion engine fuel base, solid fuels are the first non-renewable energy sources to receive scientific attention [42]. We are still quite far from the point where finding a replacement for petroleum fuel will require urgent attention. However, the fact that some of the most pessimistic predictions regarding the depletion of oil reserves by the beginning of the new millennium have not come true should not perceive as sufficiently encouraging.

Currently, price fluctuations and other changes in the global oil market are causing attention to the problem of direct combustion of coal fuels in internal combustion engines to increase from time to time, only to subside again when the situation stabilizes. However, the problem itself remains, and a satisfactory solution is currently lacking. Therefore, studying and improving methods for using solid fuels in internal combustion engines is of great practical importance for providing engines with fuel for the long term. Therefore, it is necessary to improve both existing methods of using solid fuels in internal combustion engines and to search for new ones.

2.2. Selection of the method and efficiency of using solid fuels in piston internal combustion engines

The problem of using solid fuels in internal combustion engines is not new and has several known solutions [2]:

- processing solid fuels into liquid synthetic fuels;
- gasification of solid fuels followed by use of generator gas in a gas or gas-diesel engine;
- direct combustion of solid fuel in the engine's working space.

Converting solid fuels into liquid synthetic fuels is largely a chemical engineering issue. The fuel supplied to the engines, a finished product. No fuel conversion occurs within the power plant itself, which is an undeniable advantage of this method of use. Another undeniable advantage of this method is the existing experience in the industrial production of synthetic fuels from coal. For example, during World War II, Germany annually produced approximately 600,000 tons of hydrocarbons (fuels, lubricants, and other synthetic products) [19, 21]. The most significant drawback of producing synthetic fuels is that up to 60% of the heat contained in the original fuel is lost during processing using existing technologies. Currently, synthetic fuels are more expensive than petroleum fuels, limiting their scope of use. With further improvements in processing methods, coal-based synthetic fuels could alleviate some of the problems associated with replacing petroleum [19].

Obtaining producer gas by gasifying solid fuels and then burning them in an engine is a well-established technology for using these fuels in internal combustion engines. Extensive experience exists in both the design and operation of gas generators and gas engines [6, 8]. However, the calorific value of producer gas, even with the most advanced production methods, remains quite low, and the efficiency of the gasification process typically does not exceed 40...50%.

The production of synthetic fuels and producer gases from coal is beyond the scope of this book; they covered in sufficient detail in the relevant literature.

Currently, direct combustion of solid fuels in the engine's working space considered the most efficient method of using solid fuels in internal combustion engines.

Direct combustion allows for more efficient of solid fuels and allows for the fullest realization of the advantages that distinguish internal combustion engines from other types of primary heat engines.

At the same time, this method of using solid fuels is associated with the greatest technical difficulties.

Direct combustion of solid fuels in piston engines includes methods which coal dust injected into the cylinders either directly or as part of finely dispersed mixtures with liquid motor fuel, water, or other liquids.

When discussing the advantages of direct combustion of solid fuels in the engines working space, it is necessary to evaluate their efficiency compared to other fuels or other methods of using solid fuels. This evaluation should include a broad range of issues, from extraction and primary processing to the actual generation of mechanical energy by the engine. Currently, this type of assessment is fraught with a number of objective difficulties, as reliable information on some key economic indicators characterizing this method of using solid fuels in internal combustion engines is either absent or insufficient. Specifically:

– information on the optimal characteristics of fuel suitable for use in piston engines is extremely limited. Therefore, it is quite difficult to estimate the cost of processing the initial solid fuel to acceptable parameters;

– estimating the costs of storing and transporting solid fuels is quite difficult, as there is either no or insufficient experience in transporting water-coal and pulverized fuels over long distances;

– it is difficult to estimate the costs required to modernize the entire fuel production and fuel processing infrastructure when converting a certain portion of internal combustion engines to solid fuel or its derivatives;

– it is virtually impossible to predict how the cost of solid fuels will change in the event of increased demand associated with the emergence of a large consumer;

– there is a lack of information on how operating costs will change when using liquid synthetic fuels or when directly burning solid fuels in engine cylinders.

Based on the above, any general methods for evaluating efficiency are currently quite general in nature. The economic feasibility of converting an internal combustion engine to solid fuels should assessed on a case-by-case basis based on the objectives set during engine design, taking into account its scope of application, and the specifics of subsequent operation.

A preliminary assessment of the efficiency of direct combustion of solid fuels in an internal combustion engine can performed using a method based on an analysis of the balance of the initial amount of heat contained in the original solid fuel. Although this assessment does not take into account many design, operational, and other factors, it does provide a general idea of the efficiency of a given method. The results of an assessment of the efficiency of using the initial heat of the original fuel, presented in [40], presented below. As an example, we will consider the efficiency of using the initial

heat for oil, water-coal, and liquid synthetic fuels. We will use a low-speed engine with a rotational speed of up to 120 min^{-1} as the source of mechanical energy. These engines have a high efficiency, and the thermodynamic cycle conditions within them are most favourable for the direct combustion of coal fuels.

If we take the initial heat content of the original fuel as 100% and then consider the stages of its conversion into mechanical energy, we obtain approximately the following picture:

For petroleum fuel.

During oil refining, the ratio of initial heat to the heat converted into liquid petroleum products estimated at approximately 92%. The efficiency of the petroleum product transportation process estimated at 99%. Assuming an effective engine efficiency of 41%, 37% of the initial heat of the original fuel will converted into mechanical energy.

For coal suspensions.

During the preparation, preliminary grinding, and purification of the initial solid fuel to acceptable parameters for use in suspensions, with an initial ash content of 30%, approximately 90% of the initial heat will transferred to the finished product. For fuels with an ash content of 40%, this figure will be 80%. Subsequent grinding of the purified fuel to a particle size of approximately 2 μm will transfer 86% of the heat remaining after the first processing stage to the finished coal dust. Experimental and calculated data indicate that low-speed engines can use particles up to 75 μm in size quite effectively. In this case, the amount of transferred heat estimated at 92%. As in the previous case, we assume the transport efficiency to be 99%.

It is quite difficult to estimate the efficiency of an engine operating on coal suspension. In experimental studies conducted on a Sulzer 1RSA76 low-speed engine, the efficiency reached 40%. Given the short duration of this test, it can assume that this figure will be somewhat lower in real-world operation. For our calculations, we will limit ourselves to an effective engine efficiency of 36%. Therefore, the efficiency of using coal fuel when directly burned in the engine's working space can estimated at approximately 30%.

For synthetic liquid fuels.

Depending on the production method, the efficiency of converting coal into liquid synthetic fuel ranges from 35% to 60%. Taking this average value, we estimate the heat utilization efficiency during the conversion process at 50%. Since the subsequent use of liquid synthetic fuel is little different from the use of petroleum products, we estimate the transportation costs and energy conversion efficiency in the engine at 99% and 40%, respectively.

Thus, the overall efficiency of using the initial heat of the solid fuel during its conversion into liquid synthetic fuel will be approximately 20%.

The above calculations show that direct combustion of solid fuels in low-speed engines is more efficient than their conversion into liquid synthetic fuel. A similar relationship holds for other types of power plants equipped with internal combustion engines. Naturally, this calculation is highly simplified. For a final assessment, it is necessary to take into account not only purely energy factors, but also a wider range of problems related to operational features, the distribution of solid fuel resources, the economic feasibility of their extraction and use, as well as other factors.

2.3. Areas of application of engines using direct combustion methods of solid fuel.

The most likely applications for coal-fired engines are rail transport and stationary power generation. This is where the use of this type of fuel will yield the greatest economic benefit. This largely determined by the operating conditions of the engines when running on solid fuel. A decrease in reliability (especially during the initial phase of implementation) can offset by a range of special measures aimed at maintaining the engine in working order.

In rail transport, such measures include the development of modular diesel locomotive power units that be quickly replaced to avoid locomotive downtime. The dismantled power unit undergoes maintenance and repairs in a stationary environment and then reinstalled on the locomotive. This rotation will reduce the continuous operation time of engines, thereby increasing the reliability of rolling stock. In stationary power generation, operational reliability can improved by continuously monitoring the technical condition of engines, as well as by creating reserve capacity that allows individual engines to taken out of service for maintenance and repair without reducing power plant output.

In other sectors of human activity, such as marine or truck transport, coal-fired engines will likely only introduced once their reliability and service life have been improved to acceptable levels, and a comprehensive maintenance and repair system has been established. In passenger vehicles, the use of combustion coal engines, if expected at all, will be a very distant prospect. Obviously, the challenge of replacing petroleum fuel in this type of transport will be with liquid synthetic fuels.

2.4. Economic prerequisites for the conversion of piston engines to coal fuel.

Despite the lack of information, an analysis of the entire range of issues related to the direct combustion of solid fuel in internal combustion engines

shows that this method of use will become economically viable provided the cost of preparing suspension for engines from the original solid fuel decreases to less than $2 per 1 GJ of energy content. It assumed that the price of oil at this point would be $25...30 per barrel. At this price, level, capital investments in the production of both the engines themselves and the fuel for them will prove profitable [64].

As current experience shows, oil prices already occasionally rise significantly above this level, while the price of water-coal fuel suitable for use in internal combustion engines, even when produced in relatively small batches, does not exceed $3.48 per 1 GJ of energy content. The cost of water-coal fuel made up of the cost of unprepared coal, the cost of transportation, and the cost of processing. In Table 2.2 presents approximate calculations of the price of water-coal fuel, made by specialists at General Electric, taking into account the technologies used by Otisca and AMAX [72].

Table 2.2.

Cost of WCS for three different production and consumption scenarios (USD per 1 GJ of energy content)

	Type of coal	
	Bituminous	Subbituminous
Otisca Technology:		
Coal	1.24	0.60
Production	0.83	1.36
Transportation	1.00	1.52
Amount	3.08	3.48
AMAX Technology:		
Coal	1.24	0.60
Production	0.97	1.13
Transportation	1.00	1.52
Amount	3.22	3.25
The most favorable case:		
Coal		0.37
Production		1.36
Transportation		0.00
Amount		1.73

The lower part of the table shows the cost of water-coal fuel under the most favourable scenario, when this type of fuel produced and consumed at the place of its extraction, that is, there is no transportation of unprocessed coal to the processing site and the finished product to the consumer.

Thus, in the context of constantly increasing oil prices, the solution to a range of issues related to the use of WCS in internal combustion engines, produced from relatively inexpensive coal, has potential for commercial use [48].

2.5. Prospects for the use of solid-fuel piston engines in railway transport.

An economic study of the use of water-coal fuels in rail transport conducted by Hapeman and Savkar [39] in 1986, commissioned by General Electric and the Burlenton Railroad. Their findings subsequently refined by other researchers in studies conducted between 1986 and 1992.

To study the feasibility of introducing water-coal fuels into diesel locomotive engine operation, three criteria selected technical feasibility, financial feasibility, and economic attractiveness for railroads.

Technical feasibility investigated based on a literature review, as well as laboratory tests performed by General Electric. According to the researchers, existing experience with water-coal suspensions in diesel engines, despite its contradictions, generally indicates the technical feasibility of this project.

To successfully resolve all issues associated with the use of solid fuels, five main tasks can be identified:

- determining the optimal composition of coal suspensions;
- ensuring reliable injection of WCS into the combustion chamber;
- ensuring reliable ignition and combustion of the suspension;
- reducing wear on friction parts;
- reducing harmful emissions into the atmosphere.

The studies conducted have shown that all of the above objectives can, in principle, addressed. The only issue for which sufficiently reliable data could not obtain is the impact of abrasive wear on engine performance. However, the results obtained suggest that these issues are also entirely surmountable. It is clear that the implementation of any project, especially in the initial phase, will require significant capital expenditures associated with changes in the maintenance structure and infrastructure of a number of departments within the railway system.

All costs divided into six main categories: railway infrastructure modernization, maintenance costs, research and development, capital expenditures, personnel training costs, and the cost of purchasing the WCS.

Fig. 2.3 shows a schematic diagram of the concept of a diesel locomotive with a 2950 kW engine powered by the WCS. General Electric estimates that additional equipment for storing, preparing, transporting, and injecting the WCS, as well as the engine management system, will increase the cost of the entire locomotive by approximately $280,000. The components of the locomotive modernization costs presented Table 2.3. As can be seen from the table, the majority of the costs are associated with the components of the exhaust gas toxicity management system. The second-largest cost category is associated with engine modernization [72].

Table 2.3.

Increase in the base cost of a diesel locomotive when converting it to WCS

Cost type	Cost, $USD
Engine Systems	60.171
Emission Control Systems	160.446
Diesel Locomotive Systems	58.195
Amount	278.812

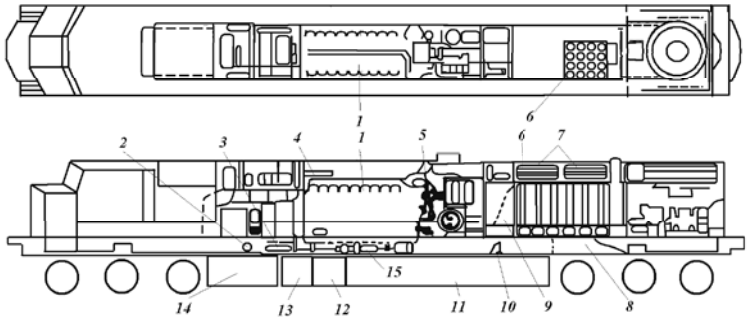

Fig. 2.3. Schematic diagram of a diesel locomotive with an engine running on water-coal fuel: 1 – engine; 2 – recirculation pump for WCS; 3 – electric heater; 4 – fuel supply regulator; 5 – centrifuge for lubricating oil purification; 6 – exhaust gas filters; 7 – automatic blinds; 8 – vacuum chamber for removing microparticles and sorbent; 9 – diffusion chamber; 10 – water pump of the cleaning system; 11 – 32,000 l tank for WCS; 12 – 950 l tank for untreated water; 13 – 950 l tank for purified water; 14 – 1,900 l tank for diesel fuel; 15 – loading pump

The locomotive's design allows for 50 hours of operation without refuelling exhaust gas toxicity reduction system cleaning. Its platform extended by three meters to accommodate a larger fuel tank capable of holding an adequate amount of fuel with a lower energy density. The additional length is also necessary to accommodate components of the exhaust gas toxicity reduction system.

At the time of this analysis, there was no commercial supply of ready-to-use water-coal fuels with characteristics suitable for use in internal combustion engines in the US or other international markets. Therefore, the most economically optimal situation is for railroads to build, maintain, and operate WCS production plants themselves. In this case, the cost of this fuel would be approximately $0.12 per liter. At the time of the main research cycle, operating costs for fuel purchases for diesel locomotive fleets on various US railroads ranged from $0.214 to $0.24 per liter of standard fuel [48]. Thus, the estimated cost of water-coal fuel was half that of diesel fuel.

The maintenance costs of one engine running on WCS will amount to $22,000 per year. The payback period for the costs associated with

converting the diesel locomotive fleet to WCS estimated at approximately 10 years.

2.6. Prospects for the use of solid-fuel piston engines in stationary power generation.

Cooper-Bessemer specialists assessed the potential for water-coal fuels in stationary diesel power plants [44]. They believe that the use of solid fuels in stationary diesel power plant engines holds great promise in the United States. The country's vast brown coal reserves make finding ways to use them in internal combustion engines for electricity generation not only a technical or economic challenge, but also a strategic one.

Fig. 2.4 shows the schematic diagram of a Cooper-Bessemer diesel power plant [41].

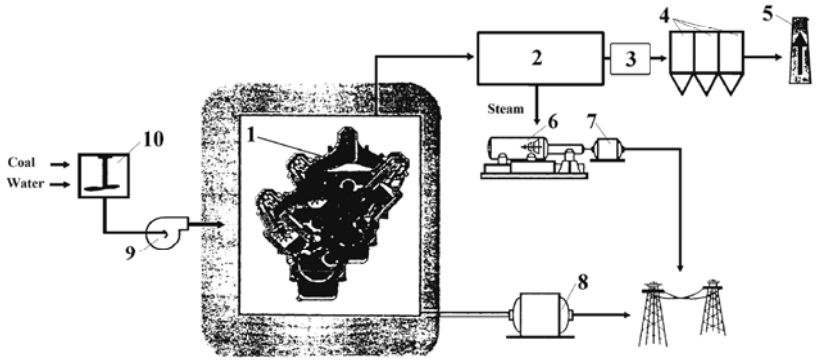

Fig. 2.4. Schematic diagram of Cooper-Bessemer diesel power plant operating on water-coal fuel. 1 – piston engine; 2 – steam generator of the heat recovery system; 3 – exhaust gases and sorbents; 4 – exhaust gas cleaning system from dust and sorbents, 5 – exhaust gas exhaust system; 6 – steam turbine; 7 – additional generator; 8 – main generator; 9 – feed pump; 10 – WCS preparation system

The economic efficiency of stationary diesel engines operating on WCS depends on a number of factors:

- increased initial engine cost, operating costs, and overhaul costs;
- costs of purchasing and pre-processing the original solid fuel and preparing the WCS;
- specific emissions' reduction costs.

According to estimates from Cooper-Bessemer [44], the use of WCS-powered internal combustion engines in stationary power generation will be feasible if energy generation costs do not exceed 5.88...7.2 cents/(kWh). Moreover, economic efficiency depends on the cost of WCS production to

greater extent than any other factor, and emissions reduction costs are the second-largest operating cost item.

Based on separate indicators of the cost of a diesel engine designed to use solid fuel and its operating costs, the relative importance of each economic parameter can be determined.

2.6.1. Increased engine cost and operating costs when using WCS. An important economic parameter for a coal-fueled engine is its effective efficiency. Test results for the JS and LSB series engines, as well as other studies, suggest that the effective efficiency of a WCS engine will be the same as that of a standard diesel engine, approximately 39%. The reduction in efficiency due to the evaporation of water contained in the WCS (2...3%) will be offset by faster heat generation and other thermodynamic factors.

To make the use of WCS economically feasible, certain design changes must made to individual engine components. However, the use of more expensive components is acceptable if this allows the creation of an engine capable of running on cheaper fuel.

Operating a WCS-fueled engine differs somewhat from operating a conventional diesel engine. The adverse effects of coal-fueled engines primarily affect moving parts, which exposed either to the fuel itself or to its combustion products.

Since there has been no long-term operation of diesel engines on WCS to date, it is quite difficult to indicate the specific type of necessary modification; however, an analysis of the cost structure and the results of the conducted research allow us to estimate, as a first approximation, the approximate increase in the cost of the engine.

For Cooper-Bessemer 6 MW stationary engines with a base price of $3.5 million, the price increase associated with the need to upgrade individual components is $1.67 million. This means that a standard engine modified for WCS estimated to cost approximately $5.2 million.

If such an engine is operated for 20 years at an average load of 80%, the cost per kWh of generated energy, including capital costs, is 1.21 cents (for an engine running on diesel or gas, the cost per kWh is estimated at 0.81 cents). Thus, the cost increase excluding the cost of emission control equipment is 0.4 cents/(kWh).

Table 2.4 shows the frequency of maintenance and repair for stationary Cooper-Bessemer engines with a capacity of 6,0 MW when operating on diesel fuel and on WCS (the assessment of operating standards is made taking into account the test results of JS and LSB series engines).

Based on the standards presented in Table 2.1, operating and capital costs will increase by 0.33 cents/(kWh). Thus, when using the WCS, the cost per

kWh for a 6 MW Cooper-Bessemer engine will be 0.73 cents higher than for the same engine running on diesel fuel.

Table 2.4.

Comparison of maintenance and repair times

Operation	Diesel Fuel Engine	WCS Engine
Injector Maintenance, hours	2000	500
Minor Routine Maintenance, hours	8000	4000
Component Overhaul, hours	25,000	12,000
Complete Engine Overhaul, hours	70000...100000	25,000

Considering that, depending on current prices, the cost of standard diesel fuel can fluctuate between 3 and 5 cents/(kWh), this increase in cost does not limit the use of the WCS. Therefore, the increase in capital, operating, and maintenance costs is within an acceptable range, regardless of the calculation method.

2.6.2. WCS production costs. The most important parameter determining the operating efficiency of a piston engine running on WCS is the cost of coal fuel purification, which essentially determines the engine's economic performance.

For over a century, the primary incentive to explore ways to use solid fuels in piston internal combustion engines has been the relatively low cost of the fuel suitable for combustion in the engine. Experience shows that, despite periodic fluctuations, the cost of petroleum fuels has steadily increased relative to coal fuels. Therefore, it can assume that the cost of WCS will be lower than that of diesel fuel. However, unlike petroleum fuels, the properties of coal fuels are poorly compatible with the operating characteristics of a piston internal combustion engine. Consequently, higher processing costs are required, which significantly reduces the economic benefit of using coal fuel.

The following calculations for the use of WCS in stationary diesel power plants based on data from AMAX, Otisca, Resource, and other companies that produce WCS, and on a subsequent independent analysis of production costs. The following important assumptions made [21]:

- the WCS production plant must simultaneously generate electricity by burning high-ash coal, a by-product of the enrichment of the original fuel;
- the plant's capacity must be 1.8 million tons per year (enough to operate 100 5 MW engines);
- the cost of coal arriving at the WCS production plant is $1.42 per 1 GJ of heat content (this includes transportation costs of $0.44 per 1 GJ, or $18.65 per ton for transportation over 1,000 km, and $27 per ton – the cost of coal at the mine site);
- electricity consumption is 175 kW/t;

- equipment depreciation is 12%, and profit is 10% per year.

Calculation results indicate that WCS suitable for use in piston ICEs will cost approximately $1.57 to $2.85 per GJ more than the original coal. Based on an average cost increase of $2.37 per GJ, we obtain that the costs of coal cleaning and WCS preparation will increase the cost of the engine's generated energy by $0.022 per kWh. This result, despite significant differences in the estimation methods, is in good agreement with the results presented in Table 2.2.

A significant potential for reducing the cost of WCS is the use of special additives and reagents that help maintain the coal particles in suspension and create optimal viscosity. The cost of such additives currently reaches 30% of the cost of WCS, but with the development of industrial production methods, the price of these additives could significantly reduced.

2.6.3. Costs of combating harmful emissions. The final economic parameter is the cost of controlling harmful emissions (sulfur oxides, particulate matter, and NO_x). Estimated treatment costs estimated in the range of $0.74...$1.69 per GJ. These costs take into account the cost of controlling particulate matter emissions, based on the results obtained during JS engine testing, and an analysis of the increasing cost of SO_x and NO_x treatment equipment.

***

The ultimate goal of the project is to create stationary engines with a capacity of 2244...5970 kW and a cylinder count of 6 to 20. The planned application for these engines is small power and electricity generation markets with a capacity of up to 50 MW. In these markets, the engines expected to be quite competitive with other types of power plants. In the US alone, this market will exceed 60,000 MW (more than 7,000 engines) by 2020. According to US Department of Energy experts, the global market is 70 times larger than the US market.

It envisaged that these engines would operate in combined-cycle power plants, with some energy generated by the internal combustion engine and some by a steam turbine, the steam for which can generated from the heat of the engine's exhaust gases. The overall efficiency of such a plant, according to the researchers, will be at least 45...48%. Table 2.5 shows the results of calculating the main economic parameters for electricity generation by a network of power plants over 20 years.

Despite the fact that, according to all estimates, operating costs for using coal fuel are higher than for using traditional fuels, all researchers agree that the use of solid fuels in internal combustion engines will become commercially viable as early as the first half of the 21st century.

Table 2.5.

Cost structure for generating 1 kW/h of energy by 100 5 MW units, taking into account depreciation (in $USA) [9, 52]

Costs, $USA	Fuel	
	Diesel fuel	WCS
Initial cost of Cooper-Bessemer diesel engines	0.0081	0.0121
Increased cost of diesel engine maintenance on WCS		0.0033
Construction of a plant for WCS production		0.0052
Coal mining and transportation		0.0131
Diesel fuel price and WCS production cost	0.05	0.022
WCS transportation		0.0027
Exhaust gas treatment		0.0103
Total energy cost	0.0581	0.0687

Chapter 3.

Solid fuels and fuel suspensions based on them used in internal combustion engines.

3.1. Raw materials for the production of pulverized coal fuel.

When using coal-based fuels, it is necessary to consider the economically challenging requirements for the fuel production process and its performance characteristics. The prospects for using a particular type of coal fuel in an internal combustion engine will determined by its cost, performance, economic characteristics, and the environmental impact of the engine using it. It is clear that the use of solid fuels in internal combustion engines requires fuel preparation, just as oil refining does.

Until recently, solid fuels in internal combustion engines used in the form of fine dust, directly injected into the engine's combustion chamber or fed with the inlet air stream, as well as in coal suspensions, with water, diesel fuel, methanol, synthetic liquid fuels, and other liquids used as carriers. Water and methanol were included in some suspension to reduce viscosity, ensure stability, and reduce corrosion. The efficiency of solid fuel use in piston internal combustion engines and their operational reliability depend on a number of important thermal characteristics of the fuels. These include the content and composition of mineral impurities, moisture content, volatile content, coke residue properties, and calorific value. All of these fuel characteristics depend on its chemical composition (Table 3.1) [26].

For engines operating on pulverized fuel, both dry and in various suspensions, suitable feedstock is including hard and brown coal, peat, wood, and mixtures thereof, as well as organic waste and soot. When choosing a feedstock, it is important to consider that the cost of pulverized fuel suitable for use in internal combustion engines largely determined by the costs of grinding it to the required particle size and removing mineral impurities. All the above-mentioned natural fuels, except for hard coal, have a fibrous structure. As a result, the cost of pulverized fuel, obtained from relatively inexpensive raw materials, can increase many times over after grinding.

Pulverized coal fuel intended for combustion in internal combustion engines should have, if possible, a high calorific value and a short ignition delay period (provided that combustion is not activated by backlighting with liquid petroleum products), as well as a relatively low self-ignition temperature. It is important to note that the combustion of coal dust, both in its pure form and in dispersed solutions with water or liquid fuel, preceded by a long period of pre-ignition reactions. This is due to the multi-stage

combustion process, during which primary chemical complexes formed on the surface of the pulverized coal particle.

Table 3.1.

Elemental chemical composition of combustible mass and main characteristics of solid fuel suitable for use in internal combustion engines

Fuel	Composition of the combustible mass. %					Ash content of dry fuel %	Volatile content %	Heat of combustion of combustible mass MJ/kg
	C	*H*	*O*	*N*	*S*			
Wood	51	6	42.6	0.5	—	1	80…90	18.9…20.1
Peat	58	6	33.0	2.5	0.5	10	65…70	21.4…24.7
Coal								
Brown	64…77	4…6	15…25	1.0	0.5…7.5	7…45	40…50	26.4…30.2
Bituminous	78…83	5…6	10…20	1.0	0.5…0.8	10…45	20…40	16.7…30.5
Lean	75…83	6…5	9…7	1.7	0.5…7.0	15…18	10…20	31.4…34.8
Anthracite	90…93	2…4	2…4	1.0	0.5…2.0	15…20	2…10	33.7…35.0

These requirements are practically incompatible with any single fuel source. For example, hard coals have a relatively high calorific value, but at the same time require relatively high activation energy for the combustion process. This virtually eliminates the possibility of spontaneous combustion of coal dust in the engine combustion chamber. The temperature reached by the air charge during compression is insufficient to overcome the energy barrier, after which the endothermic interaction between atmospheric oxygen and the carbon in the pulverized coal particle begins. Since hard coals consist of 90…95% pure carbon, the overall reaction between fuel carbon and atmospheric oxygen is heterogeneous, with the rate of surface reactions limited by diffusion.

Brown coals, wood, and other fuels contain cellulose. Unlike hard coals, they contain large amounts of hydrogen and other combustible components, known as «volatiles» (hereinafter, the word «volatiles» will use without quotation marks). Even with slight heating, volatiles are released from the pore space of the pulverized coal particle and ignite quite easily. The heat released during combustion of the volatiles leads to an increase in temperature in the combustion chamber, resulting in the coke residue of the particles heating to the activation temperature and beginning to react with oxygen. Thus, lignite, wood, and peat dust are capable of spontaneous combustion; however, these fuels have a low calorific value and typically have high ash content (see Table 3.1). As a result, the absolute fuel consumption of the engine will increase significantly, which can seriously

impede the use of these engines in transport. Furthermore, the high ash content makes cleaning such fuels quite expensive.

As well, known, mineral impurities contained in solid fuels have a significant impact on the wear of the engine's cylinder-piston assembly. However, the ash content of the fuel is not always decisive; in some cases, its composition is of primary importance. The most common mineral substances found in ash are SiO_2, Al_2O_3, CaO, Na_2O, Fe_2O_3, Na_2O_3, and K_2O. Silica and aluminum oxide together can account for up to 90% of all mineral impurities. These materials are known as excellent abrasives.

3.2. Purification of raw materials from mineral impurities.

The fuels used in the experiments had ash contents ranging from 5 to 25% in the early stages of the research, but relatively inexpensive methods for reducing this content are now known. When using coal fuel in internal combustion engines, its ash content should not exceed 1%. Several methods exist for removing mineral impurities from coal. As part of a U.S. Department of Energy program, coal powders supplied by six different companies, including Otisca, AMAX of Golden, CO, UNDERC of Grand Forks, ND, and Resource Engineering, used to conduct experiments on the combustion of various suspensions in internal combustion engines. The source coals included bituminous coal from Kentucky and Pennsylvania and subbituminous coal from Wyoming. Chemical and gravity cleaning methods were the most common. Suppliers such as AMAX and Resource Engineering used chemical enrichment of the fuel, while Otieca used a gravity method to obtain the fuel. One chemical method is the solvent coal cleaning process, the main product of which is a low-ash, low-sulfur solid fuel called SRC [45]. The SRC process originally developed Spencer Chemical in the early 1960s. The main advantages of chemical cleaning processes are their applicability to a wide range of coals and the ability significantly reduce ash content. However, chemical cleaning, compared to gravity cleaning, is more complex and more expensive.

Despite their differences, all of these methods well established in modern industry. Ultra-clean coals produced in large quantities, particularly for the metallurgical industry. Therefore, it can assumed that the production of coal fuels with minimal mineral impurity content for use in internal combustion engines does not pose a serious problem for the modern coal industry.

3.3. Use of purified pulverized coal fuel.

Until recently, two possible methods for using solid fuel in internal combustion engines considered feeding it into the engine's working space as a dry dust or in suspensions with various liquids.

The use of dry pulverized coal as a fuel was considered in the early stages of research [40]. Currently, due to the difficulties associated with creating a reliable dust feed system into the engine combustion chamber, this method of burning solid fuel in internal combustion engines been almost completely abandoned. In some studies, pulverized coal fuel fed along with the air entering the engine, but achieving a uniform distribution of particles throughout the pulsating airflow proved difficult. Furthermore, the residence time of the coal dust in the working cylinder with this feed scheme increased, and a significant portion of it settled on rubbing surfaces, forming a dense deposit that promoted active abrasive wear and increased friction in the components.

3.4. Use of coal suspensions.

Over the past three decades, all ongoing research been aimed at solving problems associated with the use of solid fuels for internal combustion engines in the form of various types of coal suspensions (CS). Unlike direct combustion of coal dust in the engine's working space, the use of CS allows for the creation of a functional fuel delivery system, solving transportation and refuelling issues, addressing environmental concerns, and ensuring fire and explosion safety.

The use of suspensions is associated with a number of difficulties, including pronounced non-Newtonian properties, especially if the mass concentration of coal particles exceeds 55...65%. Increasing the concentration, for maximum dispersion of coal, results in the suspension losing its liquid properties, making its use impossible. The viscosity of a suspension depends significantly on the particle size of its constituent particles, and increases as their size decreases. This creates another contradiction in the fuel requirements. On the one hand, particle size must be as small as possible to ensure rapid combustion. On the other hand, this leads to increased viscosity, which necessitates a reduction in the fuel weight. Otherwise, increased viscosity negatively affects fuel spraying quality and the transport of the suspension through low- and high-pressure pipelines. It also been established that, in addition to particle concentration and size, suspension viscosity is highly dependent on the particle electrical potential, pH, carrier surface tension, dust dispersion, suspension storage and mixing time, coal deposition, and a number of other factors.

The non-Newtonian properties of suspensions and the dependence of viscosity on many factors create significant challenges for their storage, transportation, delivery, and spraying. Consequently, their use poses challenges in ensuring the normal processes of mixture formation, ignition, and combustion.

3.4.1. Selecting a liquid carrier. When preparing suspensions suitable for use in internal combustion engines, the choice of liquid carrier is crucial. Diesel fuel, methyl and ethyl alcohols, vegetable oils, water, etc. can use. All carriers can divide into two groups. The first group includes suspensions obtained from flammable liquids, which, like coal dust, participate in combustion. The second group includes water, which serves only to mobilize the coal particles. The carriers of the first group, most frequently used in internal combustion engines, are diesel fuel, methanol, and SRC-II (synthetic liquid fuel obtained by liquefying brown coal).

The main properties of the liquids used to obtain suspensions belonging to the first group presented in Table 3.2. Table 3.3 presents their elemental composition [45].

The efficiency of engines operating on the FS assessed primarily comparing the performance of the same engine when operating on diesel fuel (DF) No.2. Furthermore, diesel fuel used as a carrier liquid for the FCS.

Table 3.2.

Physical properties of US-produced DF No. 2, SRC-II, and methanol

Parameter Name	DF № 2	SRC-II	Methanol
Relative Density at 20°C	0.82	0.98	0.795
Pour Point, °C	–29	below –37	–97.8
Sedimentation, Determined by Toluene Extraction, %	absent	0.05	—
Water-Mud Sedimentation (ASTM D 96-73)	absent	1.0	—
Miscibility (1:1)	mix completely	mix completely	bad
Aggressiveness Based on Copper Strip Test(ASTM D 130-75)	Low. color 1b (dark orange)	Moderate. color 2b (lavender)	—
Surface Tension at 22°C, dynes/cm	29.9	34.1	—
Oxidation Stability, mg/100 ml (ASTM D 2274)	10.7	4.0	—
Heat of Combustion, MJ/kg (ASTM D 2015-66)	45.64	39.73	19.67

Table 3.3.

Elemental composition of DF No. 2, SRC-II and methanol

	DF № 2	SRC-II	CH_3OH
Carbon, %	86.3	85.6	37.5
Hydrogen, %	13.3	8.8	12.5
Nitrogen, %	0.03	0.8	—
Sulfur, %	0.23	0.26	—
Ash, %	traces	0.014	—
Oxygen (by difference), %	0.14	4.526	50

Water is a promising carrier for suspension formation. Using WCS allows for the complete elimination of petroleum as a fuel source. Furthermore, the presence of water reduces combustion temperatures, resulting in lower exhaust emissions.

3.4.2. Rheological characteristics of the CS. Developing fuel systems for CF injection is impossible without studying their rheological properties (flowability). Designing fuel systems capable of ensuring high-quality spraying requires the ability to calculate various suspension flow regimes at the highest possible concentration of carbon particles. The study of CF rheological characteristics has received considerable attention over the past decades [38, 40, 57, 59-61, 65]. A significant amount of research into the influence of suspension rheological properties on the performance of fuel injection equipment been conducted at the Piston Engines Department of Bauman Moscow State Technical University [10, 14].

As numerous experiments show, maximum efficiency of carbon particle combustion can only achieved with good CF spraying, which can only be achieved at a certain viscosity – in the range of 0.9…3 mm^2/s. The greatest difficulty in optimizing viscosity characteristics presented by the non-Newtonian properties of the suspension (viscosity dependence on speed), as result of which these fluids exhibit a complex rheology. These patterns are quite complex and difficult to predict: at a temperature of 100°C, the viscosity stops decreasing and begins to increase, with stirring for more than 4…8 hours it begins to increase, etc. Apparent viscosity decreases sharply during steady-state motion and even more so in unsteady flow [9, 10, 14]. The suspension begins to lose fluidity at mass fillings above 55%. Depending on the additives used, the viscosity characteristics at low shear rates can be dilatant or pseudoplastic. At high shear rates, viscosity depends to greater extent on the concentration, type of carbon and the size of its particles [65]. To ensure high-quality mixture formation when operating on the suspension, increased injection pressure is required, while the length of the injection pipeline, for design reasons, can be quite large. The way the viscosity of the fuel system changes depending on its flow conditions has a decisive impact on the performance of the fuel injection system. Excessive viscosity leads to significant pressure losses (50% or more) in the high-pressure supply line system. For example, General Electric specialists tested a WCS with a carbon content of 55% by weight. The engine injection system was equipped with a separating diaphragm, which prevented carbon particles from entering the high-pressure plunger pump. During the initial tests of this system on a WCS with a high solids concentration, injection not achieved at all. To reduce viscosity, the suspension had to dilute. Fig. 3.1 shows the WCS pressure

change characteristics at the fuel pump outlet and directly in the injector. As an example, the characteristics obtained for suspensions with a carbon particle mass concentration of 53% and 48% shown. The presented dependences show that the fuel pump outlet pressure for suspensions containing 53% carbon particles is approximately 67 MPa, while the pressure in the nozzle does not exceed 31 MPa. The total pressure drop is just under 36 MPa. For suspension containing 48% carbon particles, the pressure drop is approximately 19 MPa.

Subsequently, to achieve acceptable viscosity characteristics, the carbon particle concentration maintained at 47…49%. Additionally, special water-soluble additives added to the suspension to prevent the spray needle from sticking and to prevent the agglomeration of carbon particles. The total additive content did not exceed 2.5%.

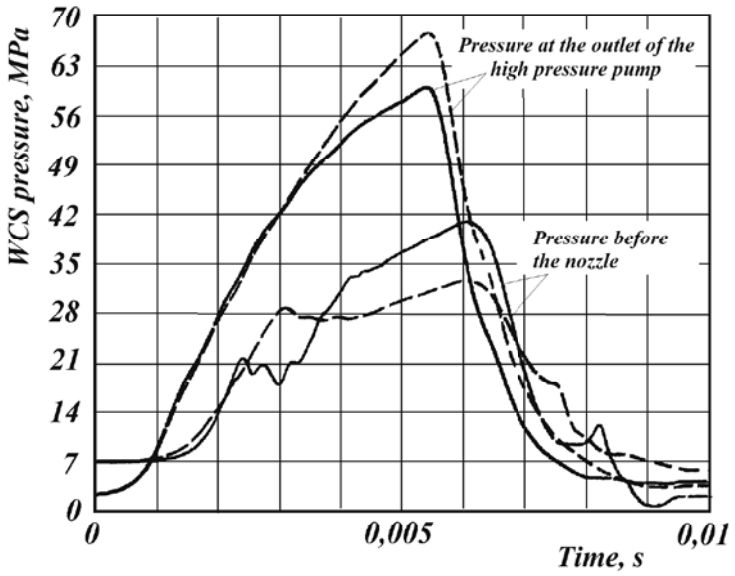

Fig. 3.1. Change in WCS pressure at the outlet of the fuel pump and in the sprayer. - - - WCS with a mass content of carbon particles of 53%; —— WCS with a mass content of carbon particles of 48%

The given example clearly illustrates the influence of the rheological properties of the WCS on the efficiency of the engine fuel supply equipment.

The influence of coal particle concentration and their fractional composition on the rheology of WCS. Fig. 3.2 shows the experimental dependences of the effect of coal particle mass concentration and shear rate

on the viscosity of three different WCSs used by Sulzer. Judging by the presented data, even small variations in solid particle concentration and coal fraction sizes can lead to changes not only in the normal viscosity but also in the rheological properties of the suspension, which, for example, changes from dilatant to pseudoplastic.

Unlike Newtonian fluids, for CS the normal viscosity ($\eta_{susp.}$), i.e. viscosity under conditions of low deformation rates, does not fully reflect their rheological properties, but it can be used to estimate the apparent viscosity (viscosity at a given rate) or relative viscosity $\overline{\eta} = \eta_{susp.}/\eta_{liquid}$ [10].

Coal dust characterized by its maximum diameter, implying a polydisperse mixture of particles ranging from this diameter to zero. To assess the impact of polydispersity and optimize the dust fractional composition, we apply the Farris multiplicativity principle. It is assumed that the WCS consist of large particles immersed in a dispersion medium formed by liquid containing small particles. Based on this assumption, for N particle fractions, we obtain:

$$\overline{\eta} = f_{\eta_1}(C^*_{V_1}) \times f_{\eta_2}(C^*_{V_2}) \times \ldots \times f_{\eta_n}(C^*_{V_n}), \qquad (3.1)$$

where $$\overline{\eta}_i = f_{\eta_i}(C^*_{V_i}); \qquad C^*_{V_i} = V_i/(V_{liquid} + \sum_{k=1}^{k=i} V_k); \qquad (3.2)$$

f_{η_i} – function of the relative viscosity of the i-th monodisperse suspension;

$C^*_{V_i}$ – relative concentration of the i-th phase in a suspension of smaller particles.

Fig. 3.3 shows the results of calculating the relative viscosity of a two-disperse suspension with variable solid phase filling $C_V = V_{solid}/(V_{solid}+V_{liquid})$ and the ratio between fractions $X_i = V_i/V_{solid}$ (X_i – the proportion of fine fractions in the total volume of the solid phase). For the calculations, D. Lee's empirical relationship for monodisperse suspensions $\overline{\eta}$ was used:

$$\overline{\eta} = 1/(1-C_V)^{(2,5+1,92C_V+C_V^2)}. \qquad (3.3)$$

Calculations show that the viscosity of a monodisperse suspension with each particle size at high C_V can be almost an order of magnitude higher than that of a two-fraction suspension. This leads to an important practical conclusion about the existence of an optimum concentration of components that ensures minimum suspension viscosity. According to Farris, the relative viscosity extremum achieved when all partial relative viscosities and partial conditional concentrations are equal.

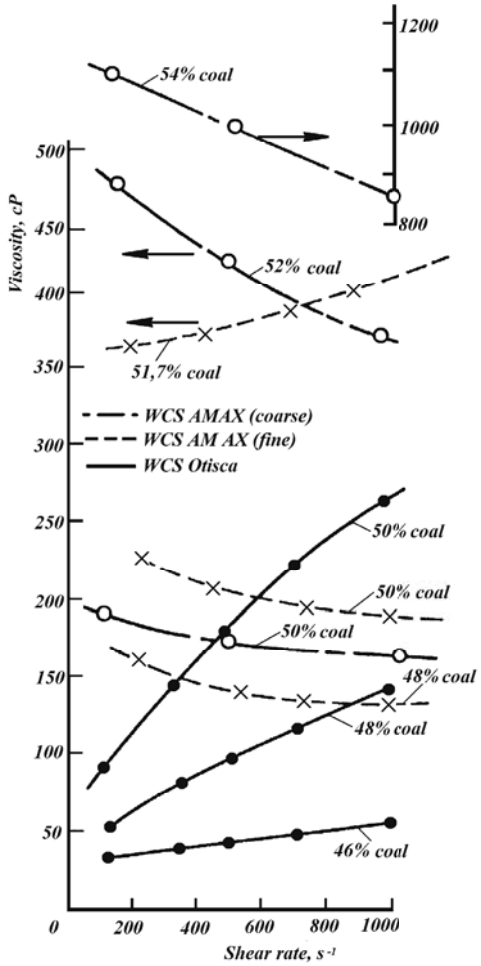

Fig. 3.2. Rheological characteristics of WCS supplied by Otisca and AMAX

An analysis of the size distribution of fractions shows that the proportions of small and large particles differ increasingly as the C_V, content of the suspension increases, with the proportion of small particles increasing relative to the total volume, while the proportion of solids decreases. This can explain by the fact that it is easier to distribute the solid phase in the liquid in large particles, whose volume is proportional to the cube of their diameter,

while the role of small particles is limited to filling the voids between large particles and ensuring their mobility.

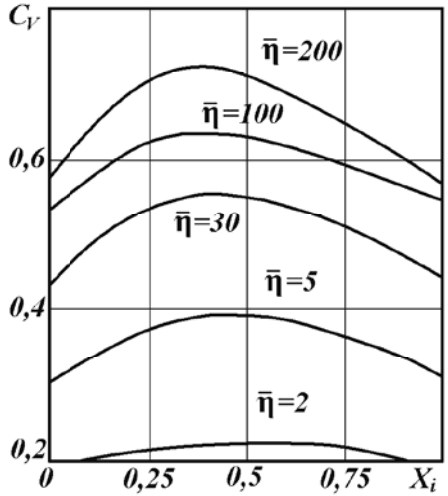

Fig. 3.3. Calculated dependence of the relative viscosity $\bar{\eta}$ of a two-disperse suspension with variable filling of the solid phase

L.V. Grekhov assessed the extent to which the actual distribution of coal fractions corresponds to the optimal one. The study included microphotography and a fractional particle count ($\bar{N}_{particle}$) for three grades of dust from hard and brown coal with a maximum particle diameter ($d^{\max}_{particle}$) of 6...15 μm. The study showed that the volume of the smallest particles is several orders of magnitude smaller than the volume of the largest, while the number of small particles in the mixture significantly predominates. Consequently, the number of small particles in the mass distribution as a function of the average particle diameter (according to Sauter) for a given fraction will increase. Fig. 3.4 shows the distributions obtained for $\bar{N}_{particle} = N^{i}_{particle} / N^{\Sigma}_{particle}$ in the function $\bar{d}_{particle} = d^{i}_{particle} / d^{\max}_{particle}$:

$$\bar{N}_{particle} = \text{const} \times \bar{d}_{particle}^{-2,38} \qquad (3.4)$$

A similar expression for the optimal distribution turned out to be little dependent on the filling of C_V and had the form:

$$\bar{N}_{particle} = 5{,}44\times10^{-8} \times \bar{d}_{particle}^{-2,9}. \qquad (3.5)$$

An analysis of expressions (3.4), (3.5) and the relationships presented in Fig. 3.4 shows that the actual distributions do not fully correspond to the optimal one. If the composition of the polyfractional dust deviates from the optimal one, the rheological properties of the suspension can be controlled by varying the content of individual fractions in the mixture. In particular, a portion of the dust can be removed and, after additional grinding, added to the original [10].

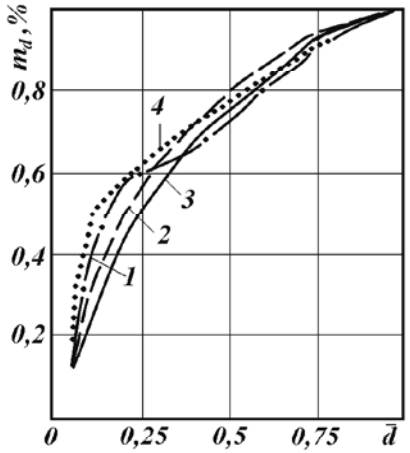

Fig. 3.4. Mass distribution of coal particles as a function of their average diameter (according to Sauter). 1, 2, 3 – particle distribution by fractions for three types of coal dust; 4 – optimal particle distribution by fractions

The difficulties associated with determining the maximum solids loading of a suspension and the effect of loading on the rheology of WCS are, on the one hand, due to the irregular shape of the particles and their absorption of liquid, and, on the other, to the polydispersity and electrification of the particles. The true density of coal determined by the increment in volume and mass upon immersion in liquid to the average loading level after degassing and vibration treatment. To determine the relative viscosity at different levels of coal particle concentration, one can use the relationships obtained by processing experimental data obtained by measuring viscosity in a capillary viscometer and by passing CS through an 8 mm diameter tube under the action of hydrostatic head, providing shear rates $\gamma < 1\ s^{-1}$ ($U < 1$ *mm/s*) [10]:

$$\left.\begin{aligned} \overline{\eta} &= \left[1 + (0{,}75 \times \overline{C}_V)/(1 - \overline{C}_V)\right]^2 \quad \text{at } \overline{C}_V \le 0{,}125; \\ \overline{\eta} &= 1{,}23 + \left[32{,}1 \times (\overline{C}_V - 0{,}125)^{2{,}3}/(1{,}125 - \overline{C}_V)\right]^2 \quad \text{at } \overline{C}_V > 0{,}125. \end{aligned}\right\} \quad (3.6)$$

This dependence $\overline{\eta} = (\overline{C}_V)$ is universal, but its use is hampered by the difficulty of preliminary estimating the maximum permissible solids concentration in the suspension ($C_V^{\max}$). The spread of this parameter, depending on a large number of factors, can be very significant. A preliminary estimate $C_V^{\max}$ can made based on the hygroscopicity of the coal. This estimate based on the experimentally established relationship between the elemental composition of coal *C/O* and its hygroscopicity (Fig. 3.5a). In this case, C_v is determined by converting from the mass concentration of solids (C_m) using the expression:

$$C_v = \left[1 + \rho_{coal}(1 - C_m)/(\rho_{liquid} C_m)\right]^{-1}.$$

Based on the established relationship, it was possible to correlate $C_m^{\max}$ with hygroscopicity, which is a reference value (Fig. 3.5*b*).

The influence of the modes of movement of the CS on the rheological characteristics. As already noted, apparent viscosity is of practical interest for calculating the pumpability and spraying of CS. Since normal viscosity tends toward apparent viscosity at an infinitely small strain rate γ, it is used as the initial value for estimating the latter. Unfortunately, the literature contains virtually no generalizations about the apparent viscosity constants $\eta_{appar} = f(\gamma)$ for concentrated CS under high shear rates. Fig. 3.6*a* presents experimental results obtained by statically pouring WCS and FCS through tubes with diameters of 2 and 8 mm under a pressure of 0.1...1.0 MPa, and Fig. 3.6*b* presents the results of processing these data.

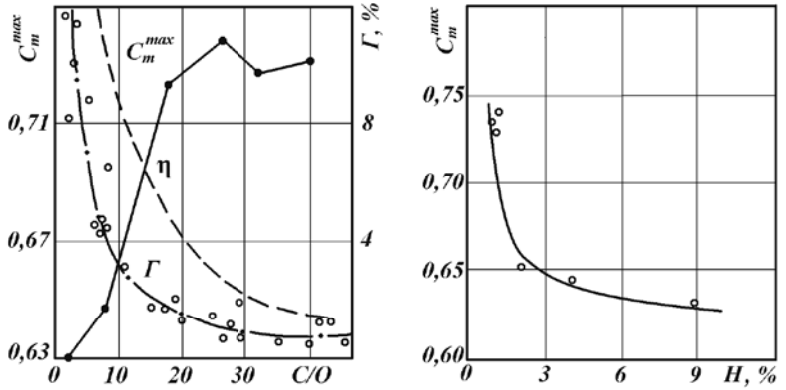

Fig. 3.5. *a* – relationship between the elemental composition of coal C/O and hygroscopicity (based on the results of data processing for 25 deposits); *b* – correlated relationship between the maximum volumetric filling of the suspension with the solid phase and the hygroscopicity of the original fuel

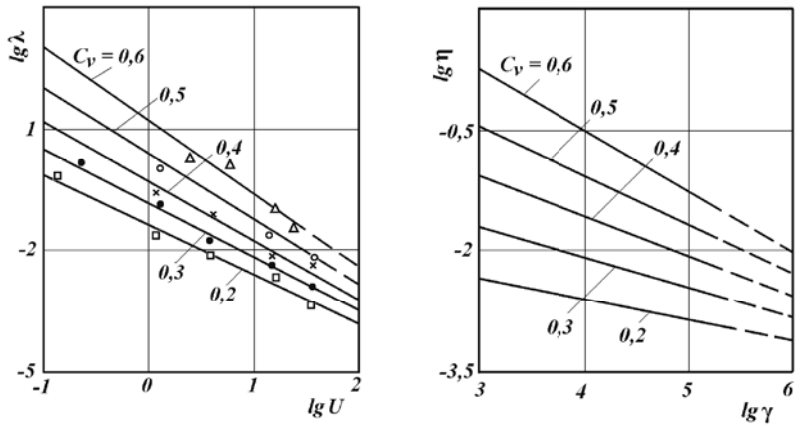

Fig. 3.6. *a* – experimental dependencies obtained by static pouring of WCS and FCS; *b* – results of experimental data processing

As can be seen from the obtained dependences, the degree of suspension dilution depends not only on the flow rate but also on its filling with a solid phase.

Taking into account the fact of the asymptotic dependence of apparent viscosity on normal viscosity, for deformation rates lying in the region $\gamma < 10^3$ s^{-1}, the expressions proposed in [10] can use:

$$\lambda = \frac{115{,}5\eta_{liquid}\overline{\eta}}{\rho U^2}\left(\frac{8U}{d_{mp}}\right)^{0{,}96-0{,}8\overline{C}_V},$$

$$\eta_{appar} = 15{,}5\eta_{liquid}\overline{\eta}\gamma^{-0{,}04-0{,}8\overline{C}_V}, \qquad (3.7)$$

where λ – coefficient of resistance to flow movement CS; ρ – density CS; d_{mp} – diameter of the pressure pipeline.

Equation (3.6) used for $\overline{\eta}$ determination. As can be seen from Fig. 3.6, CS has steeply declining curves. This pattern of rheological property change creates additional difficulties for fuel delivery and mixture formation, including a tendency to form solid plugs and clog channels. A positive aspect of this CS behavior is that they liquefy during pumping, and thicken during storage, even exhibiting thixotropic properties. This ensures the stability of the CS, and the higher their concentration, the less they stratify.

Experimental studies have shown that at high shear rates (approximately 10,000 s^{-1}) occurring during spraying, the apparent viscosity of the WCS varies almost linearly as a function of shear rate and ranges from 150 to 330 cP [57, 69].

In addition to steady-state conditions, the viscosity of the WCS under non-steady-state conditions is of interest for fuel delivery. It known that the drag coefficient during flow acceleration exceeds the quasi-steady-state value, and during deceleration, it is lower. In a cyclic process, the total friction losses are greater those in a steady-state flow with the same average velocity. For diesel fuel injection equipment, this circumstance can be significant even when delivering diesel fuel. Although non-steady-state flow movement leads to increased drag, this effect partially mitigated additional dilution of the suspension or changes in the flow pattern. This result qualitatively correlates with the possibility of a slight reduction in non-steady-state drag relative to steady-state drag at certain concentrations and fillings [10]. High-speed photography with a 15-ms exposure of flow in a transparent tube pumping a suspension of river sand in emulsion paint in steady-state and pulsating modes revealed that during unsteady flow, almost complete particle detachment from the walls is observed, forming a liquid «lubricating» layer near the walls. The combination of the effects of the non-Newtonian properties of the CS, the differences between the unsteady and steady-state boundary layer, and the particle detachment from the walls leads to complex patterns of change in apparent viscosity during unsteady flow. Thus, in unsteady flow, viscosity exhibits a hysteresis with velocity, and due to the non-Newtonian properties of the CS, this hysteresis is many times greater than would be expected if boundary layer deformation due to flow unsteadiness interpreted as the changing viscosity of a Newtonian fluid (Fig. 3.7). A quantitative description of the hysteresis in apparent viscosity requires further study.

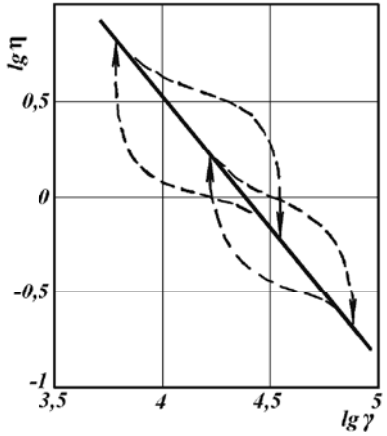

Fig. 3.7. Hysteresis of viscosity CS from velocity in unsteady flow

Influence of other factors on CS rheology. As already demonstrated, CS possess complex and even unique rheological properties. However, the list of factors influencing the rheological characteristics of CS is not limited to the solid phase content of the suspension and its particle size distribution.

The pH value, which is associated with the electric potential that enhances particle agglomeration, also influences viscosity. Long-term storage leads to oxidation of the coal, an increase in O_2 content and acidity (a decrease in pH), which leads to an increase in the viscosity of WCS (Fig. 3.8*a*).

A similar effect observed with prolonged exposure of coal to air. It follows that CS obtained from oxidized coal will have degraded viscosity properties. The viscosity of CS can reduced without reducing the solid phase concentration by alkalizing the environment or by adding surfactants, primarily with negative ions (this issue will discuss separately below).

A positive effect can also be achieved by washing the coal (Fig. 3.8*b*), which allows for an increase in the pH value. With prolonged circulation of WCS in the fuel system, a change in viscosity observed: first, the viscosity decreases, and after several hours of pumping, it begins to increase (Fig. 3.8*c*) [14].

Clearly, particle dispersion occurs at the first stage. The increase in viscosity is possibly due to more rapid oxidation and absorption of the liquid carrier by the particles, as well as a decrease in the average particle size due to their fragmentation.

To the already mentioned factors that influence the rheological properties of WCS, one can also add the anomalous dependence of normal viscosity on temperature up until the suspension completely solidifies.

This behavior of WCS first observed in studies by D.L. Siebers and T.M. Dyer [71] in 1986. When the suspension reached the temperature of the experimental chamber walls (147 °C), it solidified directly in the nozzle sprayer.

The same phenomenon subsequently noted in a study of the rheological properties of WCS conducted at the Bauman Moscow State Technical University. As the temperature increased, the viscosity of WCS initially decreased, but upon reaching 100 °C, it began to increase again (Fig. 3.9).

Based on the processing of experimental data, an expression proposed for an approximate estimate of the dynamic viscosity up to temperatures of 120...130°C [14]:

$$\overline{\eta} = \eta_t / \eta_{20} = 0{,}32 + 1{,}0625 \times 10^{-4} \times (t - 100)^2 .$$

The mechanism of such WCS behaviour remains unclear to date.

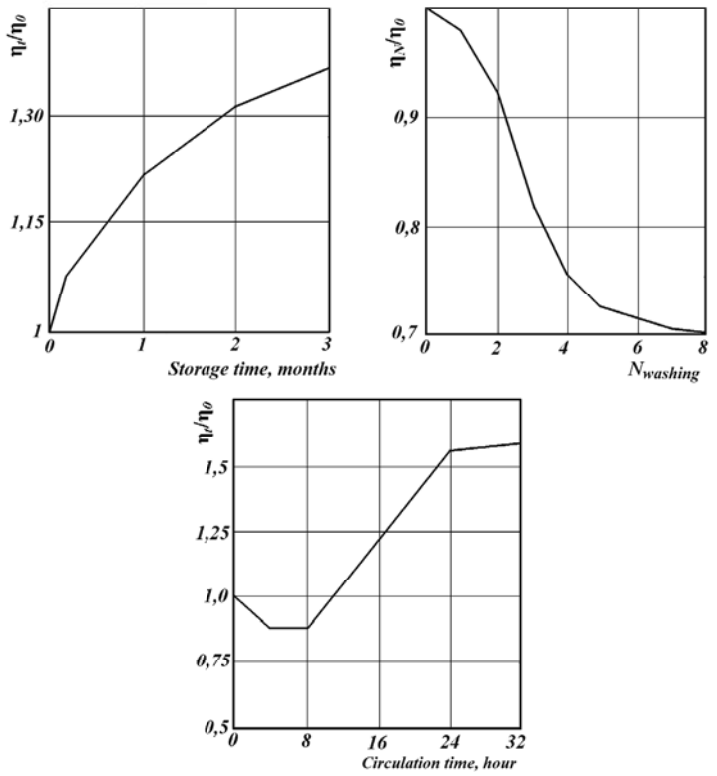

Fig. 3.8. *a* – increase in WCS viscosity depending on storage time; *b* – decrease in WCS viscosity during washing of the original fuel; *c* – change in viscosity during WCS circulation

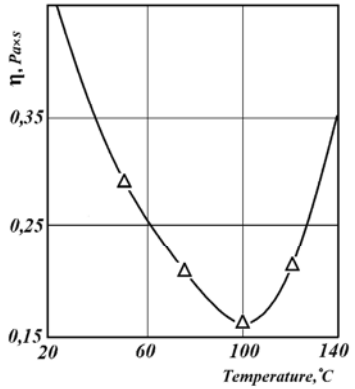

Fig. 3.9. Change in WCS viscosity depending on temperature [14]

3.5. Use of fuel-coal suspensions.

At the initial stage of experiments on the use of suspensions, mixtures produced because of diesel fuel and coal dust, which had undergone special purification, considered as the most promising fuels for internal combustion engines. It assumed that the diesel fuel included in the suspension would ensure its effective self-ignition. The attractiveness of FCS was that they use solid fuels with a high calorific value and high activation energy. However, the results of most studies indicate that the combustion nature of FCS does not agree well with the characteristics of the thermodynamic cycle of a piston internal combustion engine. When using FCS, the effective power and efficiency of the engine sharply reduced. Despite earlier injection, later ignition and slower diffusion combustion observed. The latter is clearly visible in Fig. 3.10, which shows the change in pressure and heat release rate for DF and FCS [9]. Table 3.4 presents individual results of swirl-chamber engine tests on DF and FCS.

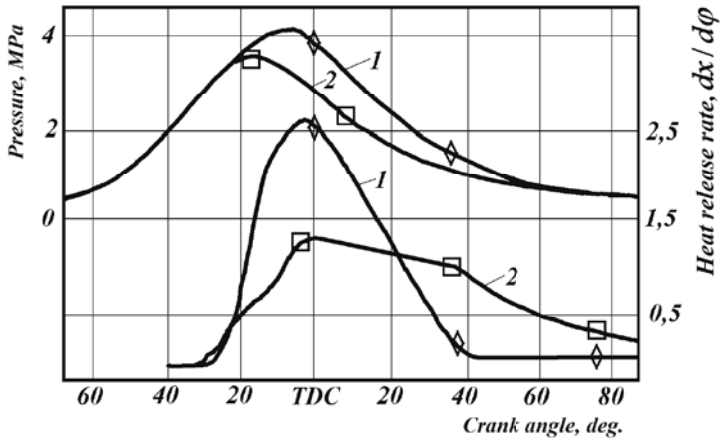

Fig. 3.10. Heat generation characteristics in a vortex-chamber engine with dimensions D/S = 85/110 mm in full load mode with a rotation speed of n = 1500 min^{-1}. 1 – when operating on DF; 2 – when operating on FCS

Even under the highly turbulent airflow conditions of a swirl-chamber engine, the combustion rate is insufficient to ensure efficient combustion of pulverized coal. Using FCS dramatically reduces the diesel engine's effective power (from 4.4 to 2.8 kW in this case) and its effective efficiency (from 0.31 to 0.19). Despite optimized, earlier fuel injection, delayed ignition and slower diffusion combustion observed. This explained by the significantly different combustion times of the liquid carrier and solid particles. As a

result, the combustion process greatly extended, and as consequence, after burning of the coal dust occurs along the expansion line. Furthermore, adjusting the onset of heat release by varying the injection angle of the fuel suspension proved ineffective in most cases.

Table 3.4.

Comparison of test results of a vortex chamber diesel engine with dimensions D/S = 85/110 mm on DF and FCS in full load mode at n = 1500 min^{-1}

Fuel	DF	FCS
Coal dust volume content, %	—	50
Optimized injection advance (geometric), deg	25	31
Engine inlet air temperature, °C	25.0	25.0
Injection start pressure, MPa	13	13
Power, kW	4.430	2.770
Mean effective pressure, MPa	0.557	0.348
Effective efficiency	0.3070	0.1917
Mean indicated pressure, MPa	0.700	0.524
Indicated efficiency	0.3859	0.2891
Excess air ratio	1.185	1.195
Maximum cycle pressure, MPa	4.110	3.540
Maximum injection pressure, MPa	18.55	16.86
Ignition delay, deg	6.430	8.200

Experimental and theoretical studies have shown that to reduce combustion time differences, the size of carbon particles should be as small as possible. For high-speed diesel engines, this should be in the range of 5…10 μm. However, reducing particle size, on the one hand, leads to increased energy consumption for grinding them, and on the other, to a significant increase in suspension viscosity. The latter circumstance leads to deterioration in the performance of the fuel injection system and a decrease in spraying quality, which further reduces fuel efficiency. Fuel burnout during FCS combustion is also affected by the fact that after evaporation of the liquid carrier, carbon particles can form agglomerates; the smaller the particle size, the more prone they are to agglomeration.

The above conclusions summarize the results of a number of studies and indicate that the use of FCS in piston internal combustion engines is associated with a number of difficulties, for which a satisfactory solution not yet been found. Low-speed engines are best suited for FCS operation. This demonstrated by tests conducted by Sulzer. The combustion time in these engines is sufficient for the almost complete burnout of carbon particles. Clearly, the future prospects for FCS applications lie specifically with engines of this type.

Some studies used carbon black as the starting solid fuel for FCS. It has a relatively high calorific value (33,494 kJ/kg), and its particle size ranges from

0.5 to 1.0 μm and contains virtually no mineral impurities. It assumed that a suspension obtained from it would not have an abrasive effect on fuel injection system components, and the small particle size would ensure their efficient burnout. In practice, these assumptions largely confirmed; however, due to agglomeration, the actual particle size entering the combustion chamber was an order of magnitude larger. The use of carbon black resulted in a more significant increase in solution viscosity than the use of carbon particles, even at elevated temperatures. Therefore, for normal engine operation, the soot content in the suspension cannot exceed 5…20%. Such a low solid fuel concentration significantly reduces the economic benefits of its use. Furthermore, soot is not a natural fuel, and its use is not an effective solution to the problem of expanding the internal combustion engine fuel base.

Fig. 3.11 shows the viscosity-temperature characteristics of a suspension of soot and DF depending on the weight filling of the liquid solution [46].

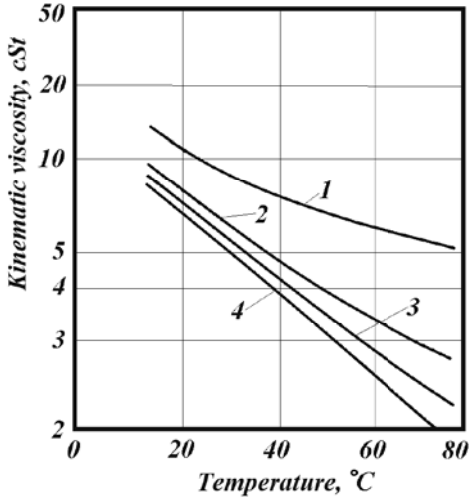

Fig. 3.11. Viscosity-temperature characteristics of the soot suspension and DF: 1, 2, 3 – weight content of soot 20%, 10%, 5%, respectively; 4 – DF

Among the synthetic liquid fuels that can use as a liquid carrier for FCS, the most interesting is a mixture produced by liquefying brown coal. Currently developed processes for coal liquefaction followed by solvent purification of the resulting products, as well as mixtures based on these products, are the most promising for industrial-scale production. In this processing technology, coal partially dissolved in a hydrocarbon mixture

consisting of aromatic compounds. This fuel marketed in the United States as SRC-II (Solvent Refined Coal) and used as a boiler fuel.

The SRC process originally developed by Spencer Chemical and used to produce ash-free pulverized coal concentrate with minimal sulfur content. This process has subsequently undergone significant modifications, resulting in two distinctly different process methods, known as the SRC-I and SRC-II processes, respectively.

The SRC-II process differs from the SRC-I process in a number of ways. The fundamental difference between them is that the final product obtained by the SPC-II process is a mixture of mainly liquid fuels. The main product obtained by the SRC-II process is a distillate liquid fuel and is a mixture of two cuts known as «middle distillate» and «heavy distillate». The boiling point ranges are 175...290°C for the middle distillate and 290...455°C for the heavy distillate. The composition and combustion characteristics of this synthetic liquid fuel depend on the relative amounts of middle and heavy distillates used to obtain the SRC fuel [45]. The characteristics of this fuel and its elemental composition are given in Tables 3.2 and 3.3. The cetane number of SRC-II is about 22 units. In a number of experiments, SRC-II was used in a mixture with lignite dust with a particle size of no more than 2 μm. The mass filling of the liquid carrier with solid fuel particles in all cases did not exceed 15%.

Overall, studies using SRC-II yielded encouraging results. However, the high viscosity of SRC-II requires significant modifications to the engine's combustion chamber fuel delivery system. To reduce viscosity during experiments, heating the suspension and mixing SRC-II with DF were used. The change in mixture viscosity as a function of temperature and DF amount is shown in Fig. 3.12. Viscosity at any ratio of combustible mixture components can be determined from the following equation:

$$log\ v = a\alpha + b,$$

where v – the kinematic viscosity (cSt); α – the ratio of the components of the combustible mixture (in percent); a and b are constants (for SRC-II and a mixture of light diesel fuel at 40°C, a = -3.35×10 and b = 0.545) [35].

Since SRC-II has a low cetin number, to achieve stable ignition it can used only in a mixture with diesel fuel or the combustion process can activated by injecting pilot diesel fuel.

The results of a number of studies have shown that the problem of using SRC-II-based suspensions has much in common with the problem of using heavy fuel oils. Consequently, such suspensions, produced by coal liquefaction, can used without any technical difficulties, but they are currently quite expensive.

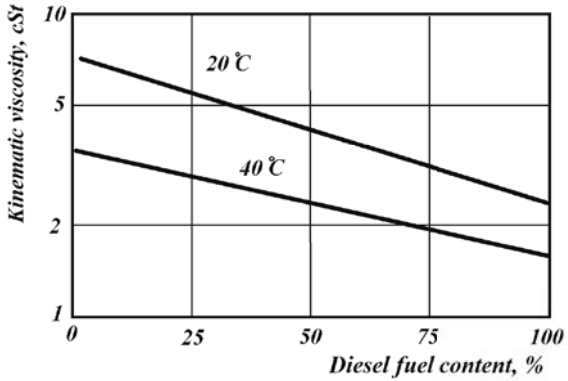

Fig. 3.12. Change in viscosity of a mixture of SRC-II and DF depending on temperature and DF concentration

3.6. Use of water-coal suspensions.

As already, noted using water as a carrier significantly reduces the cost of coal-based motor fuels completely eliminates the use of petroleum products for these purposes. Therefore, the use of WCS is the most promising direction for expanding the fuel base for piston engines. Therefore, over the past several decades, the primary efforts of solid-fuel internal combustion engine designers have focused on creating an engine capable of running on this type of fuel.

Like most other suspensions, WCS is not a simple mixture of coal and water. In such a mixture, the solid phase and water lose their normal properties. To prepare the suspension, the coal mass is finely ground – the average particle size of the coal is 1…10 μm. When atomized, the surface tension of water in the ground coal mass is so strong that it becomes virtually impossible to separate the solid particles from the water elements in the resulting dispersed colloidal mixture. Therefore, when atomized, WCS produces large droplets that have a nearly uniform structure.

Fig. 3.13 shows a micrograph of Otisca's WCS, containing 50% coal and 50% water by weight. The photograph shows that the fuel particles have an irregular, angular shape with a few exposed mineral grains.

The most important properties of WCS are a coal dust content of at least 50% by weight; low ash content; pseudoplastic rheology at high shear rates; compatibility with DF; storage stability; and reliable mixing. Therefore, for internal combustion engines, coal preparation is as necessary as oil refining, namely: particle size reduction to 5...20 μm, deashing to a level of no more than 1%, and selection of coal grade, deposit, and additives.

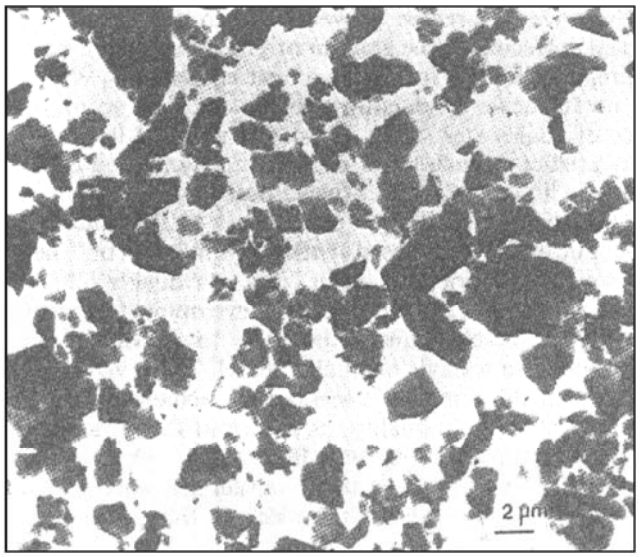

Fig. 3.13. High magnification image of WCS (average particle size 3.0 μm) [63]

Low ash content of the fuel must ensure to minimize the amount of abrasive material introduced into the working cylinder with the fuel. The requirement for pseudoplastic rheology is dictated by the need to achieve optimal WCS spraying parameters. Compatibility with DF dictated by the fact that, to avoid jamming of precision fuel injection equipment pairs, the engine must started and stopped using DF. As a result, it is periodically necessary to run the engine on a mixture of WCS and DF for some time until one fuel completely displaced by the other. When transporting and storing WCS, the most important requirement is suspension stability, which in turn depends on the transportation method. When transporting WCS in separate containers, the suspension can separate, necessitating premixing the fuel immediately before combustion in the engine.

The ash content of WCS depends on the type of original fuel and its enrichment method. The rheology of the suspension, its compatibility with liquid fuel, and its storage stability are determined primarily by the water content and, to a lesser extent, by the particle size distribution, particle size, and coal type (see Section 3.4.2).

WCS from various manufacturers tested as part of a US Department of Energy program. Their characteristics presented in Tables 3.5-3.8. Data from different researchers differ significantly in the structure of the parameters reported. They reproduced below as published.

Table 3.5.

Characteristics of the WCS used in testing the Sulzer 1RSA76 low-speed engine

WCS Characteristics	WCS type (coal grade)			
	Otisca (East Kentucky, bituminous)	**Resource** (Virginia, Wentz Mine, Wise County)	**AMAX** finely dispersed (Indiana, No. 7)	**AMAX** coarse (Indiana No. 7)
Coal Content (dry basis), %	48	46.5…48.5	50.1	54.2
Moisture, %	49.5	50.5…52.0	48.2	43.6
Additives, %	2.5	1.5	1.7	2.2
Particle Size, μm max (98% of particles)	19.5	14.5	32	47
Average Particle Size, μm	6.9	4.8	10.2	16.3
Net Heating Value, MJ/kg	14.8…15.16	14.4…15.11	15.11…15.7	16.96
Technical analysis data of coal on dry basis,%				
Ash content, %	0.05	0.78…1.1	0.53	0.52…0.60
Al_2O_3 concentration in ash, %	23.2	10.8	12.5	10.1
SiO_2 concentration in ash, %	16.0	36.9	36.6	50.9
Sulfur, %	0.74	0.84	0.78	0.98
Volatiles, %	41.2	38.0	38.2	40.5
Net heating value of dry coal, MJ/kg	31.4…32.23	33	32.32	32.32

Table 3.6.

Characteristics of the WCS used in testing the Cooper-Bessemer J-1 medium-speed engine

WCS Characteristics	**AMAX** finely dispersed	**AMAX** coarsely dispersed
Coal content (dry mass), %	53	53
Ash content, dry mass, %	0.20	0.25
Net heating value, MJ/kg	16.9	16.9
Viscosity at 38°C, cP	180	180
Particle size distribution of coal, % (by weight)	μm	μm
98	65	45
90	38	27
50	11	8
13	2	1
Technical analysis data of coal on dry mass basis, %		
Ash	0.4	0.5
Volatiles	41.5	40.9
Fixed carbon	58.1	58.6
Sulfur	1.1	1.1
Type of coal	Bituminous, «Splint» pcs. Kentucky	

Table 3.7.

Characteristics of the WCS used in testing the General Electric 7FDL engine

WCS Characteristics	**Otisca**	**Otisca**
Coal content (dry basis), %	47…49	47…49
Additives, %	2.5	2.5
Elemental analysis data, % (by weight)		
Carbon	88.59	86.15
Hydrogen	5.34	5.15
Nitrogen	2.08	1.26
Chlorine	0.18	0.11
Oxygen	7.58	6.88
Technical analysis data of coal on a dry basis		
Ash, %	1.01	0.36
Volatiles, %	41.5	40.9
Fixed carbon, %	58.1	58.6
Sulfur, %	1.01	0.36
Average particle size, μm	4.63	2.88
High heating value, MJ	34.63	35.58
Coal deposit	pcs. Kentucky	New Zealand

Table 3.8.

Characteristics of the WCS used in testing the Electro-Motive Division EMD 567B engine

WCS Characteristics	**AMAX**
Coal content (dry basis), %	50.0
Preservative (formaldehyde), %	0.10
Surfactant, %	1.50
Stabilizer, %	0.03
Water, %	48.37
Caloric value	
Gross, MJ/kg	17.4
Net, MJ/kg	15.5
Average particle size (up to 95%), μm	I5
Ash content (by weight), %	0.5
Viscosity, cPs	40
Complete elemental analysis, %	
Carbon	85.4
Hydrogen	3.22
Sulfur	0.86
Nitrogen	1.30
Oxygen	9.20
Technical analysis data of coal on a dry basis, %	
Ash	1.01
Volatile Components	34.5
Fixed Carbon	64.5

Unlike FCS, the only combustible component of WCS is coal dust, so the combustion time is determined solely by the burnout time of the solid fuel particles. The presence of water in the suspension increases the self-ignition delay period. Thus, with a water content of 50…55% by weight, self-ignition of the suspension occurs with a delay period of 20…45°C, exceeding that of diesel fuel. This is due to the time it takes for the water completely evaporates. Some of the physical heat of the charge is expended on the phase transition of water from a liquid to a vapor, resulting in a significant decrease in the charge temperature. For this reason, stable self-ignition of the suspension is possible only if the charge temperature in the cylinder is at least 900...1000 K by the end of the delay period. If the required temperature cannot achieved by the end of compression, effective ignition of the WCS can achieved injecting a pilot DF into the combustion chamber.

Despite the relatively long ignition delay, the combustion rate of WCS is significantly higher than that of FCS and DF. This pattern persists even when the combustion process is intensified using pilot fuel injected into the cylinder. Fig. 3.14 shows the heat release characteristics obtained for DF, WCS, and FCS in a high-speed swirl-chamber engine [63].

The high heat release rate explained by the fact that the long ignition delay associated with water evaporation increases the time allotted for mixing the fuel with the air charge. By the time of ignition, the dust-coal particles uniformly distributed throughout the air charge, creating the most favorable conditions for their interaction with oxygen. The rapid combustion of WCS allows for the simple optimization of heat delivery to the working fluid by selecting the optimal injection advance angle. Below we will consider some aspects that influence both the characteristics of the WCS itself and the efficiency of its combustion in an internal combustion engine.

3.6.1. Influence of source fuel characteristics on WCS properties. The properties of WCS are significantly affected the characteristics of the feedstock fuel used in its manufacture. However, any consistent patterns either absent or poorly understood. A clear example of the influence of the feedstock fuel type on engine performance provided the results of tests conducted by General Electric [52].

During the studies, the injection system parameters optimized for operation with suspension made from coal mined in Kentucky. The suspension supplied by Otisca (see Table 3.6). Since the technology used by the company did not allow the ash content of the coal to reduce below 1%, coal mined in New Zealand purchased for the experiments, which could purified to 0.4% ash using the same technology. The technical characteristics and elemental composition of both coals differed only slightly. However,

tests conducted on WCS with New Zealand coal showed a significant deterioration in engine performance. This deterioration was observed both during combustion activation by pilot fuel injection and during self-ignition. The curves of pressure change in the working cylinder, as well as the rate of heat release when using two types of initial fuel shown in Fig. 3.15-3.16, the main test results given in Table 3.9.

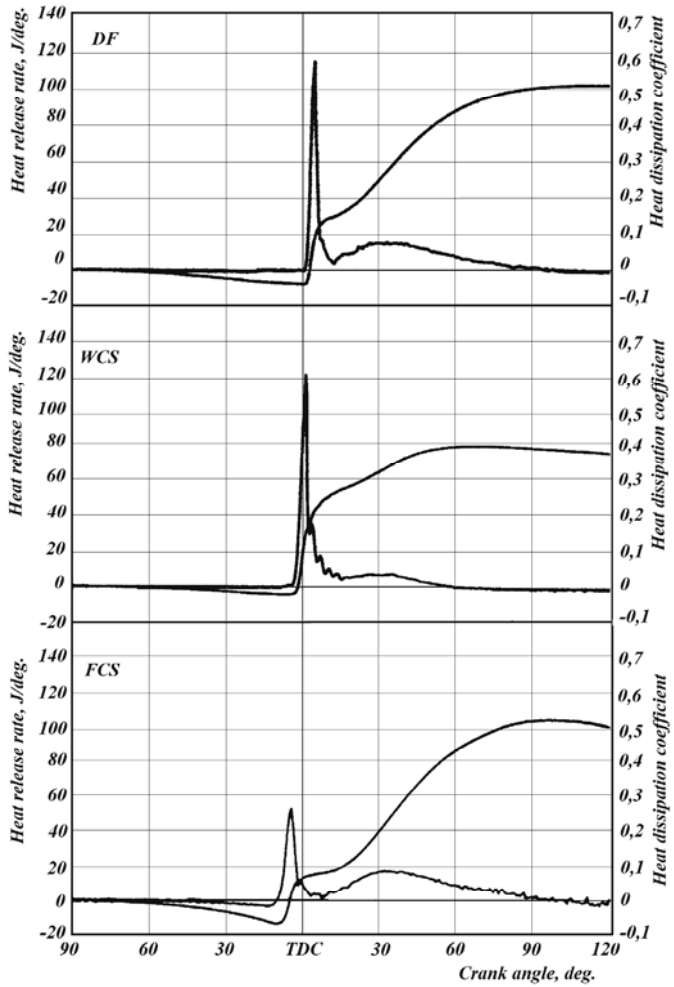

Fig. 3.14. Speed and heat release coefficient in the cylinder of a vortex-chamber engine with cylinder dimensions D/S = 96.5×95.2 mm in full load mode at a rotation speed of n = 900 min^{-1}

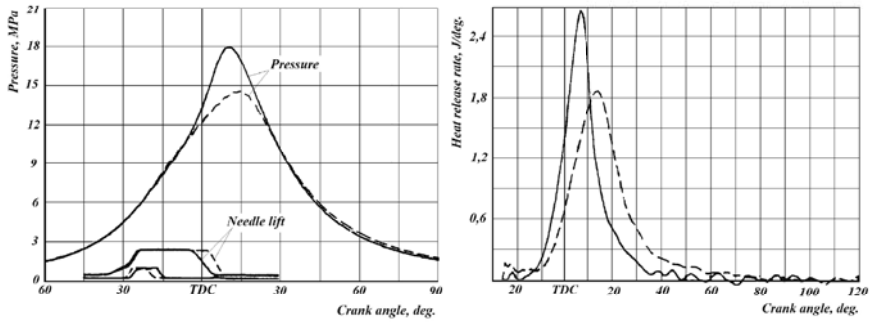

Fig. 3.15. Change in pressure and heat release rate in the cylinder of the 7FDL engine for two types of initial fuel (n=1050 min^{-1}, p_a=344 kPa, pilot ignition). —— WCS from Kentucky coal; – – – – WCS from New Zealand coal

Table 3.9.

Comparison of 7FDL engine test results on WCS made from different feedstock fuels

Type of coal	Burnout rate, %	Specific heat consumption, kJ/(kW×h)	p_{max}, MPa
Pilot fuel 3%			
Kentucky coal	91.2	8696	18.0
New Zealand coal	82.8	10153	14.6
Self-ignition			
Kentucky coal	92.1	9044	15.9
New Zealand coal	76.6	12437	11.0

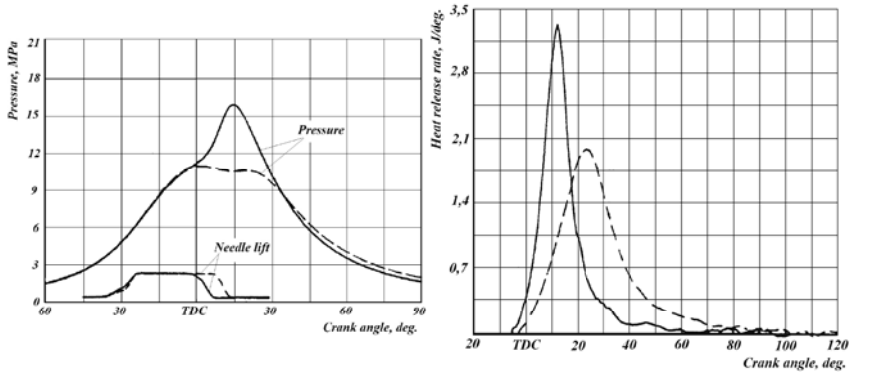

Fig. 3.16. Change in pressure and heat release rate in the 7FDL engine cylinder for two types of feedstock fuel (n=1050 min^{-1}, p_a=362 kPa, self-ignition). —— WCS obtained from Kentucky coal; - - - – WCS obtained from New Zealand coal

The objective cause of such deterioration in engine performance could not establish during the research; clearly, this issue requires further, study that is more detailed. Subsequently, by using an electronically controlled common rail fuel injection system, selecting the injection advance angles for the main and pilot fuel, as well as optimizing other operating parameters and introducing design modifications (for example, changing the nozzle orifice diameter), it was possible to achieve acceptable engine performance.

The characteristics of the WCS tested in the final stage of research conducted by General Electric, and their burnout efficiency after optimization of the operating processes, presented in Table 3.10 [72].

Table 3.10.

List of tested fuels and their combustion results

Supplier	Place of extraction of the original coal	Type of coal	Cleaning method	Average size, μm	Ash, %	Combustion efficiency, %
OTISCA	Kentucky	Bituminous	Physical	4.6	0.7	99.2
OTISCA	Kentucky	Bituminous	Physical	4.8	0.8	98.8
OTISCA	Kentucky	Bituminous	Physical	3.1	0.7	98.7
OTISCA	Kentucky	Bituminous	Physical	3.2	0.7	99.2
OTISCA	Pennsylvania	Bituminous	Physical	2.5	1.7	98.7
UNDERC	Wyoming	Subbituminosis.	Chemical	13.9	2.8	99.5
UNDERC	Wyoming	Subbituminosis.	Phys.+Chem.	14.7	2.1	99.0
UNDERC	Wyoming	Subbituminosis.	Chem.	14.9	2.8	99.2
AMAX	Kentucky	Bituminous	Phys.	8.2	2.5	97.7

3.6.2. Effect of particle size on the combustion behaviour of WCS. As already shown in Section 3.4.2, the particle sizes the suspension significantly affect the efficiency of the fuel injection system. However, particle sizes also have an equally significant effect on the combustion characteristics of the WCS. It is clear that the particle size capable of completely burning out in the engine's working space depends significantly on the amount of time allotted for the combustion process. In order to determine the maximum particle size capable of completely burning out in engines with different speeds, Caton and Rosegay conducted a theoretical study in which engine characteristics were calculated relative to particle sizes in 5 μm increments until engine performance began to deteriorate [68]. This resulted in calculated values for the indicated efficiency, injection advance angle, and mass coefficient of incomplete combustion of fuel as a function of the initial particle diameter for low-, medium-, and high-speed engines (Fig. 3.17).

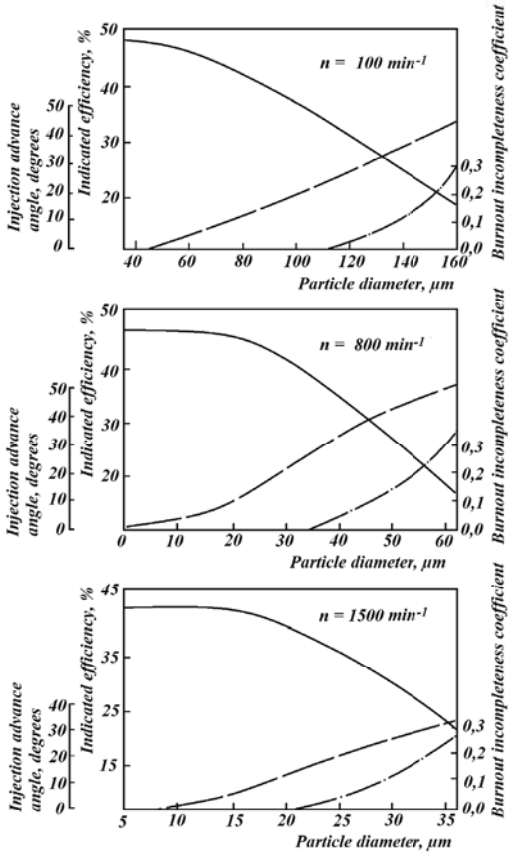

Fig. 3.17. Effect of particle size on indicated efficiency, injection advance angle and combustion incompleteness coefficient for low-, medium- and high-speed engines at 80% load. —— indicated efficiency; – – injection advance angle; – · – combustion incompleteness coefficient

In all cases, decreasing particle size resulted in an increase in the indicated efficiency. For each engine class, this trend persisted only up to a certain initial particle size. Below this value, particle size had virtually no effect on the calculated engine efficiency. In this case, particle burnout occurred within 1° of rotation angle, so fuel combustion time was determined primarily by the duration of fuel delivery to the working cylinder. The particle size at which the combustion rate and particle delivery rate are equal can be considered optimal for a given engine type. Using smaller particles in this engine class offers no thermodynamic advantages.

The calculated value of the maximum particle sizes for each engine class presented in Table 3.11.

Table 3.11.

Maximum particle size that provides optimum combustion characteristics for coal fuel in an engine [68]

Engine Class	Rotation speed, min^{-1}	η_{max}	Particle diameter for η_{max}
Low-Speed	100	47%	45 μm
Medium-Speed	750	47%	20 μm
High-Speed	1500	44%	15 μm

In addition to the lack of thermodynamic benefit from reducing particle size below a specified value, reducing their average size significantly alters the rheological properties of the WCS.

As a result, fuel viscosity increases significantly, which, in turn, disrupts the normal operation of the fuel injection system, affecting engine performance.

The curves shown in Fig. 3.18 reflect the change in the rate of heat release in the engine's working cylinder when using two types of WCS obtained from the same feedstock fuel and differing only in the average particle size of their constituents.

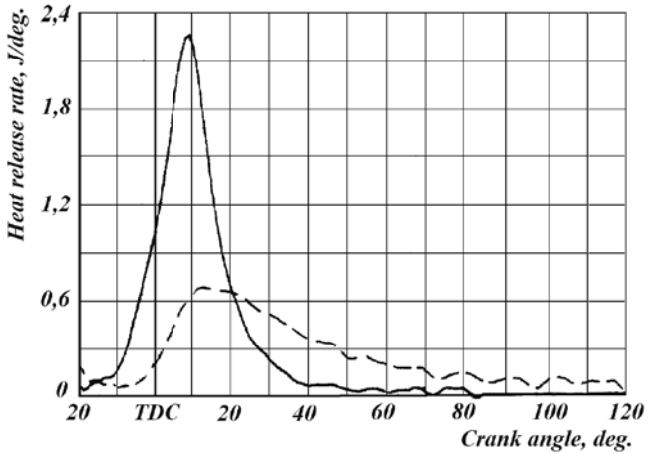

Fig. 3.18. Heat release rate in the 7DFL engine using WCS with different particle sizes (n= 1050 min^{-1}, p_a=326 kPa)

Both fuels supplied by Otisca and tested by General Electric. The characteristics of both suspensions presented in Table 3.12. The suspension for which the fuel system optimized designated as WCS No 1, while the suspension with a reduced average particle size designated as WCS No 2.

The data presented shows that with a 26% reduction in average particle size, the viscosity of the suspension increases by approximately 3.8 times. This leads to significant pressure losses in the supply line, resulting in the fuel pressure delivered to the injector being significantly lower than the pressure generated by the fuel pump.

Table 3.12.

Comparison of the performance of WCS with different average particle sizes made from pcs. Kentucky coal

Suspension	Particle size, μm	Ash,%	Viscosity, cPz	Solid particles, %
WCS No.1	4.63	1.01	123	50.1
WCS No.2	3.41	0.79	463	49.2

The nature of the change in pressure at the pump outlet and pressure in the sprayer for WCS No. 1 and WCS No. 2 shown in Fig. 3.19.

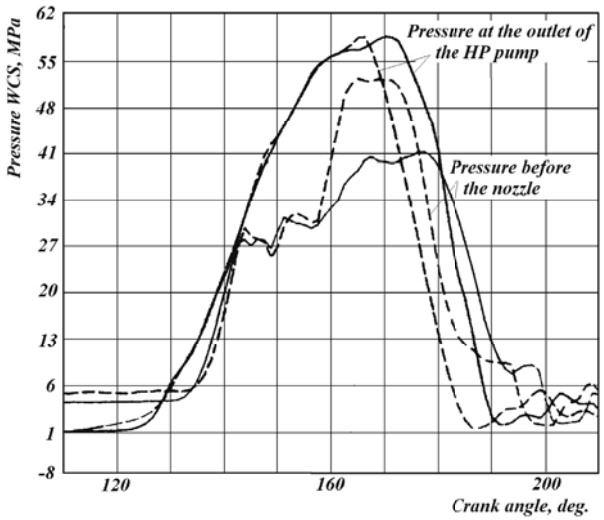

Fig. 3.19. Pressure changes at the outlet of the fuel pump and in the nozzle. - - - WCS No.1; —— WCS No. 2

While the maximum pressure developed by the fuel pump was approximately the same in both cases, at around 58 MPa, the pressure directly in the injector for WCS No.1 was approximately 52.2 MPa, and for WCS No.2 – 41 MPa. The engine test results for both suspension types presented in Table 3.13. To achieve stable injection, the mass concentration of carbon particles in the WCS had to reduce to 46.1%.

Table 3.13.

Comparison of 7FDL engine test results on WCS made from pcs. Kentucky coals with different average particle sizes

Suspension	Power, kW	Burnout rate, %	Specific heat consumption, kJ/(kWh)	p_{max}, MPa
WCS No.1	177.8	85.5	9320	16.4
WCS No.2	109.8	53.0	18925	11.5

From the above, it follows that attempts to achieve maximum combustion speeds by reducing particle size often result in deterioration of the injection system's performance, which, in turn, worsens engine performance. Thus, reducing particle size does not always improve combustion. Clearly, under certain conditions, better combustion performance can achieve by using larger particles.

3.6.3. Influence of source fuel parameters on WCS flammability. Studies of water-coal suspension combustion in internal combustion engines have shown that after water evaporation, combustion begins and occurs in the gas phase around the coal particle. For this reason, solid fuels containing higher amounts of volatile components ignite better and burn faster. Their content varies greatly depending on the type of solid fuel, its source, primary processing method, storage time, and other factors. Based on their volatile content, the following fuels ranked peat (volatile yield upon heating is approximately 75%); brown coal (approximately 50%); hard coal (approximately 25…30%); and anthracite (approximately 10%). Therefore, when using WCS, relying on high-calorific fuels is highly problematic. Their low volatile content virtually eliminates their spontaneous combustion. Based on the volatile content-calorific value ratio, brown coal is the best fuel for WCS production. Stable self-ignition of the WCS can achieve by increasing the charge temperature before the injection of the suspension. This can achieve by preheating the incoming air, increasing the compression ratio, using combustion chamber insulation, or installing glow plugs. Pre-activating the combustion process with an external open flame source or injecting pilot diesel fuel also ensures reliable and intense combustion of the suspension, especially when injecting both fuels sequentially through a common injector.

3.6.4. Use of additives to improve WCS performance. The use of various additives to WCS offers a significant opportunity to improve their rheological and performance properties.

By adding additives, the following key characteristics of WCS can significantly improve:

- increase the physical stability of WCS and reduce the tendency of the suspension to separate, especially during long-term storage;

- reduce viscosity with increased weight loading of the liquid solution with carbon particles;
- impart lubricating properties to the solution to improve the operating conditions of fuel injection equipment;
- reduce surface tension to improve fuel spraying;
- increase the self-ignition of WCS;
- lower the freezing point of WCS;
- reduce the corrosive effects of WCS on tanks and engine components.

The addition of various dispersants allows for a significant increase in the concentration of carbon particles in the liquid solution while maintaining acceptable viscosity values. As a result, the overall calorific value of the suspension increases significantly. There are two main causes of suspension stratification during long-term storage: gravitational forces and the agglomeration of coal particles into larger formations. Agglomeration intensifies the gravitational forces acting on the particles. In addition to reducing physical stability, particle agglomeration degrades the combustion characteristics of WCS, as the agglomerates burn as a single, large particle.

To reduce the tendency of coal particles to agglomerate, additives used to create a protective shell around the coal mass, preventing direct contact between individual particles. A US-produced additive, brand name TRITON X-114, has been used in several studies as such an additive. Pfizer Flocon 4800C Xanthan, a biopolymer stabilizer, added to WCS at a concentration of 0.5% to stabilize suspended particles. Bentonite also used in domestic practice to stabilize WCS [10, 59]. The effectiveness of some stabilizers is so high that suspensions can be stored for very long periods without delamination. For example, a WCS based on brown coal developed by the Research Institute of Hydrotruboprovod with bentonite stabilizer (0.5%) and C-3 plasticizer from Perm Pulp and Paper Mill (0.9%) showed no signs of delamination for a month [10].

To impart lubricating properties to the liquid solution, in some studies, the water-soluble lubricant UCON 50-HB-5100 added to the suspension; its primary purpose was to prevent the spray needle from sticking [52].

The effect of various additives on the dynamic surface tension of WCS studied Kihm K. D. and Deignan P. [59]. They concluded that the dynamic surface tension for WCS containing various additives could significantly higher than the corresponding static surface tension. They explained this by the fact that at high shear rates, the time required the surfactant to migrate to the interface is insufficient. This assumption supported by the fact that the difference between the static and dynamic surface tensions increases at higher shear rates.

Five different surfactant additives tested in the experiments. Studies have shown that, depending on specific conditions, all of these can used to reduce the surface tension of WCS. The surface-active additive SF2068 used in a number of experiments.

The primary additive used to enhance the self-ignition of WCS is DF. Some studies have shown that adding a few percent of DF to the suspension is more effective than injecting the same amount of fuel through a separate injector. The addition of DF also has a definite effect on the rheology of WCS. The introduction of DF No. 2 at a rate of 10% typically transforms even a highly plastic suspension into a pseudoplastic one [65].

Methanol has considered as an additive to lower the freezing point of WCS. It has found that adding 15% methyl alcohol to WCS reduces the freezing point to -23°C.

Formaldehydes used as preservative additives to reduce the harmful effects of WCS on metals. The optimal concentrations of additives required to impart the desired properties to WCS depend significantly on the concentration and size of the coal particles and the type of feedstock fuel. Some additives absorbed by the coal mass during storage, altering the suspension's properties. The fundamental physics of WCS spraying currently poorly understood. There is a weak theoretical basis for determining droplet size based on suspension properties. Optimizing WCS properties through the introduction of additives requires further research.

3.6.5. Storage and transportation of fuel. WCS, despite various types of additives, always remain unstable systems, if the viscosity of the liquid is relatively low and the total volume of particles is less than the volume at which the entire space of the liquid filled with contacting particles. In other words, if the suspension has the characteristics of a liquid of acceptable viscosity, the difference in density between water and carbon particles will always lead to sedimentation of the latter. This clearly seen in Table 3.14, which shows the relationships between the density changes for WCS without stabilizers with different concentrations of the solid phase. These relationships obtained from measurements in the upper and lower layers. Measurements carried out in a 500-milliliter beaker after 7 days of storage at 18°C [10].

Table 3.14.

Delamination of WCS without stabilizers in 7 days.

$\bar{C}_m$	0.18	0.51	0.77	0.87	1.0
$\Delta\rho/\rho_o$	0.145	0.13	0.043	0.01	0.0

Therefore, WCS storage systems must include special devices to maintain WCS in suspension.

Piston positive displacement pumps typically used to pump WCS from the tank to the engine and for tank recirculation [69]. WCS recirculation in storage tanks can accomplished either by pumping the suspension from the upper to the lower level or by aerating the entire tank volume.

The most common concept for long-term WCS storage in tanks is based on periodic mixing with suspension intake from the upper part of the tank using a floating intake and delivery to the lower part of the tank through a special manifold, creating two large counter-rotating fluid circulations. The flows must cover the entire lower part of the tank to avoid the formation of «dead zones» where solid particles can settle. The floating intake ensures the intake of suspension with the lowest particle concentration, regardless of the fuel level in the tank. In dimensionless form, the optimal flow condition can express as follows:

$$R_e \times H = 5{,}7,$$

Where the Reynolds number (R_e) is determined based on the tank diameter and the flow velocity at the outlet of the recirculation manifold and H is the ratio of the manifold inlet diameter to the tank diameter.

Piping systems must have smooth internal surfaces without abrupt volumetric changes or changes in flow direction. When designing piping systems, avoid using components that promote the formation of recirculation zones and volumes in which flow velocities become very low, as this can lead to particle deposition. Piping systems must also allow for flushing with water or another clean liquid.

3.6.6. Engine characteristics when running on WCS. Several studies have noted that when operating on WCS, engine efficiency decreases by 2...15%, and its power decreases by 1...25% compared to operation on diesel fuel. This is explained by the lower calorific value of water-coal fuel, deterioration of the operating cycle parameters, an increase of 3...5% in mechanical losses associated with increased friction, and a number of other factors. The high rate of heat release during combustion of WCS leads to harsher engine operation. The degree of underburning of carbon particles when using WCS is approximately 0.5...5%, which is an order of magnitude higher than the same parameter for DF. Moreover, the type of original coal fuel has a significant impact on the degree of underburning. A decrease in combustion temperature due to water evaporation leads to a decrease in NO_x emissions with exhaust gases by approximately half, and to a reduction in CH and CO emissions. No changes in emissions noted when operating on a suspension with fine or coarse coal dust. Due to high particulate matter emissions and increasing environmental performance requirements for engines, advanced installations must be equipped with particle capture and

exhaust gas-cleaning systems. The latter requirement somewhat increases the cost of both the installation itself and its operation.

3.6.7. WCS filtering. Cleaning is a separate issue when using both water- and coal-fuel suspensions. Some studies have shown that filter elements do not allow fuel particles to pass through, even if they are quite small. Standard filters become clogged within the first few hours of operation, even when filtering suspensions that use soot as a filler. Moreover, soot particles completely settle on the filters. Therefore, a fundamentally new suspension cleaning system is required to effectively protect fuel system components from mechanical impurities.

3.7. Water-methanol-coal suspensions (WMCS).

Methanol is a less studied carrier for coal suspensions used in internal combustion engines. The few attempts to use methyl alcohol have shown that using pure methanol presents a number of challenges. Its low boiling point (64.7°C) leads to rapid evaporation of the carrier, resulting in significant changes in the suspension properties during both storage and use. Methanol's poor lubricating properties lead to frequent sprayer seizures and rapid wear. In experiments [63], castor oil added to the methanol-coal suspension at a concentration of 5% to improve sprayer-operating conditions; however, the sprayer seizure rate remained unchanged. Therefore, subsequent experiments conducted with methanol mixed with water rather than pure methanol. The studies conducted in a swirl-chamber engine, which has two design variants: a standard version and one with a thermally insulated combustion chamber (Table 1.5). For both variants, power measured at full load at 900 and 1,500 min^{-1}. In addition to the water-methane-coal suspension, WCS, FCS, and DF tested under similar conditions.

The suspension compositions and initial fuel characteristics presented in Tables 3.15 and 3.16.

Fig. 3.20 shows the dependence of indicated power on suspension type and its test conditions.

In the standard version, at 900 min^{-1}, the engine did not operate at all on WMCS. In the insulated version, at 1,500 min^{-1}, it was not possible to record the characteristics due to frequent seizure of the nozzle needle.

The engine power output was significantly lower than when running on DF No. 2. This is despite the fact that the fuel injection characteristics optimized for operation with this type of suspension and, accordingly, were not optimal for DF. The power developed by the engine in both cases was almost the same, which indicates that there is no effect from the thermal insulation of the combustion chamber when using WMCS.

Table 3.15.

Composition of suspensions studied in a high-speed vortex chamber engine

Suspension type, its composition, and calorific value	Quantity
Water-coal suspension (CWS)	
Coal, %	50.0
Water, %	48.4
Surfactant SF2068, %	1.25
Formaldehyde, %	0.
Stabilizer, %	0.05
Calorific value, MJ/kg	16.3
Water-methanol-coal suspension (WMCS)	
Coal, %	50.0
Methanol, %	15.0
Water, %	35.0
Calorific value, MJ/kg	20.8
Coal-fuel suspension (CFS)	
Coal, %	50.0
Diesel fuel No. 2, %	49.0
Surfactant Span 80, %	1.0
Calorific value, MJ/kg	38.5

Table 3.16.

Characteristics of the original fuel

Technical coal analysis data on a dry basis, %	Quantity
Ash	1.0
Fixed carbon	61.60
Moisture	0.36
Volatile components	37.04
Elementary coal analysis data, % (by weight)	
Carbon	84.26
Hydrogen	5.44
Nitrogen	3.75
Sulfur	0.6
Oxygen	4.95
Ash	1.00
Gross calorific value, MJ/kg	35.12
Net calorific value, MJ/kg	33.92

The heat release diagram for WMCS in a thermally insulated engine showed Fig. 3.21. The maximum heat density for this fuel was the highest compared to the heat density from the combustion of other suspensions in a thermally insulated engine. Despite the high diffusion combustion rate of WMCS, the overall combustion efficiency was low.

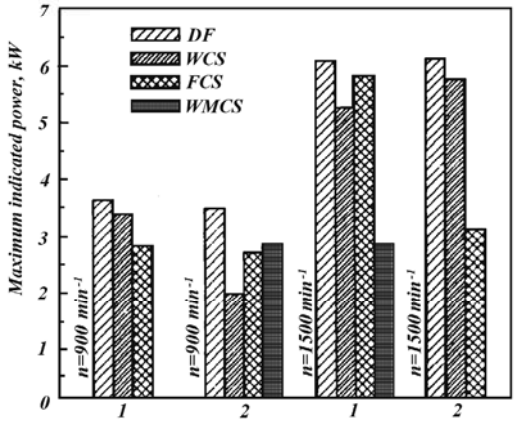

Fig. 3.20. Maximum indicated power obtained using various suspensions in a high-speed vortex-chamber engine with a cylinder size of D/S=96.5/95.2 mm (T_a=38°C). 1 – engine in a standard design; 2 – engine in a heat-insulated design

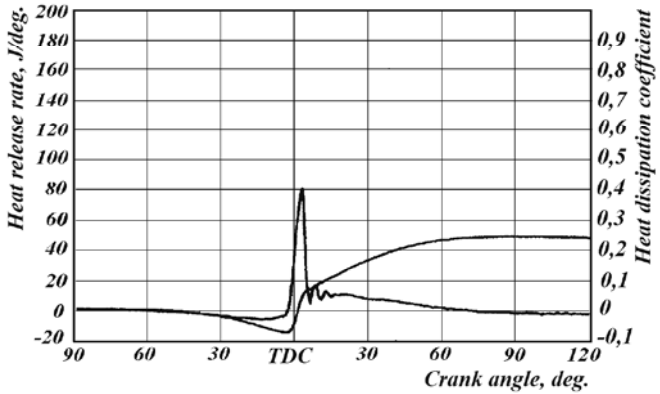

Fig. 3.21. Speed and heat release coefficient in the cylinder of a vortex chamber engine using WMCS (cylinder dimensions D/S= 96.5×95.2 mm, full load mode, rotation speed n=900 min^{-1})

Thus, the use of methanol as a carrier requires further research. Clearly, methanol is inferior to water in its characteristics as a carrier, and therefore, in the near future, it will likely use only as an additive to lower the freezing point of WCS. Unlike water, methanol is not a naturally occurring compound, so its cost will always be higher. Furthermore, methanol is quite toxic and aggressive to aluminium alloys, making operating costs higher than those of water do do.

To summarize the discussion in this chapter, the following conclusions can draw:

To summarize the discussion in this chapter, the following conclusions can draw:

- among the methods of burning solid fuel in an air charge environment, the most promising is the use of pulverized coal in various suspensions;
- the most promising suspensions are water-coal suspensions;
- optimizing the rheological characteristics of WCS, the operating process, and the parameters of the fuel injection equipment can significantly improve engine performance when operating on suspensions.

The main areas of optimization are:

– improving suspension spraying;

– refining the fuel jet directions, the start and duration of suspension and pilot diesel fuel injection;

– reducing the ignition delay period by increasing the charge temperature at the start of fuel injection to 1000 K by preheating the incoming air, increasing the compression ratio, or using combustion chamber insulation;

– increasing combustion speed by rationally organizing airflow in the combustion chamber.

Chapter 4.

Injection of suspensions into the engine combustion chamber.

4.1. Schematic and design solutions for fuel injection systems.

Early attempts to use coal suspensions as motor fuels were largely unsuccessful because researchers attempted to inject them into standard engine fuel delivery systems. However, these studies revealed that injecting suspensions into the combustion chamber of a piston engine has a number of unique characteristics that must considered when designing fuel delivery systems. These include:

- the abrasive action of both mineral impurities contained in the solid fuel and the carbon particles themselves, as it has been established that even the use of extremely fine soot particles leads to increased wear on precision fuel delivery system components;
- the presence of solid particles fills the gaps between fuel delivery system components, causing them to become unstable (stuck);
- the high viscosity of most suspensions necessitates the development of fundamentally new solutions to minimize the length of high-pressure lines;

The need to start and stop a diesel engine, as well as the need to initiate combustion by injecting a pilot liquid fuel, necessitates equipping the engine with two independent fuel supply systems, primary and secondary, or combining their functions in a single system.

The presence of two injection systems requires the creation of a dedicated control system that regulates the fuel supply to each system depending on the engine-operating mode.

When designing fuel systems, the most efficient solutions are those that minimize the number of moving parts operating under high pressure and in direct contact with the carbon suspension. Development experience shows that in some cases, the only moving part in contact with the suspension is the nozzle needle. Therefore, the nozzle is the critical element that determines the efficiency and durability of the injection system.

The most challenging aspect of creating a functional fuel supply system is the increased abrasive wear of the nozzles. High flow rates and operating pressures because nozzles made of traditional materials to fail after just a few hours of engine operation. At the same time, increasing injection pressure and, consequently, flow rates is often the only way to improve the quality of suspension spraying, which significantly influences fuel burnout.

As a rule, each specific design combines only individual advantages to ensure optimal fuel injection characteristics. Therefore, it makes sense

separately examine the application specifics of various injection system designs and configurations for the use of carbon suspensions.

4.1.1. Fuel injection system with pulse feed (plunger pumps) it is the most traditionally used system on diesel engines. The main advantages of this system include the proven design of its components and assemblies, ease of injection control, reliability, and durability. Several studies have successfully attempted to adapt standard engine injection system components for operation with coal suspension. The majority of these modifications focused on shielding the plunger-type high-pressure fuel pump from contact with carbon particles. Various separating devices used to achieve this, allowing the fuel pump to use solely as a pulse generator.

***

Cooper-Bessemer and Detroit Diesel Corporation used modified fuel systems in their developments, the main design changes of which affected the engine injectors [44, 69]. The changes aimed at increasing injection pressure while minimizing the impact of the suspension on the moving parts of the fuel system. A special extension made on the body of the JS-1 engine injector from Cooper-Bessemer, in which a separating piston installed, preventing mixing of diesel fuel and high-efficiency fuel (Fig. 4.1).

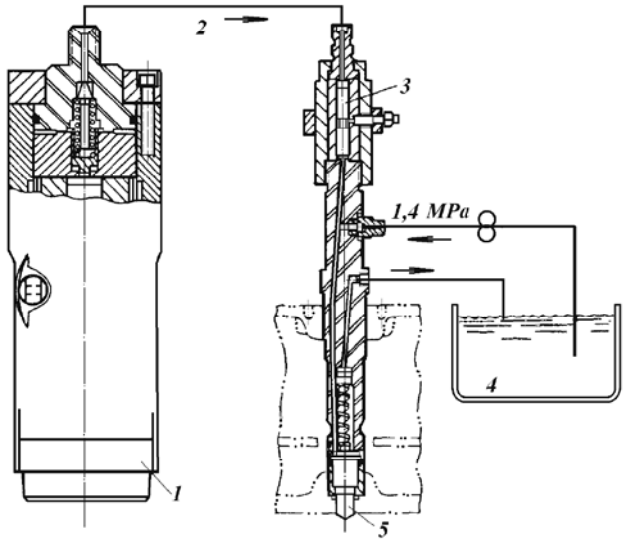

Fig. 4.1. – The design of the fuel system of the JS-1 engine converted to run on WCS. 1 – plunger-type fuel pump; 2 – high-pressure delivery line; 3 – separator piston; 4 – WCS storage tank; 5 – sprayer

The JS-1 engine's high-pressure pump delivery valve modified so that after injection, diesel fuel returned to the pump. A small drain hole was provided in the valve body for this purpose. After the pressure in the delivery line dropped, the WCS, arriving at 1.4 MPa, opened the check valve and filled the delivery chamber. At the same time, the separator piston moved to its uppermost position. Between injections, the injector maintained a pressure of 1.4 MPa, which was insufficient to raise the nozzle needle (the injection start pressure was 34.5 MPa). Seizure of the separator piston prevented a titanium nitride coating on its surface. The surface of the bushing along which the separator piston moved coated with a layer of nitralloy. In addition, oil supplied through a special channel into the gap between the piston and the sleeve, maintaining a pressure of 7…14 MPa above the maximum injection pressure. This solution prevented carbon from entering the gap between the sleeve and the piston. The initial gap size was approximately 2.5 μm; increasing it during operation by 0.2…0.5 μm prevented carbon particles from entering the gap and increased oil consumption.

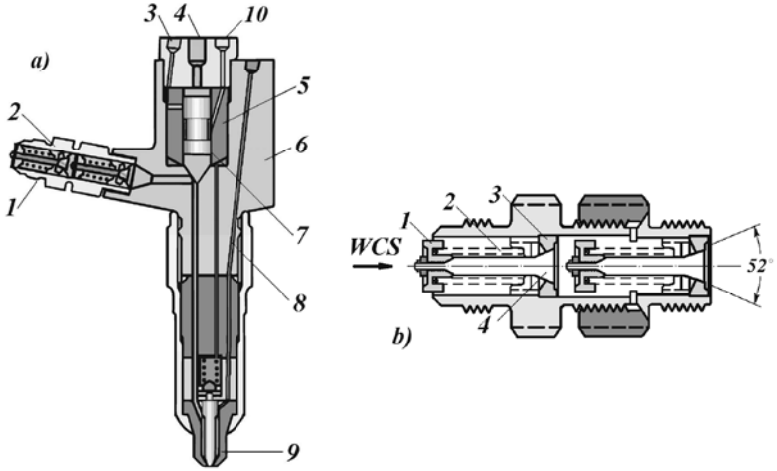

Fig. 4.2. *a* – 8V-149 engine injector designed for WCS injection: 1 – high-pressure pipeline connection nipple; 2 – check valve housing; 3 – sealing oil drain channel; 4 – channel for supplying hydraulic pulse from the high-pressure pump; 5 – separator piston guide sleeve; 6 – injector housing; 7 – separator piston; 8 – channel for supplying sealing oil to the needle valve guide; 9 – sprayer housing; 10 – sealing oil supply to the separator piston; *b* – design of the injector check valve: 1 – spring holder; 2 – spring; 3 – valve seat; 4 – valve

The suspension, under a pressure of 1.4 MPa, fed into the discharge chamber beneath the separator piston through a check valve using a dedicated booster pump. During injection, the separator piston moved downward under

the diesel fuel pressure supplied by the plunger pump. This closed the check valve, and the suspension, equal in volume to the diesel fuel, ejected from the injector under virtually the same pressure as the fuel pump. The Detroit Diesel 8V-149 engine injector (Fig. 4.2*a*) operated similarly, so the operation of the injection system will discuss below using the Cooper-Bessemer design as an example, highlighting some of the distinguishing features of both systems.

To separate the high- and low-pressure chambers in the JS-1 engine's fuel system, a two-stage, uncontrolled, poppet-type check valve with a spring located on the low-pressure side used. This design solved problems associated with sticking and leaks in the check valve, ensuring a good seal that maintains high pressure during injection, and reliably filling the WCS separator cylinder chamber after injection.

The 8V-149 engine's fuel system utilized a cluster of two poppet-type check valves with a 52-degree sealing lip angle (Fig. 4.2*b*). Both valves held closed by springs and had loose fits. To reduce wear, the sealing lips of the poppet valve and its seat were made of tungsten carbide. The injector used in the JS-1 engine experiments injected WCS at a pressure of 34.5 to 103.5 MPa through a nozzle with a more than double the number of holes, while their diameter was reduced, compared to the nozzle for diesel fuel. The size range was 0.25 to 0.40 mm and was selected based on experimental data on WCS spraying in a stationary chamber-simulating diesel combustion chamber conditions. The problem of needle valve seizure in the nozzle solved by introducing sealing oil under high pressure into the clearance of the guide portion of the bushing. The problem of carbon accumulation under the valve, between its seat and nozzle holes, solved maintaining a high flow velocity during injection in this area and using a small valve seat width (0.6 mm). Fig. 4.3 shows one version of the nozzle with 18 holes arranged in two rows.

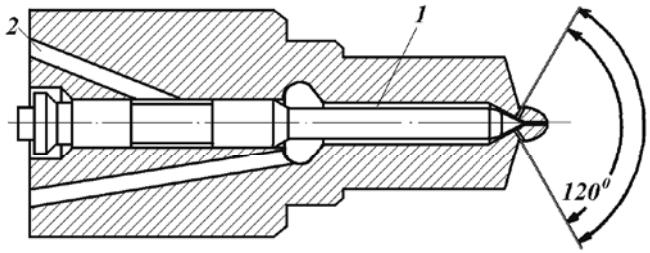

Fig. 4.3. WCS injection nozzle used in the JS-1 engine. 1 – needle valve; 2 – channel for supplying oil to the gap between the nozzle body and the valve guide

Through these holes, fuel fed into the combustion chamber along a cone-shaped 120° opening. At the end of the sprayer was a nineteenth hole, which served to prevent coal from accumulating at the valve tip.

Multi-hole sprayers provided good spraying of the WCS, resulting in sufficiently high combustion characteristics (ignition, burn rate, and fuel burnout). The only significant remaining issue was wear of the nozzle tip holes. This prompted research into the wear resistance of materials and the development of new sprayer designs. This resulted in the development of an experimental sprayer with a poppet valve (Fig. 4.4). This design allowed the use of various hard coatings for the valve seat and poppet.

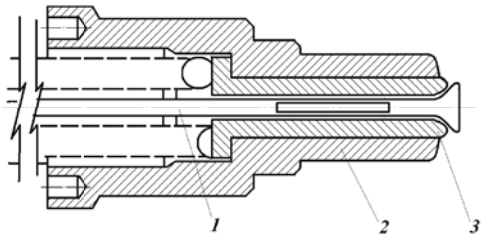

Fig. 4.4. Injector nozzle with plate valve. 1 – valve; 2 – body; 3 – valve seat insert

Fig. 4.5 shows the dependence of injection pressure on the clearance area of a poppet valve. The opening pressure of such a valve is significantly higher than with a multi-hole nozzle. On the one hand, such a valve opens quickly to a cross-section where the injection pressure maintained virtually constant. The moment when this type of valve is fully open is difficult to determine; it roughly corresponds to the value highlighted in the graph (Fig. 4.5).

On the other hand, the closing moment of such a valve is quite easy to determine: after the plate contacts the seat, only the oscillations associated with reflected waves are visible on the graph. The injection duration with this nozzle is shorter than with a multi-hole nozzle. This explained by the larger seating surface of the poppet valve, resulting in a higher average injection pressure.

During experiments with a nozzle equipped with a poppet valve, the opening pressure, spring constant, and pump plunger diameter varied.

In Fig. 4.6*a* shows the characteristic curves for the cylinder pressure of the JS-1 engine, as well as the injection pressure when using a poppet valve nozzle. Fig. 4.6*b* shows the corresponding heat release profile.

The heat release rate curve shows that when fuel is injected through a variable-area nozzle, a rapid combustion stage of premixed fuel occurs. This

is followed by a slow combustion stage limited by mixing, for which the average heat release rate is approximately 1.8 kJ/deg.

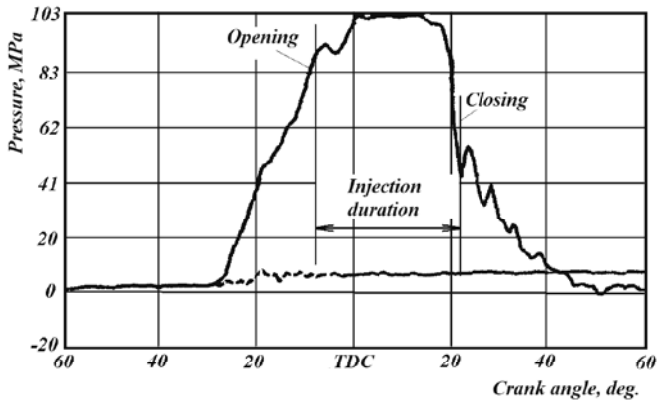

Fig. 4.5. Changing the injection pressure for a nozzle with a variable-section poppet valve

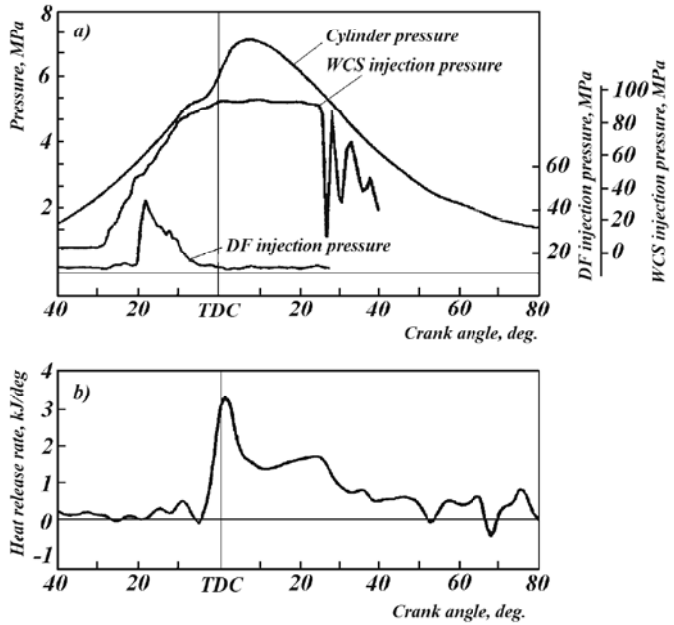

Fig. 4.6. Cylinder pressure, WCS injection pressure, pilot diesel fuel injection pressure (*a*) and heat release rate (*b*) during operation of the JS-1 engine equipped with a variable cross-section nozzle

Using a poppet-valve injector results in an extended afterburn (compared to a multi-hole injector), which begins 40° after TDC and is characterized by an average heat release rate of approximately 0.5 kJ/deg.

Experiments with a variable-area injector showed that reducing the opening pressure reduces the valve stem preload, which in turn reduces the injection pressure. This also causes injection to begin earlier, and the initial WCS velocity decreases. Reducing the spring stiffness also reduces the average injection pressure. Using a smaller-diameter plunger reduces the fuel delivery rate to the injector nozzle and increases injection duration. The experimental results presented in Table 4.1, where, for comparison, the values obtained for a multi-hole injector also presented (column 6). Preliminary experiments have shown that high injection pressure is not essential for successful operation of an engine equipped with a variable-area injector. The poppet nozzle performs better at lower injection pressures (48 MPa instead of 82 MPa), while providing comparable effective specific fuel consumption values. As can be seen from Table 4.1, the engine performance with the variable nozzle is almost as good as that with the multi-hole nozzle. The effective specific fuel consumption is 5.3 MJ/(kWh), which is essentially equivalent (within the experimental error) to the effective specific heat consumption with the standard multi-hole nozzle under the same operating conditions (5.08 MJ/(kWh)). The exhaust gas temperature is also comparable, in both cases it is approximately 450°C, indicating good combustion without significant combustion lag. Preliminary results indicate NO_x emissions of approximately 500 ppm, compared to 1200 ppm recorded for a multi-hole injector at the same engine inlet air temperature (166°C).

Table 4.1.

Test results of the Cooper-Bessemer JS-1 engine equipped with a poppet valve injector

Parameter	Experience					
	1	2	3	4	5	6
Maximum injection pressure, MPa	99.47	94.67	58.31	65.17	51.45	82.32
Average injection pressure, MPa	85.75	82.32	41.16	48.02	37.73	—
Plunger diameter, mm	26	26	26	26	22	26
Spring stiffness, kg/mm	94.73	94.73	94.73	94.73	49.15	—
Injection start (before TDC), deg	8	6	16	17	20	20
Injection duration, deg	30	31	26	28	32	37
Average effective pressure, MPa	0.86	0.97	0.93	0.90	0.93	1.03
Effective specific heat consumption, MJ/(kWh)	5.81	5.89	5.37	5.3	5.26	5.08
Exhaust gas temperature, °C	449	457	471	443	460	471
NO_x emissions, ppm	—	470	530	550	500	1200

All of the fuel system upgrades performed on the JS-1 and 8V-149 engines for WCS operation had virtually no impact on the high-pressure fuel pump (except for an upgrade to the pump delivery valve). During the experiments, a standard plunger-type fuel pump with a spool valve used to deliver diesel fuel to the separation chamber. The amount of fuel injected controlled by rotating the plunger, which causes a spiral groove on the plunger body to change its position relative to the drain hole in the plunger guide bushing.

Fuel entered the above-plunger space through the filler hole when the upper edge of the plunger was below this hole. As the engine camshaft rotated, the camshaft, via its tappet, moved the plunger. As the plunger rose, it closed the filler hole, after which a portion of fuel entered the separator chamber (Fig. 4.1). The pressure in the chamber quickly increased to a value of several tens of MPa. Under the action of the separator piston, this pressure transmitted to the WCS. As result of the pressure increase, the check valve closed, separating the separator chamber from the filler line. This led to an increase in pressure in the injector's working space, which caused the sprayer valve to open, initiating WCS injection into the engine combustion chamber.

The plunger's active stroke began when the upper edge of the filler hole closed and ended when the spiral groove on the plunger body aligned with the drain hole in the guide bushing housing. As the plunger continued to move through the spiral groove and drain whole, fuel from the above-plunger space released under pressure into the drain line. The pressure dropped, and the injector closed under the force of the spring. Between injections, the lower volume of the separating chamber filled with WCS from the filler line. Under the action of the suspension pressure on the separating piston, diesel fuel was forced out of the separating chamber through the drain hole in the discharge valve into the above-plunger space of the pump and then into the drain line.

***

General Electric. In its early developments, General Electric used a WCS supply system similar to that of Cooper-Bessemer. The main distinguishing feature was that instead of a piston separator, General Electric specialists used a diaphragm-type separator (Fig. 4.7). Fig. 4.8 shows the general arrangement of the fuel system components on an engine [52].

Since the calorific value of coal fuel lower than that of diesel fuel, to achieve the same power, all other things being equal, the WCS cycle flow rate must be higher. To achieve this, the standard 20 mm diameter plunger pair in the standard Lucas pump replaced with a larger one, 24 mm in diameter. The fuel pump operated with clean diesel fuel, which was supplied

to chamber *A*, separated from chamber *B* by a separating diaphragm. From chamber *A*, the fuel drained back into the reservoir through a calibrated orifice via a drain channel. In addition to the high-pressure plunger pump, there was a low-pressure system for continuous WCS delivery. It consisted of a screw pump, a pressure-reducing valve, a check valve, and a WCS storage tank.

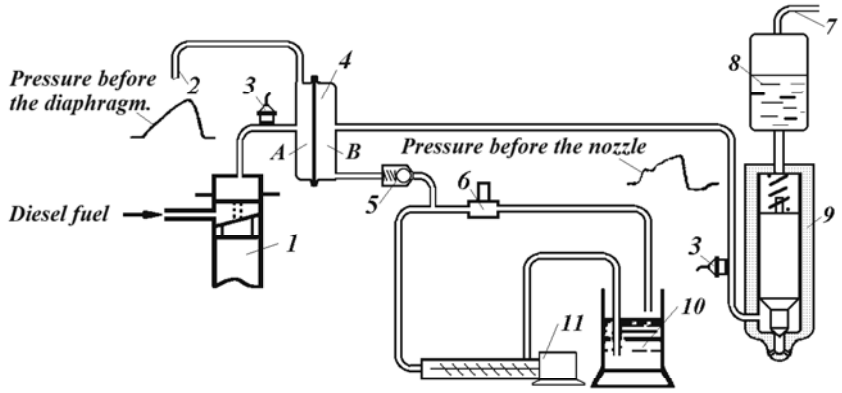

Fig. 4.7. WCS injection systems with a diaphragm-type separator: 1 – high-pressure plunger pump; 2 – diesel fuel drain channel; 3 – pressure sensor; 4 – diaphragm separator; 5 – check valve; 6 – pressure-reducing valve; 7 – pressure supply channel to the needle hydraulic locking system; 8 – nozzle needle hydraulic locking system; 9 – injector; 10 – WCS storage tank; 11 – low-pressure pump

The low-pressure fuel pump is required for continuous pumping of the WCS and for pressurizing the fuel supply system into chamber B of the diaphragm separator. The pressure-reducing valve maintains constant pressure in the system. A check valve disconnects chamber B of the diaphragm separator from the low-pressure system at the start of injection, when the pressure in chamber B exceeds the pressure set by the pressure-reducing valve. To monitor pressure changes in the high-pressure line, two sensors installed one recorded pressure changes immediately after the plunger pump, and the other, before the injector valve.

Because the pressure supplied to the injector is quite high, a hydraulic sealing system installed to ensure reliable closure of the needle valve. This not only facilitated the needle valve's compression but also prevented carbon particles from entering the gap between the needle and the injector body.

The main fuel injector, designed for WCS injection, was mounted along the cylinder axis and slightly larger than a similar injector for diesel fuel (Fig. 4.8).

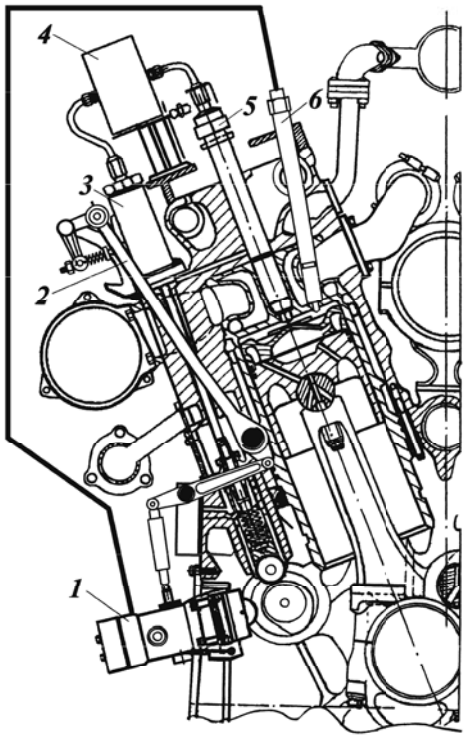

Fig. 4.8. Schematic diagram of an engine with a volumetric injection system WCS. 1 – pump for feeding pilot diesel fuel; 2 – joint pump control system; 3 – plunger pump with pulsating feed, operating on diesel fuel; 4 – diaphragm separator; 5 – injector for WCS injection; 6 – injector for injection of pilot fuel

This was done to ensure efficient fuel delivery at full load (the WCS cyclic delivery reaches up to 4 cm^3). Eight different injector types tested during preliminary studies. All had between 10 and 24 holes with diameters ranging from 0.4 to 0.63 mm, arranged along a cone-shaped generatrix with an opening angle of 120°. The pilot fuel injector nozzles had two to four holes with diameters ranging from 0.30 to 0.35 mm. All nozzles manufactured by Lucas. Except for the differences described above, the design and operation of the 7DFL engine's fuel system are generally similar to those of the Cooper-Bessemer JS-1 engine.

***

The problem of suspension injection for high-speed engines with relatively small working cylinders solved somewhat differently. In this case,

installing two independent injection systems typically unnecessarily complicates the engine design. Therefore, the most efficient approach is to combine the functions of the primary and secondary systems into a single system, so that pure diesel fuel enters the combustion chamber during engine start-up and warm-up, and then the engine switches to carbon suspension. This design is most feasible when using a FCS, as it eliminates the problem of fuel self-ignition. Using a combined WCS injection system requires additional measures to ensure stable fuel self-ignition (installing glow plugs, preheating the air at the engine inlet, insulating the combustion chamber, etc.). An example of a combined injection system is the design used by L. V. Grekhov to study the combustion of various types of coal suspensions in a small-sized swirl-chamber diesel engine S/D 11/8.5 [9, 14]. This circuit design allows the high-pressure fuel pump to operate on clean diesel fuel, relegating it to the role of a controlled pulse generator. This solves the problem of wear on the most expensive component of the fuel supply equipment (Fig. 4.9). Coal suspension and clean diesel fuel are pumped independently of each other using pumps 2 and 3. Two-way valve 4 used to switch the supply of coal suspension or diesel fuel alternately into the engine's fuel system. In the intervals between injections, one or the other fuel enters the pressure line through automatic make-up valve 5.

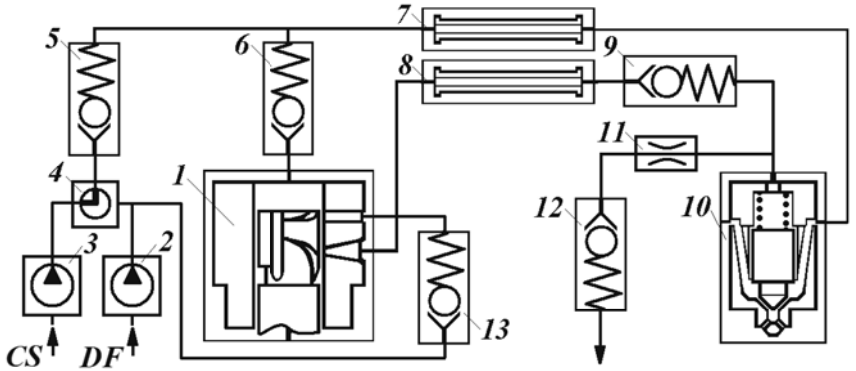

Fig. 4.9. Fuel supply equipment for injecting coal suspensions into a small-sized high-speed diesel engine. 1 – high-pressure plunger pump; 2,3 – booster pumps; 4 – two-way valve; 5 – make-up valve; 6 – discharge valve; 7 – discharge pipeline; 8 – pressure supply pipeline for hydraulic locking and cleaning of the spray needle; 9 – check valve of the needle hydraulic locking system; 10 – injector; 11 – throttle; 12 – pressure regulating valve of the needle hydraulic locking system; 13 – diesel fuel make-up valve

To compensate for heat loss supplied to the working cylinder due to the lower calorific value of the suspensions, the plungers replaced a 12 mm

plunger was installed instead of a 6.5 mm diameter plunger. This design change, along with a revised cam profile, allowed for a quadrupled injection pressure and a doubling of the flow rate. Improved spray quality achieved by narrowing the nozzles and hydraulically locking the injector needle. Injector performance ensured by hydraulically locking the needle, flushing the nozzle gap with diesel fuel via line 8, and using nozzles made of industrial diamond, cubic boron nitride, and ruby.

4.1.2. Using pump-nozzles for injection of coal suspensions. The main advantage of using pump-injectors in the WCS fuel injection system is the ability to achieve relatively high injection pressures. The most significant drawback of this fuel delivery system is that the plunger and nozzle are in direct contact with the carbon particles in the suspension.

The most extensive studies on the use of pump-injectors for WCS fuel injection were conducted Electro-Motive Division. They conducted on a two-stroke, two-cylinder EMD 567B engine. Only one cylinder of the engine was equipped with the WCS fuel injection system. It had a main pump-injector mounted along the cylinder axis, and a dual-jet pilot injectors positioned at the edge, near the cylinder wall. The second cylinder operated on diesel fuel and had single pump-injectors. The regulator disconnected from the pump-injectors, and the fuel delivery adjusted manually in each case. A MOYNO 6M1 unit injector (Fig. 4.10) [33] modified for use with WCS.

Before installing the pump-injector on the engine, tests conducted on a test bench. These tests revealed that, for normal operation (without jamming), the clearance between the plunger and the sleeve must be increased by 0.013 mm, and between the needle and the nozzle body by 0.038 mm. For reliable operation of the plunger pump on the WCS, the excess pressure at which the suspension supplied to the pump-injector must not be lower than 60 kPa. Considering the high losses in the pipelines associated with the increased viscosity of WCS, as well as the fact that water is more volatile than diesel fuel, the excess pressure in the fuel supply line maintained at approximately 400 kPa. For this purpose, the supply line was equipped with a piston pump and an adjustable pressure-reducing valve. The pump's volumetric flow rate was 2.3 l/min. Maintained pressure in the feed line prevented vaporization during filling of the pump's sub-plunger space. For increased reliability and to prevent nozzle seizure due to abnormally high viscosity (see Section 3.4.2), the pump-injector was cooled with room-temperature water. The pump-injector housing cooling system showed Fig. 4.11.

Water supplied and discharged through dedicated channels, maintaining an outlet temperature of approximately 43°C and flowing at 3.8 l/min.

Unused WCS, diverted from the pump-injector before returning to the tank, also pre-cooled.

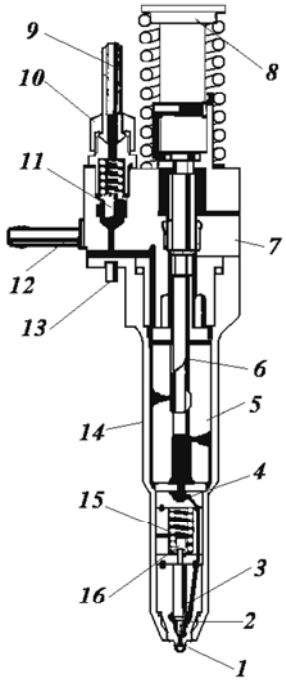

Fig. 4.10. Pump-injector adapted for operation on WCS. 1 – nozzle hole; 2 – nozzle tip; 3 – needle valve; 4 – check valve; 5 – sleeve; 6 – plunger; 7 – body; 8 – pusher; 9 – fuel supply line; 10 – fuel system nipple; 11 – filter; 12 – adjusting rack; 13 – mounting pin; 14 – mounting surface; 15 – needle valve spring; 16 – spring stop

Test results showed that when using the upgraded pump-injector for WCS injection, engine efficiency was approximately 85% of that for diesel fuel. This is obviously explained by the fact that, at a given volumetric flow rate, the injection pressure was lower than required for high-quality WCS spraying. Engine power when using the suspension was only 31…36% of the rated engine power for diesel fuel. This explained by the lower calorific value of WCS, which requires more than double the cycle delivery. The parameters of the pump-injector used did not allow this. Optimization of injection characteristics for WCS use resulted in the upgraded fuel system being tested on diesel fuel, resulting in significantly worse engine performance than with standard injection parameters. Engine test results using the upgraded injection system presented in Table 4.2.

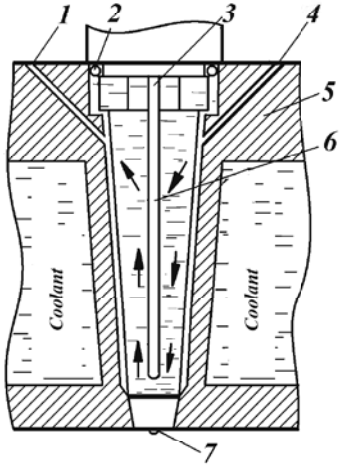

Fig. 4.11. Pump-injector cooling system. 1 – water outlet; 2 – sealing ring; 3 – spacer insert; 4 – water inlet; 5 – cylinder head; 6 – auxiliary cooling water flow; 7 – spray tip

Table 4.2.

Test results of the EMD 567B engine with a modernized injection system

The main fuel	Fuel consumption, kg/h		Effective power, kW	Efficiency, %
	main	pilot		
DF No.2	11	4.5	53.00	29
WCS	36	4.5	50.80	25
DF No.2	11	4.5	54.50	30
WCS	42	4.5	58.14	25

Based on the research results, the following conclusions can drawn:

- the use of pump-injector for WCS injection requires addressing a number of serious issues related to both nozzle wear and plunger wear;

- given the compact placement of the main components used for high-pressure fuel injection, it is quite difficult to achieve reliable operation of the pump-injector in WCS.

Based on the above, it can assume that the use of this type of injection system for coal suspensions will be very limited.

4.1.3. Accumulator fuel injection systems (Common Rail) are the most promising when using coal suspensions. They provide the necessary flexibility in terms of injection parameters, such as pressure, injection lead-time, and injection duration. With an accumulator fuel injection system, these entire parameters can vary depending on engine load and speed, both during experimental studies and during operation. This allows for the establishment of optimal injection characteristics that ensure maximum engine efficiency.

Fig. 4.12 shows a general diagram of the fuel system for a Sulzer 1RSA76 engine, used in experiments on burning coal suspensions [65].

This system utilized accumulator fuel injectors for both the main and pilot fuel injection.

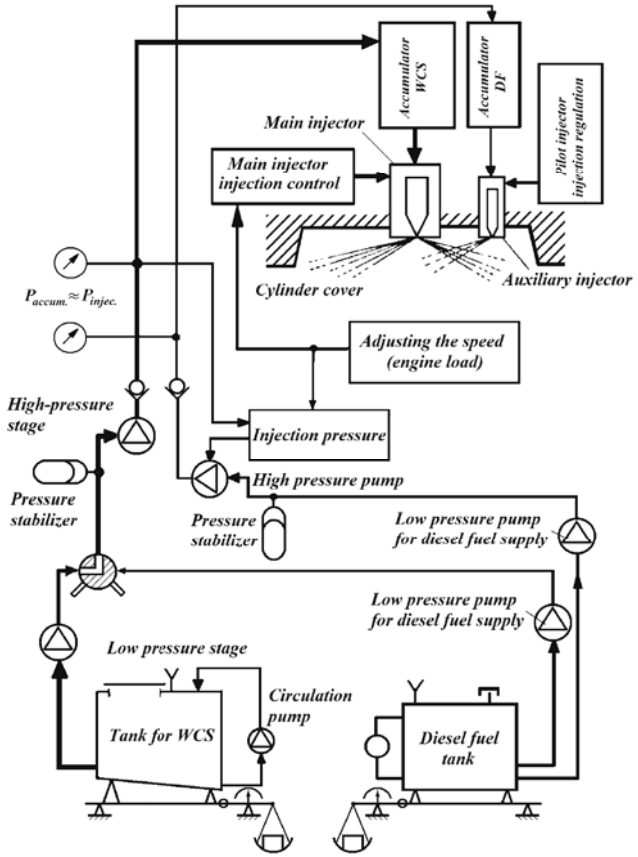

Fig. 4.12. Scheme of the experimental fuel system of the Sulzer 1RSA76 engine

After the engine had warmed up on diesel fuel and reached steady-state operating conditions, a low-pressure, positive-displacement MOYNO pump, designed for delivering WCS, activated. The pump is equipped with a rubber stator and a steel rotor. This design eliminated the need for a pressure-reducing regulator in the fuel system. When activated, this regulator crushes the carbon particles in the suspension, increasing its viscosity. The pump driven by a variable-speed electric motor, whose speed determined the

pressure in the high-pressure stage. This ensured that the booster pump delivered exactly the amount of fuel the engine actually consumed. If the fuel valve was set to the WCS position, the engine began running on suspension immediately after the diesel fuel displaced from the high-pressure storage tank. At any time during operation, the fuel valve could switch to diesel fuel, which displaced the WCS from the system. This design principle of the fuel system naturally implied compatibility between the WCS and diesel fuel.

General Electric also investigated the possibility of using accumulator water-coal fuel injection system in its development [39, 48, 55]. A series of experiments conducted on test benches and on an engine for these purposes. The conclusions drawn from the research indicate that the advantages of common-rail systems, as pointed out by Sulzer specialists, also apply to engines with rotation speeds of 450…1200 min^{-1}. Higher initial injection pressures (up to 80 MPa), which can be achieved in a common-rail system, significantly improve the quality of WCS spraying, which has a decisive impact on the ignition and combustion rate of carbon particles. The accumulator injection system allows for the effective regulation of fuel injection characteristics, which is especially important at partial loads.

Because of the research, an accumulator fuel injection system with electronic control of both the WCS and pilot diesel fuel injection processes was developed. The control system developed using microprocessor technology. To reduce losses in the high-pressure lines, the accumulator placed directly in the injector body. The fuel system circuit itself virtually identical to that used during testing of the pulse-feed fuel injection system. A diaphragm separator used during the experimental studies, but was later replaced with a piston-type separator. Fig. 4.13 shows the circuit diagram of the accumulator fuel injector [39, 55].

The injection process occurred as follows: a plunger pump supplied WCS through port 12 into the accumulator chamber of injector 6, increasing the pressure within it. The needle valve, under the influence of oil pressure acting on the top of the needle and supplied through channel 2, was held closed (initially, nitrogen supplied under pressure was used to close the injector). To prevent the needle valve from jamming in the guide, the gap between the needle and the guide sleeve was constantly flushed with water supplied through channel 3. The water pressure maintained slightly higher than the pressure in the accumulator chamber. When an electrical signal received from the control system to control valve 5, it opened and supplied oil at a pressure of 27.5 MPa from line 4 into the chamber beneath the piston, which was integral with the needle valve. Under the influence of pressure, the needle valve lifted, and WCS injected.

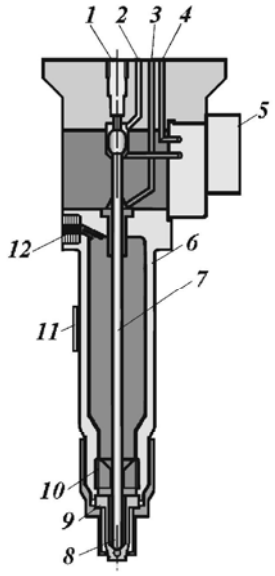

Fig. 4.13. Schematic diagram of the accumulator injector. 1 – socket for monitoring the lifting of the needle; 2 – oil supply for hydraulically locking the needle valve; 3 – water for flushing the gap between the housing and the needle; 4 – oil under pressure for lifting the needle; 5 – control valve; 6 – fuel cavity; 7 – needle; 8 – valve tip; 9 – sprayer body; 10 – lower guide of the needle valve; 11 – strain gauge; 12 – fuel supply to the accumulator

The needle lift and injection duration determined by the nature of the electrical signal supplied to the control valve. The pressure in the accumulator chamber was monitored using strain gauge 11, attached to the injector body. The diagram of the accumulator fuel system is shown in Fig. 4.14, and the location of the main components of the injection system on the engine is shown in Fig. 1.7 [25, 55, 72].

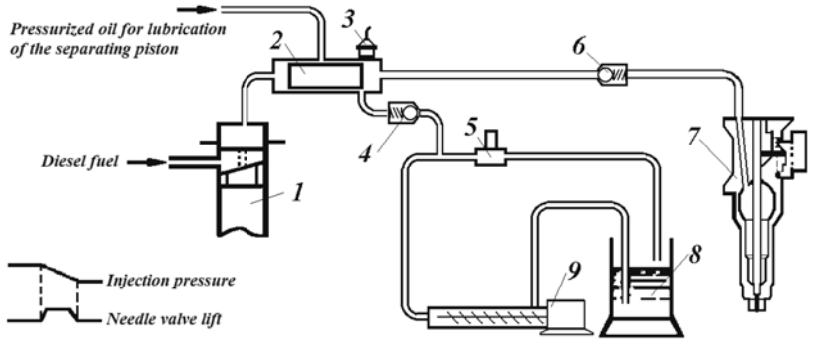

Fig. 4.14. Schematic diagram of the accumulator fuel system developed by General Electric. 1 – plunger pump; 2 – separator piston; 3 – pressure sensor; 4 – delivery valve; 5 – pressure regulating valve; 6 – check valve; 7 – injector with electronic injection control; 8 – tank with WCS; 9 – booster pump

The injector's accumulator cavity had a volume of 235 cm^3, which ensured the delivery of approximately 3 g of WCS per cycle. During bench tests, the injector pressure decreased from approximately 83 to 48 MPa, which ensured good combustion efficiency. However, during engine tests under long-term operating conditions, it was not possible to maintain the maximum injection pressure at 83 MPa. This was due to high fuel leakage rates in the diaphragm separator. Further machine tests conducted at an injection pressure of 70 MPa. At this pressure, the injector needle fully opened in approximately 0.5 ms and closed in 0.75 ms [55]. Tests conducted at maximum (1050 min^{-1}) and average speeds (785 min^{-1}). The standard engine fuel pump used as a high-pressure booster pump. The initial WCS pressure in the accumulator injector regulated by varying the delivery rate of this pump. In the early stages of research, a diaphragm separator used to separate diesel fuel from the WCS. To ensure reliable operation at high WCS flows, it was necessary to significantly increase the diaphragm area while maintaining a relatively small deflection. Otherwise, the metal diaphragm would quickly fail. Increasing the diaphragm diameter resulted in an increase in the volume of the high-pressure injection system, which reduced the maximum pressure supplied to the injector. Subsequently, the diaphragm sprayer replaced, as in other projects, with a piston-type one. This allowed injection pressure to increase to 80 MPa and above. Using a piston separator is optimal for ensuring reliable operation of both conventional and accumulator injection systems. In this regard, several design features of such systems should note. The optimal size of the separator piston should select such that its volume is approximately one and a half times greater than the volume of the injected liquid. Moreover, the larger the diameter of the separator piston, the shorter its stroke, and, consequently, the shorter the time it takes to return to its initial position, corresponding to the onset of injection. Considering that, the piston returns under pressure significantly lower than the pressure applied to it now of injection, the piston return time is extremely important, especially for high-speed engines. In all projects, the developers used the rule of thumb that the separator piston diameter should be approximately equal to the plunger diameter of the high-pressure fuel pump. The discharge cavity of the separator chamber should be 50% larger than the maximum cyclic delivery volume. This prevents mechanical contact between the piston and the separator end caps. The sealing fluid (oil) should supply through a groove in the piston. A groove made in the bushing impairs the performance of the separator.

Unlike other projects, the separator in the 7DLF engine's accumulator fuel system designed as a separate element.

Compared to the plunger-type fuel delivery system, the accumulator system demonstrated a number of significant advantages. Specifically, it maintained high injection pressure at the start of injection (67.6 MPa), dropping to 41.8 MPa at the end, while the plunger-type system had low injection pressure at the start of injection (27.6 MPa) and higher pressure (53.7 MPa) at the end. Heat release diagrams, along with needle lift curves, graphically depicting combustion characteristics associated with differences in injection conditions, shown in Fig. 4.15.

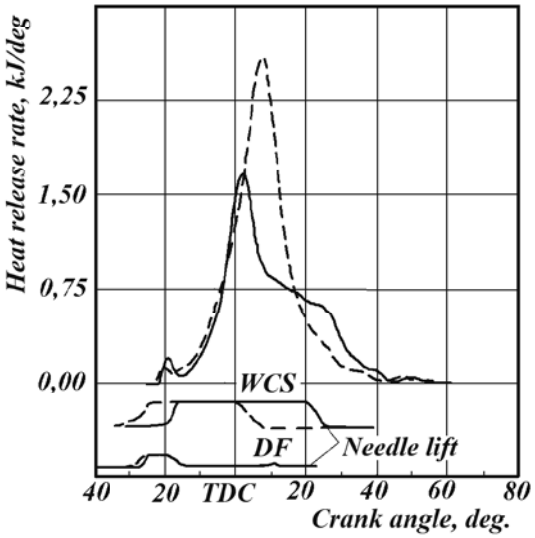

Fig. 4.15. Heat release rate when using the accumulator injection system and the plunger-type injection system. —— accumulator injection system; - - - - plunger-type injection system (rotation speed of 1050 min^{-1}, air temperature and pressure at the inlet of 85 °C and 326 kPa)

Compared to a plunger-type injection system, the use of a common rail system significantly reduced the ignition delay period and, consequently, the overall combustion time of the WCS. High pressure at the start of injection contributed to smaller aerosol droplets, which in turn reduced the ignition delay. As a result, the amount of fuel in the cylinder at ignition reduced, and the maximum pressure and thermal density decreased, while the completeness of carbon particle combustion increased from 90% to almost 100%.

The advantages of the common rail system even more pronounced at partial loads. For example, with a plunger-type system, as the engine speed dropped to 785 min^{-1}, the boost pressure decreased, reaching 46.8 MPa by the

end of the injection period. With the common rail system, injection began at a pressure of 66.4 MPa and ended at 49.5 MPa. That is, the pressure at the end of injection when using the accumulator system was higher than the maximum pressure developed by the plunger-type system. The accumulator system achieved complete burnout of carbon particles, while under similar conditions for the plunger-type system; burnout did not exceed 80%. Fig. 4.16 compares the heat dissipation characteristics of the accumulator and plunger injection systems at part-load modes, and Table 4.3 presents the main operating parameters for both systems at full and part-load modes. It should note that in the considered case, for the plunger-type system, pilot fuel injection timing should be earlier to compensate for the long WCS ignition delay.

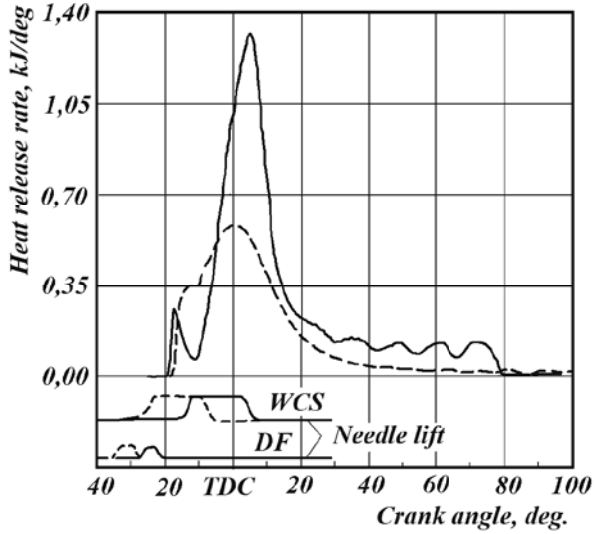

Fig. 4.16. Heat generation rate when using the accumulator injection system and the plunger injection system at part load mode. —— accumulator injection system; - - - plunger-type injection system (rotation speed 785 min^{-1}, air temperature and pressure at the inlet 85 °C and 134 kPa)

Test results on low- and high-speed engines showed that the use of accumulator systems allows for:

– significant reduction in WCS ignition delay due to increased injection pressure;

– ensuring a heat release process that eliminates a sharp increase in cylinder pressure and achieves high combustion efficiency;

– ensuring virtually complete WCS burnout at partial loads.

Table 4.3.

Comparison of accumulator and plunger fuel injection systems at full and part load modes.

Test conditions						
System type	Injection advance angle, °		Injection pressure, MPa		DF, mm^3	Power, kW
	DF	WCS	beginning	end		
Full load						
Accum.	28	22	67.6	41.8	59	145
Plun.	30	35	27.6	53.7	70	180
Partial load						
Accum.	29	26	66.4	49.5	50	69
Plun.	36	29	27.6	46.8	106	48

Combustion characteristics			
System type	P_{max}, MPa	Burnout rate, %	Specific heat consumption, kJ/(kW×h)
Full load			
Accum.	15.9	99.5	7853
Plun.	17.5	90.0	8692
Partial load			
Accum.	8.3	99.5	9840
Plun.	6.3	77.8	10734

4.2. Pilot diesel fuel injection systems.

The pilot fuel injection characteristics and delivery system must meet the following requirements:

– ensure a stable supply of a small amount of pilot fuel at full load (approximately 3...6% of the total energy released by the fuel in the cylinder);

– provide the ability to vary the fuel delivery over a sufficiently wide range: from a relatively large amount at partial load (approximately up to 40% of the total energy released by the fuel) to a complete shut-off at maximum load;

– provide the ability to deliver a large amount of fuel to enable engine starting (approximately up to 55% of the total energy released by the fuel);

– provide the ability to set injection parameters (injection advance, cyclic delivery) during engine operation that are optimal for the steady-state load condition.

Fig. 4.17 shows the location of the auxiliary injector and the nature of pilot fuel aerosol propagation in the cylinder of the 7DFL engine [48].

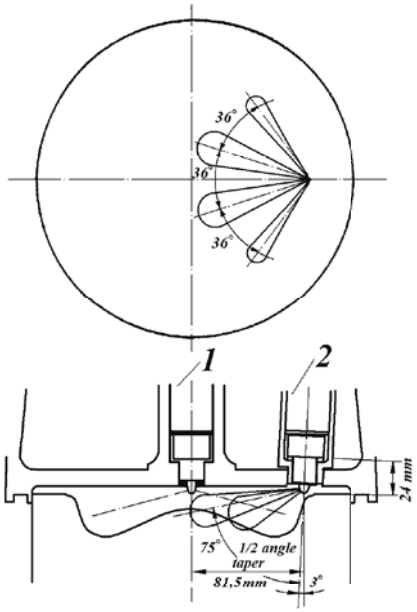

Fig. 4.17. Location of the auxiliary injector and the nature of aerosol distribution in the cylinder of the 7DFL engine. 1 – main injector for WCS injection; 2 – auxiliary injector for diesel fuel injection

The injector nozzle had four unequal holes for delivering diesel fuel to the working cylinder: two large holes directed toward the centre of the combustion chamber, and two smaller holes at the edges. This design was based on the fact that the amount of pilot fuel required for operation at close to maximum load was approximately 100 mm^3/cycle, while at partial loads, up to 600 mm^3/cycle had to be delivered to the cylinder. Under these conditions, efficient combustion of relatively large quantities of fuel was only possible with high quality mixing with air. By installing a nozzle with different holes, it was possible to achieve different spray patterns, ensuring an optimal oxygen-to-fuel ratio at all points in the combustion chamber.

In addition to the pilot fuel injection method described above, another method can used in which diesel fuel is fed by an injector into a swirl chamber, where initial ignition occurs. A plasma jet then emerges into the main combustion chamber, activating the ignition of the WCS, which then fed into the main chamber through the main fuel injector. This pilot fuel injection system design tested on the Cooper-Bessemer LSB series engine (Fig. 4.18). Pilot fuel injected into two swirl chambers located in the cylinder

head on either side of the main injector. This pilot fuel injection system allows the use of pin-type fuel injectors, which are simple and reliable, to deliver diesel fuel. The relatively poor fuel spraying quality of such injectors offset the high degree of turbulence of the air charge in the swirl chamber.

For swirl-chamber engines, the primary (WCS) and secondary (DF) fuels must supplied into the swirl chamber. This can present certain layout challenges, as both injectors and the spark plug must installed closely to each other. An example of a successful layout is the design shown in Fig. 4.19.

In this design, the secondary injector installed in place of the spark plug, and the heating elements of both spark plugs inserted along the swirl chamber axis. With this design, both injectors inject fuel directly onto the heated surface, and the spark plugs themselves have minimal influence on the swirl flow in the chamber.

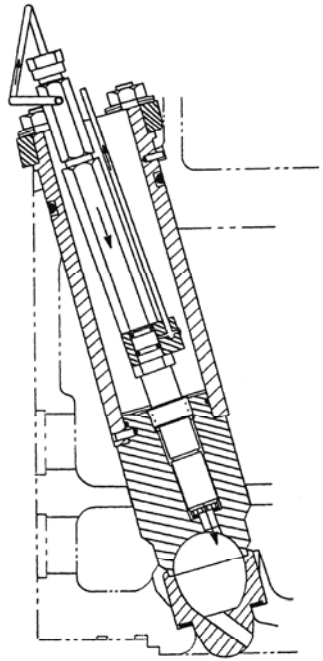

Fig. 4.18. Pilot fuel supply system in the LSB series engine from Cooper-Bessemer

To deliver high-pressure DF to the injector, plunger-type fuel pumps with the required flow rate used. To expand the injection advance angle adjustment range, the pump fasteners were modified or appropriate couplings were installed to allow for adjustment of the injection start.

A crucial aspect of the spark plug ignition system's operation is its synchronization with the WCS supply from the main injector. A decrease in load requires an increase in the supply of spark plug fuel relative to the main fuel, as the state of charge in the cylinder does not ensure effective ignition and combustion of the WCS. Conversely, as the load increases, the temperature in the working cylinder rises, increasing charge turbulence, leading to spontaneous ignition of the WCS. In this case, the pilot fuel supply may completely stop. A typical graph of the change in the supply of the main and pilot fuels with changes in engine load showed Fig. 4.20 [51]. The simplest way to coordinate the supply laws of the main and pilot fuels is to use accumulator systems with electronic control of the injection of both fuels.

Such systems allow for the optimization of not only the ratio of cyclic deliveries, but also the variation of the injection start angles and their duration to optimize the operating process.

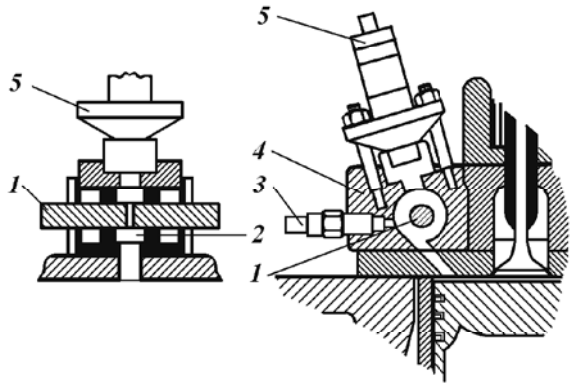

Fig. 4.19. Scheme of supply of main and pilot fuel to the engine swirl chamber: 1 – spark plug; 2 – cylindrical swirl chamber; 3 – auxiliary nozzle for supplying diesel fuel; 4 – cylinder head; 5 – main nozzle for supplying coal suspension

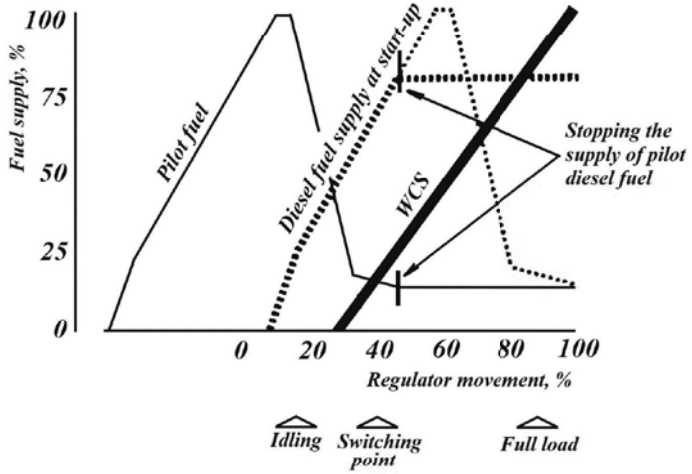

Fig. 4.20. Graph of changes in the supply of main and pilot fuel when changing engine load and when starting it

Apart from the features described above, the operation of the auxiliary pilot diesel fuel supply system is no different from that of a conventional

diesel engine. Considering that the majority of engines operate at partial loads most of the time (for example, for diesel locomotive engines, this time can reach up to 60%), the share of pilot diesel fuel in the total fuel consumption is 20...25% [51].

4.3. Research of the injection process of suspensions.

Among the first to study coal suspension injection processes separately from engine operating processes were Phaiak R.G. and Gurncy M.D. (1985). They obtained partial data on the droplet size distribution of aerosols produced by spraying FCS with coal dust mass contents of 20 and 40%. Published data from the study are very limited. It found that, for at least one operating mode, 50% of the spray mass consists of suspension particles with droplet diameters smaller than 20 μm. All measurements conducted at a single location relative to the spray length and with a single time delay.

***

Nelson L.P. et al. (1985) obtained droplet size distribution data for WCS aerosol under conditions typical of a high-speed diesel engine. The nozzle used for suspension injection modified and had six holes with a diameter of 0.35 mm. The nozzle valve opening pressure was maintained at 5.5 and 14 MPa. Measurements were conducted for a single location (32 mm from the nozzle tip) and for a single time (0.5 ms after the start of injection). It was found that during the injection of light diesel fuel, 80% of the fuel mass consisted of particles with a diameter of less than 100 μm. During WCS injection, 80% of the droplets had diameters of less than 400 μm.

***

In 1989, Yu. T. U. et al. published the results of experiments using a single-shot WCS feed system with a pneumatic drive. A needle nozzle, capable of injection at pressures of 70…170 MPa, was used to atomize the fuel. The fuel injected into a special constant-volume chamber filled with an inert gas at room temperature with a density of 17.5 kg/m^3. A laser diffraction analyzer with a beam diameter of 9 mm used to study the cloud. Two types of WCS with carbon contents of 53 and 48% by weight and three configurations of the nozzle tip studied. During the experiments, the following parameters recorded WCS injection velocity, fuel front penetration distance, light scattering as it passes through the fuel cloud, and the average droplet size. The average fuel injection velocity ranged from 220 to 450 m/s. The average aerosol droplet diameter was determined using the method proposed by Sauter. For WCS, it ranged from 25 to 54 μm, depending on the test conditions.

***

Branyon, D.P., and others (1991) reported the results of a study of continuous and intermittent injection systems. Continuous injection accomplished using a specially designed booster that utilized the hydraulic system as a power source. Intermittent injection performed using a fuel pump with a pulsating feed. It found that the cone angles of the WCS spray increased with increasing injection pressure, while this not observed for diesel fuel. Based on the experimental data, the time required for the cloud front to reach the confining surfaces of the combustion chamber of a high-speed diesel locomotive engine estimated. It found that it took 1.3 ms for the cloud to reach the piston crown and 2.1 ms to reach the cylinder walls. Furthermore, it noted that the spraying quality of the WCS was independent of the coal content in the suspension.

***

Seshadri A. K. et al. (1992) [70] conducted a series of experiments to study aerosols produced by WCS injection using a modified plunger-type system with a diaphragm separator. The injection system consisted of a pump with a pulsating feed, driven by an electric motor. A diaphragm separator used to separate the WCS from the pump and a single-orifice fuel injector. The aerosol injected into a sealed chamber equipped with windows. High-speed filming (11,000 fps) and pressure indication in the system used to study the development of the aerosol plume. This made it possible to determine the time between the start of injection and the onset of breakup of the plume core into individual droplets. For injection pressures of about 30 MPa and higher, the breakup times for WCS, diesel fuel, and water did not differ significantly. The time to flame core disintegration increased with increasing nozzle orifice cross-section and decreasing gaseous medium density into which the fuel injected. The spray cone angles depended on operating conditions and liquid properties, as well as the time and location of the measurement.

***

In 1992, Callahan T. J., Ryan T. W., et al. investigated the spray characteristics of several WCS types used by Cooper-Bessemer in their medium-speed engine development program [57]. The injection pressure range was 40...140 MPa. A high-pressure continuous spray system used for the experiments, spraying through orifices of various shapes and sizes into a continuous, high-density airflow. Detailed spray characteristics obtained, including changes in aerosol size and spray cone angles.

The penetration velocity and spray cone angles were also measured using intermittent injection into a stationary compressed gas environment. It found

that for diesel fuel, the cone angles remained relatively constant with increasing pressure, while for WCS they increased. The mixing ratios of WCS and diesel fuel increased rapidly with increasing pressure, but even at the same high injection pressures, WCS mixed with air less intensely than diesel fuel. All other factors being equal, WCS sprayed more narrowly and penetrated faster than diesel fuel. Significantly increasing the injection pressure allowed WCS to achieve the desired spray quality, while increasing diesel fuel injection pressure improved spray quality less rapidly. WCS droplets had larger average sizes than diesel fuel droplets in all cases, but by varying the nozzle orifice shape; average sizes comparable to those of diesel fuel achieved. Changing the orifice shape to converging or diverging had minimal impact on the spray characteristics.

***

Kim K. D., Terracina D. P., and Caton J. A. (1993) [58, 61] conducted an experimental study of the formation of WCS aerosols produced by an electronically controlled accumulator injection system. For this study, a special synchronization system developed that allowed the use of a laser diffraction technique to analyze the structure of the spray cone as it evolved. This technique made it possible to measure the average Sauter diameter of fuel droplets at the boundary of the aerosol front, as result of which it was possible to minimize the error due to scattering shift. WCS with a 50% coal content weight and an average particle size of 5 μm was injected into a chamber with optical access at a pressure of 28...110 MPa through replaceable nozzle tips with orifice diameters of 0.2 and 0.4 mm. Measurements were conducted in four planes perpendicular to the spray axis and located 60...120 mm from the nozzle orifice. Injection was performed into a nitrogen atmosphere under atmospheric pressure and a pressure of 2,0 MPa. The results showed that the average aerosol droplet diameter increased with distance from the nozzle orifice and with increasing gas density, and decreased with increasing injection pressure. Based on the obtained data, a correlation created to determine the average droplet diameter of WCS. A similar study, using the same experimental equipment, subsequently conducted for diesel fuel [60]. The results showed that diesel fuel aerosols, under identical injection conditions using an accumulator system, had smaller droplet diameters than WCS aerosols. Therefore, it concluded that increasing injection pressure is the primary factor in improving WCS spray quality.

***

In 1999, N.A. Ivaschenko and L.V. Grekhov published the results of research conducted at the Piston Engines Department of Bauman Moscow

State Technical University on the spraying of coal suspensions [14]. The research conducted using two independent methods: a classical method using a smoked plate; and a laser diffraction (small-angle scattering) method based on the differences in light diffraction as it passes by droplets of different sizes. The first method utilized glycerin-coated histological plates, which passed once past the measurement zone near a continuously operating nozzle. The plates then photographed under an optical microscope at a magnification of 120:1. Negatives printed at an additional magnification of 12:1 and processed manually.

The second method utilized a relatively new method of laser diffraction for studying the dispersion and concentration of atomized media. This method is applicable to opaque liquids such as FCS and WCS. This type of measurement is insensitive to the velocity, distribution of aerosol droplets, physicochemical, or other properties of the sprayed liquid. The experiments conducted on a setup developed at the Faculty of Specialized Mechanical Engineering at Bauman Moscow State Technical University. Due to the rapidity and non-reproducibility of the process, multichannel measurements performed synchronously. Good quantitative characteristics of the scattering indicatrix in transmitted light obtained diffraction of a plane monochromatic wave. The source was an LG-52-1 continuous-wave helium-neon gas laser with a power of 8 MW, generating radiation with a wavelength of $\lambda = 0.6328$ μm. Each experiment processed 300…500 time points.

The test cycle consisted of single-factor experiments for individual parameters. The average jet velocity ranged from 85 to 215 m/s, achieved by varying the average injection pressure from 9 to 59 MPa (maximum pressure, 13 to 90 MPa). The nozzle diameter varied from 0.25 to 0.5 mm, and the normal viscosity of the suspension estimated using a capillary viscometer and ranged from 26 to 800 mm^2/s. The measurement zone was located at a distance of 50 to 150 mm from the nozzle tip. The mass concentration of the solid phase in the suspensions ranged from 22 to 50%. Brown coal dust with a maximum particle size of 9 μm was used for the WCS, while coal dust with a maximum particle size of 15 μm was used for the FCS.

Differences in the results of both measurements, up to 18%, were comparable to instrumental and methodological errors, which estimated at 6 to 10% for both methods. The study showed that, under equal fuel delivery conditions, droplets produced by the FCS injection system are significantly larger. Thus, when injected at a maximum pressure of 80 MPa through 0.3 mm nozzles at a temperature of 70°C into air at a pressure of 10 MPa and a temperature of 700°C, diesel fuel droplets had an average size of 18.9 μm. For the FCS injection system with a mass filling of 50% under the same

conditions, the average droplet diameter was 26.6 μm. Analysis of the results showed that increasing the injection pressure, rather than reducing the nozzle diameter, is more effective in improving spray quality. Thus, the results of this study are in good agreement with the results obtained by Kimm K.D., Terrasina D.P., and Caton J.A., as well as Callahan T.J., Ryan T.W.

4.4. Coal suspension injection process.

In modern diesel engine fuel systems, liquid fuel supplied to the sprayer under pressure is the primary source of energy required to generate an aerosol.

Spraying is the result of the interaction of the liquid jet with the walls of the sprayer channel and the surrounding gaseous medium. This interaction creates velocity differences between individual layers of the liquid flow, ultimately breaking the flow into individual droplets.

For liquid injectors, spray quality depends on the sprayer design, fuel properties, and injection pressure. Furthermore, in diesel engines, fuel injected into a limited combustion chamber, where the airs charge is at a high temperature and under a pressure of 2…3 MPa. These factors further influence the spraying quality of liquid fuel.

Compared to DF, suspensions, especially water-coal suspensions, have a higher density. Furthermore, for almost all suspensions, viscosity is more dependent on shear rate than is observed for DF. Differences in physical properties are the main factors influencing the differences in injection patterns between DF and WCS.

4.4.1. Formation and development of the spraying plume and stages of the injection process. Fig. 4.21 and 4.22 show eight high-speed movie frames each, tracing the development of the spraying plume cone for WCS and DF, respectively, during a single injection [70]. A water-coal fuel suspension produced Otisca used. It contained 50% bituminous coal (by weight) with an average particle size of 3 μm, 48% water, 1% lignosulfonate, and 1% Triton X-114 additive. The fuel atomized through a 0.4 mm hole diameter in the sprayer at full flow. The nitrogen density in the experimental chamber was 25 kg/m^3. A Bendix pulse feed fuel pump was used to deliver fuel at a pressure of 70 MPa, with a drive shaft speed of 525 min^{-1}. The experimental setup simulated the operation of the fuel injection system in a high-speed diesel locomotive engine under full load [52, 53].

For film analysis, markers placed on the left side of each image, spaced 50 mm apart. The photographs show that the general patterns of aerosol formation are similar for WCS and DF, but the light diesel fuel aerosol is wider and somewhat more stable. For approximately the first 0.6 ms, the

spraying front propagates through the gaseous medium as a virtually uniform flow. This time represents the penetration period of the spray core.

After this initial period, the liquid core begins to disintegrate, with the detachment of small fuel droplets, resulting in the formation of an aerosol around the core. From the moment the dispersion disintegration of the spraying core begins, the formation of the main vortex begins.

The photographs show that, under the given conditions, 0.68 ms is required for the WCS spraying core to begin dispersion disintegration, while 0.82 ms is required for DF. The size of the main vortex then increases as the sprayer delivers new portions of fuel, and as the main vortex penetrates the gaseous medium. The last two frames in each figure show fully formed spray plumes for WCS and DF. These fragments clearly demonstrate the difference between the plume structure and aerosol formation for these fuels.

Analysis of the photographs, as well as the results of other spraying studies, including those with continuous injection, showed that, compared to DF, fuel-air mixing in WCS, determined by the cone-opening angle, proceeds more slowly [57].

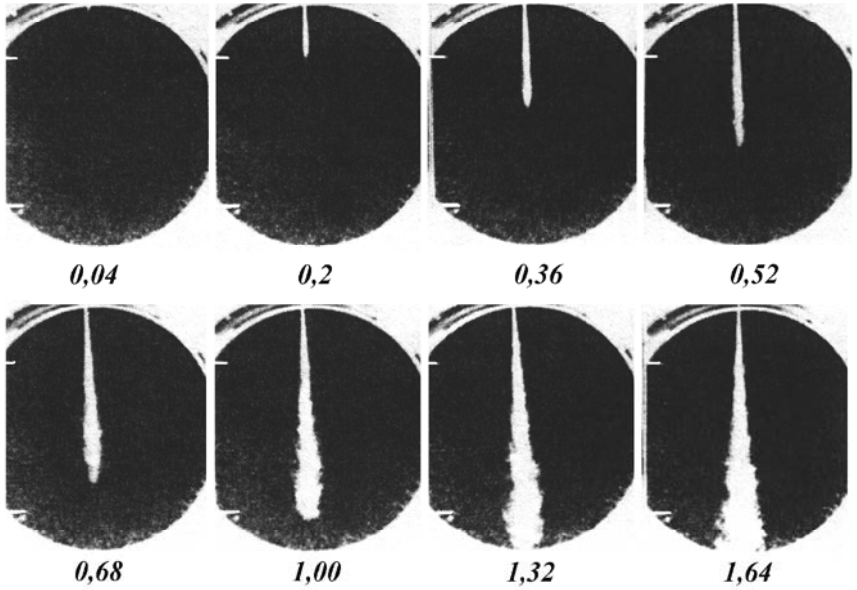

Fig. 4.21. Development of the WCS spraying plume one injection (numbers indicate time from the start of injection, ms) [70]

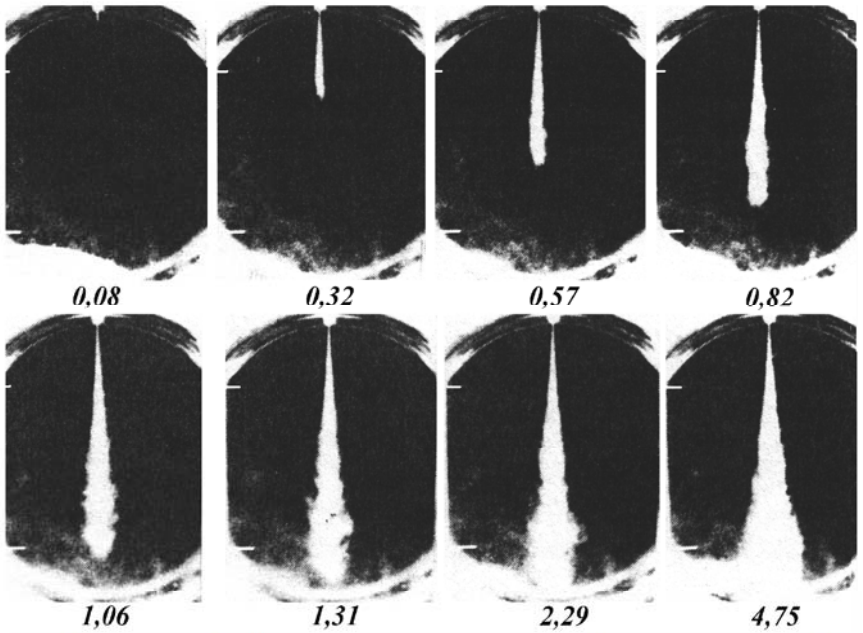

Fig. 4.22. Development of the DF spraying plume one injection (the numbers indicate the time from the start of the injection, ms) [70]

To analytically determine the plume core penetration distance and the period before its decay, the relationship proposed by Arai M., Tabaia M., et al. was used in [70].

This model allows one to determine the plume penetration parameters based on instantaneous pressure values in the fuel line. In general, this relationship expressed as follows:

$$\text{for } 0 < t < t_b,\ s = 0{,}39\left(\frac{2\Delta P}{\rho_t}\right)^{0,5} \times t, \tag{4.1}$$

$$\text{for } t > t_b,\ s = 2{,}95\left(\frac{\Delta P}{\rho_a}\right)^{0,25} \times (d \times t)^{0,5}, \tag{4.2}$$

$$t_b = 28{,}65\frac{\rho_t \times d}{(\rho_a \Delta P)^{0,5}} \quad . \tag{4.3}$$

To determine the distance from the tip of the sprayer to the localization of the plume where the decay of the nucleus begins, the work [61] proposes to use the expression:

$$L_b/d=15{,}8(\rho_t/\rho_a)^{0,5}, \qquad (4.4)$$

for *s* – локализация фронта факела; ΔP – difference between the pressure in the fuel line and the pressure in the combustion chamber; ρ_t – fuel density (for DF – 850 kg/m^3, for WCS – 1250 kg/m^3); t – time from the start of injection; ρ_a – gas density in the combustion chamber; d – diameter of the nozzle hole; t_b – time until the onset of dispersion.

This model developed for light DF, but when substituting the WCS density value, it yields results that agree well with the experimental results. For practical calculations, the power function can replaced with two linear relationships. Fig. 4.23 shows experimental data on fuel front penetration as a function of time for four sequential injections.

The dashed line represents the calculated relationship obtained from the equations above. The penetration patterns for all four cases are in good agreement with each other and with the calculated results.

Two main stages of fuel plume development can distinguished. The first stage is penetration of the unatomized liquid core, and the second is the disintegration of the liquid core to form an aerosol. For constant pressure in the supply line, fuel plume penetration is linear with time. This stage shown in Fig. 4.23 by the dashed line, for which the proportionality coefficient is equal to unity.

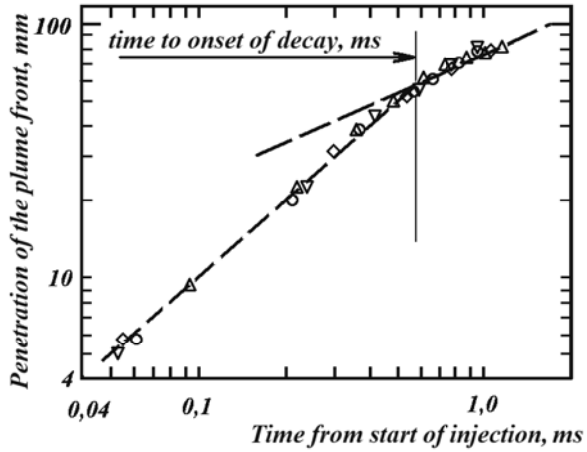

Fig. 4.23. WCS plume front penetration as a function of time (the data presented were obtained for four consecutive injections)

The second stage is aerosol formation and the onset of dispersed disintegration of the liquid core. For this stage, penetration is proportional to time as half the jet energy. In Fig. 4.23, the dotted line with a proportionality coefficient of 1/2 represents this period. The intersection of these two lines marks the onset of dispersed disintegration of the jet. For the case under consideration, this time was 0.58 ms for WCS and 0.50 ms for DF.

Research has shown that, despite significant differences in physical properties, under identical conditions, different liquids atomize in a gaseous medium according to very similar patterns. Fig. 4.24 shows the dependence of spraying plume penetration on time for WCS, DF, and water. The dotted line represents the dependence obtained analytically. The figure shows that the nature of fuel plume development for all three liquids is in good agreement with a power law, although detailed differences in plume formation do exist. In particular, the initial flow velocity of the WCS jet, under equal injection conditions, is 15% higher than for DF, and its dispersion time is 0.08 ms longer.

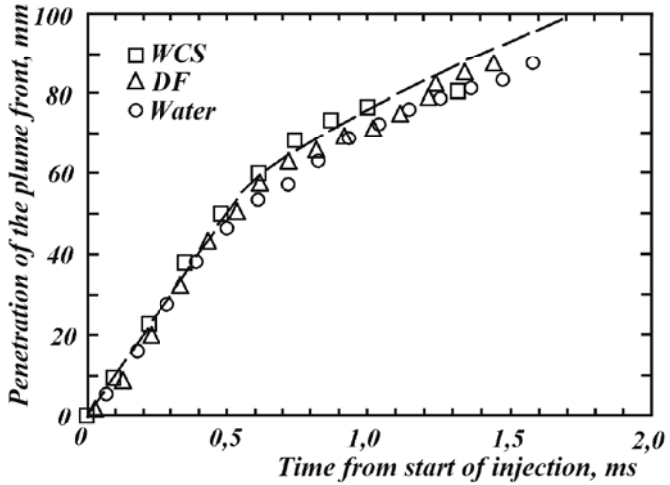

Fig. 4.24. Spray penetration as a function of time for different liquids

Studies of WCS flame development with different carbon particle concentrations also confirm the above conclusions. Fig. 4.25 shows the dispersion period as a function of carbon content for two nozzle orifice cross-sections. For WCS with different carbon contents, the time to dispersion onset varies slightly. On average, for all cases, it is within 0.55 and 0.85 ms for hole diameter of 0.4 and 0.6 mm, respectively.

Fig. 4.26 shows a model of WCS flame propagation in the combustion chamber of a General Electric 7DFL high-speed diesel locomotive engine at maximum flow rate.

This model based on electron microscopic analysis of photographs documenting aerosol development. The aerosol front is shown in the figure by lines. Each subsequent line characterizes the flame front position with a time interval of 0.101 ms. The maximum error in determining the front position does not exceed 5%. The flame development pattern shown in Fig. 4.26 is modelled taking into account the shape of the engine combustion chamber, into which the WCS is injected at an angle of 15° to the piston plane.

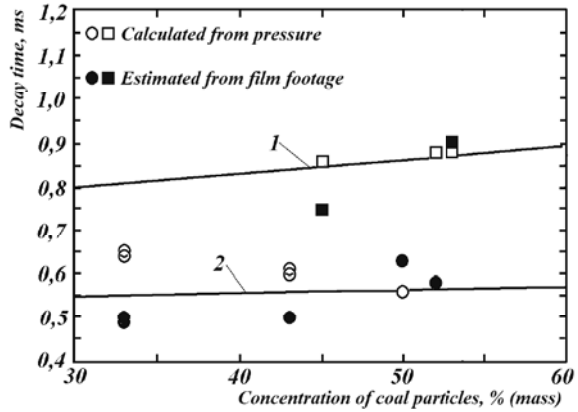

Fig. 4.25. Time to the onset of dispersion decay of the plume core as a function of the solid phase content for two spray nozzle cross-sections. 1 – hole diameter 0.4 mm; 2 – hole diameter 0.6 mm (gas medium density 25 kg/m^3)

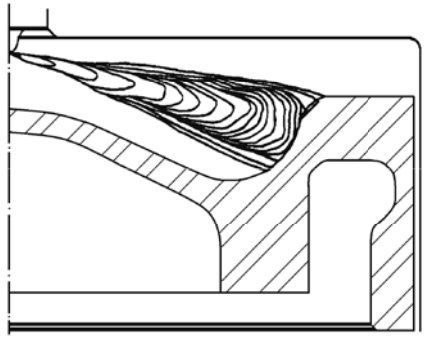

Fig. 4.26. Development of the WCS plume in the combustion chamber of a high-speed diesel locomotive engine

The figure shows that, for the case under consideration, the fuel plume will reach the piston crown approximately 1.5 ms after the start of injection. However, studies on the ignitability of water-coal fuels indicate that typical self-ignition delays for the conditions under consideration exceed 1.5 ms [71, 73]. Thus, the fuel plume will reach the piston walls before the fuel ignites. Therefore, secondary disintegration of the plume upon impact with the combustion chamber surface has a significant impact on the combustion efficiency of WCS. The influence of secondary disintegration on the combustion characteristics of WCS will discussed in more detail below.

4.4.2. Spray characteristics and aerosol droplet structure. The primary indicator of spraying quality for the average diameter of the aerosol droplets formed during injection. Droplet size has the most significant impact on the ignitability and completeness of the suspension burnout.

The most common criterion for assessing the average diameter of a suspension droplet is the Sauter method. The Sauter average diameter (SAD) defined as the size at which the volume-to-surface ratio of all measured droplets equals the average droplet size ratio. To estimate the SAD based on measurement results, the following relationship is used:

$$d_{32} = \left(\sum_i N_i D_i^3\right) / \left(\sum_i N_i D_i^2\right).$$

Unlike DF aerosols, suspension aerosol droplets have a heterogeneous structure, as they consist of components in different phase states. Using WCS as an example, we will examine the structure of a droplet of this type of aerosol. Each droplet consists of loosely packed elementary carbon particles (typically 3…5 μm in size for a high-speed engine) surrounded by a water carrier (Fig. 4.27). Water also fills the pore space of the carbon particles. A liquid film layer forms around the mass of carbon particles under the influence of surface tension. The ratio of intermediate and film water in the droplet determined by the packing coefficient, which is a function of the average size of the carbon particles. Depending on the particle size, concentration, and fuel spraying quality, the number of elementary particles in an aerosol droplet can vary widely.

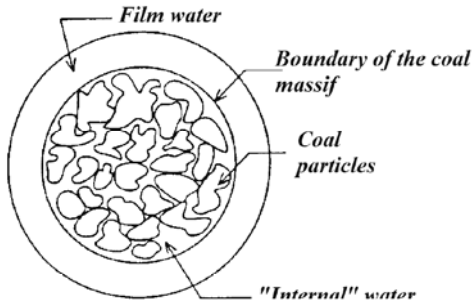

Fig. 4.27. Structure of a WCS aerosol droplet [65]

Suspension droplets with other liquid carriers have a similar structure.

Due to the structural features of aerosol droplets, the spraying patterns of coal suspensions are different from those of traditional fuels. Based on measurement data using the smoked plate method and the laser diffraction method, Grekhov [9, 14] obtained a criterion relationship for the SAD of coal suspension droplets:

$$d_{32}=495\times(\rho_a/\rho_{cs})^{0,286}\times x^{1,521}\times d_h^{0,152}\times v_{cs}^{0,44}\times U_f^{-1,2}, \quad (4.5)$$

for ρ_a, ρ_{cs} – the density of the charge and the coal suspension, respectively; v_{cs} – the viscosity of the coal suspension; x – the distance from the nozzle; d_h – the diameter of the nozzle hole; U_f – the fuel flow velocity.

Based on the data from a study of WCS injection under conditions typical of a high-speed diesel locomotive engine, a correlation of the expression for SAD for intermittent WCS spraying using an accumulator injection system performed using the regression method [61]. Because of the correlation, the expression took the form:

$$d_{32}=0,279\times\Delta P^{-0,702}\times\rho_a^{0,285}\times x^{1,521}, \quad (4.6)$$

for ΔP – injection pressure ρ_a – charge density; x – measurement location; d_{32} – SAD.

For the conditions studied, the calculation results obtained using expression (4.6) are in good agreement with the experimental data over the entire parameter range (pressures ranging from 28 to 110 MPa, gas densities from 1.2 to 25 kg/m^3, and measurement locations from 60 to 120 mm from the sprayer tip). Clearly, the expressions presented are not universal. For other spray conditions and for other types of suspensions, the correlation coefficients should be refined.

Analyzing expressions (4.5, 4.6), it should be noted that the spray quality strongly depends on the distance to the nozzle x_c, which is stronger than that observed with DF. Clearly, during DF injection, the processes of secondary droplet fragmentation and their consolidation have the same order of magnitude of velocity. The significant coarsening of droplets along x_c can be explained by the high viscosity and non-Newtonian properties of WCS, i.e., the preservation of consolidation while suppressing wave processes and secondary breakup processes [14]. In addition, other factors can influence aerosol formation, particularly the need to expend energy during the spraying process to separate closely packed particles in a relatively viscous mixture. This property is somewhat similar to surface tension and can cause a decrease in the WCS cone angle and the formation of larger droplets. It is also significant that water has approximately three times higher surface tension than DF, which also affects the quality of the WCS spray [57].

The factor limiting the size of aerosol droplets is the size of the carbon particles in the suspension. When spraying WCS, one of which contained 98% of particles no larger than 44 μm, and the other no larger than 15 μm, at the same injection pressures, the suspension containing the smaller particles always formed smaller droplets [57].

4.4.3. Change in average particle size along the spraying plume length. Fig. 4.28 shows, at an arbitrary scale, the particle size distribution determined by laser diffraction, which relies on the difference in light diffraction as it passes by droplets of different sizes. This measurement method allows one to determine the SAD of droplets based on the integral scattering characteristics. In this case, the measurement scale can eliminated, since calculating the SAD only requires finding the ratio between the light fluxes.

Fig. 4.29 shows the change in SAD of WCS and DF droplets at the boundary of the spray front for axial measurement locations from 40 to 140 mm from the nozzle tip. The dependences obtained for an injection pressure of 83 MPa, a gas density of 25 kg/m^3, and a nozzle hole diameter of 0.2 mm. Fig. 4.28 and 4.29 demonstrate that the SAD of droplets increases as the spray front penetrates the gas medium. Moreover, the increase in SAD of WCS droplets is more intense than that of DF droplets (Fig. 4.29).

For diesel fuel, the relationship between the measurement localization and SAD is practically linear (the exponent of the measurement localization component x_c in expression (4.6, 4.7) is approximately 0.9 [60]).

The exponent of the measurement localization component x_c for WCS aerosols is 1.521.

Therefore, the increase in SAD as the flame develops occurs more rapidly than for DF.

This difference in size distribution along the plume length explained by several factors:

– larger droplets carry a higher momentum and, consequently, have greater inertia, which means they penetrate deeper than smaller ones;

– even with equal sizes, CS droplets have a higher density, resulting in an inertia approximately one and a half times greater than that of DF droplets at the same injection speed;

– small droplets are relatively quickly decelerated by the gas flow, lose momentum, and lag behind larger droplets;

– as the plume front advances, some of the smaller droplets coalesce, leading to an increase in SAD at locations farther from the sprayer tip;

– the high viscosity and non-Newtonian properties of CS help suppress wave processes that impede consolidation and cause secondary droplet disintegration.

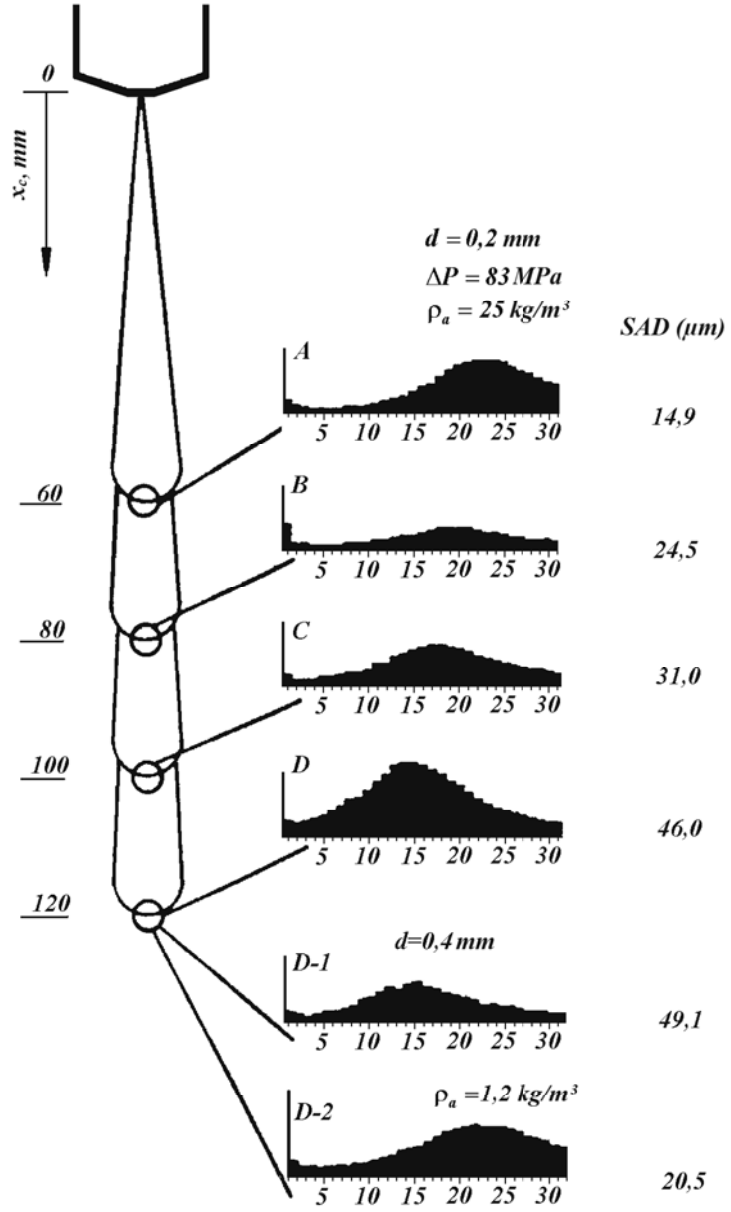

Fig. 4.28. WCS aerosol droplet size distribution for different measurement locations

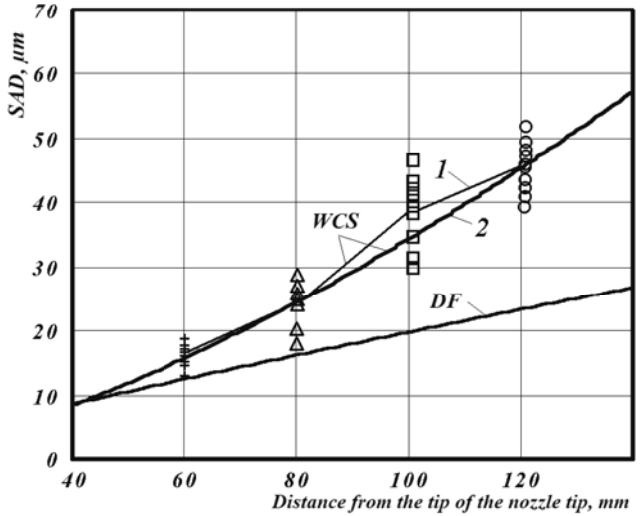

Fig. 4.29. Effect of measurement localization on the SAD of WCS and DF aerosol droplets (d_c=0.2 mm; ρ_a=25 kg/m^3; ΔP=83 MPa) [61, 70]. 1 – experimental dependence (line connects average values for a series of measurements); 2 – calculated dependence

4.4.4. Changing the spray cone angle. The CS aerosol plume does not have a clearly defined boundary surface, so there is no standard procedure for measuring its cone angle. One approach to determining the plume angle is to find the arc tangent of the half-width of the aerosol plume, measured from the centerline at the measurement location [57, 70].

Studies of continuous WCS spraying into a chamber with increased air density have shown that at pressures typical for DF injection, the development patterns of WCS and DF plumes differ significantly. While DF spraying produces a cone-shaped plume with nearly straight edges, WCS spraying produces a plume with slightly smaller initial cone angles than DF. Subsequently, as the WCS plume develops, the generatrix bends inward until it becomes nearly parallel to the plume axis (Fig. 4.30) [57]. As a result, the width of the WCS spray near the piston edge is narrower than that calculated from the initial opening angle at the spray tip.

The cone angle significantly affects the efficiency of air-fuel mixing: larger angles indicate more intense air-fuel mixing, while smaller angles imply poorer mixing. Air-fuel mixing is proportional to the spray cross-sectional area and approximately proportional to the cone angle. Therefore, WCS sprayers have significantly less efficient mixing in the spray pattern than DF sprayers.

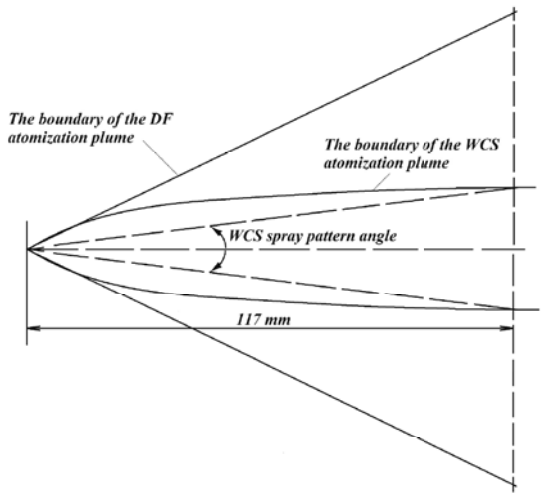

Fig. 4.30. Scheme of WCS and DF aerosol plume development and determination of cone opening angle during continuous spraying

Fig. 4.31 shows the change in spray angles for two types of WCS and DF sprayers. The cone angles for WCS sprayers are approximately 4 times smaller than for DF sprayers (Figs. 4.30, 4.31). This decrease in cone angle reduces the air-fuel ratio in the spray pattern by approximately 16 times. This indicates that, when spraying with WCS sprayers, the air charge not used efficiently by the time the spray front reaches the piston crown. It is noteworthy that the spray cone angles of the WCS spray pattern increase rapidly with increasing injection pressure, while the spray cone angles for DF are virtually independent of pressure. Thus, for sufficiently high injection pressures, WCS spray angles comparable to DF spray angles can achieve.

Benson et al. (1991) also noted a strong dependence of the spray angle on the WCS injection pressure. The cone angle can vary from 1° to 10°, depending on the pressure in the fuel supply system.

The increase in WCS cone angles with increasing injection pressure explains the need to increase the pressure supplied to the sprayer when using water-coal fuel. It also noted that suspensions with a higher solids content and higher viscosity in all cases exhibited smaller cone angles than WCS with a lower solid content and, consequently, lower viscosity.

Fig. 4.32 shows the change in cone angle as a function of time after the start of injection for WCS and DF aerosols formed at a relatively high injection pressure (70 MPa). This study used WCS with a 50% mass content of coal particles with an average particle size of 5 μm.

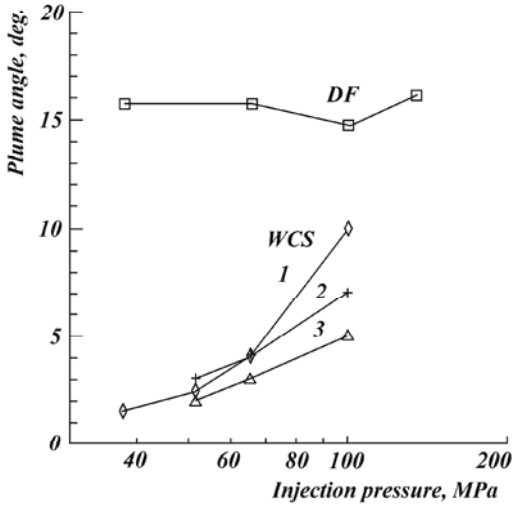

Fig. 4.31. Comparison of the spray cone angles of WCS and DF at different injection pressures. The mass content of solid particles and the average size, respectively, are 1 – 52%, 15 μm; 2 – 52%, 5 μm; 3 – 54%, 5 μm (nozzle hole 0.3 mm, air pressure 0.86 MPa, temperature 35°C)

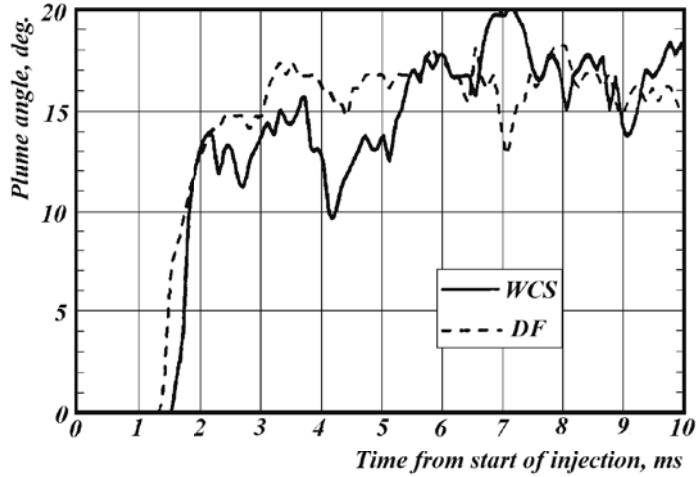

Fig. 4.32. Change in the plume angle of the WCS and DF plume (ρ_a=25 kg/m^3; x_c=80 mm) [55]

Aerosol cone angles were determined by analyzing high-speed film frames. A distance of 80 mm (200 times the nozzle orifice diameter) from the

nozzle tip chosen as the measurement location. This choice made to obtain an idea of the spray development as close as possible to the near-wall region. For diesel locomotive engines, this distance is typical for the piston crown. The spray front reaches this location approximately 1.3 ms after the start of injection. Within the next 0.5 ms, the cone angle at this location rapidly increases. During the period between 3 and 10 ms, the time-averaged cone angles for DF and WCS are within 16.3° and 15.9°, respectively. A similar result obtained for a measurement location of 60 mm (150 nozzle orifice diameters); in this case, the time-averaged cone angles for DF and WCS were 17.0° and 16.4°, respectively.

Other researchers (Seshadri et al. 1991) indicate the formation of narrower aerosol plumes under similar conditions, with time-averaged cone angles of 11.2° and 13.0° for WCS and DF, respectively. These discrepancies may be due to differences in the methodology used to estimate this parameter.

The results presented above confirm that at high injection pressures, the cone angle for WCS and DF differs only slightly. The influence of spray angle on mixture formation quality clearly demonstrated in Fig. 4.33.

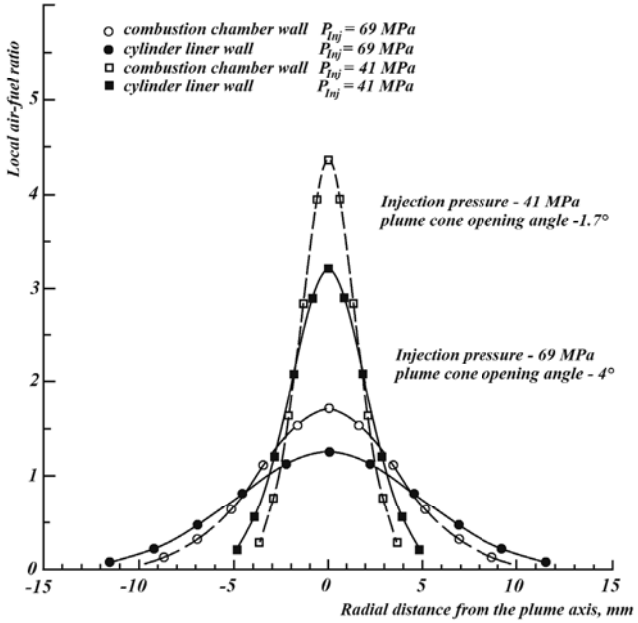

Fig. 4.33. Distribution of local air-fuel ratio in the WCS plume cone depending on pressure and localization

Fuel-air mixing within the spray plume determined the local air-fuel ratio.

$$air\text{-}fuel\ ratio = \frac{(fuel/air)_{available}}{(fuel/air)_{stoichiometric}}$$

At low injection pressures, the cone angle for WCS is so small that the air-fuel mixture is too rich to ensure efficient and complete combustion in many parts of the flame, even near the cylinder wall [57].

As can be seen from Fig. 4.32, the cone angles for both fuels are not steady over time. Several frequencies of different origins can identified within the entire spectrum of oscillatory processes occurring in the spray jet flow. High-frequency oscillations (between 5000 and 10000 Hz) observed due to the finite frame rate of high-speed filming.

Lower frequencies (approximately 600 Hz) arise from the dynamics of the sprayer needle or flow instability during spraying, as well as pressure fluctuations in the fuel supply line. For example, at a WCS injection frequency of 8.8 Hz, the pressure fluctuation is approximately 300 Hz.

It also noted that increasing air density leads to increased cone opening angles and a decrease in the WCS spray penetration velocity. For example, at air densities of 8 kg/m^3, 16.1 kg/m^3, and 24.1 kg/m^3, the initial cone angles for a 0.3 mm hole nozzle tip were 6.2°, 8.4°, and 10.0° (DF at 16.1 kg/m^3 yielded a cone angle of 13°). The differences in cone angles between WCS and diesel fuel recorded for intermittent tests were smaller than those continuous spraying. This is because the cone angles for intermittent injections were initial cone angles, while for continuous injection, measurements were made at a location 117 mm from the nozzle tip [57].

4.5. Factors affecting CS spraying quality.

Table 4.4 presents the SAD measurement results obtained for a accumulator injection system similar to that used on General Electric engines [60]. Injection control performed electronically. The injection duration in all cases was 5 ms. Each experiment was repeated 15 times, after which the obtained results were statistically processed. For comparison, Table 4.4 presents the SAD measurement data for DF.

Studies have shown that, with the same injection parameters, droplets of coal suspensions are significantly larger than those DF. This particle distribution pattern is the result of the combined effect of several factors, which together determine the nature of aerosol formation. The main factors include: injection pressure, distance from the nozzle tip to the measurement location, gas density, nozzle orifice diameter, needle lift speed, etc.

Table 4.4.

Results of SAD droplet measurements for DF No. 2 and WCS with an average particle size of 5 µm and a mass concentration of 50%

Hole diameter, mm	Fuel injection system pressure, MPa	Density of gas environment, kg/m³	Measurement localization, mm	Average diameter according to Sauter, µm	
				WCS	DF
0.4	83	25	120	49.15	25.40
0.2	83	25	120	47.22	23.28
0.4	28	25	120	92.50	39.19
0.4	55	25	120	66.89	27.10
0.4	110	25	120	31.85	—
0.2	83	1.2	120	19.37	12.67
0.2	83	25	60	15.94	12.39
0.2	83	25	80	23.81	16.33
0.2	83	25	100	38.30	20.96

The nature of the influence of some of the listed factors on the quality of suspension spraying is shown in Fig. 4.34. The presented dependencies obtained as averaged results of experimental studies of CS spraying at atmospheric pressure, conducted in the laboratory of the Piston Engines Department of Bauman Moscow State Technical University. These patterns are in good agreement with the results of other studies, in particular, those presented in Table 4.4. [14]. These dependencies will be examined in more detail below.

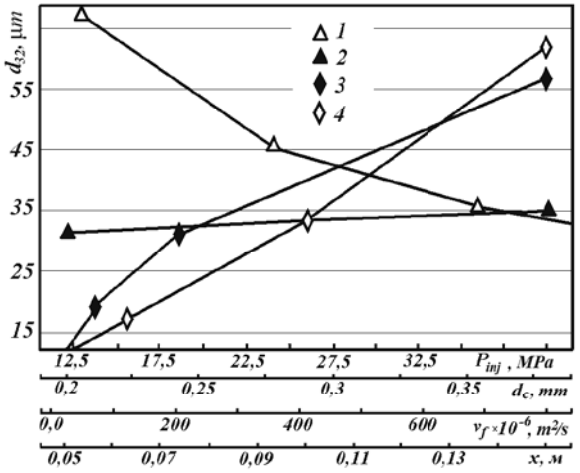

Fig. 4.34. Effect of FCS and WCS droplets on SAD during injection into the atmosphere: 1 – average injection pressure; 2 – injector nozzle diameter; 3 – normal kinematic viscosity; 4 – distance from the nozzle

4.5.1. The influence of injection pressure on the spraying quality of WCS. For WCS, the most important factor affecting spray quality is the increasing dependence of fineness on the fuel jet velocity, which in turn depends on injection pressure (the power of U_c in expression (4.5) for WCS is 1.2, while for DF it is 0.532).

As can be seen from Table 4.4 and Fig. 4.34, with increasing injection pressure, WCS spraying quality improves, resulting in a decrease in the SAD of droplets. For high quality spraying of CS, the injection pressure must be sufficiently high (above 55 MPa), due to its higher viscosity. In other words, CS requires significantly more shear energy to achieve the spraying level characteristic of DF.

This pattern also holds true when using an accumulator injection system. Fig. 4.35 shows the aerosol droplet size distribution and the change in SAD depending on injection pressure (for a measurement location of 120 mm from the nozzle tip).

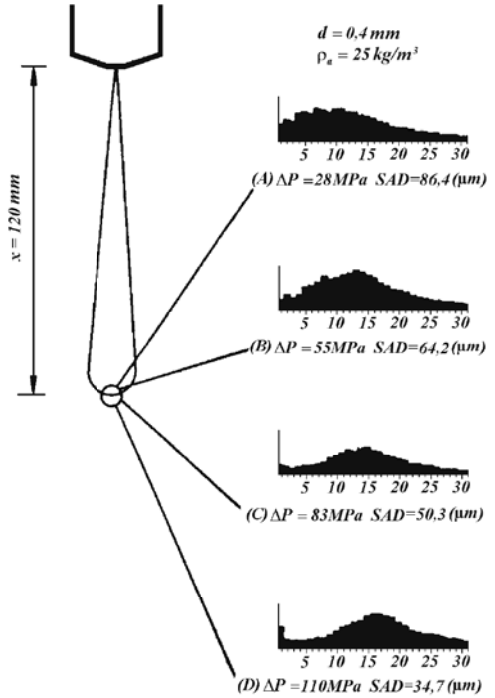

Fig. 4.35. Aerosol droplet size distribution depending on injection pressure for a measurement location of 120 mm

The SAD measurement results presented for pressures of 28, 55, 83, and 110 MPa, while other parameters held constant: the nitrogen density in the chamber maintained at 25 kg/m^3, and the nozzle orifice diameter was 0.4 mm.

Fig. 4.36 shows the calculated dependences of SAD on injection pressure for DF and WCS. The dependence for WCS (line 1) was calculated from expression (4.6), and for DF from the expressions given in [60]. The graph also includes the experimental measurement results obtained in [61]. Line 2 connects the average values for each measurement series.

It should note that at lower injection pressures, the SAD value has a wider spread. This indicates that stable aerosol formation parameters cannot achieve under these conditions. For injection pressures lower than 28 MPa, the accumulator injection system was unable to produce aerosol.

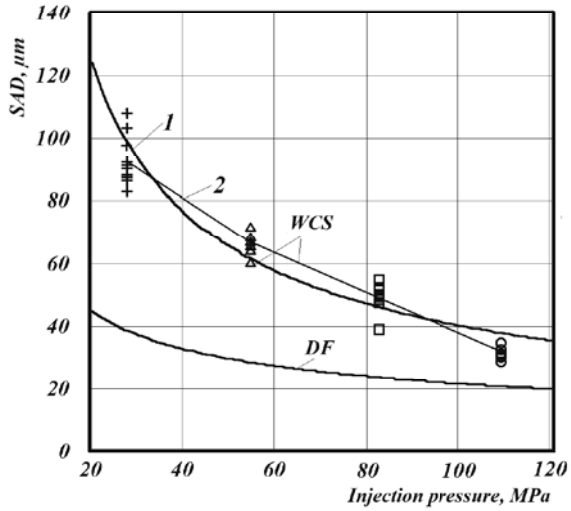

Fig. 4.36. Effect of injection pressure on SAD of WCS and DF aerosol droplets (d_c=0.4 mm; ρ_a=25 kg/m^3; x=120 mm) [59, 61]. 1 – calculated dependence; 2 – experimental dependence (the line connects the average values for a series of measurements)

As noted, the size of the carbon particles in aerosol droplets can be a limiting factor for WCS. This confirmed by the results of a study conducted by Cooper-Bessemer specialists for two types of suspensions with different particle sizes. The first had 98% of particles smaller than 44 μm, while the second had particles smaller than 15 μm. At injection pressures of 55, 69, and 103 MPa, the SAD of the droplets in the first suspension was 51, 55, and

46 μm, respectively. In other words, the droplet sizes were practically comparable to the carbon particle sizes. When testing the second suspension, the SAD of the droplets consistently decreased from 62 to 39 μm with increasing injection pressure. Thus, there a certain maximum pressure at which the droplet sizes and the sizes of the particles in the suspension become practically comparable. A further increase in injection pressure does not lead to an improvement in mixture formation.

4.5.2. The influence of air charge density on spray quality. The gas density significantly influences the WCS spraying process. At low densities, the plume has a high velocity and virtually does not disintegrate within the combustion chamber. At a charge density of 1.2 kg/m^3, the time to disintegration is 3.5 times longer than at a gas density of 25 kg/m^3. The change in the plume-gas interaction mechanism, driven rising gas density, results in an ambivalent effect of backpressure on the WCS spraying fineness. On the one hand, the higher the density, the greater the friction between the gas and the liquid flow. As a result, the velocity difference between the liquid layers increases more rapidly, leading to earlier disintegration of the plume into individual droplets. Consequently, the plume length decreases and the spray fineness increases. On the other hand, a denser environment promotes the stratification of WCS particles by velocity and an increase in the collision frequency, but fails significantly intensify the droplet oscillations that facilitate secondary disintegration.

From Fig. 4.28 shows that as the gas density decreases from 25 kg/m^3 (D) to 1.2 kg/m^3 (D-2), the SAD of WCS aerosol droplets decreases, although the relative number of large droplets in the plume front increases. As a result, the diameter of their bulk approaches the SAD. A gas medium with a higher density slows aerosol penetration and significantly shortens the dispersion length, which is proportional to the square root of the ratio of the gas and suspension densities (4.4). As a result, droplets form earlier and travel a greater distance. These two factors slower penetration and a longer penetration distance lead to the coalescence of small droplets, forming larger ones. Thus, with increasing backpressure, the SAD of WCS droplet increases.

This observation is true for aerosols formed at high injection pressures. For aerosols formed under relatively low pressure, the picture is opposite. At low injection pressure and high backpressure, a decrease in the SAD of WCS aerosols observed. The reason for this aerosol behavior has not yet been clarified.

Fig. 4.37 shows the dependence of droplet SAD on the gas medium density. The tendency for SAD to increase with increasing backpressure more pronounced for WCS aerosols than for DF.

This pattern is a consequence of the higher WCS density, which causes dispersion of the spray core to begin closer to the nozzle tip (4.4). This leads to a longer travel distance for WCS droplets, resulting in some of them coalescing. The experimental results presented here obtained for densities of 1.2 and 25 kg/m^3, corresponding to excess pressures of 0 and 2.026 MPa, respectively.

At high gas medium density, a greater spread of data observed, but the average value of this parameter is in good agreement with the calculated value. At low density of the gas environment, the calculated value has a large error, but considering that the gas density for real engines is quite high, such an error is quite acceptable.

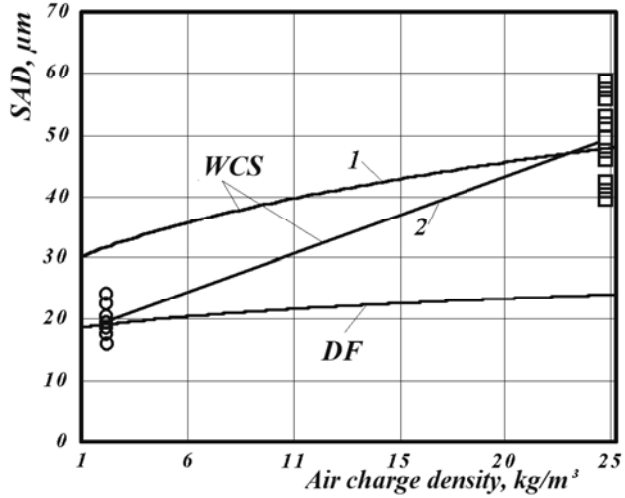

Fig. 4.37. Effect of gas medium density on the SAD of WCS and DF aerosol droplets (d_c=0.2 mm; x=120 mm; ΔP=83 MPa) [59, 61]. 1 – calculated dependence; 2 – experimental dependence (the line connects the average values for a series of measurements)

4.5.3. The influence of the geometric parameters of the sprayer hole on the quality of CS spraying and the characteristics of their combustion. In addition to density, the dispersion period depends significantly on the nozzle holes diameter: the larger the hole, the longer the time before dispersion begins. The relationship obtained for the WCS injection system with pulsating feed between the dispersion period, nozzle diameter, and air charge density shown in Fig. 4.38 (*a*) [70]. Fig. 4.38 (*b*) shows the relationship between the WCS plume core penetration depth and DF before dispersion begins, depending on the nozzle diameter and air charge density. These

relationships obtained for the accumulator injection system with an accumulator located directly in the injector body [61].

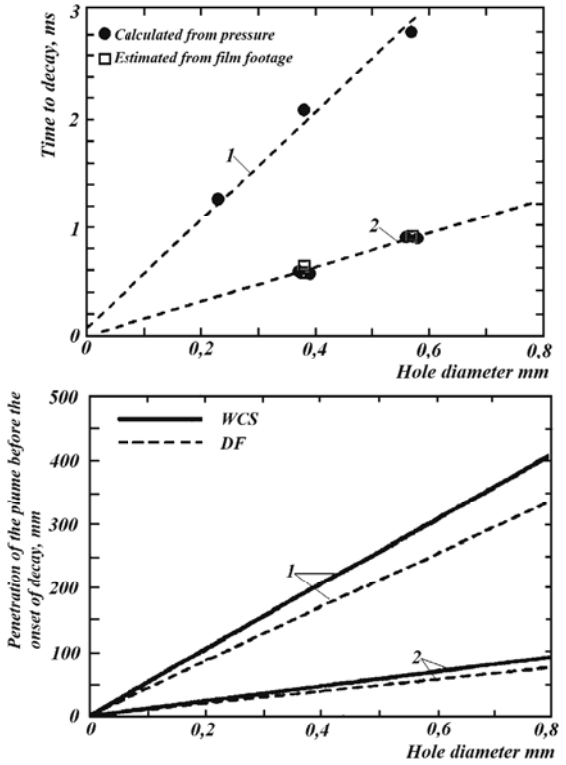

Fig. 4.38. Time (*a*) and distance (*b*) to the initiation of plume core break-up as functions of the nozzle orifice flow area for 50% mass concentration Water-Coal Slurry (WCS). 1 – gas medium density 1.2 kg/m^3; 2 – gas medium density 25 kg/m^3

The presented results demonstrate good agreement between the times to breakup determined using film recording and the analytical estimate based on instantaneous pressure measurements in the fuel line.

Fig. 4.28 shows that with an increase in the nozzle orifice diameter from 0.2 to 0.4 mm, the droplet size distribution (D-1) did not change significantly compared to the distribution (D) obtained at the same location. These results indicate that, within the considered range of orifice diameters, their size has a weak effect on the aerosol droplet size [14, 61]. Fig. 4.28 and 4.39 show that the amplitude of the SAD change for orifices of different diameters differs by only a few percent, which is well within the measurement error.

For high injection pressures, there is no clear correlation between SAD and nozzle orifice diameter. This insensitivity is particularly characteristic of the region of complete breakup of the plume core, located quite far from the dispersion onset point. This observation is consistent with similar results for diesel aerosols, except that under the same injection conditions, DF aerosol droplets are approximately half the size. This pattern explained by the fact that spraying through a small orifice produces aerosol droplets with a smaller diameter, but the dispersed disintegration of the spray core also occurs earlier. This leads to an increase in the hovering time of the droplets, during which they coalesce into larger ones. With larger orifice diameters, dispersion begins later, resulting in a shorter penetration distance and a smaller number of coalesced droplets.

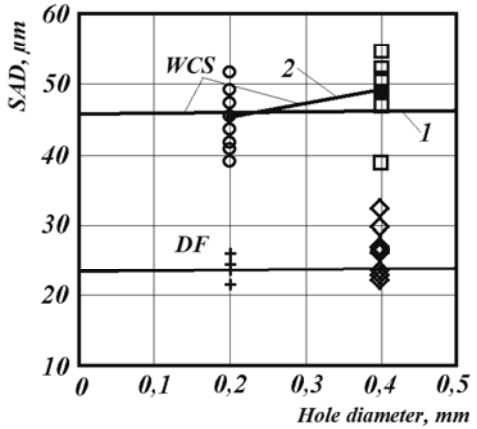

Fig. 4.39. Effect of nozzle orifice diameter on the SAD of WCS and DF aerosol droplets (ρ_a=25 kg/m^3; ΔP=83 MPa; x=120 mm) [59, 61]. 1 – calculated dependence; 2 – experimental dependence (the line connects the average values for a series of measurements)

The relatively weak influence of orifice diameter on WCS spraying quality and fuel plume cone angle, especially at low injection pressures, led to a study of the spray characteristics for twelve different orifice shapes (Fig. 4.40) [57]. The objective of this study was to determine whether, by varying orifice shape, equivalent or larger cone angles and equivalent or smaller average droplet sizes could achieved than with a standard sprayer with 0.3 mm orifice diameters at lower injection pressures. A decrease in pressure would reduce wear in the sprayer passages.

All orifice shapes tested in the pressure range of 20…69 MPa on a DF. Testing all twelve-orifice profiles at three different pressures yielded cone

opening angles ranging from 15…21°, with no significant dependence on orifice shape or injection pressure.

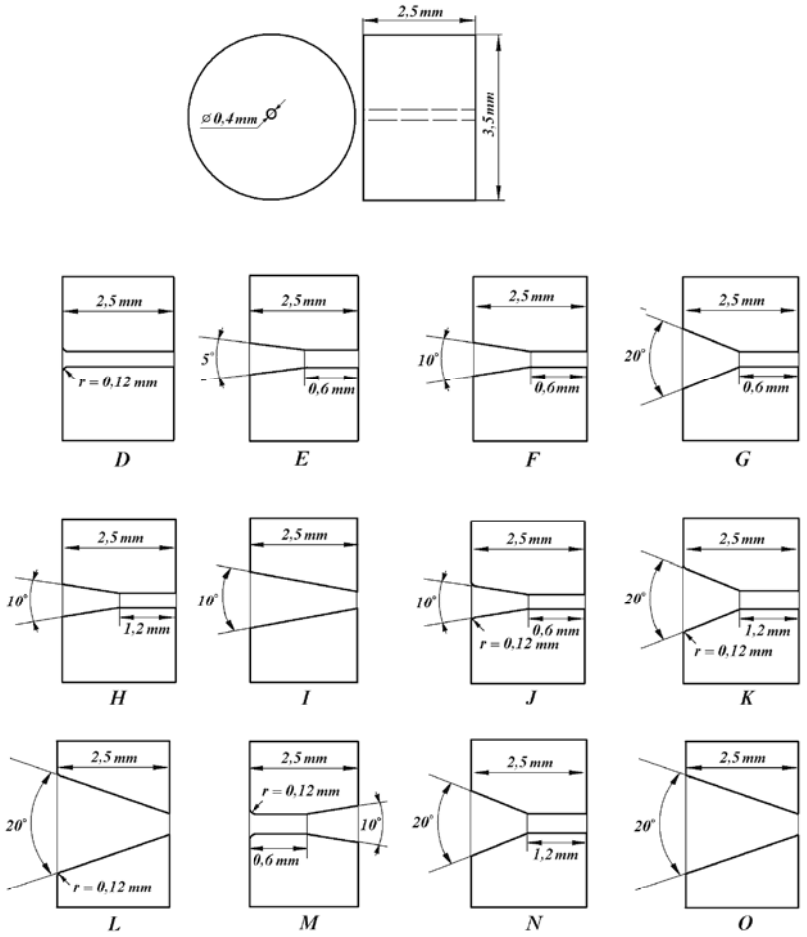

Fig. 4.40. Channel flow shapes tested to determine the influence of channel profile on DF and WCS spraying quality

The standard orifice shape D and three orifice shapes with variable radial cross-sections (G, L, and M) were tested on a WCS with a carbon particle content of 52% and an average particle size of 15 μm. The test results are shown in Fig. 4.41.

Interestingly, the standard D-profile orifice produced a smaller cone angle than other orifice shapes when spraying WCS. Orifice shape M exhibited the

largest cone angle. This difference can explain by a more efficient L/D ratio for this orifice shape.

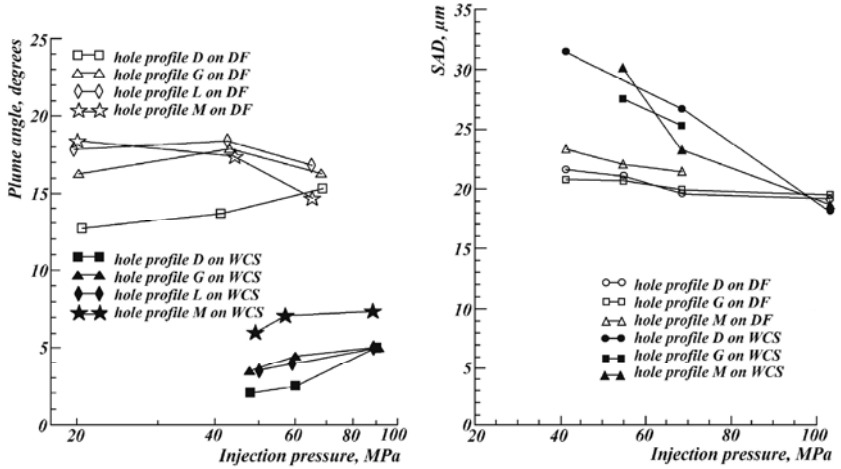
Plume angle, degrees
hole profile D on DF
hole profile G on DF
hole profile L on DF
hole profile M on DF
hole profile D on WCS
hole profile G on WCS
hole profile L on WCS
hole profile M on WCS
Injection pressure, MPa
SAD, μm
hole profile D on DF
hole profile G on DF
hole profile M on DF
hole profile D on WCS
hole profile G on WCS
hole profile M on WCS
Injection pressure, MPa

Fig. 4.41. Effect of nozzle orifice shape on the spray cone angle and SAD of aerosol droplets. WCS with a carbon particle mass content of 52% and an average size of 15 μm

Overall, the study showed that different orifice shapes did not significantly affect WCS spray quality and did not improve it at lower injection pressures. Thus, the concept of reducing orifice channel wear by lowering injection pressure while simultaneously changing orifice shape proved untenable. Of the orifice shapes tested, converging orifices had a slightly larger cone angle than others. No significant change in the reduction of SAD of aerosol droplets also observed.

Influence of the holes nozzle flow coefficient. Although the nozzle orifice shape does not significantly affect spraying quality, the design features of the nozzles still significantly influence engine performance. Fig. 4.42 shows the change in heat generation rate for two types of nozzles with low and high flow rates installed in an accumulator-type injector. Table 4.5 presents the test results for a high-speed 7FDL diesel locomotive engine.

The high-flow-coefficient sprayer had a flow area of approximately 2 mm^2 (12 holes with a diameter of 0.51 mm), while the low-flow-coefficient sprayer had a flow area of 1.2 mm^2 (10 holes with a diameter of 0.39 mm). Fig. 4.42 shows that the heat release profiles for both sprayers are significantly different. When using a high-flow-coefficient sprayer, ignition is preceded by premixing, which results in a very rapid increase in the heat release rate after ignition (the second maximum in Fig. 4.42; the first small

heat release maximum is related to the combustion of the pilot DF). This leads to increased engine harshness and an increased maximum cycle pressure. The low-flow-coefficient sprayer characterized by a diffusion-type combustion, which results in a lower maximum heat release, resulting in a decrease in harshness and maximum pressure, which is most acceptable for a coal-fuel engine. It should also noted that there is a characteristic «protrusion» on the heat release curve between crankshaft rotation angles of 10 and 30 ° after TDC.

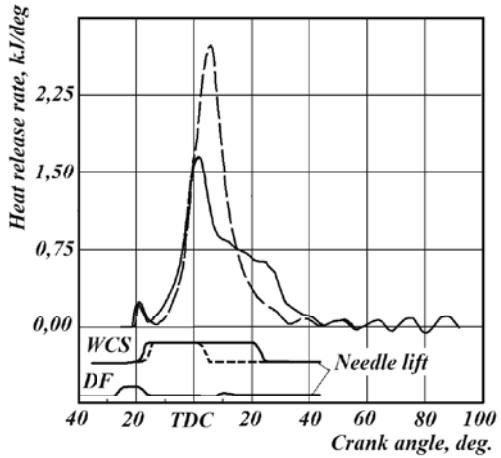

Fig. 4.42. Heat release rate when using two types of sprayers. —— low flow coefficient sprayer; – – – high flow coefficient sprayer (rotation speed 1050 min^{-1}, air temperature and pressure at the inlet 85 °C and 326 kPa)

Table 4.5.

Test results of nozzles with different flow rates

Test conditions					
Injection advance angle. deg.		Injection pressure. MPa		DF. mm^3	Power. kW
DF	WCS	beginning	end		
28	22	67.6	41.8	59	145
28	20	65.4	36.6	62	166
Combustion characteristics					
P_{max}. MPa		Burnout rate. %		Specific heat consumption. kJ/(kW×h)	
15.9		100.0		7853	
17.5		98.8		7918	

The high-flow-ratio injector provided a maximum cylinder pressure of 17.5 MPa. Using a low-flow-ratio injector, the pressure reduced to 15.9 MPa,

which is only slightly higher than the standard value for this engine when operating at DF (15.5 MPa). The decrease in the maximum heat release rate with a smaller injector flow area likely results from the fact that less fuel is in the working cylinder at the time of ignition. The injector needle lift curve shows that for the high-flow-ratio injector, all the fuel has already been injected into the cylinder by the time maximum heat release is reached. For the low-flow-ratio injector, the needle lift curve indicates that only about half of the cycle's supply has delivered to the cylinder. Fuel injected after reaching maximum heat release apparently burns in the diffusion phase, characterized by a lower burn rate. This heat generation is very similar to the result of film combustion (DF), caused by the fuel jet flowing onto the piston crown [55]. However, in the case of WCS, the dependence of the combustion rate on the needle lift time in the fuel injection system more closely indicates volume-diffusion combustion. Taking into account the error in determining incomplete combustion (3...5%), it should be noted that this indicator is virtually identical for both cases. The specific fuel consumption is also very similar. The use of a nozzle with a low flow rate at high injection pressure allows for a reduction in engine thermal stress and cylinder pressure with a sufficiently high burnout coefficient of the coal fuel.

Influence of the shape of the spray channel. When designing sprayers for WCS applications, to achieve the required wear resistance, their tips must be made of super hard materials such as artificial diamond or boron nitride. Since such materials are quite brittle, they must mounted in a metal housing, which imparts rigidity. Fig. 4.43 shows a sketch of a nozzle tip in which a hard insert mounted in a metal housing. This solution necessitates increasing the length of the nozzle channels, which affects the quality of fuel spraying. To reduce the effect of channel length on the spraying process, the outlet from the metal part of the housing is rotated 20...30°.

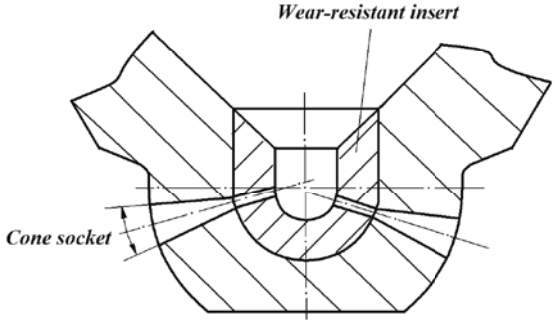

Fig. 4.43. Sprayer with a solid insert

For comparison, these sprayers were tested with an identical thin-walled sprayer without an insert (opening angle of 180°), having 12 holes with a diameter of 0.51 mm. The test results presented in Fig. 4.44 and Table 4.6. The maximum heat stress and burnout completeness for the thin-walled sprayer were much higher, and the specific fuel consumption was much lower than for the sprayer with an expanding channel.

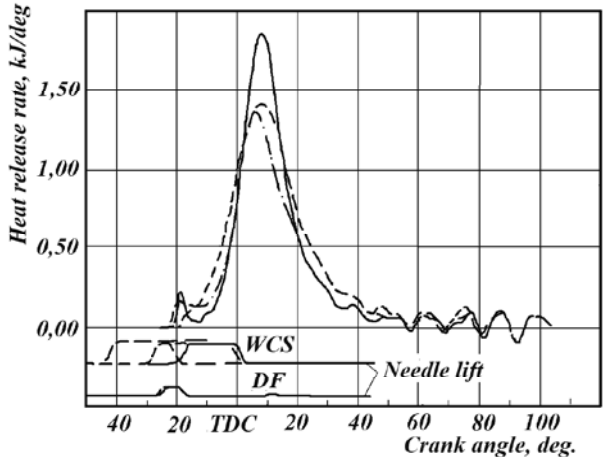

Fig. 4.44. Heat release rate when using thick-walled sprayers. — sprayer with a channel opening angle of 180°; – – – sprayer with a channel opening angle of 30°; – · – sprayer with a channel opening angle of 20° (rotation speed of 1050 min^{-1}, air temperature and pressure at the inlet of 85 °C and 326 kPa)

Table. 4.6.

Test results of sprayers with different outlet opening angles

Test conditions					
Hole opening angles. deg.	Injection advance angle. deg.		Injection pressure. MPa		DF. mm^3
	DF	WCS	beginning	end	
180	28	22	59.9	31.5	69
30	28	33	54.8	24.7	62
20	28	48	58.7	33.2	56
Combustion characteristics					
Hole opening angles. deg.	P_{max}. MPa	Burnout rate. %	Specific heat consumption. kJ/(kW×h)		
180	14.7	92.4	9537		
30	14.8	85.8	7918		
20	13.9	83.4	9570		

Influence of L/D ratio of sprayer channel. Another approach to increasing the wear resistance of the nozzle tip is the use of monolithic hard materials.

Due to the low tensile strength of these materials, the nozzle body is significantly thicker, which leads to an increase in the ratio of the length (L) of the channel to its diameter (D). The heat dissipation characteristics for the accumulator injection system using a sprayer with a high L/D ratio (15.6) shown in Fig. 4.45. Table 4.7 presents the main parameters of the operating process. For comparison, data are also provided for a sprayer with a low L/D ratio (5.6), having the same number of holes of a slightly smaller diameter (0.39 mm versus 0.41 mm).

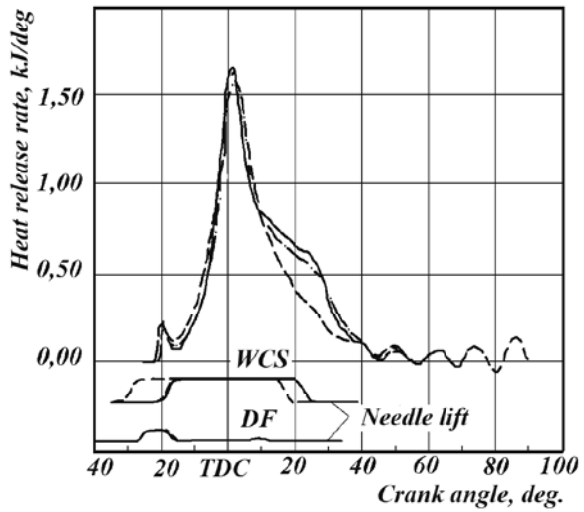

Fig. 4.45. Heat release rate when using thick-walled sprayer. —— sprayer with L/D ratio 5.6; – – – sprayer with L/D ratio 15.6; – · – sprayer with L/D ratio 15.6, operating at elevated pressure (rotation speed of 1050 min^{-1}, air temperature and pressure at the inlet of 85 °C and 326 kPa)

Table. 4.7.

Test results of a sprayer with different L/D ratios

Test conditions					
L/D ratios	Injection advance angle. deg.		Injection pressure. MPa		DF. mm^3
	DF	DF	beginning	end	
5.6	28	22	67.6	41.8	59
15.6	28	34	60.6	32.2	71
15.6	28	21	85.7	54.2	60
Характеристики сгорания					
L/D ratios	P_{max}. MPa	Burnout rate. %		Specific heat consumption. kJ/(kW×h)	
5.6	15.9	100.0		7853	
15.6	15.5	96.5		8278	
15.6	15.7	98.1		8280	

The maximum heat release and combustion onset are virtually identical for both cases. However, the needle lift curve shows that the WCS injection should have initiated earlier for the high L/D ratio nozzle. The characteristic «bump» in the heat release curve following the maximum was absent for nozzles with a high L/D ratio. This resulted in lower combustion completeness (96.5 vs. 100%) and higher specific heat consumption (8270 vs. 7853 kJ/kW). Since maximum cylinder pressure determined primarily by the onset of heat release, its value differs only slightly for these two cases.

Increasing the injection start pressure from 67.6 to 85.7 MPa improved combustion performance for the high L/D ratio nozzle, bringing the heat release profile closer to that of the low L/D ratio nozzle at lower injection pressure. Obviously, higher injection pressure can compensate for the deterioration of combustion with increasing L/D.

***

In conclusion, of this chapter, it should noted that the above conclusions are not definitive, as the injection processes of coal suspensions are currently poorly understood and require further research. In particular, the main shortcoming of all studies of WCS injection is that they have not taken into account the combined effect of temperature and air charge pressure, characteristic of the end of the compression process, on flame development. Clearly, WCS injection into a dense gas environment with a temperature of 600…750°C, and in the case of preheated air at the inlet, 800…1200°C, leads to intense evaporation of water, which is more volatile than DF. It can assume that the formation of vapor bubbles within the flame core disrupts its homogeneity and accelerates the process of dispersed decomposition. Clearly, the effect of temperature on WCS spraying requires further research.

Chapter 5.

Features of the operating process of a piston engine with self-ignition of coal-based fuels under compression.

5.1. Spontaneous self-ignition and combustion of FCS.

When using FCS, the self-ignition and combustion characteristics of the air-fuel mixture depend primarily on the self-ignition of the liquid fuel used as a carrier. Self-ignition issues for liquid fuels have been well studied and discussed in the relevant literature. When using DF as a liquid carrier, the FCS combustion process is as follows: During the self-ignition delay period, active evaporation of diesel fuel and the release of pulverized coal particles from the liquid shell occur. The delay period for FCS primarily depends on the self-ignition of the liquid carrier and the state of the working gas at the time of fuel injection. Considering that the use of high-calorific solid fuels is most rational for FCS, volatiles do not significantly, affect the self-ignition of suspensions, since their content in these fuels is very limited, and the temperature at which they actively escape is quite high. A number of researchers believe that for this type of fuel, the volatiles do not have time to escape from the particle and burn not in the gas phase, but during surface reactions.

5.2. Spontaneous self-ignition and combustion of WCS.

Recent research has shown that, from a practical standpoint, the most interesting process is the spontaneous self-ignition and subsequent combustion of pulverized coal and water-coal fuels. Moreover, the efficiency of the spontaneous self-ignition process largely determines the efficiency of the subsequent fuel combustion process and the overall efficiency of the engine's operating cycle.

5.2.1. Determination of the WCS self-ignition delay period. The self-ignition delay of the WCS entering the engine combustion chamber is a critical parameter determining the nature of the combustion process of solid fuels in internal combustion engines.

Different definitions of the self-ignition delay period can found in the literature, which introduces some confusion when assessing the impact of this parameter on the subsequent combustion process of solid fuels. Based on the chosen definition, estimates from different researchers for the same conditions can differ significantly. Most often, the self-ignition delay period understood as the time interval or crankshaft rotation angle that covers the portion of the cycle from the beginning of fuel entry into the cylinder until

the moment the cylinder pressure curve separates from the compression curve [13].

In addition to this definition, other formulations can found in foreign literature, based on various physical phenomena occurring in the combustion chamber [71]:

- the self-ignition delay period, determined by luminosity, is the time from the opening of the injector to the first flash of ignited carbon, which is recorded by a photodiode;
- the self-ignition delay, determined by pressure drop, is the time from the opening of the injector to the moment the maximum pressure drop in the engine combustion chamber is reached due to evaporation of the liquid carrier;
- the determination of the self-ignition delay by pressure recovery is because the chamber pressure drops after fuel injection due to the heat expended on evaporation of the carrier. During subsequent combustion of the fuel, the pressure rises. The self-ignition delay, determined by pressure recovery, is the time from the opening of the injector to the moment when the pressure again reaches the value that would have observed without fuel injection.

A graphical interpretation of the main definitions showed Fig. 5.1. Luminosity and injector opening expressed as fractions of a unit.

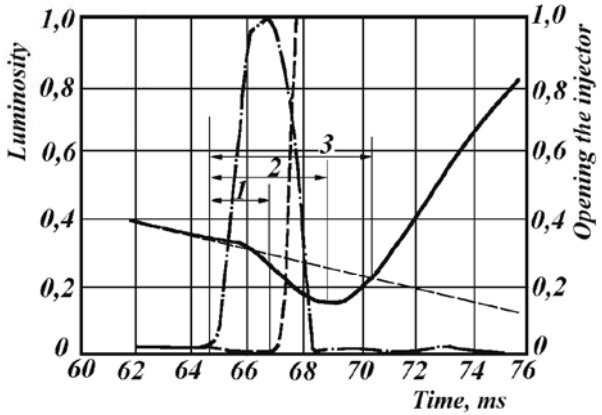

Fig. 5.1. Graphical interpretation of various definitions of the self-ignition delay period. 1 – by luminosity; 2 – by maximum pressure drop; 3 – by pressure recovery. - · - needle valve lift; - - - luminosity; —— cylinder pressure; – – – cylinder pressure without fuel supply

Regardless of the formulation, this period is characterized by the fact that during this period, the fuel enters the combustion chamber, mixes with the air

present there, and heats up, resulting in intense evaporation of the liquid carrier. When using WCS, the self-ignition process preceded by the active release of volatile substances.

5.2.2. Factors influencing the WCS self-ignition delay value. A series of experiments revealed that the self-ignition delay period for water-coal fuels increases compared to DF. This is primarily due to the presence of a relatively large amount of water in the suspension. Its evaporation results in the loss of some heat during the phase transition from liquid to vapor. The air charge temperature decreases much more significantly when using WCS than when using DF. Therefore, a longer period is required to restore cylinder pressure. This is evident from Fig. 5.2, which shows the change in pressure in the experimental chamber upon alternate injection of 20 mg of WCS and DF. The initial parameters of the gas environment at the time of injection reproduce the state of the air charge at the end of compression [71].

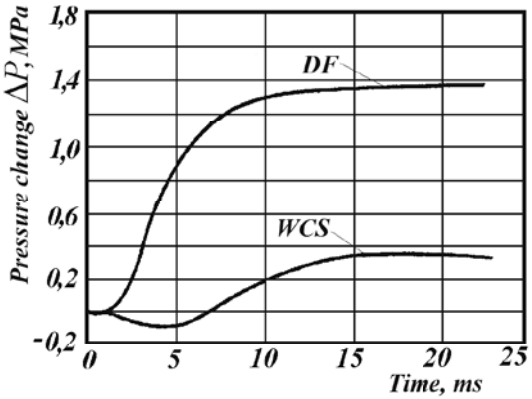

Fig. 5.2. Dependence of chamber pressure on time (counted from the start of injection) during combustion of 20 mg WCS and DF No. 2 under the same conditions (temperature 1350 K; pressure 2.9 MPa; equivalent mixture ratio of H_2, O_2, N_2 – 0.26)

The lower curve reflects the pressure change after WCS injection, while the upper curve reflects the pressure change after DF injection.

Comparison of the pressure change curves for WCS and DF combustion reveals significant differences in the self-ignition processes of these two fuels. Clearly, their combustion accompanied by very different pressure increases, heat release rates, and self-ignition delay times. In all studies, WCS released less energy and had a longer self-ignition delay than DF. Furthermore, pressure losses due to evaporation are significantly higher for WCS than for DF. As Fig. 5.2 shows, under the given conditions, it takes

almost 7.0 ms for WCS to compensate for pressure losses due to evaporation, while DF self-ignition after just 1.0 ms.

The difference in pressure is primarily because the heat of combustion of DF is 2.9 times higher than that of WCS. Furthermore, combustion of the coal particles is incomplete, as they cool upon reaching the chamber walls and no longer participates in the combustion process. Calculation results show that in the case shown in Fig. 5.2, between 5 and 15% of the coal remains unburned. This assumption of incomplete combustion confirmed the presence of coal particles adhering to the chamber wall. Moreover, the lower the chamber temperature, the more unburned coal accumulated on the wall at the end of the experiment. This result is consistent with data showing that at lower temperatures, the increased self-ignition delay leads to a larger portion of the jet reaching the chamber wall before the coal ignites. Under similar conditions, DF also reaches the wall, but unlike coal particles, it evaporates and burns.

At temperatures typical of modern diesel engines, the difference in self-ignition delay between WCS and DF becomes even more pronounced.

In Fig. 5.2, see Fig. 5.2., 5.3 presents the self-ignition delays for WCS and DF obtained from the three above-mentioned determinations as a function of temperature, under similar conditions in the experimental chamber.

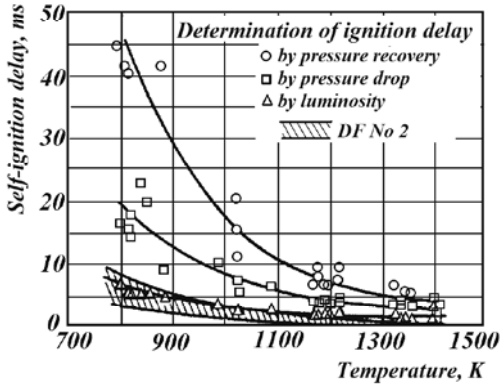

Fig. 5.3. Dependence of the self-ignition delay of WCS and DF on the temperature in the chamber

From the presented data, several characteristics of WCS self-ignition can identify:

- first, the self-ignition delay of WCS depends significantly on the chamber temperature, with the self-ignition delay becoming shorter as the temperature increases;

- second, as the temperature increases, all three self-ignition delay characteristics converge;

- third, the self-ignition delay determined by luminosity is shortest, followed by pressure drop, and finally by pressure recovery.

It should note that, under similar conditions, the self-ignition delay for WCS is always significantly longer than for DF. The self-ignition delay periods determined from pressure recovery for both fuels differ by approximately a factor of five.

Fig. 5.4 shows the logarithmic dependence of the self-ignition delay for WCS, determined from luminosity as a function of the inverse of temperature. The graph shows that the dependence of the self-ignition delay on temperature resembles the Arrhenius equation. At a chamber temperature above 800 K (or 1000/T $\leqslant$ 1.25), the effective activation energy is approximately 20 kJ/mol (versus 150 kJ/mol, the typical chemical activation energy for coal). Experimental data show that the effective activation energy increases at temperatures below 800 K. However, changes in pressure and luminosity over time indicate that very weak combustion of coal particles occurs at such temperatures. This phenomenon may explained by the fact that the typical self-ignition temperature of coal is approximately 700 K [19]. If only the coal particles on the outer surface of the plume reach this temperature, while the center remains relatively cold, then the energy released may not be enough to maintain the combustion process.

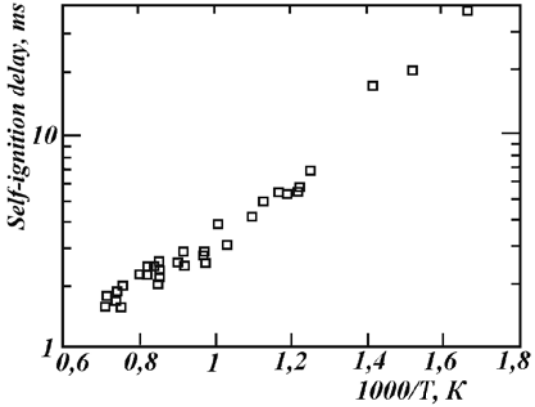

Fig. 5.4. Dependence of the self-ignition delay on temperature determined by luminosity (Arrhenius equation type)

Another explanation for the increased self-ignition delay is that the combination of the above-described effect with jet impingement on the

combustion chamber wall and the associated decrease in temperature of individual particles plays a significant role in the self-ignition process of coal fuel. At temperatures below 800 K, the self-ignition delay, determined by luminosity, is more than 7 ms, which is equivalent to the time it takes for the main part of the jet to traverse the chamber and spread along the wall. Many particles adhere to the wall and rapidly cool, preventing self-ignition, even though the chamber temperature exceeds the self-ignition temperature of coal. Fig. 5.5 shows self-ignition delay data for two temperature levels (1025 and 1200 K).

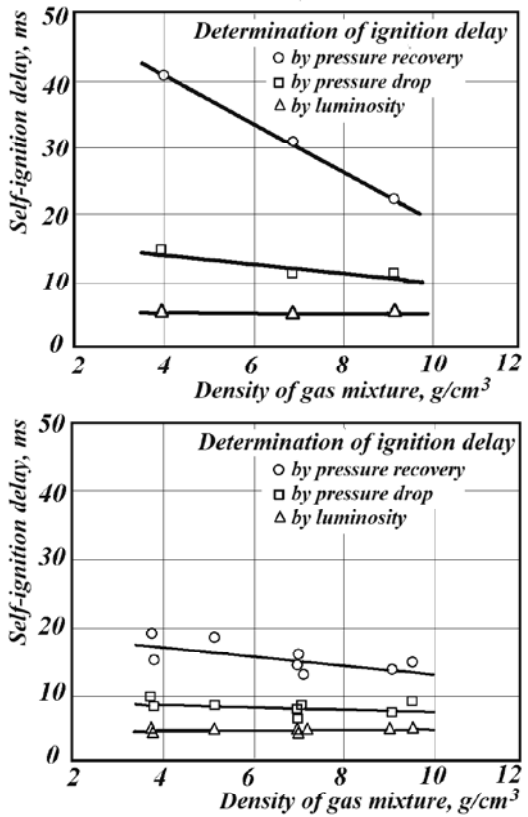

Fig. 5.5. Dependence of the self-ignition delay on the density at a temperature in the chamber of 1025 and 1200 K

The self-ignition delay period presented as a function of the density of combustion products, which at a given temperature directly related to

pressure. Self-ignition delays determined pressure decrease with increasing pressure. This relationship is strongest for self-ignition delays determined by pressure recovery. Moreover, the effect of pressure weakens with increasing temperature. Such pressure dependence is not typical for the self-ignition delay determined by luminosity.

5.3. Study of self-ignition processes of FCS and WCS.

Ryan T.W., and Dodge L.G. conducted experiments (1984) investigating the self-ignition and combustion of FCS. Coal, charcoal, and coke used as solid fuels. Diesel fuel served as the liquid carrier. During laboratory tests, the suspensions sprayed into an inert gas (nitrogen). Engine tests conducted on a single-cylinder module.

The experiments showed that properly selected fuel mixtures could have virtually the same combustion characteristics as diesel fuel.

Robben F., Brehob D. D., et al. [40] in 1984 studied the self-ignition of water-coal fuel in a setup with rapid compression of a gas mixture. They obtained some preliminary results on the self-ignition and combustion of WCS. The main conclusion drawn from the research results was that a high temperature at the end of compression is required to ensure satisfactory combustion of the mixture. A mixture of water and low-ash coal was in these studies. In 1986, Siebers D.L. and Dyer T.M. performed an experimental study of the WCS self-ignition process [71]. For their experiments, they used a constant-volume (single-use) chamber designed and manufactured by Volkswagen Research (Germany). The chamber designed to simulate combustion processes occurring near the TDC in various types of piston engines. The chamber is a cylindrical vessel equipped with 25 mm thick glass windows at both ends, which ensures the free passage of light rays throughout the chamber. The diameter of the cylindrical chamber is 80 mm, and the width between the windows is 29 mm. The outer wall of the chamber is surrounded a layer of high-temperature insulation. To simulate the cylinder wall temperature of real engines, it can heat with an electric heater to 500 K. The cross-section of the chamber showed schematically Fig. 5.6.

During the experiments, changes in combustion pressure (measured with a piezoelectric pressure sensor), changes in flame luminosity (measured with a photodiode), injection pressure, and injector needle lift recorded. High-speed cameras also used to record the chamber using shadowgraphs or conventional methods.

In the initial stages of the study, to achieve the required temperatures, the compressed air contained in the chamber heated using an electric heater

or the entire chamber placed in an oven. However, in both cases, the chamber wall temperature was equal to the air charge temperature, which was inconsistent with the conditions in real diesel engines. This particularly distorted the test results for the WCS, as the long ignition delay meant that most of the fuel reached the chamber walls long before complete combustion.

To eliminate the influence of wall temperature on chamber processes, the pressure and temperature required for the simulation were achieved using the following method: first, a pre-composed, very lean charge consisting of gaseous fuel (H_2), oxidizer (O_2), and diluent (N_2) was ignited and burned in the chamber. Depending on the temperature and pressure required for the simulation, this charge corresponded to one of three oxygen equivalent ratios: 0.23, 0.26, or 0.29. The combustion products created high pressure and temperature in the chamber. Because the charge was lean, approximately 21% oxygen remained in the combustion products, which corresponds to its content in atmospheric air. WCS injected into the resulting hot and highly compressed gas environment, resulting in spontaneous ignition and combustion of the fuel.

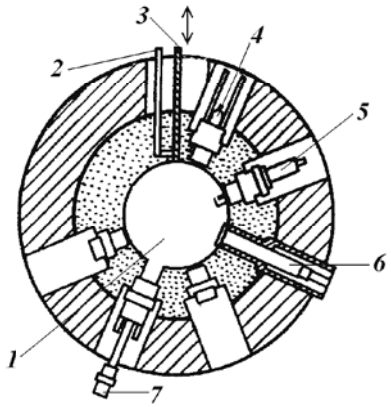

Fig. 5.6. Cross-section of the chamber. 1 – chamber; 2 – vacuum channel; 3 – manually controlled outlet valve; 4 – pressure sensor; 5 – spark plug, 6 – inlet valve; 7 – injector

Simulation of diesel engine cylinder conditions consisted of two main steps:

First, pressure and temperature typical of diesel engines near the TDC generated in a constant-volume chamber.

Second, WCS injected into the chamber under these conditions using a standard liquid fuel injector. The fuel jet ignited and burned as if it were a

separate portion of liquid fuel injected into a diesel engine with a single combustion chamber.

Using the method described above, temperatures from 700 to 1400 K and pressures from 1.0 to 3.2 MPa generated in the chamber. Furthermore, regardless of the gas temperature in the chamber, the temperature of its walls matched that of a real engine cylinder. For this purpose, the wall heated to 420 K using an electric heater.

***

A number of researchers, based on the processing of experimental data, have proposed methods for estimating the ignition delay period [36, 45, 46]. In particular, Grekhov [9] used a formula borrowed from the theory of thermal explosion in the form proposed by Pokrovsky and Adamov to determine the ignition delay period:

$$\tau_i = AP^{-n}\exp(B/T).$$

For the coal-fuel suspension, the coefficient A adjusted relative to diesel fuel; therefore, the activation energy of the coal-fuel suspension left unchanged, since its self-ignition is due specifically to diesel fuel. The discrepancy between the values for hard and brown coal explained the nearly twofold difference for volatiles. The exponent n in the calculations assumed to constant, equal to 1.19. The obtained constants presented in Table 5.1.

In [9], attention is drawn to the closeness of the obtained constants to those determined for liquefied gas $B = E/R = 4820$ K, rather than for the combustion of pure carbon (95...98%) $B \approx (10...15)\times10^3$. This emphasizes the importance of volatiles in the combustion of solid fuels primarily compounds with a molecular weight of 16...130 and higher, which consist of a complex of hydrocarbons, carbon monoxide, hydrogen, acids, resins, and other compounds. This fact indicates that the self-ignition of coal suspensions depends significantly on the rheological properties of the original fuel. The self-ignition of coal particles can vary significantly depending on the source fuel's origin, its storage method and length, and the method of pretreatment and deashing. When preparing the original fuel for WCS, it is advisable to avoid thermal treatment, as this significantly reduces the volatile content of the original fuel.

Table 5.1.

Constants for determining the self-ignition delay [9]

	Diesel fuel	FCS (50% coal by weight)	WCF (50% coal by weight)	WCF (50% coal by weight)
		Hard coal		Brown coal
$A\times10^{-6}$	39	46	77	63
$B=E/R$, K	4300	4300	5000	4800

Spadaccini and TeVelde used similar considerations as Grekhov to determine the ignition delay period of coal-fuel suspensions, presenting the expression in the following form:

$$\tau = \frac{A}{P^n}\exp\left(\frac{0{,}239E}{RT}\right),$$

where $A = 2{,}49\times10^{-9}$; $E = 174{,}17$ MJ/mol и $n = 2$.

This correlation was subsequently used Bell and Caton in modeling the thermodynamic cycle of a solid-fuel piston engine. [33].

5.4. Ways to improve the self-ignition and combustion of coal fuels.

As demonstrated above, the self-ignition conditions for coal fuels entering the engine, whether as dry coal dust or as part of a WCS, differ significantly from those for liquid fuel in the combustion chamber of a diesel engine. The activation energy of solid fuel is significantly higher than that of liquid fuel. To achieve stable self-ignition, various methods must used to create conditions conducive to stable self-ignition of the air-fuel mixture by the end of the compression process in the engine combustion chamber.

In addition to the air charge parameters in the engine combustion chamber, self-ignition characteristics depend significantly on the properties of the fuel itself. Therefore, all methods for activating the self-ignition process can roughly divide into two large groups: engine-related and fuel-related.

The first group includes changes to the engine design aimed at ensuring that by the end of the compression stroke the air charge temperature and pressure are sufficient for stable self-ignition of the air-fuel mixture.

The second group of methods includes measures aimed at reducing the activation energy of the original solid fuel or changing the composition of the suspension. In practice, various additives added to the suspension to ensure stable self-ignition in the combustion chamber.

It should note that most real-world designs typically use a combination of both methods to achieve stable self-ignition.

There are six main factors that influence the self-ignition characteristics of solid fuels:

- injection advance angle;
- air charge condition at the end of the compression process (temperature, pressure);
- particle size;
- particle distribution within the air charge;
- coal fuel properties (reactivity, volatile content);
- presence of special fuel additives.

Data obtained from laboratory studies of WCS self-ignition processes formed the basis for the development of a set of measures aimed at improving the self-ignition and combustion of water-coal fuel in real engines.

Let's consider the influence of each of these factors on the self-ignition process of solid fuels separately.

5.4.1. The influence of injection advance angle on the self-ignition and combustion characteristics of WCS. To compensate for the longer delay, fuel delivery to the combustion chamber of engines operating on WCS must occur much earlier than for DF. Fig. 5.7 shows a case of successful self-ignition of a WCS aerosol achieved by setting an earlier fuel injection point into the engine's combustion chamber.

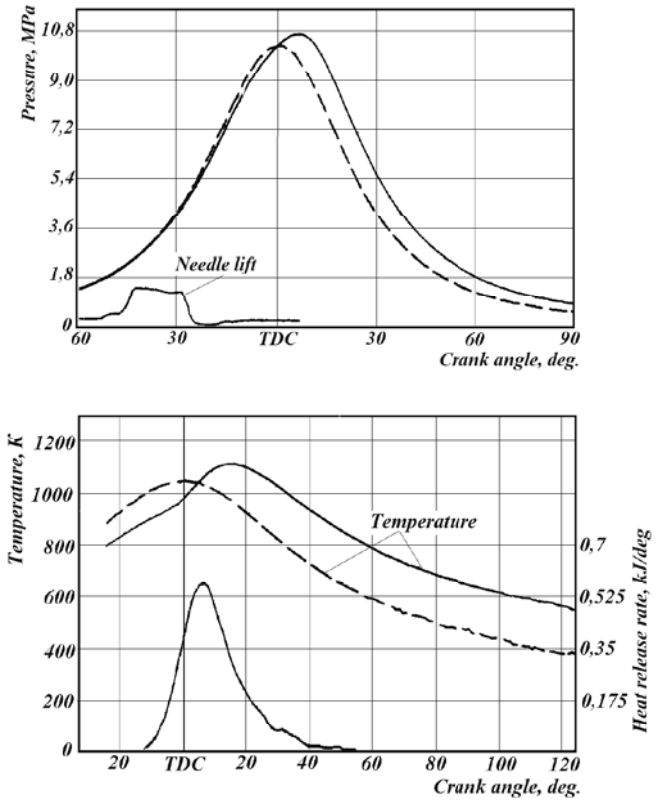

Fig. 5.7. Effect of injection start on WCS self-ignition in the General Electric 7FDL engine. - - - injection advance optimized for DF (static advance angle 26° before TDC); —— injection advance optimized for WCS (static advance angle 65° before TDC) [52]

The static injection advance increased from 26° to 65°. The dynamic injection start corresponded to 51.4° before TDC. The intake air temperature maintained at 100°C during the experiment. The pressure difference clearly shows that with the increased injection advance angle, useful work performed in the cylinder, resulting in an engine power of 45.6 kW. The calculated curves for temperature and thermal stress in the cylinder indicate that self-ignition occurs approximately 11° before TDC. The self-ignition delay was 40° of crank angle, or approximately 6.0 ms. This time almost completely coincides with the time obtained in studies of self-ignition in a simulation chamber.

5.4.2. The influence of air charge parameters at the end of the compression process on self-ignition and combustion efficiency of coal fuel. The low thermal diffusivity of coal particles (approximately 1.35 mm^2/s) means that they heat up quite slowly, and as a consequence, the time required to activate the combustion process increases [9, 52].

Increasing the air charge temperature toward the end of compression is one way to increase the rate of particle heating.

A number of studies have shown that the most favourable conditions for the self-ignition of most solid fuels created when the air charge temperature reaches 950...1300 K by the time the fuel is introduced into the combustion chamber. The lower value in this range corresponds to the use of pulverized coal fuel with a high volatile content; as the volatile content in the fuel decreases, the temperature required for stable self-ignition increases. The upper temperature corresponds to the use of WCS, since part of the air charge heat then expended on water evaporation, resulting in a charge temperature reduction of 50...70 K. The air charge parameter changes in the 7FDL high-speed engine cylinder are presented in Fig. 5.8 [52].

During testing, the WCS injection characteristics optimized to ensure combustion chamber conditions met the requirements for stable self-ignition of the DF. Despite this, no combustion observed. The same figure shows the charge temperature variation in the engine cylinder. By the time of the expected needle lift (16.5° before TDC, with no WCS injection), the average charge temperature approaches 890 K. During further compression, by the time the piston reaches TDC, its value increases to 960 K.

A comparison of the temperature curves before and after WCS injection shows that the water contained in the WCS lowers the charge temperature immediately before combustion. However, by the time, the coal fuel ignites (approximately 11° before TDC), the temperature can reach 890 K, which is necessary for stable self-ignition in this engine. According to the results of combustion studies in a bomb, this temperature is sufficient for WCS to self-

ignite within 4...5 ms. However, as motor tests have shown, the time required for self-ignition of water-coal propellant under real-world conditions is 5 ms longer than in a bomb.

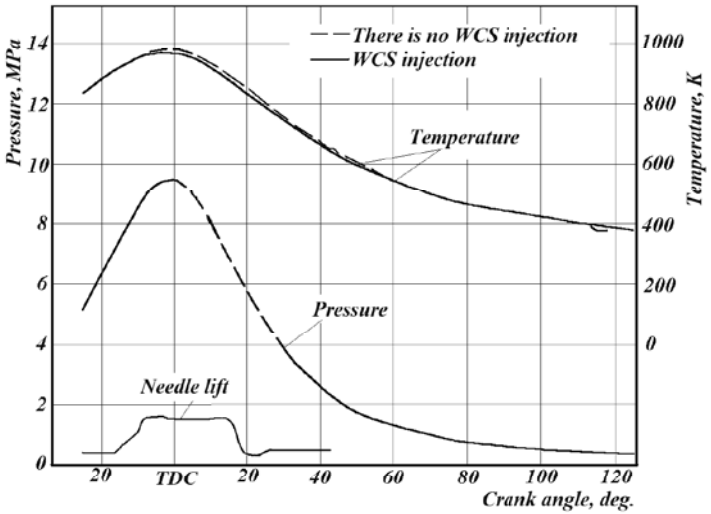

Fig. 5.8. WCS injection into an engine cylinder under conditions typical for stable DF self-ignition (n=1050 min^{-1}, inlet air pressure 329 kPa, inlet air temperature 85°C, static injection advance angle 26° before TDC)

For a given engine speed of 1050 min^{-1}, the crank rotates approximately 30° within 5 ms. The carbon particles are ready for combustion when the piston passes 15° after TDC. By this point, the average charge temperature is below 890 K, resulting in a misfire. This means that even if the charge temperature is sufficient to initiate combustion, this does not mean that the WCS can be successfully combusted in the engine's combustion chamber. The self-ignition of water-coal fuel preceded a relatively lengthy preparatory stage, during which the liquid carrier evaporates. After the water evaporates, the high temperature causes the fuel particles to heat up quickly, and volatiles begin to release. Mixing with air, they react with oxygen, forming flames. As result of the combined effect of all these factors, the ignition delay period for WCS is significantly longer than that of DF. The higher the charge temperature now of injection, the faster the pre-ignition processes and the shorter the self-ignition delays period. This, in turn, affects the engine's operating characteristics. By influencing the air charge temperature at the end of compression, it is possible to influence the self-ignition characteristics of the fuel in the engine's combustion chamber.

The most significant influence on the air charge parameters at the end of compression is exerted by the engine's geometric characteristics (compression ratio, combustion chamber volume-to-area ratio, total cylinder volume), as well as the air inlet parameters.

Attempts to increase the temperature at the end of compression solely by increasing the compression ratio have conducted in a number of studies; however, in most cases, these have proven insufficiently effective. This type of modification significantly increases the loads on the crank mechanism components, which leads to a significant reduction in the engine's mechanical efficiency.

Another method for increasing the temperature at the end of compression is thermal insulation of combustion chamber components [9, 63]. An example of such an engine design showed Fig. 5.9 [63]. The piston crown surface covered with a special 5.1 mm thick thermal insulation lining. This lining is made of a special ceramic with a thermal conductivity of 0.025 W/(cm×K). The outer surface of the cylinder liner covered with a 1.524 mm thick layer of ceramic material.

This solution generally improves the self-ignition characteristics of solid fuel, but is not effective enough on its own. Therefore, this method of increasing charge temperature usually combined with other methods.

In addition to chamber insulation, a number of researchers have considered increasing the air charge temperature at the end of the compression process by installing special uncooled combustion inserts or electric glow plugs.

All of these methods, taken together, produce positive results, but their maximum effectiveness is typically limited to a single, steady-state engine-operating mode.

Currently, the most effective way to influence self-ignition parameters and fuel combustion is to regulate the engine inlet temperature. Increasing the inlet air temperature not only ensures stable self-ignition of the coal fuel in the cylinder chamber but also achieves acceptable combustion characteristics, ensuring efficient operation of the thermodynamic cycle.

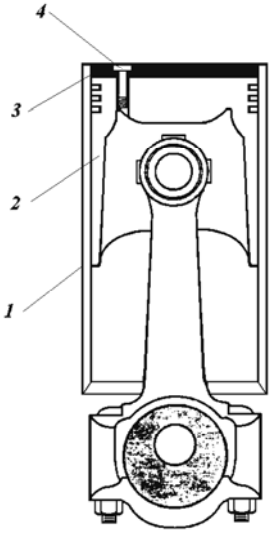

Fig. 5.9. Diagram of piston and cylinder thermal insulation. 1 – ceramic layer on the outer side of the sleeve; 2 – piston; 3 – thermal insulation lining; 4 – mounting bolt

Fig. 5.10 shows the results of a JS-1 engine test for two different inlet air temperatures.

In the first test, the engine inlet air temperature was maintained at 223°C, while in the second, it was maintained at 121°C. A nozzle with a 0.25 mm orifice diameter used for WCS injection (Table 3.6).

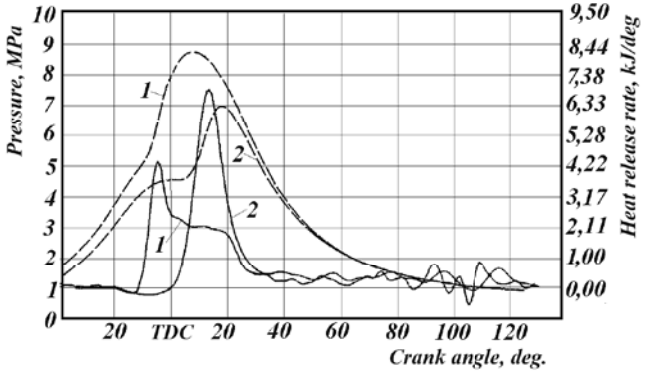

Fig. 5.10. Effect of air temperature at the inlet of the Cooper-Bessemer JS-1 engine on the change in pressure and heat generation characteristics in the working cylinder during self-ignition of the WCS [20], - - - pressure; —— heat release rate

As Fig. 5.10 shows, combustion was good at the higher temperature, with maximum cylinder pressure achieved at a crankshaft angle of 6° after TDC. The solid lines in Fig. 5.9 show the heat release pattern. In the first case, WCS combustion proceeded almost identically to DF. The maximum heat density was 4.33 kJ/deg, with all fuel burned within 20° of crankshaft rotation after TDC. The nominal specific heat consumption was 5080 kJ/(kWh).

At an inlet air temperature of approximately 121°C, the ignition delay increased from 2.5 ms to 5.4 ms (from 6° to 13° of crankshaft rotation). In this case, maximum pressure achieved at a crankshaft angle of 18° after TDC. The heat-stress curve took on a nearly triangular shape with a maximum of 6.86 kJ/deg. The longer ignition delay partially offset by higher heat release. Therefore, the specific heat consumption increased by only 3%, reaching 5230 kJ/(kWh).

Similar results obtained during testing of the 7FDL engine General Electric specialists. The studies conducted at both full and part load conditions. The operating characteristics for two different air inlet temperatures at part load presented in Table 5.2. The temperature change pattern showed Fig. 5.11.

Table 5.2.

Operating parameters of the General Electric 7FDL engine with WCS self-ignition at partial load conditions

Parameter		
Inlet air temperature, °C	110	85
Static injection start, before TDC, deg	65	65
Dynamic injection start, before TDC, deg	51.3	52.1
Combustion start, before TDC, deg	11.4	7.0
Combustion duration, deg	40.0	45.1
Temperature at end of compression, K	900	875
Maximum cycle pressure, MPa	10.7	10.8
Power, kW	45.6	45.0
Fuel burnout, %	88.2	81.2
Fuel burnout efficiency, %	94.6	91.8
Specific heat consumption, kJ/(kWh)	9510	10110

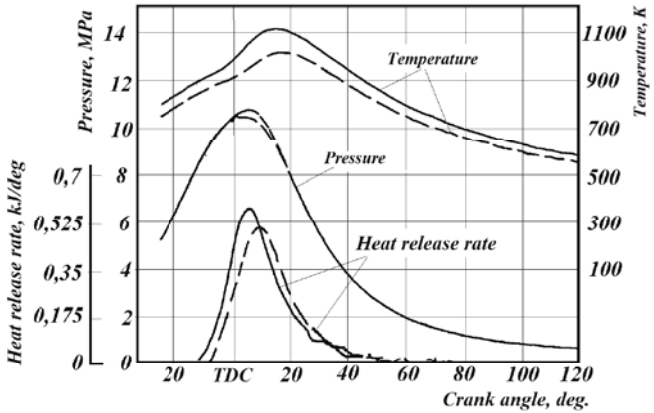

Fig. 5.11. Effect of air temperature at the inlet of the General Electric 7FDL engine on the operating cycle parameters during WCS self-ignition at partial load mode (n = 1050 min^{-1}, inlet pressure 329 kPa). - - - 85°C; —— 110°C

Fig. 5.12 shows the results of a comparison of the operating cycle parameters under full-load conditions during WCS self-ignition. The general patterns of pressure changes differ from those observed during pilot ignition.

At a lower inlet air temperature, fuel burns at a virtually constant pressure. A lower maximum heat density also observed at a lower inlet air temperature, and combustion in the cylinder begins later. Since injection timing remained constant throughout the experiments, as evidenced by the needle lift graph, the longer self-ignition delay with decreasing temperature becomes apparent. To maintain an optimal excess air ratio (approximately

1.9), the engine inlet pressure was varied to maintain a constant air density. The engine test results under full load presented in Table 5.3.

Table 5.3.

Operating parameters of the General Electric 7FDL WCS self-ignition engine at full load

Intake air			Burnout rate, %	Specific heat consumption, kJ/(kWh)	P_{max}, MPa
Temperature, °C	Density, kg/m^3	Pressure, kPa			
104	3.173	344	84.5	9426	10.6
124	3.173	362	92.1	9044	15.9

Thus, even a slight increase in intake air temperature leads to a significant improvement in solid fuel combustion characteristics and, consequently, overall engine performance. However, a significant increase in temperature, especially at maximum loads, requires an increase in intake air pressure to maintain the required charge mass for an optimal excess air ratio. Excessive intake air pressure leads to an excessive increase in maximum combustion pressure and, consequently, high mechanical loads in the engine. Therefore, the intake air pressure range should not exceed 308…377 kPa.

In most laboratory setups for naturally aspirated engines, electric heaters were used to heat the intake air to 400…600 K. When developing real designs, researchers considered the possibility of achieving the required temperature through exhaust gas recirculation. This method allows for a wide range of charge temperature control by regulating the amount of exhaust gas entering the engine inlet. Another method is to heat the intake air using the heat of the exhaust gases by installing a dedicated heat exchanger. This method allows for a more efficient balancing of heat flows in the engine, but is more complex and less reliable. Operating the heat exchanger under conditions where ash particles emitted from the exhaust gases will significantly reduce its efficiency.

It's important to note that for naturally aspirated engines, both air heating and exhaust gas recirculation degrade the mass filling of the working cylinder, resulting in reduced engine performance.

At the same time, most experimental data suggests that at operating conditions close to maximum load, the air charge in the working cylinder has parameters sufficiently close to those required for effective activation of the fuel self-ignition process. Therefore, depending on the engine operating conditions, the air temperature should vary decreasing at operating conditions close to maximum load and increasing at partial loads. Therefore, by equipping the engine with an adjustable heating system, it is possible to effectively influence the self-ignition and combustion of solid fuel. At full

load, the air can heat only slightly, resulting in no significant change in engine performance.

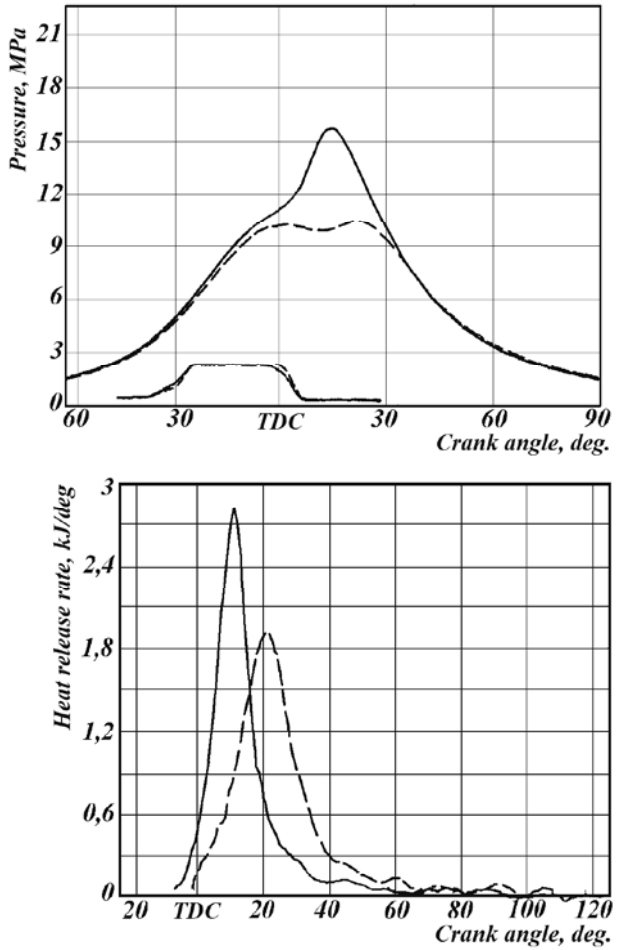

Fig. 5.12. Effect of air temperature at the inlet of the General Electric 7FDL engine on the operating cycle parameters during WCS self-ignition at full load (n = 1050 min^{-1} inlet pressure). - - - 104°C, 344 kPa; —— 124°C, 326 kPa

For turbocharged engines, it is sufficient to provide a charge air cooling system after the compressor. Furthermore, turbocharged engines exhibit a clear correlation between the efficiency of solid fuel self-ignition and the charge air pressure at the end of compression.

***

The effect of 7DFL engine inlet air pressure on WCS self-ignition and operation at part-load is shown in Fig. 5.13. For comparison, two different inlet pressures considered 329 kPa and 112 kPa. The engine speed is 1050 min^{-1}, the static injection advance angle is 47° before TDC, and the inlet air temperature is 85°C.

The temperature change shows that at 112 kPa, no combustion occurs, therefore, the heat density is zero. Increasing the pressure in the working cylinder achieves the conditions necessary for activating self-ignition and combustion of the coal fuel.

The effect of inlet air pressure can explain by several factors.

First, the mass of air entering the engine cylinder at a lower inlet pressure is less. Considering that approximately the same amount of WCS injected into the combustion chamber in both cases, approximately the same amount of heat, which removed from the air charge, consumed in water evaporation. After vaporization is complete, the temperature in the combustion chamber decreases more significantly for the lower inlet pressure case. In fact, for a pressure of 112 kPa, the maximum temperature reaches only 780 K, which is too low for self-ignition of the coal fuel.

Secondly, deterioration in the spraying quality of the WCS contributes to the ignition failure. The fuel injected into a lower-density environment, resulting in delayed dispersion of the plume core. This assumption supported by the results of studies of the combustion of WCS aerosols in a chamber simulating engine combustion conditions.

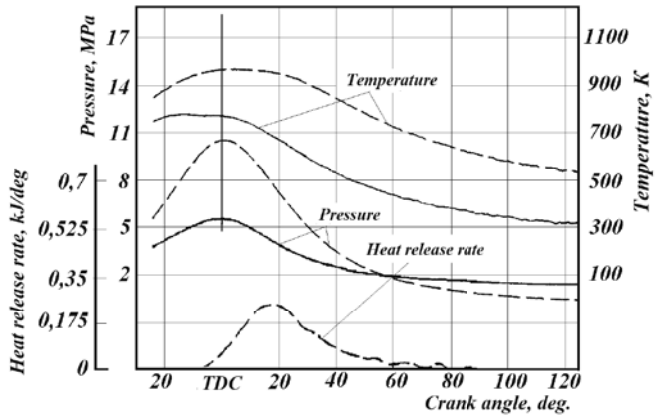

Fig. 5.13. Effect of air inlet pressure on the self-ignition and operating processes of the General Electric 7FDL engine at partial load. - - - 329 kPa; —— 112 kPa [52]

Third, the kinetics of surface reactions depends on the ambient gas pressure.

An improvement in the operating parameters with increasing inlet pressure also observed at full engine load. However, this improvement is not as significant as with increasing temperature. The results of the 7FDL engine test at full load presented in Table 5.4.

Table 5.4.

Operating parameters of the General Electric 7FDL WCS self-ignition engine at full load

Intake air			Burnout rate, %	Specific heat consumption, kJ/(kWh)	P_{max}, MPa
Temperature, °C	Density, kg/m^3	Pressure, kPa			
344	3.007	124	80.5	10756	13.0
362	3.173	124	83.6	10123	13.1

***

Bell and Caton used a process simulation to investigate the effects of temperature, inlet air pressure, and initial particle size on the thermal efficiency of a coal-fueled compression ignition engine [33]. The input parameters of the simulated engine given in Table 5.5, and those of the fuel used are given in Table 5.6.

Table 5.5.

Engine parameters adopted for modeling the operating cycle with self-ignition of coal fuel

Parameter	Meaning
Cylinder diameter, m	0.20
Piston stroke, m	0.20
Compression ratio	16.0
Rotation speed, min^{-1}	1030
Cylinder wall temperature, K	480.0
Exhaust valve opening after TDC, deg	150.0
Initial charge temperature in the working cylinder, K	450.0
Excess air ratio	1.67
Fuel injection duration, deg	20

Table 5.6.

Fuel parameters adopted for modeling the compression self-ignition cycle

Parameter	Meaning
Amount of liquid carrier (by weight), %	50
Maximum yield of volatile solids (V_{max})	0.5
Volatile content (by weight), %	50
Heat of combustion of coal, kJ/kg	33.337
Heat of combustion of volatiles, kJ/kg	35.000
Heat of combustion of coke residue, kJ/kg	32.790

Fig. 5.14 shows the dependence they obtained, which shows that increasing pressure leads to more stable self-ignition at lower engine inlet air temperatures or improves self-ignition performance at a given initial temperature. Analytical data agree with experimental data in that pressure has a lesser effect on fuel self-ignition efficiency than temperature. Nevertheless, increasing the initial gas pressure can significantly reduce the negative consequences associated with increased temperature (reduced cylinder filling efficiency, reduced engine power).

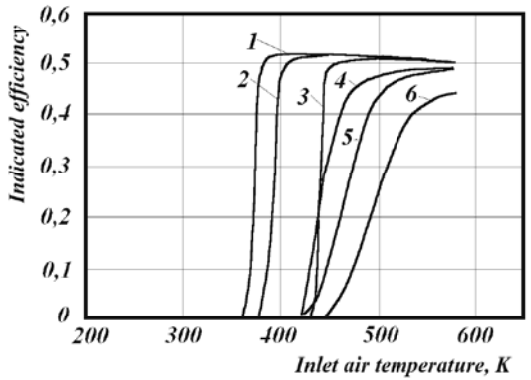

Fig. 5.14. Indicated efficiency as a function of air temperature at the engine inlet depending on the initial pressure and the size of the fuel particles included in the WCS: 1 – (10 μm, 200 kPa); 2 – (10 μm, 100 kPa); 3 – (10 μm, 50 kPa); 4 – (30 μm, 200 kPa); 5 – (30 μm, 100 kPa); 6 – (30 μm, 50 kPa)

5.4.3. The influence of particle size and polydispersity of coal fuel on its self-ignition and completeness of combustion. Modern technologies make it possible to produce coal fuel with a particle polydispersity range of 2...10 μm. It is an established fact that as particle size decreases, their self-ignition efficiency increases, while the ignition delay period decreases. However, this relationship is nonlinear, and after a certain value reached, further particle size reduction becomes impractical for a given engine. During injection, individual fuel particles can form agglomerates, the size of which is two to three times larger than the original particles. These agglomerates ignite and burn as a single, relatively large particle. Thus, the actual particle sizes entering the engine cylinder can differ significantly from the initial ones. As a result, the polydispersity range of the particles actually involved in self-ignition and combustion increases.

In addition to increasing self-ignition efficiency, reducing particle size leads to a reduction in the ignition delay period. This explained by their faster

heating and larger reaction surface area. In polydisperse mixtures, smaller particles ignite spontaneously earlier, causing the pressure and temperature of the working gas rapidly increase. This, in turn, leads to the active ignition of larger particles. Fig. 5.15 shows the relationship between the calculated indicated engine efficiency and the initial air charge temperature as a function of the initial particle sizes [33].

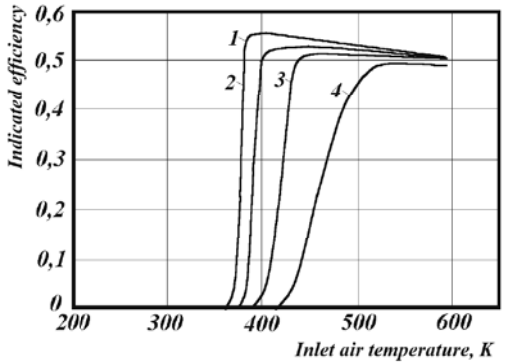

Fig. 5.15. Indicated efficiency as a function of the initial gas temperature (in TDC) for particles with a mono-size of 5, 10, 20, and 30 μm (1, 2, 3, 4 – respectively)

Fig. 5.16 shows the same dependence for a polydisperse mixture consisting of 20% particles with sizes of 10 μm, 60% particles with sizes of 15 μm, and 20% particles with sizes of 30 μm.

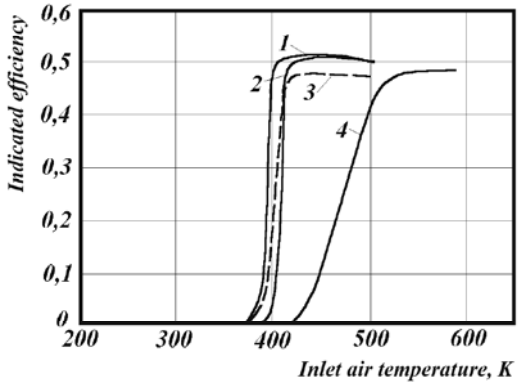

Fig. 5.16. Indicator efficiency as a function of the initial gas temperature (at TDC): 1 – for particles with a uniform size of 5 μm; 2 – for particles with a uniform size of 10 μm; 3 – for a polydisperse mixture consisting of 20% of 20 μm particles (by weight), 60% of 10 μm particles, and 20% of 15 μm particles; 4 – for particles with a uniform size of 30 μm

5.4.4. The influence of coal fuel properties on their self-ignition and combustion efficiency. The reactivity of solid fuels, like the volatile content, affects their self-ignition. Fig. 5.17 shows the relationship between the analytically obtained thermal efficiency, the initial air temperature at the cylinder inlet, and the surface reaction coefficient [33]. The fuel used was WCS, consisting of monofractional particles 15 μm in size with varying degrees of reactivity.

As the fuel reactivity increases, the initial gas temperature at which maximum engine efficiency is achieved decreases. For example, if the surface reaction coefficient A_i is 50, then maximum engine efficiency can achieved at an inlet temperature of 325 K. With an A_i value of 1, the initial air temperature at the cylinder inlet must be at least 400 K.

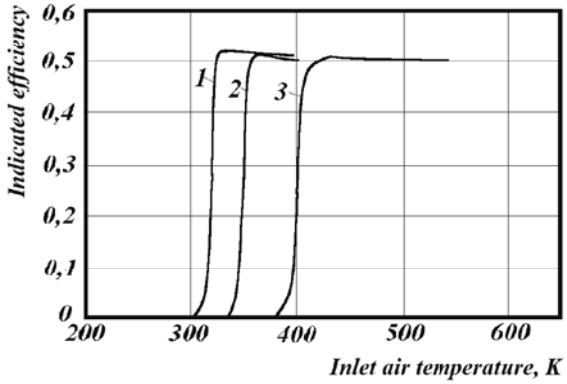

Fig. 5.17. Indicated efficiency as a function of the initial air temperature (in TDC) for WCS with 15 μm monofraction particles depending on the surface reaction coefficient. 1 – A_i=1; 2 – A_i=10; 3 – A_i=50

Thus, with a 50-fold increase in the surface reaction coefficient, the engine inlet temperature required for stable self-ignition decreases by only approximately 20%. This suggests that reactivity has a negligible effect on the self-ignition efficiency of solid fuel. This supports the hypothesis that the combustion process of coke residue in the working cylinder is diffusion-based. Furthermore, with increasing fuel reactivity, the self-ignition delay period decreases.

5.4.5. Increasing the self-ignition of WCS by adding additives. In some cases, various additives are added to WCS to improve its self-ignition characteristics, including methanol, diesel fuel, and other petroleum products. The results of an analytical study of the self-ignition characteristics of WCS in a high-speed locomotive diesel engine presented [33].

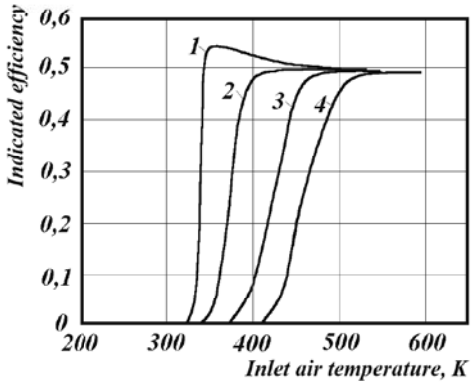

Fig. 5.18. Thermal efficiency as a function of initial air temperature for WCS with the following composition (by weight): 1 – coal 50%, DF 50%; 2 – coal 50%, water 45%, DF 5%; 3 – coal 50%, water 48%, DF 2%; 4 – coal 50%, water 50%

Combustion process modeling established a relationship between thermal efficiency and the initial air temperature at the engine inlet for four different types of coal suspensions. The resulting relationships presented in Fig. 5.18, showing that the addition of a relatively small amount of diesel fuel (approximately 5% by weight) reduces the initial air temperature required for stable self-ignition by 80 K.

Furthermore, the presence of diesel fuel in the suspension leads to a decrease in the self-ignition delay. Siebers and Dyer found that with increasing amounts of diesel fuel in the suspension, the self-ignition delay period decreases, but this trend persists up to a certain point. At high gas temperatures, the self-ignition delay reaches a constant value and then remains virtually unchanged.

Chapter 6.

Operating process of a coal-based forced ignition piston engine.

6.1. Forced combustion activation. Ignition coefficient.

After solid fuel, particles are into the combustion chamber of a solid-fuel diesel engine, their temperature increases to approximately 320…350°C because of heat exchange with the air charge. At these temperatures, reaction rates remain insignificant, resulting in no combustion activation. In this case, the coal particles initially simply heat up and then cool with virtually no change in size (no combustion).

As noted, the volatiles released during particle heating play a crucial role in the ignition of coal fuels in the engine cylinder. Igniting and burning in the gas phase, the volatiles contribute to an increase in the temperature in the active zone, thereby supplying the particles with the energy necessary to activate surface reactions that burn off the coke residue. When using high-calorific coals with a low volatile content, to overcome the activation threshold, as well as for coals with a moderate volatile content, to stabilize the ignition process, a pre-injection of a small portion of pilot liquid fuel or some other external open flame source into the working cylinder is used. Calculations show that for the successful combustion of high-calorific solid fuels in an engine with a rotational speed of approximately 1500 min^{-1}, the combustion activation threshold must overcome within the first two degrees of crankshaft rotation [33]. To obtain the thermal effect from the reactions between atmospheric oxygen and the carbon in the fuel, a certain amount of heat must supply to the working cylinder beforehand. The activation rate of the combustion process is an important parameter. Given the limited time available for the combustion process, the completeness of fuel burnout depends on the activation rate, which ultimately significantly affects the thermal efficiency of the engine. The energy ratio between the heat released as result of combustion of the ignition fuel and the total heat required to carry out the thermodynamic cycle characterized by the ignition coefficient:

$$\chi = \frac{Q_{pil}}{Q_{cycl}},$$

where Q_{pil} – the heat obtained as a result of combustion of the pilot fuel; Q_{cycl} – the total heat released during the cycle.

6.2. Methods of forced ignition of coal fuel in the combustion chamber of a piston engine and their influence on the working process.

Existing methods of forced ignition of solid fuel in the engine's combustion chamber can roughly divided into the following groups:

- coal fuel ignites due to interaction with an air charge, the temperature of which is pre-injected with a portion of the DF. In this case, all of the DF burns before the coal fuel injected into the cylinder (thermal ignition method);
- pilot DF injection is carried out through a separate injector. This injector delivers the DF in such a way that the injection of the pilot and main fuels overlaps in timing (pilot ignition method);
- stratified pilot fuel injection, in which the pilot DF is injected into the working cylinder through the main injector before or after the injection of the main fuel (stratified pilot ignition method);
- the combustion process is activated by introducing a plasma jet into the combustion chamber, obtained in a separate chamber by forced ignition (for example, from an electric spark) of a gas-air or petrol-air mixture (plasma ignition method).

6.2.1. Thermal ignition method. During the course of WCS combustion studies in a low-speed Sulzer engine, a so-called thermal ignition method studied. To implement this method, auxiliary fuel injection advanced so that all auxiliary DF had time to burn completely before the WCS delivered. With this ignition method, the role of the auxiliary fuel was to increase the air charge temperature to a value sufficient for WCS self-ignition. These tests showed that achieving stable ignition parameters using this method is quite difficult [65]. Fig. 6.1 illustrates an inverted oscillogram showing the pressure change over ten operating cycles in a low-speed 1RSA76 Sulzer engine.

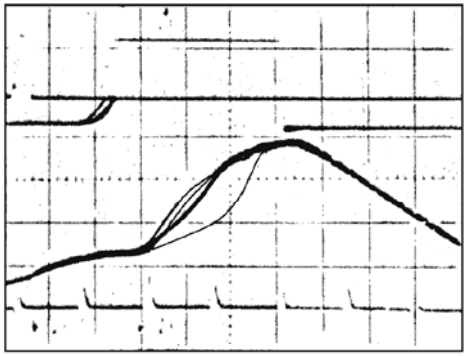

Fig. 6.1. Change in pressure in the working cylinder of the 1RSA76 engine from Sulzer over ten cycles using the thermal ignition method (based on the results of processing the oscillograms given in [65])

In the mode under consideration, the auxiliary DF consumption is 3...4%, and the engine load is approximately 50%. As can be seen from the figure,

the spread of the curves for this ignition method is quite large, indicating instability of the ignition process, resulting in poorer engine performance than with other ignition methods. In particular, the specific fuel consumption increases by an average of 5% compared to the pilot ignition method.

6.2.2. Pilot ignition method. Injecting a small amount of pilot liquid fuel into the combustion chamber intensifies the ignition process of coal particles. The ignition activation mechanism, which injects liquid diesel fuel simultaneously with the introduction of coal fuel into the cylinder, has two components. First, the ignited diesel fuel heats the air charge, which accelerates the heating of the coal particles and the release of volatile components, as well as accelerates reactions on the particle surface and in the gas phase. Secondly, the presence of an open flame accelerates the ignition of volatile components, which have a relatively low cetane number (15...19).

Depending on which factor predominates in the ignition process of the coal particles, pilot fuel injection may begin with the introduction of coal fuel into the combustion chamber or toward the end of the introduction. For high-calorific fuels, where volatiles play a minor role in the ignition process, it obviously makes sense to inject pilot fuel at the start of the carbon fuel injection. For fuels with a high volatile content and low volatile release temperature, pilot fuel should inject closer to the end of the main fuel injection. In this case, the volatiles will released from the carbon particles due to the heat of the charge, and the formation of an open flame will lead to their rapid ignition. In all cases, pilot ignition been noted to provide a more stable ignition characteristic, resulting in reduced pressure fluctuations from cycle to cycle. Fig. 6.2 shows pressure oscillograms for ten consecutive cycles in a Sulzer 1RSA76 low-speed engine using pilot ignition.

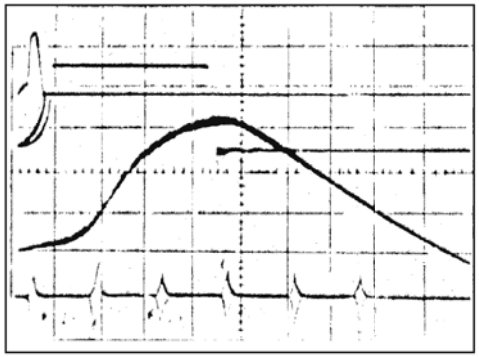

Fig. 6.2. Change in pressure in the working cylinder of the 1RSA76 engine from Sulzer over ten cycles using the pilot ignition method (based on the results of processing the oscillograms given in [65])

Unlike thermal ignition (Fig. 6.1), pressure fluctuations are minimal.

The effect of pilot ignition on the operating process of the 7FDL diesel engine, when operating on WCS in partial load mode, demonstrated in Fig. 6.3. The main operating process indicators presented in Table 6.1.

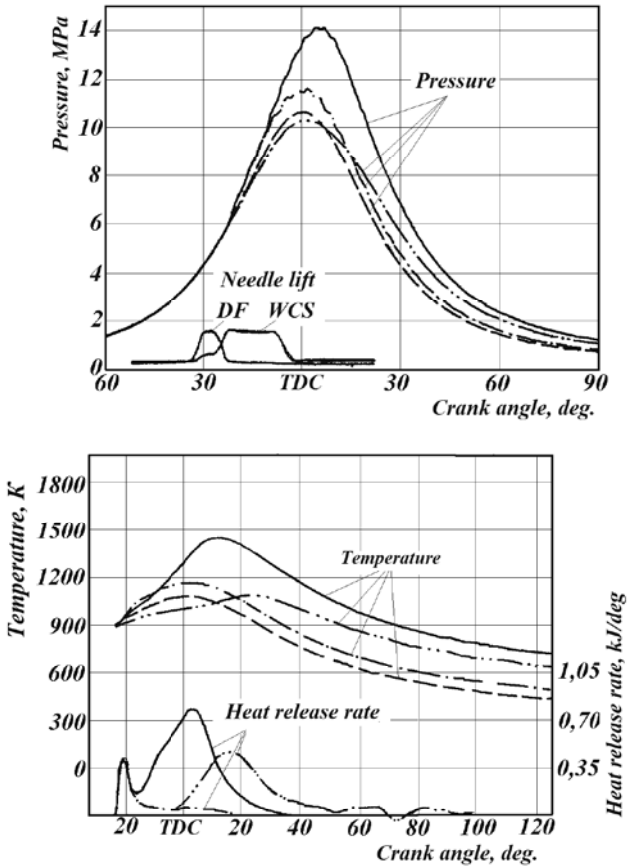

Fig. 6.3. Effect of pilot ignition on the working process in the 7FDL diesel engine from General Electric (main fuel WCS, pilot fuel DF). – – no fuel; – · – pilot DF; —— pilot DF+WCS; – · · – WCS

The amount of pilot fuel supplied to the combustion chamber was 90 mm^3 per cycle. In energy terms, this is approximately 6…7% of the energy required by the engine at maximum load. Four cases considered for comparison: no main and pilot fuel supply (curve 1); only pilot fuel supplied

to the cylinder (curve 2); pilot fuel and WCS supplied (curve 3); no pilot fuel supply (curve 4).

Table 6.1.

The influence of pilot ignition on the operating process of the General Electric 7FDL engine (partial load mode)

Fuel	Ignition characteristics*							Combustion characteristics			
	Dynamic injection angle (before TDC), deg		Ignition (to TDC), deg		Ignition delay, deg		WCS combustion start temperature, K	P_{max}, *MPa*	Power, kW	Fuel burnout efficiency, %	Specific heat consumption, kJ/(kWh)
	DF	WCS	DF	WCS	DF	WCS					
No fuel	——	——	——	——	——	——	——	10.6	-23.3	——	——
DF	33.8	——	24.0	——	9.8	——	——	11.6	5.3	100	17329
DF + WCS	33.8	32.4	24.0	18.0	9.8	14.4	1011	14.1	76.6	98.7	8038
WCS	——	32.4	——	7.0	——	25.4	983	10.1	43.1	75.5	12079

* n = 1050 min^{-1}, inlet air temperature 110°C; inlet air pressure 329 kPa; static injection angle of pilot fuel – 47° before TDC; static injection angle of WCS – 47° before TDC.

Fig. 6.3*a* and Table 6.1 demonstrate that using pilot ignition to initiate the WCS combustion process allows for maximum cylinder pressure. While a separate pilot fuel injection increases pressure to 11.6 MPa, a separate WCS injection increases pressure to 10.2 MPa, and the combined injection of these two fuels allows for a maximum cylinder pressure of approximately 14 MPa. When only WCS is injected into the combustion chamber, the maximum cycle pressure is reduced to a value lower than without any fuel injection. At the same time, fuel combustion occurred, as pressure waves recorded by the sensor. During operation, a sound typical of diesel engines operating with extremely early DF injection or with a long ignition delay was audible.

Fig. 6.3*b* shows the calculated cylinder temperature and heat release rate. With pilot fuel injection alone, heat release began approximately 24°C before TDC, with the heat release curve typical of early DF injection. All the fuel burned almost immediately after ignition. When WCS and pilot DF injected into the combustion chamber, the first portion of the heat release curve remained unchanged. This occurred because some WCS injected into the cylinder before DF ignition. WCS ignition characterized by the appearance of a second peak in the heat release curve. It should noted that without pilot fuel, WCS self-ignition 7°C before TDC, while with pilot fuel, this occurred 18°C before TDC. It should also note that with pilot ignition, the maximum heat release of WCS combustion is much higher than with self-ignition.

From the Table 6.1 shows that the combined combustion of pilot fuel and WCS results in significantly higher power (76.6 kW) than that achieved with either fuel type alone. This explained not only by the combined thermal effect of combustion but also by the nature of the heat release. When using pilot fuel and WCS, heat release is concentrated in the immediate vicinity of the TDC, while in other cases, maximum heat release achieved well beyond the TDC. Without pilot fuel, the WCS ignition delay is 25.4° of crankshaft rotation; with pilot ignition, the delay reduced to 14.4°. The temperature dependences show that the WCS is exposed to a higher average charge temperature before ignition. Clearly, by the time the first solid fuel particles ignite, the local temperature affecting the particle is even higher.

6.2.3. Stratified ignition method. Stratified ignition can only loosely identify as a separate method for activating the ignition process of coal fuel in the working cylinder of a piston engine. Its main difference from thermal ignition is that WCS injection occurs immediately after the pilot fuel injection, and activation occurs not only due to an increase in the air charge temperature but also through direct contact of the volatile products of coal decomposition with an open flame.

Stratified ignition differs from pilot ignition in those clearly defined zones of distribution of the fuel-air mixture with the pilot fuel and WCS formed within the air charge.

The use of stratified pilot fuel injection to activate WCS ignition was investigated General Electric on the 7FDL diesel locomotive engine [52]. Pilot fuel injection performed through the main injector, located along the axis of the working cylinder. The studies conducted at an engine speed of 1050 min^{-1}, with the inlet air temperature and pressure maintained at 110°C and 329 kPa, respectively, and the static injection start at 52° before TDC. The test results are shown Fig. 6.4 and Table 6.2.

Table 6.2.

The effect of stratified ignition on the operation of the General Electric 7FDL engine

Fuel	Ignition characteristics*				Combustion characteristics			
	Dynamic injection angle (before TDC), deg	Ignition (to TDC), deg	Ignition delay, deg	WCS combustion start temperature, K	P_{max}, *MPa*	Power, kW	Fuel burnout efficiency, %	Specific heat consumption, kJ/(kWh)
No fuel	——	——	——	——	10.6	-8.7	——	——
Stratified fuse	40.4	10.0	30.4	972	13.1	69.9	94.0	8124

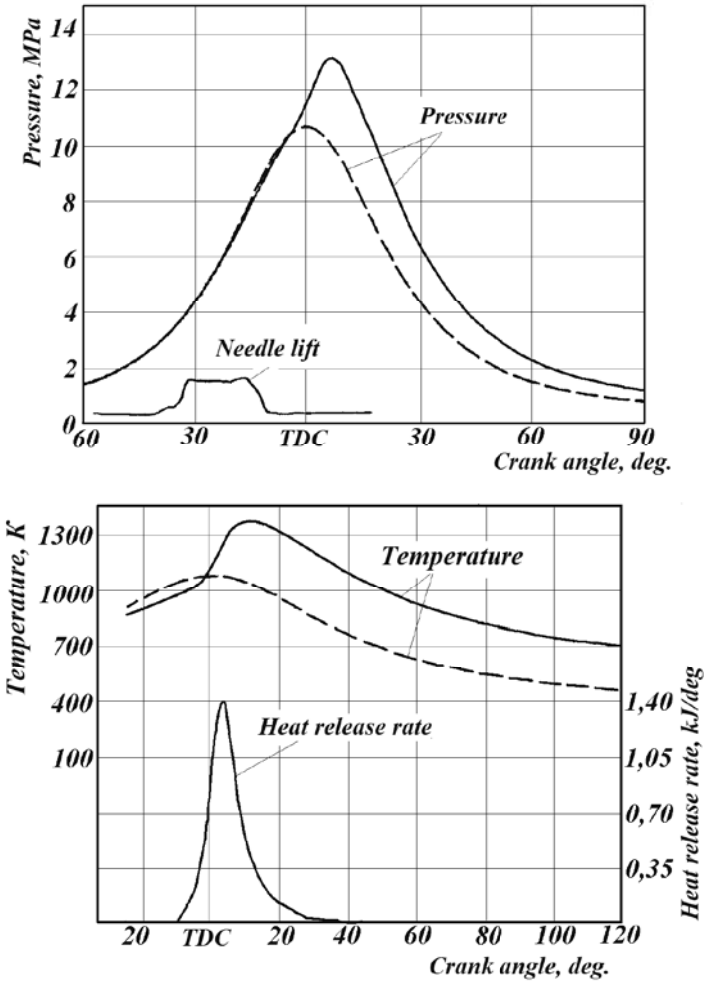

Fig. 6.4. Change in pressure, heat release rate and temperature in the working cylinder of the General Electric 7FDL engine with stratified ignition WCS. —— pilot fuel supply through the main injector; – – – no pilot fuel supply

Studies have shown that, compared to WCS self-ignition, the ignition delay with stratified ignition reduced from 40° to approximately 30°. This is apparently because diesel fuel injected into the combustion chamber before the WCS. Moreover, the conditions for pilot fuel self-ignition are virtually identical to those in DF-fueled engines. With stratified pilot fuel injection,

pressure fluctuations were absent during pressure changes, which is explained by the sequential combustion of both fuels, with DF pilot combustion smoothly transitioning to WCS combustion. Stratified ignition, compared to other forced-ignition methods, demonstrated the highest heat release rate in the engine's working cylinder, reaching up to 1.4 kJ/deg.

Table 6.3.

Operating parameters of the 7FDL engine of General Electric at partial loads with different methods of activating the ignition process of the combustion chamber

Parameter	Ignition method		
	Compression self-ignition	Pilot ignition	Stratified ignition
Heat release rate, kJ/deg	0.57	0.77	1.39
Fuel burnout rate, %	88.2	98.7	94.0
Heat utilization rate, %	94.6	96.8	97.9
Specific effective heat consumption, kJ/(kWh)	9508	8038	8124
Effective power, kW	45.6	76.6	69.9

Fig. 6.5 and Table 6.3 compare the operating parameters of the 7FDL engine at partial loads with the stratified and pilot ignition methods of WCS ignition activation, as well as during self-ignition. Fig. 6.6 and Table 6.4 similarly present the operating parameters for full load mode.

Table 6.4.

Operating parameters of the General Electric 7FDL engine at full load conditions with different WCS ignition process activation methods

Parameter	Ignition method			
	Stratified ignition	Pilot ignition	Compression self-ignition	Diesel fuel
Ignition coefficient	0.05	0.06	0	1.0
Specific heat consumption, kJ/(kWh)	8721	8400	9044	8141
Burnout efficiency, %	90.3	93.8	92.1	100
P_{max}, (MPa)	17.5	16.5	15.9	15.4
Effective power, kW	182	181	185	197

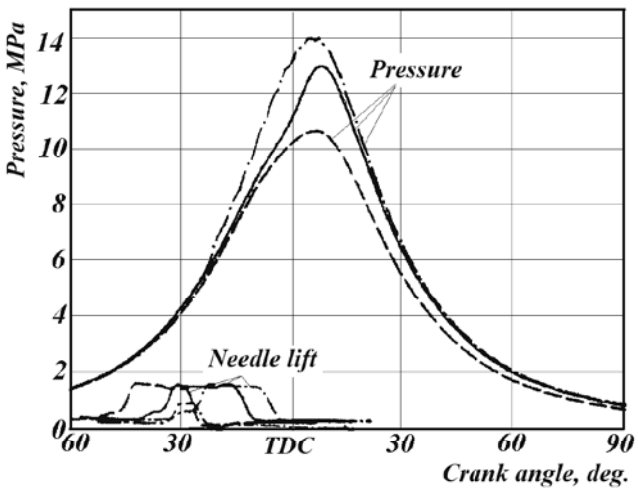

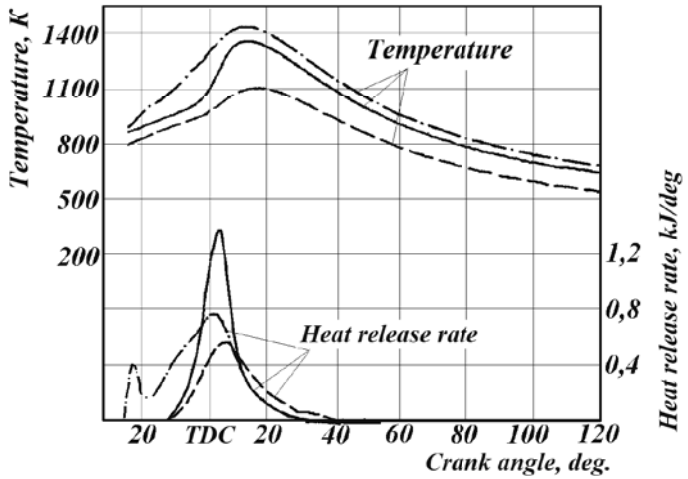

Fig. 6.5. Change in pressure, heat release rate and temperature in the working cylinder of the General Electric 7FDL engine with different WCS ignition activation methods (partial load mode). —— stratified ignition; – – – self-ignition; – · – pilot ignition

For comparison, the tables and figures provide data for the self-ignition of coal fuel; in addition, Table 6.4 provides the engine characteristics when operating on DF No. 2.

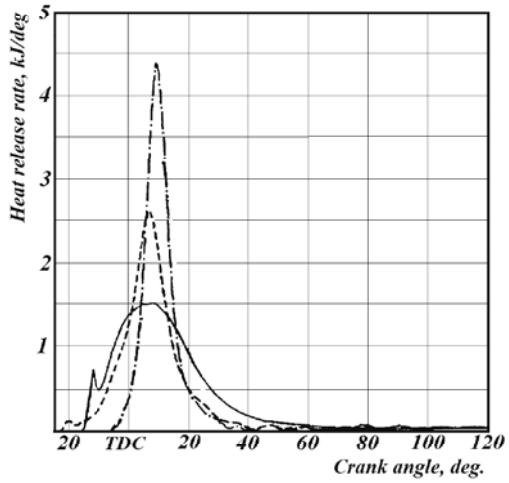

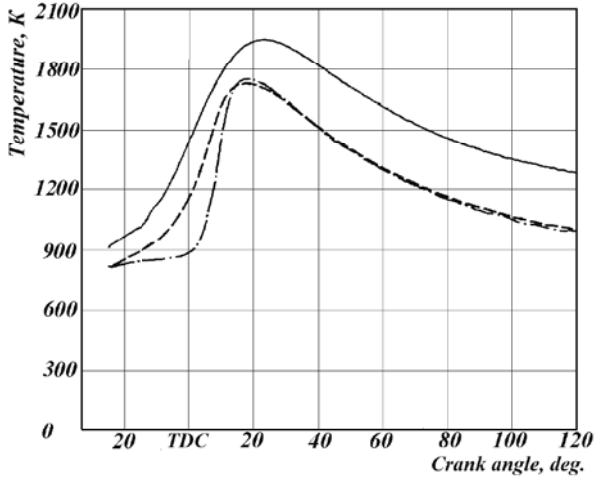

Fig. 6.6. Change in the rate of heat release and temperature in the working cylinder of the General Electric 7FDL engine with different methods of WCS ignition activation (full load mode). —— DF; – – – WCS + pilot ignition; — · — WCS + stratified ignition

6.2.4. Plasma ignition method. The possibility of using the plasma ignition method for WCS was investigated specialists at Cooper-Bessemer [44]. A four-stroke, single-cylinder JS-1 engine, which in its basic version designed to operate on natural gas, diesel fuel, or a combination of both, was used for these experiments.

For the plasma ignition experiments with WCS, a special cylinder head designed and manufactured, a cross-section of which shown in Fig. 6.7. In addition to the main and auxiliary nozzles, a jet gas burner for flare combustion of natural gas installed in it.

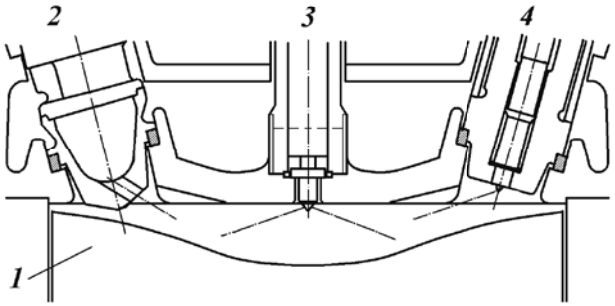

Fig. 6.7. Design of the cylinder head of the JS-1 engine by Cooper-Bessemer. 1 – working piston; 2 – jet gas pre-chamber; 3 – main injector; 4 – injector for supplying pilot DF

Gas enters the pre-chamber through the supply valve during a period when the pressure in the natural gas supply line is greater than the cylinder pressure. During the compression stroke, air enters the pre-chamber from the working cylinder, forming a combustible mixture. This mixture is ignited by a spark plug in the jet pre-chamber, after which the hot combustion products enter the main combustion chamber as a jet, which acts as the ignition source.

Fig. 6.8 shows that the jet gas igniters ignites and provides combustion parameters similar to pilot ignition-using DF supplied through a three-hole auxiliary nozzle. As with plasma ignition, the ignition coefficient of natural gas is only 0.04...0.05.

In both cases, maximum cylinder pressure reached 9° after TDC and approximately 8.2 MPa. Experiments with pilot ignition resulted in a slightly shorter ignition delay and, consequently, a lower heat release rate. Specific fuel consumption and exhaust gas temperatures during dynamometer testing were nearly identical for both cases.

Thus, plasma ignition allows for quite acceptable engine operating cycle parameters with a relatively simple igniters design.

Plasma ignition eliminates the need for a complex and expensive pilot fuel injection system, replacing it with a simpler and more proven system for preparing a gas-air or fuel-air mixture. Furthermore, the use of a plasma plume and ignition of the combustible mixture by an electric spark allows for wide control of the fuel ignition process in the engine's combustion chamber, both during development and during operation.

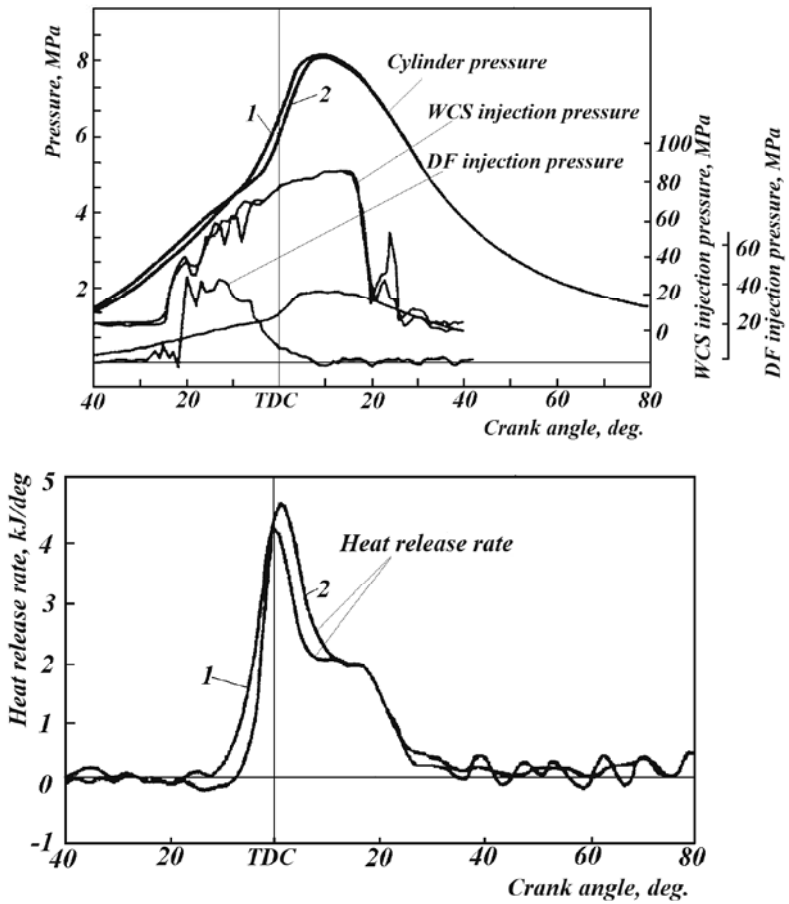

Fig. 6.8. Change in pressure and rate of heat release in the working cylinder of the Cooper-Bessemer JS-1 engine during WCS ignition by the pilot and plasma methods. 1 – pilot ignition; 2 – plasma ignition

6.3. The influence of air charge parameters at the engine inlet on the efficiency of the working process.

As with the spontaneous combustion of coal fuel by compression, for forced-ignition engines, a significant potential for improving operating efficiency lies in manipulating the air charge parameters at the engine inlet. Depending on the objectives, changing one or more air parameters at the engine inlet can improve fuel combustion efficiency and thermodynamic cycle parameters.

In further consideration of the various factors influencing engine operation, the primary focus will be on the use of water-coal fuel. This is because this fuel offers greater potential in terms of reducing dependence on oil and is more theoretically interesting. Consequently, the greatest amount of research been conducted on this fuel recently.

6.3.1. The influence of excess air coefficient on the efficiency of the engine working process. Theoretically, due to the higher carbon-to-hydrogen ratio, stoichiometric combustion of coal-based fuel requires 3...5% more air than DF combustion. However, a longer ignition delay allows for prolonged mixing of the coal particles with the air charge, resulting in a more homogeneous mixture by the time of ignition. With optimal selection of main and pilot fuel injection parameters, this enables efficient combustion of solid fuels at lower excess air ratios (α) than in engines operating on DF. During WCS combustion experiments in a 7FDL engine at full load at 1050 min^{-1}, an indicated power of over 190 kW/cyl (p_i = 2.0 MPa) was achieved with α = 1.6. When using DF, reducing α below 1.9 resulted in a significant deterioration in combustion performance in this engine. It might expect that with increasing α, combustion efficiency will increase, and heat losses in the engine's working cylinder will decrease. However, calculations show that with $\alpha \geq 2$, fuel combustion efficiency begins to decline. This behavior explained by the uniform distribution of particles within the air charge. With uneven mixing, fuel combustion would occur in specific zones, resulting in a localized temperature increase within these zones around groups of burning carbon particles. Thus, higher reaction rates would maintain in localized zones separated from the main portion of the cooler working gas. If the mixing of fuel particles and the air charge is uniform, the gradients within the working space of the cylinder are insignificant, and the particles surrounded by gas with a lower temperature. This leads to more intense heat exchange and a decrease in particle temperature. Therefore, despite the excess oxygen, reaction rates are quite low. Increased combustion time and the associated incomplete burnout of the fuel lead to a decrease in overall engine efficiency.

All of the above is also true for engines operating with self-ignition of coal fuel. Thus, the combustion efficiency of solid fuel depends largely on the excess air ratio in the engine cylinder. To maintain engine performance, especially at full load, any influence on the intake air parameters must carry out in such a way that α remains close to the optimal value for the given engine.

6.3.2. Effect of engine inlet air temperature on WCS combustion efficiency. As noted, the ignition of the WCS introduced into the combustion chamber is preceded water vaporization and the release of volatiles from the

coal. To cover the heat losses in these processes, the temperature at the end of compression must be sufficiently high. An optimal and relatively simple method for influencing the temperature at the end of compression is to preheat the inlet air.

As discussed in Chapter 5, increasing intake air temperature improves ignition and combustion of the coal-fueled fuel in compression ignition engines. The main factor contributing to more efficient fuel combustion in such engines is the compensation of heat losses due to water evaporation through increased temperature and, consequently, a reduction in the ignition delay period. In pilot-ignition engines, the delay period significantly depends on the method and characteristics of pilot ignition. Therefore, the effect of preheating the intake air is not as clear-cut as for compression self-ignition engines.

At maximum load conditions, to maintain the required charge mass, an increase in temperature must accompanied by an increase in intake air pressure. However, excessive intake air pressure leads to an excessive increase in maximum combustion pressure and, consequently, high mechanical loads in the engine. Increasing intake air temperature without compensating for charge density at the engine intake leads to a decrease in cylinder mass filling, which impacts fuel combustion efficiency. Based on the above, two methods for heating the charge at the engine intake can distinguish: with a constant charge density and with a constant pressure. Depending on the intake air heating method, as well as the temperature range used, the effect of charge heating at the engine intake can vary significantly.

***

At a constant charge density, the engine inlet temperature limited, on the one hand, by the need to maintain an optimal excess air ratio, and on the other hand, by the permissible boost pressure. For the General Electric 7FDL engine with α = 2 and a boost pressure of 308...377 kPa, the intake air temperature range was selected from 65° to 145°C. In this range, a higher temperature (and, accordingly, a higher pressure) improves fuel combustion and leads to a decrease in its specific consumption. An increase in intake air temperature also promotes optimal heat release (in the TDC region) and an increase in cylinder pressure, which is clearly visible in Fig. 6.9, which shows the change in pressure and heat release rate in the 7FDL engine working cylinder. Considering that the air charge density is constant for both temperatures and the carbon fuel injection adjustment is the same, it can assume that the fuel spraying conditions for the considered cases are very similar. A higher temperature allows for better-indicated characteristics of the working process. This is primarily because increasing inlet pressure leads to

an increase in the maximum combustion pressure. It can reach values of approximately 15.5 MPa, significantly exceeding the equivalent value for this engine when operating on DF. However, as can be seen from Fig. 6.9, the difference in maximum pressures is insignificant.

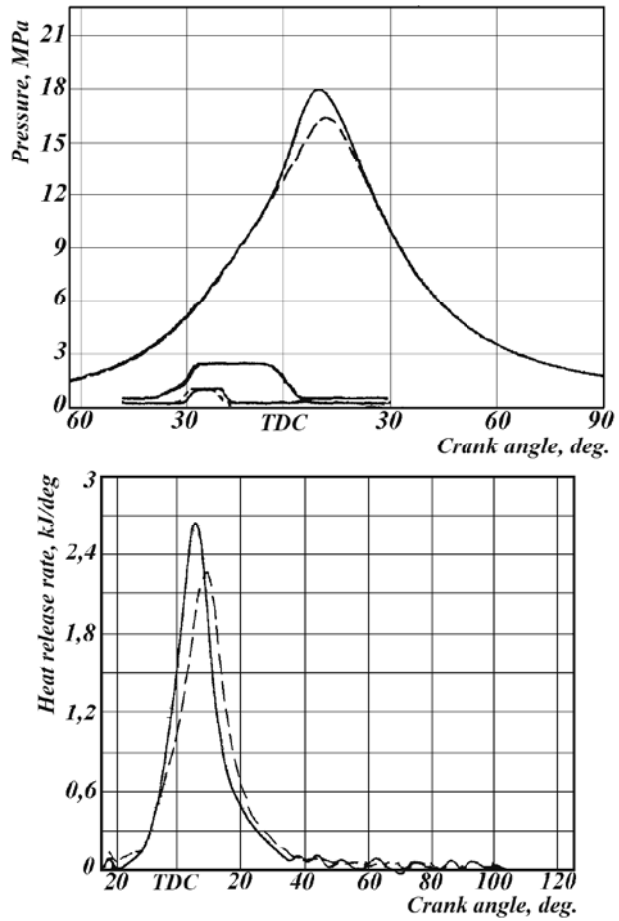

Fig. 6.9. Change in pressure and rate of heat release in the working cylinder of the 7FDL engine of General Electric at constant density and different air inlet temperatures (pilot ignition, full load).——— 104°C; – – – 85°C

On the heat release curve, the first small peaks reflect the combustion of the pilot fuel. The second large peaks are due to the combustion of the coal fuel. They increase significantly with increasing inlet air temperature. It is

important to note that as temperature decreases, the maximum heat release shifts toward expansion, indicating a decrease in the combustion rate of the WCS. The main operating characteristics of the 7FDL engine for different temperatures at a constant charge density presented Table 6.5.

Table 6.5.

Operating parameters of the General Electric 7FDL engine at constant density and various supply air heating temperatures (full load mode)

Method of ignition	Engine inlet air			Burnout rate, %	Specific heat consumption, kJ/(kWh)	P_{max}, MPa
	Density, kg/m^3	Temperature, °C	Pressure, kPa			
PI	3.173	85	326	85.5	9320	16.4
PI	3.173	104	344	91.2	8696	18.0
SI	3.173	104	344	76.0	11721	13.0
SI	3.173	124	362	79.3	11026	16.2

PI – pilot ignition; SI – stratified ignition.

***

At constant pressure, a higher temperature (and, consequently, lower air charge density) allows for virtually the same complete combustion of coal fuel as a lower temperature (higher air charge density). Clearly, the effects of temperature and density on coal fuel burnout are balanced. Within the considered parameter range, a change in temperature has a greater impact on specific fuel consumption than a change in density. It should note that heat release efficiency (optimal heat release relative to TDC) increases with increasing air inlet temperature. The large difference in maximum pressure values is also explained the influence of temperature, which has a greater effect than density. Fig. 6.10 compares pressures and heat release in the cylinder of a 7FDL engine.

Due to the low inlet air temperature, pilot fuel combustion begins later, although pilot fuel injection timing is identical for both cases. However, improved pilot fuel spraying and WCS due to the higher air charge density obviously cannot compensate for the lower thermal efficiency of the combustion process. As can be seen from Fig. 6.10, heat release occurs very slowly, with the majority of it released in the expansion line. Some operating characteristics of the 7FDL engine for different temperatures at constant inlet pressure presented Table 6.6.

The above data demonstrates that the performance of engines operating on WCS is extremely sensitive to inlet air temperature. It should also note that, at a constant pressure, increasing inlet temperature up to a certain point leads to an increase in engine efficiency. As temperature increases further, other combustion mechanisms may become more prominent, resulting in a decrease in cycle efficiency.

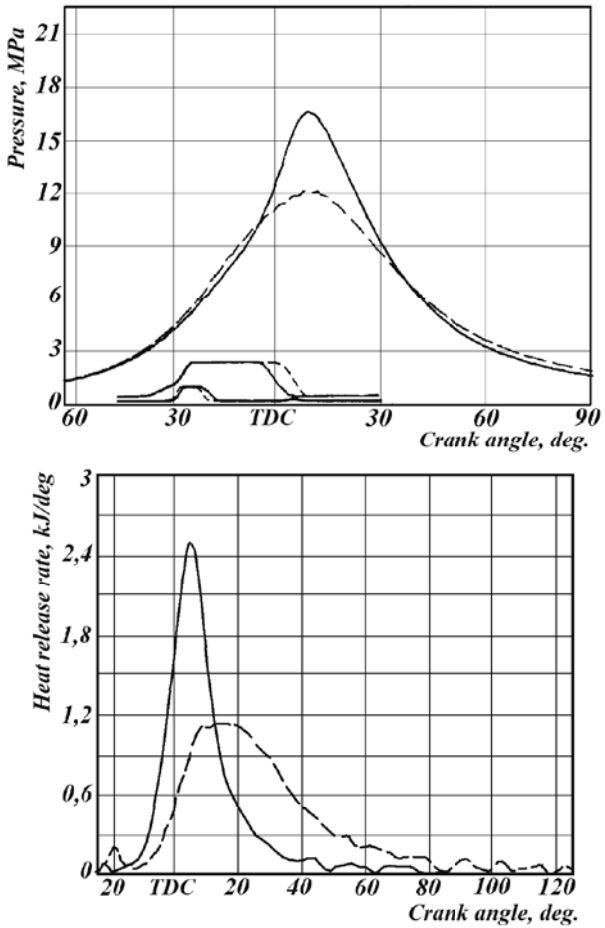

Fig. 6.10. Change in pressure and rate of heat release in the working cylinder of the 7FDL engine from General Electric at constant pressure and different air inlet temperatures (pilot ignition, full load). ——— 104°C; – – – 66°C

Table 6.6.

Operating parameters of the General Electric 7FDL engine at constant pressure and various supply air heating temperatures (full load mode, pilot ignition)

Engine inlet air			Burnout rate, %	Specific heat consumption, kJ/(kWh)	P_{max}, MPa
Pressure, kPa	Temperature, °C	Density, kg/m^3			
308	104	2.842	86.2	9260	16.7
308	66	3.173	86.5	10392	12.1

Thus, a significant increase in supply air temperature will significantly reduce the ignition delay period, causing combustion to begin long before the fuel particles uniformly distributed throughout the air charge. In this case, combustion of the particles will occur in localized zones due to a lack of oxygen. As a result, the combustion process will be longer and less efficient.

An example of the effect of high supply air temperature at constant pressure on the efficiency of an engine operating under WCS pilot ignition showed Fig. 6.11. The characteristics obtained during testing of the Cooper-Bessemer JS-1 medium-speed engine [66].

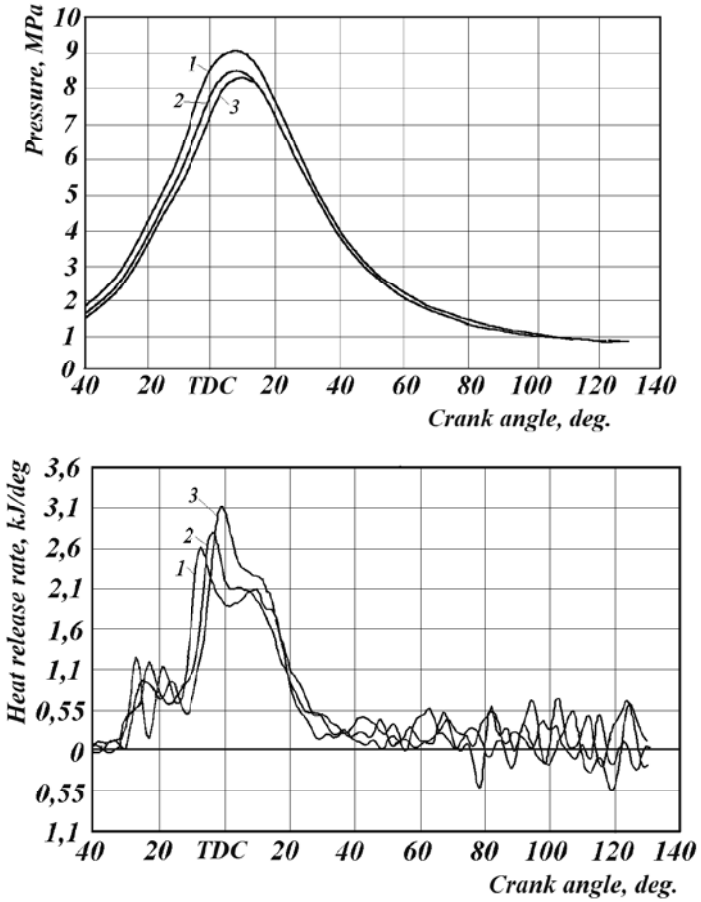

Fig. 6.11. Change in pressure and rate of heat release depending on the air temperature at the inlet of the Cooper-Bessemer JS-1 engine. 1 – 226°C; 2 – 176°C; 3 – 144°C

During engine testing, WCS (Table 3.6) used as the primary fuel, and DF was used as the pilot fuel. Engine inlet air temperature varied from 144 to 262°C. The pilot fuel and WCS injection times were 35° and 18° before TDC, respectively, while the WCS injection pressure maintained at 82 MPa.

As can be seen in Fig. 6.11, the maximum combustion pressure increased with increasing temperature within the range of 8.6…9.3 MPa, while the maximum heat density decreased from 3.16 to 2.64 kJ/deg.

The decrease in heat release rate with increasing inlet air temperature is primarily due to a gradual decrease in the WCS ignition delay from 7° to 4°.

The increase in heat release rate with decreasing inlet air temperature partially offsets the heat losses associated with fuel ignition delay, even at engine inlet air temperatures of approximately 144°C. This is also confirmed by the fact that the specific heat consumption per unit of power output remained virtually constant for different temperatures (5.3 MJ/(kWh)).

These tests conducted for two types of suspensions with average particle sizes of 11 μm and 8 μm. In both cases, the above-described pattern was maintained; the only difference was that when using WCS with smaller particles, the specific heat consumption increased to 5.6 MJ/(kWh), which is 4% higher than when using WCS with larger particles. This is obviously, because larger particles, having greater inertia, more evenly distributed within the air charge.

Unlike the case where combustion initiated by self-ignition, with pilot ignition, the effect of increasing the air, charge temperature depends significantly on a number of additional factors. Under certain conditions, heating the inlet air can improve combustion. However, it should note that increasing the temperature leads to increased nitrogen oxide levels in the exhaust gases.

6.3.3. The influence of engine inlet air pressure on the WCS ignition process. At higher pressure (and, consequently, higher density), the efficiency of coal combustion increases, the specific heat consumption decreases, and the maximum cylinder pressure increases. Higher air charge density improves pilot fuel and WCS spraying, resulting in increased ignition and combustion efficiency of coal particles. This leads to a decrease in heat consumption per unit of power output. At lower pressures, due to poorer atomization, a longer ignition delay observed, resulting in a significant difference in the pilot fuel combustion heat release rate curve from the curve obtained at higher inlet air pressure. This is evident in Fig. 6.12 and Table 6.7, which display the results of a 7FDL engine test at part-load.

The increased ignition delay of the DF pilot fuel also occurs because the water contained in the WCS suppresses the initial high combustion rate of the

DF pilot fuel. However, the latter remains high enough effectively initiate the WCS ignition process.

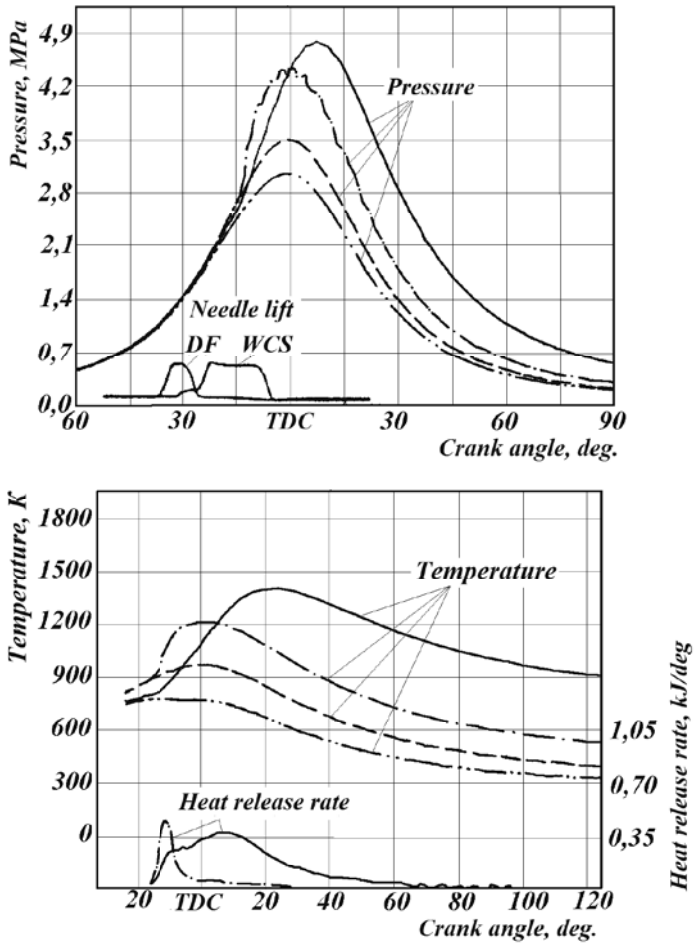

Fig. 6.12. Engine operating process in part load mode at reduced air inlet pressure (n=1050 min^{-1}, air inlet temperature 85°C; air inlet pressure – 112 kPa; static angle of pilot fuel injection and WCS, respectively, – 49° and 47° before TDC). – – – no fuel injection; – · – pilot DF; —— WCS + DF; – ·· – WCS

As can be seen from the heat release graph, WCS ignition delayed in the same way as DF pilot ignition. WCS combustion begins approximately 4° before TDC, while the maximum temperature during the combined

combustion of WCS and DF pilot remains almost as high as for the higher-pressure case (Table 6.5).

Table 6.7.

The effect of reduced air pressure at the engine inlet on the operating process with the pilot ignition method (partial load)

Fuel	Ignition characteristics*							Combustion characteristics			
	Dynamic injection angle (before TDC), deg		Ignition (to TDC), deg		Ignition delay, deg		WCS combustion start temperature, K	P_{max}, *MPa*	Power, kW	Fuel burnout efficiency, %	Specific heat consumption, kJ/(kWh)
	DF	WCS	DF	WCS	DF	WCS					
No fuel	——	——	——	——	——	——	——	3.5	-6	——	——
DF	36.6	——	16.3	——	20.3	——	——	4.4	9.3	100	12072
DF + WCS	36.6	31.1	16.3	4.0	20.3	27.1	1000	4.8	49.7	72.3	12009
WCS	——	31.1	——	no	——	no	780	3.1	-11.0	0	no

A somewhat different effect of increased inlet pressure on the engine's performance observed when the engine is operating at full load. Typical pressure and heat generation relationships in the cylinder for various inlet pressures showed Fig. 6.13. Table 6.8 presents the main operating parameters.

Table 6.8.

Operating parameters of the General Electric 7FDL engine at constant temperature and various supply air pressures (full load mode, pilot ignition)

Engine inlet air			Burnout rate, %	Specific heat consumption, kJ/(kWh)	P_{max}, *MPa*
Pressure, kPa	Temperature, °C	Density, kg/m^3			
308	104	2.842	86.2	9260	16.7
344	104	3.173	91.2	8696	18.0

Here, there is virtually no difference in ignition delay, and the difference between maximum pressures is not as great as in the case of elevated temperature at constant charge density. There are virtually no differences in the nature of heat release, other than the maximum value. Since the nature of heat input has a predominant influence on the maximum pressure developed in the cylinder, the difference in maximum cycle pressures caused solely by the difference in inlet pressures.

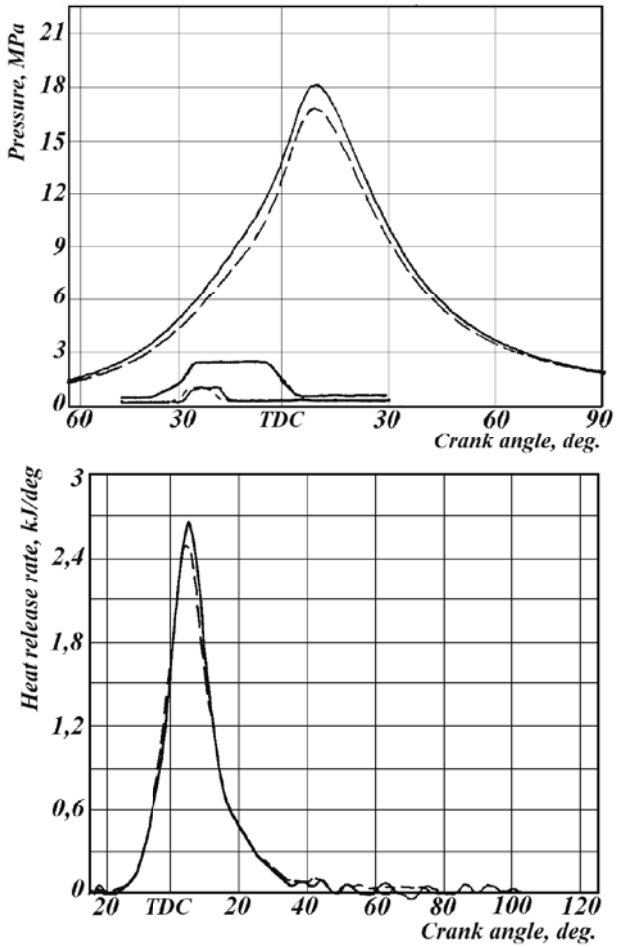

Fig. 6.13. Change in pressure and heat generation in the cylinder at full load at different values of air inlet pressure. (n = 1050 min^{-1}, air inlet temperature 104°C). —— air inlet pressure 344 kPa; – – air inlet pressure 308 kPa

6.4. The influence of the injection angle of the pilot DF and WCS on the efficiency of the working process of the engine with pilot ignition.

Adjusting the fuel injection advance angle (IAA) is one of the most effective ways to influence both the ignition and subsequent combustion of the coal fuel, as well as the entire engine operation. This method is particularly convenient in operation, as it allows the operating process to

influence by simply adjusting the fuel injection angle. This may be necessary, for example, when changing the original fuel included in the WCS (as already noted, the properties of the original fuels can differ significantly).

The combined injection of two fuels into the working cylinder can adjusted in three ways:

- by adjusting the WCS supply while maintaining the pilot fuel IAA;
- by adjusting the pilot fuel IAA while maintaining the WCS injection angle;
- by changing the injection advance angles of both fuels.

In the initial stages of studying the characteristics of WCS positive ignition in diesel engines, Bell and Caton [33] investigated the pilot ignition process in a high-speed locomotive engine using mathematical modeling. Two cases simulated in the first, pilot diesel, fuel was injected simultaneously with the first 25% of the WCS (during the first 5° from the start of injection); in the second, pilot fuel was injected together with the last 25% of the WCS (during the last 5° until the end of injection). After comparing the two methods, the researchers concluded that, for the conditions under consideration, the best result could achieved by injecting pilot fuel together with the first 25% of the WCS. In this case, the minimum ignition delay was achieved if the ignition coefficient was at least 0.05. Subsequently, Wahiduzzaman, Blumberg et al. performed analytical studies of the sensitivity of the operating process to adjusting the injection advance angles of pilot fuel and WCS. In this case, the injection angle of one fuel varied, while the injection angle of the second fuel remained constant. To test the model, the parameters of the General Electric 7FDL engine were as a prototype. When simulating the working process, the consumption of the main and ignition fuel taken to be 85.05 kg/hour and 5.623 kg/hour, respectively (ignition coefficient 0.19).

The main patterns of pressure changes during the operating process when regulating the supply of both fuels shown in Figs. 6.14 and 6.15 [62]. In the first case, the pilot fuel injection advance assumed to constant at 30° before TDC, while the WCS injection advance is varied. In the second case, the WCS injection advance is fixed (40° before TDC), and the pilot fuel injection angle is varied.

In addition to the expected increase in pressure and more efficient heat input at TDC, other trends are observed with increasing IAA. For the case with a fixed pilot fuel supply (Fig. 6.14), at the minimum WCS injection advance (10° before TDC), ignition begins well after TDC, combustion occurs on the expansion line, which leads to increased incomplete combustion of the coal fuel. Compared to cases of optimal control, the

incomplete combustion of the WCS primarily reduces the maximum pressure and temperature of the cycle. As the WCS injection advance angle increases, ignition occurs earlier, and higher maximum pressures and temperatures achieved. However, after increasing the IAA by more than 40° (before TDC), only an increase in maximum pressure is observed. Thus, for an injection advance of 40°, WCS ignition occurs 0.5° before TDC, and for an injection advance of 50°, it occurs 2.3° before TDC. The convergence of combustion onset for these two cases, despite a difference in WCS injection advance of 10°, occurs due to the approximately identical evaporation and ignition conditions that affect the WCS during pilot injection.

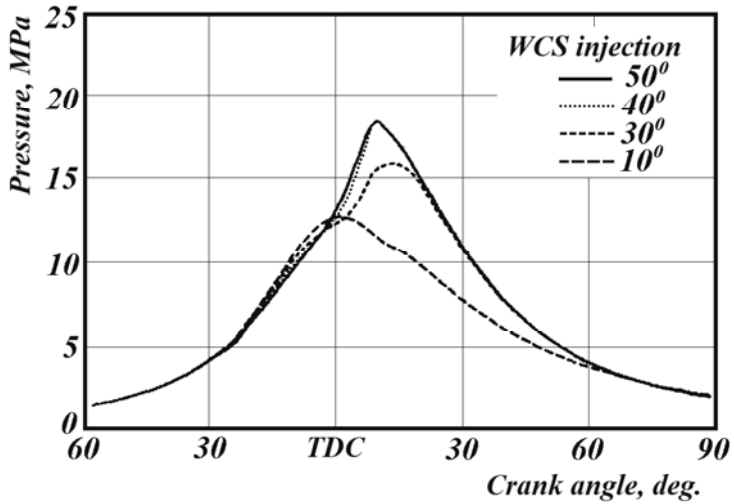

Fig. 6.14. Calculated change in pressure in the General Electric 7FDL engine at full load with a change in the WCS injection angle (start of pilot DF injection 30° before TDC; n = 1050 min^{-1}; amount of supplied WCS 85.05 kg/h; amount of supplied DF 5.623 kg/h; pressure and temperature at the engine inlet 420 kPa and 420 K, respectively)

A similar, but less pronounced, trend also observed when adjusting the pilot fuel IAA at a constant WCS injection angle. As can be seen Fig. 6.15, with a change in the pilot fuel injection advance angle (IAA WCS 40° to TDC), the maximum pressures increase as result of earlier ignition and more complete combustion of the carbon fuel particles. This occurs due to a reduction in the time for the water contained in the WCS to evaporate due to more conditions that from in favourable the air charge environment mixed with the combustion products of the pilot fuel. A further increase in the pilot fuel IAA leads to a decrease in the efficiency of the combustion process in

the cylinder. This explained, on the one hand, by the fact that pilot fuel combustion is complete before the WCS injected into the cylinder. As a result, ignition is of a thermal rather than pilot nature. On the other hand, the evaporation rate is determined the parameters of the gas environment, which, in turn, depend on changes in the air charge temperature during compression. The basic principles for pilot fuel IAA control shown in Fig. 6.15.

Fig. 6.16 *a* and 6.16 *b* present the above considerations in a slightly different form. The combustion duration of a given portion of the solid fuel presented as a function of the angular interval during which the carbon particles burn out, depending on the WCS (Fig. 6.16 *a*) and pilot fuel (Fig. 6.16 *b*) injection angle.

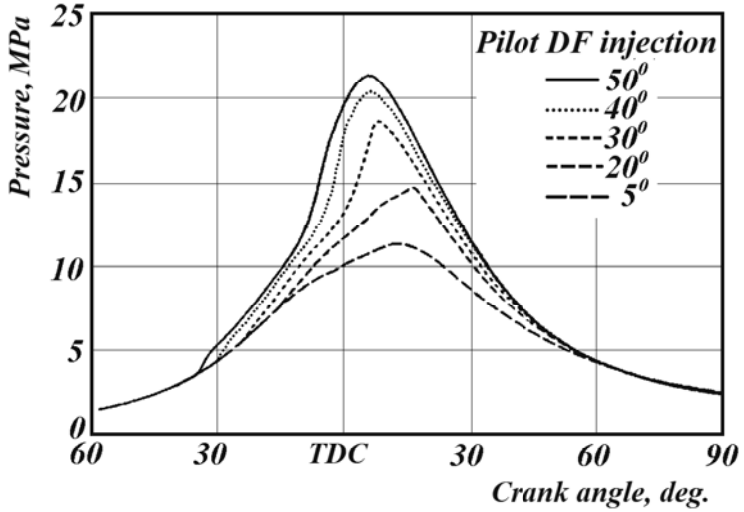

Fig. 6.15. Calculated change in pressure in the General Electric 7FDL engine at full load with a change in the pilot DF injection angle (WCS injection start 40° before TDC; n = 1050 min^{-1}; WCS supplied quantity 85.05 kg/h; DF supplied quantity 5.623 kg/h; pressure and temperature at the engine inlet 420 kPa and 420 K, respectively)

In the case under consideration, 90% of the particles burned out faster with increasing IAA for both fuels. However, achieving a significant reduction in combustion time, especially by increasing the WCS advance angle, is impossible; as combustion duration reaches a certain value and becomes virtually constant, (the reasons for this will discuss in more detail below). Therefore, a more optimal way to influence the combustion process is to adjust the IAA of the pilot fuel, since burnout times, although slightly, decrease with increasing advance angle (Fig. 6.16 *b*).

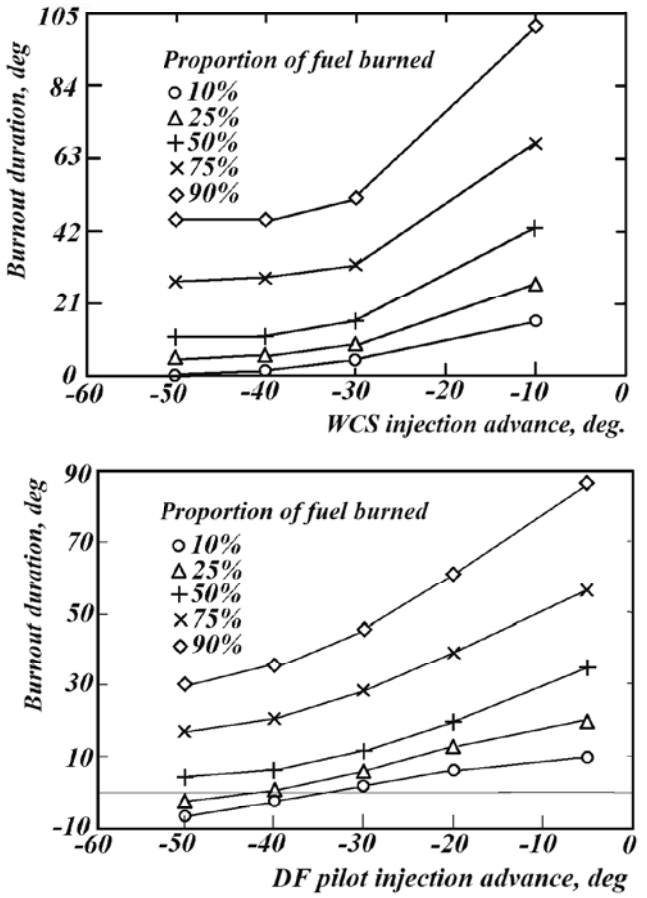

Fig. 6.16. Burnout duration as a function of injection advance control: *a* – WCS at a fixed pilot fuel injection angle of 30° before TDC; *b* – DF at a fixed WCS injection angle of 40° before TDC

Another noteworthy trend is that at later injection angles, the WCS burnout efficiency becomes increasingly nonlinear with respect to the optimal injection control parameters. This occurs primarily due to the weakening influence of surface reactions. Combustion occurs along the expansion line, preventing high temperatures from achieved in the combustion zone.

Incomplete combustion of the WCS through surface reactions leads to an increased concentration of unburned particles in the engine exhaust gases.

Fig. 6.17 *a* shows the burnout efficiency curves for both control cases, showing that with optimal IAA, a burnout efficiency of over 99% can theoretically achieve.

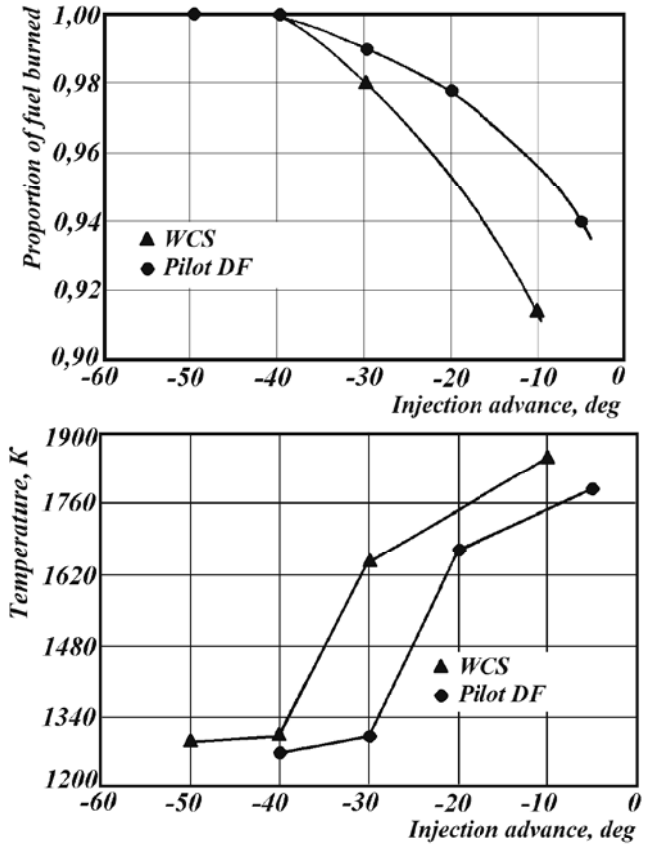

Fig. 6.17. Burnout (*a*) and exhaust gas temperature (*b*) as a function of IAA WCS and pilot fuel

Increased combustion duration associated with later injection advance leads to an increase in exhaust gas temperature, as shown in Fig. 6.17 *b*, where exhaust temperature plotted as a function of IAA WCS and DF. At low injection advance angles, combustion begins too late, and virtually all the heat released during expansion, leading to a significant increase in exhaust temperature. As the retard angle increases, the increase in exhaust gas temperature first decreases sharply and then virtually stabilizes.

Based on the above, it follows that:

- fuel injection timing can effectively influence engine operation;
- pilot fuel injection advance timing has a much greater impact on solid fuel combustion in an engine than WCS timing.

Based on these findings, most experimental studies have investigated the effect of pilot fuel injection advance timing on combustion efficiency.

This approach was also justified by the fact that the pilot fuel injection system installed additionally on the engine for the studies. This upgrade allowed for wide pilot fuel injection angle adjustment, while the WCS injection utilized a modified stock fuel injection system, which allowed for narrow advance angle adjustments. Consequently, research into the impact of WCS injection angle on engine performance with a fixed pilot fuel injection angle has been limited. However, a wealth of experimental data exists on pilot fuel IAA adjustment and the combined adjustment of both fuels. Some of this data will discuss below.

6.4.1. The influence of the pilot fuel IAA on the efficiency of the working process over a wide range of changes in this parameter investigated during tests of the high-speed diesel locomotive engine 645 EMD [75]. Two cases considered with an increased pilot fuel supply (ignition coefficient of 0.5); with a reduced supply (ignition coefficient of 0.177).

An increased ignition coefficient adopted to more clearly demonstrate the effect of separate injection of the two fuels on the WCS combustion process at various pilot fuel injection angles.

Fig. 6.18.1 *a*, *b* and 6.18.2 *c*, *d* shows the dependences of pressure (*a*), temperature (*b*), heat release rate (*c*), and relative heat release (*d*) as a function of crankshaft angle.

The WCS injected into the combustion chamber 20° before TDC, and the pilot fuel injection advance varied between 58 and 28°. Depending on the pilot fuel injection angle, ignition was either thermal or ignition. The figures selectively show the dependences for pilot fuel IAAs of 46°, 40°, 34°, and 28° before TDC. Engine test results for the case with a higher pilot coefficient presented in Table 6.9.

The combustion of water-coal fuel using pilot ignition can divided into five main stages (Fig. 6.18.1 *a*, *b* and 6.18.2 *c*, *d*):

A) ignition and combustion of the pilot fuel;

B) vaporization of water, which is part of the WCS, and heating of the particles;

C) release, ignition, and combustion of volatiles in the gas phase;

D) diffusion burnout of the pure oblique-angled residue;

E) combustion attenuation during expansion of the working fluid.

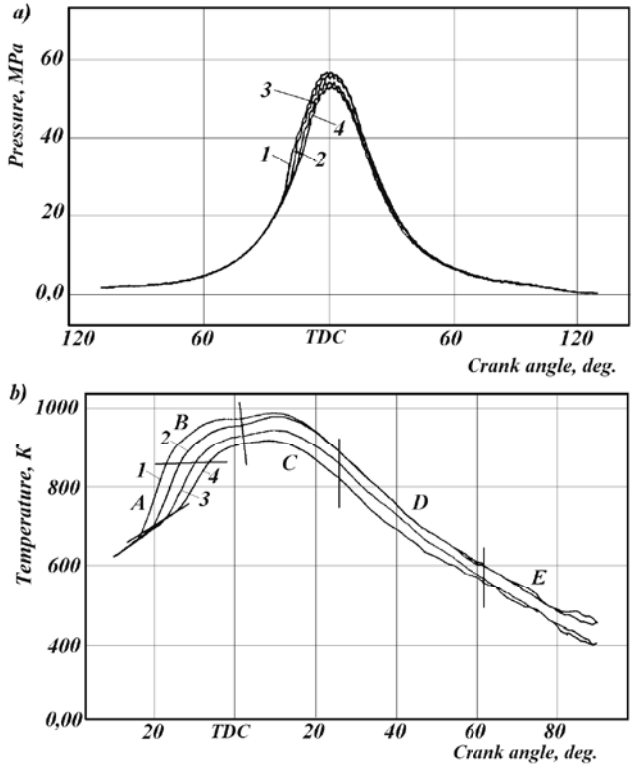

Fig. 6.18.1 Effect of pilot fuel IAA on changes in pressure (*a*), temperature (*b*) during co-combustion of pilot fuel and WCS. 1 – 40°; 2 – 34°; 3 – 28°; 4 – 24° (n = 834 min^{-1}; WCS amount – 210 mm^3/cycle; pilot fuel amount – 100 mm^3/cycle; WCS injection – 20° before TDC; ignition coefficient 0.5)

Table 6.9.

Main operating parameters of the 645 EMD engine depending on the pilot fuel injection advance angle*

Pilot fuel injection advance, deg	P_{max}, MPa	T_{max}, K	T_{out}, K	Relative heat release (maximum), kJ/kg	Combustion efficiency, %
24	5.3	916.8	423.82	148.8	32.7
28	5.42	942.9	435.98	180.0	39.7
34	5.57	977.9	446.54	210.0	46.0
40	5.67	987.0	447.10	210.0	45.2
46	5.67	979.9	446.32	211.2	45.7
52	5.73	990.0	440.32	203.8	44.1
58	5.64	965.9	431.82	183.8	39.8

* Ignition coefficient 0.5

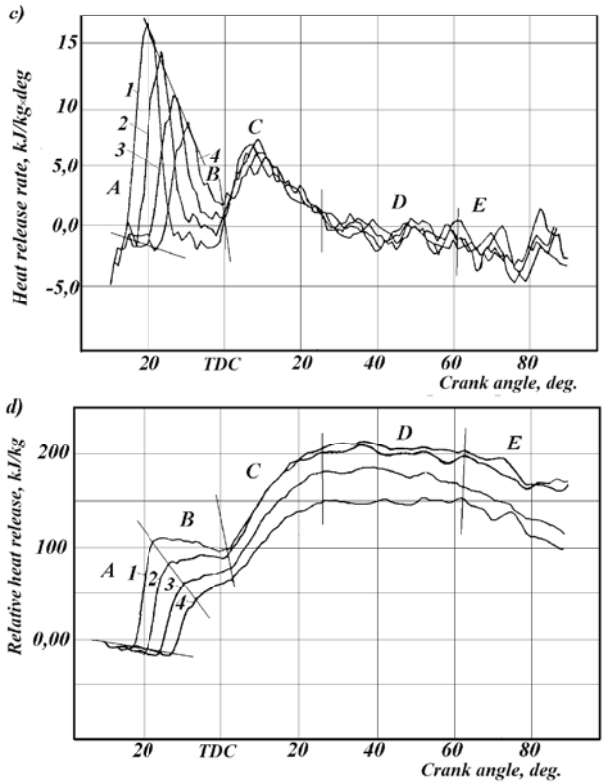

Fig. 6.18.2 Effect of IAA of pilot fuel on changes in: heat intensity (*c*) and relative heat release (*d*) during co-combustion of pilot fuel and WCS. 1 – 40°; 2 – 34°; 3 – 28°; 4 – 24° (n = 834 min^{-1}; WCS amount – 210 mm^3/cycle; pilot fuel amount – 100 mm^3/cycle; WCS injection – 20° before TDC; ignition coefficient 0.5)

Analyzing the presented data, we can conclude that as the IAA changes from 58 to 28° before TDC, the exhaust gas temperature initially increases to a maximum, which corresponds to approximately 40° before TDC, and then begins to decrease. It fluctuates slightly around this maximum.

As the IAA of the pilot fuel increases, the maximum cylinder pressure increases, and it begins to rise significantly even before the piston reaches TDC, which, in turn, leads to a decrease in power and a reduction in the engine's thermal efficiency. Injecting the pilot fuel too early results in a pressure change accompanied wave processes (Fig. 6.18 *a*).

Due to earlier combustion of the pilot fuel at earlier crankshaft rotation angles, the maximum charge temperature increases with increasing IAA of

the pilot fuel. This occurs despite the evaporation of water, which is part of the WCS, which reduces the rate of temperature rise inside the cylinder. WCS combustion begins only after the charge temperature reaches 880...920 K. The region where the temperature remains close to the maximum is located in the immediate vicinity of the TDC and persists for a relatively large crankshaft rotation angle. This is apparently because the rate of heat release during WCS combustion is only sufficient to compensate for the external work performed by the piston. Thus, under these conditions, the heat release process can considered approximately isothermal. Fig. 6.18 *b* shows that increasing the pilot injection IAA increases the period during which the cylinder temperature remains virtually constant. A further increase in IAA leads to a decrease in the maximum temperature due to vaporization preceding WCS combustion.

The heat release rate curves exhibit two maxima, while the total heat release curves exhibit two sections with a sharp increase in heat input, corresponding to the combustion of pilot and water-coal fuels. These processes can, in principle, overlap: in the WCS combustion section, pilot fuel after burning can occur. In this case, ignition transitions from thermal to pilot ignition.

With injection advance up to 40°, heat release from pilot fuel combustion occurs at earlier crankshaft rotation angles and the heat release rate increases. The location of the heat release maxima changes by almost the same amount as the injection advance. As the heat, release rate increases, the pilot fuel combustion period decreases, covering smaller crankshaft rotation amplitude. All this indicates faster combustion of diesel fuel. Interestingly, the minimum points of the DF combustion heat release rate curve have a dislocation that is little dependent on the IAA of the pilot fuel. This confirms the hypothesis that at high pilot fuel IAA values, changing it has little effect on the onset of WCS combustion. For pilot fuel IAA greater than 34°, the relative heat release in the region corresponding to water evaporation becomes negative; indicating that heat loss due to vaporization predominates overheat release from pilot fuel combustion. A relationship also observed between the pilot fuel IAA and the maximum heat release from WCS combustion. In the IAA range from 24 to 40°, the maximum heat release shifts closer to the TDC. This suggests that there is an optimal pilot fuel injection time that promotes earlier WCS combustion (relative to the TDC). Injecting the pilot fuel too late results in delayed WCS combustion. Injecting the WCS too early results in delayed combustion. Injecting the pilot fuel even 40° before the TDC does not bring the maximum heat release from WCS combustion closer to the TDC. As a result, the contribution to piston work from WCS combustion is

less than that from pilot fuel combustion. The maximum total heat release also changes with the pilot fuel injection angle. In the IAA range from 40 to 24°, the maximum total heat release initially increases and then decreases.

Fig. 6.18.2 *b*, *d* show that the boundary between water evaporation, WCS ignition, and solid fuel combustion and afterburning varies little with the pilot fuel IAA. The maximum exhaust gas temperature (Table 6.10) reached when the IAA is within 40°C of the TDC. Moreover, the maximum exhaust gas temperature is not very sensitive to changes in pilot fuel injection timing and remains nearly constant over a wide range of IAA variations. Its maximum corresponds to the greatest heat release in the working cylinder. This indicates that exhaust gas temperature can use as a criterion for determining maximum heat utilization efficiency.

Comparing Fig. 6.18.2 *b* and 6.18.2 *d*, it can be noted that the pilot fuel IAA at which the maximum working fluid temperature is reached also corresponds to the maximum heat release in the engine cylinder. Despite the high ignition coefficient, the combustion efficiency of the solid fuel in this process remained quite low. As can be seen from Table 6.10, it reached a maximum of 46%. This can explain by the combined effect of several factors, namely:

- injecting a large amount of pilot fuel too early leads to significant heat losses, resulting in the maximum temperature by the end of combustion remaining low enough to effectively activate the combustion process of the WCS;
- combustion of a large amount of pilot fuel results in the WCS being injected into an environment with a reduced oxygen concentration, resulting in less intense surface reactions;
- a sufficiently long WCS ignition delay allows the particles to disperse throughout the combustion chamber. Given the small total number of particles, their concentration in the charge environment will be comparatively low, reducing the mutual influence of burning particles on each other.

A reduced ignition coefficient allows for engine characteristics that differ significantly from those considered in the first case. The key operating parameters of the 645 EMD engine with a pilot coefficient of 0.177 are given in Table 6.10. In this case, the IAA varied within the range of 46...18° up to TDC. The effect of pilot fuel IAA selection on pressure, temperature, instantaneous heat release, and relative heat release in the cylinder shown in Fig. 6.19.1 *a*, *b* and 6.19.2 *c*, *d*, respectively. The graphed curves correspond to pilot fuel IAAs of 41°, 34°, 28°, and 24°.

It should note that with a small pilot fuel amount, the rate of heat release from WCS combustion is much higher than with a high ignition coefficient.

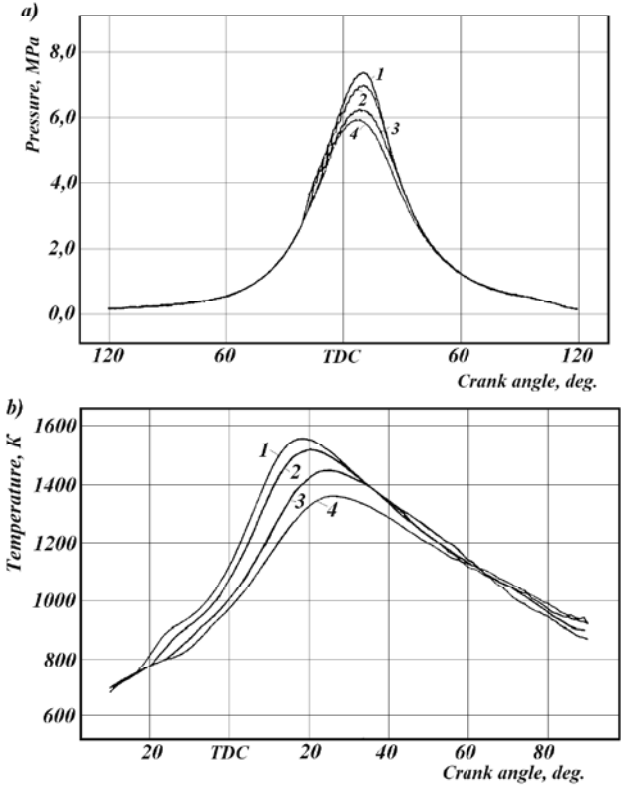

Fig. 6.19.1. Effect of pilot fuel IAA on changes in pressure (*a*), temperature (*b*) during co-combustion of pilot fuel and WCS. 1 – 41°; 2 – 34°; 3 – 28°; 4 – 24° (n = 837 min^{-1}; WCS amount – 787.5 mm^3/cycle; pilot fuel amount – 80 mm^3/cycle; WCS injection – 20° before TDC; ignition coefficient 0.177)

Table 6.10.

Main operating parameters of the 645 EMD engine depending on the pilot fuel injection advance angle *

Pilot fuel injection advance, deg	P_{max}, MPa	T_{max}, K	T_{out}, K	Relative heat release (maximum), kJ/kg	Combustion efficiency, %
46	8.07	1597	625.43	862.5	91.1
41	7.40	1353	619.98	811.3	85.7
34	7.02	1514	592.72	846.3	89.4
28	6.28	1443	629.15	837.5	88.5
24	5.93	1356	615.04	788.8	83.3
18	5.31	1118	544.04	570.0	60.7

* Ignition coefficient 0,177

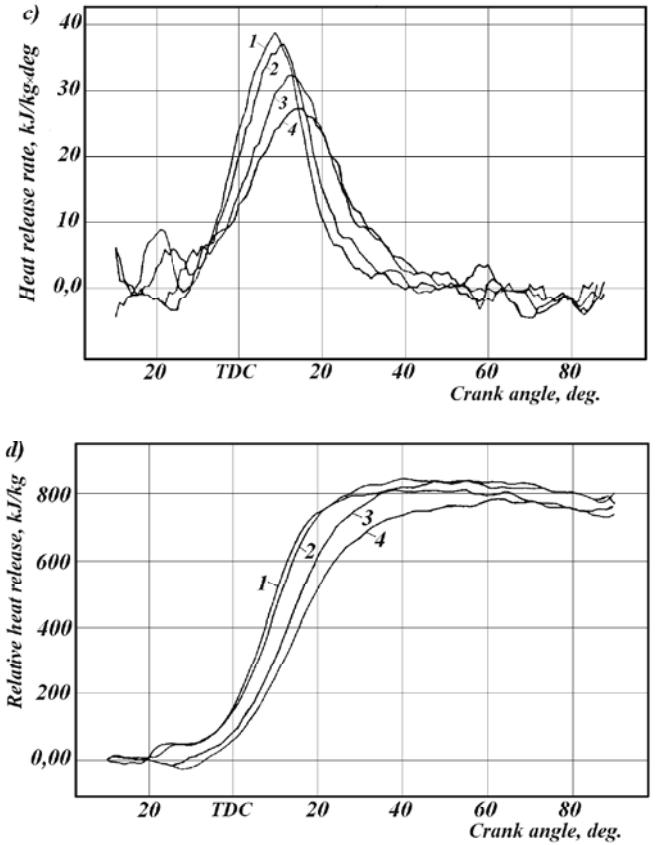

Fig. 6.19.2. Effect of IAA of pilot fuel on changes in heat stress (*c*) and relative heat release (*d*) during co-combustion of pilot fuel and WCS. 1 – 41°; 2 – 34°; 3 – 28°; 4 – 24° (n = 837 min^{-1}; WCS amount – 787.5 mm^3/cycle; pilot fuel amount – 80 mm^3/cycle; WCS injection – 20° before TDC; ignition coefficient 0.177)

The maximum rate of heat release during WCS combustion achieved when the IAA is approximately 40°, while the lowest is 24°. As the IAA increases, the combustion period decreases with respect to crankshaft angle. As the IAA decreases, the maximum heat density not only increases but also shifts toward the TDC.

As in the previous case, the onset of WCS combustion depends little on the IAA of the pilot fuel. During the initial stage of combustion, the heat release rate decreases due to the vaporization of water contained in the WCS. This delays the ignition of the suspension, so at low IAA values, combustion

occurs during expansion. As the IAA of the pilot fuel increases, the maximum temperatures increase, and the maximum point shifts toward the TDC. As a result, the afterburning period of the solid fuel on the expansion line reduced. Similar relationships are characteristic of pressure changes. Thus, at a low ignition coefficient, increasing IAA increases the efficiency of solid fuel combustion.

During testing of the JS-1 medium-speed engine, Cooper-Bessemer obtained results somewhat different from those obtained during testing of the 645 EMD engine; however, the main patterns of the influence of the IAA pilot fuel on the operating process can be observed in this case as well [66]. These differences only confirm that the efficiency of using solid fuel in piston internal combustion engines depends on a large number of factors, the combination of which leads to one result or another.

During experiments to optimize the operating process of the JS-1 engine, the pilot fuel injection angle varied such that the difference between its injection and the WCS injection reached 14°. The main dependencies obtained during the experiments shown in Fig. 6.20.

The results of the study indicate that, within a given range of change in the start of injection, the WCS ignition delay remained practically constant and lay in the range of 4.5...5.4 ms (11...13° of crankshaft rotation angle). Maximum combustion pressures (7.34...7.58 MPa) were achieved in the range of 16...18°C after TDC. Heat release curves show that the heat density reaches a maximum of 6.86 kJ/deg when the start of pilot fuel injection coincides with the start of WCS injection (19°C before TDC).

As the pilot fuel IAA increased, the maximum heat density decreased to 6.0...5.6 kJ/deg. In all cases, the heat release curves have a steep maximum, indicating that combustion begins after good mixing of the fuel particles with the air charge. The optimal timing of the pilot and main fuel injection for this engine also ensured by the fact that the specific heat consumption for power generation is minimal for this particular case. Fig. 6.21 shows that when the pilot injection starts at 18° before TDC, the heat consumption is 5.12 MJ/(kWh). Increasing the pilot fuel injection start angle increases the heat consumption to 5.52 MJ/(kWh). Thus, the savings may be because the heat obtained from the combustion of the pilot fuel actually transferred to the working fluid during this reduction, producing negative work.

It should noted that in all the cases discussed above, only the static fuel injection angle was determined, which does not adequately reflect the nature of the interaction between the pilot and main fuel. This does not allow for an objective comparison of the study results, but only allows for the tracing of the main combustion process patterns.

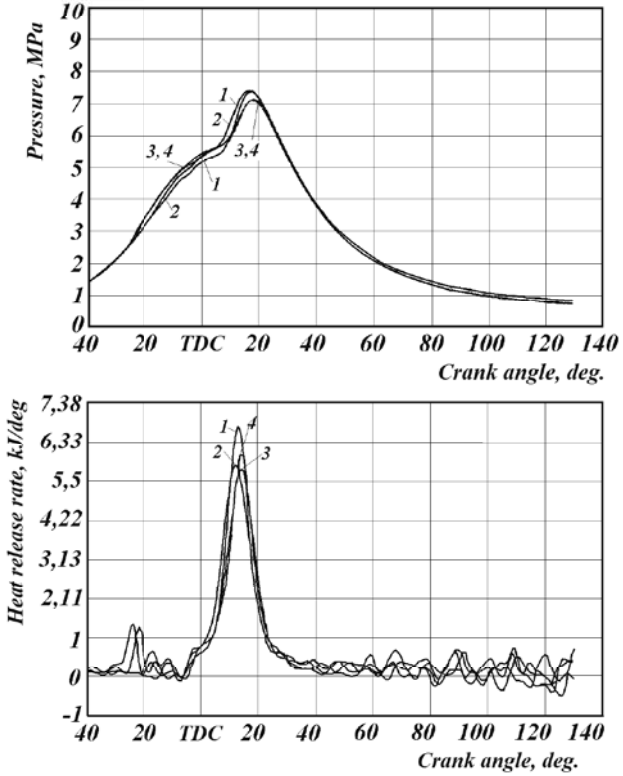

Fig. 6.20. Change in pressure and rate of heat release depending on the angle of the start of pilot DF injection in the Cooper-Bessemer JS-1 engine (air temperature at the engine inlet 126°C; average particle diameter 11 μm; nozzle hole diameter 0.25 mm; maximum injection pressure 75.8 MPa; pilot fuel cyclic injection 229 mm^3). 1 – 18°; 2 – 23°; 3 – 30°; 4 – 33° (before TDC)

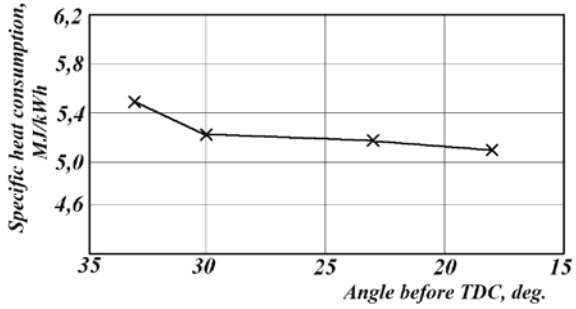

Fig. 6.21. Effect of pilot fuel injection start on specific heat consumption in the Cooper-Bessemer J-1 engine

In the cases examined, optimization performed only for the pilot fuel injection angle, while the WCS injection angle remained close to optimal for DF injection. Considering that the majority of combustion time is spent burning out the coal fuel, it is clear that the best result can be achieved by jointly optimizing both the pilot fuel injection timing and the WCS injection timing. This confirmed by the results of tests conducted by General Electric.

***

In the early stages of research, General Electric conducted part-load testing of the 7FDL engine at various pilot fuel injection angles [52]. Based on preliminary calculations, the static WCS injection angle was set at 47° before TDC, and the pilot fuel IAA varied within the range of 41...49°. Fig. 6.22 and Table 6.11 show the results of these tests.

The data presented demonstrates that with increasing injection advance, the maximum cylinder pressure increases. Moreover, as in the 645 EMD engines, the pressure change accompanied by wave processes, which are provoked by premature combustion of the pilot fuel. Moreover, the wave processes persist even in cases where the pilot fuel injected into the engine cylinder after WCS injection (41°, 44° before TDC).

Table 6.11.

The influence of the pilot fuel injection start angle on engine performance when operating in WCS (partial load mode)

Pilot diesel injection angle (before TDC), degrees	Ignition characteristics*							Combustion characteristics			
	Dynamic injection angle (before TDC), deg		Ignition (to TDC), deg		Ignition delay, deg		WCS combustion start temperature, K	P_{max}, MPa	Power, kW	Fuel burnout efficiency, %	Specific heat consumption, kJ/(kWh)
	DF	WCS	DF	WCS	DF	WCS					
no	——	32.9	——	6.8	——	26.1	987	10.2	37.5	71.3	13000
41	25.2	32.3	19.3	13.3	5.9	19.0	994	12.3	67.8	91.8	8718
44	31.0	32.7	22.2	15.3	8.8	17.4	1017	13.5	74.2	97.5	7966
47	33.8	32.3	24.2	16.5	9.6	15.8	1022	14.1	76.6	98.7	8038
49	36.9	32.0	25.5	18.0	11.4	14.0	1006	14.5	70.8	97.9	8162

*n = 1050 min^{-1}; inlet air temperature 110°C; inlet air pressure 329 kPa; WCS static feed angle – 47° to TDC.

As can be seen from the heat stress graphs, the onset of pilot fuel ignition depends on the moment of its injection into the working cylinder, while the onset of WCS combustion varies in each specific case, despite the fact that

the water-coal fuel injection angle remained constant in all cases. The WCS ignition delay becomes shorter as the pilot fuel injection advance angle increases. Interestingly, the temperature at which WCS ignition occurs varied very little in all cases.

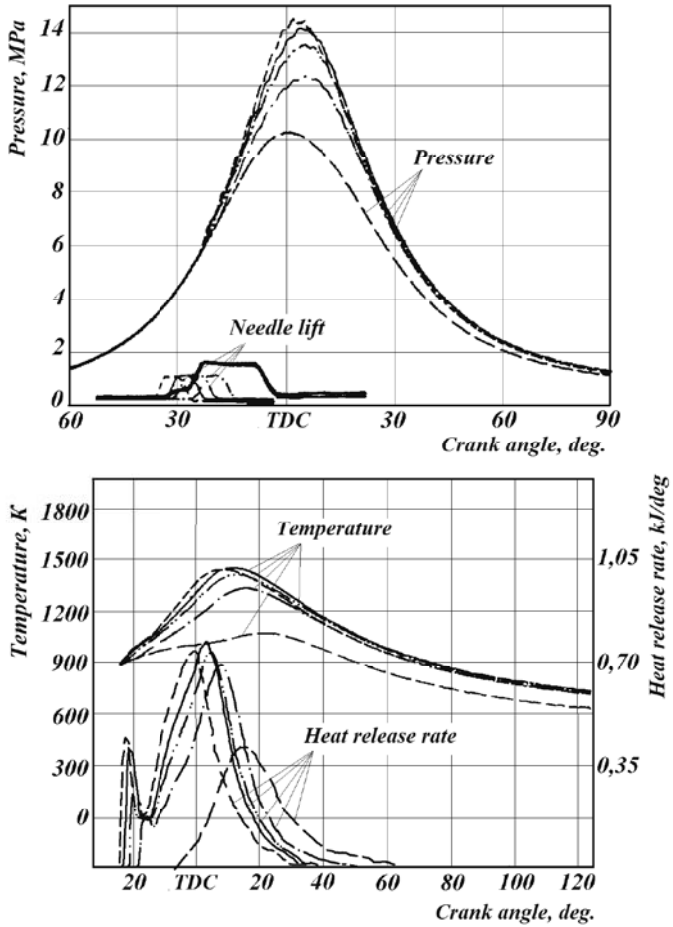

Fig. 6.22. Effect of pilot DF injection angle on the WCS ignition and combustion process in the General Electric 7FDL diesel engine (WCS main fuel, DF pilot fuel). – – no igniter; – · – 41°; – · · – 44°; —— 47°; - - - 49° (before TDC)

Since heat release curves vary in shape and relative position relative to the TDC, heat utilization efficiency will vary in all cases. The presented

relationships demonstrate that extremely early and very late heat releases are equally detrimental, so there is an optimal pilot fuel injection angle. For this case, this angle is between 44° and 47°.

Combined optimization of the main and pilot fuel injection angles allows for burnout completeness approaching 99%.

A study of the influence of pilot fuel IAA under full-load conditions conducted by General Electric confirmed the previously established patterns and identified some additional trends. Injection performed using an electronically controlled accumulator injection system with a constant WCS injection angle 25° before the TDC, while pilot fuel injected at 35°, 25°, and 15° before the TDC. Table 6.12 presents the test conditions and combustion results for the engine cylinder. Changes in pressure, temperature, and heat release rate shown in Fig. 6.23.

Table. 6.12.

Test conditions and combustion results of fuel in the cylinder of the 7FDL engine at different IAA of pilot fuel at full load mode

Pilot diesel injection	Test conditions					
	Injection start, deg (before TDC)		Injection pressure, MPa.		DF volume, mm^3.	Power, kW.
	DF	WCS	WCS	DF		
Late	15	25	60.8	38,0	73	188
Middle	25	25	69.8	37,7	71	192
Early	35	25	69.7	36,5	71	192
Combustion results						
	P_{max}. MPa	Burnout efficiency. %		Specific heat consumption. kJ/kW		
Late	15.4	99.3		8414		
Middle	16.1	99.2		8655		
Early	16.5	99.0		9008		

Injecting pilot fuel 15° before TDC yielded the best results. The maximum cylinder pressure and specific heat consumption were the lowest, while the combustion efficiency was the highest. Analysis of the heat release curves helps explain this result. The highest maximum pressure (for the pilot fuel injection 35° before TDC) was caused a large amount of fuel burning well before TDC. The lowest heat consumption (for the pilot fuel injection 15° before TDC) can explain by the combustion of a large amount of fuel close to TDC. At the end of the heat release period, the highest maximum temperature is reached (30...40° after TDC), which likely contributed to the highest combustion efficiency [54, 56].

The difference in the shape of the three heat release curves caused by the difference in the residence time of the WCS in the combustion chamber before ignition onset (Table 6.13). The residence time of the WCS before

ignition onset is somewhat similar to the «ignition delay» for DF. However, these processes differ significantly. When operating on DF, during the ignition delay period, the physical process of vaporization and kinetic processes of chemical reaction occur (the latter are predominant).

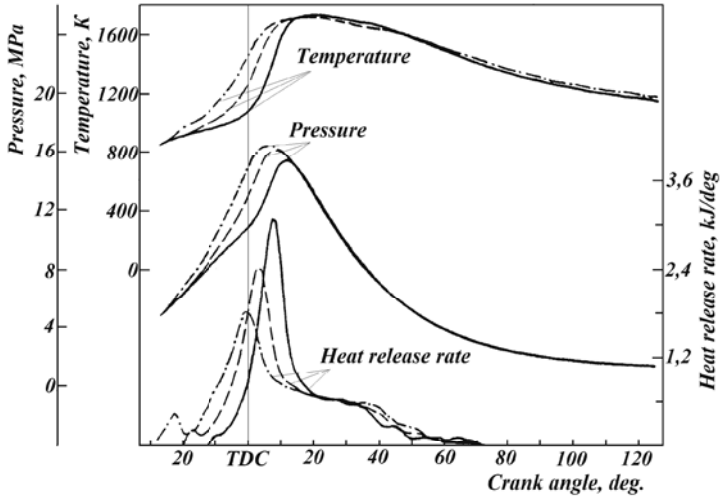

Fig. 6.23. Change in pressure, temperature and heat release rate in the cylinder of the 7FDL engine at different IAA of pilot fuel at full load mode (rotation speed 1050 min^{-1}; air inlet pressure and temperature 320 kPa and 360 K, respectively)

Table 6.13.

WCS residence time and average charge temperature in the cylinder before ignition

IAA DF, deg (before TDC)	WCS residence time before ignition, deg (ms)	Temperature of gases in the working cylinder, K
35	6 (0.95)	940
25	11 (1.74)	930
15	15 (2.38)	920

In the period from the start of injection to the onset of combustion, water vaporization and the release of volatiles primarily occur. Water vaporization is the primary limiting factor determining the ignition delay time. The amount of dehydrated coal fuel available for combustion by the time of ignition depends on the amount of water evaporated by that time. Clearly, the longer the residence time of the WCS in the cylinder before ignition, the more water will evaporate due to the heat of the charge and, consequently, the more dehydrated coal will be in the combustion chamber at the onset of

combustion. This can lead to very high thermal stress in the combustion process.

As already noted, with early pilot fuel injection, the average cylinder temperature rises more rapidly due to its combustion, which can accelerate the vaporization process. However, a higher temperature has a lesser effect on vaporization than the residence time of the WCS in the combustion chamber. This is evident from the simplified dependence for droplet vaporization [54]:

$$dW = k_1 \times dt \times ln(k_2 \times T_{cham} + C),$$

where dW – mass of evaporated water; dt – time; T_{cham} – temperature in the combustion chamber; $k_1=f$ (droplet diameter, thermal conductivity, density); $k_2=f$ (specific heat capacity, latent heat of vaporization); $C=f$ (specific heat capacity, latent heat, droplet temperature).

The above expression demonstrates that cylinder temperature affects the vaporization process exponentially, while residence time has a directly proportional effect. Table 6.13 shows that the difference in average gas temperature for the three cases considered is very small, no more than 2%, while the difference in residence time is an order of magnitude greater (increasing from 0.95 to 2.38 ms, or approximately 250%). Thus, for the case of pilot fuel injection 15° before TDC, the maximum amount of dehydrated carbon ready for ignition results in the maximum thermal stress in the cylinder.

When operating with late pilot fuel injection, near-self-ignition of the WCS occurs. In such cases, the pilot fuel does not so much ignite the carbon particles as accelerate their combustion after self-ignition. This does not adversely affect the combustion process or engine performance.

6.4.2. The influence of IAA WCS on the efficiency of the engine working process.

As demonstrated in previous sections, increasing the residence time of the WCS in the combustion chamber before ignition significantly influences combustion efficiency. The easiest way to extend the time to self-ignition is by increasing the WCS injection advance angle. However, engine test results at full load with extremely late injection timing showed deterioration in combustion (Fig. 6.24). The experimental results presented in Table 6.14.

Comparing the combustion results with WCS injection at 22° and 32° before TDC, it should noted that the specific heat consumption for the case of suspension injection at 32° is significantly lower than for the case of later regulation. The combustion efficiency for these two cases is almost the same, while the maximum pressure for the later regulation is much lower. The

decrease in the maximum pressure was due to the relatively low heat density due to the ignition delay of the coal fuel. However, this trend did not persist with a further increase in the WCS injection advance angle from 32° to 42° before TDC. Although the maximum pressure remained virtually unchanged for the latter experiment, a deterioration in combustion efficiency and an increase in the specific heat consumption were noted (from 99.5 to 99.1% and from 8054 to 8876 kJ/(kWh), respectively). Further increasing the WCS injection start to 47° before TDC (not shown in the figure) reduced the combustion efficiency to 98% and the specific heat consumption increased to 9100 kJ/(kWh).

Table. 6.14.

Test conditions and combustion results of fuel in the cylinder of the 7FDL engine at various IAA WCS at full load mode

Pilot diesel injection	Test conditions					
	Injection start, deg (before TDC)		Injection pressure, MPa.		DF volume, mm^3.	Power, kW.
	DF	WCS	WCS	DF		
Late	12	22	88.1	50.9	71	187
Middle	12	32	82.9	52.6	74	192
Early	12	42	82.8	52.6	93	178
	Combustion results					
	P_{max}, MPa		Burnout efficiency, %		Specific heat consumption, kJ/kW	
Late	15.3		99.5		8509	
Middle	17.2		99.5		8054	
Early	17.2		99.1		8876	

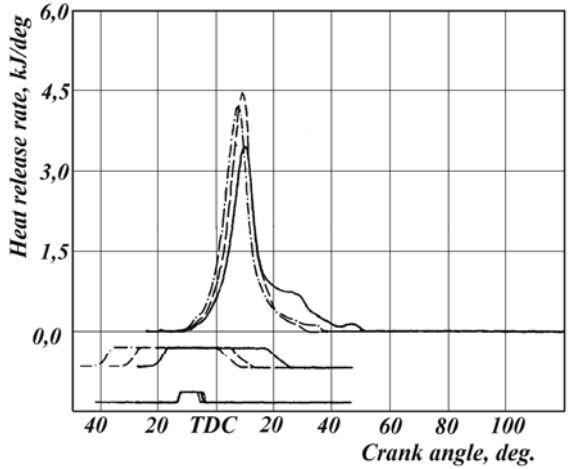

Fig. 6.24. Heat release rates in the 7FDL engine cylinder at different IAA WCS at full load. —— 22° before TDC; – – – 32° before TDC; – · – 42° before TDC

The deterioration in combustion cannot explain by conventional DF use. Excessively late injection timing leads to DF combustion well before the TDC, resulting in increased peak pressure, harshness, and reduced efficiency.

In the engine running on WCS, excessively early combustion not observed. This can explain by two mechanisms operating almost simultaneously. On the one hand, with earlier injection, the WCS enter a gas environment that has not yet reached its maximum temperature. The resulting vaporization processes reduce the average cylinder temperature. Consequently, the evaporation process is less intense, resulting in increased ignition delay. On the other hand, an analysis of fuel spraying processes shows that with later WCS injection, the spray plume enters the working cylinder well before the piston reaches TDC. The high initial velocity and long ignition delay cause the jet to impact the cylinder liner wall. By this point, the flame velocity significantly decreases, which impairs its secondary decomposition, and the low cylinder wall temperature does not promote intensive water evaporation. This development further increases ignition delay and impairs the combustion efficiency of the WCS.

With an injection advance of 32° before TDC, the WCS flame reaches the piston crown at a crank angle of approximately 5°. However, the WCS does not ignite until at least 20° after the start of injection, i.e., approximately 10° before TDC. Therefore, impact with the piston crown occurs well before ignition. The increased efficiency of the combustion process with this control, explained by the relatively high temperature of the combustion chamber wall, which is formed in the piston. This promotes efficient evaporation of water, which is also more volatile than DF. At the same time, the high jet velocity now of impact with the piston promotes intensive secondary flame decomposition. It is obvious that during combustion of WCS, the process of secondary disintegration of the spray torch upon impact with the piston is of the same, and perhaps even more important, significance than the disintegration of the torch because of dispersion.

The role of secondary decomposition in WCS combustion first hypothesized by B. D. Hsu, G. L. Confer, and Z. J. Shen. In 1992, during a study of late WCS injection, they observed traces of the flame affecting the piston [54]. Subsequently, combustion in an engine cylinder studied using high-speed filming through an insert providing optical access to the combustion chamber (B. D. Hsu, D. P. Branyon). In the frames obtained with the late WCS injection setting, the reverse movement of burning particles from the walls of the combustion chamber to its axis was clearly visible [56]. Fig. 6.25 shows the dependences of the optimal ratio of the start of WCS injection and pilot DF at maximum load for the 7FDL engine.

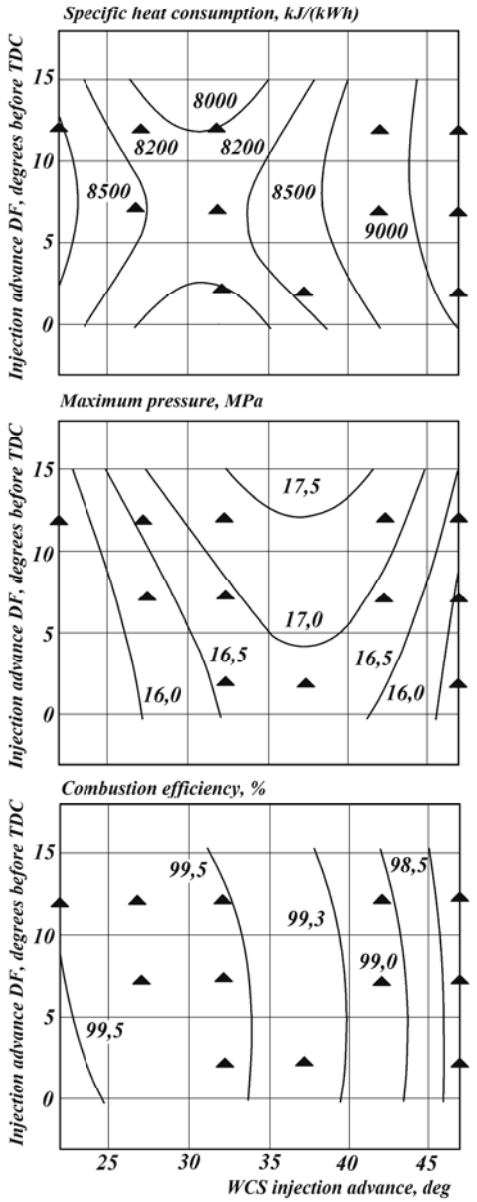

Fig. 6.25. Dependencies for determining the optimal regulation of the WCS and pilot DF feed start angles at maximum load for the 7FDL engine

These dependences make it possible to optimize the operating process in terms of specific heat consumption, maximum pressure, and fuel efficiency. They obtained by constructing isometric lines based on actual experimental results (triangles in the figure). At full load, the pilot fuel IAA has no significant effect on all three parameters. This is because combustion in the cylinder occurs primarily through self-ignition of the charcoal fuel. When WCS injection begins approximately 37° before TDC, the highest maximum pressure can expected for any pilot fuel IAA. The later the pilot fuel injected, the smaller its contribution to the increase in maximum pressure during combustion after TDC. When WCS injected earlier than 37° before TDC, the maximum pressure decreases due to the impact of the fuel spray on the cylinder liner. As can be seen from Fig. 6.25, the optimal WCS and DF injection settings differ for all parameters. Optimum combustion efficiency depends primarily on the in-cylinder temperature, while the specific heat consumption depends on the heat release concentration at TDC. The presented relationships allow adjustments to make for pilot fuel and WCS injection with an acceptable compromise. For the case under consideration, the optimal injection is the pilot DF injection 12° and the WCS injection 35° before TDC.

To summarize this section, it should be noted that the WCS combustion process can be optimized through two fundamentally different mechanisms:

- by reducing the WCS ignition delay by activating the combustion process by introducing pilot fuel into the cylinder early enough;
- by intensifying the self-ignition process of the coal fuel by introducing pilot fuel toward the end of the WCS self-ignition delay.

6.5. The influence of spark angle on the efficiency of the working process of an engine with plasma ignition.

The effect of the spark advance angle in the plasma pre-chamber on the combustion process studied on the JS-1 engine Cooper-Bessemer [44]. The key parameters influencing the efficiency of WCS plasma ignition were the ignition timing (spark delivery) and the amount of natural gas supplied to the pre-chamber.

Fig. 6.26 shows the change in cylinder pressure, WCS injection pressure, and pre-chamber pressure for three ignition advance timings (26, 20, and 13° before TDC). Table 6.15 presents the ignition and combustion parameters in the engine's working cylinder from the ignition timing in the pre-chamber.

The ignition timing of a pre-chamber (similar to the pilot fuel injection timing) influences the interaction between the hot gas jet exiting the pre-chamber and the WCS flame supplied by the main nozzle. WCS injection

was performed 20° before TDC, the shaft speed was 400 min^{-1}, and the natural gas pressure in the supply line was 0.27 MPa. The ignition timing of the gas-air mixture in the pre-chamber varied between 26° and 13° before TDC (6° before and 7° after the start of WCS injection).

Table 6.15.

Dependence of cylinder pressure on ignition moment in a jet gas pre-chamber

Ignition timing (before TDC), degrees	WCS ignition delay, deg	Maximum cylinder pressure, MPa	Moment of reaching maximum pressure (after TDC), deg
13	16	7.48	14.0
20	13	7.75	12.5
26	16	7.48	15.0

The pressure dependence in a pre-chamber illustrates the time delay between ignition and the pressure increase within the burner. This delay is approximately 2° of shaft rotation (approximately 1 ms). Before reaching maximum combustion pressure in the pre-chamber, the motor shaft rotates an additional 5° (approximately 2 ms). Research has shown that the delay between ignition and the moment the jet penetrates the main combustion chamber ranges from 3 to 5° of shaft rotation.

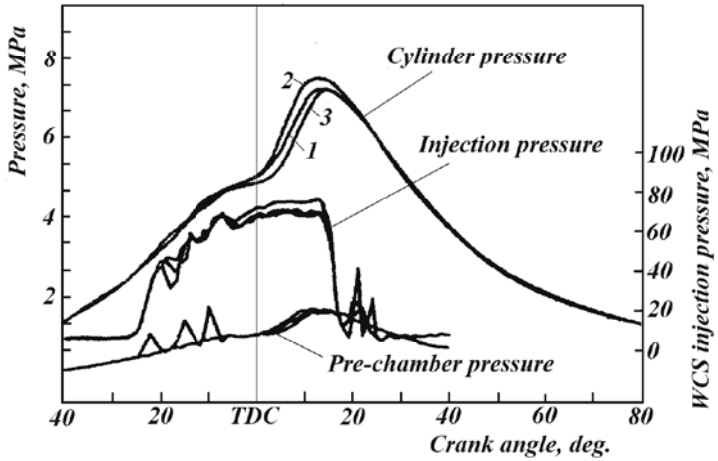

Fig. 6.26. Change in pressure in the working cylinder of the JS-1 engine from Cooper-Bessemer depending on the ignition moment in the pre-chamber. 1 – 13°; 2 – 20°; 3 – 26° (before TDC)

Fig. 6.26 and Table 6.15 demonstrate that applying the spark to the pre-chamber 20° before TDC results in the shortest ignition delay, the highest

maximum cylinder pressure, and the most optimal pattern of pressure change. This indicates that this ignition timing, for the conditions under consideration, is closest to optimal. Plasma jet ignition efficiency of the WCS is maintained with a natural gas contribution to the total heat of combustion of approximately 3%; however, the most reliable ignition and best engine performance were achieved when this share was 5%.

6.6. The influence of pilot fuel quantity on the efficiency of the pilot-ignition engine.

The amount of pilot fuel is another important component that influences both the thermodynamic cycle and the combustion efficiency of solid fuel. As demonstrated above, the completeness of solid fuel burnout in a piston engine's working space depends significantly on the ignition coefficient. Calculations show that for fuels with a low volatile content, ignition is extremely unstable at a ignition coefficient of less than 0.06, and engine performance is extremely sensitive to the ignition coefficient. Starting from approximately 0.07 to 0.2, thermal efficiency is essentially independent of the ignition coefficient. Therefore, when using high-calorific fuels, to effectively activate the combustion process, at least 7% of the total heat required for the thermodynamic cycle must be supplied to the cylinder with the pilot fuel. For fuels containing volatile fuels, the ignition coefficient can significantly reduced. Thus, with a volatile content of approximately 50% in solid fuel, the pilot coefficient value can be only about 0.01.

Fig. 6.27 shows the dependence of the burnout efficiency and effective power of the 7FDL engine on the pilot coefficient value.

The main patterns associated with the pilot coefficient value quite fully traced based on the test results of the 645 EMD engines of General Motors [75].

The dependencies for pressure, temperature, heat stress and heat release by the crankshaft rotation angle shown in Figs. 6.28.1 *a*, *b* and 6.28.2 *c*, *d*.

During the study, the amount of pilot fuel supplied to the cylinder varied from 20 to 80 mm^3. The engine test results presented in Table 6.16. For the cases shown in the figures, the ignition coefficient is 0.178; 0.089; 0.0572; 0.0512.

The engine operated quite successfully with a pilot coefficient of 0.0512, but significant cycle-to-cycle parameter fluctuations and high exhaust smoke observed.

The maximum cylinder gas temperature increased steadily with increasing pilot coefficient, and the maximum point shifted toward the TDC. All this indicates an earlier onset of WCS combustion. This also indicated by

the pressure curves. It should note that the sufficiently intense temperature increase associated with WCS combustion occurs only after the cylinder temperature exceeds 900 K.

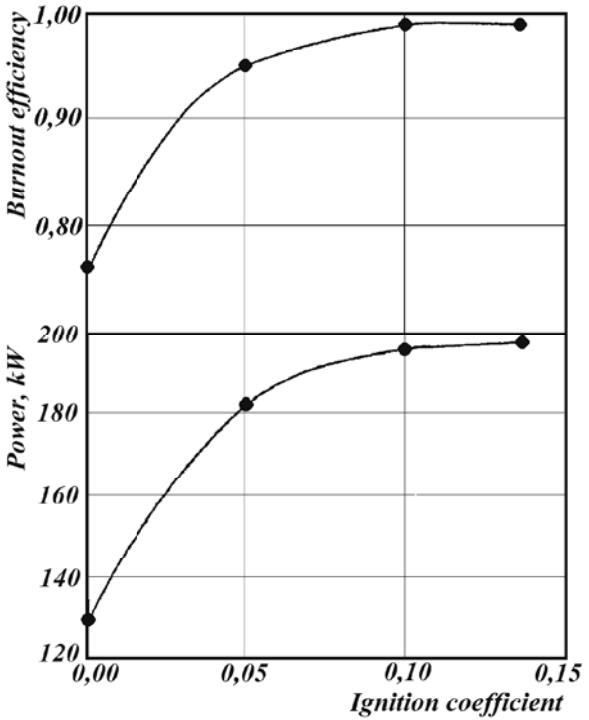

Fig. 6.27. Burnout efficiency and effective power of the 7FDL engine as a function of the ignition coefficient (IAA of the pilot fuel and WCS is 45°; carbon to hydrogen ratio is 1:0.8)

The maximum heat output from coal combustion increases with increasing ignition coefficient, and the angle at which this maximum value reached correspondingly decreases. As a result, the maximum heat release shifts toward earlier crank angles, approaching the TDC, while the amount of heat released during subsequent expansion decreases.

Relative heat release increases with increasing ignition coefficient. The portion of the curve corresponding to pilot fuel combustion becomes more pronounced as its amount increases, but the pilot fuel's contribution to the overall heat of combustion is significantly less than the WCS. The crank angle at which pilot fuel combustion is complete (the curve flattens out) shifts toward earlier crank angles.

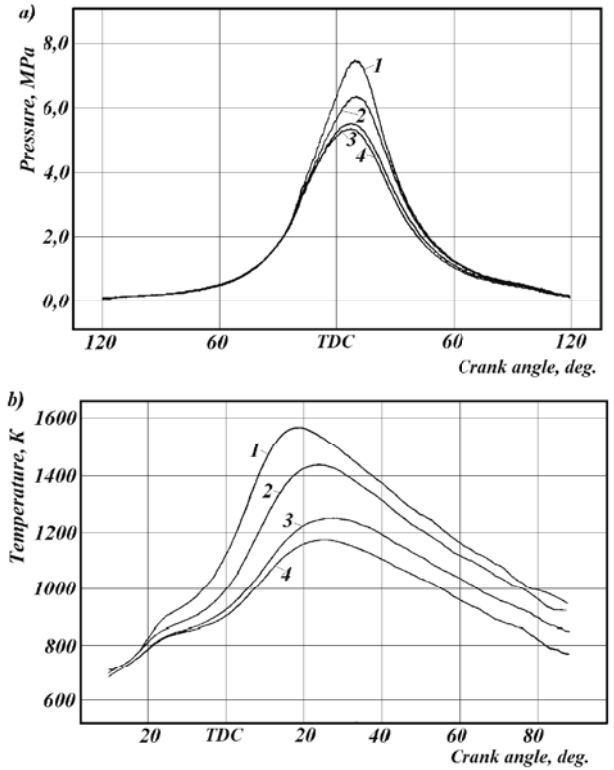

Fig. 6.28.1 Effect of ignition coefficient on changes in pressure (*a*) and temperature (*b*) during co-combustion of pilot fuel and WCS. 1 – 0.178; 2 – 0.089; 3 – 0.0572; 4 – 0.0512 (n = 837 min^{-1}; WCS amount – 814.6 mm^3/cycle; WCS injection – 20°; pilot fuel injection – 40° (before TDC))

Table 6.16.

The main operating parameters of the 645 EMD engine from General Motors, depending on the ignition coefficient value *

Ignition coefficient	Amount of pilot fuel, mm^3	P_{max}, *MPa.*	T_{max}, *K*	T_{exh}, *K*	Relative heat release (maximum), kJ/kg	Combustion efficiency, %
0.17750	80.00	7.79	1572	627.37	860.0	88.7
0.13630	58.50	6.96	1422	621.15	788.7	85.8
0.08810	35.80	7.38	1438	616.09	780.0	90.1
0.0749	30.00	6.48	1366	606.15	738.8	86.8
0.0584	22.05	5.79	1254	589.15	661.0	79.4
0.0512	20.00	5.52	1179	554.15	571.2	69.0

* WCS cyclic feed 814.6 mm^3

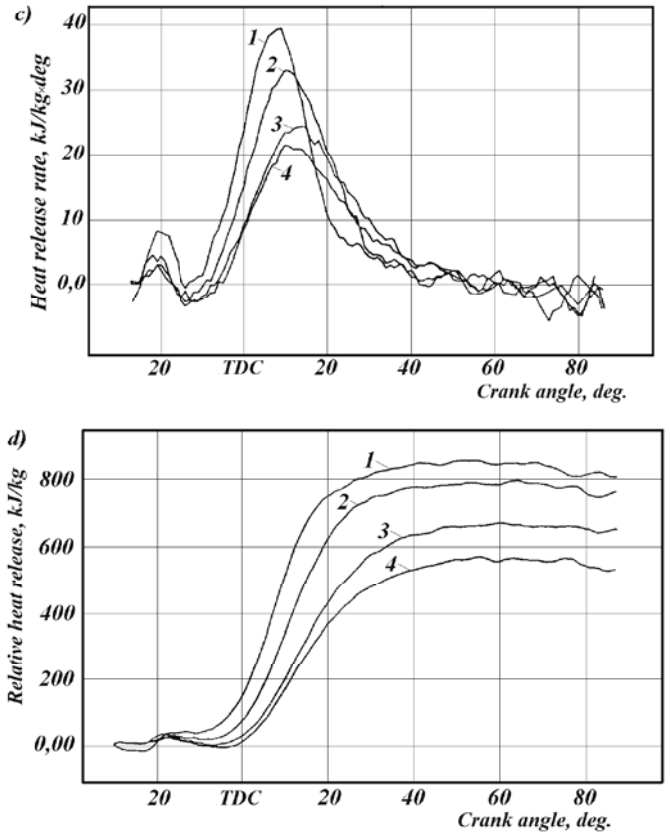

Fig. 6.28.2 Effect of the ignition coefficient on changes in heat density (*c*) and relative heat release (*d*) during co-combustion of pilot fuel and WCS. 1 – 0.178; 2 – 0.089; 3 – 0.0572; 4 – 0.0512 (n = 837 min^{-1}; WCS amount – 814.6 mm^3/cycle; WCS injection – 20°; pilot fuel injection – 40° (before TDC))

At low pilot fuel quantities, a decrease in total heat release observed. This indicates that the heat released during pilot fuel combustion is less than the latent heat of vaporization of the water contained in the WCS. However, the gas temperature remains high enough to activate the combustion of carbon particles. This obviously increases the ignition delay, and the amount of WCS burned during the expansion period increases. This leads to a decrease in cylinder pressure and temperature.

Similar patterns observed during testing of the Cooper-Bessemer JS-1 engine.

WCS with an average particle size of 11 μm used as the main fuel, and DF No. 2 was used as the pilot fuel. Inlet air temperature maintained between 174 and 177°C, and injection pressure maintained between 62 and 69 MPa. With an increase in the ignition coefficient from 0.07 to 0.16, the ignition delay decreased from 6.2 to 5.4 ms (from 15 to 13° CV). The maximum cycle pressure was 8.27 MPa. Although the ignition delay changed only slightly, with an increase in the ignition coefficient, the maximum heat density increased from 3.59 to 7.4 kJ/deg, and the specific heat consumption decreased from 5.31 to 5.04 MJ/(kWh).

The trends described above indicate that with a sufficiently early pilot fuel injection, reducing its amount leads to an increase in the WCS ignition delay. At the same time, the temperature and pressure in the cylinder decrease, and the efficiency of carbon particle combustion deteriorates. Clearly, to eliminate these drawbacks, when reducing the pilot fuel amount, the injection start angle must shift toward the TDC.

6.7. Regulation of engines operating on WCS.

The control process for WCS-powered engines is more complex than for conventional diesel engines. This is due to the extremely high sensitivity of the combustion process of carbon particles to the air charge parameters at the end of compression and at the start of fuel injection. The combustion efficiency of solid fuel in the engine's working space is significantly dependent on a large number of factors, including:

- characteristics of the feedstock fuel and the WCS;
- air charge parameters at the engine inlet;
- the nature and characteristics of the compression process;
- features of the combustion process and air charge turbulence;
- parameters of the main and pilot fuel injection process.

As has already been shown, deviation of even one of the above parameters from the optimal value leads to a decrease in fuel combustion efficiency and the entire engine operation process. Therefore, engine control must carry out taking into account the above factors: changing one parameter must accompany by adjustments to the others. The main parameter, allowing for a wide range of power control, is changing the WCS cyclic delivery. In this respect, engines running on WCS are similar to conventional diesel engines; however, varying the primary fuel cycle delivery results in certain combustion characteristics unique to this type of engine. Adjusting the amount of primary fuel delivered to the cylinder allows for a wide range of engine power control, as illustrated in Fig. 6.29.1 *a*, *b* and Fig. 6.29.2 *c*, *d*, which illustrate the patterns characteristic of such control.

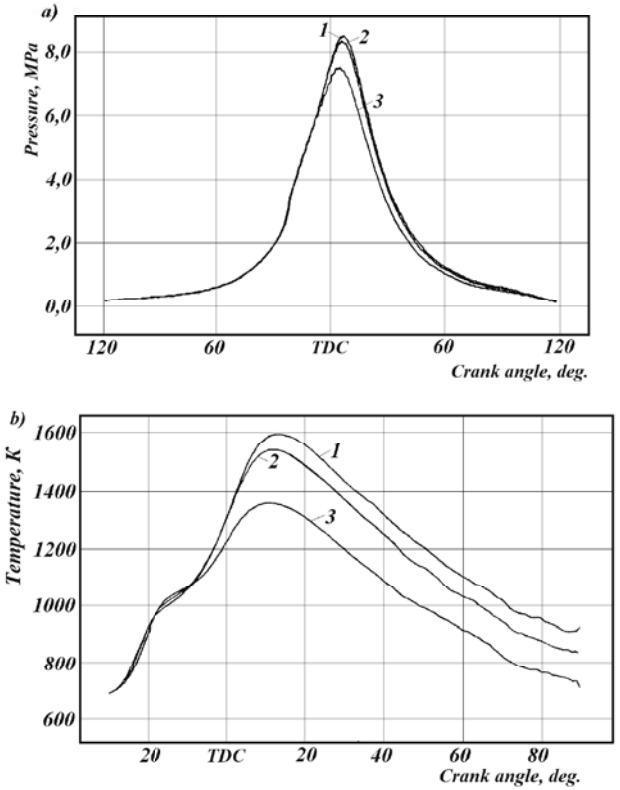

Fig. 6.29.1 Regulating the power of the 645 EMD engine by changing the WCS cyclic feed. Change in pressure (*a*) and temperature (*b*) in the process of co-combustion of pilot fuel and WCS. 1– 824.0 mm^3; 2 – 688.5 mm^3; 3 – 405.5 mm^3 (n = 837 min^{-1}; amount of pilot fuel 100 mm^3/cycle; WCS injection – 11° (to TDC); pilot fuel injection – 40° (to TDC))

The figures show the main dependencies for the working process of the General Motors 645 EMD engine. When the WCS supply decreases from 824.0 to 405.5 mm^3/cycle and the amount of pilot fuel is unchanged (100 mm^3/cycle), the value of the ignition coefficient increases from 0.17 to 0.343. This determines some features of the engine's working process at partial loads.

The increase in pressure in the working cylinder is practically directly proportional to the increase in cyclic WCS feed, while the maximum pressure values shifted to later angles of rotation of the crank.

The temperature of the gas inside the cylinder, as well as the pressure, increases in proportion to the increase in cyclic WCS supply, but the

maximum temperature of the working body reached at later angles of rotation of the crank than the maximum pressure.

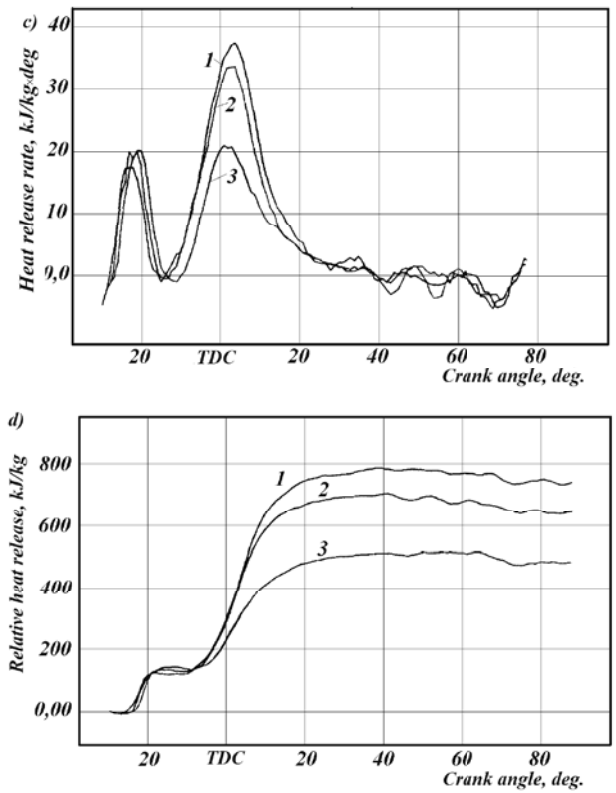

Fig. 6.29.2 Regulating the power of the 645 EMD engine by changing the WCS cyclic feed. Change in thermal tension (*c*) and relative heat release (*d*) in the process of joint combustion of pilot fuel and WCS. 1– 824.0 mm^3; 2 – 688.5 mm^3; 3 – 405.5 mm^3 (n = 837 min^{-1}; amount of pilot fuel 100 mm^3/cycle; WCS injection – 11° (to TDC); pilot fuel injection – 40° (to TDC))

Heat stress and heat release, because of the combustion of hydrocarbon fuel, increase with an increase in its quantity. At the same time, an earlier combustion of the pilot fuel observed, and the maximum thermal stress from the combustion of the WCS shifts to later angles of rotation of the crank. In all cases, the release of heat stops approximately 25° after TDC. In contrast to changes in pressure and temperature, the heat release during combustion of WCS is disproportionate to the increase in its quantity. With large supplies of

hydrocarbon fuel, due to evaporation of water, the ignition delay increases, because of which the combustion efficiency deteriorates.

When the cyclic supply reduced and the parameters of the air charge are unchanged, the coefficient of excess air increases, because of which the efficiency of fuel combustion deteriorates. The mechanism of the process of deterioration of solid fuel combustion with a large excess of air considered in paragraph 6.2.1. It should note that it is possible to significantly increase the efficiency of combustion at partial load modes by increasing the temperature of the air entering the engine. Thus, for effective engine regulation, in addition to the WCS supply change system, it is necessary to provide a system for regulating the temperature of the air supplied to the engine. Additionally, the parameters of the working process can adjust according to the IAA of the pilot and main fuel.

A significant reserve in increasing the efficiency of engine regulation is the use of WCS injection accumulator systems. As shown by the results of tests of the 7FDL engine of the General Electric Company, the use of such systems allows increasing the injection pressure. At the same time, there are opportunities to obtain not only finer aerosol, but also to achieve its optimal distribution in the space of the air charge. In addition, the electronic control of the injection process allows you to change the cyclic supply, the advance angle of the main fuel injection, and the duration of the fuel supply to the combustion chamber. Evaluation of the optimal combination of regulation parameters can carry out using microprocessor technology, which will significantly increase the efficiency of regulation.

As studies have shown, when the load increases, the optimal injection advance and the required amount of pilot fuel decrease, while an increase in IAA is observed for WCS. At full load, late supply of pilot fuel is optimal. In this case, favorable conditions created for self-ignition of coal fuel, and ignition pilot fuel only intensifies combustion. At the same time, the release of heat is concentrated in the immediate vicinity of TDC, which has a favorable effect on the parameters of the engine's working process (Fig. 6.30a). The change in operating parameters and combustion parameters when the load changes is presented in the table. 6.17.

Lowering the load characterized by very low boost pressure or its complete absence in the intake manifold. Under such conditions, the temperature after evaporation of water decreases, and self-ignition of WCS becomes impossible. The heat of combustion of the pilot DF spent on increasing the temperature. A typical characteristic of heat release during the combustion of two fuels at partial load (620 min^{-1}, average indicator pressure 0.3 MPa) is shown in Fig. 6.30 *b*. The first peak of heat generation

corresponds to the combustion of pilot diesel fuel, which in this case releases approximately 24% of the total energy, compared to 4% at full engine load. The combustion efficiency drops to 93%, and the maximum combustion temperature does not exceed 1560 K, which is much lower than the temperature at full engine load (1900 K).

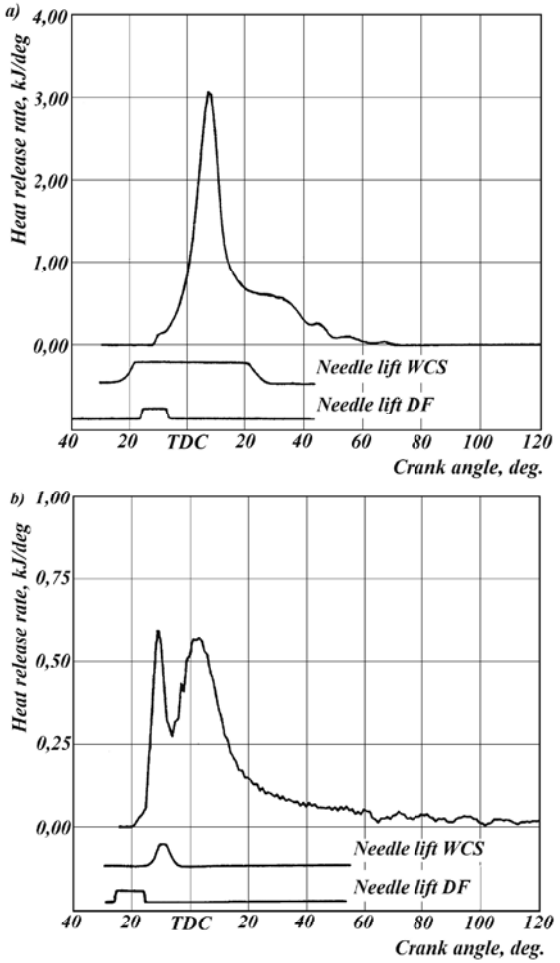

Fig. 6.30. Change in the rate of heat release in the working cylinder of the 7FDL engine of the General Electric Company. *a* – at full load mode (rotational frequency – 1050 min^{-1}; air pressure and temperature at the inlet 360 kPa and 360 K, respectively); *b* – in partial load mode (rotation frequency – 620 min^{-1}; pressure and temperature of air at the inlet 102 kPa and 332 K, respectively)

Table 6.17.

Optimized operating parameters and combustion parameters during operation of the General Electric 7FDL engine in various modes.

Ignition characteristics						Combustion characteristics		
Speed of rotation, min^{-1}	The mean effective pressure, MPa	Injection start angle, degrees		Contribution of fuel to the process of heat release, %		P_{max}, MPa	Combustion efficiency, %	Specific heat consumption, kJ/(kWh)
		DF	WCS	DF	WCS			
620	0.30	24	15	23.8	76.2	4.9	92.8	12165
880	0.49	23	15	23.9	76.1	5.5	94.9	10450
880	0.56	22	15	16.9	83.1	5.9	96.5	9255
960	1.03	20	20	9.2	90.8	8.2	97.5	8560
960	1.35	19	20	6.7	93.3	9.9	98.5	8258
960	1.71	18	25	5.0	95.0	12.3	99.0	8403
1050	1.98	12	35	4.0	96.0	17.1	99.5	8159

6.8. Fuel consumption in engines working on WCS.

The efficiency of using solid fuel in reciprocating internal combustion engines depends on two main factors: the completeness of combustion of coal particles and the nature of heat release during fuel combustion. The latter has a significant impact on the effective and specific performance of the engine, including specific fuel consumption.

At the initial stage of the modern stage of research on the combustion of coal suspensions in piston engines, the efficiency of burning solid fuel did not exceed 50...85%. More recent studies have shown that the amount of fuel that managed to burn in the working space of the engine can be 92...99.5%. At the same time, theoretical calculations show that, in principle, it is possible to burn up to 100% of fuel under the conditions of an engine with a rotation frequency of about 1000 min^{-1}.

The effective performance of engines largely depends on how the release of heat from the combustion of solid fuel is consistent with the parameters of its thermodynamic cycle. Studies have shown that, despite the fundamental differences in the combustion mechanisms of solid and DF, it is possible to obtain such combustion characteristics that allow you to preserve, and in some cases even improve the efficiency of the engine's working process. The most complete coal fuel can burned in low-speed engines with a large cylinder volume with the pilot ignition method.

It should note that, as a rule, specific fuel consumption for engines operating on WCS with pilot ignition calculated based on the total heat released in the working cylinder. Such a technique does not allow to

objectively estimate separately the consumption of main and pilot fuel, therefore, when evaluating the efficiency of fuel use, it is necessary to take into account the value of the ignition coefficient.

The specific fuel consumption values for various types of WCS, obtained during testing of the Sulzer low-speed engine 1RSA76, shown in Fig. 6.31 [65]. Data on the consumption of the main and pilot fuel are on the standard heat of combustion of 42.7 MJ/kg.

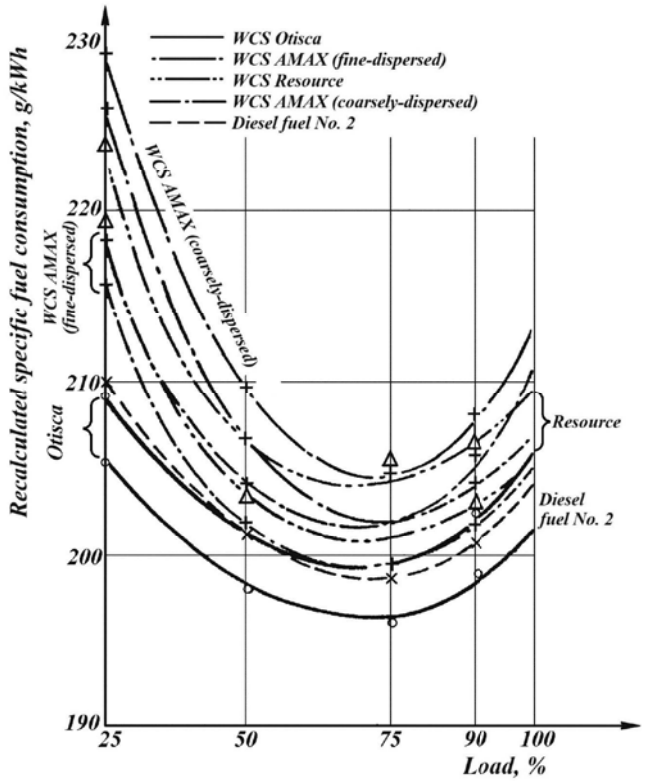

Fig. 6.31. Specific fuel consumption in engine 1 RSA 76 (experimental data), recalculated the heat of combustion 42.7 MJ/kg

Each WCS characterized by two curves, of which the lower one shows the fuel consumption at the heat of combustion, determined according to the methodology of the Swiss Federal Institute for Materials Testing (FIIM); the upper one – according to the heat of combustion, determined based on the

methodology developed by the company Resource. The discrepancy in the values of the heat of combustion explained by the fact that the suspension is an inhomogeneous product, so the definition of its calorific value is more difficult than for DF. The discrepancy for both methods is less than 2%, and the values obtained by the FIIM method are invariably lower. Measurements carried out at 90-, 75-, 50-, and 25% load at a shaft rotation frequency of 120 min-1. Data on fuel consumption at higher loads could not obtained, since the heat of combustion of the fuel was lower than the value of 16.75 MJ/kg used in the calculation of the injection system.

The specific fuel consumption values shown in Fig. 6.31 include data on diesel fuel, which mixed with the main fuel in the form of leaks. Leaks for 4...6% of the total heat supply at loads of 50...90% are caused by the design features of the Sulzer fuel injection system.

The WCS of the Otisca Company gives a fuel consumption that does not exceed a similar figure for DF No. 2. Next, in the order of increasing consumption, WCS AMAX (fine-dispersed), Resource and AMAX (coarse-dispersed) follow. The maximum relative to DF No. 2 is the consumption of coarsely dispersed AMAX suspension (about 3...8% depending on the load). It is interesting to note that the consumption of the Resource suspension, which has the minimum particle size, is greater, while WCS Otisca, obtained by the method of gravity enrichment, shows the minimum consumption.

***

The results of both theoretical and experimental studies considered above suggest that the thermodynamic aspects of the problem of using solid fuels practically solved now. The use of solid fuels in the composition of WCS makes it possible to obtain stable performance indicators of engines. Even now, they are not inferior to engines running on petroleum products in terms of fuel efficiency. For commercial use, it remains to solve the problem of wear of the main engine parts and the problem of reducing harmful emissions into the environment.

Chapter 7

Theoretical foundations of burning coal fuel in the working space of a piston engine

7.1. The process of combustion of solid fuel in the working space of the engine

The actual combustion mechanisms of coal particles, especially in the solid phase, within the space of the combustion chamber are currently insufficiently studied. The influence of solid fuel parameters (elemental composition, particle sizes, their shape, internal structure, volatile content, etc.) on engine characteristics is also poorly studied. When choosing the initial conditions necessary for the effective use of one or another type of solid fuel, the task complicated by the fact that the parameters of particle combustion must be consistent with the characteristics of the thermodynamic cycle of the engine.

At present, only qualitative characteristics known, indicating the influence of turbulence, coefficient of excess air, engine speed, and pressure in the cylinder, temperature and intensity of heating of fuel particles on the combustion process of pulverized coal fuel. There is uncertainty regarding the role of kinetic and diffusion processes on the total thermal effect of the fuel combustion reaction. This complicates the process of determining the time required for the complete combustion of a coal particle in the working space of the engine. This time limits the maximum possible engine speed and the efficiency of fuel combustion, and therefore the efficiency of the entire thermodynamic cycle as a whole.

In order to optimize combustion processes, additional research needed, which directly concerns the preparation and combustion of fuel in the engine cylinders, namely:

- optimization of the fuel system, which includes the search for rational sprayer designs, the determination of the most effective spray angles of the fuel torch, the optimal pressure and nature of the injection, as well as its duration;
- optimization of ignition delay and combustion characteristics of coal fuels;
- optimization of the shape of the combustion chamber, including studies of the possibilities of using pre-chambers and stratified charge;
- optimization of methods of activation of the combustion process, which can be used spark ignition, compression ignition, use of flammable liquid fuel;

- reduction of slag formation and other types of deposits associated with incomplete combustion of coal fuel on engine parts.

In addition to the thermodynamic characteristics of the engine, the completeness of the combustion of fuel particles has a significant effect on the content of toxic substances and soot in the exhaust gases.

In order to get a general idea of the combustion process of solid fuel in the working space of a piston engine, further, in the most general form, we will consider the combustion process from the point of view of the thermodynamic cycle of the engine, individual stages of the combustion process and factors affecting the efficiency of solid fuel combustion.

7.2. Model of the state of the working body in the engine cylinder.

As can be seen from Fig. 7.1, the state of the working body in the engine cylinder, depending on the angle of rotation of the crankshaft, is influenced by the following thermodynamic factors: changes in the work done on the gas from the side of the piston, heat transfer from the working body to the cylinder walls, combustion of fuel particles and heat and mass exchange of the working cylinder with the environment. To describe the instantaneous thermodynamic state of the gas in the cylinder, the first law of thermodynamics (Fig. 7.1) applied to the control volume [35, 68].

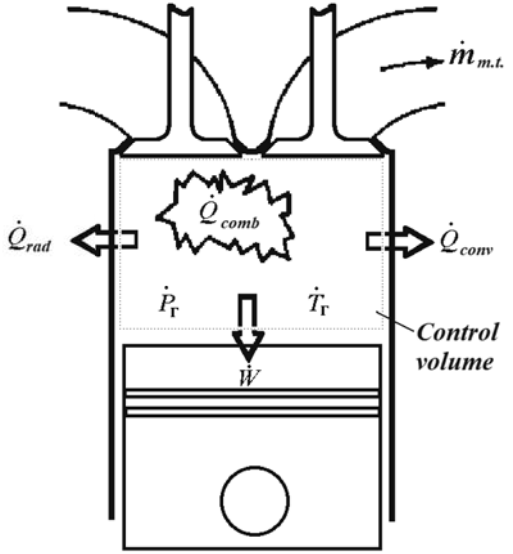

Fig. 7.1. Components of the closed thermodynamic system of the working cylinder

Having written down the first law of thermodynamics for the control volume in differential form, we get:

$$\frac{dE_{cv}}{dt} = \dot{Q}_{comb} - \dot{W} - \dot{Q}_{conv} - \dot{Q}_{rad} - \dot{m}_{m.t.}, \qquad (7.1)$$

where $\dot{Q}_{comb}$ – the amount of heat; released during fuel combustion; $\dot{W}$ – the term of the equation equivalent to the heat expended on the work performed by the piston; $\dot{Q}_{conv}$ – the term of the equation that takes into account the heat transfer between the gas and the walls of the combustion chamber; $\dot{Q}_{rad}$ – the term of the equation that takes into account radiation heat transfer between fuel particles and the walls of the combustion chamber; $\dot{m}_{m.t.}$ – energy losses due to mass exchange with the environment.

To take into account the uneven distribution of various components, the contents of the cylinder must divided into separate areas and zones (see below). In the process of gas exchange of the working cylinder with the environment, three main areas formed one for air, the second for combustion products, and the third for a mixture of these two components (air and combustion products). Equation (7.1) must apply to each of the areas during blowdown, to each of the zones during combustion, and to the entire contents of the cylinder during compression and expansion.

Equation (7.1) does not take into account the heat losses associated with radiation from the gas, since according to a number of estimates; they make up a relatively small amount in the overall balance of heat losses [46]. The change in internal energy in the control volume can also write as the sum of the change in internal energy of gas and fuel particles:

$$\frac{dE_{cv}}{dt} = \dot{U}_g + \dot{U}_p. \qquad (7.2)$$

Having transformed equation (7.2) taking into account the specific heat capacities, we get:

$$\frac{dE_{cv}}{dt} = \dot{m}_g c_{v_g} T_g + m_g c_{v_g} \dot{T}_g + \dot{m}_p c T_p + m_p c \dot{T}_p. \qquad (7.3)$$

Solving this equation relative to the value of the instantaneous temperature of the working gas for each region during purging and for each zone during combustion, equating equations (7.1, 7.3) and integrating, we have:

$$\dot{T}_g = \frac{1}{m_g c_{v_g}} \{\dot{Q}_{comb} - \dot{W} - \dot{Q}_{conv} - \dot{Q}_{rad} - \dot{m}_{m.t.} - \\ - \dot{m}_g c_{v_g} T_g - \dot{m}_p c T_p - m_p c \dot{T}_p\}. \qquad (7.4)$$

The resulting equation (7.4) allows you to determine the instantaneous value of the temperature at any moment of time by the angle of rotation of the crankshaft.

When determining the state of the working body during compression until the moment of fuel injection, the equation is simplified, in particular, such parameters as; $\dot{Q}_{comb}$, $\dot{Q}_{rad}$, $\dot{m}_g c_{v_g} T_g$, $\dot{m}_p c T_p$, $m_p c \dot{T}_p$ and $\dot{m}_{m.t.}$ are taken equal to zero.

Depending on the type of liquid carrier and the method of activation of the combustion process, the total heat $\dot{Q}_{comb}$ released during the fuel combustion cycle consists of several components. They characterize the heat release from the combustion of pilot fuel or a combustible liquid carrier, as well as the heat release from the combustion of volatiles and oblique residue. When using WCS, the heat spent on the evaporation of the water carrier $\dot{Q}_{wat}$ is also included in the indicator with a minus sign.

7.3. Stages of the combustion process of coal suspensions in the working space of a piston engine.

Preparation of coal fuel for combustion begins at the stage of its spraying. As already noted earlier, the characteristics of spraying suspensions have a significant impact on the process of ignition of coal fuel and on the process of its subsequent combustion. The most important parameters from the point of view of efficient burning of coal fuel are: the size of the aerosol droplets and the nature of their distribution in the space of the combustion chamber, the thermodynamic state of the gas medium in the cylinder, the size and composition of coal particles, the nature of heat and mass exchange between the fuel particles and the gas medium, the heat exchange process between the fuel particles and the cylinder walls.

The nature of heat release as result of combustion of pilot fuel and coal suspension in the working cylinder of the engine largely depends on the type of carrier used and the method of activation of the combustion process. The largest number of stages of the combustion process observed when using WCS and the thermal method of ignition. Separate stages of the WCS combustion process can clearly trace by the characteristic of the change in the rate of heat release, which shown in Fig. 7.2. The following dependencies obtained based on the test results of the EMD 645 diesel engine.

In the case under consideration, an increased cyclic supply of pilot fuel used. This done in order to more clearly trace the effect of separate supply of pilot and main fuel on the combustion process in the working cylinder. From fig. 7.2 it can be seen that there are two maxima on the curves of the instantaneous rate of heat release, which correspond to the combustion of

pilot and coal fuel. Both processes, in principle, can superimpose on each other, while pilot fuel burnout can take place in the WCS combustion area (with the pilot method of ignition).

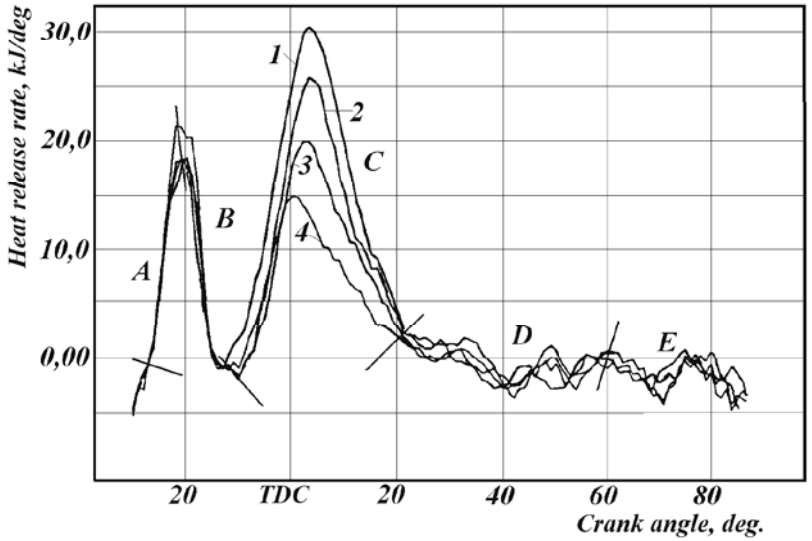

Fig. 7.2. Change in the rate of heat release in the EMD 645 engine when using WCS with thermal ignition (amount and start of pilot DF injection 100 mm^3/cycle and 40° to TDC, respectively; WCS injection 11° to TDC; WCS amount: 1 – 806 mm^3/cycle; 2 – 711 mm^3/cycle; 3 – 495 mm^3/cycle; 4 – 394 mm^3/cycle)

As it already noted in chapter 6, in the process of joint combustion of two fuels (main WCS and pilot DF), five main stages can distinguish.

For other types of suspensions and methods of activation, the number and sequence of individual stages can be significant. Some stages may overlap or occur simultaneously.

Thus, the burning of solid fuel must considered as a set of simultaneous and sequential physical and chemical processes that depend on the instantaneous state of all components of the thermodynamic system and on the speed of surface-kinetic reactions. As an example, in Fig. 7.3 in the most general form shows the scheme of the processes of physical and chemical interaction between WCS aerosol droplets and the gas medium during the pilot method of ignition [76]. The model considered further allows taking into account the influence of combustion of pilot fuel, evaporation of the liquid carrier, release and combustion of volatiles, and burning of coking-coal residue.

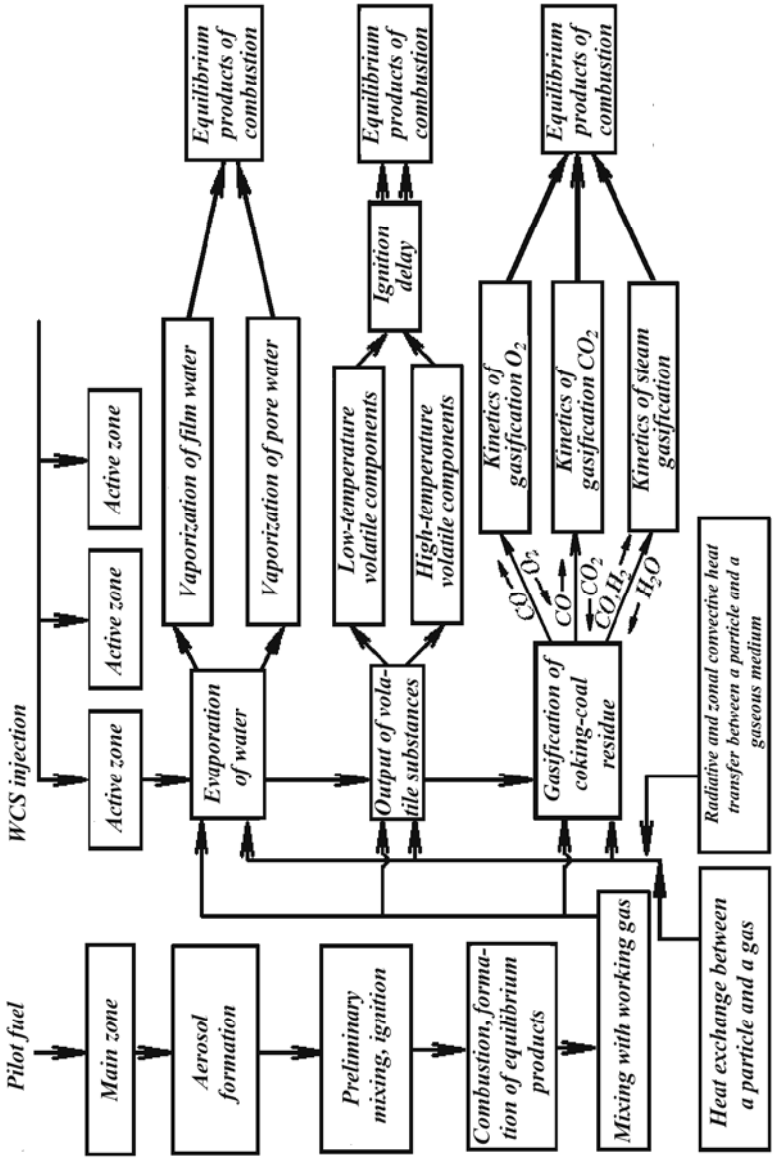

Fig. 7.3. Scheme of the WCS combustion process in the engine cylinder during pilot ignition

7.4. Formation of active zones.

The fuel, consisting of a mixture of liquid carrier and coal particles, injected into the combustion chamber of the engine. Fuel particles, in turn, consist of the corresponding mass fractions of coking coal substance, volatile components, and ash residue. As an aerosol formed, individual droplets, spreading within a certain space, mix with the air, involving it in a complex vortex motion. Sprayed fuel goes through certain stages in the process of preparation for combustion and can exist in several forms. Due to the difference in density, during spraying, coal particles can be released from the liquid carrier with the formation of separate liquid and solid droplets; several coal particles can be grouped together within one droplet and, finally, each particle can surrounded by a liquid shell. Probably, all these forms exist together, at least at the initial stage of aerosol formation. The process of penetration and mixing of various fuel components with the air charge is stretched over time, due to which there is an in homogeneity in the distribution of fuel particles in the volume of the combustion chamber. This in homogeneity has a significant impact on both the ignition process and subsequent fuel combustion.

Analytical studies to account for the uneven distribution of aerosol in the space of the combustion chamber of the engine usually consider a set of separate spatial zones [34, 36, 62, 68, 76]. These zones formed as fuel injected into the gas environment. The entire portion of injected fuel is divided into separate «packages» (hereinafter the word «package» will be used without quotation marks), containing equal masses of injected fuel. Then the mass of fuel in each package divided into a number of drops and particles of a certain diameter. Based on different injection conditions and characteristics of the initial solid fuel, the droplet size can vary between 30...100 μm, and the particle size 2...10 μm. At each angle of rotation of the crank, from one to several packets can inject into the cylinder. Schematically, the process of forming packets and their classification showed Fig. 7.4.

As soon as the packets introduced into the cylinder, they begin to sink into the gaseous contents of the combustion chamber, resulting in the formation of active zones. The size of these zones, the nature of the interaction between the aerosol droplets and the gaseous medium, changes both as the active zone moves within the volume of the combustion chamber and over time. Each package or zone identified by the time of entry into the cylinder and according to his or her position relative to the torch core.

This classification because the mass of entrained air must related to the mass of the unburned mixture. At the same time, the mass of entrained air should increase as the plume develops during the injection process. The

attached mass of air in the active zone depends on two layer numbers: by the time it enters the cylinder and by its location. The mass of fuel components in each active zone preserved during the entire combustion process, that is, the products of fuel combustion in each zone interact with unburned fuel and the associated mass of gas.

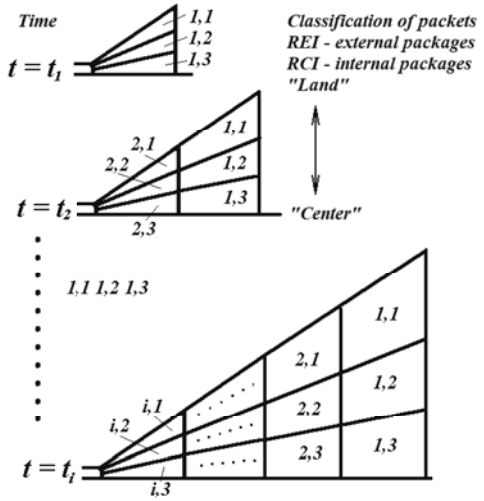

Fig. 7.4. Injection of individual fuel packages and formation of active zones [36]

The attached mass of gas m_{att} can determine by a simple exponential expression of involvement, which proposed in [34]. Despite its simplicity, this expression formulated taking into account the main features of the involvement process.

$$m_{att}(I,J) = K\frac{m_{im}}{I_t J_t (Y+1)}\left(\frac{\Delta\theta_{ts}}{\theta_b}\right)\exp\left\{-\frac{I}{I_t}\frac{J}{J_t}\right\},$$

where K – the coefficient of involvement; Y – the duration of fuel injection; I – package number (by the time it hits the cylinder); J – package number (according to the classification scheme); θ_b – constant involvement; m_{im} – instantaneous mass of the unburned zone; I_t – the total number of packets (by the time they hit the cylinder); J_t – the total number of packets (according to the classification scheme); $\Delta\theta_{ts}$ – the time step of the calculation scheme in time (in degrees above sea level). Each package is described by numbers I (according to the time of hitting the cylinder) and J (according to the classification scheme). The first packets injected into the

cylinder have the number 1, the second – number 2, etc. The packets of each number (by the time they hit the cylinder) designated according to the classification scheme (for example, 1, 2...).

Constant involvement θ_b, is the time required for complete coverage of the surrounding gas space by aerosol jets or the time set for the jet to cover the entire volume of the combustion chamber. The estimation of the time required for the aerosol to cover the surrounding gas environment can made because of the time required for the aerosol to reach the edge of the piston, based on the plume penetration equation.

7.5. Evaporation of the liquid carrier.

In the process of formation of active zones, the suspension sprayed in a gas medium with high density and temperature, while the liquid carrier begins to evaporate. It generally accepted that the combustion process of solid fuel, which is a part of WCS, begins only after all the water evaporates from the surface of the particle. This leads to longer ignition delays.

For FCS, the beginning of the combustion process is determined based on the self-ignition conditions of DF, which is a liquid carrier. Therefore, the ignition mechanism for WCS and FCS is different. At the same time, it largely determines the course of the further combustion process. These issues discussed in detail in chapter 6.

7.5.1. Evaporation of DF when using FCS. To estimate the evaporation of DF, which is part of FCS, the vaporization model proposed by Spalding can use. It based on the theory of vaporization of droplets in equilibrium conditions. This model used in their work on modeling the FCS combustion process in a piston engine, Bell and Caton [35]. Expressions of the energy equation in spherical coordinates for a droplet have the form:

$$\frac{d}{dr}\left(k_g 4\pi r^2 \frac{dT}{dr}\right) - \frac{d}{dr}(W 4\pi r^2) c_p T = 0$$

and

$$\frac{d}{dr}\left(\rho_g D_f 4\pi r^2 \frac{dY_f}{dr}\right) - \frac{d}{dr}(W 4\pi r^2) Y_f = 0,$$

where W – the mass flow of evaporated fuel; r – the radius of the droplet; k_g – thermal conductivity of gas; T – temperature; c_p – isobaric heat capacity of gas; ρ_g – gas density; D_f – diffusion coefficient DF; Y_f – the fraction of fuel in the gas phase.

After double integration of the above equations using boundary conditions, the expression obtained:

$$W_w = \frac{\rho_g k_g}{R_d} \ln(B+1),$$

where R_d – the instantaneous radius of the droplet; B is the mass transfer coefficient (for conditions close to critical, taking into account the surface temperature, the coefficient can be taken as 0.9).

7.5.2. Evaporation of water when using WCS. Despite the possible diversity in the structure of WCS aerosol droplets, the most common case represented by droplets consisting of several particles of coal fuel (coal array) a water envelope. With such a structure (Fig. 4.27), the liquid fraction of a WCS droplet can divided into a film fraction and a pore fraction, that is, it can considered as a set of water molecules around and within the coal massif, respectively. The process of evaporation of film and pore water has some differences.

The specific conditions of the evaporation process in the combustion chamber of a piston engine do not allow us to consider the vaporization process as an equilibrium phenomenon, that is, a process in which the heat transfer coefficient dictated and balanced only by the evaporation rate. To determine the time required for the evaporation of film water, it is necessary to take into account the sensitivity of vapor formation to the prevailing external conditions in the zone immediately adjacent to the surface of the droplet, as well as the heat of the phase transition and mass transfer processes. Evaporation of a water carrier can represented as a series of sequential physical processes that affect the total evaporation coefficient. These include initial heating of the droplet when the evaporation rate is low, and equilibrium or boiling vapor formation when the evaporation rate is high. The temperature of the surface of the droplet depends to large extent on its composition, since the heat supplied to it distributed between the water film, pore water, and coal massif. The corresponding vapor formation mechanism dictated by the surface temperature of the droplet and the prevailing conditions of the active zone.

As soon as the film water evaporates, the second stage of steam formation begins, during which the pore water evaporates. The second phase begins with a lower evaporation coefficient, primarily due to the simultaneous supply of heat to the water and the coal massif. At this stage of vaporization, the WCS droplet size remains almost constant, individual elementary coal particles within the droplet agglomerate held together by the surface tension of water and can considered as a single porous particle. The size of the agglomerate, its surface area and the period of existence at the second stage of vaporization determined the size of the coal massif. Vaporization of pore

water can considered as an evaporation process, in which pore water penetrates through the coal massif to the surface, where it evaporates.

Fig. 7.5 shows the calculated dependence for the evaporation rate taking into account all the factors listed above [76].

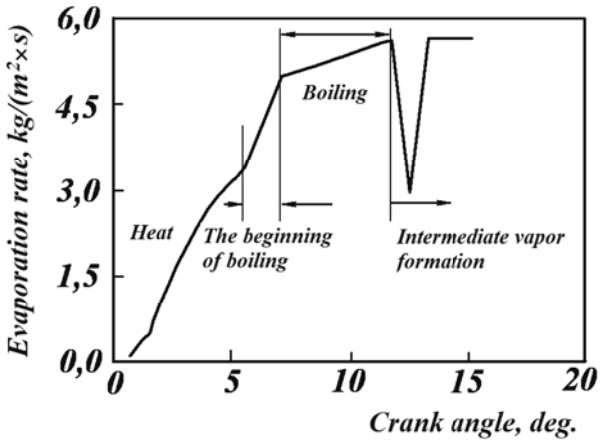

Fig. 7.5. Evaporation rate of a WCS droplet with a diameter of 30 μm (ambient pressure 1.0 MPa; temperature 1500 K)

As the pore water evaporates, the coal massif disintegrates into individual particles, which begin to heat up intensely and release volatile components.

7.6. Removal of volatile substances.

The combustion process of coal particles consists of two main phases. The first phase is the removal and combustion of volatile substances and the second phase is the burnout of the coke-coal residue.

The most common understanding of the nature of volatile substance removal is that gaseous products locally removed from the surface in a jet and burn in the gas phase far from the fuel particle, without hindering surface reactions (Fig. 7.6). This assumption supported by several experimental observations [35]. Another model of the volatile substance removal process based on the assumption that surface reactions preceded to processes leading to the complete removal of volatile substances. Some researchers believe that during the combustion of small particles (approximately 20 μm), volatile components do not have time to leave the coal particle and are burned during surface reactions. Obviously, all the described mechanisms for volatile substance release reactions can occur during particle combustion in the engine's working space.

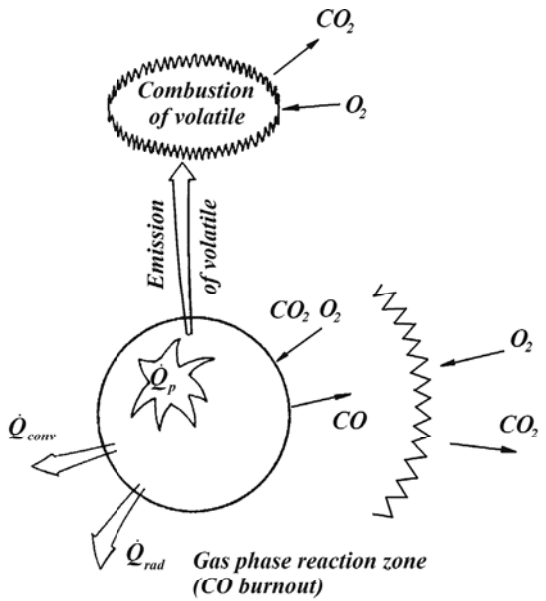

Fig. 7.6. Scheme of combustion of coal particle [35]

It is currently unknown which model best describes the processes of volatile matter removal from the surface of carbon particles under piston engine conditions. Model selection further complicated by the fact that no studies of volatile matter removal under conditions identical to those of piston internal combustion engines been conducted. Specific conditions include engine cylinder pressure from 1 to 15 MPa, gas temperature from 600 to 3500 K, and fuel particle heating rate from 5000 to more than 10^6 K/sec. Furthermore, the time allotted for complete combustion of a carbon particle (including volatile matter removal) typically does not exceed 10 ms for high-speed engines.

Due to the lack of experimental data, several researchers have attempted to model the volatile matter removal process and evaluate its impact on solid fuel combustion efficiency. The studies conducted using mathematical and physical modeling methods. The first attempt to model coal fuel combustion in an engine cylinder performed by Caton et al. [35, 70]. His proposed model of particle-gas interaction based on the mechanism depicted in Fig. 7.6. Wahiduzzaman, Blumberg, and others subsequently refined this model [76].

The multifactorial nature of the devolatilization process significantly complicates the development of fundamental mechanistic expressions for the

volatile yield coefficient, so Caton's model utilized an empirical relationship approximated by a first-order equation:

$$\frac{dV}{dt} = (a_1 k_1 + a_2 k_2) F (V_{max} - V), \quad (7.5)$$

where V_{max} – the maximum content of volatiles in the fuel; k_i – are constant coefficients (determined from the Arrhenius expression):

$$k_i = A_i \exp\left(\frac{-E_i}{RT}\right). \quad (7.6)$$

To assess the impact of volatile emissions on solid fuel combustion, data from four studies collected from the literature. None of these studies corresponded to engine conditions, but each reproduced some parameters relatively close to the target ones.

To adjust for process pressure, a correction factor F used:

$$F = B_1 + \frac{B_2 - B_1}{1 + aP},$$

where $B_1 = 0{,}766$; $B_2 = 1{,}085$ and $a = 0{,}138$ MPa.

Table 7.1 presents the kinetic parameters for estimating the removal of volatile matter from coal fuel (see equations (7.5) and (7.6))

To balance the carbon and hydrogen ratio with the available oxygen, all volatile matter treated as cyclopentane (C_5H_{10}) in further calculations. The calorific value of the volatile matter was assumed be 35 MJ/kg.

Table 7.1.

Kinetic parameters for assessing volatiles removal

Parameter	*Badzioch and Hawksley*	*Kobayashi and others*	*Suuherg and others*	*Ubhayakar and others*
a_1	1.0	0.3	1.0	0.39
A_1, s^{-1}	1.14×10^5	2×10^5	8.7×10^5	3.7×10^5
E_1, *kJ/mol*	74.1	104.7	55.27	73.7
a_2	0	1.0	0	0.8
A_2, s^{-1}	—	1.3×10^7	—	1.46×10^{13}
E_2, *kJ/mol*		167.5		251.2

The enthalpy of the volatiles was considered as a linear function of the fuel particle temperature:

$$h_v = c_{pv} T_p,$$

where $c_{pv} = 1{,}67$ kJ/(kg×K)

Subsequently, Wahiduzzaman and Blumberg described the volatile removal mechanism based on the model proposed by Kobayashi [76]. In this

model, degassing hydrocarbons represented by two species with fixed H/C ratios (~2.29 and ~1.02 for coal with a total H/C ratio of 0.8). Each of these hydrocarbon species produced a corresponding, highly precise reaction. One of the reactions (H/C ~ 2.29) characterizes the low-temperature release of volatiles, the other (H/C ~ 1.02) the high-temperature release. The ratio of hydrocarbon species and the temperature of the coal massif depend on the ratio of the two types of volatile removal reactions, which, in turn, independently depend on the mass temperature. The model predicts that for typical air charge parameters a cylinder, the low-temperature reaction initially predominates, dominating the process of volatile component release. Later, as the temperature rises, the second reaction becomes dominant, and the total hydrocarbon ratio significantly increases with the amount of volatile compounds produced by the second type of volatile release reaction.

Fig. 7.7 shows the calculated volatile release reaction rates as a function of the ambient gas temperature and the initial conditions adopted from a number of studies.

Considering that the volatile release patterns can vary significantly for different fuels, even with the same volatile content, all four relationships can be valid when using WCS. This implies that the combustion behavior of carbon particles depends more on the volatile release rate than on their content in the fuel.

Applied to the combustion chamber conditions of a piston engine with inlet air heating, the calculated dependence of volatile release on crankshaft angle shown Fig. 7.8.

In addition to the calculated curves, Fig. 7.8 shows the point at which the volatile release reaches 50% of the total amount contained in the fuel. The obtained results are in good agreement with the experimental data. Since the removal of volatiles can occur simultaneously with surface reactions, some of them burn directly on the particle surface. The first three dependences (A, B, C) of volatile removal correspond to their complete removal before the onset of surface reactions, while the fourth dependence (D) indicates only partial release. The remaining portion consumed during surface reactions.

The release and combustion of volatiles significantly influences the overall combustion process of coal fuel. On the one hand, the released volatile matter mixes with the gaseous content of the corresponding active zone, after which it begins to burn out, forming equilibrium combustion products. This increases the temperature in the active zone and accelerates the heating of the coal massif, which further accelerates the release of volatiles also promotes the acceleration of coke-coal residue burnout reactions. On the other hand, the volatile components quickly burn out,

forming equilibrium products, resulting in a decrease in the oxygen concentration in the active zone and a slight reduction in the rate of solid-phase reactions.

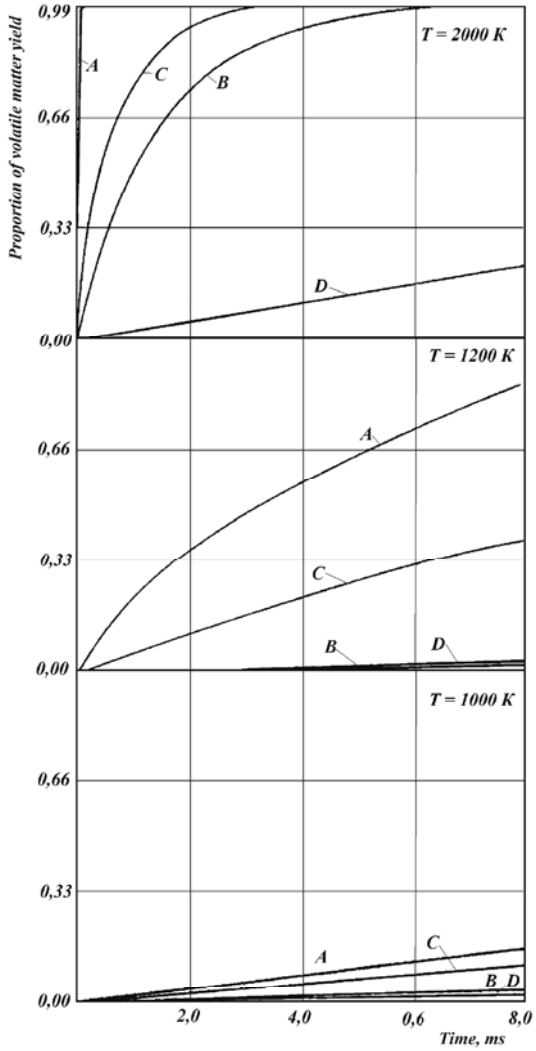

Fig. 7.7. Calculated volatile yield as a function of time for temperatures of 1000, 1200, and 2000 K and a pressure of 3 MPa, obtained depending on the initial conditions adopted from the results of four studies. *A* – Ubhayakar, et al.; *B* – Badzioch and Hawksley; *C* – Kobayashi; *D* – Suuherg et al.

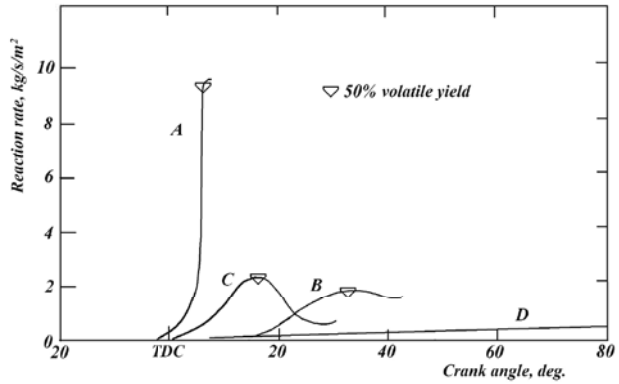

Fig. 7.8. The yield of volatile substances as a function of the crankshaft rotation angle for the particles of the first packet (D/S = 220/260 mm; n = 1000 min^{-1}; V_{max} = 0.7; T_a = 450 K)

Fig. 7.9 and 7.10 illustrate how the combustion characteristics of volatiles affect the total burnout of coal particles within the first set of data. Fig. 7.9 shows the solid phase reaction rate as a function of the crankshaft rotation angle for the four cases considered earlier.

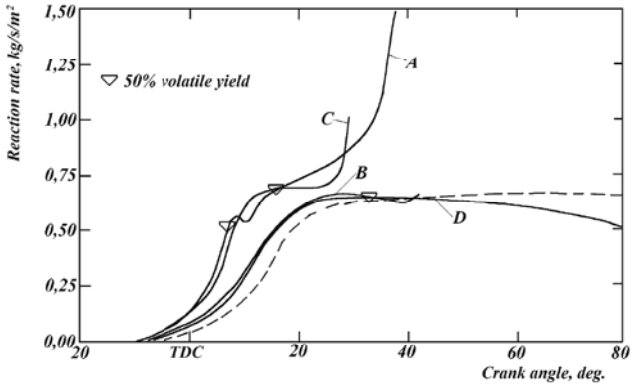

Fig. 7.9. The reaction rate of the solid phase as a function of the crankshaft rotation angle for the particles of the first packet (D/S = 220/260 mm; n = 1000 min^{-1}; V_{max} = 0.7; T_a = 450 K)

Fig. 7.10 shows the change in the diameter of the fuel particles in the first packet during burnout as a function of the crankshaft angle. The dotted line in both figures shows the case of burnout of a fuel particle burning without the release of volatile components (coke particles). The figure shows that in fuels with a high volatile content and high volatile release rate, the total combustion time of a fuel particle significantly reduced.

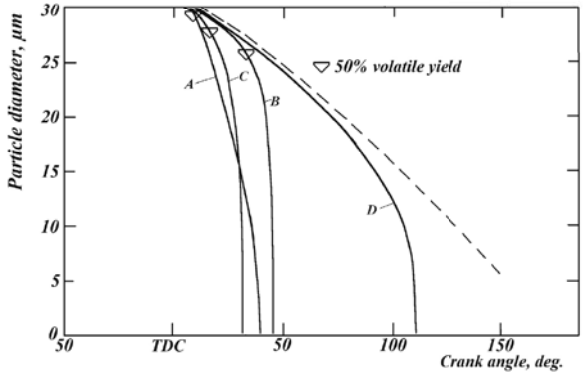

Fig. 7.10. Change in the diameter of a fuel particle as a function of the crankshaft rotation angle for particles of the first packet (D/S = 220/260 mm; n = 1000 min^{-1}; V_{max} = 0.7; T_a = 450 K)

Calculated and experimental data show that the higher the potential volatile release rate, the higher the indicated engine efficiency. The rate of volatile combustion reactions exceeds the rate of surface reactions by approximately four times. The higher the volatile content and the higher the volatile release rate, the higher the thermal stress in the working cylinder. This type of heat release leads not only to increased fuel combustion efficiency but also to more efficient heat utilization, since most of the heat released in the immediate vicinity of TDC. The calculated relationship between the volatile content, release rate, and engine thermal efficiency showed Fig. 7.11.

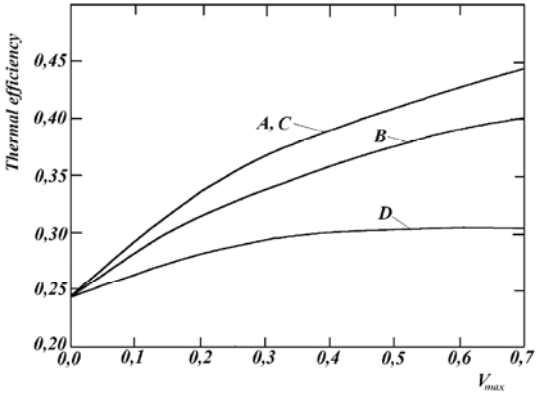

Fig. 7.11. Thermal efficiency as a function of the crankshaft rotation angle for the particles of the first package (D/S = 220/260 mm; n = 1000 min^{-1}; T_a = 450 K)

7.7. Burnout of coke-coal residue.

The first stage of coal particle combustion ends with the removal of volatile matter. The porous mass remaining after this stage consists primarily of carbon (coke) and non-combustible materials (ash). Combustion of the coke residue is the primary stage, the intensity of which determines the rate of fuel burnout and the efficiency of the engine's operating cycle as a whole. The crucial role of carbon burnout explained by the following:

- solid carbon contained in the fuel is the main combustible component of almost all natural solid fuels;
- coke residue burnout is the longest of all stages and can account for up to 90% of the total combustion time.

For the efficient use of solid fuels in piston internal combustion engines, it is necessary to create optimal conditions for carbon combustion. This requires considering the main factors acting during coke residue combustion [30, 31].

The combustion of pulverized fuels based on the chemical reaction of the combustible components of the fuel with oxygen in the air charge. Chemical combustion reactions in the engine's working space, as already noted, occur during the extremely short residence time of the fuel and oxidizer (5...80 ms). These reactions occur under conditions of strong mutual influence with simultaneous physical processes. These processes include:

- turbulent and molecular diffusion and convective transfer of the starting materials and reaction products in the gas flow, as well as the transfer of gas reactants to dispersed particles;
- heat exchange between the gas flows of combustion products and the starting mixture;
- heat exchange between the gas and the fuel particles contained therein;
- radiative heat exchange of the particles with the gas environment and the screen surfaces of the combustion chamber.

Thus, the combustion of coke-coal particles is a complex physicochemical process consisting of chemical reactions and physical processes occurring in conditions of mutual interaction and mutual influence.

Before the chemical combustion of the coke-coal residue can occur, the oxidizer must diffuse through the boundary layer to reach the reacting surface. Therefore, carbon combustion must consider a complex heterogeneous physicochemical process consisting of two stages: the supply of oxygen to the particle surface through molecular diffusion and the chemical reaction on its surface.

Let us consider the general scheme of heterogeneous combustion, assuming the following conditions:

- the oxygen concentration is uniform across the entire particle surface;

- the rate of oxygen reaction with carbon is proportional to the oxygen concentration at the surface (i.e., a first-order reaction occurs, which is most likely for heterogeneous processes);

- the reaction occurs on the particle surface, forming the final combustion products.

Given the adopted simplifications, the rate of carbon combustion can represented as dependent on the rate of two main stages of the process: namely, the rate of oxidizer supply to the coke-coal particles and the rate of the chemical reaction itself occurring on the surface. The interaction of these processes results in a dynamic equilibrium between the amount of oxidizer delivered by diffusion and consumed in chemical reactions at a certain concentration on the surface of the coke-coal particles. In its most general form, coke carbon burnout characterized by gasification processes and determined by a set of heterogeneous surface reactions during which carbon converted into gaseous products by interacting with O_2, CO_2, and H_2O according to the following reactions:

$$C + ½O_2 = CO, \quad (7.5)$$

$$C + CO_2 = 2CO, \quad (7.6)$$

$$C + H_2O = CO + H_2. \quad (7.7)$$

The consumption of the coke-coal massif depends on the local concentrations of reactants on the coke-coal particles, consistent with the reaction rates for the described mechanisms, as well as the nature of mass transfer in the gas phase. The products of heterogeneous reactions (CO and H_2) then oxidized in the gas phase within the core. In this case, oxidation reactions in the gas phase approach the equilibrium limit if the pressure, temperature, and water vapor concentrations in the core are sufficiently high. Therefore, with regard to engine conditions, equilibrium reaction conditions yield more realistic results than nonequilibrium ones [76]. Given the diffusion nature of surface reactions, heterogeneous combustion products may be present at any point in the core at some distance from the coke-coal massif. These products will interact with the oxidizer distributed within the core, forming equilibrium combustion products in accordance with the thermochemical conditions existing at a given point.

At temperatures above 2000 K, gasification reactions with carbon dioxide and steam begin. In this region, the combustion zone removed from the surface of the mass, and oxygen gasification reactions virtually cease due to the lack of oxygen at the surface. At the pressures encountered in diesel engines, the role of CO_2 and H_2O gasification will increase significantly, as

temperatures rise above 2000 K, resulting in an increased rate of fuel consumption.

7.7.1. Burnout of a single coke-coal massif in the working space of a piston engine. To gain a more general understanding of the solid fuel burnout process in the working cylinder of a piston engine, let us consider this process using a single coke coal massif as an example.

The main parameter of the coke-coal massif burnout process in the working cylinder of a piston engine is its mass loss. Considering that the role of the steam gasification reaction increases at temperatures above 2000 K, we will limit the entire burnout process to only two surface reactions according to equations (7.5) and (7.6). Furthermore, to consider the burnout process, we will make the following assumptions:

- the mass temperature is constant throughout the entire volume (i.e., there are no internal temperature gradients in the mass);

- we will assume that the coke coal massif has a regular spherical shape and maintains this shape throughout the burnout process;

- all reactions occur on the mass surface (there is no intrapore reaction);

- the mass properties remain constant during burnout.

As experimental data show, despite a significant simplification in the consideration of processes, such an analysis allows for adequate determination of the influence of various factors acting in the cylinder on fuel carbon burnout and on the engine thermodynamic cycle parameters [34, 36, 62].

Given the small size of the masses, it can assume that they all suspended during combustion and move with the flow of the working gas contained in the cylinder. Thus, the relative velocity between the gas and the coke-coal masses is zero. Heat released on the mass surface transferred to the gas solely by thermal conductivity, and surface reactions occur in the diffusion region. During carbon burnout in the working gas, the CO_2 concentration increases and the oxygen concentration decreases.

A schematic of the coke-coal massif burnout model shown in Fig. 7.12.

The combustion velocity of a coal particle is determined as the sum of the velocities for equations 7.5 and 7.6. In the immediate vicinity of the coal massif surface, no reactions occur in the gas phase, and the resulting carbon monoxide dissipates far from the massif surface, where its final oxidation occurs in the gas phase, according to the equation:

$$CO + ½O_2 \rightarrow CO_2. \quad (7.8)$$

The rate of reaction (7.8) limited by the rate of carbon monoxide formation and therefore depends on the rate of reactions on the surface of the

coke-coal massif. Thus, the rate of mass burnout determined solely by the rate of surface reactions.

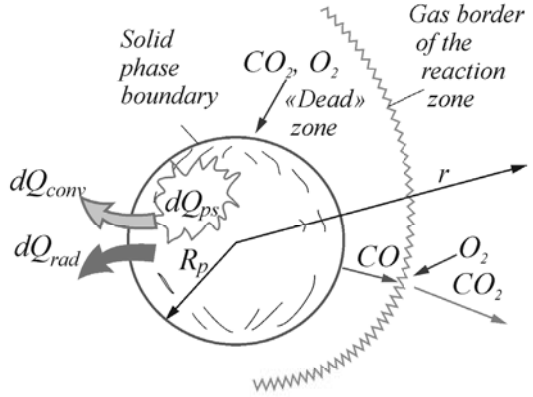

Fig. 7.12. Scheme of coke-coal massif burnout

The reaction rates for equations (7.5) and (7.6) must simultaneously satisfy the mass conservation equation for a steady-state radial oxygen flow, motionless relative to the particle mass, a carbon dioxide flow to the particle surface, and surface chemical kinetics. Considering this, under conditions of mass conservation, the reaction rates for equations (7.5) and (7.6) are determined:

$$\dot{W}_{O_2} = \frac{\rho_g D}{R_p} \ln\left(\frac{1 + f_{O_2} Y_{O_{2\infty}}}{1 + f_{O_2} Y_{O_{2R}}}\right), \tag{7.9}$$

and

$$\dot{W}_{CO_2} = \frac{\rho_g D}{R_p} \ln\left(\frac{1 + f_{CO_2} Y_{CO_{2\infty}}}{1 + f_{CO_2} Y_{CO_{2R}}}\right). \tag{7.10}$$

where $\rho_г$ – is the gas density; D – the molecular diffusion coefficient; R_p – the particle radius; f – the mass ratio of fuel to oxidizer; Y – the mass of the gas.

Rewriting these equations in Arrhenius form yields:

$$\dot{W}_{O_2} = A_{O_2} Y_{O_{2R}} p_g \exp(-E_{O_2} / R_u T_p), \tag{7.11}$$

$$\dot{W}_{CO_2} = A_{CO_2} Y_{CO_{2R}} p_g \exp(-E_{CO_2} / R_u T_p), \tag{7.12}$$

where A_{O_2}, A_{CO_2}, E_{O_2}, E_{CO_2} are reaction constants, the values of which are included in Table 7.2.

By iterating the value $Y_{O_{2R}}$ through substitution in equations 7.9 and 7.11, a single value of $\dot{W}_{O_2}$ can obtained.

Table 7.2.

Parameters and constants of combustion reactions

Subscript	Reaction	Localization	f_i	$A_i\left(\frac{kg}{m^2 \times kPa \times s}\right)$	E_i/R_u	$Q_{V_i}\left(\frac{MJ}{kg}\right)$
O_2	C+ ½O_2→CO	Surface of a coke-coal particle	0,75	882,30	18000	9,28
CO_2	C+ CO_2→2CO	Surface of a coke-coal particle	0,273	25,00	21050	-14,24
—	CO+ ½O_2→CO_2	Gas phase boundary	—	*	*	10,07

* There is no need to estimate; the reaction rate is assumed to be equal to infinity.

The value of $\dot{W}_{CO_2}$ can be obtained in the same way (by substituting $Y_{CO_{2R}}$ in equations 7.10 and 7.12).

Using this procedure, the corresponding reaction rates can obtained regardless of whether chemical or diffusion factors are predominant in the combustion process. Knowing the reaction rates of $\dot{W}_{O_2}$ and $\dot{W}_{CO_2}$, we determine the rate of carbon monoxide formation:

$$\dot{W}_{CO} = 2{,}33\dot{W}_{O_2} + 4{,}66\dot{W}_{CO_2}. \tag{7.13}$$

Теплота, выделившаяся в ходе сгорания, частично получена за счет поверхностных реакций, частично – в ходе реакции газовой фазы:

$$Q_{comb} = A_p(\dot{W}_{O_2} Q_{V_{O_2}} + \dot{W}_{CO_2} Q_{V_{CO_2}} + \dot{W}_{CO} Q_{V_{CO}}), \tag{7.14}$$

where A_p – the surface area of the coke-coal massif, Q_V – the heat of reaction (Table 7.2).

Knowing the burnout rate of a coal particle, one can determine the instantaneous rate of oxygen and carbon dioxide consumption in the control volume adjacent to the coal particle, as well as its temperature and instantaneous radius. The mass concentration of free oxygen and carbon dioxide changes over time, according to:

$$\dot{Y}_{O_{2\infty}} = \frac{A_p}{0{,}375 m_g}(\dot{W}_{O_2} + \dot{W}_{CO_2}), \tag{7.15}$$

$$\dot{Y}_{CO_{2\infty}} = \frac{A_p}{0{,}273 m_g}(\dot{W}_{O_2} + \dot{W}_{CO_2}), \tag{7.16}$$

where the constants for the ratio of the masses of oxygen and carbon dioxide used are divided by the mass of reacted carbon.

The reduction in the radius of a coke particle is determined by:

$$\dot{R}_p = (\dot{W}_{O_2} + \dot{W}_{CO_2})/\rho_p, \tag{7.17}$$

where ρ_p – the density of the coke-coal particle.

To determine the magnitude of the change in the mass temperature, we write the energy balance equation for the control volume, as shown in Fig. 7.2. To do this, we determine the heat supplied to the control volume during surface reactions, obtaining it from the equation:

$$\dot{Q}_{ps} = A_p(\dot{W}_{O_2} Q_{V_{O_2}} + \dot{W}_{CO_2} Q_{V_{CO_2}}). \tag{7.18}$$

Burning particles lose their energy through heat transfer to the gas and by radiation to the surfaces enclosing the working volume. Fuel particles entering the cylinder for a very short period are cooler than the gas inside the cylinder and its walls. During this period, the particles gain energy through heat transfer. The heat exchange between the particle and the gas can be determined from the equation:

$$\dot{Q}_{heat} = \frac{Nuk_g}{2R_p} A_p(T_p^4 - T_g^4). \tag{7.19}$$

Based on the assumption that the relative velocity between the gas and the particles is zero, the Nusselt number (Nu) can taken to be 2. The magnitude of the radiative heat exchange between the particle and the walls of the confining volume is found from the equation:

$$\dot{Q}_{rad} = \varepsilon\sigma A_p(T_p - T_w), \tag{7.20}$$

where T_w – the temperature of the combustion chamber wall; ε – the emissivity coefficient, which can be taken as constant – equal to 0.8; σ – the Stefan-Boltzmann constant.

Changes in internal energy in the control volume:

$$\dot{U}_{cv} = \dot{Q}_{ps} - \dot{Q}_{heat} - \dot{Q}_{rad}. \tag{7.21}$$

Knowing the heat capacity of a coal particle, we find the instantaneous temperature value:

$$\dot{T}_p = \frac{1}{m_p c}(\dot{Q}_{ps} - \dot{Q}_{heat} - \dot{Q}_{rad}). \tag{7.22}$$

Integrating equation 7.22 over time allows one to determine the temperature of the coal particle as a function of the crankshaft rotation angle based on the adopted geometry of the working cylinder.

When considering the combustion of coke-coal from the perspective of diffusion processes occurring in the immediate vicinity of the fuel particle

surface, it should noted that most of the combustion process is influenced by diffusion. It is diffusion, rather than the intrinsic rate of surface reactions, that limits the rate of combustion of fuel particles in the engine's working space.

The equivalent heat expended in the work performed by the piston can estimated from the expression:

$$\dot{W} = p_g(dV/dt) \tag{7.23}$$

where p_g – the current pressure in the engine cylinder; and dV/dt – the change in cylinder volume.

The convective component of heat transfer for the given temperature level remained insignificant during the given time.

$$Q_{conv} = hA_w(T_g - T_w) \tag{7.24}$$

where A_w – the area of the combustion chamber walls; h – the heat transfer coefficient.

7.8. The combined effect of various factors on the combustion process of coal-water fuel in the engine working space.

Fig. 7.13 shows calculated data for changes in key parameters during combustion of the first and last coal-water fuel packets introduced into the engine combustion chamber.

All values presented as a function of the crankshaft angle at an injection timing setting that ensures optimal engine performance. The data presented correspond to packets entering the cylinder at the initial and final injection stages and assigned an average number according to the classification scheme. The presented curves characterize the change in temperature of the entire packet and individual particles, as well as the diameters of aerosol droplets and solid fuel particles. In addition, graphs presented for the change in the oxygen surface reaction coefficient (G_1), the carbon dioxide surface reaction coefficient (G_2), and the volatile matter removal coefficient (G_4).

All packages behave similarly, but have their own individual characteristics determined by the crankshaft rotation angle during injection and their position according to the classification scheme. The change in gas pressure and temperature in the cylinder, determined by the total thermal effect of the combustion of all fuel packets injected into the working cylinder.

After injection, the liquid carrier (water) begins to evaporate almost immediately due to the high temperature of the gas in the cylinder. Liquid evaporation leads to a decrease in the local temperature of the combustion chamber, but this process is short-lived. Volatiles released from the coal particles. When they begin to burn (upon reaching the appropriate local

equivalence ratios), the temperatures of both the gas and the combustion chamber particles increase. As local gas temperatures continue to increase, the particle temperature rises to a level that causes intense release of volatiles and the combustion of the coke-coal massif begins.

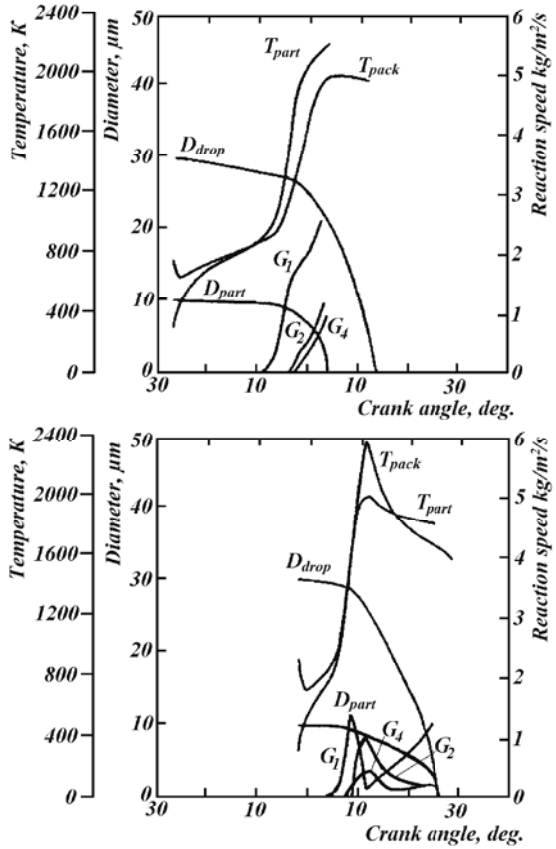

Fig. 7.13. Calculated data on the change in the temperature of the packet (T_{pack}); particles (T_{part}); aerosol droplet diameters (D_{drop}); solid fuel particles (D_{part}); oxygen surface reaction coefficient (G_1); carbon dioxide (G_2); volatile matter removal coefficient (G_4) during the combustion of the first and last packets of coal-water fuel introduced into the engine combustion chamber (D/S = 229/267 mm, n = 1050 min^{-1}, ε = 11.5)

The initial rapid increase in temperature of the coke-coal mass and its decrease in radius occur immediately after evaporation of the liquid carrier. The combustion rate at this stage is approximately 2...3 kg/m^2/s. The process

of particle heating continues for approximately 2...3° of crank angle. At the end of the forced ignition phases, all parameters of the gas thermal state determined solely by the burnout of the coal particles.

Fig. 7.13 illustrates that for the first packet, coke-coal particle size is unaffected by the evaporation stage. A continuous decline in diameter only occurs following the onset of the temperature rise, spanning duration of 13°.

Unlike the burnout of the first packet, which occurs within 43° after it introduced into the cylinder, ignition of the coal particles in the last packet occurs in a gas heated to a high temperature due to the combustion energy of the preceding packets. Therefore, during the initial combustion stage, the temperature of the particles in the last packet increases much more rapidly than in the first. Despite this, the combustion of the last packet turns out to be less efficient, since it occurs in conditions of an already cooling working fluid with limited oxygen content.

7.9. The influence of rotational speed on the efficiency of the engine working process.

Rotation speed is a key parameter affecting the efficiency of coal fuel combustion. On the one hand, the time allocated to the combustion process in the engine depends on the rotation speed. On the other hand, the thermal efficiency of the engine largely depends on the relative heat transfer to the combustion chamber walls to the total amount of heat released during fuel combustion. By optimizing the start of fuel injection, maximum thermal efficiency can achieved for each engine speed. However, for speeds above 1500 min-1, thermal efficiency steadily decreases, which is primarily due to the limited combustion rate. Fig. 7.14 presents calculated data on the effect of rotation speed on the combustion efficiency of high-calorific coal fuel in the cylinder of an engine with pilot ignition [68].

Calculations show that if the exhaust valve opens 150° after TDC, at a rotation speed of 1500 min^{-1}, all particles entering the cylinder have time to burn before the exhaust valve opens.

At a speed of 3000 min^{-1}, 7% of the fuel particle mass fails to burn and expelled with the exhaust gases. As a result, the calculated indicated engine efficiency decreases by 14%. However, the decrease in thermal efficiency less pronounced, as relative heat losses decrease from 22 to 16% with increasing speed. At speeds below 1500 min^{-1}, thermal efficiency remains essentially constant, as a balance established between heat generation and heat losses in the working cylinder's baffle surfaces. Radiative transfer is approximately 2% across the entire speed range, and its share of the overall heat loss balance is between 8 and 11%.

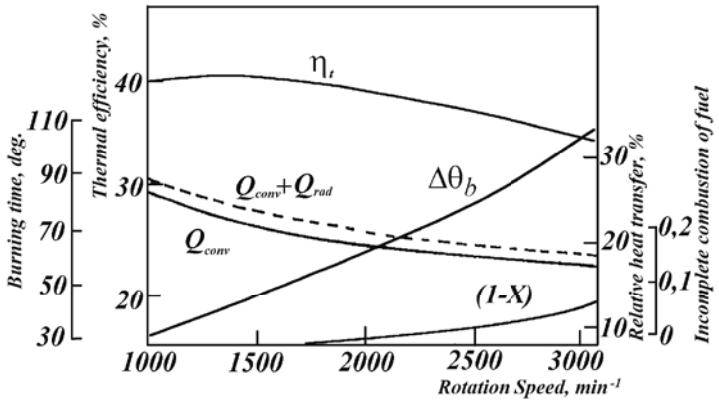

Fig. 7.14. Calculated dependence of combustion duration ($\Delta\theta_b$); thermal efficiency (η_t); total heat losses (Q_{conv} + Q_{rad}) and the coefficient of incomplete combustion (1-X) on the engine speed (D/S=82/80 mm, ε=18)

Chapter 8.

Wear and mitigation methods for solid fuel-based piston engines

8.1. Wear mechanisms operating in solid fuel-based ICEs.

The most important issue that needs to address for the practical use of coal-fired engines is increased wear. Wear rapidly reduces the mechanical and thermal efficiency of the engine, necessitating maintenance that is more frequent, repairs, and adjustments.

The increased wear is caused by abrasive particles, both within the natural fuel and formed during its combustion, as well as coke particles deposited on the internal surfaces of the engine's working space as a result of incomplete combustion.

Table 8.1 shows the typical composition of the mineral portion of the original fuel used in CS production. It contains large amounts of metals, including iron and calcium, which are bound to softer minerals. X-ray analysis of the ash reveals the presence of quartz, kaolinite, calcium, dolomite, anhydrite, and other minerals. Quartz, the hardest of these minerals, is present in small quantities, while softer clays form the bulk of the mineral matter.

Table 8.1.

Mineral composition of the ash from the original coal used by Otisca for the production of WCS.

Compounds	Content
SiO_2	22,4%
Al_2O_3	29,15%
TiO	1,80%
Fe_2O_3	28,54%
CaO	9,86%
MgO	3,00%
K_2O	0,17%
Na_2O	0,54%
SO_3	0,62%
P_2O_5	0,33%
SrO	1,09%
BaO	0,67%
MnO	0,04%

The second source of wear is combustion products. Particles collected from the engine exhaust tract, shown in Fig. 8.1. Four types of combustion products observed: molten ash, unburned coke, metal vapors, and soot. The

last two components have particle sizes of 5…50 μm and are most likely formed by vapor condensation during the expansion of the working gas.

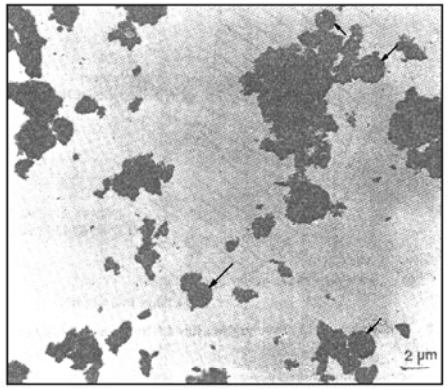

Fig. 8.1. High magnification photograph of particles in the exhaust of a diesel engine running on WCS

Ash particles, in the form of glass spheroids (shown by arrows in the image), were initially fused in the flame and then solidified. Their rounded, glassy nature obviously reduces their contribution to wear compared to their angular crystalline precursors. They average 1.1 μm in diameter. Each spheroid has a unique composition due to its local mineral content, formed in the air charge during combustion.

Even if it were possible to efficiently separate mineral impurities from the combustible components of the fuel, this would not solve the wear problem. Increased wear caused not only by the relatively hard mineral impurity particles contained in the ash, but also by the relatively fragile coke particles. When trapped between rubbing surfaces, they disrupt the lubrication system by absorbing oil from the working surfaces and increasing mechanical losses. Even with combustion efficiency of at least 99%, coke-coal matter actually constitutes the overwhelming majority of solid combustion products. Experiments have shown that, due to their high porosity and hollow shell, coke particles form a large abrasive surface in the friction zone of the ring and liner.

In addition to abrasive wear during combustion of natural solid fuels, engine wear can cause by chemical corrosion resulting from the formation of various organic and mineral acids.

The presence of abrasive and chemically active materials leads to wear and corrosion of both moving and stationary engine parts, but the degree of impact of various factors on individual engine components varies. The

impact of chemical corrosion on individual engine components is currently difficult to determine, as all known tests have been relatively short-term. Data from German companies that have conducted long-term tests of solid fuel engines is either unreliable or unavailable. Known research studies have not noted any significant impact of chemical corrosion on engine components; however, this does not mean that such a problem cannot arise during long-term operation of this type of engine. Issues of abrasive wear have more thoroughly studied. The results of these studies suggest that the unresolved problem of abrasive wear is the main obstacle to the introduction of solid-fuel engines into practical operation [49]. Clearly, for the successful use of coal-fueled engines, special measures must take to protect their components from excessive abrasive wear.

All wear control methods can roughly divided into three groups:

- measures aimed at limiting contact between engine parts and abrasive particles, including reducing mineral impurities in the feedstock fuel;
- design changes aimed at reducing the impact of increased wear on engine operation;
- measures to select appropriate, more wear-resistant materials (including non-metallic ones).

In most cases, all of these measures used in combination to reduce the harmful effects of abrasive wear.

Therefore, it is possible to increase the service life of a coal-fuel engine simultaneously in two ways: by improving the quality of the fuel used and by improving the engine design. The first approach leads to an increase in the cost of the fuel, while the second leads to an increase in the cost of the engine itself, which, in turn, reduces the profits from burning cheaper fuel. Fig. 8.2 shows both components as functions of fuel quality. These components of the service life of a coal-fuel engine will properly optimize at the minimum point.

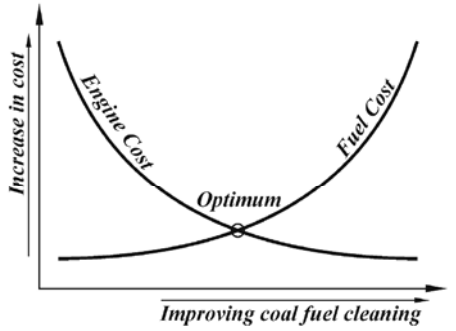

Fig. 8.2. The relationship between the level of fuel purification and the cost of its use

8.2. Wear of injection system elements.

Fuel system components fuel pumps, valve seals, and injector needles are subject to significant wear due to direct contact with carbon particles. This leads to changes in fuel injection parameters, pressure loss, and valve leaks, which, in turn, reduces overall engine efficiency. To reduce the harmful effects of carbon fuel on fuel system components, a number of design solutions exist to limit the impact of carbon particles on key fuel system components. Some of the available design solutions discussed in Chapter 4. These developments allow the fuel injection process to organize in such a way that the only fuel system component operating under high WCS pressure is the injector nozzle. In such designs, nozzle wear determines the reliability of the fuel injection system. The high impact of abrasive particles on the nozzle components leads to an increase in WCS flow through the nozzle openings during engine operation, resulting in a change in the injection pressure characteristic. This leads to deterioration in the operating parameters of the fuel process. This clearly demonstrated by the results of a study conducted on the 7FDL engine, in the initial testing stage of which nozzle bodies made of ordinary steel were used [52]. The maximum pressure in the fuel injection system with a new injector nozzle was approximately 52 MPa. The nozzle tip had 16 holes with a diameter of 0.5 mm. Due to wear of the nozzle holes during the tests, the injection pressure dropped to 47 MPa, resulting in a deterioration in engine performance. Table 8.2 shows the results of a comparison of the operating process parameters with a new and worn nozzle. Fig. 8.3 shows the pattern of changes in cylinder pressure, injection pressure, and thermal stress for the cases under consideration.

Table 8.2.

The influence of injection pressure on the working process of the 7 FDL engine

Maximum injection pressure, MPa	Burnout rate, %	Specific heat consumption, kJ/(kWh)	P_{max}, *MPa*
52,2	88,8	9114	17,2
46,9	81,1	10432	14,7

The heat stress graph shows that the WCS combustion phase slows as pressure decreases due to nozzle wear. This occurs because the injected fuel droplets are larger, reducing the reaction surface area and increasing the time required for complete combustion.

Therefore, in modified injection systems, nozzle erosion is a critical factor limiting the maximum continuous engine operating time with WCS. Nozzle elements must withstand high pressures and flow rates to produce fine droplets that can ignite and burn within the engine's time allocated for

this process. This is one of the most highly loaded and shortest sections of a diesel engine's operating cycle.

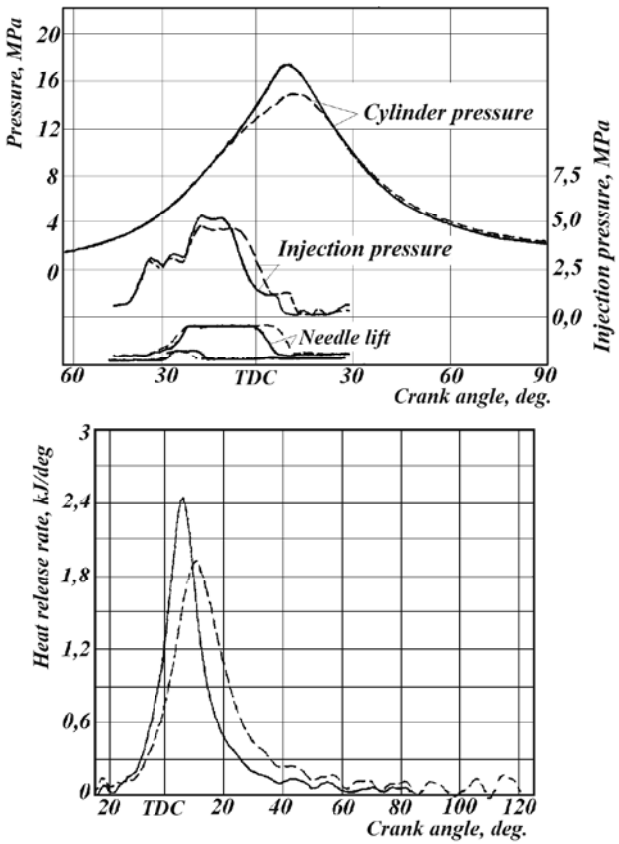

Fig. 8.3. Changing the parameters of the working process depending on the injection pressure WCS.—— injection pressure 52 MPa; – – – injection pressure 47 MPa

The operating pressure in the nozzle ranges between 70 and 140 MPa. To achieve better fuel spraying, a WCS engine will operate at the upper end of this range. Direct injection diesel engines use nozzles with multiple holes. The velocity of the fluid through these holes in WCS engines reaches 250 m/s, while in engines running on petroleum fuels it does not exceed 200 m/s. When using steels typically used for standard sprayers, significant wear of the flow path of the sprayer holes and the valve seat observed after just two hours of engine operation on WCS. The wear mechanism is a

combination of cavitation and erosion under the action of solid particles. Fig. 8.4 shows a micrograph of a section of the sprayer of a JS-1 engine that operated for 40 min on WCS with ash content in the original fuel of 0.6%, as well as a micrograph of the surface of the flow path of the hole, obtained at high magnification using a scanning electron microscope [44].

For WCS with an ash content of less than 1%, the wear of the holes is non-uniform both in size and in the mechanism. Fig. 8.5 shows a longitudinal section of a nozzle made of hardened carbon steel with 12 holes of 0.55 mm in diameter after 4.5 hours of operation on WCS with an ash content of 0.9% [49]. As can be seen from Figs. 8.4 and 8.5, the hole outlet wears more than the inlet. Cavitation damage, resulting from an abrupt decrease in fluid pressure, explains the funneling effect observed at the hole outlets. Wear initially spreads along the diameter and then along the hole towards its inlet end. The front of material carryover is clearly visible in the micrograph (Fig. 8.4*b*). In the mid-section of the channel, the surface morphology consists of prominent relief features created by the depletion of material between martensite arrays, coupled with the partial etching of the martensitic structures themselves. Here, no erosion grooves observed, as is the case at the entrance. Here, particle impacts create scratches, resulting in the sharp edge at the hole entrance rounded off. This is clearly visible in the electron micrograph (Fig. 8.6).

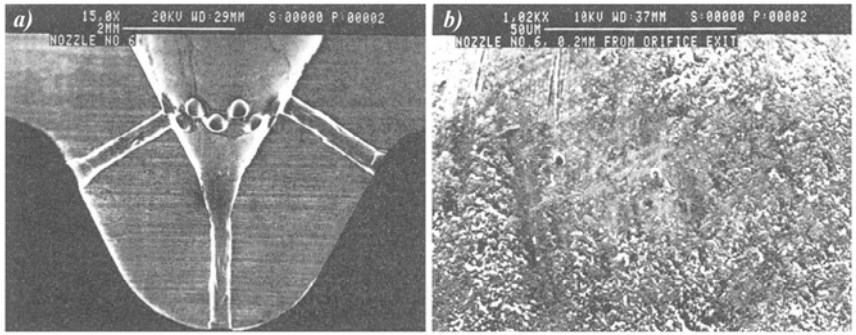

Fig. 8.4. *a* – section of a nozzle with several holes (carburized nitrided steel grade 8620) after 40 minutes of operation on low-ash WCS (dry coal ash content 0.6%); *b* – surface of the spray nozzle hole after operation on low-ash WCS (at high magnification)

An increase in the ash content of the original fuel leads not only to an increase in wear, but also to a change in the nature of its formation. Fig. 8.7 shows a micrograph of a section of the tip of the sprayer after 40 minutes of operation on fuel with an ash content of 3.8%, as well as a micrograph of the surface of the flow channel [44].

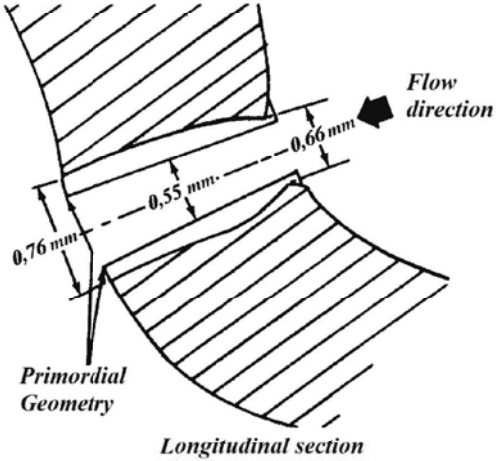

Fig. 8.5. Cross-section of a steel nozzle tip after 4.5 hours of operation on WCS with an ash content of the original fuel of 0.9% (maximum load)

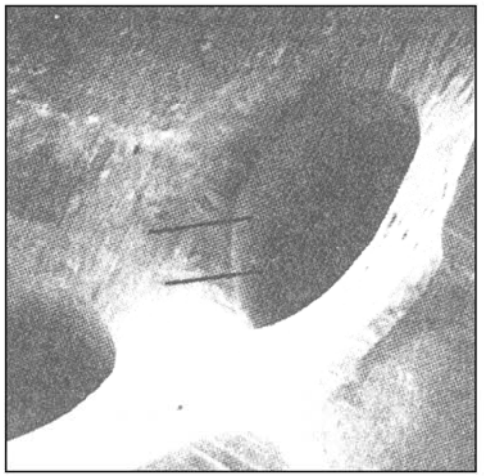

Fig. 8.6. Micrograph of the fuel tip bore entrance shown in Fig. 8.5. The bore edge rounded, with clearly visible scratches. The change in appearance after entry indicates a change in the wear mechanism

Here, a gradual increase in the hole diameter observed from the inlet to the outlet. In this instance, material loss driven by ash-induced erosion, as evidenced by the high-magnification micrograph of the outlet showed in Fig. 8.3 *b*.

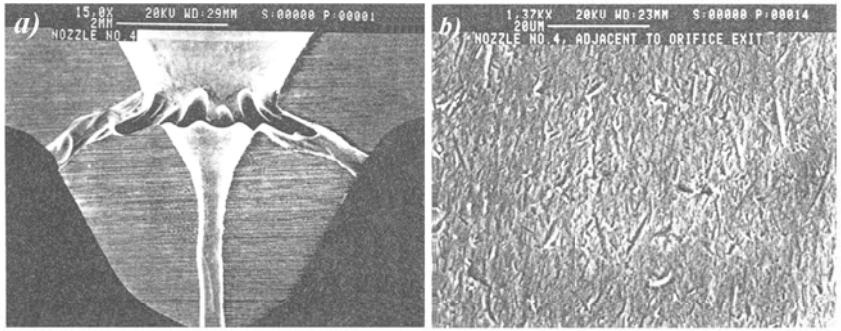

Fig. 8.7. *a* – section of a sprayer with several holes (carburized nitrided steel grade 8620) after 40 minutes of operation on high-ash WCS (ash content of dry coal 3.8%); *b* – surface of the sprayer hole after operation on high-ash WCS (at high magnification)

Most studies using standard injector nozzles made from common materials conducted with fuels with an ash content of no more than 1%. Typically, within the first hour of operation, the outlet orifice size increased by 50% compared to the initial value. Therefore, to increase service life to a practically acceptable level, it is necessary to use highly resistant materials or fundamentally new injector designs capable of operating under conditions of increased wear.

Fuel ash content is the primary, but not the only, factor determining injector nozzle service life. As demonstrated by the results of testing the Sulzer 1RSA76 engine, at elevated fuel injection pressures, the size of the carbon particles significantly influences injector nozzle wear [65]. It found that, under the studied conditions, the decisive factor in the erosive destruction of the material (as opposed to its abrasive wear) was the impact force, not the particle hardness. To increase the service life of the injector during the studies, its tip was made of sintered tungsten carbide and cobalt (94% WC 6% Co). However, even using this material allowed the engine to operate continuously for only 5…10 hours. Injectors failed due to fatigue failure of the injector or enlargement of the injection orifice cross-section (although this damage did not lead to catastrophic failure, as occurred with steel injectors).

The selection of injector tip materials was a major focus for all researchers involved in the development of solid-fuel diesel engines. Typically, injector materials pre-tested in a WCS flow pumped through small orifices. The wear criterion used in these tests was the change in the effective orifice cross-sectional area, determined as a function of the flow coefficient and the geometric cross-sectional area. Such wear assessments are traditional

when selecting injector material for diesel engines running on petroleum products. Fig. 8.8 presents the results of a test performed in a steady-state WCS flow supplied at a pressure of 28 MPa [49]. The change in the flow area was determined every 5 minutes by passing water through the orifice under a pressure of 0.7 MPa. Although this experiment did not reflect the expected service life of the sprayer in the engine, it nevertheless provided an opportunity to compare the wear dynamics of various materials in the erosive flow.

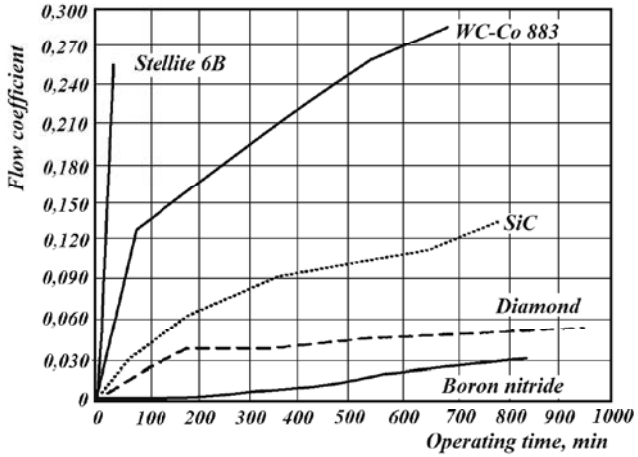

Fig. 8.8. Results of hole wear study

It should note that the change in flow area not linearly related to the volumetric loss of material in the sprayer channel. This is the result of a rapid increase in the flow coefficient as the sharp edges of the orifice become rounded. The material that wore most rapidly, Stellite 6B, had a completely rounded entrance, and its diameter varied from 0.46 to 0.61 mm over the course of 40 minutes of testing. Synthetic diamond and cubic boron nitride demonstrated high resistance to erosive wear. Synthetic diamond used as a finished product, typically used in wire drawing dies. It showed very little wear after an initial short period of time during which the diamond grains were ground by the flow. The wear mechanism of cubic boron nitride differed somewhat from that of diamond. The sharp edge of the orifice wore evenly but extremely slowly. Apparently, after the initial intense wear associated with high flow acceleration around the sharp edge of the orifice ceased, the abrasion rate of the cubic boron nitride specimen decreased significantly. The sharp edge of the orifice in the sintered silicon carbide

specimen wore at a rate significantly higher than that of the boron nitride specimen. However, like cubic boron nitride, no noticeable change in orifice diameter observed. Sintered tungsten carbide with 6% cobalt, despite being an order of magnitude more resistant to erosion than Stellite 6B, still wore too quickly. Therefore, the most suitable materials for use in the manufacture of nozzles for CS engines are cubic boron nitride and synthetic diamond. Both of these materials are quite brittle, so they can only used as inserts in the nozzle channel.

An example of the successful use of new materials to increase the service life of an injector is a design developed by General Electric [48]. To prevent wear on the body, standard diamond gauges used in wire drawing installed at the outlet ends of the holes. The drawing gauge is a standard product consisting of a diamond insert placed in a tungsten carbide cylinder. A cross-section of the injector body with inserts shown Fig. 8.9. The injector body was made of stainless steel, and the inserts secured in it by soldering. To increase the wear resistance of the needle valve seat, it made in the form of a tungsten carbide insert, which pressed into the steel body. To provide sufficient clearance between the diamond inserts, the hole count reduced relative to a baseline injector, resulting in a configuration of 10 holes with a diameter of 0.4 mm. Two injectors of this design worked for 40 hours on a 7DFL engine, after which the injectors dismantled and tested on a test bench. Tests showed that the injector's performance remained virtually unchanged. Disassembly revealed that the diamond inserts had not undergone any changes, and the steel sections of the channels showed minor wear.

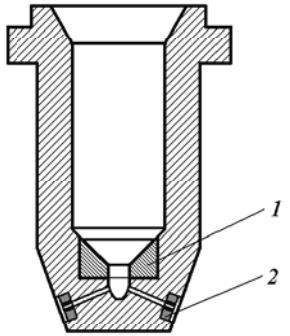

Fig. 8.9. Spray nozzle body with diamond inserts. 1 – tungsten carbide valve seat; 2 – diamond insert

To assess the service life of injectors with diamond inserts, accelerated testing conducted on a separate element simulating the flow path of the channel. Fig. 8.10 shows a schematic of the control sample. The test conducted on a WCS circulating flow system at ambient temperature and a pressure of 41.5 MPa. The suspension pumped continuously through the sample orifice, which made it possible to speed up the testing process (on a real engine, the injection process takes only 1/20th of the working cycle).

The experiment lasted for a period equivalent to 600 hours of engine operation. During this time, the nozzle flow rate increased by only 0.25%

(Fig. 8.11). Further testing, conducted on a 12-cylinder engine, used only nozzles with diamond inserts. In total, including laboratory and road tests, the engine with these nozzles operated for approximately 1,000 hours. No serious nozzle failures recorded.

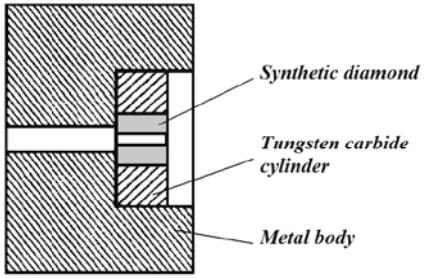

Fig. 8.10. An element simulating the flow part of a channel used for accelerated testing of the service life of a sprayer with diamond inserts

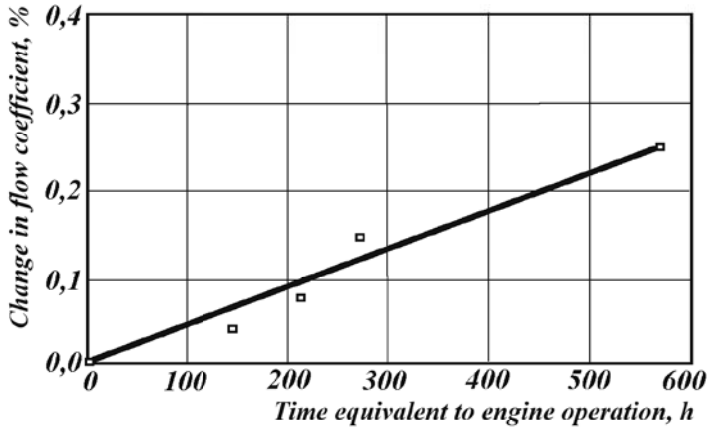

Fig. 8.11. Changing the flow coefficient for a single-hole diamond insert

An example of a design solution aimed at reducing the impact of wear on the performance of the sprayer is the design proposed by Cooper-Bessemer (Chapter 4, Fig. 4.3).

The use of a poppet valve allows, on the one hand, increasing the contact area of the sealing surfaces, and on the other, to compensate for the increase in clearance as wear occurs by raising the valve. Another advantage of a variable-cross-section sprayer is the ease of applying a coating to surfaces subject to wear.

Testing of an engine equipped with a poppet valve sprayer yielded results similar to those for an sprayer with multiple holes [44]. Fig. 8.12 shows a micrograph of the wear of a poppet valve seat after approximately one hour of operation on a WCS with an initial fuel ash content of 0.6%. The valve shown in the photograph coated with a thin layer of titanium nitride, traces of which are visible in some areas of the valve seat. It remains unclear whether the seat coating damaged by cavitation and erosion from solid particles or by impact loading during repeated opening and closing of the valve. Comparable wear can expected with this type of nozzle, as the hydrodynamic flow conditions pressure drop and velocity in this design are very similar to those observed in a multi-orifice nozzle. However, automatic adjustment of the flow area can extend the service life of the nozzle.

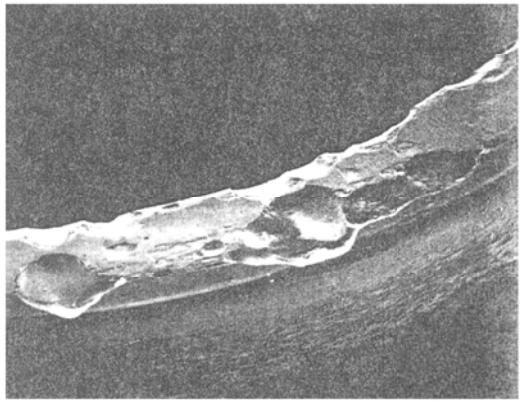

Fig. 8.12. Micrograph of a plate valve seat after one hour of operation on a WCS with an ash content of the original fuel of 0.6%

8.3. Wear of engine components.

The impact of abrasive particles on engine parts can divide into direct and secondary. Parts that come into direct contact with solid fuel combustion products directly exposed to abrasive particles. These include cylinder liners, piston rings, piston skirts, valve seats, valve plates, valve guides, and turbocharger blades. Protecting these parts from increased wear is both the most important and the most challenging task.

Elevated concentrations of soot and metallic wear debris in the lubricant compromise filtration efficiency, eventually resulting in total filter occlusion. In addition to large particles, the oil also accumulates particles so small that they not captured by the filter elements. These particles have a secondary abrasive effect; they constantly circulate with the oil flow and lead to

increased wear on engine components lubricated under pressure. Furthermore, the presence of these particles increases friction in engine mechanisms, resulting in a decrease in mechanical efficiency. Fig. 8.13 shows a micrograph of a deposit sample collected from a 7DFL engine lubricating oil centrifuge. Note the presence of coke-coal fragments and ash spheres in concentrations comparable to those found in exhaust. Both forms of the macroparticles, coke-coal and ash, serve as evidence of wear; the edges of the coke-coal fragments rounded, while the ash spheres are somewhat deformed.

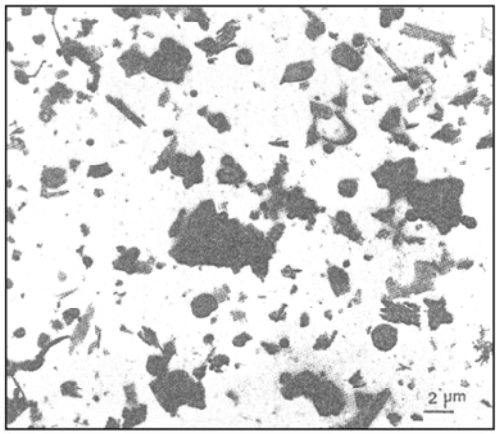

Fig. 8.13. High magnification photograph of particles present in the lubricating oil of a diesel engine running on WCS

To prevent mineral and coke particles from entering the lubricating oil, the most effective method is to isolate the sub-piston space from the engine crankcase. This type of isolation most easily achieved in crosshead engines; however, their design is more complex and their applicability is limited. Another method for reducing abrasive wear is to reduce the time the friction surfaces are in contact with abrasive particles. Special systems used to remove abrasive particles from friction surfaces. In the early stages of research (most of which was conducted in Germany on the eve of World War II), compressed air blasts or flushing with liquid petroleum products were used to clean surfaces, cylinders, piston rings, and valve seats. Adjusting piston ring offset used to reduce the impact of wear on engine performance. The effectiveness of these wear control methods is unknown, as no reliable data on this type of research exists.

It can assumed that even with highly effective fuel purification and high burnout rates, microparticles of ash and carbon will always be present in both

the combustion products and the lubricating oil. Abrasive wear caused by their presence must minimize. This can achieve by selecting special wear-resistant materials, including non-metallic ones. Furthermore, individual components can subject to special heat treatment and coated to enhance their wear resistance.

Of all engine components directly exposed to abrasive particles, compression rings operate under the harshest conditions. Using materials common to standard diesel engines, the service life of a piston ring set estimated at 5 to 30 hours. The piston ring and cylinder liner form the primary tribological pair in the engine. This friction pair between the stationary and moving engine parts accounts for the majority of friction losses. It must also seal the working space during compression and combustion and retain lubricants in the crankcase. The worst wear conditions occur when the piston passes TDC. This is the hottest part of the liner and the farthest from the lubricants. Gas pressure at this point reaches its maximum, and ring velocity crosses zero as the piston reverses direction. The combination of these factors leads to significant wear of the liner near the stop of the top piston ring. The most significant ring wear also occurs during this part of the cycle.

Fig. 8.14 shows the dependence of the increase in the clearance of the upper compression ring of the JS-1 engine on the time of operation on a WCS [44]. These data correspond to a ring made of malleable cast iron with a hardness of 400 kg/mm^2 and a chrome-plated cylinder liner. The wear rate was not constant, since the engine tested for 25 hours under various conditions, including during break-in.

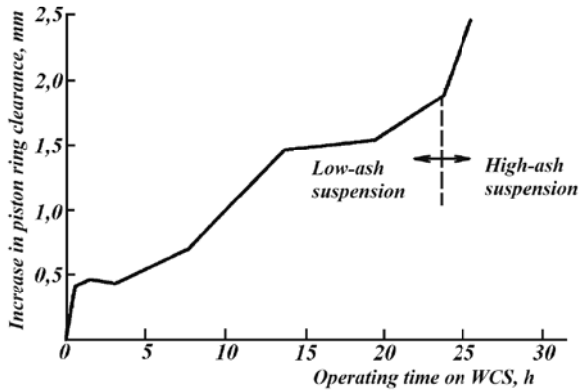

Fig. 8.14. Dependence of wear of the upper compression ring on time (ring made of malleable cast iron, sleeve with chrome coating)

One of the main differences in operating conditions during individual test phases was the ash content of the original fuel. The abrasive effect of ash particles increased both with higher-ash original fuel and with increasing carbon burnout. The mechanism of direct abrasive particle action is roughly as follows: burnt-out carbon particles settle on the oil film that coats the cylinder walls, causing wear on the piston ring set as they move. The crucial role of ash residue on wear is confirmed by the fact that during the final hour of operation of the JS-1 engine, WCS with an ash content of 3.8% was used (as opposed to the previously used original fuel with an ash content of 0.4…0.6%). The figure shows that the slope of the curve describing the change in ring gap over time increased sharply during this period.

The resulting change in final gap after 24 hours of operation for four compression rings shown Table 8.3. No data obtained for the oil scraper rings, and no noticeable wear observed for the chrome-plated sleeve.

Table 8.3.

Wear rate of compression rings of the JS-1 engine after 24 hours of operation on coal fuel with an ash content of 0.4...0.6%

Ring	Change in clearance,* mm	Wear rate, mm/h
1 (top)	1,88	0,078
2	0,36	0,015
3	0,48	0,020
4	0,30	0,012

* Change in piston ring clearance in 1 hour.

Table 8.4 presents the wear rates of standard liner-piston mating components for four types of suspensions tested in the Sulzer 1RSA76 low-speed engine [65]. In the standard design, all cylinder-piston components are made of conventional GG-25 gray cast iron.

The wear rate data for engine operation on DF compared with similar data, systematized by wear rates of piston rings and cylinder liners when burning different types of WCS. Fig. 8.15 illustrates this comparison graphically. For comparison, the results obtained for FCS with a carbon particle content of 32% by weight shown.

It should note that the cylinder liner wears 3…10 times slower than the piston rings. Otisca and AMAX (fine) WCS suspension exhibit approximately equal cylinder liner and piston ring wear rates, the lowest among all four suspensions. When burning Resource WCS, the cylinder liner rate is the highest, and the top piston ring wear rate is the second highest among all the slurries suspension. When using AMAX (fine) WCS, the top piston ring wears almost twice as fast as when burning Otisca and AMAX

(coarse) WCS, while the cylinder liner rate for these three WCS is approximately the same.

Based on the results of experiments with all four-suspension types, average wear rates for standard cylinder liner and piston rings can derived. When using SAE 40 mineral oil for cylinder lubrication (consumption rate of 1.0 g/(kWh)) cylinder liner wear occurred on average 22 times faster than when the engine was running on diesel fuel (range 13…42). Piston rings wore on average 90 times more intensely (range 56…160).

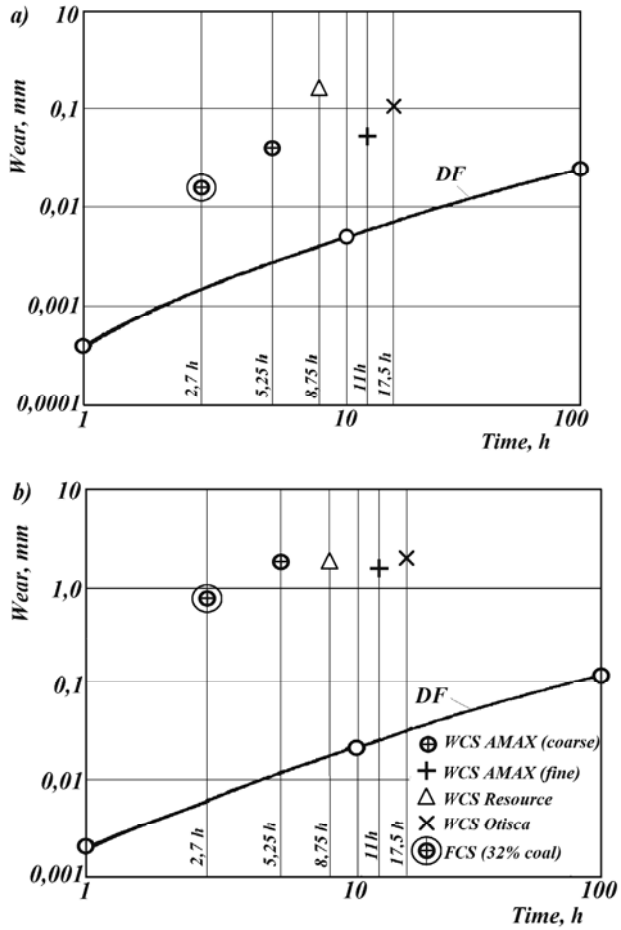

Fig. 8.15. Comparison of cylinder liner (*a*) and piston ring (*b*) wear of an engine burning diesel fuel, FCS and different types of WCS

Table 8.4.

Wear rate of single-cylinder diesel engine 1RSA76 components when burning different types of WCS

Fuel Type	Total engine operating time, h	Upper piston ring			Cylinder liner		
		Radial wear, mm	Wear rate, mm/h	Relative wear rate *	Diametrical wear, mm	Wear rate, mm/h	Relative wear rate *
Otisca	17.5	2.05	0.117	56	0.12	0.00686	16
AMAX Coarse	11.0	1.575	0.143	68	0.06	0.00545	13
Resource	8.75	1.763	0.301	96	0.155	0.0177	42
AMAX Fine	5.85	1.78	0.339	61	0.04	0.0076	18

* Calculated based on the estimated wear rate during the first 20 hours of engine operation (after installing a new cylinder liner) on DF No. 2; in the case of the upper piston ring, this rate is taken to be 0.0021, and in the case of the cylinder liner, 0.00042 mm/h.

8.3.1. The influence of particle size and ash content on the wear rate of cylinder-piston group parts. Experiments conducted on the 1RSA76 engine involved testing various suspensions with widely varying particle size distributions. This allowed us to observe the influence of not only the ash content of the original fuel but also the particle size of the WCS on wear characteristics. Fig. 8.16 shows the dependence of wear rate on the average particle size and ash content of the coal.

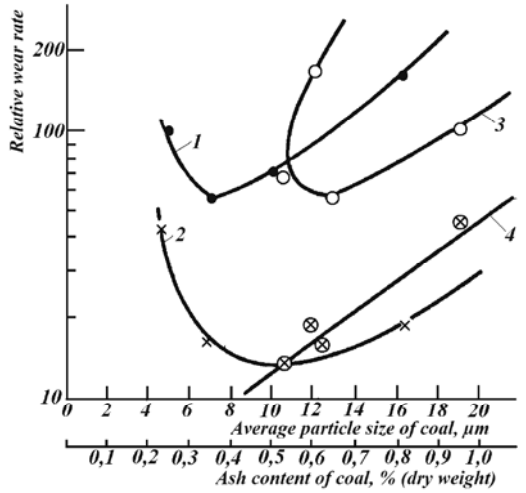

Fig. 8.16. Dependence of the wear rate of piston rings and cylinder liners on the average size of coal particles (1 and 2, respectively) and its ash content (3, 4, respectively). The wear rate is defined as the ratio of the wear rates when the engine is running on WCS and on DF

The wear rate curves for the upper piston ring and cylinder liner versus the average particle size have minima in the range of 6…10 μm. A linear relationship observed between cylinder liner rate and ash content of the coal, while no systematic relationship observed between piston ring wear rate and ash content. The relationship between coal particle size and ash content is random for the three WCS types. Ignoring the wear rate data for engines running on WCS Resource, we can see a strong influence of particle size on piston ring wear rate and a weak influence on cylinder liner rate. The relationship between wear rate and coal ash content remains virtually unchanged for all four-suspension types.

The fact that WCS Resource produces results that are different from the other three WCSs may be because the coal included in the suspension has the smallest particle size and the highest ash content.

8.3.2. Composition of mineral residues and their influence on the rate of engine wear. As already noted in Chapter 3 and Table 8.1, the ash of natural solid fuels contains a large number of different elements and compounds. Among all the mineral components of ash, silicon and aluminum oxides have the greatest hardness. Their presence largely determines the wear rate of the cylinder-piston group components of an engine running on coal fuel. During testing of the 1RSA76 engine, the dependences of the wear rate of piston rings and cylinder liner on the alumina content (Al_2O_3) and the total content of silica and alumina (SiO_2 + Al_2O_3) in the original fuel obtained (Fig. 8.17) [65]. In the case of Al_2O_3, the dependences of the cylinder liner and piston ring wear rates are non-systematic. At the same time, in the case of SiO_2+Al_2O_3, a strict dependence found for the piston ring wear rate. If we ignore the data for WCS Resource, we can state a strict monotonic increase in piston ring wear as the total concentration of SiO_2+Al_2O_3 in the coal increases. The absence of a systematic dependence for the piston ring wear rate on the concentration of Al_2O_3 and a more or less strict dependence on the concentration of SiO_2+Al_2O_3 can be explained by the fact that alumina and silica are present in the ash in a bound state in the form of aluminosilicates, the hardness of which is usually less than that of alumina (2100 kg/mm^2), but greater than that of silica (800 kg/mm^2).

The analytical dependence of the wear rate on the size (diameter d) of coal particles and its ash content can be estimated as the product of the total concentration of SiO_2+Al_2O_3 and the average particle diameter raised to the power m. Based on the results of tests on the low-speed 1RSA76 engine, the cylinder liner wear rate, for the conditions under consideration, is most accurately approximated by the expression (SiO_2+Al_2O_3)×$d^{-0.2}$, and the piston ring wear rate by the expression (SiO_2+Al_2O_3)×$d^{-0.5}$.

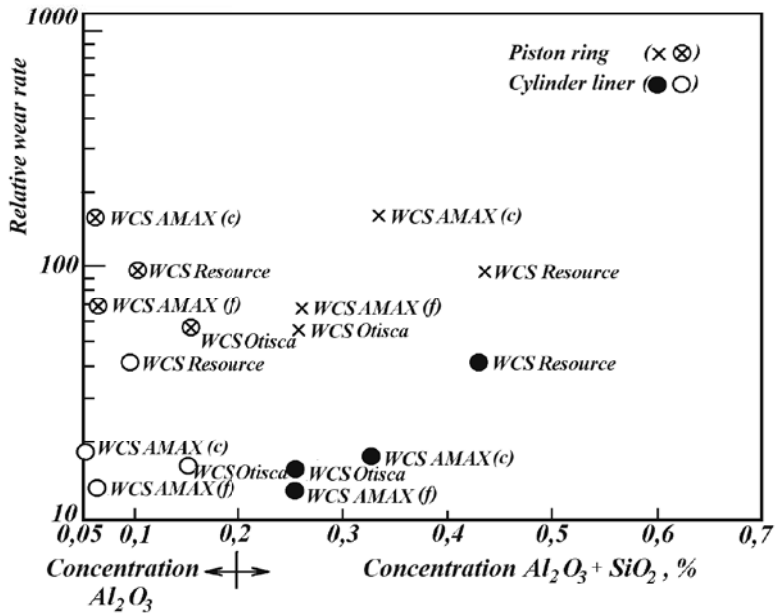

Fig. 8.17. Dependence of the wear rate of piston rings and cylinder liner on the concentration of SiO_2 and Al_2O_3 in coal (the wear rate is determined as the ratio of the wear rates when the engine is running on WCS and on DF No. 2)

An analysis of the presented dependencies suggests that cylinder liner wear depends primarily on the total concentration of silica and alumina in the carbon, while piston ring wear depends not only on the SiO_2+Al_2O_3 concentration, but also on the diameter of the carbon particles. This feature suggests that carbon particles or ash adhere to the cylinder liner walls either as result of their softening or due to the adhesive capacity of the oil film, so that these particles abrade the piston ring rather than rolling between it and the cylinder liner.

Based on the data presented in Table 8.4, an expression can written that allows for an approximate assessment of the influence of various factors on the wear mechanism by calculating the order of magnitude using the following equation [65]:

$$W=KLD/H,$$

where W – the volume of material removed as a result of wear; L – the applied load; D – the sliding distance; H – the indentation resistance; K – the dimensionless wear coefficient.

The essence of the method is as follows: first, using experimental data and the equation above, the coefficient K is calculated, then compared with the characteristic wear coefficients inherent in a given wear mechanism.

Fig. 8.18 shows the calculated values and ranges of wear coefficients characteristic of various cylinder liner and piston ring wear mechanisms.

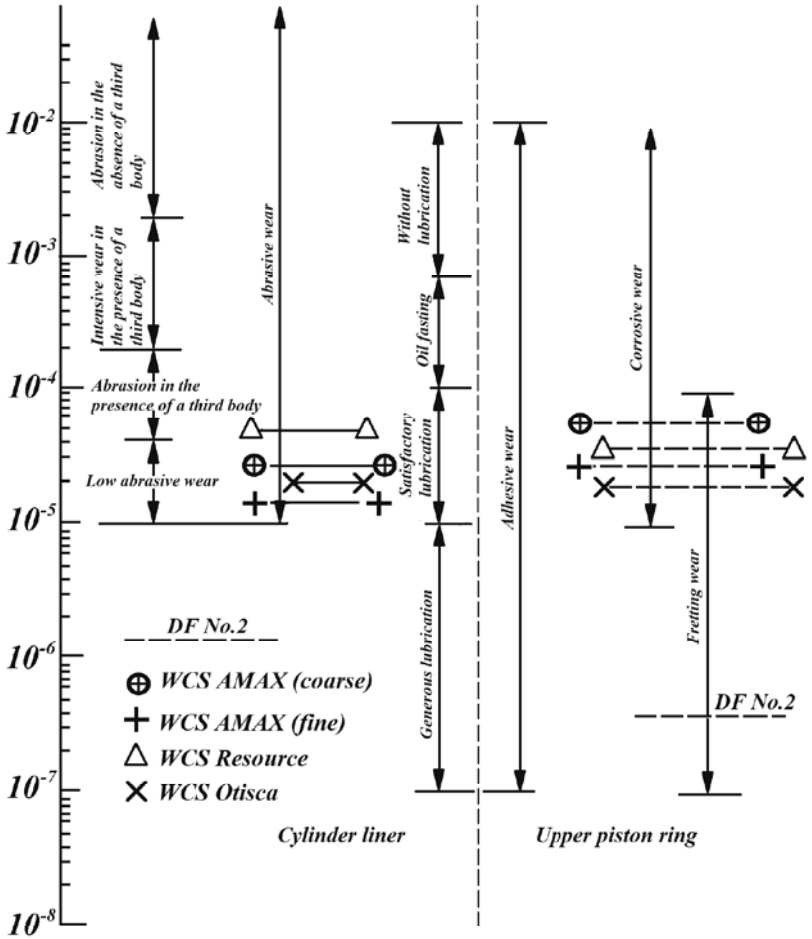

Fig. 8.18. Comparative analysis of typical wear coefficient values obtained by burning WCS for the same metal-on-metal friction pairs

The calculated wear coefficients for WCS are generally located in the zone of light abrasive wear, as well as in the region of adhesive wear with

satisfactory lubrication. It should noted that when using DF No. 2, all calculated wear coefficients lie in the region of adhesive wear with abundant lubrication, with no signs of corrosive or fretting wear. From the above, it follows that a certain reduction in wear can achieved by improving the lubrication mechanism of the rubbing surfaces, as well as by efficiently removing mineral particles and other products of incomplete combustion of coal from the working cylinder. It should note that the swirling motion of the charge during combustion and expansion could lead to increased deposition of abrasive particles on the cylinder walls.

8.3.3. The mechanism of wear of engine elements in direct contact with abrasive materials. Micrograph analysis of piston ring and cylinder liner surfaces reveals that the interaction of friction surfaces in the presence of mineral and coke-coal particles produces signs of both adhesive wear (torn surfaces, plastic deformation, metallic wear debris) and abrasive wear (clear, straight grooves). Adhesive wear predominates when solid fuel and ash particles settle on the walls, adsorbing and absorbing the oil film from the cylinder liner walls, resulting in oil starvation. If abrasive wear predominates, the groove tips on the mating surfaces of the friction pair may interact with each other as the piston ring moves, resulting in jagged marks on these surfaces.

If we assume that solid particles of coal and ash adhere to the cylinder liner walls, the appearance of jagged marks on the rubbing surfaces may also be the result of the rolling of the solid particle between the rubbing surfaces. In some cases, the combined adhesive and abrasive action of ash particles leads to signs of plastic flow, which results in the destruction of both the piston ring and cylinder liner surface itself and the lubricant film applied to them.

8.4. Ways to reduce wear in engines running on solid fuels.

8.4.1. Selection of materials for elements of the engine cylinder-piston group. A promising approach to improving solid-fuel engine components to reduce wear is the use of hard coatings produced by plasma spraying. Various companies have investigated several different types of coatings applied to the surfaces of piston rings and cylinder liners. Generally, all studies divided into laboratory studies, using setups simulating friction conditions in a real engine, and direct testing of the coatings on engines. In some cases, engine tests were of a simulation nature, with the engine running on standard fuel and the abrasive material introduced into the cylinder either with the fuel or with the lubricating oil. These types of tests typically utilized engines smaller those used in the primary study. In most cases, the studies

were comprehensive, utilizing all of the above methods. To determine the suitability of a particular coating for use in an engine, General Electric conducted two types of tests [48, 49], the general methodology for which is shown Fig. 8.19 and 8.21.

The pin-on-disc test conducted at room temperature (21°C) with mineral oil as a lubricant. The materials used in the test manufactured as pins and/or discs, either as coatings or as monoliths. The monolithic materials tested to establish a baseline wear rate for comparison with coating wear data of the same or similar compositions. Coatings applied by a variety of methods, including plasma deposition, chemical vapor deposition, and electroplating.

The pins were 1.27 cm long and 4.75 mm in diameter with polished hemispherical ends of 4.75 mm radius. The pins moved relative to a stationary disc at a speed of 18.8 cm/s and pressed against it with a specific force of 0.28 kg/cm^2. All tests were conducted with standard 75 cSt mineral oil, which was contained in a container surrounding the stationary disk and rotating control pin. Alumina (Al_2O_3) with an average particle size of 2.0 μm used a contaminant, added to the mineral oil at a rate of 2 g/l.

The addition of Al_2O_3 to the lubricant resulted in a significant increase in the wear rate of the surfaces. The wear rate of 440C stainless steel with the addition of Al_2O_3 increased approximately 100-fold (Fig. 8.20). The increase in wear with the addition of alumina depended on the hardness of the friction pair components. The wear of tungsten carbide on a disc made of the same material after the addition of alumina in-creased only by a factor of 2. Approximately 100 different friction pairs considered as potential materials, which included the following components: Al_2O_3, WC + Co, Cr_2O_3, Cr_3C_2, TiC, and Si3N4. Of these materials, tungsten carbide (WC 96%) with cobalt (Co 6%) sprayed on the surfaces consistently showed the best performance. In addition, several proven coating methods exist for this group of materials.

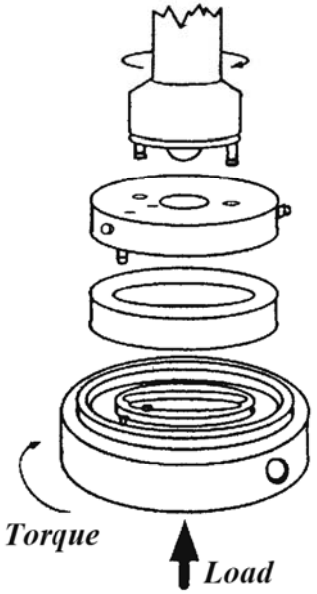

Fig. 8.19. Schematic diagram of the pin-on-disk test rig used to evaluate the optimal combination of liner and ring coatings

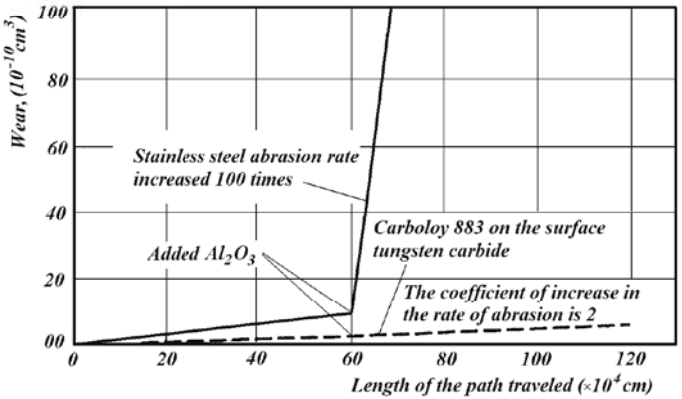

Fig. 8.20. Pin-on-disc test result for 440C stainless steel and sintered tungsten carbide

The best results obtained for samples provided by APS and Sermatech. The coating test results presented in Table 8.5.

Table 8.5.

Pin-on-Disc Test Results

Coating manufacturer	Degree of wear *
APS	0,05
Sermatech	0,09
Plasma Technology	0,15
Plasma Technic	0,3
Union Carbide	0,6

* The degree of wear is determined relative to the wear of the chrome plate when interacting with the WC-Co coating without abrasives.

Piston ring segment tests conducted at 177°C. Standard motor oil used as the lubricant. As in the first case, alumina with an average particle size of 2 μm was used as an abrasive, added to the lubricating oil at a rate of 2 grams per liter. The test scheme for this type of test shown in Fig. 8.21, and the test conditions are given Table 8.6.

Table 8.6.

Conditions for conducting a segment-on-ring test

Oil	Mobil Bulk Motor Oil
Temperature	177°C
Abrasive	Al_2O_3 (2 μm); 2 g/liter
Specific load	1,4 kg/cm^2
R_1	17,5 mm
R_2	50,8 mm
R_3	38,1 mm
Ring rotation angle	75°
Maximum speed	366 mm/s

Plasma-sprayed ring segments positioned against a polished monolithic ring of sintered tungsten carbide and cobalt. The ring subjected to rotational motion in both directions. Wear intensity was assessed by comparison with the wear of a chromium segment tested in uncontaminated oil.

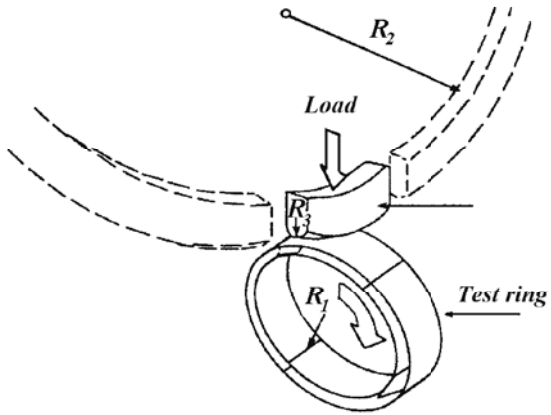

Fig. 8.21. Segment-on-ring test to determine the degree of wear of piston ring coatings

In this series of tests, the best results shown by the samples provided by APS and Union Carbide (Table 8.7).

Table 8.7.

Results of the segment-on-ring test

Coating manufacturer	Degree of wear
APS	3
Union Carbide	9
Plasma Technology	11
Sermatech	13
Plasma Technic	16

Based on laboratory data, coatings from APS, Sermatech, and Union Carbide selected for further testing. Tests conducted on a compact, four-stroke, and single-cylinder Yanmar diesel engine producing 9 kW at 2100 min^{-1}. For these tests, Kaydon Corporation (a division of Plasma Technology) manufactured several sets of 101.6 mm diameter piston rings. These rings, in various combinations with cylinder liner material, operated for 500 hours. Standard DF fuel with the addition of coal ash or octamethylcyclotetrasiloxane (OMTS) used. Upon combustion, this additive formed colloidal silicon dioxide, which, like coal ash, deposited on the cylinder liner and rings during engine operation.

The first series of tests conducted with standard fuel. The new engine used to establish baseline characteristics. In the second series of tests, 2.0% OMTS (by weight) were added to the diesel fuel. In the final stage of testing, 0.2% coal ash, which obtained by burning Otisca bituminous coal in an air stream, was added to the diesel fuel. The results of the machine tests presented in Table 8.8. A total 50 different combinations of materials were tested. The cylinder liner and piston rings made of monolithic tungsten carbide with cobalt tested on diesel fuel with the OMTS additive. As shown in Table 8.8 (item 6), the monolithic materials proved to be extremely hard. Their wear rate when working with abrasives was less than the wear of standard elements on pure fuel. Plasma-sprayed rings, when working in tandem with a monolithic tungsten carbide liner (item 7), also showed low wear rates. Interestingly, in the absence of abrasives, the chrome ring showed significantly less wear when paired with a solid tungsten carbide liner (item 8) than when paired with an iron liner (item 3). The plasma-sprayed cylinder liner proved to be extremely rigid. When running on diesel fuel, this resulted in significant ring wear.

Table 8.8.

Yanmar's small-size engine test results

Item	Ring Material	Sleeve Material	Ring Wear Rate, mm^3/h
No pollution			
1	Chrome	Cast iron	$1{,}80\times10^{-5}$
2	*WC+Co* (ST)	*WC+Co* (LPPD)	$1{,}40\times10^{-5}$
Pollutant, OMTC (2%)			
3	Chrome	Cast iron	$41{,}50\times10^{-5}$
4	*WC+Co* (ST)	*WC+Co* (LPPD)	$55{,}00\times10^{-5}$
5	*WC+Co* (PT)	*WC+Co* (LPPD)	$64{,}00\times10^{-5}$
6	*WC+Co* (K96)	*WC+Co* (K703)	$0{,}80\times10^{-5}$
7	*WC+Co* (ST)	*WC+Co* (K703)	$3{,}50\times10^{-5}$
8	Chrome	*WC+Co* (K703)	$7{,}10\times10^{-5}$
9	Chrome	Cast iron	$28{,}80\times10^{-5}$
10	Cr_3C_2+*Mo* (K1008)	*WC+Co* (703)	$24{,}50\times10^{-5}$
Pollutant, Otlisca ash (2%)			
11	*WC+Co* (K96)	*WC+Co* (K703)	$1{,}43\times10^{-5}$
12	*WC+Co* (ST)	*WC+Co* (K703)	$7{,}00\times10^{-5}$
13	Chrome	Cast iron	$250{,}00\times10^{-5}$
Type of technology			
ST – Serma Tech (Plasma spraying)			
PT – Dlasma Technics (Plasma spraying)			
LPPD – CRD (Low pressure plasma deposition)			
K96 – Kennametal (Monolithic carbide)			
K703 – Kennametal (Monolithic carbide)			

With the addition of ash to DF, the wear rate of standard materials increased by approximately 100 times (item 13). In contrast, a monolithic tungsten carbide ring, when paired with a monolithic liner made of the same material, showed good results (item 11).

After completing the full test cycle, no signs of coating cracking or damage detected at the microstructural level. Therefore, the selected coatings applied to 228.6 mm diameter rings, which subsequently used in testing in the 7FDL engine.

Initially, the new cylinder liner was run-in on diesel fuel. After a break-in period of 8.5 hours, rapid wear of the upper and lower piston rings observed. Further testing showed a rapid decrease in the wear rate until it stabilized at approximately 20 µm per 1,000 hours at maximum load. Initially, commercially available tungsten carbide plasma spraying used to coat the cylinder liner. In the first phase, the following tested on the WCS: a chromium carbide-coated top piston ring, chromium-plated middle rings, and iron oil scraper rings. In the next phase of testing, rings with galvanic coatings installed: the top coated with tungsten carbide, and the lower rings with chromium. During both periods (each test series lasted 13 hours), liner wear with the WCS was significantly lower than with cast iron liners. The wear rate in the area of the top ring was only twice as high as that of cast iron liners when running on DF (Fig. 8.22). The wear rate near the bottom dead centre was very low, within the error limits of the measuring instruments used.

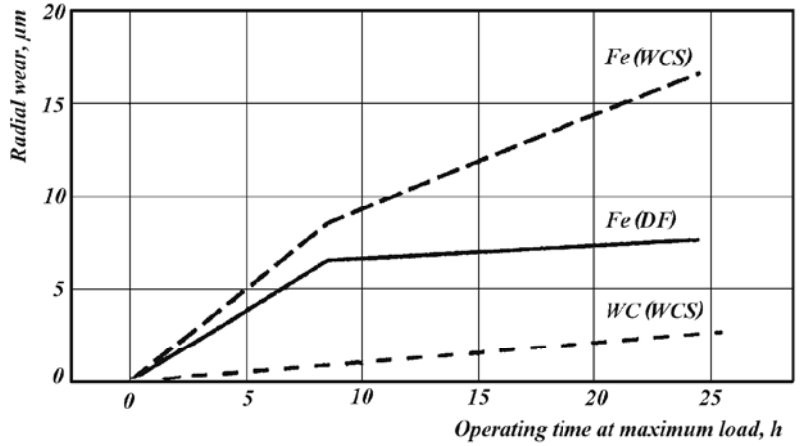

Fig. 8.22. Cylinder liners wear at the top of the ring stroke. Cast iron liner and liner with plasma spraying of tungsten carbide

Although preliminary tests showed that, the wear rate of the hardened cylinder surface was twice that of diesel fuel, it could assume that the cylinder liner problem can addressed within the limits of existing materials technology.

Ring wear studied using a similar methodology to the cylinder liner. To understand the differences in wear mechanisms, the materials were first tested on diesel fuel and then on WCS. When running on diesel fuel, all three rings exhibited typical break-in behavior.

The first attempt to increase the durability of the top ring was by plasma-spraying it with a chromium carbide coating with added molybdenum. This ring previously tested in conjunction with a tungsten carbide liner running on diesel fuel. The wear rate of this ring on WCS was twice that of a standard chromium-plated ring (Fig. 8.23).

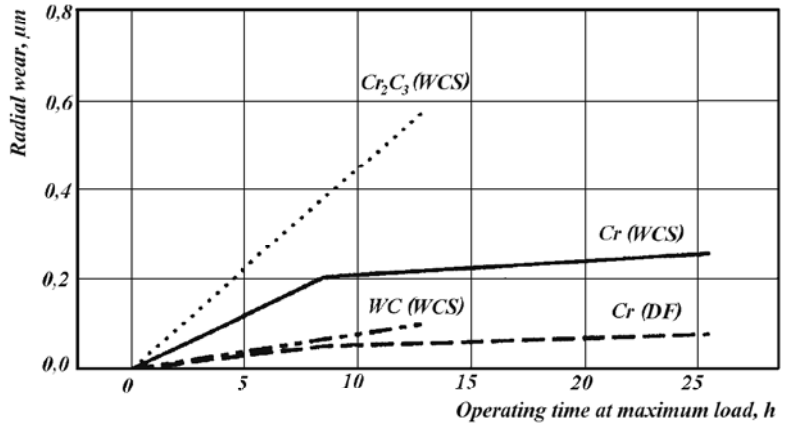

Fig. 8.23. Wear of the upper ring. Chrome-plated ring when working on DF and WCS. Plasma spraying of chromium carbide and tungsten carbide when working on WCS

The top ring, coated with tungsten carbide by plasma spraying, performed well in WCS applications. Its wear rate was only approximately twice that of a standard chrome-plated ring when running on DF.

The wear rates of the middle and oil scraper rings significantly reduced by chrome plating. Over 13 hours, the chrome-plated middle ring showed very little wear. Its wear rate was approximately one-quarter that of the iron middle ring when running on DF. The chrome-plated oil scraper ring showed no noticeable wear at all.

These ring wear reduction results provide grounds for optimism. As with the cylinder liner, advances in materials technology now make it possible to achieve wear rates comparable to those of engines running on DF.

***

Aiming to determine the wear resistance of multiple coating types, Cooper-Bessemer specialists carried out a research program focused specifically on piston rings and cylinder liners. They conducted their studies on three setups: a JS-1 series engine, a smaller gas-fueled engine, and a laboratory setup [44].

To determine the wear resistance of various ring and liner materials and coatings, a diesel engine with a cylinder D/S=104/125 mm and a speed of 1000 min^{-1}, converted to gas fuel, used. Simulation tests conducted primarily to study the wear mechanism during reciprocating motion. Abrasive wear conditions typical of a coal-fired engine simulated injecting suspension of 20% ash coal and SAE 20W oil through the cylinder sidewall. Experiments were performed with cast iron rings and a chrome-plated cylinder liner (the materials used in standard JS-series engines), as well as with rings coated with tungsten carbide and cobalt and a cast iron cylinder liner. All ring coatings achieved using plasma spraying. The wear rates of the upper compression ring for these two cases presented in Table 8.9.

Table 8.9.

Wear rate of the upper compression ring during simulation tests

Liner material	Ring material	Operating time, h	Change in thermal gap, mm	Wear rate*, mm/h
Chrome	Cast iron	40	0,89	0,022
Cast iron	WC-Co	98	0,13	0,001

* Change in thermal gap in 1 hour.

Simulation test results showed that wear on the small engine was approximately one-third that of the JS-1 engine. Tungsten carbide-coated rings found to be 20 times more wear-resistant than cast iron rings. No noticeable wear on the cylinder surface detected. Furthermore, the studies confirmed a linear relationship between wear and the ash content of the original fuel and the abrasive concentration in the oil.

8.4.2. Protection of valve timing components, turbocharger blades and pressure-lubricated parts.

Solid particles formed in the engine during coal combustion have a detrimental effect not only on cylinder-piston components but also on valve train components. Furthermore, they can damage the turbocharger and heat exchange equipment. By depositing on the surfaces of the engine's exhaust tract, they reduce the flow area, leading to increased exhaust backpressure.

The effects of abrasive particles and chemical corrosion on valve train components currently poorly understood. In the early stages of research, several cases were noted where solid particles trapped between friction

surfaces resulted in exhaust valve seizure. However, the percentage of coal fuel burnout in these experiments was very low, so the number of particles in the exhaust gases was quite high. In later studies, when burnout rates reached 90…99.5%, no significant wear of valve train components observed, although all experiments were of relatively short duration. Based on available data, it can conclude that the wear rate of valve train components is at least several times lower than that of cylinder-piston components. This suggests that by selecting wear-resistant materials and using appropriate design solutions, the wear rate of exhaust system components can reduce to a level acceptable for the commercial use of this type of engine.

The optimal design solution for minimizing the impact of valve train wear on engine reliability and efficiency is the use of a slide valve timing system with a loop scavenging system. The complete absence of valves eliminates the problem of valve wear, which inevitably occurs during operation of four-stroke engines or two-stroke engines with straight-through valve scavenging. Furthermore, loop scavenging prevents the formation of an axial vortex, which throws ash particles toward the cylinder walls, thereby increasing liner and piston ring wear. For engines with valve timing, compressed air can used to blow off the friction surfaces, or the friction pairs can be flushed with petroleum products. With the appropriate selection of materials, the clearances in the guide bushing can be flushed with water, and the valve seats and working faces can be flushed with steam. Steam can generated by recovering heat from the air cooler or exhaust gases. With this cleaning this method minimizes the consumption of liquid petroleum products.

In addition to the abrasive effect on valve timing components, high-velocity solid particles in the exhaust gas flow have a destructive effect on the turbocharger guide vanes and blades. Therefore, it is desirable to remove solid particles from the flow between the engine outlet and the turbocharger inlet. Temperatures in this section can reach 540°C, requiring the use of hot gas cleaning methods, which somewhat complicates the task.

Some research been conducted to date on removing solid particles from hot gas flows. The equipment under consideration includes barrier filters, granular bed filters, cyclones, and electrostatic precipitators. However, little large-scale research been conducted on removing solid particles from exhaust gases in coal-fired diesel engines. The most promising cleaning method currently considered to a compact, high-temperature barrier filter made of ceramic or other non-metallic material and installed in folds across the flow. The presence of carbon and ash particles in engine oil, as well as the accumulation of wear products in the oil, leads to rapid clogging of filter elements. The presence of ultrafine particles in the oil, which not captured by

filters, leads to increased wear throughout the engine. Bearings and crankshaft journals, as well as other friction pairs lubricated under pressure, are particularly susceptible to the effects of abrasive particles. Reducing wear on these components can achieved by:

- reducing the ash content of the original fuel;
- selecting appropriate, more wear-resistant materials;
- reducing the amount of abrasive material entering the engine's sub-piston space;
- reducing the contact of abrasive particles with engine components.

As already noted, even with minimal ash content in the fuel, some amount of carbon and coke particles will always be present in the lubricating oil. Therefore, their effects should minimize. This can achieve by using wear-resistant materials such as new alloys or non-metallic materials for the corresponding engine components. Additionally, appropriate heat treatment or various coatings, including those used for cylinder liners and rings, can be used to increase the hardness of friction surfaces.

To reduce the ingress of abrasive particles into the sub-piston space, a special system for isolating the engine crankcase from the working cylinder can used. This separation most easily achieved in crosshead engines. This design allows for the installation of an additional seal between the cylinder and the crankcase. Furthermore, this design feature allows for the use of two separate lubrication systems, preventing contamination of the oil used to lubricate the crankshaft bearings and allowing for the selection of the optimal lubricant grade for different friction pairs. A separate lubrication system is also possible in engines in which the piston directly connected to the connecting rod. In such engines, the seal can mounted directly on the piston. There are several different piston designs with this type of separator system.

Clearly, engines running on solid fuels require an upgraded lubricating oil purification system to more effectively remove solid particles and wear debris. In some designs, the standard lubrication system upgraded, with additional pumps and filters installed for oil purification, as well as magnetic separators and centrifugal cleaners.

Combating secondary wear in coal-fueled engines must be comprehensive; all of the above wear reduction methods may be present in each specific design. Many issues related to secondary wear been poorly researched and require further investigation.

Chapter 9.

Environmental aspects of direct combustion of solid fuels in piston internal combustion engines. Methods for reducing harmful emissions.

9.1. Content of harmful substances in the exhaust gases of piston engines using coal fuel.

Criticism of internal combustion engines as a source of mechanical energy primarily comes from two sources: the consumption of petroleum products and environmental pollution from toxic exhaust gases and carbon dioxide. The latter considered the cause of the «greenhouse effect» in the Earth's atmosphere [29]. Therefore, when discussing the use of coal as an alternative fuel for internal combustion engines, one cannot ignore the environmental impact of coal-fueled engines.

Preliminary results of studies conducted under a US Department of Energy program, as well as other studies, have shown that diesel engines running on coal-water slurry emit significantly lower amounts of nitrogen oxides (NO_x), although emissions of particulate matter and sulfur oxides (SO_x) may be higher. This depends largely on the ash content and sulfur content of the original fuel. At the same time, an analysis of existing combustion product purification methods indicates that there is a real opportunity to meet not only current standards for the main types of pollutants but also more stringent standards that will be introduced in the future. The development of installations using solid fuels will require the use of hot gas purification from pollutants to ensure environmentally sound combustion of coal. The objectives of this chapter are an analysis of the problem of harmful emissions; an analysis of approaches and methods for cleaning engine exhaust gases from pollutants; and an analysis of the design of equipment that can used to clean combustion products so that a diesel engine using WCS fuel will meet current and future environmental standards.

Currently available data indicate that sulfur oxides and particulate matter will play a primary role in engine emissions from coal-water fuel. Nitrogen oxides, due to the combustion characteristics of WCS, will play a secondary role and, according to preliminary data, will not cause significant problems. The high combustion efficiency of coal fuel currently achieved suggests that carbon monoxide and some hydrocarbons may form only during engine start-up or during engine malfunctions. During normal operation, the content of these harmful compounds will be below the levels typical of conventional installations using DF. Table 9.1 shows the test results of the low-speed engine 1RSA76 from Sulzer [65]. The tests conducted using four types of initial fuels, the ash and sulfur content of which did not exceed 1%.

Table 9.1.

Emissions of harmful substances based on the results of tests of the low-speed engine 1RSA76 from Sulzer at a speed of 120 min^{-1}

Fuel	WCS AMAX (fin. dispersed)				WCS *Resource*				WCS AMAX (coars. dispersed)				DF No.2			
Load, %	90	75	50	25	90	75	50	25	90	75	50	25	90	75	50	25
NO_x, ppm	610	760	740	370	430	640	600	380	480	590	590	315	1565	1780	1695	1520
CO, ppm	82	63	40	60	90	50	53	68	94	70	77	147	110	58	84	90
CH, ppm	60	60	85	80	70	60	74	80	55	50	53	70	76	80	100	100
Partic., mg/m^3	99	—	—	—	135	116	168	102	82	69	69	78	—	—	—	—

As the table shows, when using coal-water fuel in low-speed engines, NO_x levels are approximately half those of DF No.2. Moreover, hydrocarbon emissions are below the levels typical for DF. The data on the CH content in the exhaust gases of a low-speed engine do not agree well with the results of other studies on higher-speed engines. This discrepancy can explained the more optimal conditions for solid fuel combustion in low-speed engines. This confirmed by the low CO content in the exhaust gases, which does not exceed that of DF. SO_x measurements not conducted during the 1RSA76 engine test. Particulate emissions measured, but the obtained value was lower than the ash content of the fuel. This suggests that not all of the ash generated captured. At 90% load, approximately half of the ash contained in the fuel captured as particulate matter. Similar data obtained in other well-known experiments. The results of exhaust gas composition studies for engines of various purposes and designs are presented below.

The available data vary in their completeness and presentation. They reproduced here in the form in which they published by the researchers themselves.

Table 9.2 presents the results of testing a Cooper-Bessemer JS-1 medium-speed diesel engine [44, 79].

With pilot ignition (ignition coefficient of 0.14) and with WCS autoignition, the NO_x, CO, and CO_2 levels were very similar. A slight increase in CO content without pilot ignition indicates less complete fuel combustion. Exhaust gas analysis revealed no significant difference in NO_x, CO, and CO_2 content.

For the cases examined, the CO/CO_2 ratio was less than 0.5%, indicating very high fuel burnout efficiency.

Table 9.3 presents the test results for the EMD 567 two-stroke locomotive engine [79]. The data obtained during the study demonstrate the same trend as the Sulzer data, with the exception of HC emissions, which were higher in this case. NO_x levels were almost half those observed when the engine was running on DF No.2, while CO emissions were virtually comparable.

Table 9.2.

Exhaust gas composition of the Cooper-Bessemer JS-1 engine depending on test conditions

Fuel	The diameter of the spray holes and their number, mm×pcs	Inlet air temperature, °C	CO_2 %	O_2 %	CO ppm	NO_x ppm		Excess air coefficient	CO/CO_2 ratio
						measurement	at 15% O_2		
Basic DF No.2	0.30×8	169	9.0	8.75	800	850	403	1.68	0.009
WCS + pilot	0.30×8	173	8.7	10.6	360	750	426	2.00	0.004
Basic DF No.2	0.25×8	227	7.8	10.4	—	1250	697	1.92	—
WCS + pilot	0.25×8	226	8.5	11.2	210	1200	725	2.08	0.002
WCS + fpilot	0.30×8	223	8.4	11.5	95	1650	1029	1.16	0.001
WCS	0.25×8	223	8.3	11.6	150	1440	907	2.20	0.002
WCS + pilot	0.25×8	176	8.9	10.8	200	1080	626	2.00	0.02
Basic DF No.2	0.25×8	218	7.6	10.7	510	1325	864	1.98	0.007
WCS + pilot	0.25×8	219	8.8	10.8	108	1200	695	2.00	0.001

All tests conducted at a shaft speed of 400 min^{-1} and a mean effective pressure of 1.06 MPa. Changes in excess air pressure are due to boost instability. DF No.2 used as the pilot fuel.

Table 9.3.

Results of a study of harmful emissions during operation of the General Motors EMD 567 diesel engine at WCS

Fuel Type	DF No.2			DF No.2 and WCS			
Shaft Speed, min^{-1}	806	801	804	806	806	794	805
Power, kW	106	108.2	107.5	103	112	100	103
Diesel Fuel Consumption, kg/h	31.8	31.8	31.8	—	—	—	—
Auxiliary Fuel Consumption, kg/h	—	—	—	4.6	4.7	4.6	4.3
DF Pilot IAA, deg	—	—	—	35	35	45	55
WCS Consumption, kg/h	—	—	—	35.7	42.2	36.5	36.1
Hydrocarbons (measured), ppm	140	198	169	190	260	218	240
Hydrocarbons (converted to coal), ppm	—	—	—	240	322	267	311
CO (measured), ppm	817	992	904	—	—	779	—
CO (converted to coal*), ppm	—	—	—	—	—	858	—
NO_x (measured), ppm	947	786	866	676	601	601	671
NO_x (converted to coal*), ppm	—	—	—	486	336	336	476
Particulate Matter (measured), ppm	57.2	102.8	79.8	459.1	1144.2	1126.5	953.5
Particulate Matter (converted to coal**), mg/m^3	—	—	—	837.0	2207.2	2171.8	1829.3

* Average data.
** Including pilot fuel.

Particulate matter emissions during engine operation on WCS were 10…30 times higher than when running on DF No.2. These figures are higher than those obtained by Sulzer, but they are still lower than expected, given that the ash content of the coal is two orders of magnitude higher than in DF No.2.

Analysis of various test results shows that the combustion gases of engines running on WCS and DF consist of the same components, but the quantitative contents of these components differ.

Table 8.4 shows approximate ratios of harmful emissions from a diesel locomotive engine operating on WCS and DF. Emission levels calculated at the Southwest Research Institute (USA) based on experimental data. The SO_x level was determined based on the assumption that during combustion, most of the sulfur contained in the fuel converted to SO_x.

Table 9.4.

Expected level of harmful emissions from a diesel locomotive when operating on WCS (for comparison, a similar indicator for diesel fuel is given)

	Emission level (without cleaning), g/(kWh)	
	Engine on WCS	Engine on DF No.2
Hydrocarbons	0.765	0.765
CO	3.45	3.45
NO_x	4.92	9.84
SO_x	2.08...3.72	0.60
Particulate Matter	1.04...6.27	0.36

The data presented correspond to units not equipped with emission reduction devices. The table shows that when the engine operates on WCS, NO_x emissions reduced by approximately 50%. SO_x emissions increase, with the rate of increase varying depending on the calorific value of the original fuel (ranging from 30 to 33 MJ/kg) and its sulfur content (0.6 to 1.0 wt %). Particulate matter emissions increase approximately fivefold compared to DF No. 2. Therefore, when burning WCS, the engine emits approximately 4.9 g/(kWh) less NO_x, 1.5 to 3.1 g/(kWh) more SO_x, and 0.68 to 5.91 g/(kWh) more macroparticles.

It should note that the SO_x emission level meets NSPS requirements for stationary boilers burning high-sulfur coal. However, it cannot ruled out that engines running on WCS may require a SO_x capture system capable of regulating exhaust gas composition based on the sulfur content of the original fuel, as well as a particulate capture system.

Below, we will examine in more detail the formation mechanisms of various harmful components found in exhaust gases and methods for reducing their emissions.

9.1.1. Nitrogen oxide content in exhaust gases. Almost all WCS combustion experiments in piston engines have shown that NO_x emissions reduced by 32…68% compared to DF. Fig. 9.1 shows the dependence of NO_x concentration change on load for a low-speed 1RSA76 Sulzer engine using various types of WCS and DF [65, 79].

The reduction in nitrogen oxide content occurs despite the fact that the concentration of nitrogen-containing compounds in coals is 1.5…2% (by dry weight), while DF contains virtually no bound nitrogen. Thus, the reduction for compounds formed from atmospheric nitrogen appears even more significant.

The reduction in NO_x content occurs primarily due to the action of water, present in the suspension as a carrier. Water lowers the local flame temperature, thereby suppressing the formation of thermal NO_x oxides. The decisive role of reducing the temperature in the combustion zone in reducing the NO_x content in the exhaust gases confirmed by the fact that an increase in the temperature of the supply air in all cases leads to an increase in the formation of NO_x during the combustion process.

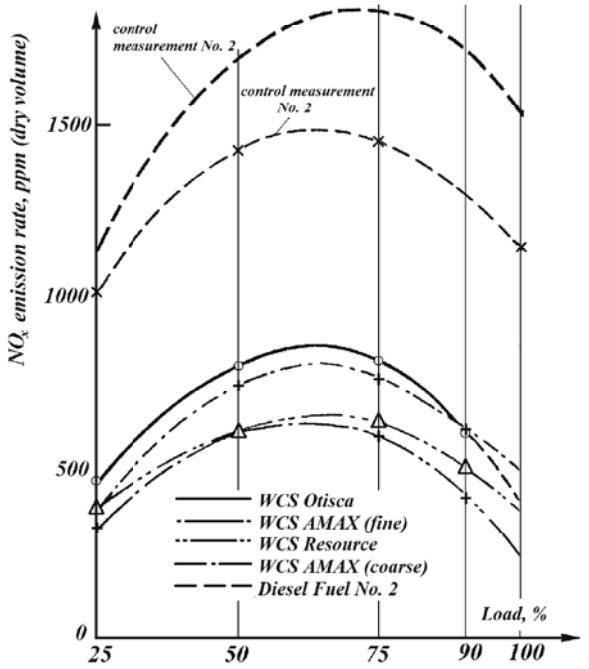

Fig. 9.1. Intensity of NO_x emissions from exhaust gases of the 1RSA76 engine

In early tests conducted by Cooper-Bessemer at a supply air temperature of 95°C, the NO_x concentration was no more than 380 ppm. Increasing the temperature to 222°C increased the NO_x content to 1650 ppm. Fig. 9.2 demonstrates the effect of air temperature on NO_x content during particulate combustion in a JS-1 medium-speed engine.

It should note that in tests conducted at elevated supply air temperatures (166...227°C), the NO_x content differed only slightly between WCS and DF No. 2 (Table 9.2). It is also interesting that increasing the nozzle whole size from 0.25 to 0.30 mm reduced NO_x formation by 30%. No difference in NO_x emissions observed between WCS with standard and ultra-fine grinding.

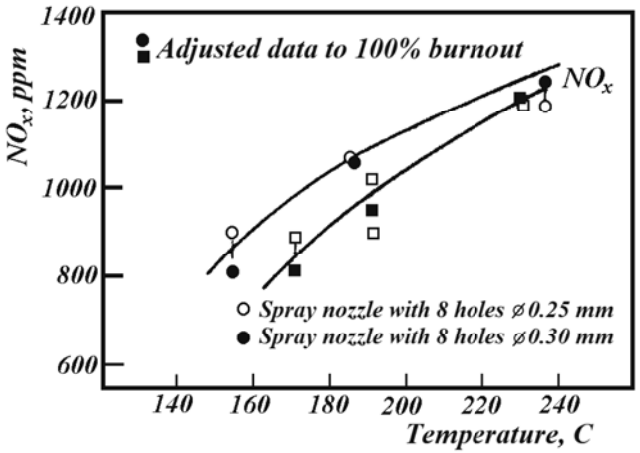

Fig. 9.2. The influence of supply air temperature on the NO_x content in exhaust gases

From the above, it follows that solid fuel engines operating at a sufficiently high efficiency can achieve NO_x emissions of less than 600 ppm (based on 35% efficiency and 15% O_2 concentration) without compromising performance. This complies with standards established by the U.S. Environmental Protection Agency and national agencies in other countries.

If NO_x requirements are further increased, a number of methods can used to reduce nitrogen oxide emissions, including afterburning, catalytic gas purification, the Raprenox process, and NO_x OUT. Let us briefly review the essence of these methods [47, 79].

***

Afterburning. An additional portion of fuel added to the gas engine's combustion chamber, creating fuel-rich zones in which the oxygen concentration decreases. This results in the detachment of oxygen atoms from

nitrogen oxide molecules and the reduction of NO_x to N_2 by hydrocarbon radicals, resulting in a «low-temperature» flame. NO_x reductions of 50...90% have been achieved in the laboratory using natural gas for reburning under conditions typical of boiler furnaces and heaters [47]. Although this method has not yet been applied to diesel engines, when combined with combined cycle gas turbines, its use can reduce the N_2 content in exhaust gases by up to 50%. At this gas temperature, conditions for heat recovery provided.

Preliminary test results suggest that this same method could be used in internal combustion engines. The low cost of reburning, combined with more efficient heat recovery and more complete combustion of coke-coal massif, makes this process quite attractive.

***

Catalytic gas purification. There are two modifications to this NO_x reduction process. The first uses carbon from exhaust particulates as a catalyst. This method involves the direct injection of ammonia into the exhaust stream. Porous filters operating at 200°C serve to capture carbon particulates, effectively increasing the contact time between the chemical reactants.

If the residence time is insufficient, the exhaust system can be equipped with a special reactor to ensure better contact between the gas and particulates. Using a reactor slightly increases the cost of the purification process; however, operating costs remain relatively low and determined primarily by the cost of ammonia.

The second modification of the ammonia-based NO_x reduction method called the «Shell/UOP process». Ammonia injected into the gas flow over the catalyst, which decomposes NO_x into nitrogen and water. This method successfully used to reduce NO_x and SO_2 in exhaust gases. Its use in coal-fired diesel engines may pose some difficulties because catalytic decomposition occurs within a narrow temperature range. At low temperatures, catalytic cleaning reactions slow down or do not occur at all, and at high temperatures, the metal catalyst fails. Capital costs for this method are quite high, but since the process reduces NO_x, SO_2, and possibly particulate matter, the cost of a cleaning system using this process could be comparable to the other systems considered. Operating costs are high primarily due to the need for catalyst regeneration, which performed using expensive hydrogen. If this process used to reduce NO_x and particulate matter, expensive regeneration can avoided. However, it remains to be determined whether the particulate material reduces catalyst activity at exhaust gas temperatures. If this method is preferred in the future, the effect of particulate matter on catalyst service life should further investigate.

Experience with this method in stationary installations shows that it capable of providing significant NO_x reduction. However, methods using ammonia in the presence of a metal catalyst are more expensive.

***

The Raprenox process. This relatively new process uses cyanuric acid to remove NO_x. The process is still under development, and its practical use for cleaning diesel engine exhaust gases from NO_x will require significant research.

***

The NO_x OUT process involves injecting an aqueous urea solution into various points of the engine exhaust tract. The process can successfully used at temperatures ranging from 400 to 1100°C.

9.1.2. Content of carbon monoxide and hydrocarbons in combustion products. The carbon monoxide and hydrocarbon content of the exhaust gases largely depends on the combustion efficiency of the coal fuel. Analysis of the exhaust gas composition based on various studies shows that the currently achieved coal fuel burnout efficiencies of 92...99.5% allow for a very low CO/CO_2 ratio. This confirms the high efficiency of coal combustion. Despite the higher carbon-hydrogen ratio in WCS, actual CO emission levels are often lower than for DF No. 2.

As already noted, the completeness of fuel combustion largely depends on the air temperature at the engine inlet. The dependence of exhaust CO emissions on the inlet air temperature depicted Fig. 9.3.

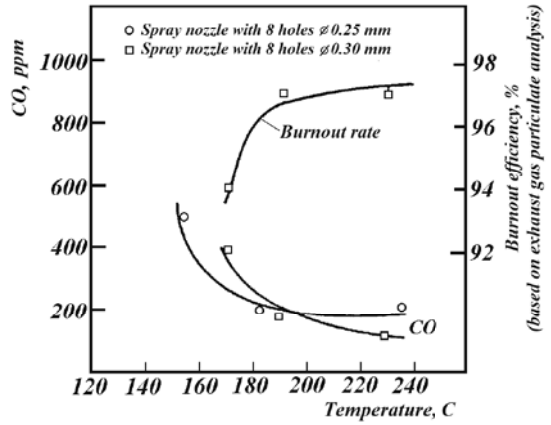

Fig. 9.3. Relationship between CO content in exhaust gases, completeness of combustion and air temperature at the engine inlet

The same figure also shows the relationship between the inlet air temperature and the completeness of fuel combustion. The data obtained during testing of the Cooper-Bessemer JS-1 medium-speed engine [44].

Even lower values of CO content in the exhaust gases observed in low-speed engines, especially at partial load conditions. This indicates that this type of engine creates the most favorable conditions for the combustion of coal fuel. Fig. 9.4 shows the dependence of CO content in the exhaust gases of the 1RSA76 engine from Sulzer at various load conditions [65, 79].

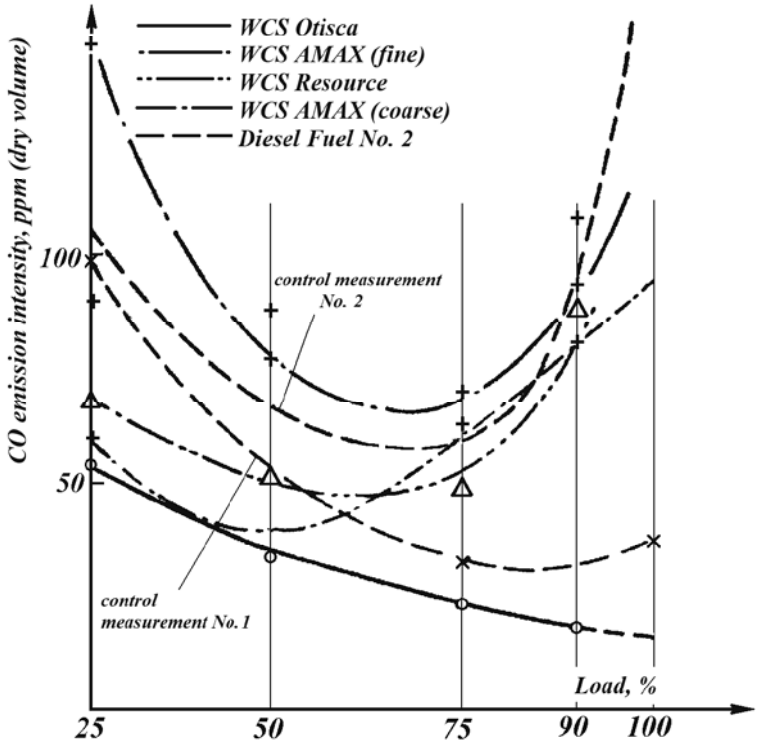

Fig. 9.4. Intensity of CO emissions in exhaust gases of the 1RSA76 engine

The combustion process of coal fuel in a piston engine cylinder precedes in such a way that hydrocarbon compounds burned out in the early stages. The pilot fuel burns out first, followed by the volatile compounds. The majority of the combustion process spent burning out the coke residue. Almost all gaseous hydrocarbon combustion reactions completed simultaneously with the coke carbon burnout. Therefore, their content in the

exhaust gases does not exceed, and in some cases is even lower than, the same value for the same engine running on DF.

Fig. 9.5 illustrates the HC emission intensity levels for the Sulzer 1RSA76 low-speed engine.

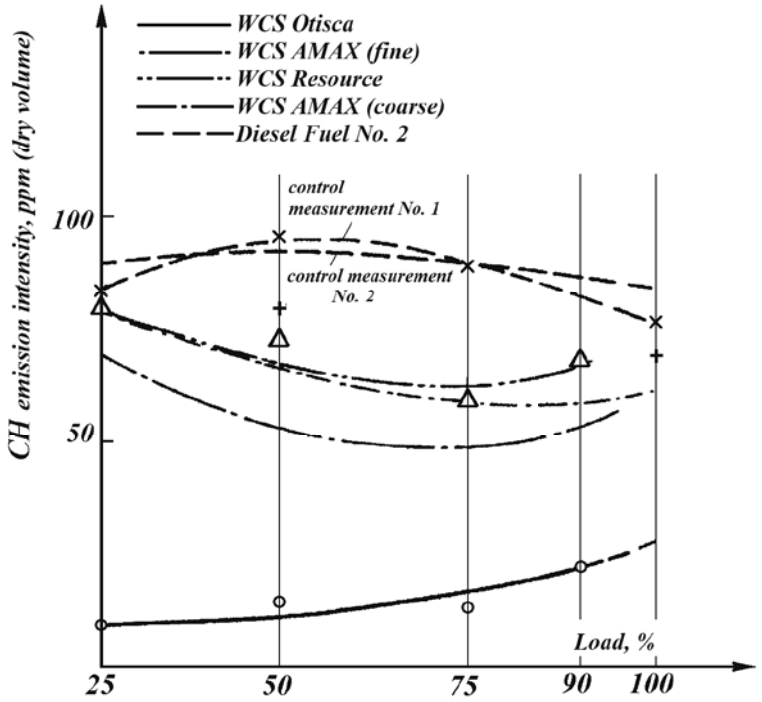

Fig. 9.5. Intensity of CH emissions with exhaust gases of the 1RSA76 engine

A rough analysis of the composition of solid particles emitted from the working cylinder with the exhaust gas flow indicates the presence of volatile components. The presence of 11...20% volatiles explained by their presence in the portion of the carbon that escapes unburned from the engine. The presence of volatiles may also indicate that their release slowed by high pressure or due to the short residence time of the carbon in the cylinder. At high temperatures and pressures in the cylinder, combustion of the coke-coal substance likely occurs on the surface, and complete release of volatiles and their combustion in the gas phase does not necessarily follow.

Of all the hydrocarbons potentially present in the solid exhaust of an engine operating on WCS, polycyclic aromatic hydrocarbon compounds are

of greatest interest due to their potential carcinogenicity. The content of compounds in this group for five tests presented Table 9.5, which shows that molecules containing approximately 2..4 benzene rings are present in exhaust gases in quantities of 1...70 ng/l. Heavier molecules (5...6 rings) are present in quantities not exceeding 0.1...0.5 ng/l.

Table 9.5.

Content of polycyclic aromatic hydrocarbon compounds in the exhaust of the Cooper-Bessemer JS-1 engine

Compounds	Aromatic rings	Experience				
		1	2	3	4	5
Naphthalene	2	40	30	10	30	40
Acenaphthalene	2-1/2	<1	<1	<1	<1	<1
Acenaphthene	2-1/2	<6	100	40	70	90
Fluorene	2-1/2	<1	2	<1	<1	2
Phenanthrene	3	<4	10	4	6	<4
Anthracene	3	<1	2	<1	<1	<1
Fluoranthene	3-1/2	7	6	10	4	6
Pirin	4	<5	70	<5	20	9
Benzo(a)anthracene	4	6	2	2	10	30
Krizin	4	20	20	10	20	7
Benzo(b)fluoranthene	4-1/2	<0,2	<0,2	0,6	<0,2	0,5
Benzo(k)fluoranthene	4-1/2	<0,1	<0,1	<0,1	<0,1	<0,1
Benzo(a)pyrine	5	<0,4	<0,4	<0,4	0,5	<0,4
Dibenz (a, h) anthracene	5	<0,4	<0,4	<0,4	<0,4	<0,4
Benzo (g, h, i) perylene	6	<0,5	<0,5	<0,5	<0,5	<0,5
Indeno (l,2,3-c,d)pyrine	6	<1	<1	1	<1	1

A comparison of the results using DF and WCS indicates a similar or slightly higher content of polycyclic hydrocarbon compounds in the particulate matter contained in the exhaust gases when the engine is running on WCS. However, since the total content of particulate matter in the exhaust is ten times higher for WCS than for DF, the specific concentration of these compounds per unit mass is approximately ten times lower for WCS than for DF [47].

9.1.3. Sulfur oxide content in exhaust gases. The residual sulfur content in WCS depends on the amount of organic sulfur in the original fuel and the coal pre-cleaning method. Modern physical and chemical coal cleaning methods can effectively remove most of the pyrite sulfur. However, since the characteristics of the original coal vary greatly depending on a large number of factors, the sulfur content of WCS expected to vary as well. In coals tested to date, dry cleaning typically reduces the sulfur content to less than 1% by weight. During coal combustion, sulfur converted into SO_x oxides.

All methods for reducing SO_x content in engine exhaust gases can roughly divide into those that reduce the sulfur content in the original fuel before combustion and those that rely on the extraction of sulfur oxides from combustion products. In the following, the focus will be on methods aimed at extracting sulfur oxides directly from engine exhaust gases.

The most efficient method is to extract sulfur compounds before the turbocharger, but this may not always be practical. Of the several sulfur oxide reduction methods developed for use in other types of systems, one of the most suitable for internal combustion engines is the addition of a calcium-based sorbent. Calcium hydroxide ($Ca(OH)_2$) is used as an effective sulfur absorbent in thermal power plants. It sprayed at the inlet of the economizer, operates in the temperature range typical of diesel engine exhaust gases (500...540°C).

Although the chemistry of sulfur removal from hot gas streams is well known, applying this cleaning method to diesel engine systems requires further consideration of a number of issues related to the specific operating characteristics of power plants using coal-fired internal combustion engines, in particular:

- the limited response time available for sulfur absorption within the exhaust tract;
- insufficient knowledge of the effect of water on reactions at exhaust gas temperatures;
- the lack of information on the mechanism of interaction between solid particles and various types of absorbents and filter elements.

To answer these questions, two types of calcium-based sorbents tested in a tubular reactor developed at the University of Utah [48]. The reactor, shown in Fig. 9.6, purged with a gas mixture containing SO_2 in the range of 200 to 500 ppm.

Dry powdered $Ca(OH)_2$ and $CaMg(OH)_4$ were introduced into the reactor through a Venturi tube. To determine the rate of SO_2 uptake by the sorbent, gas samples were collected at several points along the upstream flow.

Fig. 9.7 shows the kinetics of SO_2 uptake for both sorbents over time. The total interaction time between the sorbent and the gas flow was 500 ms. As can be seen in Fig. 9.5, at 500 °C and a Ca/S ratio of 2, the largest amount of SO_2 was captured by $Ca(OH)_2$ (approximately 500 ppm). For CaMg(OH), this value did not exceed 200 ppm. It should note that both sorbents almost completely cease to react with the gas flow after 300 ms, and the maximum reaction rate achieved within the first 50 ms.

Testing of sorbents based on calcium compounds showed good results. Considering the low cost of these sorbents ($Ca(OH)_2$ is ordinary slaked lime),

it can be assumed that in the future this method of cleaning exhaust gases will be used in diesel power plants running on solid fuel.

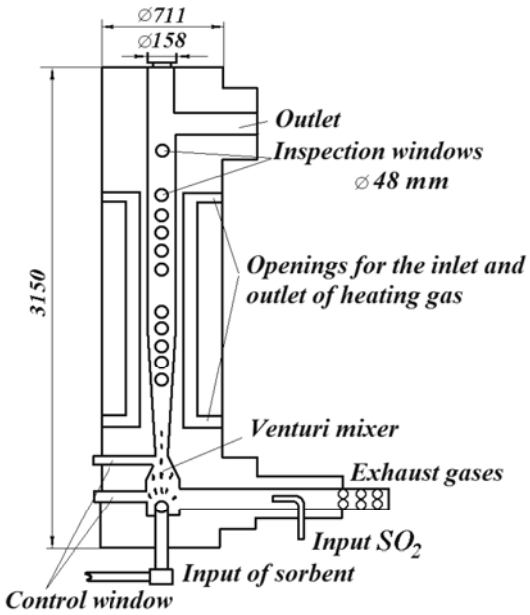

Fig. 9.6. Cross-section of a reactor developed at the University of Utah for testing various sorbents

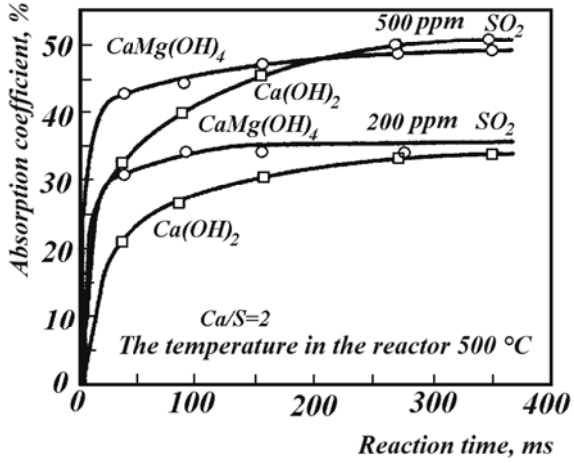

Fig. 9.7. Kinetics of SO_2 absorption by calcium sorbents in an experimental reactor

Another promising method for removing sulfur compounds from exhaust gases is by passing them through a granular copper oxide catalyst bed. Several granular copper oxide sorbents tested in a laboratory setup simulating a bed-type catalyst reactor [48]. Granules containing 5.4% copper oxide (CuO) supported on porous alumina successfully adsorbed SO_2 and subsequently recovered. Engine exhausts gases simulated by mixing O_2, CO_2, N_2, and 300 ppm SO_2 in appropriate proportions, and heating the mixture to 425 °C. SO_2 levels measured at a depth of 150 mm in the reactor (Fig. 9.8).

The level of sulfur oxide adsorption studied as a function of the gas filtration rate through the sorbent bed. At a flow rate of 500 mm/s, the reaction time was insufficient for complete SO_2 absorption within the bed, and the absorption rate was not constant throughout the experiment. At this bed flow rate, the absorption rate averaged 80%. When the flow rate reduced to 120 mm/s, the absorption rate stabilized briefly at 93% and remained constant for over 20 hours.

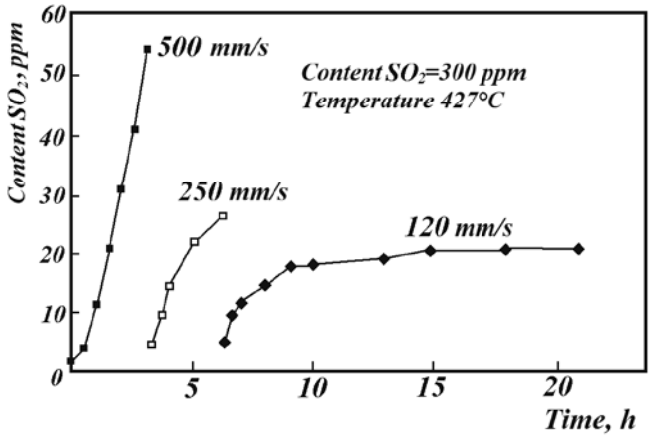

Fig. 9.8. Effect of gas flow velocity on SO_2 absorption by a granular layer of copper oxide

Copper oxide, unlike lime, is a expensive sorbent (approximately $10/kg). This high cost necessitates its regeneration for reuse. Regeneration can accomplish by reducing metallic copper from sulfate by reaction with methane. The SO_2 released during reduction as a gas can be collected in a special tank and further processed. The metallic copper can reoxidized and reused a sorbent.

In addition to the methods described above, which have already found some application in various types of power plants, others can identify that have potential for use in future developments.

We discussed the Shell/UOP method for the comprehensive reduction of NO_x and SO_2 content above.

In the long term, methods for absorbing sulfur compounds during the combustion of solid fuel in the working cylinder could used to reduce sulfur oxides. In particular, calcium compounds (calcium acetate), injected into the engine as a fine aerosol, can capture sulfur at temperatures of 1000…2000°C. This method requires no additional equipment and implemented simply by adding calcium acetate to the WCS [47].

Carbon-containing particles in engine exhaust gases can use as a sorbent for SO_2 absorption. This method is relatively inexpensive, but the amount of sulfur that can captured this way has not been determined, and the issue of carbonate residue disposal also remains unresolved.

9.1.4. Content of solid particles in exhaust gases. Solid particles formed as result of coal combustion in a diesel engine. They not only pollute the environment but can also damage the turbocharger and heat exchange equipment. Therefore, it is most desirable to remove solid particles immediately at the engine outlet. The temperature in this region ranges from 500 to 540°C, requiring specialized cleaning methods to remove solid particles from the hot gases.

The mechanism of solid particle formation and their composition remain poorly understood. These particles primarily consist of mineral impurities contained in the original fuel and unreacted coke residue. It is clear that under high temperatures and pressures, certain compounds present in the ash can undergo various changes, which ultimately affect the composition of the solid residue emitted with the exhaust gases. Measurement results show that the concentration of particulate matter in the exhaust gases of engines operating on WCS is approximately 10 times higher than when operating on DF (102...103 mg/L).

Fig. 9.9 shows a micrograph of particulate matter collected from the filter of a JS-1 engine operating on WCS. A number of characteristic particle shapes observed. Small spherical particles are mineral substances liberated and fused in the flame during combustion of the coal fuel; they have sizes of approximately 2 μm and below. X-ray diffraction analysis revealed that these particles contain aluminum, silicon, iron, calcium, sulfur, and titanium. There are also some sharp particles resembling the original coal. The fact that 45% of the original coal particles were larger than 10 μm suggests that most of this fraction may be particles of unburned coal, which only slightly reduced in size during combustion of the coke-coal substance. The macroparticles observed in the image are chain-like or agglomerated formations of smaller carbon particles, ranging in size from 5 to 10 μm. X-ray analysis revealed

that these macroparticles are almost completely free of mineral components. Most of this material may be an agglomerate of carbon particles that burned and bonded together [47]. It is also possible that a small number of particles formed in the engine exhaust port; these are primarily agglomerates of soot particles and condensed metal vapors.

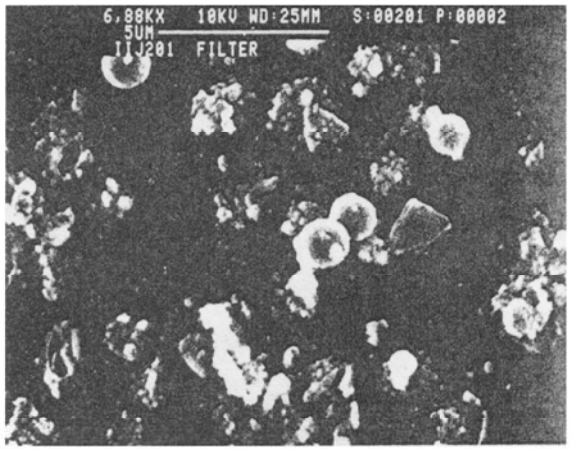

Fig. 9.9. Close-up of diesel engine exhaust particulates

A number of researchers have noted that even very good cleaning, the total number of retained particles is lower than the ash content of the original fuel. Fig. 9.10 shows the results of measuring the content of solid particles in the exhaust gases of a 1RSA76 Sulzer engine [65].

For comparison, Fig. 9.10 shows the curves for the concentration of solid particles in the exhaust gases, constructed based on the ash content of the original fuel (solid lines). The curves for the actually measured amount of solid particles are invariably located below these values, despite the fact that the experiments were repeated multiple times, and their results were distinguished by good reproducibility (especially at 50 and 75% load modes) [65]. The lower concentration of solid particles during the experimental studies is possibly the result of either the adhesion of some particles to engine components and the walls of the exhaust pipes, or their removal into the space under the piston along with the cylinder lubricant. It also cannot ruled out that the lower particulate matter content in the exhaust gases is due to the engine's combustion temperature significantly exceeding 815°C, the standard deashing temperature for carbon (ASTM standards). At such high temperatures, oxides present in the exhaust gases lose their oxygen content and reduced to metals. It is also possible that alkali metals evaporate, forming

fine particulate matter, which condenses and passes through the filter. This hypothesis supported by the fact that higher particulate matter concentrations observed at loads of 25...50% (compared to loads of 75...90%). This may be due to lower combustion temperatures at low loads.

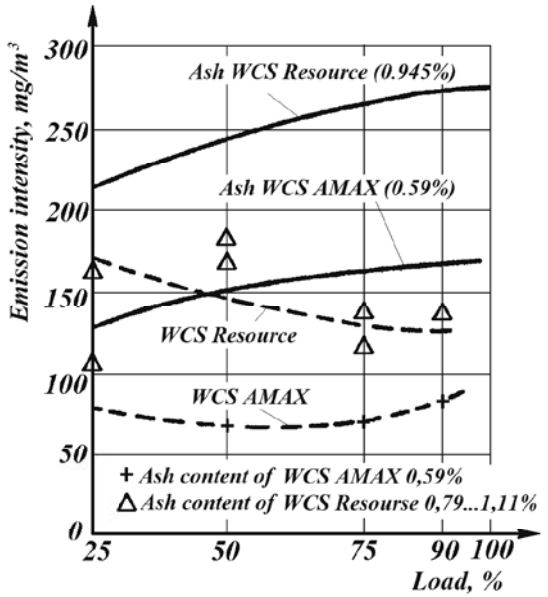

Fig. 9.10. Calculated and experimental intensity of emissions of solid particles with exhaust gases of the 1RSA76 engine

To date, a number of studies have conducted on removing particulate matter from exhaust gas streams. Equipment used for hot gas cleaning includes barrier filters, granular bed filters, cyclones, and electrostatic precipitators. To effectively remove particulate matter from exhaust gases, a number of issues must be addressed, including:

- selecting optimal cleaning methods and filter designs for separating ash and unburned coke-coal particles from the gas stream based on the engine's application and environmental requirements;
- preventing the re-entrainment of particulate matter into the gas stream due to pressure fluctuations in the cleaning system;
- selecting materials for filter and filter shell manufacturing, taking into account operation at high temperatures and in a fairly aggressive environment (especially when using some of the exhaust gas toxicity reduction methods described above);

- organizing filter cleaning during operation to prevent increased resistance on the filter device as it becomes clogged.

Clearly, methods for removing particulate matter from exhaust gases must be comprehensive. On the one hand, this is due to the high load on the filter elements, and on the other hand, to the fact that the particulate matter contained in the exhaust has a bimodal size distribution and consists of relatively large carbon aggregates (<10 μm), much smaller carbon fragments, and mineral particles (>10 μm). The proportion of large coal fractions can account for 20...40% of the total mass of exhaust macroparticles.

Therefore, it is difficult to use a single method that would effectively separate both fairly large and small particles from the gas flow. Fig. 9.11 shows the particle size distribution in the exhaust gases of a General Electric 7FDL engine [48].

During testing, the engine operated on WCS containing purified bituminous coal with an ash content of 0.8% on a dry basis. The accumulator injection system with a diamond-tipped sprayer ensured high solid fuel burnout throughout the test. The engine produced 187 kW/cyl at 1050 min^{-1}.

The smaller ash particles had an average size of 3 μm. The larger particles, typically composed of unburned coke and coal, had an average size of 9 μm.

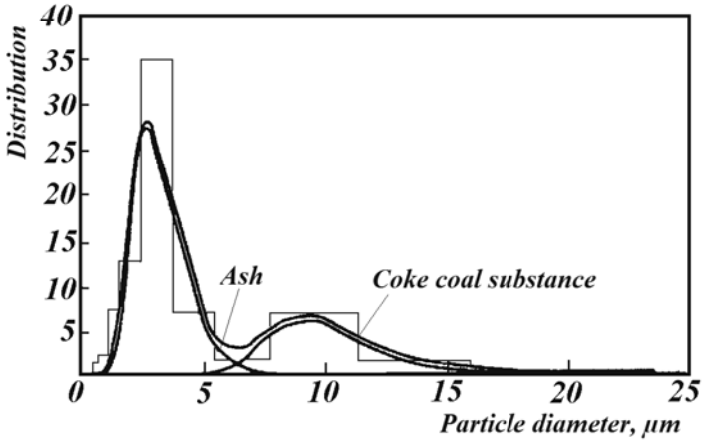

Fig. 9.11. Particle size distribution in the exhaust gases of a General Electric 7FDL engine modified to run on WCS

Fig. 9.12 shows a schematic diagram of a device used by General Electric to study various methods for removing particulate matter from coal-fueled engine exhaust gases.

Fig. 9.12 shows a schematic diagram of a device used by General Electric to study various methods for removing particulate matter from coal-fueled engine exhaust gases.

The purification system consists of a cyclone, a granular bed filter, a metal filter, and a porous filter. An additional fabric filter for collecting particulate matter installed at the outlet of the device to determine the efficiency of each method. A portion of the 7FDL engine exhaust flow sampled for testing. A valve system allowed the gas flow to pass through a cyclone, a granular bed filter, or a porous filter, either individually or in various combinations. The gas for analysis collected after final cleaning.

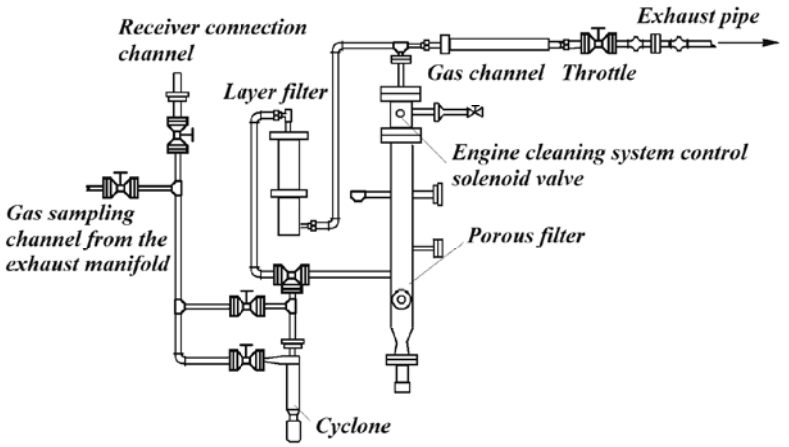

Fig. 9.12. Device for studying methods of cleaning engine exhaust gases

Experimental studies have shown that the cyclone removes virtually all particles larger than 5 μm from the gas flow, the majority of which are unreacted coke particles. At the same time, it allows the majority of ash particles smaller than 3 μm to pass through (Fig. 9.13).

Cyclone cleaning efficiency reaches approximately 75%. Given the simplicity of this method and minimal resistance to gas flow, a cyclone can used as the first stage of cleaning and installed before a granular or porous filter.

Stainless steel mesh filters with multiple pore sizes can retain over 99% of particles contained in exhaust gases. However, small ash and coke particles quickly clog the filter pores, leading to increased backpressure at the outlet. This occurs especially intensely if a calcium-based dust sorbent added to the exhaust gases to remove sulfur oxides from the gas stream. Clogged

pores can clear by pulsed purges of the filters with compressed air. Brief purges of the filter elements can repeatedly reduce filter resistance to several tens of centimeters of water column (Fig. 9.14).

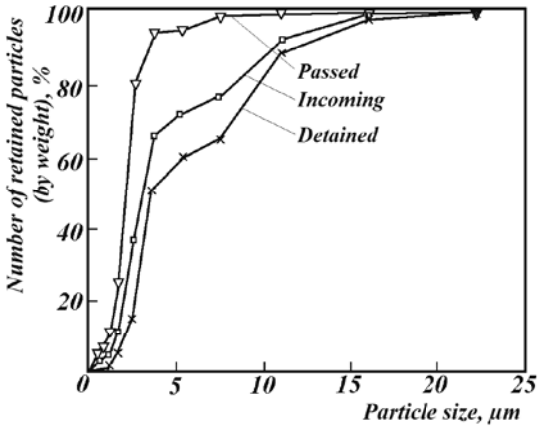

Fig. 9.13. Characteristics of cleaning exhaust gases of a coal-fuel engine using a cyclone

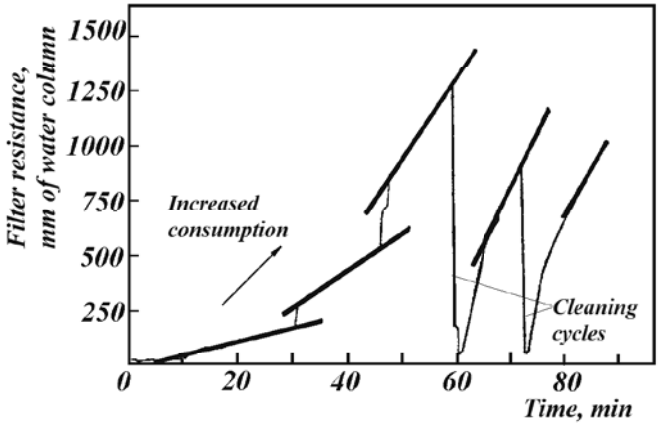

Fig. 9.14. Resistance of a stainless steel mesh filter during pulse cleaning with compressed air

The use of an exhaust gas cleaning system, especially in vehicle power plants, requires a simple and reliable device with low resistance and compact dimensions. For example, a 12-cylinder locomotive engine with a power output of 2200 kW produces approximately 4 kg of exhaust gas per second. The gas backpressure at the turbocharger outlet must not exceed 2600 Pa

(254 mm H_2O). The device must be able to handle high gas emissions within acceptable high-temperature range (510°C upstream of the turbine and 400°C downstream of the turbine). If the device installed between the engine and the turbocharger, its size must be limited to maintain acceptable inertia.

The device must design to clean exhaust gases for 50 hours (the typical duration of a single trip). During this period, depending on the ash content of the original fuel, between 130 and 200 kg of particulate matter and sorbents used to reduce SO_2 content will accumulate in the storage bin.

Fig. 9.15 shows a schematic diagram of the exhaust gas cleaning system used in the power plant of a locomotive equipped with a 12-cylinder General Electric 7FDL engine running on WCS [39].

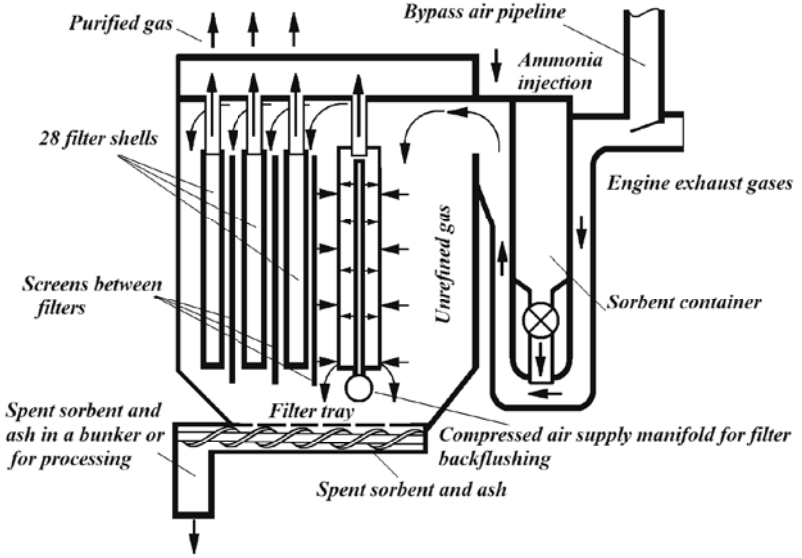

Fig. 9.15. Schematic diagram of a complex filter element for cleaning exhaust gases from engines from sulfur oxides and solid particles

The engine was equipped with an accumulator injection system and diamond-tipped sprayers. The high injection pressure provided by this system enabled efficient combustion of solid fuel throughout the entire test, which lasted approximately 1,000 hours. It was found that NO_x and CO emissions were reduced by more than 90%, and the exhaust gas cleaning system, using sorbents, and reduced sulfur dioxide content by 85%.

The basic diagram of the toxicity reduction and cleaning system for a coal-fueled diesel engine operating in a diesel power plant showed Fig. 9.16.

It includes a high-temperature cyclone collector protecting the turbocharger; reburning after the turbocharger; a heat recovery steam generator; sorbent spraying (slaked lime for SO_2, ammonia for NO_x) at 150°C; a porous filter for final purification from particles and sorbents, NO_x and SO_2 absorbers; an exhaust fan that ensures guaranteed emission of gases through the chimney. The expected characteristics of these devices presented in Table 9.6 [47].

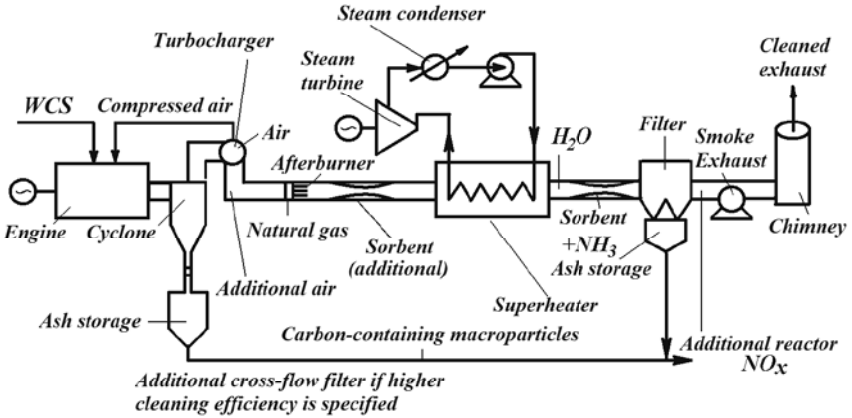

Fig. 9.16. Coal-fueled diesel engine for combined power generation

Table 9.6.

Preliminary performance of an emission control system for a 5 MW coal-fired diesel power plant

Emissions Control System Element	Solid particles, g/(kWh)			SO_2, g/(kWh)			NO_x, g/(kWh)		
	before	after	reduction, %	before	after	reduction, %	before	after	reduction, %
Cyclone (including ash removal)	0.97	0.45	54	1.03	1.03	0.00	1.55	1.55	0.00
Re-combustion	0.45	0.28	36	1.03	0.83	20	1.55	0.62	60
Low-temperature lime spray	0.28	1.64	—	0.83	0.65	20	0.62	0.62	0.00
Porous filter and NH_3 injection (including ash removal)	1.64	0.02	98.8	0.65	0.32	50	0.62	0.39	38

Another configuration may involve placing a reburner before the turbocharger. As noted, reburning is effective in reducing both NO_x and particulate matter. Using natural gas for reburning will dilute the combustion products and reduce harmful emissions by approximately 20%. NO_x

destruction in the reburner flame can reach up to 50%. Furthermore, further combustion of carbon particles expected, with a total reduction of up to 36%. SO_2 reduction occurs through the spraying of slaked lime using porous filters to collect the particles. The porous filters, in turn, increase the contact surface for the reaction between ammonia and carbon-containing particles, which can be catalytically active in this reaction.

***

The above considerations suggest that burning coal-based fuel in piston engines can accomplished without adverse environmental impacts. The development of suitable exhaust gas cleaning methods will result in power plants powered by WCS engines producing less pollution than currently used diesel engines.

Chapter 10.

Layered combustion of solid fuels in reciprocating internal combustion engines

10.1. The method of cyclic gasification of solid fuel in the working space of a piston engine.

In 1993, the American inventor Joseph C. Firey proposed a fundamentally new method of burning solid fuels in the working space of an internal combustion engine – by blowing an air charge through a layer of heated fuel [24]. It should note right away that the design developed by Ferey has a number of significant shortcomings, which are unlikely to allow using solid fuels effectively in the internal combustion engine. The main merit of the inventor is that he first proposed to change the approach to the principle of obtaining a working body for the implementation of a thermodynamic cycle. For quite a long time, the main attention of researchers directed to the burning of finely atomized coal fuel in the volume of the air charge. Ferey proposed to obtain generator gas, and then the products of complete combustion in the working space of the engine by blowing an air charge through a layer of fuel heated to the temperature of activation of oxidation-reduction reactions. The essence of the proposed method illustrated in Fig. 10.1.

Air fills the engine cylinder in the process of gas exchange with the surrounding environment. Solid fuel, preheated to a temperature of about 1000°C, is located in a special remote reactor, which is connected to the working space of the engine through a system of channels. Because of the compression of the air charge in the working cylinder, the initial mass of the charge redistributed between the volumes communicating with the working cylinder. As a result, part of the air enters the primary chamber of the reactor through a special channel, and then the charge passes through the fuel layer and enters the secondary chamber. At the same time, air oxygen enters into a series of successive reactions with heated fuel. The thickness of the heated layer and the distribution of temperatures in it selected in such a way that generator gas formed at the exit from the layer, which fills the secondary chamber of the reactor.

When the piston in the working cylinder moves from TDC to BDC, the generator gas from the secondary chamber of the reactor enters the working cylinder of the engine. At the same time, it can again pass through the fuel layer or directly enter the working cylinder of the engine. Because of repeated passage of gas through the fuel layer, an additional amount of

combustible components formed. The movement of gas flows controlled by means of special gas distribution bodies.

In the working cylinder, the generator gas mixes with the unreacted oxygen of the air in the primary chamber, forming a combustible mixture that ignites with the help of an electric spark or by injecting pilot fuel. Under the action of pressure from the combustion products, the piston makes a working stroke.

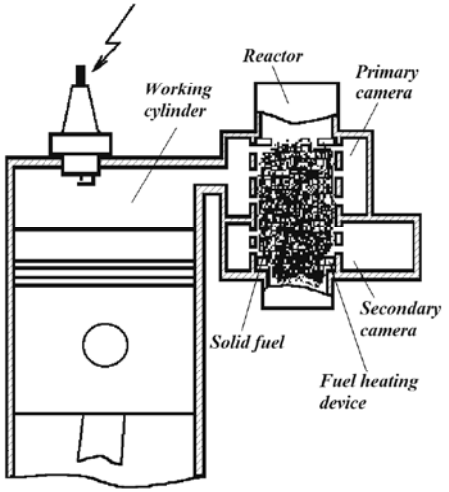

Fig. 10.1. Scheme of the engine with layered combustion of fuel by cyclic gasification and afterburning of generator gas

As already noted, the method described above has a number of significant disadvantages, namely:

– in the process of compression, part of the air, passing through a layer of heated fuel and entering into a reaction with it, heats up significantly, which leads to a sharper increase in pressure. As a result, the negative work of compression increases;

– the fuel combustion process proceeds through a number of intermediate reactions in which heat is not only released, but also absorbed, as a result of which a significant part of it is lost;

– the flow of generator gas from the secondary chamber of the reactor and the formation of a combustible mixture continues throughout the expansion process. As a result, the heat supply stretched over the entire working stroke, which leads to an increase in the temperature of the exhaust gases, reduces the efficiency of heat use, and makes it impossible for the engine to operate according to the most rational thermodynamic cycles.

Despite the listed disadvantages, the layered method of burning solid fuel has good prospects for use in solid fuel internal combustion engines. The fuel, which is located in a layer with a sufficiently high initial temperature, almost immediately enters oxidation-reduction reactions, which allows avoiding the preparatory stages of particle heating during blowing with air. This, in turn, allows reducing the time of pre-flame processes. The specified circumstances lead to a significant increase in the rate of reaction and more efficient use fuel. Thus, layer combustion, provided the method is improved, has a number of significant advantages over bulk combustion.

10.2. The process of layer burning of solid fuel in an internal combustion engine by means of forced purging of the layer.

To reduce the cost of work on compressing the air charge, it is advisable to blow the layer not during the entire compression process, but only when the working piston in the immediate vicinity of TDC. To do this, the reactor must be equipped with a special displacement device that allows forced blowing of the heated fuel layer. At the same time, the control of gas flows inside the working space carried out by redistributing volumes between the primary and secondary chambers of the combustion device according to a predetermined law [23]. This method of controlling gas flows and thermodynamic processes is widely used in Stirling engines, where it has proven itself quite well [27]. Installation of an additional displacement piston in the reactor allows not only to limit the ingress of air charge into the fuel layer during the compression stroke, but also to control the process of heat supply to the working body during the period when the working piston is at TDC, as well as during the expansion process. At the same time, the engine, equipped with a reactor for stratified combustion of solid fuel, may fully or partially retain the ability to operate on liquid fuel.

The above approach allows not only to get rid of most of the disadvantages inherent in the cyclic gasification method considered earlier, but also to obtain significant advantages in the organization of rational burning of solid fuel.

The diagram of an engine equipped with a reactor for stratified combustion of solid fuel by means of forced purging shown in Fig. 10.2, and ego work in Fig. 10.3.

Depending on the organization of gas exchange with the environment, this method is applicable to both two- and four-stroke engines.

In general, the operation of the engine looks like this:

Air fills working cylinder 1 through gas distribution bodies. On the compression stroke, under the action of the piston in the working cylinder 1,

air is forced into the primary (displacement) chamber of the reactor 4 through a special channel 2 equipped with a shut-off device 3, which remains open during the compression stroke. By the end of compression, all or a certain part of the air is concentrated in the primary chamber 4.

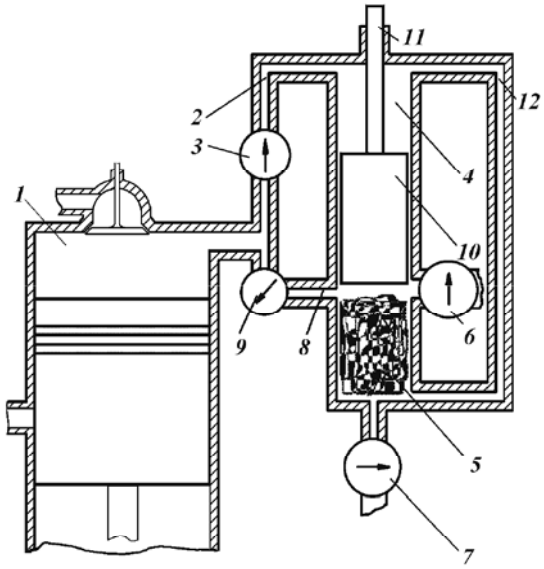

Fig. 10.2. Scheme of the device for supplying heat to the working body by forced blowing of the air charge through a layer of burning fuel: 1 – working cylinder of the engine; 2 – connecting channel of the displacement chamber of the reactor and the working cylinder; 3 – locking device; 4 – primary (displacement) chamber of the reactor; 5 – secondary (burner) reactor chamber filled with heated fuel; 6 – fuel supply device; 7 – ash removal device; 8 – the connecting channel of the reactor combustion chamber and the working cylinder; 9 – locking device; 10 – mechanical air displacer; 11 – displacer drive rod; 12 – connecting channel between the displacement and furnace chambers of the reactor

The combustion chamber is an insulated container, part of which filled with solid fuel. Fuel, with the help of a special device (not shown in the figure), is preheated to the temperature of activation of reactions between combustible components and oxygen in the air. This part is a secondary (fuel) chamber of reactor 5.

In addition to the fuel tank, the secondary chamber 5 is equipped with a device 6 for feeding it to the container and a device for removing ash 7. The design of these devices should ensure the reactor's tightness during the compression cycle and the operating cycle. The secondary chamber 5 communicates with the working cylinder 1 through a special channel 8 equipped with a locking device 9, driven by the crankshaft of the engine (not

shown in the figure). In addition, a device for cleaning combustion products or generator gas (not shown in the figure) can install in the channel.

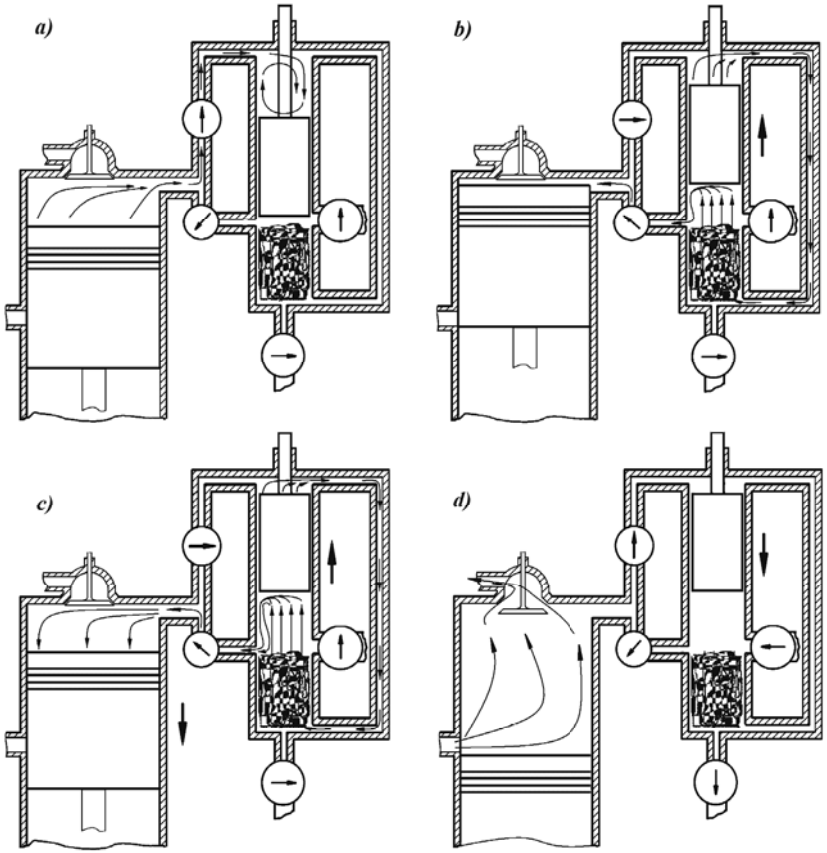

Fig. 10.3. The working cycle of a piston engine with layered combustion of solid fuel by the method of forced blow-by: *a* – compression process; *b* – heat supply; *c* – working course; *d* – gas exchange process of the working cylinder with the environment

The second part of the reactor separated from the first by a displacement piston (displacer) 10. The displacer driven from the engine through a rod 11. The part of the reactor space free from the displacer and solid fuel forms the primary (displacement) chamber 4, where air accumulates during the compression process. At the same time, during compression, only an insignificant part of the air, equal to the volume of the free space between the fuel particles, reacts with the fuel.

In the process of air compression by the working piston 1, the displacer 10 remains motionless (Fig. 10.3 *a*). When the piston in the working cylinder 1 on the compression stroke reaches TDC, the shut-off device 3 of the channel of the primary chamber 4 closes. At the same time, the locking device 9 of the secondary camera 5 is opened (Fig. 10.3 *b*). At the same time, the displacer 10 begins to move, reducing the volume of the primary chamber of the reactor 4 and increasing the volume of the secondary chamber 5. Both reactor chambers communicate with each other through a special connecting channel 12 in such a way that the air displaced from the primary chamber 4 passes through a layer of heated fuel and fills the space vacated by the displacer 10. When passing through the fuel layer, oxygen in the air reacts with combustible components. At the same time, the final product of the reaction can be both generator gas and pure combustion products. The latter largely depends on the thickness of the fuel layer and the temperature distribution in it.

The heat released during the reaction partially used to maintain the temperature regime of the fuel layer, and the main part used to increase the internal energy of the combustion products. This, in turn, leads to an increase in the pressure in the reactor and in the working cylinder 1.

Further, the combustion products through the channel 8, which connects the secondary chamber of the reactor 5 with the working cylinder of the engine 1, through the open shut-off device 9, enter the working cylinder 1, where when the piston moves from TDC to BDC, they perform useful work (Fig. 10.3 *c*).

Then the combustion products are removed through the gas distribution of the engine, after which the cycle is repeated (Fig. 10.3 *d*).

Since all the volumes of the engine and the reactor are constantly communicating with each other, the pressure, accordingly, in all volumes increases approximately the same (if the gas-dynamic resistance of the channels not taken into account). For this reason, the drive of the displacer will not require significant energy expenditure.

For the successful implementation of the working process in a solid-fuel piston engine (SFPE), two basic conditions must meet:

- the thermal inertia of the layer should be sufficient to maintain the solid fuel in an activated state during the period between purges;
- the rate of heterogeneous reactions in the conditions of the of the SFPE reactor should be sufficient to ensure an effective supply of heat to the working body during the time intervals allocated to the purging of the layer.

A special case of implementation of the technology of layer burning of solid fuels by the method of forced purging of the layer is the use of a

displacement piston to control gas flows. A variant of such an engine and the sequence of its operation showed Fig. 10.4.

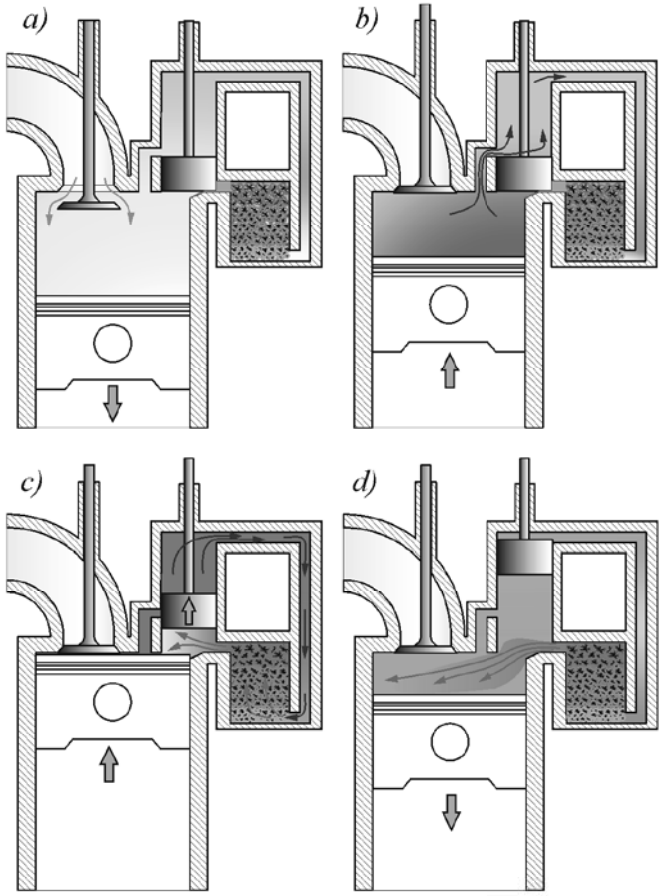

Fig. 10.4 – The working cycle of a piston engine with layered combustion of solid fuel by the forced blowing method: *a* – intake process; *b* – compression process; *c* – heat supply; *d* – power stroke

The first study of solid fuel combustion using the forced-blast bed method conducted at the Ukrainian State Marine Technical University. The experimental portion of the study was conducted on a prototype SFPE, based on a S/D = 5.1/4 piston engine [1, 3-5].

The main parameters of the experimental engine are given Table 10.1, and Fig. 10.5 shows the general view of the installation.

Table. 10.1.

Main parameters of an experimental engine with layered combustion of solid fuel using the forced-blow method

Parameter	Parameter value
Working cylinder diameter, cm	5.1
Working piston stroke, cm	4.0
Displacement volume, cm^3	81.7
Displacement chamber diameter, cm	3.0
Displacement piston stroke, cm	1.4
Displacement chamber volume, cm^3	9.9
Dead volume (volume of connecting channels), cm^3	0.8…1.2*
Combustion chamber volume, cm^3	8
Combustion chamber filling factor	0.6…0.8**
Geometric compression ratio	8.36…8.63*
Actual compression ratio	5.3…7.3(*)**
Forced rotation speed, min^{-1}	120…500

* depending on the type of combustion device.
** depending on the volume of fuel used.

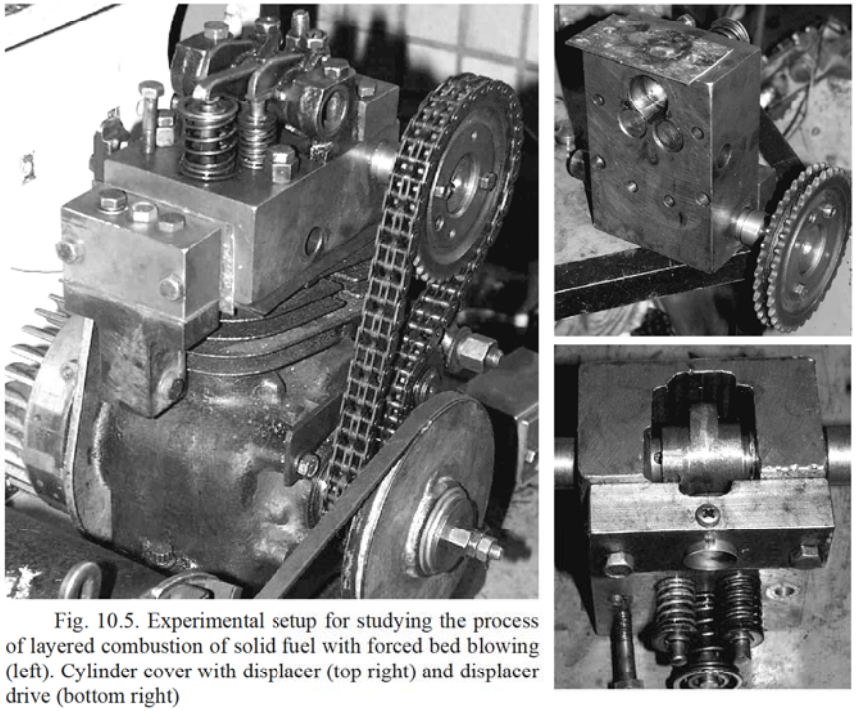

Fig. 10.5. Experimental setup for studying the process of layered combustion of solid fuel with forced bed blowing (left). Cylinder cover with displacer (top right) and displacer drive (bottom right)

The experimental engine's cylinder cover featured a valve timing mechanism driven by a camshaft located in the crankcase, as well as a removable combustion chamber, allowing the same cover to use for experiments with different combustion chamber types. Two combustion chamber designs tested one with a vertical fuel channel, the other with a horizontal one. In the first case, the fuel on the grate held by its own weight; in the second, the grate prevented fuel particles from entering the connecting channel to the working cylinder. In addition to the valve timing mechanism, the cover housed the reactor's displacement chamber with a displacer piston located within it, and the displacer drive mechanism (Fig. 10.5). The displacer drive camshaft was driven a double-row chain from the engine crankshaft. In the design under consideration, gas flow control achieved a displacement piston (Fig. 10.4), which also served as a spool valve. This solution not only simplified the design but also reduced the length of the connecting passages. The latter circumstance is particularly important for reducing heat loss in the passage through which hot combustion products return to the working cylinder, as the small size of the unit precluded the necessary thermal insulation of this passage.

To reduce bed aerodynamic drag, fuel with a narrow particle size distribution used in the experiments. For the main series of studies, fuel particles were obtained by sifting through a 2 mm sieve and then through a 1 mm sieve.

For simplicity of design, both combustion chambers lacked fuel feeders and slag removal devices. Therefore, fuel burnout in the combustion chamber resulted in an increase in dead volume, which significantly distorted the study results. Therefore, all data collected within the first few tens of seconds after the setup started. In order to circumvent grate coking issues, petroleum coke selected as the primary fuel for the experimental trials. With a net heating value of 35 MJ/kg, it had an ash content of approximately 0.3...0.5%. Heating of the solid fuel to the activation temperature of oxidation-reduction reactions accomplished using an electric coil located in the combustion chamber body and in direct contact with the fuel. This accelerated the heating of the fuel to the activation temperature. Inside, all combustion chambers had a ceramic body, which served both as a heat insulator for the combustion chamber and as an electrical insulator.

10.3. Flow of the working process in SFPE with forced controlled blowing of the layer.

Despite the general similarity in the processes occurring in SFPE and ICE, there are some differences, in particular in the thermodynamic processes

of compression and heat supply, as well as in the technological processes of feeding fuel into the reactor combustion chamber and removing ash residues.

10.3.1. Compression process. On the one hand, the presence of fairly long connecting channels between the various volumes of the engine's working space leads to significant losses of initial heat by the air charge. This, in turn, leads to a decrease in temperature and pressure at the end of compression. On the other hand, during compression, the oxygen concentration in all engine volumes increases, causing a certain amount of oxygen to enter from the working cylinder and fill the free space between the heated fuel particles in the reactor's combustion chamber. During this process, the oxygen chemically reacts with the hot fuel particles, resulting in a certain amount of heat being supplied to the working gas. Since all engine volumes interconnected, the additional heat input leads to a sharper increase in pressure and temperature throughout the entire SFPE working space.

These two factors compensate for each other to some extent, but under certain conditions, each can have a predominant effect. Analyzing the specifics of the SFPE thermodynamic cycle, we can conclude that reducing the temperature by removing some of the heat from the air charge not only won't affect the efficiency of the combustion process, but will actually lead to a reduction in the mechanical energy required to compress the air charge. Unlike diesel engines, where combustion is activated the heat of the air charge, and spark-ignition engines, where charge temperature has a significant impact on the quality of mixture formation, in SFPE, the charge temperature at the end of compression doesn't play such a decisive role. Combustion in such an engine activated not by the heat of the air charge, but by the heat accumulated in the fuel bed, and mixture formation in the conventional sense of the term is completely absent. The air temperature at the bed inlet can be quite low without any detriment to the completeness of fuel combustion. Therefore, in SFPE, it is entirely feasible to remove some of the heat from the air charge during its compression, thereby bringing the process closer to isothermal. To remove heat, air flowing from the working cylinder to the displacement chamber can pass through a special heat exchanger or be cooled by spraying water into the air charge. It is interesting to note that the latter method of air charge cooling considered by R. Diesel in his original patent [11, 12].

In an experimental study conducted on a small engine, charge cooling achieved by utilizing the high heat capacity of the cylinder head. To achieve this, the head itself, which houses the channel for airflow from the working cylinder to the displacement chamber, made quite massive. Since each test was relatively short-lived and no layer activation performed (a series of

experiments in which the layer remained cold), the large mass of metal adjacent to the channel ensured effective heat dissipation, especially during the initial stages of the compression process, when the heat flux density remained relatively low.

To reduce charge leakage through the piston rings in this series of experiments, the oil scraper ring replaced with a solid rubber seal.

Figs. 10.6 show the decoded $p\varphi$-oscillograms obtained from five different test series. During this series of experiments, bed purging not performed. To achieve this, the displacer drive disconnected, and the displacer itself fixed in a position corresponding to the maximum volume of the secondary chamber. This allowed us to obtain data on the compression process without the influence of purging (with the displacer drive engaged, purging began before the piston reached TDC, resulting in heat input superimposed on the compression process).

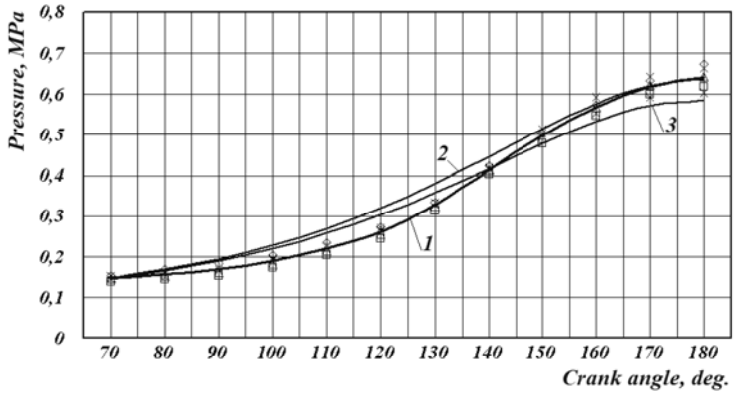

Fig. 10.6. The compression process in an experimental engine with a deactivated layer. 1 – compression line constructed based on the results of 5 experiments; 2 – calculated value of the compression line based on the pressure at the end of the process; 3 – calculated compression line constructed based on the equality of the work expended on charge compression

In addition to the experimentally obtained compression curve, the graphs show the calculated pressure changes, calculated using a standard method based on the average value of the polytropic exponent.

The following trends can noted. At the beginning of the compression process, the heat flux density and temperature change insignificantly. This is because the gas flow, passing through the connecting channel, manages to release a significant portion of its heat. As the flow density increases, despite the rising temperature and increasing thermal gradient, the heat transfer rate is insufficient effectively remove heat from the gas flow. Consequently, the

pressure curve begins to rise sharply, approaching the analytically obtained curve.

Due to the redistribution of the air charge mass between the engine volumes during compression, some air enters the interlayer space between the fuel particles. At this point, atmospheric oxygen undergoes oxidation-reduction reactions, releasing heat, leading to unproductive fuel combustion and a more intense pressure increase.

Fig. 10.7 shows the pressure change pattern during the compression process with an activated fuel bed. Otherwise, the experimental conditions were the same as in the previous case.

Analysis of the diagrams shows that, under the conditions under consideration, the charge cooling process predominates over heat addition in the bed. In earlier experiments with larger fuel sizes, heat addition due to fuel burnout in the bed observed to have a predominant effect on pressure changes [1]. Thus, the bed density, as well the combustion chamber size, significantly influence the compression process in SFPE. In general, heat addition during compression leads to a more intense pressure increase.

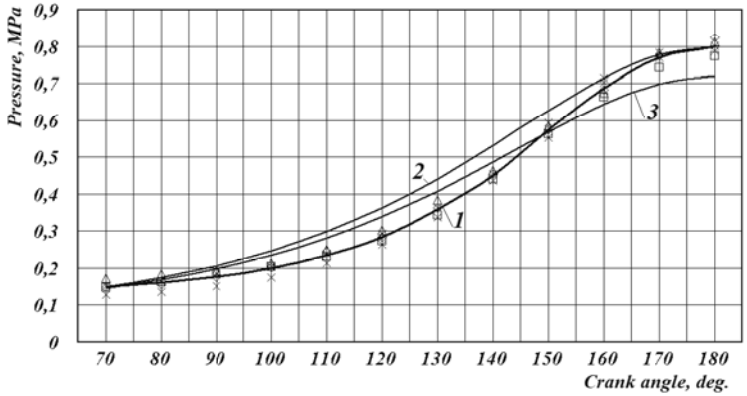

Fig. 10.7. The compression process in an experimental engine with an activated layer. 1 – compression line constructed based on the results of 5 experiments; 2 – calculated value of the compression line based on the pressure at the end of the process; 3 – calculated compression line constructed based on the equality of the work expended on charge compression

Air ingestion into the bed during the compression stroke is a parasitic factor, which is why reactor design must incorporate a range of measures to reduce unproductive fuel burnup.

As calculations show, the fuel bed density, as well as the ratio of the initial volumes of the reactor's displacement chamber to the combustion chamber, significantly influence the compression process. Reducing the fuel

bed density and increasing the combustion chamber volume leads to increased compression losses and unproductive fuel burnup.

Based on the analysis presented in [1], several ways to reduce unproductive fuel burnup during the compression process can identified.

Losses can reduce in several ways. One is to increase the density of the fuel bed. This will reduce the volume of free space between fuel particles – V_{fuel}. However, increased density leads to increased aerodynamic drag of the fuel bed, which largely depends on the geometric parameters of the combustion chamber. This latter circumstance allows for some flexibility in the choice of a specific design.

A second approach is to increase fuel density by creating a «boiling» bed. At a specific flow velocity, the bed transitions into a pseudo-boiling state, this shift characterized by a significant reduction in drag as the particles become suspended. In other cases, including during the compression stroke, fuel particles, under their own weight, packed tightly onto the grate of the reactor combustion chamber.

A third approach is rationally utilizing the engine's «dead volumes» associated with the combustion chamber. Specifically, distribute the "dead volumes" of adjacent channels relative to the combustion chamber so that during the compression stroke, the combustion chamber fed not by fresh propellant but by residual gases from the connecting channels, which contain significantly less oxygen. As a result, pre-combustion will be less intense.

A fourth option is to install an additional shut-off device that will restrict the air charge from entering the reactor combustion chamber during compression. This approach may prove the most efficient, but its use complicates the design of both the reactor itself and the engine as a whole.

10.3.2. The process of heat supply. As analysis shows, the factors operating in SFPE elevated pressure and temperature, high concentrations of reactants, and forced fuel bed blowing lead to accelerated oxidation-reduction reactions. This, in turn, promotes more efficient fuel burnout in SFPE reactor conditions. However, all known studies of layer combustion have focused primarily on steady-state bed blowing. Therefore, before discussing the feasibility and effectiveness of layer combustion of solid fuels in internal combustion engines, it is necessary to determine how combustion will proceed in the bed during pulsed blowing. This is especially important, as the bed cools during pauses between blowing cycles, which could potentially lead to a decrease in the activation energy of fuel particles and a complete cessation of combustion. To a significant extent, the loss of bed activity depends not only on the pause time between blowing cycles, but also on the quality of the combustion chamber thermal insulation, the bed parameters,

and a number of other factors. In a SFPE combustion device, the active bed blowdown time can be 12 to 25 times shorter than the pause time for four-stroke engines and 6 to 12 times shorter for two-stroke engines.

Preliminary test results performed on an experimental setup (Fig. 10.5) demonstrated that the combustion rate of coal fuel in forced blowdown mode is sufficient effectively supply heat to the working fluid during engine operation. Bed cooling did not occur even at the minimum engine speed (120 min^{-1}). Thus, it established that the bed's inertia allows it to maintain in an activated state even when the pause time between blowdowns is ten times shorter than the blowdown time itself. As the speed increased to 480 min^{-1}, an increase in temperature observed in the reactor's combustion chamber, indicating an increase in reaction rates the bed.

Fig. 10.8 shows the oscillogram decoding results, and Fig. 10.9 shows a fragment of the pV-diagram for the process under consideration.

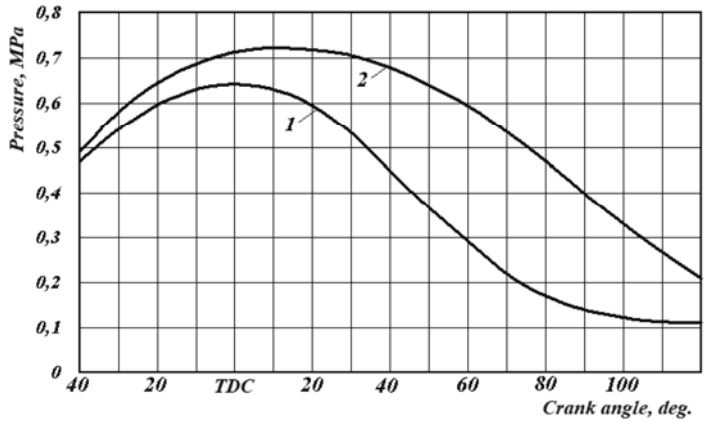

Fig. 10.8. Heat supply in experimental SFPE: 1 – layer not activated; 2 – layer activated

The oscillogram decoding results show that during solid fuel combustion in the SFPE combustion device, heat input occurs almost isobarically over a range of 180° to 220° of crankshaft rotation.

The measurement instruments used did not allow monitoring the change in cylinder pressure until the engine exhaust valve opened. However, during fuel combustion experiments in the combustion device, supersonic pops were heard when the exhaust valve opened, indicating that the pressure at which the exhaust valve opened was at least 0.182 MPa. To avoid errors due to charge leakage, the compression ratio of the setup for this series of experiments was limited to 4.3 to 4.6.

The studies described above, despite the limited amount of data obtained, nonetheless allow us to answer a number of key questions related to the implementation of layer combustion in piston engines. Their results indicate that the solid-fuel piston engine's operating process has a positive work balance, confirming its operability. Fuel ignition and combustion occur stably over a wide range of scavenging conditions, which makes it possible to implement a layer combustion process in low- and medium-speed engines, and potentially in high-speed engines.

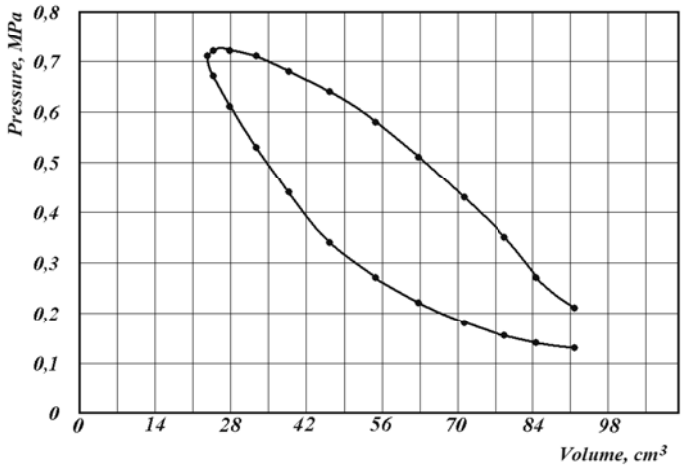

Fig. 10.9. Fragment of a *pV*-diagram of the working process in an experimental engine

10.3.3. The influence of the layer blowing mode on the nature of heat supply in the thermodynamic cycle. The heat input feature associated with forced bed blowdown allows for the implementation of various thermodynamic cycles in SFPE, both those implemented in conventional internal combustion engines and those specially designed [5]. The primary factor influencing the nature of heat input is the phase relationship between the displacement piston and the working piston. Since the working piston moves according to a predetermined relationship, the problem reduced to determining the law of displacement of the displacer piston.

When considering both ideal and real processes (except isochoric), the amount of heat supplied to the working fluid is determined by the amount of oxygen passing through the heated fuel bed. As the working piston moves, the oxygen concentration in all engine volumes changes. Consequently, at each discrete interval, the displacer must move relative to the working piston, accounting for the change in the volumetric oxygen concentration.

10.4. The process of feeding fuel into the SFPE combustion device.

Unlike the volumetric combustion of solid fuels, the bed method involves a large quantity of fuel in the combustion process, sufficient to complete several dozen or even hundreds of combustion cycles. The onset and nature of heat transfer to the working fluid are independent of the fuel injection process, but determined by the onset and nature of forced purge. These circumstances indicate that fuel can supply to the combustion chamber independently of the combustion process or synchronously with periods when the pressure in the combustion cycle is low (for example, during the exhaust or intake process). This will significantly reduce the requirements for fuel supply and ash removal devices. Currently, it is difficult to predict what these devices might look like. However, it can be stated with a reasonable degree of certainty that these devices will have lower requirements than fuel supply devices for engines operating on suspensions or diesel fuel.

The chemical industry has accumulated extensive experience in creating such devices and systems for feeding bulk materials into high-pressure cavities. Here, relatively large volumes of various bulk solids (catalysts, reagents, reaction products) are continuously fed to and withdrawn from reaction columns operating under pressures of up to 20 MPa. Certainly, some of this experience can be used in the design of fuel feed and slag removal devices for the SFPE reactor.

Fig. 10.10 shows a diagram of a slide valve device for feeding fuel into the reactor.

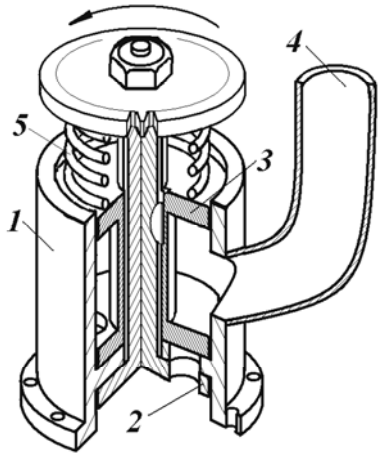

Fig.10.10. Spool valve device for feeding solid fuel into the engine reactor without depressurization. 1 – housing; 2 – lower spool washer; 3 – upper spool; 4 – channel for feeding solid fuel; 5 – pressure spring

Fuel flows under its own weight through channel 4 into the cavity formed by the upper slide valve and the device body. Some of the fuel enters the opening in the upper slide valve washer. As both slide valves rotate together, the opening in the upper slide valve aligns with the opening in the middle slide valve washer, which is integral with housing 1. As a result, fuel spills into the cavity between the housing and the lower slide valve. The opening in the housing then aligns with the opening in the lower slide valve washer 2, causing the fuel to spill into the combustion chamber. The slide valves pressed against the middle slide valve by spring 5. Thus, the fuel alternately sluiced relative to the central slide valve. The capacity of the feeding device depends on the size of the openings in the slide valves and their number on each slide valve.

This device allows fuel to feed into the reactor combustion chamber without depressurizing it. Despite this, it is desirable to synchronize the rotation speed of the spool valves so that the opening in the lower washer aligns with the opening in the middle washer when the cylinder is not at maximum pressure.

A device for removing ash residues from the reactor can have a similar design.

In addition to continuous fuel supply, intermittent fuel supply to the reactor can use. In this case, the reactor is equipped with two combustion chambers that operate and replenished with fuel alternately.

10.5. Fuels for layer combustion in SFPE.

As has been noted previously, during the volumetric combustion of solid fuels, especially in coal-fired combustion systems, volatile components play a decisive role in the autoignition and combustion process. Therefore, when selecting feedstock for preparing slurries, preference should give to bituminous coals, which have a sufficiently high volatile content and an acceptable calorific value. All other things being equal, the use of these coals, whose calorific value is 2.5 to 3 times lower than that of diesel fuel, leads to an increase in absolute fuel consumption. When such an engine used in a vehicle's powertrain, the increased fuel consumption reduces its autonomy. This is a significant drawback of the volumetric combustion method. Furthermore, the preparation of coal dust requires significant energy for grinding, which increases the cost of pulverized coal fuel.

With layered combustion, the fuel is constantly in an activated state, and volatiles do not have a decisive influence on the combustion process. Therefore, high-calorific solid fuels of both natural (anthracite) and synthetic (coke) origin are most suitable for bed-fed combustion. The absence of a

liquid carrier eliminates the need for inert ballast (as is the case with WCS), which also leads to a reduction in absolute fuel consumption.

As already, noted, bed-fed combustion requires fuel consisting of large pieces (from a few millimeters to several centimeters, depending on the engine type) of approximately uniform size. Therefore, to obtain the required fractions, it is sufficient to crush the feedstock fuel a process that is less expensive than grinding to produce coal dust. After crushing, the feedstock fuel can sieved through sieves of varying mesh sizes to select the desired fractions. The remaining fuel after sifting can be ground and burned in stationary pulverized coal-fired boilers.

The main drawback of this fuel production method is the difficulty of removing mineral impurities during production. Current fuel enrichment methods mostly rely on pre-grinding. However, fuel combustion in SFPE occurs outside the engine cylinder, and the bed itself acts as a filter. This results in a significant portion of the resulting ash remaining in the combustion chamber, from where it can remove. Furthermore, as hot combustion products flow from the combustion chamber to the working cylinder, gases can hot cleaned, for example, using insulated microcyclones.

In some cases, it may be practical to use special granulated solid fuel obtained from purified coal dust. This will minimize the ash content of the fuel, but will significantly increase its cost.

Regardless of the type and method of fuel production for bed-fed combustion, it can produced using existing technologies that have mastered on an industrial scale, which could facilitate the rapid implementation of bed-fed combustion.

10.6. The burnout process of solid fuel in a SFPE reactor.

10.6.1. General characteristics of the solid fuel combustion process. Layer structure. Given that the process of solid fuel combustion in a bed has not yet considered for internal combustion engines, it makes sense to briefly review its specific features and examine the specialized terminology associated with the bed combustion process.

As already noted, the process of generating the working fluid during bed combustion of solid fuel in an SFPE reactor can carried out in a single-stage or two-stage manner. In single-stage combustion, the interaction of atmospheric oxygen and fuel carbon produces complete oxidation products, which expand directly in the working cylinder. In two-stage combustion, complete oxidation products are formed first, and then, as result of their interaction with fuel carbon, a generator gas is formed, which is forcibly ignited and burns in the engine's working space. For single-stage combustion,

the interaction between fuel and atmospheric oxygen can represented as follows: air, forced out of the primary reactor chamber, passes through the grate openings, enters a layer of hot slag, and, heated there, enters the coke-burning zone. Here, oxygen reacts with the fuel carbon, forming primarily carbon dioxide and a relatively small amount of carbon monoxide. As the air moves along the bed, its carbon dioxide and carbon monoxide content increases. This accompanied by an increase in the temperature of the gas mixture and a decrease in its oxygen content. The section of the bed where reactions between atmospheric oxygen and solid fuel occur called the oxygen zone. With single-stage heat input, the removal of combustion products from the reactor to the working cylinder must occur immediately after the oxygen zone.

With two-stage combustion, the thickness of the fuel layer on the grate must maintain above the oxygen zone. In this case, the burnout process leads to the complete disappearance of free oxygen. The carbon dioxide content increases to a certain maximum, and the temperature rises to 1500...1600 °C [22, 30]. In the absence of oxygen, the resulting carbon dioxide begins to react with the carbon in the coke located above according to the reaction:

$$CO_2+C=2CO.$$

As a result, the carbon dioxide content of the gases passing through the bed begins to decrease, while the amount of carbon monoxide rapidly increases. The section of the bed where carbon dioxide reduction occurs called the reduction zone. Because the reaction proceeds with heat absorption, the temperature in the reduction zone begins to decrease. The reaction ends with the almost complete reduction of CO_2 to CO.

Above the reduction zone begins a zone of inert, heated coke, through which passes a gas mixture consisting of approximately 34% carbon monoxide and 65% nitrogen. In this zone, no reaction occurs between the gaseous products and the carbon in the coke. As result of heat exchange with the gas flow, the coke acquires the temperature of the gaseous products.

Above the heated coke zone is a layer of freshly charged fuel, where drying and gasification occur under the influence of the sensible heat of the generator gas. Volatile fuel substances and evaporated moisture added to the gas flow. The resulting oxygen-free mixture escapes into the space above the bed and then into the engine's working cylinder. Mixing with residual air, the generator gas forms a combustible mixture, which ignited by an electric spark or by pilot fuel injection.

Both of the above methods can, in principle, implemented in a SFPE; however, for a number of reasons, listed below, preference should give to the single-stage combustion method:

- combustion of fuel only within the oxygen zone allows for a reduction in the bed height, and consequently, the dimensions of the combustion device. This is a significant advantage not only in terms of weight and size, but also in terms of reducing the intralayer space, which, as has been shown, leads to unproductive fuel burnout during the compression process;
- reducing the volume of fuel used reduces unproductive heat loss to the combustion chamber walls;
- the production and subsequent expansion of the products of complete combustion allows for the complete elimination of the forced ignition system of the gas-air mixture, simplifying the overall engine design;
- obtaining complete combustion products through forced blowdown allows for control of heat input and the implementation of the most efficient thermodynamic cycles in the engine.

Based on the above considerations, further attention will paid to the combustion method that produces the working fluid directly at the bed exit.

10.6.2. Methods of organizing layered combustion of fuel in a SFPE reactor and their influence on the rate of formation, composition and properties of combustion products. Combustion of solid fuel in a combustion engine reactor can accomplish in several ways. The choice of the appropriate combustion system influences not only the design of the reactor's combustion chamber but also the combustion rate, composition, and characteristics of the resulting working fluid.

A combustion system where fuel fed into the reactor from above and retained on the grate by gravity, while air purges the bed from below, defined as counter-current combustion [22]. This system is relatively simple and ensures stable ignition by introducing fresh fuel into the hot burning bed. In this process, newly incoming fuel particles heated, dried, and ignited by the heat transferred by the flow of hot gases leaving the active combustion zone, as well as by radiation from the bed and flame.

A disadvantage of this combustion method is that increasing the purging rate leads to active rearrangement of the fuel particles and an increase in the removal of increasingly larger particles from the bed. Relatively large fuel particles no longer have time to burn in flight within the combustion chamber, leading to a sharp increase in mechanical underburning and the entry of unburned particles into the engine's working cylinder. Upon reaching a certain blowdown velocity, the entire bed transitions to a fluidized state, characterized by the random movement of particles over the grate surface. Loss of aerodynamic stability in the bed is the main factor preventing an increase in the heat density of the combustion zone in the reactor, limiting the speed of combustion processes in the SFPE reactor. With counter-current

combustion, fuel with a narrow particle size distribution is preferable to reduce the carryover of fine particles.

Another bed combustion scheme that can implemented in an SFPE reactor is clamped-bed combustion. With this method, fuel fed into the reactor and blown either from one side or crosswise. In this case, the fuel pressed against the grate not only by gravity but also by aerodynamic resistance to the oncoming flow of scavenging air. In this case, the grate prevents disruption of the bed's aerodynamic stability at increased blowdown rates [22]. Combustion products generated in this combustion method formed within the oxygen zone, so they are virtually free of volatile components and products of incomplete combustion at the bed outlet, and have a relatively high temperature. The furnace shaft can be either horizontal or vertical. Furnaces of this type significantly enhance combustion acceleration and increase the bed blowdown rate, thereby reducing blowdown time and increasing the rate of heat supply to the working fluid. Since the grate elements in this combustion system are located in the high-temperature zone, the use of special heat-resistant materials is necessary for their long-term operation.

10.6.3. The process of combustion of solid fuel within the oxygen zone. Unlike steady state, bed-fed combustion processes, in SFPE, the air charge blown through the fuel bed periodically. The nature of combustion and the rate of chemical reactions depend significantly on the chemical activity of the fuel, its fractional composition, ballast content, the behavior of the oxidation zone and coke residue, bed parameters, the frequency and method of blowing, and a number of other factors.

During single-stage countercurrent combustion of solid fuel in an SFPE reactor, the gas flow passing through the fuel bed resting on the grate must ensure both complete combustion of the coke in the bed and complete combustion of volatiles in the combustion space above the bed. During combustion, products of complete combustion, unburned products of thermal decomposition, and small fuel particles carried into the combustion space. These particles then burned out in the space above the bed or in the working cylinder. Based on this, the size of the fuel particles and the blowdown rate must be selected to avoid losses due to chemical and mechanical incomplete combustion and, especially, to avoid the removal of fuel particles into the engine's working cylinder. For effective afterburning of the products of incomplete combustion and coke particles, the mixture of gaseous products that have passed through the burning coke bed and exited into the above-bed space must contain a sufficient amount of oxygen. This can achieve by removing the gas mixture from the bed before the end of the oxygen zone or

by organizing a secondary blow along the bed surface. With this combustion organization, the reducing zone is completely absent, and a zone of inert coke is located immediately above the oxidizing zone. Newly incoming fuel ignites primarily under the action of heat transferred by the underlying layer of hot burning coke [22, 26]. This ignition is quite effective, since it occurs as result of the combined action of heat transferred by conduction from the burning particles and heat transferred by convection from the heated gaseous combustion products. In addition, the loaded fuel ignited by the heat emitted by the flame of volatile substances burning in the interlayer space. The combined effect of all of these factors leads to the effective activation of newly introduced fuel. Favorable ignition conditions determine the ability to efficiently burn solid fuel in a reactor, even with high humidity.

In terms of combustion intensity and rate, the bed process offers significant advantages over other methods of burning solid fuel in internal combustion engines. Forced blowing of the bed enables high relative velocities to achieve between the filtered gas flow and the bed skeleton. This, in turn, significantly reduces diffusion resistance and transfers the combustion process to the high-temperature kinetic region. Estimates of the combustion surface intensity for stationary bed combustion devices show that the bed has an almost fifty-fold reserve compared to the achieved limit values [22]. Several key prerequisites enable a significant increase in combustion intensity within the SFPE reactor: a high volumetric concentration of combustible material, where dense particle packing provides mutual thermal shielding; the achievement of high relative velocities between the air and the burning particles; and the elevated oxygen concentration and pressure resulting from the compression of the working fluid.

The combined effect of the above factors results in a significantly higher rate of heat and mass transfer in a bed than during bulk combustion of solid fuel in the working space of an internal combustion engine. This facilitated by the high velocities of the purge airflow relative to the stationary fuel, well as the turbulent effect of the bed. Particles entering the reactor combustion chamber intensely heated, during which they are dried. As the temperature increases, complex chemical processes begin within the particle, accompanied by the decomposition of unstable organic compounds with the release of volatiles. The particle becomes more porous, its internal surface and pore size change. The flow of volatile components actively interacts with the incoming oxygen flow, preventing the interaction of oxygen with the coke residue. When the particle is heated to a temperature of 800...850°C, the release of volatiles almost completely ceases, and its coking is completed [22, 30, 31]. At bed heights within the oxidation zone, the presence of free

oxygen leads to ignition and combustion of volatiles above the bed surface. Intense heat and mass transfer between the particles and the gas flow leads to a rapid increase in the surface temperature of the coke residue. As the release of volatiles ceases, the carbon in the coke residue begins actively, interact with the residual oxygen in the purge air.

It is difficult clearly define the oxygen zone boundary in the bed, as these boundaries overlap due to the bed's structural features. This is especially challenging under conditions of periodic fuel purge, as the parameters of the purge agent vary not only along the bed's thickness but also over time. At the same time, as already noted, ensuring combustion in the SFPE reactor confined to the oxygen zone is crucial. The absence of reducing reactions determines the purity of the combustion products at the bed outlet. The maximum working fluid temperature, as well as the maximum carbon dioxide content the combustion products; correspond to the end of the oxygen zone.

Under the influence of high temperatures, the ash of most fuels melts. The resulting slag droplets flow downwards, counteracting the flow of combustion products and air, entering a region of lower temperatures. Intense heat exchange with the comparatively cold oncoming flow leads to the solidification and granulation of the slag in the lower sections of the layer [22]. Gradually, the slag granules fall beneath the grate, where they accumulate. Slag removal from the combustion chamber can perform either continuously or periodically.

10.6.4. The rate of reactions in the layer. A comparison of the individual stages of particle combustion reveals that, in both bulk and bed combustion, the burnout stage of the carbon in the coke residue takes the longest time. Oxygen, with its high chemical activity, plays a key role in fuel combustion. Most of the bed's height occupied by the carbon burnout zone. Depending on a number of factors, the reactions within the oxygen zone can vary.

At low blowing rates and high temperatures, typical of most of the coke burnout zone in bed combustion, secondary reactions are active. These reactions result in the final combustion products being formed not on the surface of the coal particle, but at some distance from it. The region in which gas-phase reactions occur, called the boundary layer. In this combustion mode, oxygen does not reach the carbon mass, but diffuses into the boundary layer. Under these conditions, the large thickness of the diffusion zone and the high process temperature result in an intense homogeneous CO afterburning reaction at the boundary of the gas zone. Carbon combustion proceeds solely via a reduction reaction.

$$C + CO_2 = 2CO.$$

These conditions for carbon particle combustion called a burning boundary layer [31]. The particle combustion rate in this case is independent of the rate of surface reactions, but determined by the rate of oxygen diffusion. Thus, at low flow rates, the combustion process is diffusion-based.

During intense flow, the boundary layer collapses due to the high relative velocity of the gas flow. In this instance, the rate of carbon combustion primarily governed by the mass transfer between the gas flow and the surface of the particles. Atmospheric oxygen directly reacts with the carbon, and the rates of chemical combustion reactions become so high that they pose virtually no limit to the particle combustion rate. Thus, with increasing flow rate and oxygen volume concentration, the combustion rate increases significantly, and the combustion process enters the kinetic region [22]. In this case, the combustion rate is determined not by the rate of oxygen diffusion, but by the rate of surface reactions. Simply put, the carbon combustion rate depends on the rate of oxygen supply to its surface and the rate of removal of reaction products. Consequently, with intensive blowdown, the rate of heat input into the SFPE reactor depends significantly not on the oxygen diffusion rate, as occurs with volumetric combustion, but on the gas flow parameters and velocity. Shifting the coke carbon combustion process from the diffusion to the kinetic region offers a significant potential for increasing the heat release rate in the SFPE reactor.

Numerical assessment of the influence of solid fuel combustion reaction rates on the heat release process in solid fuel piston engines and the nature of the working process. The fundamental feature of the SFPE working process is that the fuel burned not in the working cylinder, but in a special remote device – a reactor, which consists of a reactor and a displacement chamber separated by a displacement piston, which simultaneously performs the functions of a spool distributor.

As already noted, the peculiarities of the organization of the working process in SFPE lead to the fact that the charge temperature at the end of compression not of fundamental importance and can reduced by cooling it during compression, for example, by spraying water in the space of the working cylinder. This allows you to reduce the cost of work on compression and bring the process closer to isothermal, as well as implement the Miller cycle working process in such engines, without the need to obtain a sufficiently high temperature at the end of compression sufficient for self-ignition of liquid fuel.

The presence of a displacement piston allows, by changing the law of its motion, to optimize the heat supply process to obtain maximum efficiency of the thermodynamic cycle.

The main limiting factor determining the efficiency of the combustion process in the engine under consideration is the rate of fuel burnout reactions in the engine's reactor chamber. Because piston engines provide a very limited duration for combustion, it is essential to compare the ideal heat release profile (Q_{comb}) against the actual chemical reaction rates (Q'_{comb}). This comparison determines whether the fuel can burn fast enough to satisfy the requirements of the thermodynamic cycle.

In other words, Q'_{comb} the maximum possible rate of reaction under given conditions limited by the laws of chemical kinetics, and Q_{comb} is the heat release associated with the supply of the oxidant to the reactor surface, i.e. a purely physical process associated with the rate of purging the fuel layer by means of a displacing piston. It is clear that in the case of physical processes prevailing over chemical processes, the release rate Q_{comb} will be greater than Q'_{comb}, the oxygen supplied to the phase interface will not have time to react completely with carbon, because of which incomplete combustion products will formed at the exit from the layer. Thus, the condition for effective combustion of solid fuel in SFPE is the superiority of the limitations of the rate of heat release of a chemical nature over the limitations of a physical nature, i.e. Q'_{comb} must be greater than Q_{comb}.

It is clear that the inherent reaction rates (in the case under consideration, reactions 7.5, 7.6, 7.8) must be greater than the theoretical rate of heat supply in the thermodynamic cycle. Otherwise, it will be impossible to obtain the final reaction products and effectively use the heat from fuel combustion. The process of solid fuel burnout on the surface of a coking coal massif proceeds through a number of intermediate reactions; however, to determine the fuel burnout rate, it is sufficient to estimate the rate of reactions that occur on the phase interface. As the above analysis showed, these reactions limit the rate of the burnout process. The method for determining the rate of reactions on the surface of the coking coal massif given in subsection 7.7. The study of the influence of these factors on the nature of the thermodynamic cycles in the SFPE can be performed numerical modeling of the physicochemical processes occurring in the engine working space using the considered method. To date, such studies have conducted only for pulverized coal fuel. To assess the influence of the rates of limiting reactions of solid fuel burnout in the SFPE working space on the theoretical heat release rate Q'_{comb}, a submodel for calculating reaction rates was developed using the method described above. This submodel integrated into the SFPE working process model, which allowed not only to determine the theoretical rates of the fuel burnout process based on the main reactions of the interaction of combustible components of solid fuel with air oxygen, but also to assess the influence of

the kinetics of these reactions on the rate of their occurrence in the SFPE working space.

The following are the results of the modeling performed to assess the influence of the rates of combustion reactions (7.5, 7.6, 7.8) of solid fuel on the heat release process in SFPE and the nature of its working process.

To assess the influence of the theoretical rates of Q'_{comb} reactions on the fuel burnout process, the working process of a small-sized high-speed four-stroke engine simulated, the main characteristics of which given in Table. 10.2.

Table 10.2

Input data for workflow modeling

Parameter	Value	Parameter	Value
Cylinder diameter, m	0,105	Residue gas temperature, K	910,0
Piston stroke, m	0,11	Residual gas pressure, MPa	0,123
Working volume, dm^3	0,952	Residual gas coefficient	0,039
Part of lost stroke	0,0450	Engine inlet pressure, MPa	0,103
Combustion chamber volume, dm^3	0,063	Inlet pressure loss, MPa	0,022
Geometric compression ratio	16	Inlet end pressure, MPa	0,081
Actual compression ratio	15,31	Filling coefficient	0,667
Speed, min^{-1}	1800	Inlet air density, kg/m^3	0,782
Ambient pressure, MPa	0,103	End of gas exchange temperature, K	360,5
Ambient temperature, K	293		

The results of the study of the process of burning solid fuel during bed purging shown Fig. 10.11. In the case under consideration, it assumed that purging (displacer movement) begins 18° before TDC and ends 42° after TDC.

A characteristic feature of the heat release process in a SFPE is that during compression the density of the gas phase increases. This leads to an increase in the oxygen concentration at the boundary of the solid phase and unproductive burning of part of the fuel in the reactor chamber. As a result, the increase in pressure and temperature on the compression line is more intense than during compression in classical piston engines. Thus, now of the start of purging, a certain amount of heat already been supplied to the gas phase. With the start of purging, the forced supply of the gas phase to the surface of the fuel particles begins. As a result, surface reactions (7.5, 7.6) and reactions at the boundary of the gas reactor zone (7.8) intensify.

As can be seen from the figures presented in Fig. 3.15 graphs, with the start of purging, the theoretical intensity of heat release Q'_{comb}, limited by the reaction rates, increases much faster than the amount of heat Q_{comb} required for the thermodynamic cycle to proceed according to the given law.

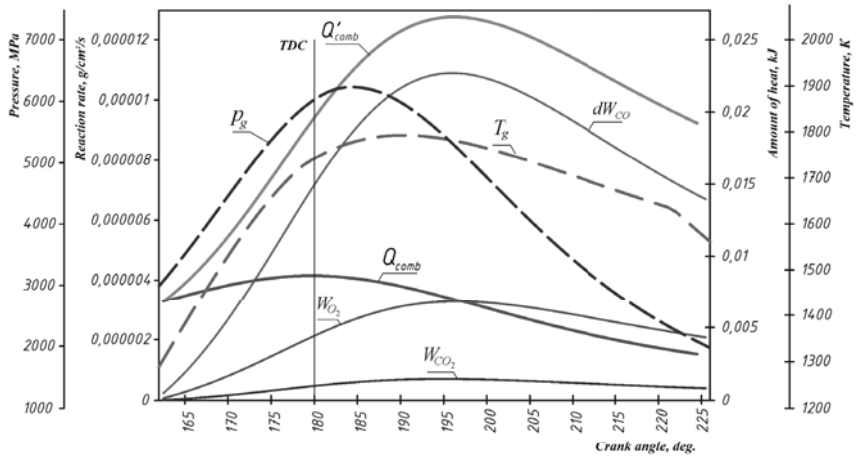

Fig. 10.11 – Results of modeling the process of burning solid fuel during bed purging

The maximum speed for reaction (7.5) reached 14° after TDC, and for reaction (7.6) – 16°. The maximum heat release corresponds to the same range.

Changes in the elemental composition and properties of the gas phase in the engine cylinder during the cycle presented in Fig. 10.11.

The molecular weight of the gas mixture and its gas constant depend only on the partial pressures of the individual components that make up its composition, while the molecular heat capacity has a rather strong dependence on temperature.

During compression, the consumption of oxygen and the concentration of reaction products in the layer lead to a decrease in the molecular weight of the charge.

During the purging of the layer, due to fuel burnout reactions in the reactor (7.5, 7.6, 7.8), the amount of oxygen in the gas mixture begins to decrease intensively and the CO_2 content increases. The gradual saturation of the gas mixture with carbon dioxide CO_2 with a molecular weight of 44 g/mol leads to an increase in the molecular and total mass of the entire mixture (Fig. 10.12).

After the completion of the layer purge, the composition, molecular weight and gas charge constant stabilize, and only the molecular heat capacity continues to decrease with a decrease in the temperature of the gas mixture (Fig. 10.12). It should noted that the considered model does not take into account the influence of forced layer purge on the stability of the

diffusion region; however, obviously, the role of diffusion processes during purge will weaken.

The turbulizing effect of the layer and the high speed of the airflow around the solid fuel particles will contribute to a decrease in the thickness of the diffusion region, increasing the rate of penetration of the oxidant to the surface of the coking coal massif. However, at this stage of the study, the lack of experimental data does not allow us to assess the degree of influence of this factor on the rate of reactions.

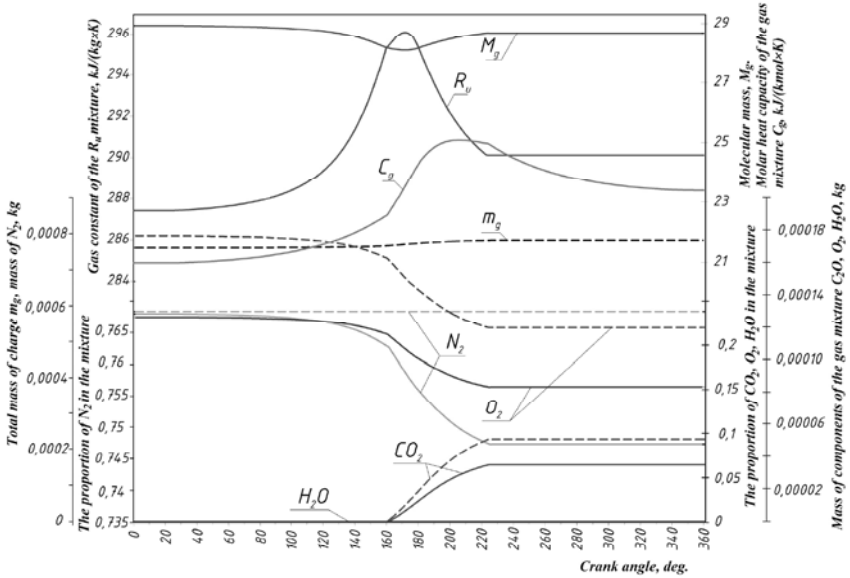
Total mass of charge m_g, mass of N_2, kg
Gas constant of the R_u mixture, kJ/(kg·K)
The proportion of N_2 in the mixture
Molecular mass, M_g
Molar heat capacity of the gas mixture C_g, kJ/(kmol×K)
The proportion of CO_2, O_2, H_2O in the mixture
Mass of components of the gas mixture CO, O_2, H_2O, kg
M_g
R_u
C_g
m_g
N_2
O_2
CO_2
H_2O
Crank angle, deg.

Fig. 10.12. Change in the properties and composition of the gas phase during the thermodynamic cycle

Based on the results of modeling the solid fuel burnout process in the SFPE reactor with determination of the limiting reaction rates, a number of conclusions can drawn:

- for the considered case, conditions are created in the working space that ensure the rate of surface reactions of solid fuel burnout, which is 2.3 times higher than the rate of heat supply required for the implementation of the thermodynamic cycle;

- the results of modeling the working process of a high-speed engine allow us to assume that in other types of ship engines, in which the time allocated to the combustion process is much greater (by an order of magnitude in medium-speed engines and by two orders of magnitude in low-

speed engines), the limitations associated with the reaction rates will not affect the efficiency of fuel burnout in any way;

- the use of supercharging, which is characteristic of the vast majority of modern engines, leads to an increase in the concentration of reacting components on the reaction surface, which leads to a shift in the kinetic constants of reactions towards their acceleration;

- given the results obtained, it can be assumed that when calculating the combustion process of solid fuel, the amount of heat released in the forced blowing section can be determined based on the thermal effect of the main reactions without taking into account the limitations on their rate of occurrence. That is, the main limiting factor in the burnout process of solid fuel is the rate of oxygen supply to the reactor surface, and not the reaction rate itself.

The latter statement is in good agreement with the conclusions obtained for industrial furnace devices with layered combustion.

10.6.5. Activation of the fuel layer. As temperature increases, the rate of chemical combustion reactions increases very rapidly [22], because most molecules are in an activated state. Active molecules formed endothermically from normal molecules. The process by which the energy of molecules changes without chemical transformation called activation, and the heat absorbed during the formation of active molecules is the heat of activation. In other words, for reactions between the carbon in the coke and the oxygen in the air to begin, a preliminary energy expenditure corresponding to the activation energy is required.

Chemical combustion reactions in the layer do not proceed according to stoichiometric equations, but rather through a series of intermediate states corresponding to the formation of active intermediates. The formation of intermediates in the form of atoms and radicals is associated with energy expenditure. Consequently, one can imagine that the reaction impeded by an energy barrier, which requires activation energy to overcome. Unlike internal combustion engines, where combustion reactions activated by an increase in charge temperature during compression, in SFPE, combustion activated by an external source, which preheats the layer. When starting the engine, an electric coil, directly either in contact with the fuel or embedded in the combustion chamber lining can serve as an external heat source. Initial heating of the fuel can also achieved by passing a high-density electric current through it.Renewed fuel activated by heat transferred by radiation from hotter fuel particles, as well as by the heat of the gas flow filtering through the bed. During operation, the bed maintained in an activated state because not all the heat released during combustion reactions carried away

from the bed with the combustion products. Between blowdowns, the bed temperature is maintained by the heat accumulated the bed during the blowdown. Some of the released heat expended in preparing the newly incoming fuel for combustion, i.e., activating it.

If the periods between blowdowns are sufficiently long, heat loss from the bed may exceed the amount accumulated during the blowdown. As a result, the bed temperature will decrease, and consequently, fuel activation will decrease, eventually leading to the complete cessation of combustion reactions. As the periods between purges become shorter and their duration increases, the fuel bed become more activated. This will lead to an increase in temperature, a growth of the oxygen zone, and, consequently, to more efficient fuel utilization in the SFPE.

10.6.6. The influence of pressure at the end of the compression process and charge density on the fuel burnout process in the SFPE reactor. The rates of both homogeneous and heterogeneous reactions occurring in the bed depend on the temperature and concentration of the reactants. Since the bed has a relatively high thermal inertia, the reactions occurring within it can consider isothermal. The rate of such reactions is highest at the beginning of the process and then decreases proportionally to the effective concentration. At a constant temperature, the highest rate corresponds to the initial moment and decreases as the reaction progresses due to decreasing concentrations of the reactants.

The dependence of the rate of a chemical reaction on the concentrations of the reactants is expressed the law of mass action. An increase in pressure during compression, which precedes combustion, leads to an increase in the charge density and, consequently, to an increase in the oxygen concentration in the SFPE combustion device.

When expressing the reaction products in terms of relative concentrations, the rate of a monomolecular reaction is independent of pressure, the rate of a bimolecular reaction is proportional to the pressure, and the rate of a trimolecular reaction is proportional to the square of the pressure. Since all reactions occurring in the SFPE combustion device are bimolecular or higher, increasing the pressure at the end of compression will lead to a significant increase in the combustion rate in the combustion device [30]. This dependence allows for influencing the combustion reaction rate by varying the pressure at the end of compression. It can assume that the higher the rotational speed of the designed engine, the higher the compression ratio should be in order to both improve efficiency and accelerate combustion processes. Under the limited time allotted for combustion in SFPE, fuel

burnout will occur more completely due to an increase in the concentration of reactants.

Forced purging allows for maintaining the concentration of reactants in the combustion zone at a sufficiently high level. Throughout the entire period of heat input, the concentration of reactants will depend on the speed and initial period of purging, as well as on the effective charge density. Termination of the forced oxidizer supply will lead to a rapid attenuation of reactions in the combustion device.

10.6.7. Fuel layer aerodynamics in the SFPE reactor and its influence on the process of working fluid production. Efficient operation of a SFPE is only possible if the energy expenditure required to overcome the aerodynamic drag of the fuel bed is minimal. For this reason, when designing a SFPE, it is necessary to consider the variation in bed drag depending on its state. In a real-world packed bed, the pressure drop (drag) is a function of the flow velocity, determined specifically by the kinetic energy developed within the void channels of the fuel bed. Experimental data have shown that there is no pressure recovery in the jet, and therefore, the kinetic energy acquired during the flow through the lumen is lost. The drag of a burning fuel bed differs significantly from that of a cold bed. This explained the increased temperature and the resulting change in gas density and viscosity. Furthermore, the bed drags significantly affected by changes in particle size due to their burnout.

The drag of a burning bed is sometimes 8...10 times higher than that of a cold bed. Experimental data indicate that the sharp increase in drag of a burning bed caused by its non-isothermal nature, which leads to a significant change in physical constants.

To reduce purging costs, the flow velocity through the fuel bed must reduce. On the one hand, this will reduce the turbulence of the bed, but on the other hand, it will increase the contact time between the fuel's reaction surface and atmospheric oxygen (the combustion reaction approaches isothermal). A reduction in speed can only achieved by reducing the volume of the displacement chamber, i.e., by increasing the engine's compression ratio. At the same time, the oxygen concentration in the displacement chamber will increase towards the end of compression, meaning that a smaller volume of air will need to pass through the bed to produce the same amount of heat.

10.7. Ways to improve SFPE with layered combustion of fuel.

The characteristics of the SFPE process, namely, combustion activation due to the bed heat and the ability to control the heat supply process, enable

the implementation of a number of specialized, highly efficient thermodynamic cycles in this engine, in particular, cycles with isothermal compression of the air charge and isothermal heat supply. The efficiency benefits of isothermal compression over adiabatic or polytropic alternatives established by Carnot and recognized by early heat engine designers. Attempts to implement such compression have made repeatedly, but none has achieved significant success. As is well known, Diesel, developing the theoretical foundations of a rational engine, emphasized the preferable use of isothermal preliminary compression of the working fluid in the engine cylinder [11]. In his proposed design, air compression in the first part of the piston stroke was to occur along an isothermal line. This achieved by spraying water within the air charge. During the second part of the stroke, water injection ceased, and compression then proceeded adiabatically until the air charge temperature reached the fuel's autoignition temperature. After this, coal dust gradually injected into the working cylinder so that combustion occurred without a temperature increase (isothermally). At a certain point in the stroke, the fuel supply ceased, after which the combustion products began to expand.

To practically implement this working cycle with acceptable energy parameters, it was necessary to compress the air to a high pressure of approximately 25 MPa, which is practically unattainable with single-stage compression. To reduce the pressure to a realistically achievable level and still achieve a temperature at the end of compression sufficient for fuel ignition, Diesel had to abandon isothermal compression and immediately switch to adiabatic compression. Otherwise, heat removal from the working fluid would not have allowed self-ignition of the fuel in a real engine, and this was the second most important principle in his concept for creating a rational engine.

Unlike a diesel engine, in a SFPE the temperature of the air charge at the end of compression does not play such a significant role, since the combustion process activated not by the heat of the air charge, but by the heat accumulated by the fuel layer. Thus, during the compression process, the air charge can cooled, for example, by intensively removing heat from the channel connecting the working cylinder with the displacement chamber (Fig. 10.2) or by injecting water into the displacement chamber. This will make the compression process closer to isothermal (hereinafter, for simplicity of presentation, we will refer to a process close to isothermal as isothermal). Cooling the working fluid in a thermodynamic cycle makes it possible significantly reduce the work expended on compression. Cooling the working fluid makes it possible to reduce mechanical work costs by 25...50% at the

same compression ratio, or to increase the compression ratio by 1.5...2 times at the same final compression pressure. In the first case, it becomes possible to reduce the maximum cycle temperature while maintaining a virtually unchanged pressure ratio, without reducing useful work. In the second case, increasing the compression ratio will improve engine efficiency with final combustion fluid parameters similar to those of a diesel engine.

10.8. Advantages of layer combustion of solid fuels in internal combustion engines over other methods.

It should noted that the stratified combustion of solid fuels in the working space of a piston engine using pulsed bed blowing has been relatively poorly studied to date. Despite this, an analysis of the factors acting during engine operation reveals a number of advantages of stratified combustion of solid fuels in piston engines over other methods.

A significant advantage of forced blowing over cyclic gasification is that this process can produce not only generator gas but also products of complete combustion, which, entering directly into the working cylinder, perform useful work there. Unlike the method proposed by Firey, this eliminates the need for afterburning of the generator gas in the working cylinder.

Compared to the bulk combustion of pulverized fuel in a FCS or WCS, stratified combustion with forced blowing offers a number of thermodynamic and purely technical advantages. In terms of thermodynamic cycle management, this method allows for:

- reducing pre-flame reaction times, since the fuel is already activated by the time it is blown through the bed, and combustion reactions begin immediately upon blowing, without requiring additional liquid fuel;
- increasing combustion speed and efficiency, since the fuel bed exerts a significant turbulent effect on the gas flow filtering through it, and the high relative velocity difference between the flow and the fuel particles accelerates the delivery of oxidizer to the reaction surface. As a result, reactions are more kinetic in nature, rather than diffusional, as is observed with pulverized coal combustion. The combined effect of these factors leads to more complete utilization of atmospheric oxygen and significantly reduces the excess air ratio without significantly impairing combustion, which, in turn, improves the engine's weight and size by 1.3 to 2 times;
- reduce the loss of combustible fuel components, as the same particle participates in combustion over several blowdowns until all the carbon it contains is burned out (with the volumetric combustion method, the pulverized coal particle is removed from the working cylinder, regardless of the degree of burnout);

- affect the heat supply process, which allows engine operation to organize according to the most efficient thermodynamic cycles;
- reduce the mechanical work required to compress the air charge by cooling it.

The following technical and technological advantages, characteristic of the layered combustion method compared to the volumetric combustion method, include:

- the use of coal dust requires significant efforts to protect the main components of the fuel system and the engine itself from abrasive wear. With layered combustion, the combustion process occurs outside the working cylinder, which significantly reduces the amount of abrasive material carried into the cylinder, and the layer itself has a filtering effect. If necessary, combustion products can hot clean directly in the reactor or in the channel connecting the reactor to the working cylinder;
– coal dust preparation requires significant energy expenditure for milling. To obtain the fuel fractions required for stratified combustion, it is sufficient to subject the fuel to a less expensive process – crushing;
- solid fuel suitable for stratified combustion has high physical stability and requires no additional storage costs. The preparation and maintenance of colloidal solutions in suspension requires significant energy, which increases the cost of their use, especially during long-term storage;
- fuel feeder requirements for stratified combustion are significantly lower, since fuel loading and ash removal occur periodically during the exhaust and intake strokes, when the pressure in the engine's working space is minimal;
- SFPE can developed using existing piston engines, significantly reducing design costs.

List of references

1. Белоусов Е. В. Использование твердых топлив в двигателях внутреннего сгорания // Проблемы создания новых машин и технологий : науч. труды КГПИ. Кременчуг : КГПИ, 2000. № 1 (8). С. 420–422.

2. Белоусов Е. В., Белоусова Т. П. Особенности протекания политропного процесса сжатия в твердотопливных поршневых двигателях со слоевым сжиганием топлива // Сб. науч. трудов УГМТУ. Николаев : УГМТУ, 2001. № 3 (375). С. 84–89.

3. Белоусов Е. В. Слоевой метод сжигания твердых топлив в двигателе внутреннего сгорания // Сб. науч. трудов УГМТУ. Николаев : УГМТУ, 2000. № 3 (369). С. 66–70.

4. Белоусов Е .В. Слоевой способ прямого сжигания твердых топлив в двигателях внутреннего сгорания // Энергетика: экономика, технологии, экология : сб. науч. трудов НТУ Украины «КПИ». К. : Знання, 2000. № 4. С. 62–65.

5. Белоусов Е. В., Тимошевский Б. Г., Белоусова Т. П. Усовершенствование слоевого метода сжигания твердых топлив в двигателях внутреннего сгорания // Сб. науч. трудов УГМТУ. Николаев : УГМТУ, 2001. № 6 (378). С. 68–77.

6. Глаголев Н. М. Испытание газовых двигателей. Харьков ; Киев : Гос. науч.-техн. изд-во Украины, 1934. 426 с.

7. Глобальная энергетическая проблема / Александрова И. И., Байков Н. М., Бесчинский А. А. и др. М. : Мысль, 1985. 239 с.

8. Головина Е. С. Высокотемпературное горение и газификация углерода. М. : Энергоатомнздат, 1983. 180 с.

9. Грехов Л. В. Создание и исследование дизеля, работающего на угольных суспензиях // Вестн. МГТУ нм. Баумана. Сер.: Машиностроение. 1998. № 1. С. 47–59.

10. Грехов Л. В. Результаты исследования реологических свойств водоугольных и топливоугольных суспензий как перспективных топлив для дизелей // Автомобильные и тракторные двигатели : межвуз. сб. науч. тр. МАМИ. 1998. Вып. XIV. С. 48–61.

11. Гумилевский Л. И. Рудольф Дизель. М. ; Л. : ГОНТИ, 1938. 292 с.

12. Гюльднер Г. Двигатели внутреннего сгорания: их работа, конструкция и проектирование: в 2 т. Т. 2. М. : МАКИЗ, 1928.

13. Дизели : справочник. Л. : Машиностроение, 1977. 480 с.

14. Иващенко Н. А., Грехов Л. В. Исследование распыливания угольных суспензий и интенсификация их сжигания в дизеле // Автомобильные и тракторные двигатели : межвуз. сб. науч. тр. МАМИ. 1999. Вып. XV. С. 214–225.

15. Канило П. М., Бей И. С., Ровенский А. И. Автомобиль и окружающая среда. Харьков : Прапор, 2000. 304 с.

16. Коллеров Л. К. Применение угольного топлива в дизелях // Двигателестроенне. 1982. № 2. С. 51–53.

17. Круглов М. Г., Грехов Л. В., Иващенко Н. А. Применение низкосортных и твердых видов топлива в ДВС // Тез. докл. науч.-тех. конф., 21–23 ноября 1995 г. / МГТУ им. Баумана. М., 1995. Ч. 1. С. 110.

18. Кузнецов Б. Развитие тепловых двигателей. М. ; Л. : Госэнергонздат, 1953. 588 с.

19. Лапидус А. Л., Крылова А. Ю. Уголь и природный газ – источники для получения искусственного жидкого топлива и химического производства. М. : Знание, 1986. 47 с.

20. Моделирование процесса выгорания твердого топлива в реакторе твердотопливного поршневого двигателя внутреннего сгорания со слоевым методом сжигания / Белоусов Е. В., Майстренко Ю. А., Пацков В. П., Пацкова Т. В. // Сб. науч. трудов УГМТУ. Николаев : УГМТУ. 2001. № 4 (376). С. 93–104.

21. Моторные топлива из альтернативных сырьевых ресурсов / Терентьев Г. А., Тюков В. М., Смаль Ф. В. М. : Химия, 1989. 271 с.

22. Основы практической теории горения / Померанцев В. В., Арефьев К. М., Ахмедов Д. Б. и др. Л : Энергия, 1973. 263 с.

23. Пат. 32644 Украина. МКВ 7 F02B 45/02 Способ сжигания твердых топлив в двигателе внутреннего сгорания / Белоусов Е. В. (Украина) : Заявлено 17.02.2000 ; Опубликовано 15.02.2001. 4 с.

24. Пат. 5216928 США. МКИ F02B 45/02 Product gas reservoirs for cyclic char burning engines and gasifies / Joseph C. Firev (США) : Заявл. 30.04. 92 ; Опубл. 08.06.93. 14 с.

25. Пат. 5271357 США. МКИ F02B 45/00 Method of combustion for dual fuel engine General Electric (США) : Заявл. 24.01.92 ; Опубл 21.12.93. 14 с.

26. Равич М. Б. Топливо и эффективность его использования. М. : Наука, 1971. 358 с.

27. Райдер Г., Хупер Ч. Двигатели Стирлинга. М. : Мир, 1986. 464 с.

28. Рудольф Дизель – изобретатель и финансист // Автоинформ плюс. 2001. № 10. С. 96–100.

29. Семиноженко В. П., Канило П. М., Ровенский А. И. Энергия и жизнь. Экология и будущее. Харьков : Фолио, 1997. 176 с.

30. Теория топочных процессов / Кноре Г. Ф., Арефьев К. М., Блох А. Г. и др. М. : Л. : Энергия, 1966. 491 с.

31. Хзмалян Д. М., Каган Я. А. Тсория горсния и топочныс устройства. М. : Энергия, 1976. 488 с.

32. Шкаливоа В. П., Патрахальцев Н. Н. Применение нетрадиционных топлив в дизелях. М. : Изд. Университета дружбы народов, 1986. 54 с.

33. Bell S. R., Caton J. A. Diesel engines: analytical evaluations of ignition options. Twenty-first Symposium (International) on Combustion / The Combustion Institute. 1986. P. 389–397.

34. Bell S. R., Caton J. A. Numerical simulation of a coal-fueled compression-ignition engine // Fuel. 1988. Vol. 67. P. 474–481.

35. Bell S. R., Caton J. A. Cycle Simulations of a Coal Fueled. Reciprocating, Internal Combustion Engine: the Role of Volatiles and Liquid Carriers // Combust Science and Technology. 1986. Vol. 50. P. 185–203.

36. Branyon D. P., Caton J., Annamalai K. Coal-Fueled Diesel Cycle Simulation: The Role of Group Effects // ASME Transactions : Journal of Engineering for Gas Turbines and Power. 1990. Vol. 112, No. 3. P. 391–397.

37. Caton J. A., Rosegay K. H. An Analysis of Solid Particle Combustion in an IC Engine Environment. Central States Section // The Combustion Institute. CSS. 1983. March. P. 83–102.

38. Caton J. A. The Development of Coal-Fueled Diesel Engines: A Brief Review // Energy Information Annual. 1992. Vol. 17. P. A89–A97.

39. Caton J. A., Hsu B. D. The General Electric Coal-Fueled Diesel Engine Program (1982-1993): A Technical Review // ASME Transaction : Journal of Engineering for Gas Turbines and Power. 1994. Vol. 116, No. 1. P. 749–757.

40. Caton J. A., Rosegay K. H. A Review and Comparison of Reciprocating Engine Operation Using Solid Fuels // Transactions of the Society of Automotive Engineers. 1984. Vol. 82, No. 831362. P. 1108–1124.

41. Clean Coal Technology Demonstration Program / U. S. Department of Energy Secretary for Fossil Energy. Washington, DC 20585. 1995. April. 3 p.

42. Coal Slurries-Oil Substitutes // Mechanical Engineering. 1980. Vol. 102, No. 12. 50 p.

43. COM and SRC-II as alternative fuels for diesel engines / Murayama Tadashi, Miyamoto Noboru, Chikahisa Takemi et al. // Bulletin Marine Engineering Society Japan. 1986. Vol. 14, No. 1. P. 29–36.

44. Cooper-Bessemer coal-fueled engine system – progress report / Rao A. K., Wilson R. P., Balles E. N. et al. // ASME Transactions : Journal of Engineering for Gas Turbines and Power. 1988. Vol. 110. No. 3. P. 498–506.

45. Downs W., Vecci S. J., Barsin J. A., Rovesti W. C. Characterization and Combustion of SRC- II Fuel Oil // ASME Transactions : Journal of Engineering for Gas Turbines and Power. 1980. Vol. 102, No. 3. P. 672–678.

46. Efficient and low-smoke combustion of various low-grade fuel in high-speed small diesel engines / Murayama R., Miyamoto N., Chikahisa R., Tosaka S. // ASME Transactions : Journal of Engineering for Gas Turbines and Power. 1988. Vol. 110, No. 3. P. 385–392.

47. Emission Characteristics and Control Technology for Stationary Coal-Fueled Diesel Engines / Benedek K. R., Menzies K. T., Johnson S. A. et al. // ASME Transactions : Journal of Engineering for Gas Turbines and Power. 1989. Vol. 111, No. 3. P. 507–515.

48. Flynn P. L., Hsu B. D., Leonard G. L. Coal-Fueled Diesel Engine Progress at GE Transportation Systems // ASME Transactions : Journal of Engineering for Gas Turbines and Power. 1990. Vol. 112, No. 3. P. 369–375.

49. Flynn P .L., Leonard G. L., Mehan R. L. Component wear in coal-fueled diesel engines // ASME Transactions : Journal of Engineering for Gas Turbines and Power. 1989. Vol. 111, No. 3. P. 521–529.

50. Gandhidasan P., Ertas A., Anderson E. E. Review of methanol and compressed natural gas (CNG) as alternative for transportation fuel // ASME Transactions : Journal of Engineering for Gas Turbines and Power. 1991. Vol. 113, No. 3. P. 101–109.

51. Hsu B. D. Coal-Fueled Diesel Engine Development Update at GE Transportation Systems // ASME Transactions : Journal of Engineering for Gas Turbines and Power. 1992. Vol. 114, No. 3. P. 502–508.

52. Hsu B. D. Progress on the investigation of coal-water slurry fuel combustion in a medium speed diesel engine P. 1. Ignition studies // ASME Transactions : Journal of Engineering for Gas Turbines and Power. 1988. Vol. 110, No. 3. P. 415–422.

53. Hsu B. D. Progress on the investigation of coal-water slurry fuel combustion in medium speed diesel engine P. 2. Preliminary full load test // ASME Transactions : Journal of Engineering for Gas Turbines and Power. 1988. Vol. 110, No. 3. P. 425–430.

54. Hsu B. D., Confer G. L., Shen Z. J. Progress on the Investigation of Coal Water Slurry Fuel Combustion in a Medium Speed Diesel Engine: P. 5 // Combustion Studies, in Coal-Fueled Diesel Engines. 1992. Vol. 16. P. 39–46.

55. Hsu B.D., Leonard Q.L., Johnson R.N. Progress on the investigation of coal-water-slurry fuel combustion in a diesel engine P. 3. Accumulator in Coal-Fueled Diesel Engines // Energy-sources and Technology Conference and Exhibition – Houston, TX, Vol. 7. January 1989. – P. 19-25.

56. Hsu B. D., Branyon D. P. Progress on the Investigation of Coal-Water Slurry Fuel Combustion in a Medium-Speed Diesel Engine: P. 6. In-Cylinder Combustion Photography Studies // ASME Transactions : Journal of Engineering for Gas Turbines and Power. 1993. Vol. 115, No. 3. P. 790–797.

57. Injection Characteristics of Coal-Water Slurries in Medium-Speed Diesel Equipment / Callahan T. J., Ryan R. W., Schwalb J. A. et al. // ASME Transactions : Journal of Engineering for Gas Turbines and Power. 1992. Vol. 114, No. 3. P. 522–527.

58. Kihm K. D., Caton J. A. Synchronization of a Laser Diffraction Drop Sizing Technique with Intermittent Spray Systems // Journal of Applied Optics. 1992. Vol. 31, No. 23. P. 1914–1916.

59. Kihm K. D., Deignan P. Dynamic surface tension of coal-water slurry fuels // Fuel. 1995. Vol. 74, No. 2. P. 295–300.

60. Kihm K. D., Terracina D. P., Caton J .A. Spray-tip droplet SMDs of intermittent high-pressure sprays of diesel fuel compared with coal-water slurry sprays // Journal of the Institute of Energy. 1995. Vol. 65, No. 3. P. 57–64.

61. Kihm K. D., Terracina D. P., Caton J. A. Synchronised droplet size measurements for coal-water slurry sprays generated from a high-pressure diesel injection system // Journal of the Institute of Energy. 1994. Vol. 67, No. 3. P. 2–9.

62. Kishan S., Bell S. R., Caton J. A. Numerical Simulations of Two-Strops Cycle Engines Using Coal Fuels // ASME Transactions : Journal of Engineering for Gas Turbines and Power. 1986. P. Vol. 108. P. 661–668.

63. Likos W. E., Ruan T. W. Experiments with coal fuels in a high temperature diesel engine // ASME Transactions : Journal of Engineering for Gas Turbines and Power. 1988. Vol. 110, No. 3. P. 444–452.

64. McMillian M. H., Webb H. A. Coal-fueled diesels: systems development // ASME Transactions : Journal of Engineering for Gas Turbines and Power. 1989. Vol. 111, No. 3. P. 485–490.

65. Nydick S. E., Prochet F., Steiger H. A. Continued Development of a Coal Water Slurry Fired Slow-Speed Diesel Engine A Review of Recent Test Results // ASME Transactions : Journal of Engineering for Gas Turbines and Power. 1987. Vol. 109, No. 3. P. 465–476.

66. Operating results of the Cooper-Bessemer JS-1 engine on coal-water slurry / Rao A. K., Melcner C. H., Wilson R.P. et al. // ASME Transactions : Journal of Engineering for Gas Turbines and Power. 1988. Vol. 110, No. 3. P. 431–436.

67. Rao A. K., Balles E. N. Wilson R. P. Features and Performance Data of Cooper-Bessemer Coat-Fueled Six-Cylinder LSB Engine // Coal-Fueled Diesel Engines. 1992. Vol. 16. P. 11–16.

68. Rosegay K. H., Caton J. A. Cycle Simulation of Coal Particle Fueled Reciprocating Internal-Combustion Engines // M. S. Thesis. Texas A&M University. 1982. Paper No. 831699, December. P. 895–908.

69. Ryan T. W. Coal-Fueled Diesel Development: A Technical Review // ASME Transactions : Journal of Engineering for Gas Turbines and Power. 1994. Vol. 116, No. 3. P. 740–748.

70. Seshadri A. K., Caton J. A., Kihm K. D. Coal-Water Slurry Spray Characteristics of a Positive Displacement Fuel Injection System // ASME Transactions : Journal of Engineering for Gas Turbines and Power. 1992. Vol. 114, No. 3. P. 528–533.

71. Siebers D. L., Dyer T. M. The Autoignition and Combustion of Coal-Water Slurry Under Simulated Diesel Engine Conditions // ASME Transactions : Journal of Engineering for Gas Turbines and Power. 1986. Vol. 108, No. 3. P. 652–660.

72. Slurry-fueled diesels seen beneficial to cogeneration // Cogeneration. 1985. Vol. 2, No. 4. P. 11–12.

73. Tataiah K., Wood C. U. Performance of coal slurry fuel in a diesel engine // SAE. Technical Paper Series. 1980. No. 800329. P. 12–18.

74. Urban C. M., Mecredy H. E., Ryan T. W., Angeles M. N. Coal-Water Slurry Operation in an EMD Diesel Engine // ASME Transactions : Journal of Engineering for Gas Turbines and Power. 1988. Vol. 110, No. 3. P. 437–443.

75. Uzkan R., Horton C. E. Combustion of Coal-Water Slurry in a Two-Cycle Diesel Engine: Effects of Fuel Amount and Timing // ASME Transactions : Journal of Engineering for Gas Turbines and Power. 1990. Vol. 112, No. 3. P. 376–383.

76. Wahiduzzaman S., Blumberg P. N., Keribar R., Rackmil C. I. A Comprehensive Model for Pilot-Ignited, Coal-Water Mixture Combustion in a Direct-Injection Diesel Engine // ASME Transactions : Journal of Engineering for Gas Turbines and Power. 1990. Vol. 112, No. 3. P. 384–390.

77. Wakenell J. F. Performance of Carbon/Diesel Fuel Slurries in a Medium – Speed Diesel Engine // SAE. Technical Paper Series. 1983. No. 830554. P. 67–75.

78. Weber R. Der Dieselmotor lauft mit Kohlestaub und Wasser // VDI-Nachrichten. 1980. Vol. 34, No. 47. P. 7–12.

79. Williams M. C., Holcombe N. T., McMillian M. Environmental aspects of coal-fueled diesel engines // ASME Transactions : Journal of Engineering for Gas Turbines and Power. 1989. Vol. 111, No. 3. P. 491–497.

List of references containing information regarding the direct combustion of solid fuels in piston internal combustion engines.

1. Гюльднер Г. Двигатели внутреннего сгорания: их работа, конструкция и проектирование : в 2 т. Т. 2. М. : МАКИЗ, 1928.
2. Morrison L. H. The Coal Dust Engine: Details of the Design // Power. 1928. Vol. 68.
3. Pawlikowski R. The Coal Dust Engine Upsets Traditions // Power. 1928. Vol. 68.
4. Радциг А. А. Современные достижения теплотехники. Л. : Госэнергоиздат, 1933.
5. Hanse O. J. Coal-Oil Mixture as a Diesel Fuel // Master of Science Thesis / University of North Carolina, 1949.
6. Есин В. В. Исследование процесса распиливания твердого топлива в связи с проблемой непосредственного сжигания последнего в стационарных и автотракторных двигателях внутреннего сгорания : автореф. дис. ... канд. техн. наук / МИМЭСХ. М.,1952. 19 с.
7. Tracy E. W. Feasibility Study of the Use of Powdered Coal as a Fuel for Diesel Engines. SwRi Report No. 8-681-1 / Southwest Research Institute, Nov. 1957.
8. Marshall H. P., Shelton C. The Coal Burning Piston Engine, Bulletin of the Virginia Polytechnic Institute // Engineering Experiment Station. 1959. No. 135, Vol. 53.
9. Sittauer H. Diesel eine erfindun erobert sich die welt // Transpress. S. Nr., 1961. P. 95.
10. Rich L. L., Walker M. L. Pulverized Coal Burning Diesel Engine / Howard University // Office of Coal – Research, RD. USGPO. Washington, D.C., 1969.Report No. 46.
11. Tipler W. Prospects for the Operation of Diesel Engines on Coal or Its Derivatives / Institution of Mechanical Engineers. 1975. Paper No. C17/75.
12. Soehngen E. E. The Development of the Coal Burning Diesel in Germany // US ERDA Report. 1976. No. WA76-3387.
13. Marshall H. P., Walters D. C. An Experimental Investigation of Coal Slurry Fueled Diesel Engine // SAE. 1977. Paper No. 770795.
14. Sulzer developing coal-fueled slow-speed diesel engine // Zosen. 1978. No. 6. P. 23.
15. Tataiah K., Lestz S. J. Influence of MICO Fuels n Engine Performance, Exhaust Emissions, and Endurance // Interim Report AFLR. U.S. Army Fuels and Lubricants Research Laboratory, Southwest Research Institute. San Antonio, Texas, 1979. No. 125.
16. Dunlay J. B., Davis J. P., Steiger H. A., Eberle M. K. Economic and Technological Assessment of Diesel Engines Using Coal Based Fuels for Electric Power Generation 8 Thermo Electron Corp. 1979. Report No. TE 4234 P. 37-80.
17. Rentz R. L., Renner R. A. Solid Fuel Applications to Transportation Engines, DOE Report No. CS-56051-T2, Prepared by Mueller Associates, Inc. – 1980.
18. Tataiah K., Wood C.O. Performance of Coal Slurry Fuel in a Diesel Engine // SAE. 1980. Paper No. 800329. 12 p.
19. Ryan T. W., Likos W. E., Moses C. A. The Use of Hybrid Fuel in a Single-Cylinder Diesel Engine, Central State Section // The Combustion Institute. 1980. Paper No. CSS/CI-80-06.

20. Ryan T. W., Likos W. E., Moses C. A. The Use of Hybrid Fuel in a Single-Cylinder Diesel Engine // SAE. 1980. Paper No. 801380.
21. Dunlay J. B., Davis J. P., Steiger H. A., Eberle M. K. Performance Tests of a Slow Speed Two Stroke Diesel Engine Using Coal Based Fuels / Thermo Electron Corp. 1980. Report No. TE 7905-267-80.
22. Fortschritte bei Versucnen mit Kuhlenschlamm-Brennstoffen bei langsamlaufenden Sulzer – Dieselmoioren // MTZ. 1980. 41, No. 9. 370 s.
23. Coal Slurries-Oil Substitutes // Mechanical Engineering. 1980. (102) No. 12. P. 50.
24. Weber R. Der Diesel motor lauft mit Kohlestaub und Wasser // VDI – Nachrichten. 1980. 34, No. 47. 7 s .
25. Coal slurries in diesel engines // Fairplay Int. Shipp Weekly. 1980. 275, No. 5057. 26 p.
26. Fortschritte bei Versuchen mit Kohlenschlamm-Brennstoffen bei langsamlaufenden Sulrer-Diesel motren // MTZ. 1980. No. 9. S. 41.
27. Rentz R .L., Timbario T. J., Renner H. A. Solid Fuel Applications to Transportation Engines // SAE. 1981. Paper 81044.
28. Dunlay J. B. Coal: Diesel Fuel of the Future? // Power. 1981.Vol. 12.
29. Dunlay J. B., Davis J. P., Steiger H. A., Eberle M. K. Slow-Speed Two Stroke Diesel Engine Tests Using Coal-Based Fuels // ASME. 1981. Paper 81-DQP-12.
30. Marshall H. P., Bhat S. M., Mulvaney S. T., Sevelli J. F. Performance of Diesel Engine Operating on Raw Coal-Diesel Fuel Slurries // SAE. 1981. Paper No. 810253.
31. Коллеров Л. К. Применение угольного топлива в дизелях // Двигателестроение. 1982. № 2. С. 51–53.
32. Ryan T. W., Callahan T. J., Dodge L. G., Moses C. A. Injection, Atomization and Combustion of Carbon Slurry Fuels // SAE. 1982. Paper No. 821199.
33. Rosegay K. H., Caton J. A. Cycle Simulation of Coal Particle Fueled Reciprocating Internal-Combustion Engines // M.S. Thesis. Texas A&M University. 1982. Paper No. 831699, December. P. 895–908.
34. Wakenell J. F. Performance of Carbon-Diesel Fuel Slurries in a Medium-Speed Diesel Engine // SAE. 1983. Paper 830554. P. 67–75.
35. Energy and Environmental Research Corporation, Research Engine Test of Coal Slurry Fuels, work plan for U. S. Department of Energy Contract DE-AC19-82BC10T29. 1983. January.
36. Robben F. Coal-Fueled Diesel Engines // SAE. 1983. Paper No. 831747.
37. Phatak R. G. Investigation of diesel Fuel Injection Equipment Response to Coal-Slurry Fuels / Southwest Research Institute. 1983. Report No. SwRI-7328, November.
38. Caton J. A., Rosegay K. H. An Analysis of Solid Particle Combustion in an IC Engine Environment / Central States Section Spring Meeting of the Combustion Institute. 1983.Paper No. CSS / CI83-02, March.
39. Rosegay K. H., Caton J. A. Cycle Simulation of Coal Particle Fueled Reciprocating Internal-Combustion Engines, in Proceedings: A Worldwide View of Diesel Combustion, Emissions, and Analysis, at the International Off Highway Meeting and Exposition, Society of Automotive Engineer. Milwaukee, 1983. Vol. 1, 12–15, September. P. 123–136.

40. Caton J. A., Rosegay K. H. A Review and Comparison of Reciprocating Engine Operation Using Solid Fuels // Transactions of the Society of Automotive Engineers. 1984. Paper No. 831362, Vol. 92. P. 1108–1124.
41. Gurney M. D., Clingenpeel J. M., Eccleston D. B. A Program to Examine the Use of Coal Slurry Fuels in Diesel Engines // ASME. 1984. Paper No. 84-DGP-9.
42. Clingenpeel J. M., Gurney M. D., Eccleston D. B. A Combustion and Wear Analysis of a Compression-Ignition Engine Using Coal Slurry Fuels // ASME. 1984. Paper No. 84-DGP-8.
43. Robben F., Brehob D. D., Narnazian M. et al. Coal-Fueled Diesel Engines // Proceedings of The Sixth International Symposium on Coal Slurry Combustion and Technology, FL; also, Lawrence Berkeley Laboratory. 1984. Report No. LBL-17721. P. 767–775.
44. Crouse F. W. Proceedings of the First Annual Heat Engines Contractors Review Meeting / Topical Report prepared by DOE-METC. 1984. Report No. DOE–METC-84-31, November.
45. Caton J. A. Cycle Simulation of a Coal-Particle-Fueled, Reciprocating, Locomotive Engine // 7-th Annual Energy-sources Technology Conference and Exhibition, American Society of Mechanical Engineers. 1984. Paper No. 84-DGP-19.
46. Rosegay K. H., Caton J. A. Cycle Simulation of Coal Particle Fueled, Reciprocating Internal-Combustion Engines // Transactions of the Society of Automotive Engineers. 1984. Paper No. 831299, Vol. 92. P. 895–908.
47. Bell S. R., Caton J. A. Cycle Simulation for a Reciprocating, Internal- Combustion Engine Using a Coal Slurry Fuel: The Role of Volatiles, 1984 // American Flame Research Committee Fall Symposium. 1984. Paper No. 41, October.
48. Caton J. A. Cycle Simulation for a Coal-Fueled Diesel Engine // Proceedings of the First Annual Heat Engines Contractors Meeting, US Department of Energy, Morgantown Energy Technology Center. 1984. November. P. 245–258.
49. Nelson L .P., Heap M. T., Sampson T. W., Seeker W. R. The Combustion Characteristics of Slurred Fuels in Diesel Engines: Detailed Measurements end Analysis : presented at the Energy-sources and Technology Conference and Exhibition, Dallas, TX // ASME. 1985. Paper No. 85-DGP-19, February.
50. Brehob D. D. Compress on Ignition of Coal Slurry Fuels, Ph.D // Thesis, University of Berkeley, Department of Mechanical Engineering, also Lawrence Berkeley Laboratory. 1985. Report No. LBL-20710, November.
51. Siebers D. L., Dyer T. M. The Autoignition and Combustion of Coal-Water Slurry Under Simulated Diesel Engine Conditions : presented at the Energy-sources and Technology Conference and Exhibition, Dallas, TX // ASME. 1985. Paper No. 85-DGP-15, February.
52. Phatak R. G., Gurney M. D. Investigation of diesel Fuel Injection Equipment Response to Coal-Slurry Fuels : presented at the Energy-sources and Technology Conference and Exhibition, Dallas, TX // ASME. 1985. Paper No. 85-DGP-17 February.
53. Carpenter L. K., Grouse F. W. Coal-Fueled Diesel Engines, Fossil Energy Activities : presented at the Energy-sources and Technology Conference and Exhibition, Dallas, TX // ASME. 1985. Paper No. 85-DGP-18 February.

54. Grouse F. W. Proceedings of the Second Annual Heat Engines Contractors Review Meeting // Topical Report prepared by DOE-METC. 1985. Report No. DOE-METC-85-6023.
55. Kishan S., Caton J. A. Simulation of a Two-Stroke Cycle, Locomotive Engine Using Diesel or Coal Fuels, Joint Central and Western Slates Sections/Combustion Institute Spring Meeting, Paper No. 1-1A, April 1985.
56. Bell S. R., Caton J. A. Cycle Simulation of Reciprocating, Internal-Combustion Engines Using Coal Slurry Fuels, Joint Central and Western States Sections // Combustion Institute Spring Meeting. 1985. Paper No. 2-1 A, April.
57. Caton J. A., Bell S. R. Coal-Fueled Diesel: Cycle Simulation Study // Proceedings of the Second Annual Heat Engines Contractors Meeting, U.S. Department of Energy, Morgantown Energy Technology Center. 1985. May. P. 250–266.
58. Bell S. R., Caton J. A. Analytical Evaluations of Ignition Options for a Coal // Water Slurry Fueled Engine, 1985, American Flame Research Committee Fall Symposium. 1985. October.
59. Slurry-fueled diesels seen beneficial to cogeneration // Cogeneration. 1985. No. 4. P. 11–12.
60. Tests positive with coal derived fuels // Diesel and Gas Turbine Worldwide. 1985. No. 5. P. 52–53.
61. Шкаливоа В. П., Потрархальцев Н. Н. Применение нетрадиционных топлив в дизелях. М. : Изд. Университета дружбы народов, 1986. 54 с.
62. Carpenter L. K., Grouse F. W. Coal-Fueled Diesels: Challenges and Progress :presented at Energy-sources and Technology Conference and Exhibition, New Orleans, LA // ASME. 1986. Paper № 86-ICE-6, February.
63. Grouse F. W. Proceedings of the Third Annual Heat Engines Contractors Review Meeting // Topical Report prepared by DOE-METC. 1986. Report No. DOE–METC-86-6041, May.
64. Hapeman M., Savkar S. Coal Fired Diesel System Application to Locomotive Power plants : presented at Energy-sources and Technology Conference and Exhibition, New Orleans, LA // ASME. 1986. Paper No. 86-ICE-14, February.
65. Leonard G. L., Fiske G. H. Combustion Characteristics of a Coal-Water Mixture in a Simulated Medium Speed Diesel Engine Environment : presented at Energy-sources and Technology Conference and Exhibition, New Orleans, LA // ASME. 1986. Paper No. 86-ICE-15, February.
66. Koch R. L., Curry C. E., Slezinger J. O. Commercialization Considerations for a Coal-Fueled Diesel Locomotive : presented LA // ASME. 1986. Paper No. 86-ICE-S, February.
67. Ryan R. W., Likos W. E., Vinyard S. Combustion Characteristics of Coal Fuel in an Insulated High Temperature Diesel Engine : presented at Energy-sources and Technology Conference and Exhibition, (oral only) New Orleans, LA. 1986.
68. Kishan S., Bell S. R., Caton J. A. Numerical Simulations of Two-Stroke Cycle Engines Using Coal Fuels // Ninth Annual Energy-sources Technology Conference and Exhibition, American Society of Mechanical Engineers, Internal Combustion Engine Division Symposium. 1986. Paper No. 86-ICE-13, 25 February.

69. Bell S. R., Caton J. A. Coal-Fueled Diesel Engines: Analytical Evaluations of Ignition Options // Twenty-First (International) Symposium on Combustion. 1986. P. 389–397.
70. Bell S. R., Caton J. A. Cycle Simulations of a Coal-Fueled, Reciprocating Internal Combustion Engine: the Role of Volatiles and Liquid Carriers // Combustion Science and Technology. 1986. Vol. 50, No. 4–6. P. 185–203.
71. Bell S. R., Caton J. A. Coal-Fueled Diesel: Simulation Study // Proceedings of the Third Annual Heat Engines Contractors Meeting, US Department of Energy, Morgantown Energy Technology Center. 1986. May. P. 308–319.
72. Kishan S., Bell S. R., Caton J. A. Numerical Simulations of Two-Stroke Cycle Engines Using Coal Fuels // ASME Transactions : Journal of Engineering for Gas Turbines and Power. 1986. Vol. 108, No. 4, October. P. 661–668.
73. Kamo R., Kakwani R., Carpenter L. K. Introduction of Micronized Coal In the Intake Air of a Medium-speed Adiabatic Diesel Engine : presented at Energy-sources and Technology Conference and Exhibition, New Orleans, LA // ASME. 1986. Paper No. 86-ICE-19, February.
74. COM and SRC-II as alternative fuels for diesel engines / Murayama R., Miyamoto N., Chikahisa R. et al. // Bulletin Marine Engineering Society Japan. 1986. Vol. 14, No. 1. P. 29–36.
75. Siebers D. L., Dyer T. M. The Auto ignition and Combustion of Coal-Water Slurry Under Simulated Diesel Engine Conditions // ASME Transactions : Journal of Engineering for Gas Turbines and Power. 1986. Vol. 108, No. 3. P. 652–660.
76. Byam J. W., Markel K. E. Proceedings of the Annual Heat Engines and Gas Stream Cleanup Systems Contractors Review Meeting. Topical Report prepared by DOE-METC. 1987. Report No. DOE-METC-87-6077, April.
77. Balles E. N., Benedek K. R., Wilson R. P., Rao A. K. Analysis of Cylinder Pressure and Combustion Products from an Experimental Coal-Fueled Diesel Engine : presented at the Internal Combustion Engine Division Technical Conference, Kansas City, MO // New Engine Technology for Cogeneration / ed. J. M. Bailey. 1987. ICE-Vol.-2, October. P. 75–81.
78. Ryan T. W., Callahan T. J., Mecredy H. E. et al. Coal Slurry Combustion – Bomb and Small Engine Test Results : presented at the Energy-sources and Technology Conference and Exhibition, Dallas, TX // ASME. 1987. Paper No. 87-ICE-31.
79. Likos E., Ryan T. W. Combustion Characteristics of Coal Fuels in a High Temperatures Diesel Engine : presented at the Energy-sources and Technology Conference and Exhibition, Dallas, TX // ASME. 1987. Paper No. 87-ICE-56.
80. Caton J. A., Bell S. R., Richardson K. D., Koncke K. F. Autoignition Characteristics of Coal-Water Slurry Fuels for Diesel Engine Conditions. Numerical Results // Proceedings of the 1987 ASME-JSME Thermal Engineering Joint Conferenc / Mario P. J., Tanasawa L., eds. 1987. Vol. 1, March. P. 217–223.
81. Caton J. A., Annamalai K. Performance and Emissions of Coal-Fueled Engines Using Group Combustion Theory // Proceedings of the Annual Heat Engines and Gas Stream Cleanup Systems Contractors Review Meeting, US Department of Energy, Morgantown Energy Technology Center. 1987. April. P. 190–196.

82. Caton J. A., Annamalai K. Performance and Emissions of Coal-Fueled Engines Using Group Combustion Theory // Proceedings of the AR&TO Direct Utilization, and Instrumentation and Diagnostic Contractors Review Meeting, US Department of Energy. 1987. October. P. 31–40.
83. Nydick S. E., Prochet F., Stieger H. A. Continued Development of a Coal Water Slurry Fired Slow-Speed Diesel Engine a Review of Recent Test Results : presented at the Energy-sources and Technology Conference and Exhibition, Dallas, TX // ASME. 1987. Paper No. 87-ICE-10, February.
84. Brehob D. D., Sawyer R. F. Compression Ignition of Coal Slurry Fuels : presented at the Energy-sources and Technology Conference and Exhibition, Dallas, TX // ASME. 1987. Paper No. 87-ICE-11, February.
85. Lai M .C., Zhou B., Cheng W. K. et al. Parametric Studies of Coal-Water Slurry Combustion in a Rapid Compression Machine : presented at the Energy-sources and Technology Conference and Exhibition, Dallas, TX // ASME. 1987. Paper No. 87-ICE-9, February.
86. Nydick S. E., Prochet F., Steiger H. A. Continued Development of a Coal Water Slurry Fired Slow-Speed Diesel Engine A Review of Recent Test Results // ASME Transactions : Journal of Engineering for Gas Turbines and Power. 1987. Vol. 109, No. 3. P. 465–476.
87. Dellefield R. J., Webb H. A. Proceedings of the Annual Heat Engines and Gas Cleanup Systems Contractors Review Meeting. Topical Report prepared by DOE-METC. 1988. Report-No. DOE-METC-88-6094, June.
88. Hsu B. D. Progress on the Investigation of Coal-Water Slurry Fuel Combustion in a Medium Speed Diesel Engine. Part 1: Ignition Studies : presented at the Energy-sources and Technology Conference and Exhibition, New Orleans, LA // ASME. 1988. Paper No. 68-ICE-4, January.
89. Hsu B. D. Progress on the Investigation of Coal-Water Slurry Fuel Combustion in a Medium-Speed Diesel Engine. Part 2: Preliminary Full Load Test : presented at the Energy-sources and Technology Conference and Exhibition, New Orleans, LA // ASME. 1988. Paper No. 88-ICE-5, January.
90. Flynn P. L., Hsu B. D. Coal Fueled Diesel Developments // SAE. 1988. Paper 881159.
91. Benedek K. R., Menzies K. T., Johnson S. A. et al. Emission Characteristics and Control Technology for Stationary. Coal-Fueled Diesel Engine, in Engine Emissions Technology for the 1990s : presented at the Internal Combustion Engine Division Conference, San Antonio, TX / ed. Springer K. J. // ICE. 1988. Vol. 4, October. P. 169–176.
92. Urban C. M., Mecredy H. E., Ryan T. W., Angeles M. N. Coal-Water Slurry Operation in an EMD Diesel Engine : presented at the Energy-sources and Technology Conference and Exhibition, New Orleans, LA // ASME. 1988. Paper No. 88-ICE-28, January.
93. Likos W. E., Ryan T. W. Experiments with Coal Fuels in a High Temperature Diesel Engine : presented at the Energy-sources and Technology Conference and Exhibition, New Orleans, LA // ASME. 1988. Paper No. 88-ICE-29, January.

94. Caton J. A., Schmidt J., Roth J. et al. Nitric Oxide Emissions from a Coal-Fueled Engine: Numerical Results // Energy-sources : Technology Conference and Exhibition, American Society of Mechanical Engineers, Internal Combustion Engine Division Symposium. 1988. Paper No. 88-ICE-22, January.
95. Bell S. R., Caton J. A. Numerical Simulation of a Coal-Fueled, Compression-Ignition Engine // Fuel. 1988. Vol. 67, April. P. 474–481.
96. Caton J. A., Annamalai K. Performance and Emissions of Coal-Fueled Engines Using Group Combustion Theory // Proceedings of the Annual Heat Engines and Gas Stream Cleanup Systems Contractors Review Meeting, US Department of Energy, Morgan town Energy Technology Center. 1988 June. P. 173–178.
97. Caton J. A., Annamalai K. Performance and Emissions of Coal-Fueled Engines Using Group Combustion // Proceedings of the Advanced Research and Technology Development (AR&TD) Direct Utilization, and Instrumentation and Diagnostics Contractors Review Meeting, US Department of Energy, Pittsburgh Energy Technology Center. 1988. September. P. 657–668.
98. Cooper-Bessemer coal-fueled engine system – progress report / Rao A. K., Wilson R. P., Balles E. N. et al. // ASME Transactions : Journal of Engineering for Gas Turbines and Power. 1988. Vol. 110, No. 3. P. 498–506.
99. Murayama R., Miyamoto N., Chikahisa R., Tosaka S. Efficient and low- smoke combustion of various low-grade fuel in high-speed small diesel engines // ASME Transactions : Journal of Engineering for Gas Turbines and Power. 1988. Vol. 110, No. 3. P. 385–392.
100. Likos W. E., Ruan T. W. Experiments with coal fuels in a high temperature diesel engine // ASME Transactions : Journal of Engineering for Gas Turbines and Power. 1988. Vol. 110, No. 3. P. 444–452.
101. Hsu B. D. Progress on the investigation of coal – water slurry fuel combustion in a medium speed diesel engine. P. 1: Ignition studies // ASME Transactions : Journal of Engineering for Gas Turbines and Power» – Vol. 110, No. 3. – 1988. P. 415-422.
102. Hsu B.D. Progress on the investigation of coal-water slurry fuel combustion in medium speed diesel engine. P.2. – Preliminary full load test // «ASME Transactions – Journal of Engineering for Gas Turbines and Power. 1988. Vol. 110, No. 3. P. 425–430.
103. Operating results of the Cooper-Bessemer JS-1 engine on coal – water slurry / Rao A. K., Melcner C. H., Wilson R. P. et al. // ASME Transactions : Journal of Engineering for Gas Turbines and Power. 1988. Vol. 110, No. 3. P. 431–436.
104. Coal-water slurry operation in an EMD diesel engine / Urban C. M., Mecredy H. E., Ryan T.W. et al. // ASME Transactions : Journal of Engineering for Gas Turbines and Power. 1988. Vol. 110, No. 3. P. 437–443.
105. Webb H. A., McMillian M. H. Coal Fueled Diesels: Systems Development : presented at the Energy-sources and Technology Conference and Exhibition, Houston, TX // Coal-Fueled Diesel Engines /eds. McMillian M. H., Webb H. A. 1989. Vol. 7, January. P. 1–8.
106. Emission Characteristics and Control Technology for Stationary Coal-Fueled Diesel Engine / Benedek K. R., Menzies K. T., Johnson S. A. et al. // ASME Transactions : Journal of Engineering for Gas Turbines and Power. 1989. Vol. 110, No. 3. P. 507–515.
107. Williams M. C., Holcombe N. T., McMillian M. H. Environmental Aspects of Coal-Fueled Diesel Engines : presented at the Energy-sources Technology Conference and Exhibition, Houston, TX. 1989. January.
108. Bedick R. C., Dorchak T. P., Rekos N. F., Webb H. A. Proceedings of the Sixth Annual Coal-Fueled Heat Engines and Gas Stream Cleanup Systems Contractors Review Meeting, Meeting. Topical Report prepared by DOE-METC. 1989. Report No. DOE-METC-89-6101, March.
109. Hsu B. D., Leonard G. L., Johnson R. N. Progress On the Investigation of Coal-Water-Slurry Fuel Combustion in a Diesel Engine. Part 3: Accumulator : presented at the Energy-sources and Technology Conference and Exhibition, Houston, TX // Coal-Fueled Diesel Engines / eds. McMillian M. H., Webb H. A. 1989. Vol. 7, P. 19–25, January.
110. Rao A. K., Wilson R. P., Balles E. et al. Cooper-Bessemer Coal-Fuel ed Diesel Systems: Progress Report : presented at the Energy-sources and Technology Conference and Exhibition, Houston, TX // Coal-Fuel ed Diesel Engines / eds. McMillian M. H., Webb H. A. 1989. Vol. 7, January. P. 9–18.
111. Ryan T. W., Likos W. E., Moulton D. S., Bauer H. F. Characterization, Processing, end Diesel Engine Evaluation of Coal Liquid Fuels : presented at the Energy-sources and Technology Conference and Exhibition, Houston, TX // Coal-Fueled Diesel Engines / eds. McMillian M. H., Webb H. A. 1989. Vol. 7, January. P. 43-50.
112. Caton J. A., Annamalai K. Performance and Emissions of Coal-Fueled Engines Using Group Combustion Theory // Proceedings of the Sixth Annual Coal-Fueled Heat Engines and Gas Stream Cleanup Systems Contractors Review Meeting, US Department of Energy. Morgantown Energy Technology Center. 1989. March. P. 346–357.
113.Ryan W., Annamalai K., Caton J. Relation Between Group Combustion and Drop Array Studies, Proceedings of the Central States Section // Combustion Institute Spring Technical Meeting. 1989. Paper No. 20, May. P. 261–267.
114. Kakwani R. M., Kamo R., Smith W. C., Cutlip R. G. Combustion Characteristics of a Dry Coal Powder Fueled Adiabatic Diesel Engine : presented at the Energy-sources and Technology Conference and Exhibition, Houston, TX // Coal-Fueled Diesel Engines / eds. McMillian M. H., Webb H. A. 1989. Vol. 7, P. 27-34, January.
115. Bell S. R., Choi G. H. Numerical Evaluation of the Carbon-Water Reaction in a Coal-Water Fueled Engine : presented at the Energy- sources and Technology Conference and Exhibition, Houston, TX // Coal-Fueled Diesel Engines / eds. McMillian M. H., Webb H. A. 1989. Vol. 7, January. P. 35–42.
116. Yu T. U., Beer J. M., Cheng W. K. Injection and Atomization of Coal-Water Slurry in High Pressure Diesel Engine Environment : presented at the Energy-sources and Technology Conference and Exhibition, Houston, TX // Coal-Fueled Diesel Engines / eds. McMillian M. H., Webb H. A. 1989. Vol. 7, January. P. 51–60.

117. Khandare S. S. Cycle Simulation of Volatile Coal-Fueled Diesel Engine with Coal-Dust Induction System : presented at the Energy-sources and Technology Conference and Exhibition, Houston, TX // Coal-Fueled Diesel Engines / eds. McMillian M. H., Webb H. A. 1989. Vol. 7, January. P. 61–74.
118. Likos W. E., Ryan T. Coal fuels for diesel and gas turbine engines // SAE. Technical Paper Series. 1989. No. 890866. P. 9.
119. McMillian M. H., Webb H. A. Coal-fueled diesels: systems development // ASME Transactions : Journal of Engineering for Gas Turbines and Power. 1989. Vol. 111, No. 3. P. 485–490.
120. Flynn P. L., Leonard G. L., Mehan R. L. Component wear in coal-fueled diesel engines, // ASME Transactions : Journal of Engineering for Gas Turbines and Power. 1989. Vol. 111, No. 3. P. 521–529.
121. Hsu B. D., Leonard G. L., Johnson R. N. Progress on the investigation of coal-water-slurry fuel combustion in a medium-speed diesel engine. Part 3: Accumulator injector performance // ASME Transactions : Journal of Engineering for Gas Turbines and Power. 1989. Vol. 111, No. 3. P. 516–520.
122. Williams M. C., Holcombe N. T., McMillian M. Environmental aspects of coal-fueled diesel engines // ASME Transactions : Journal of Engineering for Gas Turbines and Power. 1989. Vol. 111, No. 3. P. 491–497.
123. Webb H. A., Rekos N. F., Kofhari V. P., Bedick R. C. Proceedings of the Seventh Annual Coal-Fueled Heat Engines and Gas Stream Cleanup Systems Contractors Review Meeting Topical Report prepared by DOE– METC. 1990. Report No. DOE-METC-90-6110, March.
124. Flynn P. L., Hsu B. D., Leonard G. L. Coal Fueled Diesel Engine Progress at GE Transportation Systems : presented at the Energy-sources and Technology Conference and Exhibition, New Orleans, LA // Coal-Fueled Diesel Engines / ed. Caton J. A. 1990. ICE-Vol. 12, January. P. 1–9.
125. Slaughter D., Cohen M., Samuel E.et al. Control of Emissions in the Coal Fueled Diesel Locomotive : presented at the LA // Coal-Fueled Diesel Engines / ed. Caton J. A. 1990. ICE-Vol. 12, January. P. 11–16.
126. Mayville R. A., Rao A. K., Wilson R. P. Cooper-Bessemer Coal Fueled Engine System: Recent Developments in Durable Components : presented at the Energy-sources and Technology Conference and Exhibition, New Orleans, LA // Coal-Fueled Diesel Engines / ed. Caton J. A. 1990. ICE-Vol. 12, January. P. 17–22.
127. Uzkan R., Horton C. E. Combustion of Coal-Water Slurry in a Two-cycle Diesel Engine: Test System Design : presented at the Energy- sources and Technology Conference and Exhibition, New Orleans, LA // Coal-Fueled Diesel Engines / ed. Caton J. A. 1990. ICE-Vol. 12, January. P. 23–30.
128. Uzkan R., Horton C. E. Combustion of Coal-Water Slurry In a Two-Cycle Diesel Engine: Effects of Fuel Amount and Timing : presented at the Energy-sources and Technology Conference and Exhibition, New Orleans, LA // Coal-Fueled Diesel Engines / ed. Caton J. A. 1990. ICE-Vol. 12, January. P. 31–40.
129. Schwalb J. A., Ryan T. W., Smith W. C. Lube Oil Contamination Induced Wear in Coal Fueled Diesel Engines : presented at the Energy-sources and Technology

Conference and Exhibition, New Orleans, LA // Coal-Fueled Diesel Engines / ed. Caton J. A.1990. ICE-Vol. 12, January. P. 51–58.
130. Branyon D. P., Caton J., Annamalai K. Coal Fueled Diesel Cycle Simulation: The Role of Group Effects : presented at the Energy-sources and Technology Conference and Exhibition, New Orleans, LA // ASME Transactions : Journal of Engineering for Gas Turbines and Power. Vol. 112, No. 3. P. 391–397; Coal-Fueled Diesel Engines / ed. Caton J. A. 1990. ICE-Vol. 12, January. P. 77–84.
131. Kakwani R. M., Badgley P. R., Smith W. C. Development of Fuel Injection and Combustion Systems for Coal-Water-Slurry Fueled Diesel Engines : presented at the Energy-sources and Technology Conference and Exhibition, New Orleans, LA // Coal-Fueled Diesel Engines / ed. Caton J. A. 1990. ICE-Vol. 12, January. P. 41–50.
132. Wahiduzzaman S., Blumberg P. N., Keribar R., Rackmil C. I. A Comprehensive Model for Pilot-Ignited, Coal-Water Mixture Combustion in a Direct Injection Diesel Engine : presented at the Energy-sources and Technology Conference and Exhibition, New Orleans, LA // Coal-Fueled Diesel Engines / ed. Caton J. A. 1990. ICE-Vol. 12, January. P. 59–68.
133. Bell S. R., Choi G. H. Numerical Evaluation of Fuel Atomization : presented at the Energy-sources and Technology Conference and Exhibition, New Orleans, LA // Coal-Fueled Diesel Engines / ed. Caton J. A. 1990. ICE-Vol. 12, January. P. 69–76.
134. Weber R. MitKohie staub and Wasser // Schweizer Mashinenmarkt. 1990. Vol. 90, No. 27. P. 84–87.
135. Flynn P. L., Hsu B. D., Leonard G. L. Coal-Fueled Diesel Engine Progress at GE Transportation Systems // ASME Transactions : Journal of Engineering for Gas Turbines and Power. 1990. Vol. 112, No. 3. P. 369–375.
136. Uzkan T., Horton C. E. Combustion of Coal-Water Slurry in a Two-cycle Diesel Engine: Effects of Fuel Amount and Timing // ASME Transactions : Journal of Engineering for Gas Turbines and Power. 1990. Vol. 112, No. 3. P. 376–383.
137. Wahiduzzaman S., Blumberg P. M., Keribar R., Rackmil C. I. A Comprehensive Model for Pilot-Ignited, Coal-Water Mixture Combustion in a Direct-Injection Diesel Engine // ASME Transactions : Journal of Engineering for Gas Turbines and Power. 1990. Vol. 112, No. 3. P. 384–390.
138. Webb H. A., Bedick R. C., Gelling D. W., Cicero D. C. Proceedings of the Eighth Annual Heat Engines and Gas Cleanup Systems Contractors Review Meeting Topical Report prepared by DOE-METC. 1991. Report No. DOE-METC-91-6122, July.
139. Hsu B. D., Confer G. L. Progress on the Investigation of Coal-Water-Slurry Fuel Combustion in a Medium Speed Diesel Engine. Part 4: Fuels Effect : presented at the Energy-sources and Technology Conference and Exhibition, Houston, TX // Coal-Fueled Diesel Engines / eds. Caton J. A., Webb H. A. 1991. ICE-Vol. 14, January. P. 1–8.
140. Mayville R. A., Rao A. K., Wilson H. P. Durable Component Development Progress for the Cooper-Bessemer Coal-Fueled Diesel Engine : presented at the Energy-sources and Technology Conference and Exhibition, Houston, TX // Coal-

Fueled Diesel Engines / eds. Caton J. A., Webb H. A.1991. ICE-Vol. 14, January. P. 23–28.
141. Uzkan R., Morton C. E. Effects of Engine Speed, Inlet Air Heating and Slurry Timing on the Combustion of Coal-Water Slurry in a Diesel Engine : presented at the Energy-sources and Technology Conference and Exhibition, Houston, TX // Coal-Fueled Diesel Engines / eds. Caton J. A., Webb H. A. 1991. ICE-Vol. 14, January. P. 9–16.
142. Greenhalgh M. L. High-Pressure Coal Fuel Processor. Engine Development : presented at the Energy-sources and Technology Conference and Exhibition, Houston, TX // Coal-Fueled Diesel Engines / eds. Caton J. A., Webb H. A. 1991. ICE-Vol. 14, January 1991. P. 49–55.
143. Schwalb J. A., Ryan T. W. Surface Finish and Particle Size Effects on Wear in Coal-Fueled Diesel Engines : presented at the Energy-sources and Technology Conference and Exhibition, Houston, TX // Coal-Fueled Diesel Engines / eds. Caton J. A., Webb H. A. 1991. ICE-Vol. 14, January. P. 29–38.
144. Caton J. A., Kihm K. D., Seshadrt A. K., Zicterman G. Micronized-Coal-Water Slurry Sprays from a Diesel Engine Positive Displacement Fuel Injection System // Proceedings of the Central States Section. Combustion Institute Spring Technical Meeting. 1991. Paper No. 58, April. P. 361–366.
145. Caton J. A., Kihm K. D. Coal-Water Slurry Atomization Characteristics // Proceedings of the Eighth Annual Coal-Fueled Heat Engines and Gas Stream Cleanup Systems Contractors Review Meeting, U.S. Department of Energy, Morgantown Energy Technology Center. 1991. July. P. 273–282.
146. Badgley P. R., Doup D. C. Combustion Optimization of High-Speed Coal-Water-Slurry Fueled Diesel Engine : presented at the Energy-sources and Technology Conference and Exhibition, Houston, TX // Coal-Fueled Diesel Engines / eds. Caton J. A., Webb H. A. 1991. ICE-Vol. 14, January. P. 17–22.
147. Wahiduzzaman S., Blumberg P. N., Hsu B. D. Simulation of Significant Design and Operating Characteristics of a Coal Fueled Locomotive Diesel Engine : presented at the Energy-sources and Technology Conference and Exhibition, Houston, TX // Coal-Fueled Diesel Engines / eds. Caton J. A., Webb H. A. 1991. ICE-Vol. 14, January. P. 39–48.
148. Webb H. A. Proceedings of the Ninth Annual Heat Engines Contractors Review Meeting, to be available. Topical Report prepared by DOE-METC. 1992. October.
149. Hsu B. D. Coal-Fueled Diesel Engine Development Update at GE Transportation Systems : presented at the Energy-sources and Technology Conference and Exhibition, Houston, TX // Coal-Fueled Diesel Engines / eds. Caton J. A., Webb H. A. 1992. ICE-Vol. 16, January. P. 1–10.
150. Hsu B. D. Coal-Fueled Diesel Engine Development Update at GE Transportation Systems // ASME Transactions : Journal of Engineering for Gas Turbines and Power. 1992. Vol. 114, No. 3. P. 502–508.
151. McDowell R. E., Basic S .L., Confer G. L. Design and Operation of a Medium Sized 12-CyUnder Coal-Fueled Diesel Engine : presented at the Energy-sources and Technology Conference and Exhibition, Houston, TX // Coal-Fueled Diesel Engines / eds. Caton J. A., Webb H. A.1992. Vol. 16, January. P. 33–38.

152. Hsu B. D., Confer G. L., Shen Z. J. Progress on the Investigation of Coal Water Slurry Fuel Combustion in a Medium Speed Diesel Engine. Part 5: Combustion Studies : presented at the Energy-sources and Technology Conference and Exhibition, Houston, TX // Coal-Fueled Diesel Engines / eds. Caton J. A., Webb H. A. 1992. Vol. 16, January. P. 39–46.
153. Hsu B. D., Confer G. L., Shen Z. J. Progress on the Investigation of Coal-Water Slurry Fuel Combustion in a Medium-Speed Diesel Engine. Part 5: Combustion Studies // ASME Transactions : Journal of Engineering for Gas Turbines and Power. 1992. Vol. 114, No. 3. P. 515–521.
154. Hsu B. D., Shen Z., Caton J. A. Combustion Characteristics of Coal-Water Slurry Fuel in a Medium Speed Diesel Engine // Proceedings of the Ninth Annual International Pittsburgh Coal Conference, Coal-Energy and the Environment, Pittsburgh, PA. 1992. 12–16 October. P. 335–340.
155. Rao A .K., Balles E. N., Wilson R. P. Features and Performance Data of Cooper-Bessemer Coat-Fueled Six-Cylinder LSB Engine : presented at the Energy-sources and Technology Conference and Exhibition, Houston, TX // Coal-Fueled Diesel Engines / eds. Caton J. A., Webb H. A.1992. ICE-Vol. 16, January. P. 11–16.
156. Rao A. K., Balles E. N., Wilson R. P. Features and Performance Data of Cooper-Bessemer Coal-Fueled Six-Cylinder LSB Engine // ASME Transactions : Journal of Engineering for Gas Turbines and Power. 1992. Vol. 114, No. 3. P. 509–514.
157. Greenhalgh M. L. Preliminary Test Data and Systems Analysis of a High- Pressure Coal Fuel Processor Engine System Concept : presented at the Energy-sources and Technology Conference and Exhibition, Houston, TX // Coal-Fueled Diesel Engines / eds. Caton J.A., Webb H. A.1992. ICE-Vol. 16, January. P. 17–24.
158. Kakwani R. M., Winsor R. E., Wahiduzzaman S. et al. Study for Coal-Water Slurry Fuel Combustion in a High-Speed Diesel Engine : presented at the Energy-sources and Technology Conference and Exhibition, Houston, TX // Coal-Fueled Diesel Engines / eds. Caton J. A., Webb H. A. 1992. ICE-Vol. 16. P. 25–32.
159. Callahan T. J., Ryan T. W., Schwalb J. A. et al. Injection Characteristics of Coal-Water Slurries in Medium-Speed Diesel Equipment. // ASME Transactions : Journal of Engineering for Gas Turbines and Power. 1992. Vol. 114, No. 3. P. 522–527.
160. Dodge L. G., Callahan T. J., Ryan T.W. et al. Injection Characteristics of Coal-Water Slurries in Medium-Speed Diesel Equipment : presented at the Energy-sources and Technology Conference and Exhibition, Houston, TX // Coal-Fueled Diesel Engines / eds. Caton J. A., Webb H. A. 1992. Vol. 16, January. P. 47–54.
161. Schwalb J. A., Ryan T. W. Investigation of Break-In Wear, Ring Loading, and Oil Supply Configuration Effects on Wear In Coal-Fueled Diesel Engines : presented at the Energy-sources and Technology Conference and Exhibition, Houston, TX // Coal-Fueled Diesel Engines / eds. Caton J. A., Webb H. A.1992. Vol. 16, January. P. 69–78.
162. Seshadri A. K., Caton J. A., Kihm K. D. Coal-Water Slurry Spray Characteristics of a Positive Displacement Fuel Injection System : Energy-sources Technology Conference and Exhibition, American Society of Mechanical Engineers, Internal

Combustion Engine Division Symposium, Houston, TX // Coal-Fueled Diesel Engines / eds. Caton J. A., Webb H. A. 1992. ICE-Vol. 16, January. P. 55–62.
163. Caton J. A., Seshadri A .K., Kihm K. D. Spray Tip Penetration and Cone Angles for Coal-Water Slurry Using a Modified Medium-Speed Diesel Engine Injection System // Proceedings of the Central States Section. Combustion Institute Spring Technical Meeting. 1992. April. P. 234–239.
164. Seshadri A. K., Caton J. A., Kihm K .D. Coal-Water Slurry Spray Characteristics of a Positive Displacement Fuel Injection System // ASME Transactions : Journal of Engineering for Gas Turbines and Power. 1992. Vol. 114, No. 3. P. 528–533.
165. Doup D. C., Badgley P. R. Novel Injector Techniques for Coal-Fueled Diesel Engines : presented at the Energy-sources and Technology Conference and Exhibition, Houston, TX // Coal-Fueled Diesel Engines / eds. Caton J. A., Webb H. A. 1992. Vol. 16, January. P. 63–68.
166. Caton J. A. The Development of Coal-Fueled Diesel Engines: A Brief Review // Energy Information Annual. 1992. Vol. 17. P. A89–A97.
167. Kihm K. D., Caton J. A. Synchronization of a Laser Diffraction Drop Sizing Technique with Intermittent Spray Systems // Journal of Applied Optics. 1992. Vol. 31, No. 23. P. 1914–1916.
168. Hsu B. D., Najewicz D. J., Cook C. S. Coal-Fueled Diesel Engines for Locomotive Applications to be published in the Proceedings of the Joint Contractors Meeting (FE/EE Advanced Turbine Systems Conference // FE Fuel Cells and Coal-Fired Heat Engines Conference), U. S. Department of Energy, Morgan town Energy Technology Center, Morgantown, WV. 1993. Aug. P. 3–5.
169. Hsu B. D., Branyon D. P. Progress on the Investigation of Coal-Water Slurry Fuel Combustion in a Medium-Speed Diesel Engine. P. 6–In-Cy Under Combustion Photography Studies // ASME Transactions : Journal of Engineering for Gas Turbines and Power. 1993. Vol. 115, No. 3. P. 790–797.
170. Schwalb J., Ryan T.W., Kakwani R., Winsor R. Study of Coal-Water Slurry Fuel Combustion in a High-Speed Diesel Engine: P. 2 – Bench Test Results and Engine Setup, to be presented at the 1993 Energy-sources Technology Conference and Exhibition, Houston, TX, February 1993.
171. Caton J. A., Payne S. E., Terracina D. P., Kihm K. D. Coal-Water Slurry Spray Characteristics of an Electronically-Controlled Accumulator Fuel Injection System, accepted for publication : Energy-sources Technology Conference and Exhibition, American Society of Mechanical Engineers, Internal Combustion Engine Division Symposium, Houston, TX // Coal-Fueled Diesel Engines / eds. Caton J. A., Webb H. A. February 1993.
172. Kihm K. D., Terracina D. P., Payne S. E., Caton J. A. Synchronized Droplet Size Measurements for Coal-Water Slurry (CWS) Diesel Sprays of an Electronically-Controlled Fuel Injection System, accepted for publication : Energy-sources Technology Conference and Exhibition, American Society of Mechanical Engineers, Internal Combustion Engine Division Symposium, Houston, TX // Coal-Fueled Diesel Engines / eds. Caton J. A., Webb H. A. 1993. February.

173. Studium możliwości zastosowania zawicsiny sadzy w olcju napçdowym jako paliwa dla silnika wysokopręznego : monogr. / Szlachta Z. P. Krak., 1993. No. 154.
174. Terracina D. P. Synchronized droplet size measurements for intermittent sprays of an electronically-controlled fuel injection system for both diesel and coal-water slurry, fuels MSc thesis. Texas : A&M University, 1993.
175. Kihm K. D., Terracina D. P., Payne S. E., Caton J. A. Properly Synchronized Droplet Sizing for Intermittent High-Pressure Coal-Water Slurry (CWS) Sprays Using the Light Extinction as a Triggering Source // 29-th National Heat Transfer Conference, the American Society of Mechanical Engineers, Proceedings of the Heat Transfer in Fire and Combustion Systems / eds. Farouk B., Menguc M. P., Viskanta R., Presser C., Chellaiah S. Atlanta, GA, 1993. HTD-Vol. 250, August. P. 93–100.
176. Kihm K. D., Terracina D. P., Payne S. E., Caton J. A. Properly Synchronized Measurements of Droplet Sizes for High-Pressure Intermittent Coal-Water Slurry Fuel Sprays // Proceedings of the 1993 Joint Central and Eastern States Section/Combustion Institute Spring Technical Meeting. New Orleans, LA. 1993. Paper No. 50, March. P. 271–275.
177. Caton J. A., Payne S. E., Terracina D. P., Kihm K. D. Coal-Water Slurry Sprays from an Electronically-Controlled Accumulator Fuel Injection System // Break-up Distances and Times Proceedings of the 1993 Joint Central and Eastern States Section / Combustion Institute Spring Technical Meeting. New Orleans, LA, 1993. Paper No. 76, March. P. 405–409.
178. Caton J. A., Hsu B. D. The General Electric Coal-Fueled Diesel Engine Program (1982–1993): A Technical Review // ASME Transactions : Journal of Engineering for Gas Turbines and Power. 1994. Vol. 116, No. 1. P. 749–757.
179. Hsu B. D., Confe G. L., McDowell R. E. et al. Design and Operation of a Medium Speed 12-Cy Under Coal-Fueled Diesel Engine : presented at the ASME Energy-Sources and Technology Conference and Exhibition. New Orleans, LA, 1994. 23–27 Jan.
180. McDowell R. E., Giammarise A. W., Branyon D. P. Durability Testing of Medium Speed Diesel Engine Components Designed for Operating On Coal-Water Slurry Fuel : presented at the ASME Energy-Sources and Technology Conference and Exhibition. New Orleans, LA, 1994. 23–27 Jan.
181. Kihm K. D., Terracina D. P., Payne S. E., Caton J. A. Synchronised droplet size measurements for coal-water slurry sprays generated from a high-pressure diesel injection system // Journal of the Institute of Energy. 1994. Vol. 67, No. 3. P. 2–9.
182. Caton J. A., Payne S. E., Terracina D. P., Kihm K. D. Cone angles and spray tip penetrations for coal-water slurry using an electronically-controlled accumulator fuel injection system. Western States Section / Combustion Institute Spring Technical Meeting. Davis, California, 1994. Paper No. WSS/CIS 94-037.
183. Ryan T. W. Coal-Fueled Diesel Development: A Technical Review // ASME Transactions : Journal of Engineering for Gas Turbines and Power. 1994. Vol. 116, No. 3. P. 74–748.

184. Круглов М. Г., Грехов Л. В., Иващенко Н. А. Применение низкосортных и твердых видов топлива в ДВС // Тез. Доклада науч.-тех. конф. 21–23 ноября 1995 г. М. : МГТУ им. Баумана. 1995. Ч. 1. С. 110.
185. Clean Coal Technology Demonstration Program // U. S. Department of Energy Secretary for Fossil Energy. Washington, DC 20585, 1995. April. 3 p.
186. Kihm K. D., Terracina D. P., Caton J. A. Spray-tip droplet SMDs of intermittent high-pressure sprays of diesel fuel compared with coal-water slurry sprays // Journal of the Institute of Energy. 1995. Vol. 65, No. 3. P. 57–64.
187. Грехов Л. В. Реология угольных суспензий как топлив для дизелей // Совершенствование мощностных, экономических и экологических показателей ДВС : матер. VI междунар. науч.-практ. семинара. Владимир, 1997. С. 104–105.
188. Грехов Л. В. Результаты исследования реологических свойств водоугольных и топливоугольных суспензий как перспективных топлив для дизелей // Автомобильные и тракторные двигатели : межвуз. сб. науч. тр. МАМИ. 1998. Вып. XIV. С. 48–61.
189. Грехов Л. В. Создание и исследование дизеля, работающего на топливных суспензиях // Вестник МВТУ. Сер. : Машиностроение. 1998. № 1. С. 47–59.
190. Иващенко Н. А., Грехов Л. В. Исследование распиливания угольных суспензий и интенсификация их сжигания в дизеле // Автомобильные и тракторные двигатели : межвуз. сб. науч. тр. МАМИ. 1999. Вып. XV. С. 214–225.
191. Белоусов Е. В. Использование твердых топлив в двигателях внутреннего сгорания // Проблемы создания новых машин и технологий : науч. тр. КГПИ. Кременчуг : КГПИ. 2000. № 1 (8). С. 420–422.
192. Белоусов Е. В. Слоевой метод сжигания твердых топлив в двигателе внутреннего сгорания // Сб. науч. трудов УГМТУ. Николаев : УГМТУ, 2000. № 3 (369). С. 66–70.
193. Белоусов Е. В. Слоевой способ прямого сжигания твердых топлив в двигателях внутреннего сгорания // Энергетика: экономика, технологии, экология : сб. науч. тр. НТУ Украины «КПИ». Киев : Знання, 2000. № 4. С. 62–65.
194. Белоусов Е. В., Белоусова Т. П. Особенности протекания политропного процесса сжатия в твердотопливных поршневых двигателях со слоевым сжиганием топлива // Сб. науч. трудов УГМТУ. Николаев : УГМТУ, 2001. № 3 (375). С. 84–89.
195. Белоусов Е. В., Тимошевский Б. Г., Белоусова Т. П. Усовершенствование слоевого метода сжигания твердых топлив в двигателях внутреннего сгорания // Сб. науч. трудов УГМТУ. Николаев : УГМТУ, 2001. № 6 (378). С. 68–77.
196. Моделирование процесса выгорания твердого топлива в реакторе твердотопливного поршневого двигателя внутреннего сгорания со слоевым методом сжигания / Белоусов Е. В., Майстренко Ю. А., Пацков В. П., Пацкова Т. В. // Сб. науч. тр. УГМТУ. Николаев : УГМТУ, 2001. № 4 (376). С. 93–104.

Наукове видання

БІЛОУСОВ Євген Вікторович

СТВОРЕННЯ ТА ВДОСКОНАЛЕННЯ ПОРШНЕВИХ ДВИГУНІВ ВНУТРІШНЬОГО ЗГОРЯННЯ НА ТВЕРДОМУ ПАЛИВІ

Монографія

Англійською мовою

Надруковано в авторській редакції
з готового оригінал-макета

Завідувачка редакції *Т. М. Забанова*

Формат 60x84/16. Ум. друк. арк. 23,25.
Тираж 100 прим. Зам. № 5 (1).

Видавництво і друкарня «Астропринт»
65091, м. Одеса, вул. Разумовська, 21
Тел.: (0482) 37-14-25, 33-07-17, (048) 7-855-855
e-mail: astro_print@ukr.net; www.astroprint.ua
Свідоцтво суб'єкта видавничої справи ДК № 1373 від 28.05.2003 р.

Visit our team of authors' website. There you'll find much useful information for your studies, work, and research. Follow the **QR-code** or link: **Modern marine engines**

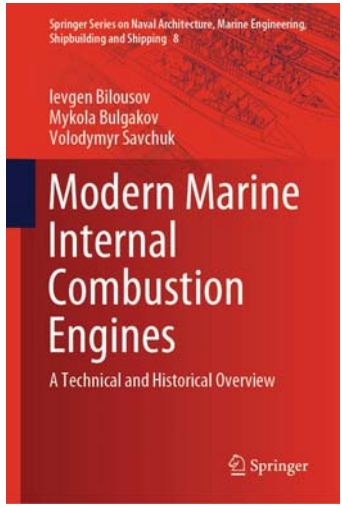
Springer Series on Naval Architecture, Marine Engineering, Shipbuilding and Shipping 8
Ievgen Bilousov
Mykola Bulgakov
Volodymyr Savchuk
Modern Marine Internal Combustion Engines
A Technical and Historical Overview
Springer

This book offers a unique, self-contained reference guide for engineers and professionals involved in shipbuilding. At the same time, it is intended to support students at maritime academies and university students in naval architecture/marine engineering with their design projects at both master and graduate levels, thus filling an important gap in the literature.

We have put our more than 20 years of experience in training marine engineer officers into practice by writing a textbook for maritime educational institutions that meets the requirements of STCW and IMO model courses (7.02 and 7.04) to the best of our ability. The textbook is illustrated with more than 500 high-quality black-and-white and color drawings that fully facilitate the assimilation of the material. In addition, this book will be useful for existing engineers, as well as for teachers conducting advanced training courses.